



The Development of Novel Antibiotics Using Chemical Evolution

by

Hany Fathy Nour

A thesis submitted in partial fulfillment
of the requirements for the degree of
Doctor of Philosophy
in Chemistry

Approved, Thesis Committee

Prof. Dr. Nikolai Kuhnert

Professor of Organic Chemistry, Jacobs University

Prof. Dr. Marcelo Fernández-Lahore

Professor of Biochemical Engineering, Jacobs University

Prof. Dr. Sijbren Otto

Professor of Organic Chemistry, Groningen University

Date of Defence: 04.09.2012

School of Engineering and Science

“Success is a decision”



Declaration of Authorship

I, Hany Nour, hereby certify that the thesis I am submitting is entirely my own original work except where otherwise indicated. Any use of the works of any other author, in any form, is properly acknowledged at their point of use.

Bremen, July 2012

Place, date

Signed

Acknowledgements

First and foremost, I would like to express my deepest praises and gratitude to Allah for His blessing in accomplishing this thesis.

My sincere gratitude and appreciation goes to my advisor Prof. Dr. Nikolai Kuhnert for continues support, motivation, encouragement throughout the course of this work and for his immense knowledge. I could not have imagined having a better advisor for my PhD work. I would like to record my sincere thanks to Prof. Dr. Marcelo Fernández-Lahore and Prof. Dr. Sijbren Otto for accepting to be members of the dissertation committee. I would like to thank Prof. Dr. Mohamed Hegab and Prof. Dr. Nabil Yousef who supervised my M.Sc. thesis and taught me how to work independently. Sincere thanks to my laboratory colleagues for their help and support during my study in particular Dr. Nadim Hourani and Ms. Agnieszka Golon. It would not have been possible to accomplish this work without their continuous help and assistance. I also would like to thank Mrs. Anja Müller for laboratory assistance.

I am most grateful to DAAD (Deutscher Akademischer Austausch Dienst) for giving me the opportunity to carry out my PhD research in Germany and for offering me a preparatory German course at Goethe Institute in Goettingen. I would like to thank deeply my German teachers at Goethe Institute in particular Mr. Andreas Hübner, Mrs. Susanna and Mrs. Susan. I would like to record my sincere gratitude to Mrs. Senay Caput who helped me during my study in Germany. I'm so glad to have come to know her and her daughter Defne. Last but not least, I would like to thank my family for supporting me spiritually throughout my life.

Abstract

Over the past few decades, bacterial resistance against antibiotics has emerged as a real threat to human health. Both mutation and most importantly the rapid exchange in genetic information between bacteria have resulted in multidrug resistant strains. A statement of the world health organization (WHO) predicts that by year 2020, 30% of all bacterial infections will not be successfully treated because of resistance. Accordingly, there is an urgent demand to develop innovative approaches for discovering new antibiotics. In an attempt to provide such approach, a novel class of chiral non-racemic macrocycles has been synthesized in [2+2]-cyclocondensation reactions of chiral dioxolane dihydrazides obtained from commercially available tartaric acids with aromatic dialdehydes. The novel macrocycles were named *tetra*-carbohydrazide cyclophanes and can be readily available in both enantiomeric forms (*R* or *S*). Three macrocycles underwent successfully dynamic exchange to generate a small dynamic combinatorial library (DCL) of eight members. Electrospray ionization time-of-flight mass spectrometry (ESI-TOF/MS) and tandem MS showed potential recognition of a one member from the generated DCL to AcNH-L-Lys-D-Ala-D-Ala-Gly-COOH oligopeptide which mimics bacterial cell wall structure. Reactions of dioxolane dihydrazides with aromatic diiso- and isocyanates afforded novel classes of *tetra*-(hydrazinecarboxamide) cyclophanes and *bis-N*-substituted hydrazinecarboxamide receptors, which also showed potential recognition to a wide selection of chiral carboxylic acids and oligopeptides as confirmed by ESI-TOF/MS.

Contents

Declaration of Authorship	iii
Acknowledgements	iv
Abstract	v
Contents	vi
List of Figures	viii
Publications	x
Abbreviations	xi
Introduction	1
Chapter I	1
1.1 Bacterial Resistance to Antibiotics	1
1.2 Dynamic Combinatorial Chemistry	2
1.3 Reversible Reactions Commonly Used in Generation of DCLs	3
1.3.1 Imine exchange	3
1.3.2 Hydrazone exchange	5
1.3.3 Disulfide exchange	7
1.3.4 Acetal exchange	7
1.3.5 Thioester and ester exchange	8
1.3.6 Pyrazolotriazinone metathesis	9
1.3.7 Michael addition	10
1.3.8 Alkene metathesis	11
1.3.9 Catalytic transamidation	12
1.3.10 Thiazolidine exchange	13
1.3.11 Boronic ester exchange	14
1.3.12 Non-covalent exchange	14
1.3.13 Metal-ligand non-covalent exchange	15
1.3.14 Other reactions used in generation of DCLs	15
References	16

Chapter 2 Trianglimine Chemistry	19
2.1. Synthesis and conformational structure	19
2.2. Applications of trianglimines	21
References	25
Aim of Thesis	27
Scope of Work	28
Paper 1	35
Paper 2	50
Paper 3	62
Paper 4	72
Paper 5	80
Paper 6	103
Paper 7	110
Conclusion	119
Appendix	120
Letters of Permission	273
Curriculum Vitae	277

List of Figures

Figure 1.1 A graphical representation showing amplification of a host molecule in a DCL ...	3
Figure 1.2 An exchange reaction between imine 1 and aniline 2	3
Figure 1.3 A small DCL formed by reacting diamines 5 and 7 with dialdehyde 6	4
Figure 1.4 Molecular amplification in a DCL of <i>poly</i> -imine macrocycles by metal salts	5
Figure 1.5 DCLs of cyclic oligomers of peptide-hydrazones	5
Figure 1.6 DCLs of an equilibrating mixture of hydrazone isomers	6
Figure 1.7 DCLs of water soluble disulfide linked cages	7
Figure 1.8 Generation of a DCL of cyclophane formaldehyde acetals	8
Figure 1.9 A DCL generated by transthioesterification approach	8
Figure 1.10 Dynamic reversibility of macrocycles 39 and 40	9
Figure 1.11 Synthetic route and dynamic reversibility of pyrazolotriazinones 48	10
Figure 1.12 A DCL generated from GSH analogues 49-52 and EA	11
Figure 1.13 Generation of a DCL <i>via</i> cross metathesis approach	12
Figure 1.14 Catalytic transamidation reaction	12
Figure 1.15 Exchange reaction of Thiazolidine 70 with aldehydes 66-69	13
Figure 1.16 Dynamic self-assembly of boronic ester using solvents as template guests	14
Figure 1.17 Self-duplication of homodimer 82 from a DCL	15
Figure 1.18 Copper (I) assisted self-assembly of copper-(I)- <i>bis</i> -(dimine) 85	15
Figure 2.1 [3+3]-cyclocondensation reaction of (1 <i>R</i> ,2 <i>R</i>)- 1 and dialdehydes 2	19
Figure 2.2 Energy-minimized structure of trianglimine 4 at the MM+ level	20
Figure 2.3 Formation of functionalized trianglimines 9 from dialdehydes 8	20

Figure 2.4 Trianglimines 10-12 with different cavity sizes	21
Figure 2.5 Trianglimine 4 forming interlocked structure with β -cyclodextrin 14	22
Figure 2.6 Energy-minimized structure for host/guest complex 4/20 at the MM+ level	23
Figure 2.7 Enantioselective Henry reaction catalyzed by Trianglimine-Cu(OAc) ₂	23
Figure 2.8 Asymmetric hydrosilylation of ketimine 28	24
Figure 3.1 Molecular recognition of Vancomycin to D-Ala-D-Ala	29
Figure 3.2 C ₃ -symmetrical 5 and non-symmetrical 6 trianglimines obtained from 2	30
Figure 3.3 Modification of the core structure of trianglimine 7	31
Figure 3.4 Structures of trianglimine 7 and <i>tetra</i> -carbohydrazide cyclophane 10	32
Figure 3.5 Computed structure for host/guest complex 12/11 at the MM+ level	32
Figure 3.6 Macrocycle 13 and receptor 14 which bind with oligopeptides	33

Publications

1. H. Nour, M. Matei, B. Bassil, U. Kortz, N. Kuhnert, Synthesis of tri-substituted biaryl based trianglimines: formation of C_3 -symmetrical and non-symmetrical regioisomers, *Org. Biomol. Chem.*, **2011**, 9, 3258.
2. H. Nour, A. López-Periago, N. Kuhnert, Probing the mechanism and dynamic reversibility of trianglimine formation using real-time electrospray ionization time-of-flight mass spectrometry, *Rapid Commun. Mass Spectrom.*, **2012**, 26, 1070.
3. H. Nour, N. Hourani, N. Kuhnert, Synthesis of novel enantiomerically pure tetra-carbohydrazide cyclophane macrocycles, *Org. Biomol. Chem.*, **2012**, 10, 4381.
4. H. Nour, A. Golon, A. Le-Gresley, N. Kuhnert, Novel synthesis of enantiomerically pure dioxaspiro[4.5]decane tetra-carbohydrazide cyclophane macrocycles, *Chem. Eur. J.*, **2012**, *submitted manuscript*.
5. H. Nour, T. Islam, M. Fernández-Lahore, N. Kuhnert, Probing the dynamic reversibility and generation of dynamic combinatorial libraries in the presence of bacterial model oligopeptides as templating guests of tetra-carbohydrazide macrocycles using electrospray mass spectrometry, *Rapid Commun. Mass Spectrom.*, **2012**, *accepted manuscript*.
6. H. Nour, A. Golon, T. Islam, M. Fernández-Lahore, N. Kuhnert, Synthesis and ESI-MS complexation studies of novel chiral tetra-(hydrazinecarboxamide) cyclophane macrocycles, *manuscript*.
7. H. Nour, A. Golon, T. Islam, M. Fernández-Lahore, N. Kuhnert, Synthesis, self-assembly and ESI-MS complexation studies of novel chiral *bis-N*-substituted-hydrazinecarboxamide receptors, *manuscript*.

Abbreviations

ACN	Acetonitrile
AcOH	Acetic acid
Ala	Alanine
AM1	Austin model 1
AMBER	Assisted model building with energy refinement
APCI	Atmospheric pressure chemical ionization
CA	Carbonic anhydrase II
CC	Column chromatography
CD	Circular dichroism
COSY	Correlation spectroscopy
DCC	Dynamic combinatorial chemistry
<i>N,N'</i> -DCC	<i>N,N'</i> -Dicyclohexylcarbodiimide
DCL	Dynamic combinatorial library
DCM	Dichloromethane
DEPT	Distortionless enhancement by polarization transfer
DIEA	<i>N,N</i> -Diisopropylethylamine
DMF	<i>N,N</i> -Dimethylformamide
DMSO	Dimethyl sulfoxide
EA	Ethacrynic acid
EDT	1,2-Ethanedithiol

MS	Mass spectrometry
MS/MS	Tandem mass spectrometry
ESI-MS	Electrospray ionization mass spectrometry
ESI-TOF/MS	Electrospray ionization time-of-flight mass spectrometry
FT-IR	Fourier transform infrared spectroscopy
GSH	Glutathione
Gly	Glycine
HBTU	<i>N,N,N',N'</i> -tetramethyluronium hexafluorophosphate
HMBC	Heteronuclear multiple bond correlation
HMQC	Heteronuclear multiple quantum correlation
HOBt	<i>O</i> -(Benzotriazol-1-yl)-hydroxybenzotriazole
HPLC	High performance liquid chromatography
HRMS	High resolution mass spectrometry
Lac	Lactate
Lys	Lysine
MM+	Molecular mechanics
NMP	<i>N</i> -Methylpyrrolidone
NMR	Nuclear magnetic resonance
Otf	Trifluoromethanesulfonate
PM3	Parameterized Model number 3
PTSA	<i>p</i> -Toluenesulfonic acid

RMS	Root-mean square
ROESY	Rotating frame nuclear overhauser effect correlation spectroscopy
SjGST	Schistosoma japonicum glutathione- <i>S</i> -transferase
TFA	Trifluoroacetic acid
THF	Tetrahydrofuran
TLC	Thin layer chromatography
TMS	Tetra-methylsilane
TOCSY	Total correlation spectroscopy
UV	Ultraviolet
VT-NMR	Variable temperature nuclear magnetic resonance
WHO	World health organization

Chapter 1

1.1 Bacterial Resistance to Antibiotics

Over the past decades, bacterial resistance to antibiotics has emerged as a real threat to mankind. Both mutation and most importantly the rapid exchange in genetic information between bacteria have resulted in multi-drug resistant strains. Antibiotics are vital drugs, which treat infections caused by bacteria without harming the person being treated. In 1930s, sulfonamides were developed as the first and most effective antibacterial drugs against a limited number of bacterial species. Sir Alexander Fleming, a microbiologist at St. Mary's Hospital in London, discovered the well known antibiotic Penicillin in 1928. Penicillin belongs to a class of β -lactam antibiotics, which contains a chemically activated β -lactam ring. This ring is critically important for the function of the antibiotic. Penicillin was biologically active against a deadly human pathogen called *Staphylococcus aureus*. The use of penicillin saved millions of lives worldwide and revolutionized the practice of medicine. In 1940, Edward Abraham and Ernst Chain reported the existence of an enzyme in *Escherichia coli*, which inactivated penicillin by hydrolyzing the β -lactam ring. Penicillin became ineffective in less than ten years from its use for treating some bacterial infections caused by *Staphylococcus aureus*. There are fortunately great differences between bacterial and human cells. Accordingly, there are many targets on bacterial cells on which the antibiotic drugs can work without affecting human cells. Many classes of drugs have been introduced into the market to satisfy the urgent demand for antibiotics. Some antibiotics such as quinolones prevent replication of DNA. Others prevent bacteria from making RNA, which is essential for many cellular processes. The lack of RNA is lethal for the cell. Polymyxin causes damage of bacterial membrane, which is essential for regulating the movements of materials in and out of the cells. Tetracyclines, aminoglycosides and macrolides are a group of antibiotics, which prevent bacteria from making proteins. Bacteria unable to make their protein will no longer grow and will eventually die. Bacterial cell wall constitutes an important target for antibiotic drugs. Bacteria cannot survive without an intact cell wall. Penicillin inhibits transpeptidation, Vancomycin inhibits both transpeptidation and transglycosylation, while Bacitracin makes disruption of the carriers required for moving *N*-acetyl glucosamine and *N*-acetylmuramic acid across the membrane. Bacteria have developed resistance to almost all different classes of antibiotics discovered to date. Bacteria resist Vancomycin by making a

Introduction •

complete remodel of the cell wall *via* replacing the part D-Ala-D-Ala by D-Ala-D-Lac. They acquire resistance to Penicillin as previously mentioned by releasing β -lactamases, which hydrolyze the β -lactam ring. Bacteria get nutrients through pores of proteins. These pores are the same portals for entry of antibiotics into the cell. Bacteria synthesize proteins, which form smaller pores, thus permitting nutrients to enter the cell and excluding antibiotics with larger size. Bacteria resist Streptomycin by making modification of the chemical structure of the antibiotic though addition of some groups into its structural framework, thus preventing it from doing its proper task. Protein pumps are one of the most efficient mechanisms by which bacteria resist antibiotics. *Staphylococcus aureus* resists Ciprofloxacin and Tetracycline antibiotics by pumping the antibiotic out of cells faster than it comes in. The rapid development of antibiotic resistance has led to a continual need to discover novel drugs using innovative approaches. Dynamic combinatorial chemistry (DCC) can provide such approach.

1.2 Dynamic Combinatorial Chemistry

Over the past two decades, DCC has attracted considerable and growing interest in supramolecular chemistry.¹⁻⁷ Unlike conventional synthesis, DCC involves generation of an equilibrating mixture of interchanging species in solution forming in reversible reactions. The mixture of library members, which forms in a DCC, constitutes a dynamic combinatorial library (DCL). In DCC, library members are formed under thermodynamic control. The composition of the DCL is subject to change by addition of an external guest acting as a trigger, which acts by shifting the equilibrium towards the preferential formation of the most stable host/guest complexes, in other words ideally from the DCL mixture of compounds one host molecule is formed selectively that is able to recognize the guest. In DCC therefore, amplified targets can form in high yields with sufficient purity in covalent reversible reactions (Figure 1.1).

DCC allows generation of a diverse collection of structurally unique compounds, which cannot be obtained by other classical synthetic approaches. Direct screening of the DCL can be achieved by electrospray ionization time-of-flight mass spectrometry (ESI-TOF/MS). Electrospray mass spectrometry (ESI-MS) showed considerable promise in the analysis of DCLs as a soft ionization technique due its ability to provide precise mass values, high resolution and little or almost no fragmentations. High performance liquid chromatography (HPLC) is another sophisticated tool, which can be used to monitor the exchange and amplification processes in DCLs. The

Introduction •

combination of DCC and supramolecular chemistry along with rapid screening of library members or host/guest complexes by mass spectrometry (MS) can lead to discovery of novel drugs with intriguing structures. Literature is rich with different examples of reversible reactions used in generation of DCLs. These reactions are described here in details.

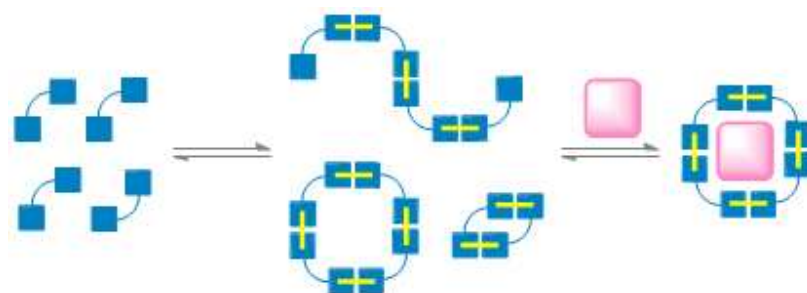


Figure 1.1 A graphical representation showing amplification of a host molecule in a DCL.

1.3 Reversible Reactions Commonly Used in Generation of DCLs

1.3.1 Imine exchange

Azomethine linkages ($\text{CH}=\text{N}$) form in a simple reversible reaction of aldehydes or ketones with primary amines.⁸ The dynamic reversibility of the imine bond makes it an ideal choice for the generation of DCLs as firstly demonstrated and explored by Huc and Lehn (Figure 1.2).⁹ Imine exchange reactions can lead to polymerization or macrocyclization depending on the overall concentration of the components. Furthermore, the functional groups that are able to form non-covalent interactions with the external template and the molecular geometries of the interconverting components may shift the imine DCL towards a single compound.

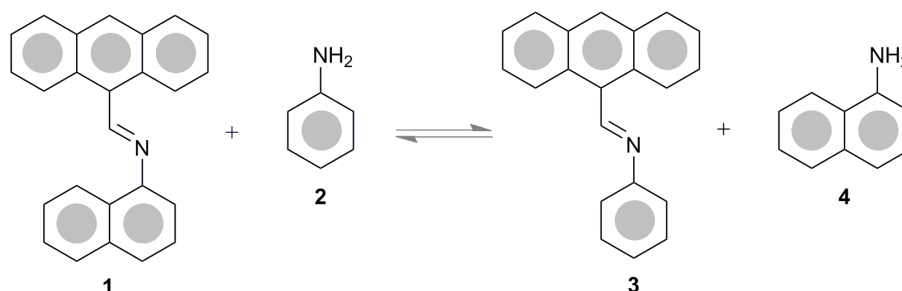


Figure 1.2 An exchange reaction between imine **1** and aniline **2**.

Imine containing Schiff base macrocycles have been extensively studied due to the ability of the lone pairs on the imine nitrogen atoms to interact with anionic guests through ion bridges

Introduction •

following protonation. An advantage of the carbon-nitrogen double bond of imine is its ability to undergo reduction to the corresponding amine, which is more kinetically stable and offer a good opportunity for the analysis of products from imine exchange reactions. An interesting example for the formation of a small dynamic library of interchanging imine macrocycles has been demonstrated by Wessjohann and co-workers (Figure 1.3).¹⁰ Wessjohann *et al.* introduced an innovative approach for quenching the imine exchange reaction based on Ugi four component reactions as an alternative to the typical reduction procedure with borohydrides.¹⁰ The quenching process takes place by addition of an isocyanate and a carboxylic acid with stirring the mixture at room temperature. The authors demonstrated that addition of Mg^{II} followed by subsequent quenching resulted in amplification of macrocycle **8** obtained through a [1+1]-cyclocondensation reaction at the expense of the products obtained through [2+2]-cyclocondensation reactions, while addition of Ba^{II} , which has larger radius, resulted in formation of all library members without preferential amplification.

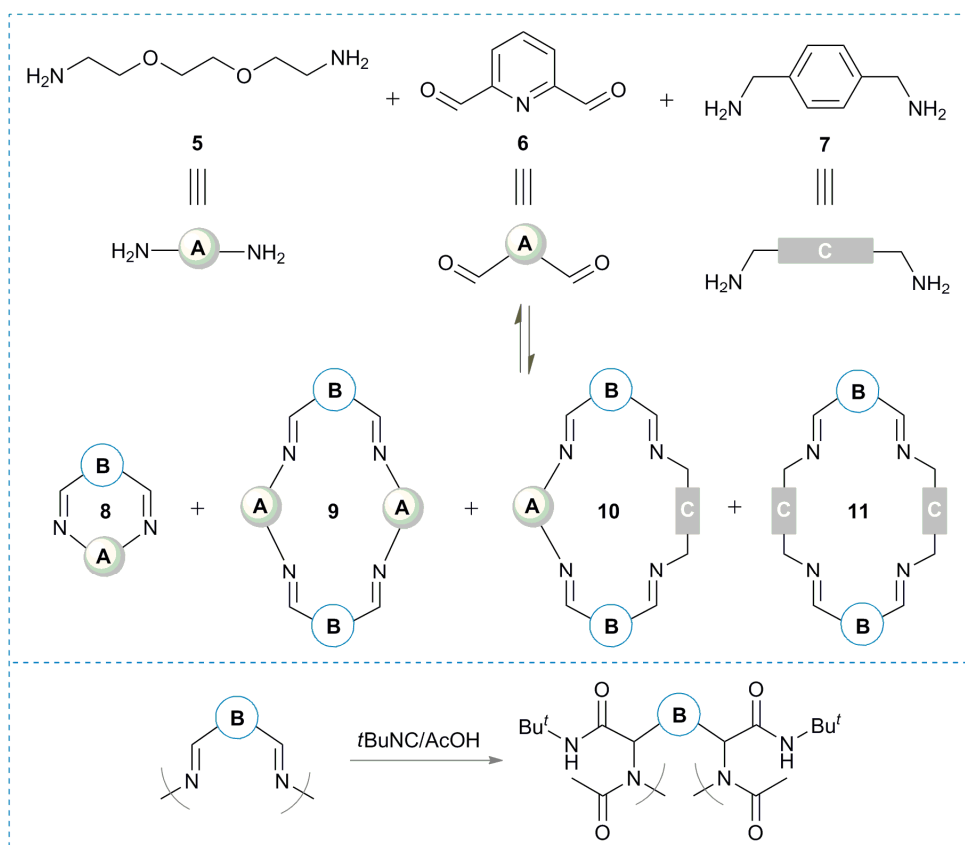


Figure 1.3 A small DCL formed by reacting diamines **5** and **7** with dialdehyde **6**.

Introduction •

Molecular amplification in a DCL of imine macrocycles through addition of metal ions has been demonstrated by Gotor and co-workers.¹¹ Reaction of *trans*-(1*R*,2*R*)-1,2-diaminocyclohexane **12** with pyridine-2,6-dicarbaldehyde **6** forms a DCL of six *poly*-imine macrocycles **13**. Addition of metal salts shifts the equilibrium towards the best complementary of hosts and guests. Amplification of macrocycles **14** and **15** obtained through [3+3]- and [2+2]-cyclocondensation reactions take places by addition of Cd²⁺ and Ba²⁺, respectively (Figure 1.4).¹¹ Interestingly, when an excess of Cd²⁺ was added to complex **15**, the equilibration shifts towards the [3+3]-adduct **14**.

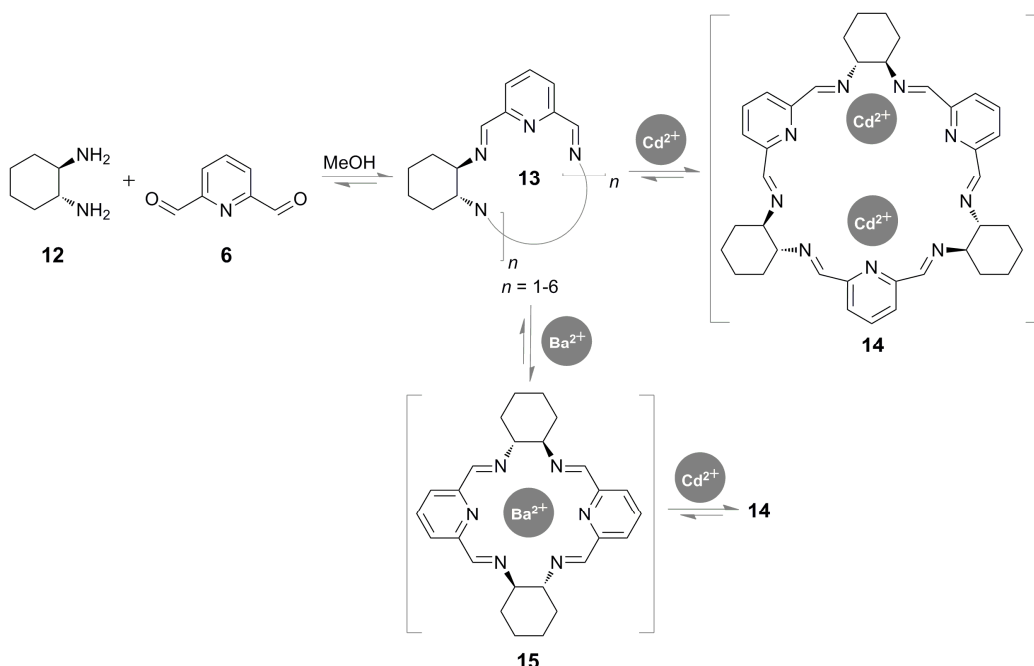


Figure 1.4 Molecular amplification in a DCL of *poly*-imine macrocycles by metal salts.

1.3.2 Hydrazone exchange

Sanders and co-workers reported in many occasions the formation of DCLs from peptide-hydrazone building blocks and amplification of some members of the libraries by addition of external templates (Figure 1.5).¹²⁻²²

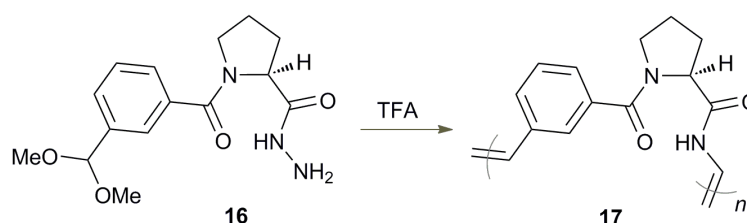


Figure 1.5 DCLs of cyclic oligomers of peptide-hydrazones.

Introduction •

Lehn and co-workers reported an early example for the generation of a DCL of hydrazones from 5,5-dimethyl-1,3-cyclohexanedione **18** and 2-hydrazinopyridine **19** (Figure 1.6).²³ Addition of dibutylbarbiturate **26** to the DCL mixture of isomers **20-25** shifts the equilibration towards host **25**, which forms the most stable complex with the guest, in this case by formation of four hydrogen bonds.

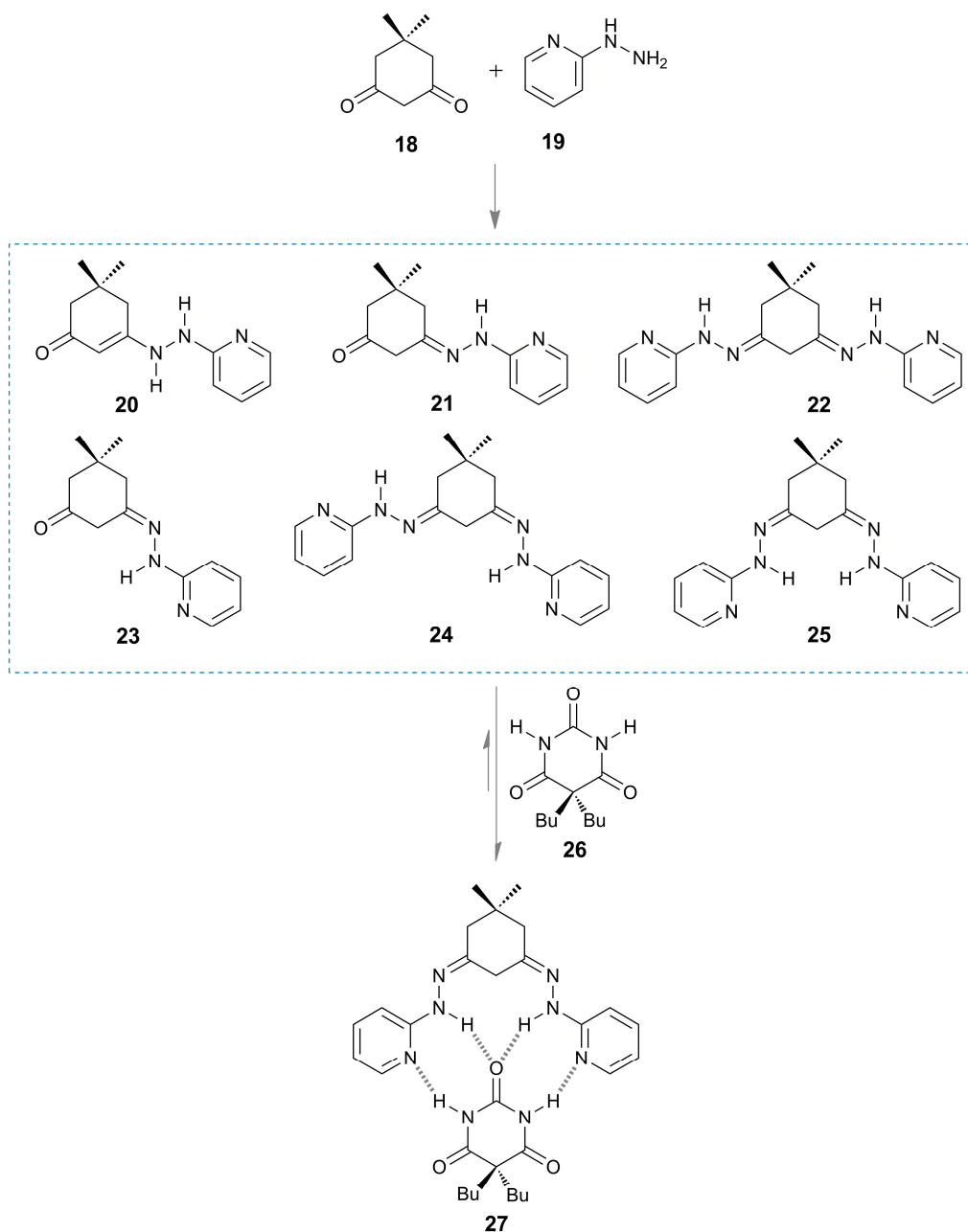


Figure 1.6 DCLs of an equilibrating mixture of hydrazone isomers.

1.3.3 Disulfide exchange

Disulfide exchange has been thoroughly investigated in generation of DCLs.²⁴⁻³⁸ Otto *et al.* reported the generation of a DCL having cage-like structures made from di- and trithiols **28-30** under thermodynamic control (Figure 1.7).³⁸ The interlocked disulfides **31-33** form by oxidation of an aqueous solution of the thiols upon exposure to air in the presence of a thiolate. Quenching of the DCL took place under acidic condition or by removing the thiolate.³⁹

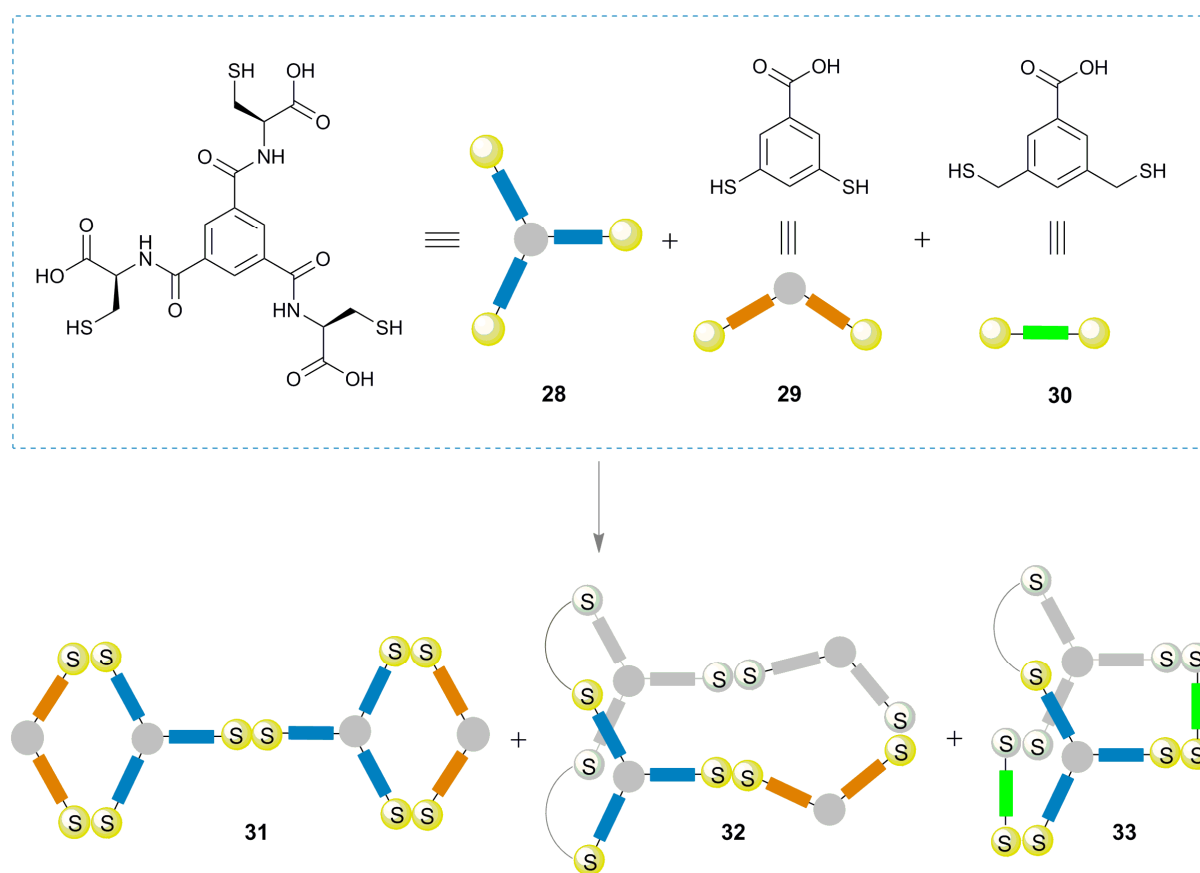


Figure 1.7 DCLs of water soluble disulfide linked cages.

1.3.4 Acetal exchange

There are few examples reported in literature, which describe generation of DCC from acetals.^{40,41} Mandolini and co-workers reported on the acid-catalyzed transacetalation reaction of formaldehyde acetals with generation of a DCL of interchangeable cyclophane-type oligomers under mild conditions.⁴²⁻⁴⁵ The authors suggested the mechanism shown in Figure 1.8 for the transacetalation process, which took place through a ring-fusion/ring-fission S_N2 pathway.

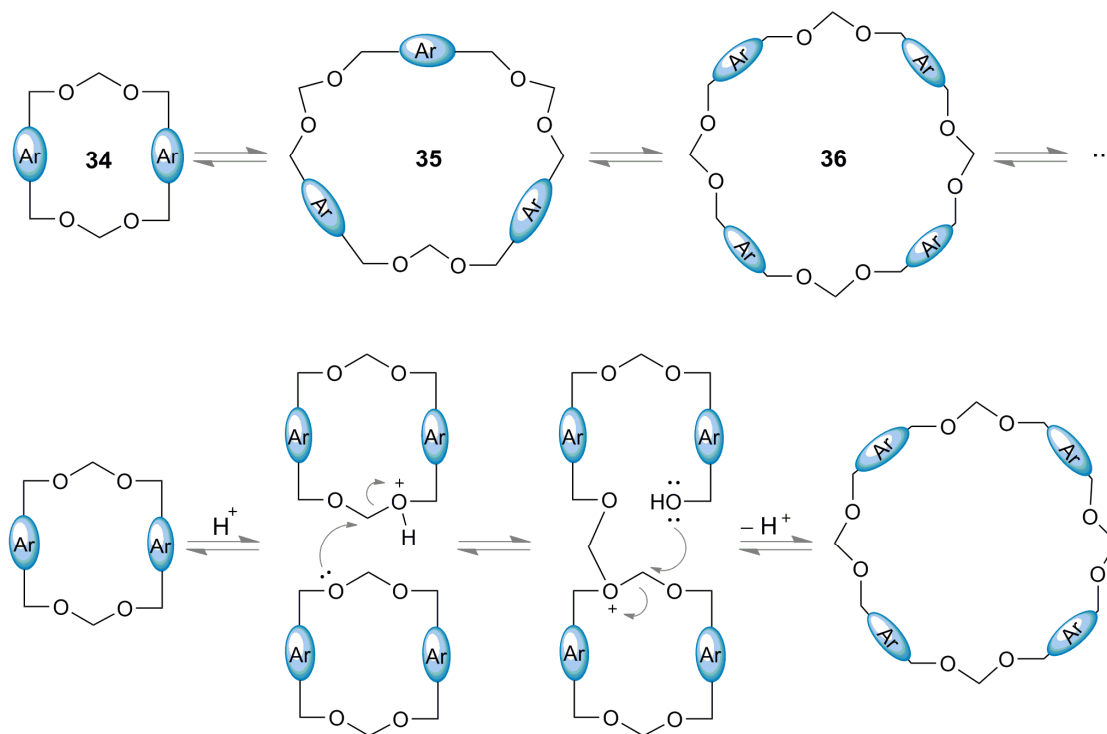


Figure 1.8 Generation of a DCL of cyclophane formaldehyde acetals.

1.3.5 Thioester and ester exchange

Ramström and Larsson reported on the generation of a DCL *via* transthioesterification in aqueous media under mild conditions (Figure 1.9).^{46,47} The library members were subjected to recognition by acetylcholineesterase. Compounds **37** and **38** were recognized and hydrolyzed by the enzyme from the screened library. This approach is of a great importance for discovering new catalytic systems of organic and inorganic reactions using DCLs.

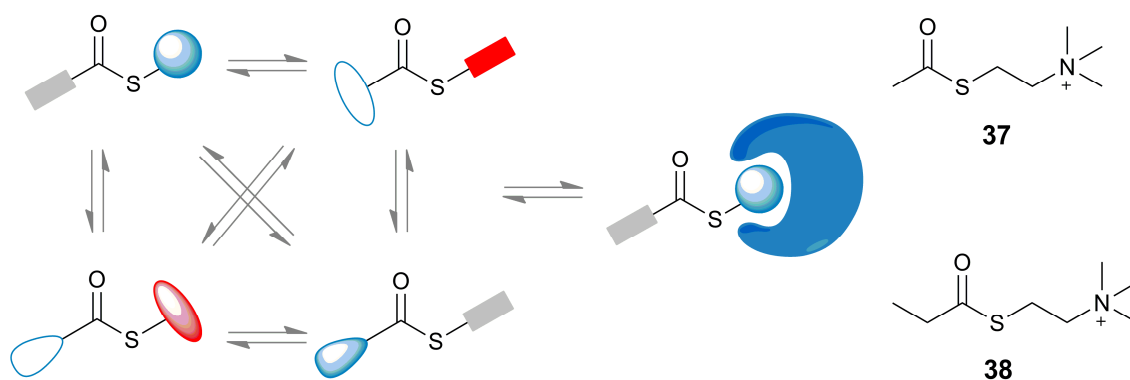


Figure 1.9 A DCL generated by transthioesterification approach.

Introduction •

The dynamic reversibility of macrocycles **39** and **40**, which are derived from cinchona alkaloid, has been demonstrated by Sanders and Rowan.⁴⁸ Transesterification of macrocycles **39** and **40** was achieved by refluxing the compounds in toluene in the presence of potassium methoxide-crown ether complex to form the four symmetrically mixed products **39-42** shown in Figure 1.10.

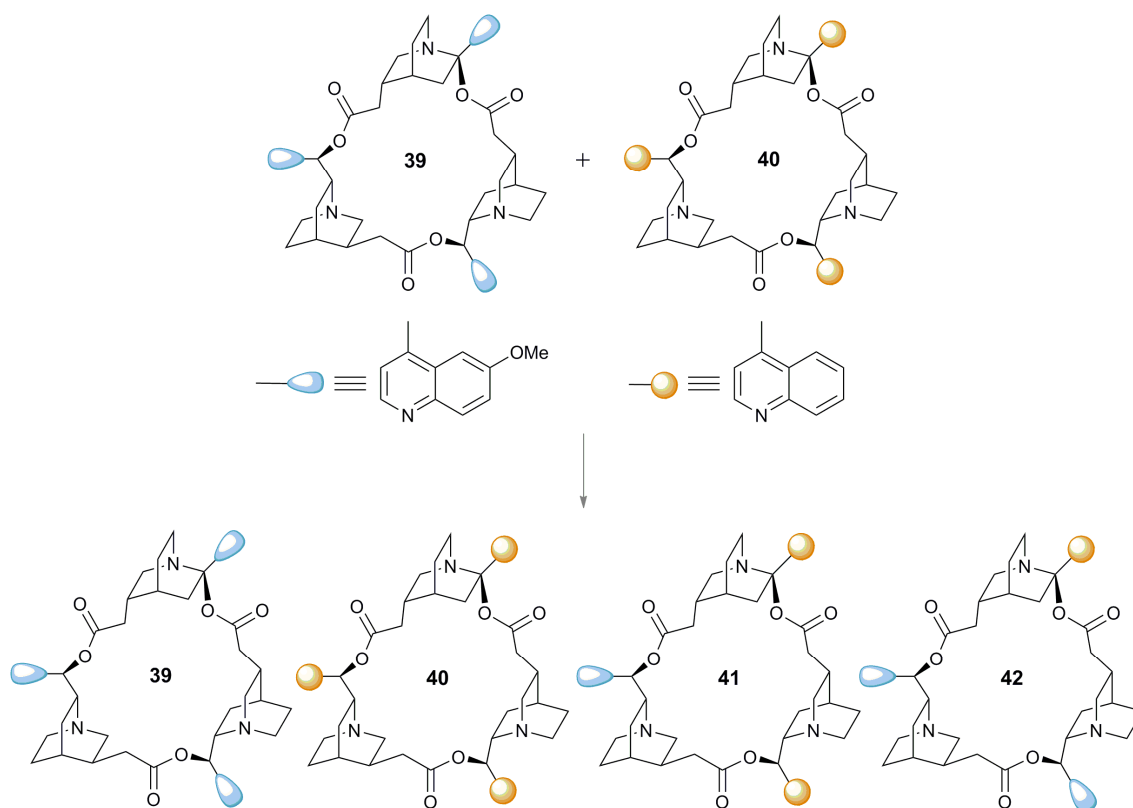


Figure 1.10 Dynamic reversibility of macrocycles **39** and **40**.

1.3.6 Pyrazolotriazinone metathesis

Wipf *et al.* reported the reversible metathesis reaction of pyrazolotriazinones **48** and aliphatic aldehydes. A DCL of heterocycles (*a-d*) was generated in an aqueous phosphate buffered solution.⁴⁹ Pyrazolotriazinones **48** were synthesized in multistep reactions involving Aldol condensation of acetone **43** with diethyloxalate **44** to form **45**. Cyclocondensation of **45** with hydrazine monohydrate afforded pyrazole **46**, which upon reaction with methyl hydrazine in the presence of *N,N'*-dicyclohexylcarbodiimide (*N,N'*-DCC) gave compound **47**. Condensation of **47** with aliphatic aldehydes gave pyrazolotriazinones **48** (Figure 1.11).

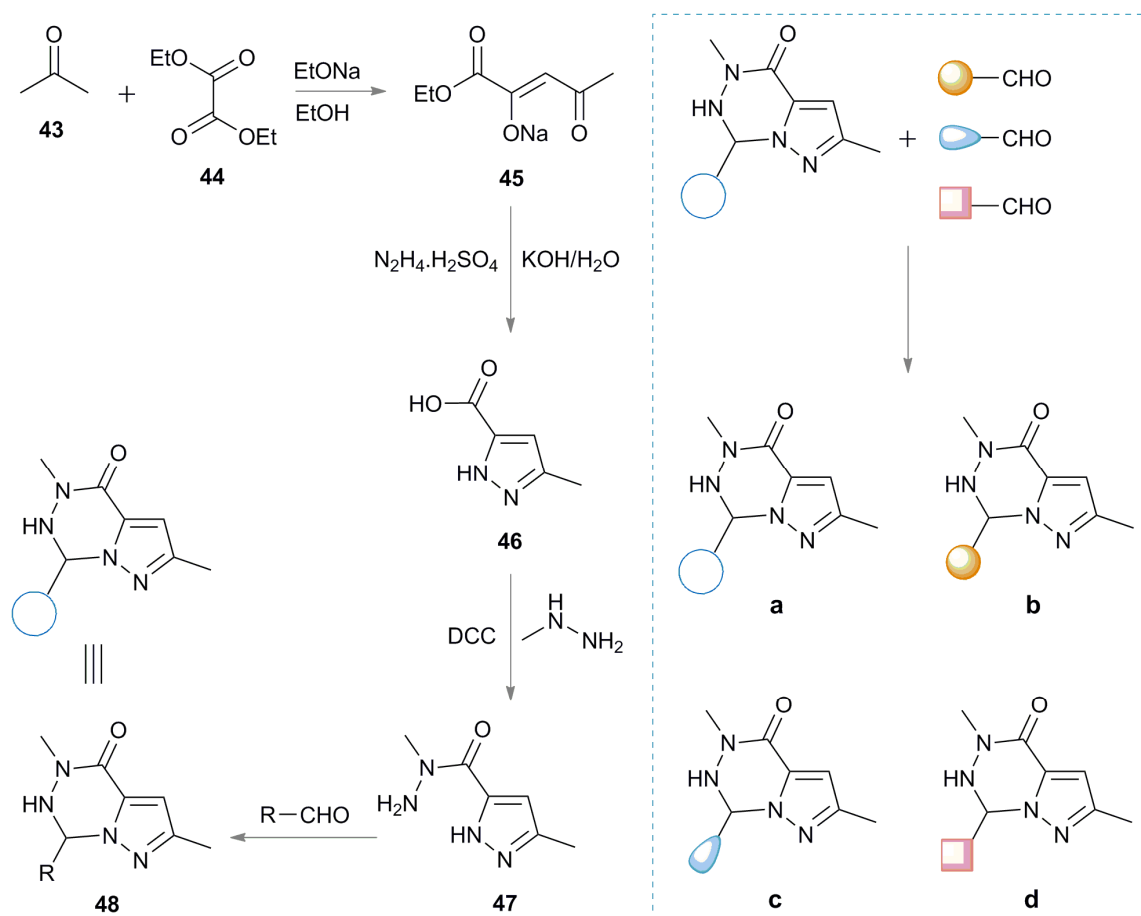


Figure 1.11 Synthetic route and dynamic reversibility of pyrazolotriazinones **48**.

1.3.7 Michael addition

The 1,4-conjugate addition of a nucleophile to an α,β -unsaturated carbonyl compound is known as Michael addition. The reaction is reversible at a pH of 7-8 and takes place at room temperature in water making it suitable for different DCC applications. Addition of proteins or biological targets is possible under such mild conditions.^{50,51} Glutathione GSH-**49** is a thiol containing tripeptide existing in eukaryotic cells. It is an important antioxidant, which prevents damage of cellular components caused by peroxides and other toxic electrophiles. It acts by scavenging toxic electrophiles, enhancing their water solubility and thus eliminating them out from the cell. Ethacrynic acid (EA) contains an α,β -unsaturated carbonyl functionality making it suitable for the Michael addition reaction. Campopiano and co-workers reported on generation of a DCL from GSH analogues **49-52** and EA **53** via Michael addition reaction (Figure 1.12).

Introduction •

Addition of *Schistosoma japonicum* glutathione-*S*-transferase (SjGST) amplifies library member **54**. This approach is a good example for enzyme-directed amplification in a DCL. At low pH the reaction becomes slow and irreversible allowing switching off the DCL.

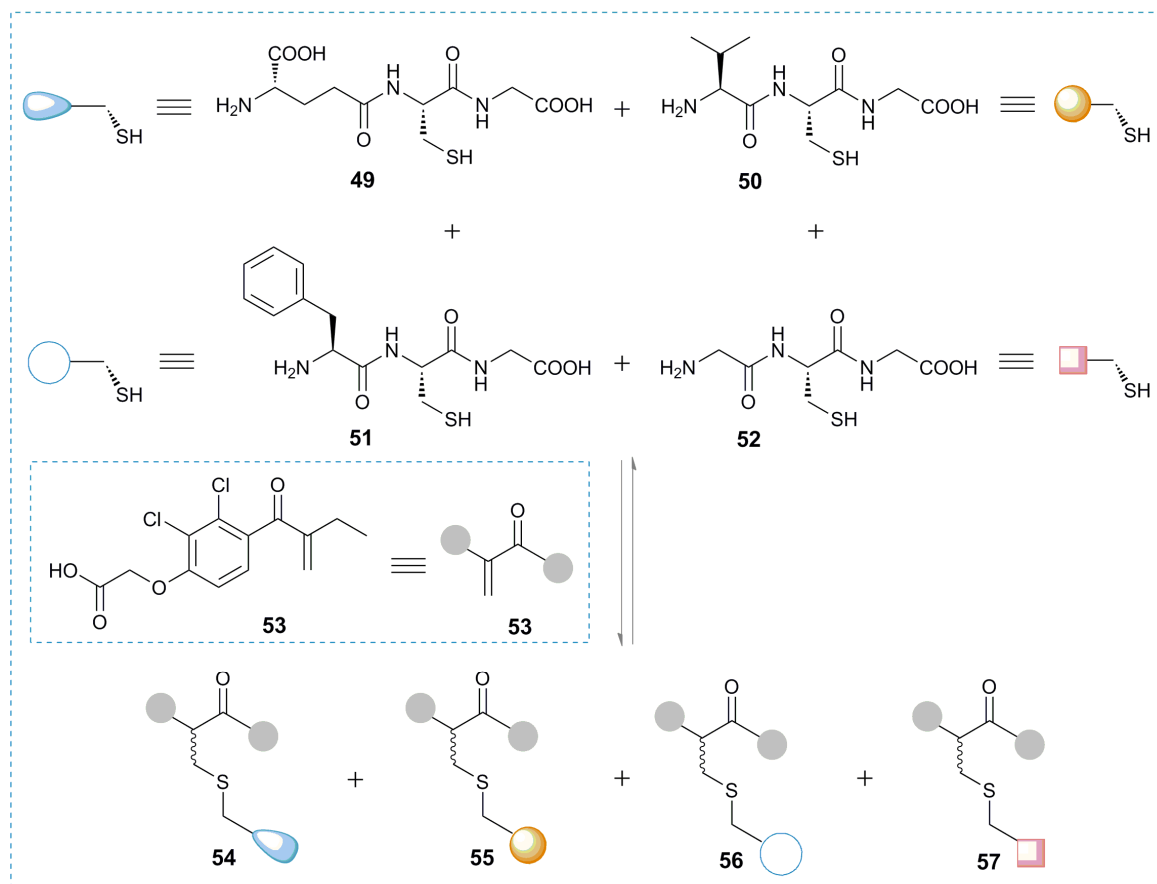


Figure 1.12 A DCL generated from GSH analogues **49-52** and EA.

1.3.8 Alkene metathesis

Carbonic anhydrase II (CA) are family of Zn-containing enzymes, which catalyze the interconversions of bicarbonate ions (HCO_3^-) and carbon dioxide, which forms in high levels in almost all metabolic processes. Some antitumor drugs function by inhibiting Zn-containing enzymes. The mechanism of inhibition for CA proceeds through recognition of the sulfonamide moiety in the structure core of the inhibitor. Poulson and Bornaghi reported on generation of a DCL *via* cross metathesis olefin approach using an immobilized Grubbs first generation catalyst.⁵² The authors demonstrated the recognition affinity of **58** to CA enzyme from the screened library members (Figure 1.13).

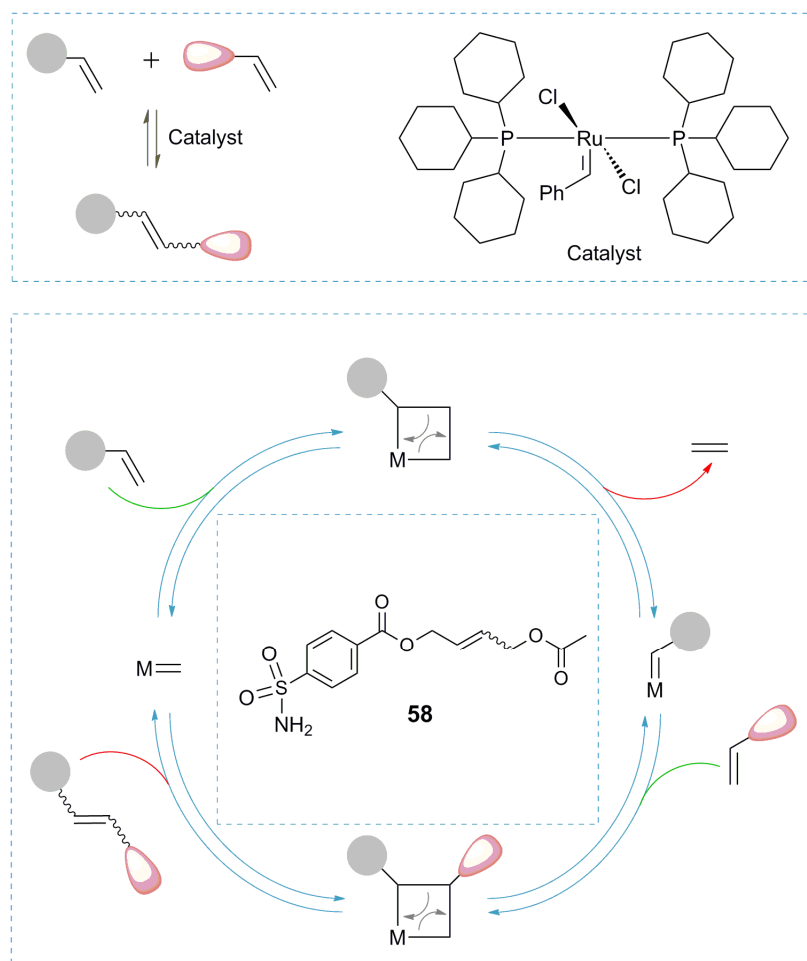


Figure 1.13 Generation of a DCL *via* cross metathesis approach.

1.3.9 Catalytic transamidation

Carboxamide group is known to be chemically stable and cannot undergo reversible reactions under normal reaction conditions. Stahl and co-workers reported an efficient strategy, which promotes transamidation mediated by catalysts under moderate reaction conditions (Figure 1.14).⁵³ The transamidation reaction took place in toluene in the presence of a Lewis-acid catalyst such as $\text{Ti}(\text{NMe}_2)_4$, $\text{Al}_2(\text{NMe}_2)_6$ and $\text{Sc}(\text{OTf})_3$ (OTf, trifluoromethane sulfonate).

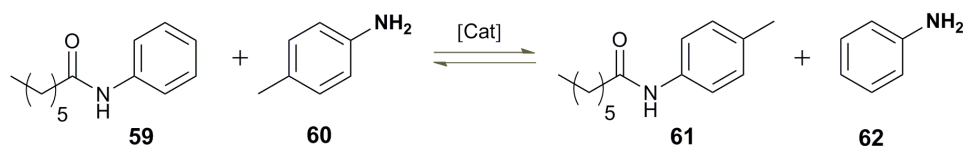


Figure 1.14 Catalytic transamidation reaction.

1.3.10 Thiazolidine exchange

Thiazolidines can undergo reversible reactions at room temperature in aqueous acidic media (pH 4-5) to generate DCLs of interconverting species under thermodynamic control.⁵⁴ Condensation of aldehydes **64** with chiral cysteine ethyl ester **63** in ethanol affords thiazolidine **65** (Figure 1.15). Thiazolidine **70** undergoes a reversible aminothiols exchange reaction with *m*- and *p*-substituted aromatic aldehydes **66-69**. Quenching the dynamic exchange process takes place simply by raising the pH of the reaction to 7. The equilibration process proceeds faster at elevated temperature, but with hydrolysis of **65** to **63**.

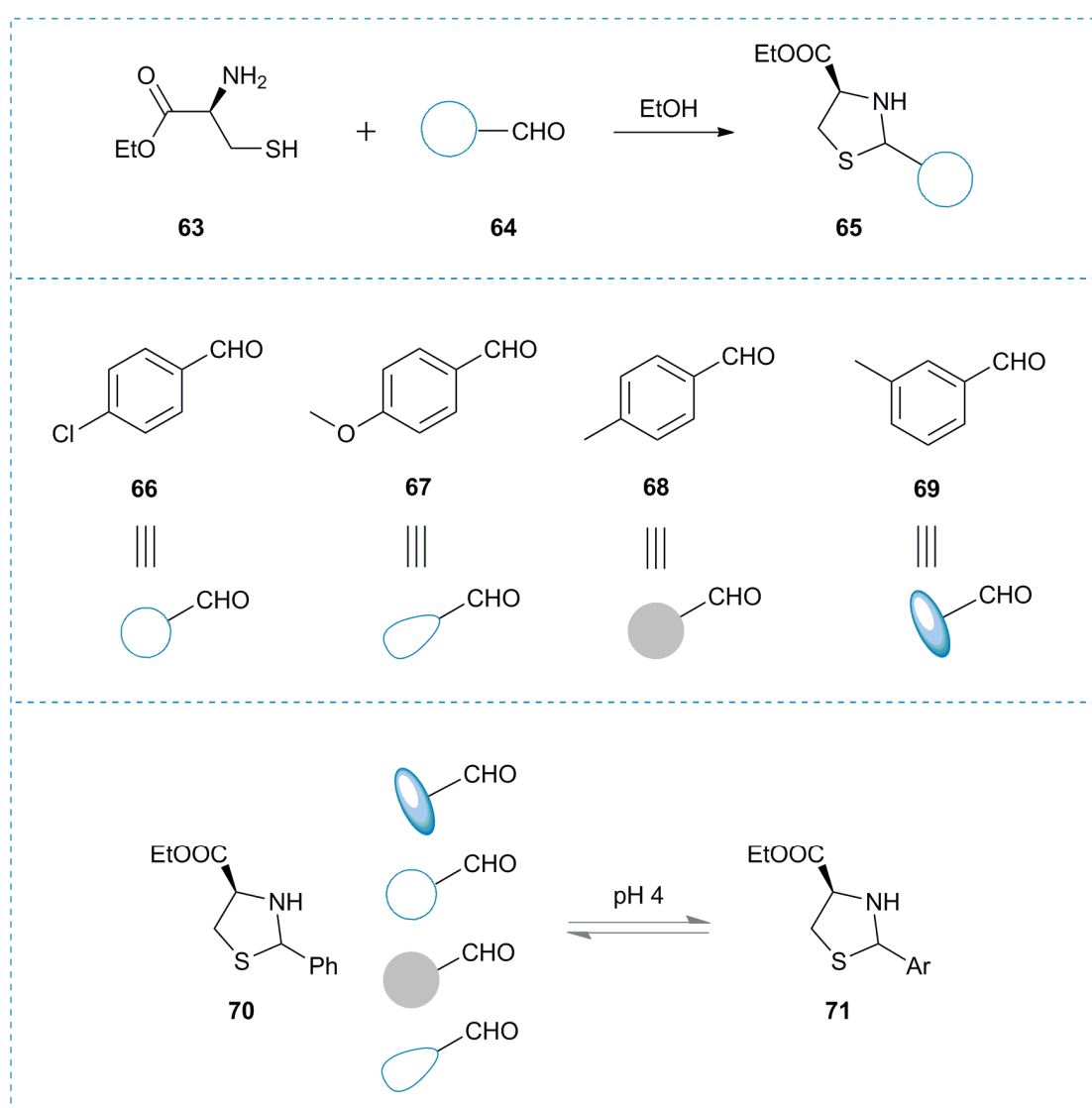


Figure 1.15 Exchange reaction of Thiazolidine **70** with aldehydes **66-69**.

1.3.11 Boronic ester exchange

The reaction of racemic tetrol **72** with structurally rigid 1,4-benzenedi(boronic acid) **73** has been reported by Iwasawa and Takahagi (Figure 1.16).⁵⁵ The authors showed the vital role of the solvent of the reaction in determining the type of the supramolecular product obtained. Aromatic solvents act as templates, which facilitate formation of supramolecular structures and stabilize them *via* π - π stacking interactions. Thus, reaction of **72** and **73** in MeOH forms polymer **75**. Tetrol **72** and **73** react in a mixture of MeOH/naphthalene to form an inclusion complex of the [2+2]-macrocycle **74** in high yield. Triphenylene, which has larger size assisted formation of [3+3]-macrocycle **76**. The authors also showed the possibility of interconversion between the **74** and **76** macrocycles in the presence of MeOH and the appropriate aromatic guest molecules.⁵⁵

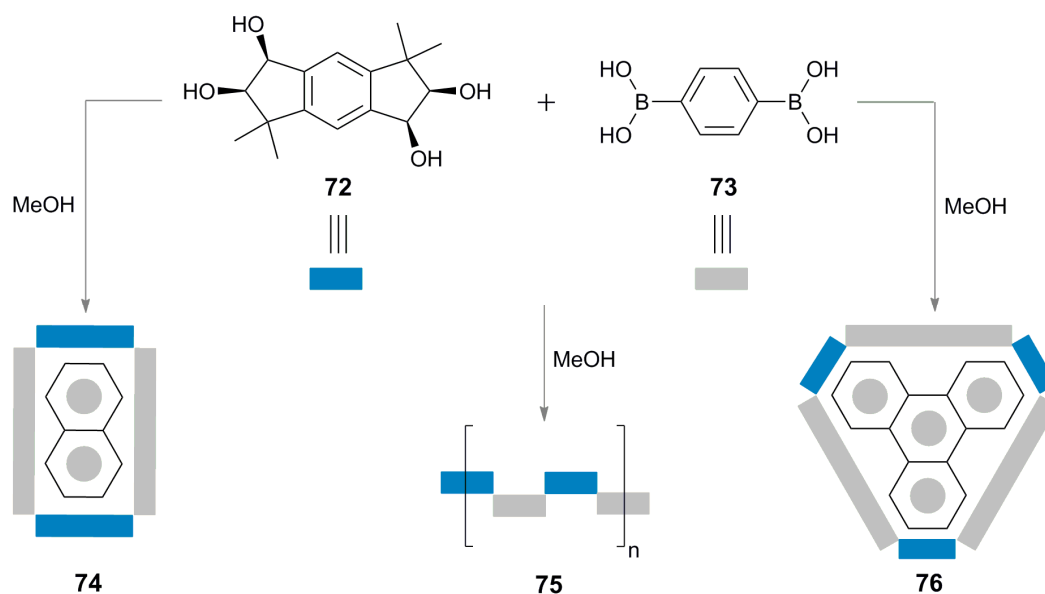


Figure 1.16 Dynamic self-assembly of boronic ester using solvents as template guests.

1.3.12 Non-covalent exchange

Giuseppone and Xu reported on generation of a DCL composed of eleven library members by reacting aldehydes **78**, **79** and **81** with amines **77** and **80** in CDCl_3 (Figure 1.17).⁵⁶ Amplification of the homodimer **82** took place at the expense of other library members due to its ability to form complementary supramolecular units with self-recognition properties. Homodimer **82** possesses two imine moieties to permit dynamic reversibility through covalent bonds, thus facilitating the interconversion between the different library members.

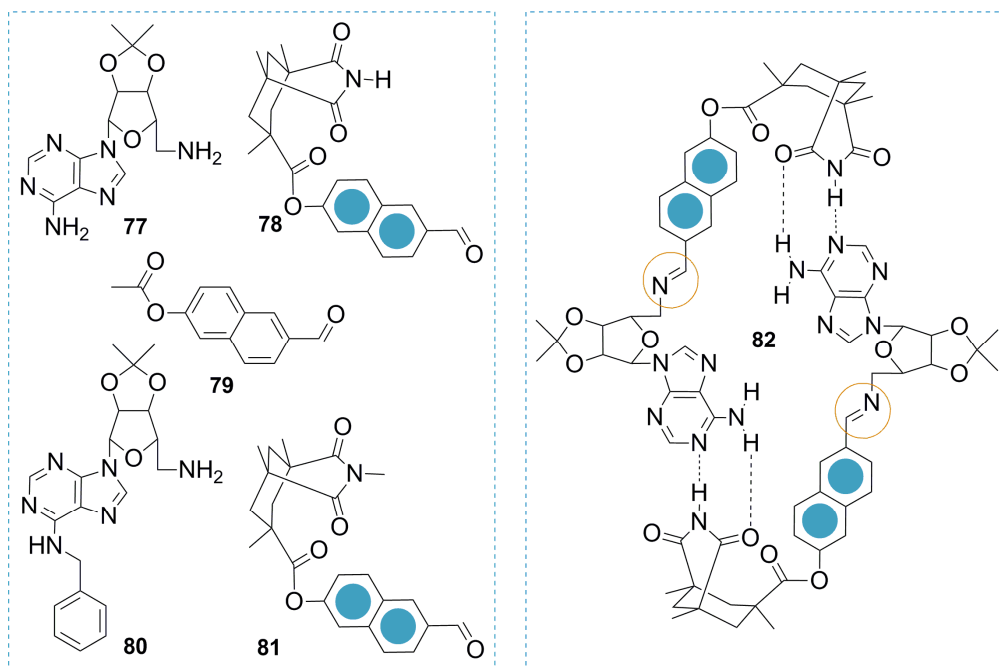


Figure 1.17 Self-duplication of homodimer **82** from a DCL.

1.3.13 Metal-ligand non-covalent exchange

2-Aminoethanesulfonic acid **83** reacted with pyridine-2-carboxaldehyde **84** in D_2O to afford a mixture of interconverting products, which upon addition of Cu_2O collapsed down to give copper(I)-*bis*-(dimine) **85**. Cu^I ions act as templating guests, which stabilize **85** (Figure 1.18).⁵⁷

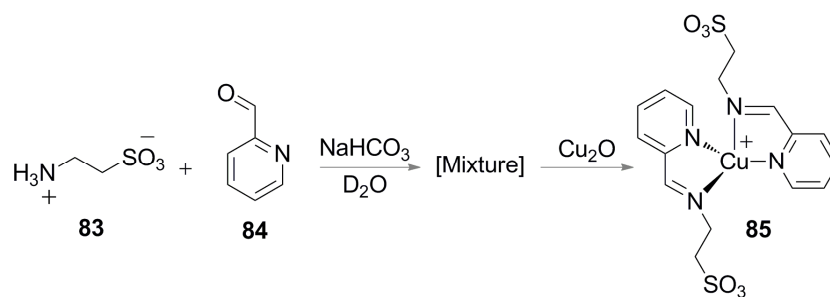


Figure 1.18 Copper (I) assisted self-assembly of copper(I)-*bis*-(dimine) **85**.

1.3.14 Other reactions used in generation of DCLs

Further reversible reactions, which involve generation of interchanging members in DCLs are Diels-Alder,⁵⁸ nitrones exchange,⁵⁹ amine exchange,⁶⁰ photoinversion of sulfoxides⁶¹ and metal-ligand exchange.⁶²⁻⁷¹

References

1. E. Moulin, G. Cormos, N. Giuseppone, *Chem. Soc. Rev.*, **2012**, *41*, 1031.
2. L. Hunter, G. Condie, M. Harding, *Tetrahedron Lett.*, **2010**, *51*, 5064.
3. J. Sun, B. Patrick, J. Sherman, *Tetrahedron*, **2009**, *65*, 7296.
4. M. Cancilla, M. He, N. Viswanathan, R. Simmons, M. Taylor, A. Fung, K. Cao, D. Erlanson, *Bioorg. Med. Chem. Lett.*, **2008**, *18*, 3978.
5. S. Ladame, *Org. Biomol. Chem.*, **2008**, *6*, 219.
6. J.-M. Lehn, *Chem. Euro. J.*, **1999**, *5*, 2455.
7. P. Corbett, J. Leclaire, L. Vial, K. West, J.-L. Wietor, J. Sanders, S. Otto, *Chem. Rev.*, **2006**, *106*, 3652.
8. H. Schiff, *Ann. Chem. Pharm.*, **1864**, *131*, 118.
9. I. Huc, J.-M. Lehn, *Proc. Natl. Acad. Sci. USA*, **1997**, *94*, 2106.
10. L. A. Wessjohann, D. G. Rivera, F. León, *Org. Lett.*, **2007**, *9*, 4733.
11. A. González-Álvarez, I. Alfonso, F. López-Ortiz, Á. Aguirre, S. García-Granda, V. Gotor, *Eur. J. Org. Chem.*, **2004**, 1117.
12. R. Furlan, Y.-F. Ng, G. Cousins, J. Redman, J. Sanders, *Tetrahedron*, **2002**, *58*, 771.
13. R. Lam, A. Belenguer, S. Roberts, C. Naumann, T. Jarroson, S. Otto, J. Sanders, *Science*, **2005**, *308*, 667.
14. S.-A. Poulsen, P. Gates, G. Cousins, J. Sanders, *Rapid Commun. Mass Spectrom.*, **2000**, *14*, 44.
15. S. Roberts, R. Furlan, G. Cousins, J. Sanders, *Chem. Commun.*, **2002**, 938.
16. F. Bulos, S. Roberts, R. Furlan, J. Sanders, *Chem. Commun.*, **2007**, 3092.
17. R. Furlan, Y.-F. Ng, S. Otto, J. Sanders, *J. Am. Chem. Soc.*, **2001**, *123*, 8876.
18. G. Cousins, S.-A. Poulsen, J. Sanders, *Chem. Commun.*, **1999**, 1575.
19. G. Cousins, R. Furlan, Y.-F. Ng, J. Redman, J. Sanders, *Angew. Chem. Int. Ed.*, **2001**, *40*, 423.
20. S. Roberts, R. Furlan, S. Otto, J. Sanders, *Org. Biomol. Chem.*, **2003**, *1*, 1625.
21. R. Furlan, G. Cousins, J. Sanders, *Chem. Commun.*, **2000**, 1761.
22. J. Liu, K. West, C. Bondy, J. Sanders, *Org. Biomol. Chem.*, **2007**, *5*, 778.
23. V. Berl, I. Huc, J.-M. Lehn, A. De Cian, J. Fischer, *Eur. J. Org. Chem.*, **1999**, 3089.
24. S. Sando, A. Narita, Y. Aoyama, *Bioorg. Med. Chem. Lett.*, **2004**, *14*, 2835.

25. K. Nicolaou, R. Hughes, S. Cho, N. Winssinger, H. Labischinski, R. Endermann, *Chem. Eur. J.*, **2001**, 7, 3824.
26. L. Vial, J. Sanders, S. Otto, *New J. Chem.*, **2005**, 29, 1001.
27. L. Vial, R. Ludlow, J. Leclaire, R. Pérez-Fernández, S. Otto, *J. Am. Chem. Soc.*, **2006**, 128, 10253.
28. B. Danieli, A. Giardini, G. Lesma, D. Passarella, B. Peretto, A. Sacchetti, A. Silvani, G. Pratesi, F. Zunino, *J. Org. Chem.*, **2006**, 71, 2848.
29. B. Brisig, J. Sanders, S. Otto, *Angew. Chem. Int. Ed.*, **2003**, 42, 1270.
30. T. Hotchkiss, H. Kramer, K. Doores, D. Gamblin, N. Oldham, B. Davis, *Chem. Commun.*, **2005**, 4264.
31. O. Ramström, J.-M. Lehn, *ChemBioChem.*, **2000**, 1, 41.
32. F. Cougnon, H. Au-Yeung, G. Pantoş, J. Sanders, *J. Am. Chem. Soc.*, **2011**, 133, 3198.
33. S. Otto, R. Furlan, J. Sanders, *Science*, **2002**, 297, 590.
34. S. Otto, S. Kubik, *J. Am. Chem. Soc.*, **2003**, 125, 7804.
35. A. Kieran, A. Bond, A. Belenguer, J. Sanders, *Chem. Commun.*, **2003**, 2674.
36. P. Corbett, L. Tong, J. Sanders, S. Otto, *J. Am. Chem. Soc.*, **2005**, 127, 8902.
37. P. Corbett, J. Sanders, S. Otto, *J. Am. Chem. Soc.*, **2005**, 127, 9390.
38. K. R. West, K. D. Bake, S. Otto, *Org. Lett.*, **2005**, 7, 2615.
39. S. Otto, R. L. E. Furlan, J. K. M. Sanders, *J. Am. Chem. Soc.*, **2000**, 122, 12063.
40. B. Fuchs, A. Nelson, A. Star, J. F. Stoddart, S. Vidal, *Angew. Chem.*, **2003**, 115, 4352.
41. D. Berkovich-Berger, N. Lemcoff, *Chem. Commun.*, **2008**, 1686.
42. R. Cacciapaglia, S. Di Stefano, L. Mandolini, *J. Am. Chem. Soc.*, **2005**, 127, 13666.
43. R. Cacciapaglia, S. Di Stefano, L. Mandolini, *Chem. Eur. J.*, **2006**, 12, 8566.
44. J. A. Berrocal, R. Cacciapaglia, S. Di Stefano, *Org. Biomol. Chem.*, **2011**, 9, 8190.
45. J. A. Berrocal, R. Cacciapaglia, S. Di Stefano, L. Mandolini, *New J. Chem.*, **2012**, 36, 40.
46. R. Larsson, O. Ramström, *Eur. J. Org. Chem.*, **2006**, 285.
47. R. Larsson, Z. Pei, O. Ramström, *Angew. Chem. Int. Ed.*, **2004**, 43, 3716.
48. S. J. Rowan, J. K. M. Sanders, *J. Org. Chem.*, **1998**, 63, 1536.
49. P. Wipf, S. G. Mahler, K. Okumura, *Org. Lett.*, **2005**, 7, 4483.
50. B. Shi, R. Stevenson, D. J. Campopiano, M. F. Greaney, *J. Am. Chem. Soc.*, **2006**, 128, 8459.

51. B. Shi, M. F. Greaney, *Chem. Commun.*, **2005**, 886.
52. S.-A. Poulsen, L. F. Bornaghi, *Bioorg. Med. Chem.*, **2006**, *14*, 3275.
53. S. E. Eldred, D. A. Stone, S. H. Gellman, S. S. Stahl, *J. Am. Chem. Soc.*, **2003**, *125*, 3422.
54. C. Saiz, P. Wipf, E. Manta, G. Mahler, *Org. Lett.*, **2009**, *11*, 3170.
55. N. Iwasawa, H. Takahagi, *J. Am. Chem. Soc.*, **2007**, *129*, 7754.
56. S. Xu, N. Giuseppone, *J. Am. Chem. Soc.*, **2008**, *130*, 1826.
57. J. Nitschke, *Angew. Chem. Int. Ed.*, **2004**, *43*, 3073.
58. P. Boul, P. Reutenauer, J.-M. Lehn, *Org. Lett.*, **2005**, *7*, 15.
59. S. Turega, C. Lorenz, J. Sadownik, D. Philp, *Chem. Commun.*, **2008**, 4076.
60. A. Paul, S. Ladame, *Org. Lett.*, **2009**, *11*, 4894.
61. S. Di Stefano, M. Mazzonna, E. Bodo, L. Mandolini, O. Lanzalunga, *Org. Lett.*, **2011**, *13*, 142.
62. I. Huc, M. Krische, D. Funeriu, J.-M. Lehn, *Eur. J. Inorg. Chem.*, **1999**, 1415.
63. S. Hiraoka, Y. Kubota, M. Fujita, *Chem. Commun.*, **2000**, 1509.
64. C. Campos-Fernández, B. Schottel, H. Chifotides, J. Bera, J. Bacsá, J. Koomen, D. Russell, K. Dunbar, *J. Am. Chem. Soc.*, **2005**, *127*, 12909.
65. M. Cai, X. Shi, V. Sidorov, D. Fabris, Y.-F. Lam, J. Davis, *Tetrahedron*, **2002**, *58*, 661.
66. M. Albrecht, O. Blau, R. Fröhlich, *Chem. Eur. J.*, **1999**, *5*, 48.
67. P. Baxter, R. Khoury, J.-M. Lehn, G. Baum, D. Fenske, *Chem. Eur. J.*, **2000**, *6*, 4140.
68. B. Hasenknopf, J.-M. Lehn, N. Boumediene, A. Dupont-Gervais, A. Van Dorselaer, B. Kneisel, D. Fenske, *J. Am. Chem. Soc.*, **1997**, *119*, 10956.
69. E. Stulz, Y.-F. Ng, S. Scott, J. Sanders, *Chem. Commun.*, **2002**, 524.
70. S. Hiraoka, M. Fujita, *J. Am. Chem. Soc.*, **1999**, *121*, 10239.
71. E. Stulz, S. Scott, A. Bond, S. Teat, J. Sanders, *Chem. Eur. J.*, **2003**, *9*, 6039.

Chapter 2 Trianglimine Chemistry

2.1. Synthesis and conformational structure

Trianglimines form a class of chiral enantiomerically pure macrocycles, which are obtained in [3+3]-cyclocondensation reactions of chiral (1*R*,2*R*)-1,2-diaminocyclohexane **1** and aromatic or aliphatic dialdehydes **2** (Figure 2.1).^{1,2} The cyclocondensation reaction involves formation of six imine bonds in a single reaction. The first member of trianglimines has been synthesized by Gawroński *et al.* a decade ago.¹ The macrocycles form in almost quantitative yields at relatively high concentration of the reactants without using external templates to direct cyclocondensation or applying high dilution conditions to avoid polymerization. Hexa-amine macrocycles, which constitute reduced versions of their hexa-imine analogues are referred to as trianglamines.^{3,4} The amino moieties in **1** are equatorially oriented with formation an angle of 60° for C–N bonds, which after repetition of this structural moiety results in selective formation of the triangular shaped [3+3]-cyclocondensation product through conformational bias. In the intermediate open chain macrocyclization precursor conformational constraints result in a spatial close proximity of the nucleophilic primary amine and the electrophilic carbonyl resulting in a ring closure reaction. Reactions of **1** with planar dialdehydes, which have a dihedral angle of 180° of the two carbonyl moieties form preferentially [3+3]-macrocycles. Deviation from a 180° angle favors formation of a mixture of [3+3]- and [2+2]-macrocycles.^{5,6} Gawroński pointed out that the imine bonds assume *E* conformation and the torsion angle H–C–N=C (ω) is *syn* as shown in Figure 2.1.¹

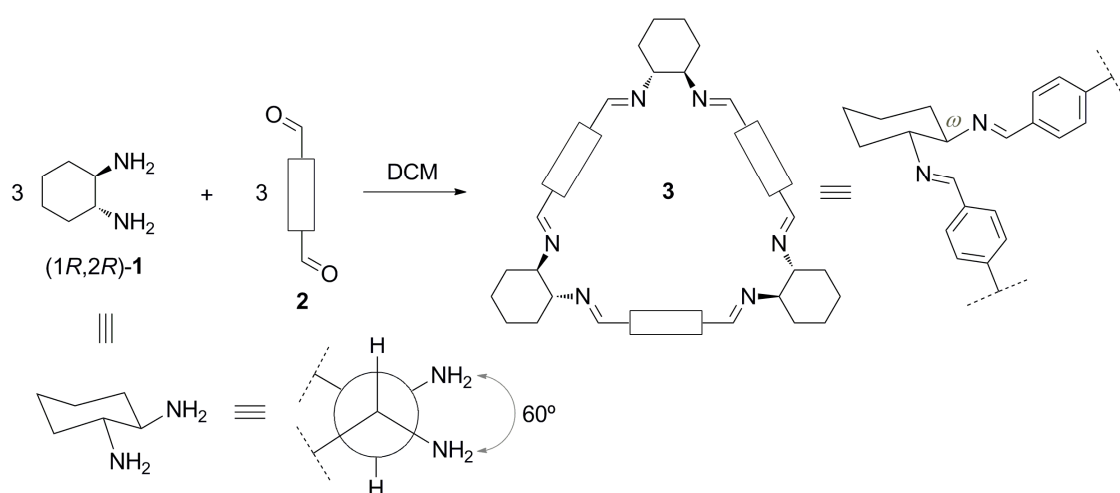


Figure 2.1 [3+3]-cyclocondensation reaction of (1*R*,2*R*)-**1** and dialdehydes **2**.

Introduction •

Figure 2.2 shows computed structure for **4** based on previously reported X-ray structure.¹ Kuhnert *et al.* reported an efficient protocol for the synthesis of trianglimine macrocycles bearing different functionalities (Figure 2.3).^{7,8} Alkylation of 4-methoxyphenol **5** affords diethers **6**, which upon bromination with two equivalents of bromine in a mixture of AcOH/ NaOAc yields dibromide diether **7**.

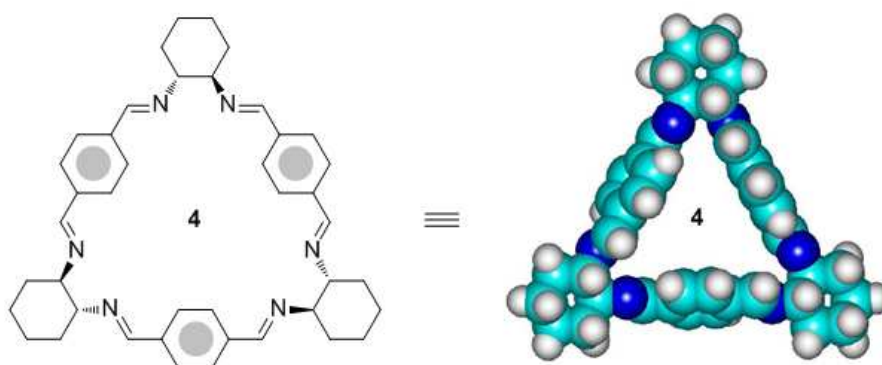


Figure 2.2 Energy-minimized structure of trianglimine **4** at the MM+ level.

Dilithiation of substituted dibromide **7** gives dicarbaldehydes **8** with D_{2h} symmetry. The [3+3]-cyclocondensation reactions of aromatic dialdehydes **8** with (1*R*,2*R*)-1,2-diaminocyclohexane **1** form D_{3h} symmetrical trianglimines **9**. The yields of the crude trianglimines are high; however repeated recrystallization reduces the yields of the isolated products.

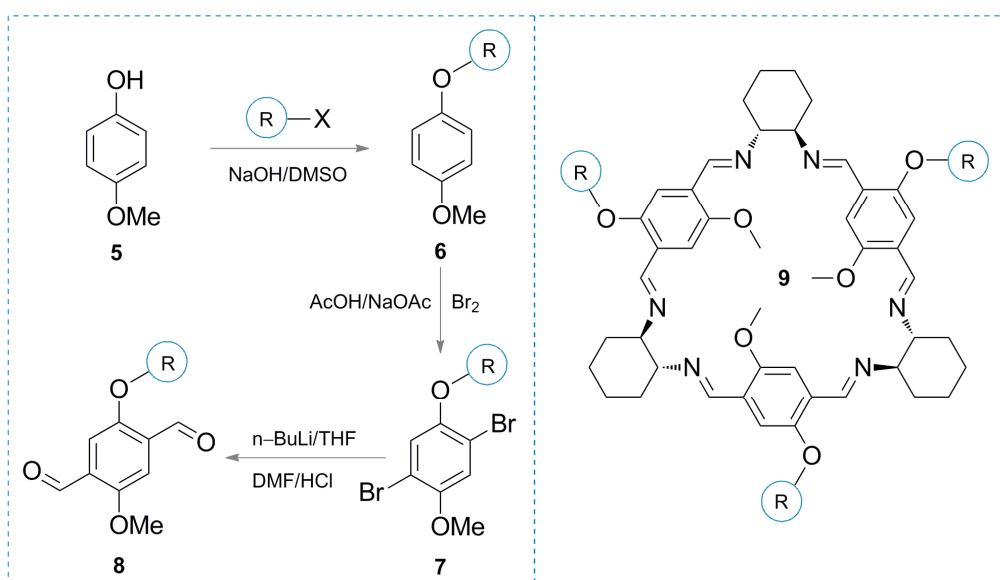


Figure 2.3 Formation of functionalized trianglimines **9** from dialdehydes **8**.

Introduction •

Trianglimines with different cavity sizes (*i.e.*, **10-12**) can be prepared by simple choice of the target dialdehyde component.^{9,10} Changing the distance between the two carbonyl moieties varies the size of the central hole of trianglimines. An efficient strategy for the synthesis of dialdehydes with different sizes is the Suzuki coupling of formylboronic acids with different bromophenyls. Macrocycle **10** is an example of a small size trianglimine obtained in reaction of 2,5-diformylfuran with (1*R*,2*R*)-1,2-diaminocyclohexane **1**. Unlike the case with trianglimine **4**, macrocycle **10** assumes a *s-syn* conformation due to repulsion between the sp^2 -lone pairs at oxygen and nitrogen atoms. Macrocycles **11** and **12**, which constitute medium and large size trianglimines, can be obtained by reacting 4,4'-biphenyldicarboxaldehyde and *bis*-(4-formylbenzene)-4,4'-biphenyl with **1** (Figure 2.4).

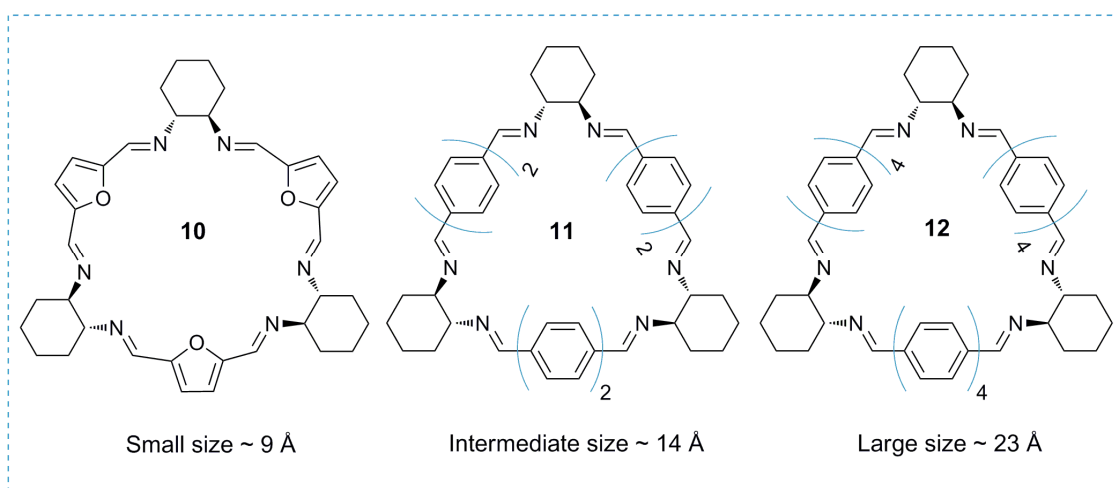


Figure 2.4 Trianglimines **10-12** with different cavity sizes.

2.2. Applications of trianglimines

The [3+3]-cyclocondensation reaction (*i.e.*, for trianglimine macrocycles) has attracted considerable attention in supramolecular chemistry.^{11,12} Trianglimines have been synthesized a decade ago, however only few examples describing their applications are reported in literature. The recognition ability of trianglimines has been initially described by Gawroński and co-workers.¹ The authors reported the X-ray structure for a 1:1 inclusion complex of trianglimine/ethylacetate. The ability of trianglimines or trianglamines to host small size neutral organic guests and metal ions was reported in many occasions.¹³⁻¹⁶ Varying the cavity dimensions of trianglimine has led to the synthesis of more sophisticated structures of trianglimine, which

Introduction •

incorporate β -cyclodextrin units.¹⁷ Terephthalaldehyde **13** forms inclusion complexes with β -cyclodextrin **14** in water.¹⁸ β -Cyclodextrin **14** was reported to have a diameter of 7.8 Å, while the cavity size of trianglimine **4** was reported to be 10.5 Å.^{9,10,19} Trianglimine **4** and β -cyclodextrin **14** have accordingly complement in their sizes. The [3+3]-cyclocondensation reaction of inclusion complex **15** with (1*R*,2*R*)-1,2-diaminocyclohexane **1** forms an interlocked catenane-like intermediate structure, which upon *in situ* reduction with sodium borohydrides (NaBH_4) gives **16** (Figure 2.5).

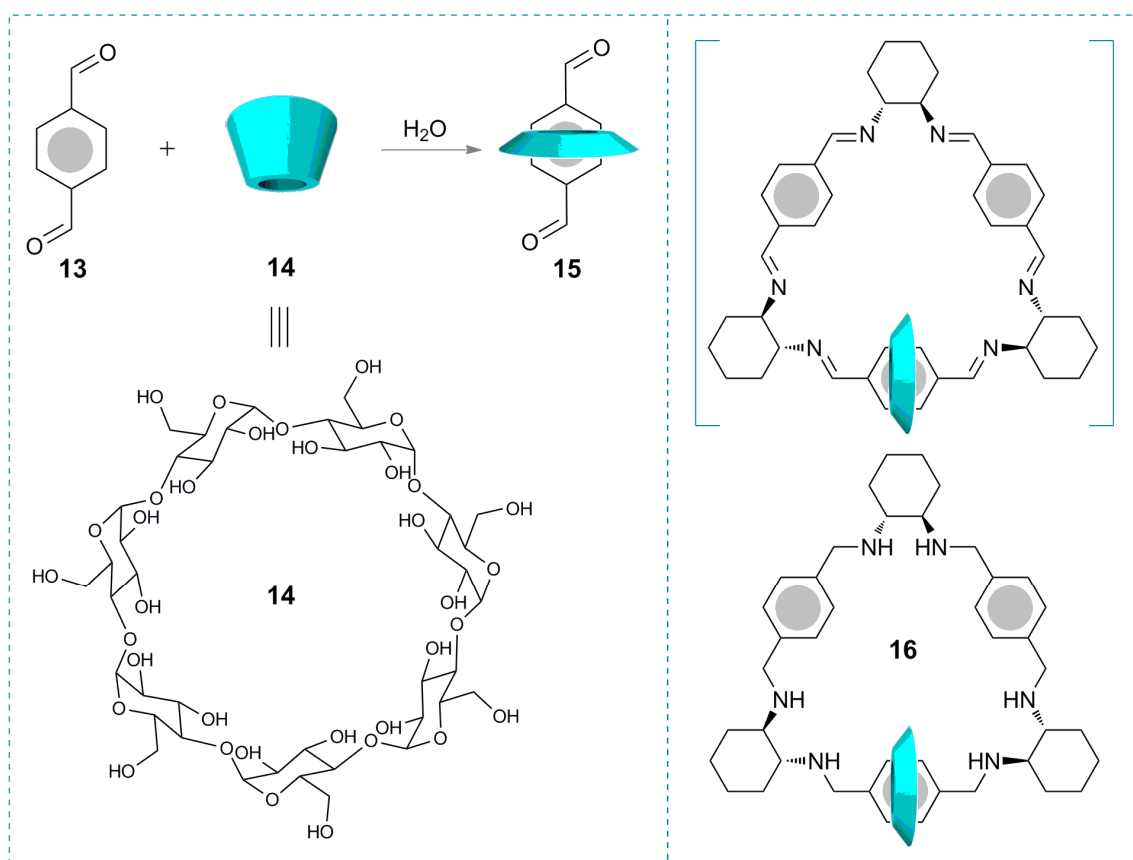


Figure 2.5 Trianglimine **4** forming interlocked structure with β -cyclodextrin **14**.

Trianglimines have been used as chiral probes for recognition of chiral carboxylic acids **17-22** both in the gas phase and in solution (Figure 2.6).²⁰⁻²² Molecular recognition in the gas phase was investigated by ESI-MS and MS/MS by observing the molecular ion peaks corresponding to the host/guest complexes (*i.e.*, **23**). Changes in CD-spectra (Circular dichroism) and titration NMR confirm molecular recognition in solution.

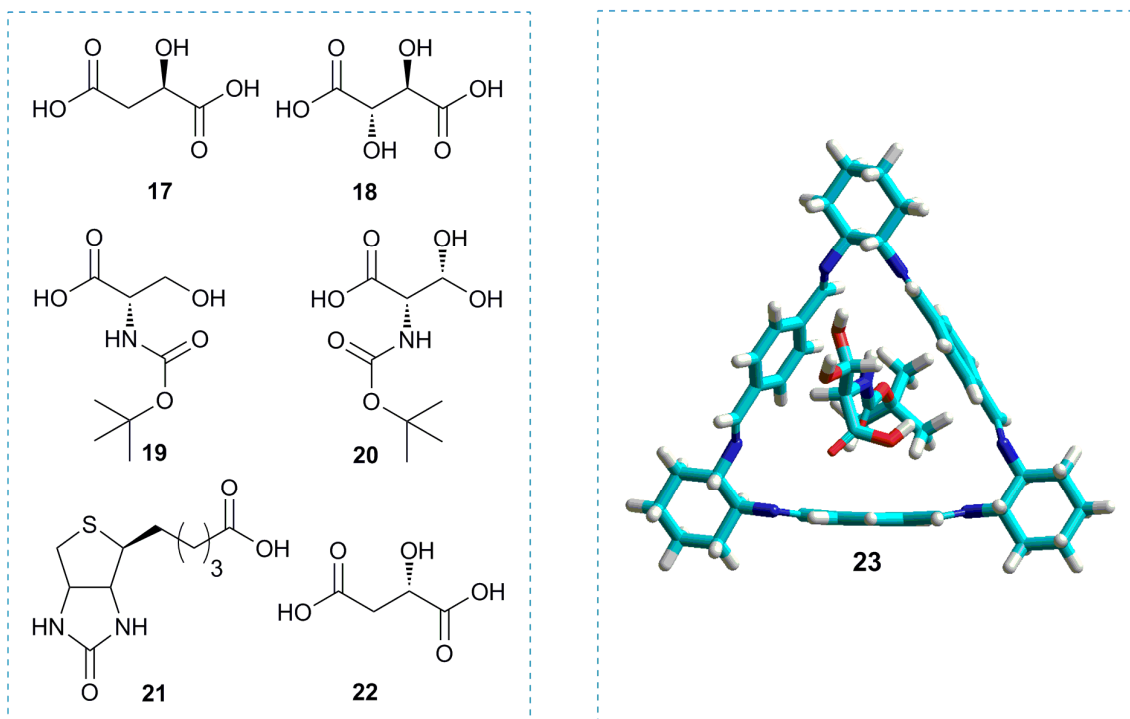


Figure 2.6 Energy-minimized structure for host/guest complex **4/20** at the MM+ level.

Trianglamine-Cu(OAc)₂ complex, obtained by stirring of trianglamine **27** (*All-S*) and Cu(OAc)₂ in dichloromethane (DCM) at room temperature, has been used as an efficient catalyst for the Henry reaction of aldehydes (*i.e.*, **24**) and nitromethane **25**.²³ The β-hydroxynitroalkanes (*i.e.*, **26**) obtained by this approach form with high enantioselectivity (82-93% ee) under mild solvent free condition. The products from the reactions were obtained in the (*R*)-form (Figure 2.7).

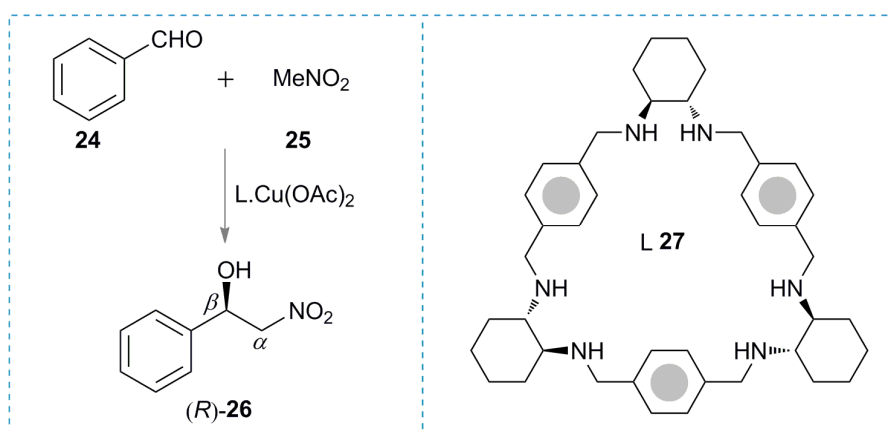


Figure 2.7 Enantioselective Henry reaction catalyzed by Trianglamine-Cu(OAc)₂.

Introduction •

Trianglamine-Zn(R)₂ complexes have been recently used as efficient catalytic systems for asymmetric hydrosilylation of ketimines (*i.e.*, **28**) and ketones. The products from the catalytic reaction were obtained in high enantiomeric excess.^{24,25} Addition of silane or a protic solvent was essential to facilitate the cleavage of the Zn-N bonds. Proposed mechanism for the hydrosilylation reaction is shown in Figure 2.8.²⁴

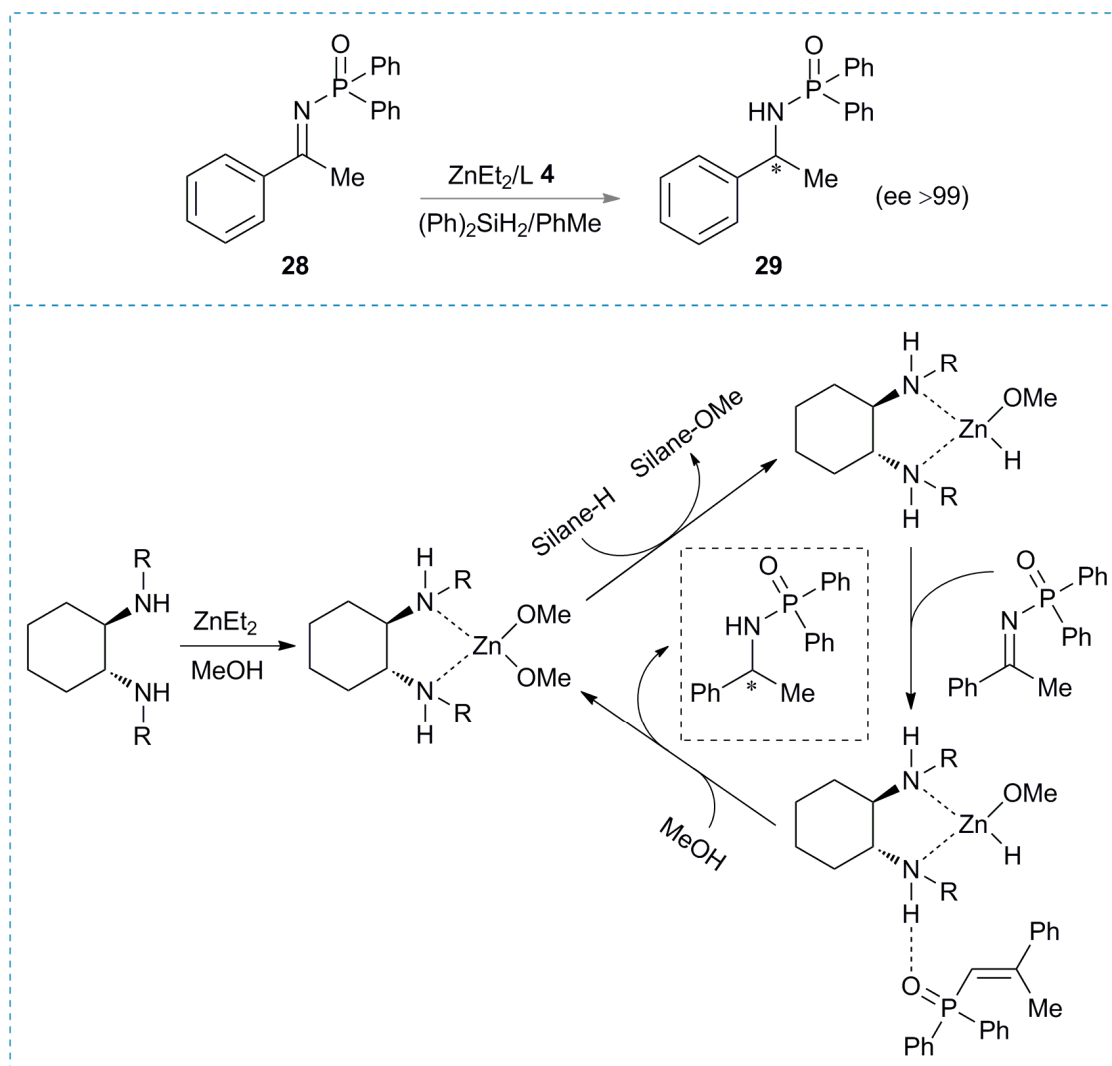


Figure 2.8 Asymmetric hydrosilylation of ketimine **28**.

References

1. J. Gawroński, H. Kołbon, M. Kwit, A. Katrusiak, *J. Org. Chem.*, **2000**, *65*, 5768.
2. M. Kwit, A. Plutecka, U. Rychlewska, J. Gawroński, A. Khlebnikov, S. Kozhushkov, K. Rauch, A. de Meijere, *Chem. Eur. J.*, **2007**, *13*, 8688.
3. N. Kuhnert, A. López-Periago, *Tetrahedron Lett.*, **2002**, *43*, 3329.
4. N. Kuhnert, A. López-Periago, *Tetrahedron Lett.*, **2002**, *43*, 3329.
5. J. Gawroński, M. Kwit, J. Grajewski, J. Gajewy, A. Długokińska, *Tetrahedron: Asymm.*, **2007**, *18*, 2632.
6. N. Kuhnert, C. Patel, F. Jami, *Tetrahedron Lett.*, **2005**, *46*, 7575.
7. N. Kuhnert, A. López-Periago, G. Rossignolo, *Org. Biomol. Chem.*, **2005**, *3*, 524.
8. N. Kuhnert, G. Rossignolo, A. López-Periago, *Org. Biomol. Chem.*, **2003**, *1*, 1157.
9. N. Kuhnert, N. Burzlaff, C. Patel, A. López-Periago, *Org. Biomol. Chem.*, **2005**, *3*, 1911.
10. N. Kuhnert, C. Straßnig, A. López-Periago, *Tetrahedron: Asymm.*, **2002**, *13*, 123.
11. Jana Hodačová, M. Buděšínský, *Org. Lett.*, **2007**, *9*, 5641.
12. J. Gawroński, M. Brzostowska, M. Kwit, A. Plutecka, U. Rychlewska, *J. Org. Chem.*, **2005**, *70*, 10147.
13. J. Gawroński, K. Gawronska, J. Grajewski, M. Kwit, A. Plutecka, U. Rychlewska, *Chem. Eur. J.*, **2006**, *12*, 1807.
14. J. Gregoliński, T. Lis, M. Cyganik, J. Lisowski, *Inorg. Chem.*, **2008**, *47*, 11527.
15. K. Tanaka, S. Fukuoka, H. Miyaniishi, H. Takahashi, *Tetrahedron Lett.*, **2010**, *51*, 2693.
16. M. Kwit, B. Zabicka, J. Gawroński, *Dalton Trans.*, **2009**, 6783.
17. N. Kuhnert, B. Tang, *Tetrahedron Lett.*, **2006**, *47*, 2985.
18. C. Simionescu, M. Grigoras, A. Farcas, A. Stoleru, *Macromol. Chem. Phys.*, **1998**, *7*, 1301.
19. H.-J. Schneider, F. Hacket, V. Rüdiger, H. Ikeda, *Chem. Rev.*, **1998**, *98*, 1755.
20. N. Kuhnert, D. Marsh, D. Nicolau, *Tetrahedron Asymm.*, **2007**, *18*, 1648.
21. A. Gualandi, S. Grilli, D. Savoia, M. Kwit, J. Gawroński, *Org. Biomol. Chem.*, **2011**, *9*, 4234.
22. J. Hodačová, M. Chadim, J. Závada, J. Aguilar, E. García-España, S. Luis, J. Miravet, *J. Org. Chem.*, **2005**, *70*, 2042.
23. K. Tanaka, S. Hachiken, *Tetrahedron Lett.*, **2008**, *49*, 2533.

Introduction •

24. J. Gajewy, J. Gawroński, M. Kwit, *Org. Biomol. Chem.*, **2011**, 9, 3863.
25. D. Savoia, A. Gualandia, H. Stoeckli-Evans, *Org. Biomol. Chem.*, **2010**, 8, 3992.

Aim of Thesis

The first objective of the thesis is to synthesize highly functionalized imine containing macrocycles, which can undergo imine exchange reactions to generate a DCL of macrocycles existing in continuous interconversion. The chemistry of trianglimine will be used in attempts to achieve this purpose by introducing functionalities into the aromatic side walls of the triangular macrocycles. An alternative to this approach will be replacing the (1*R*,2*R*)-1,2-diaminocyclohexane units in trianglimines by dihydrazides obtained from tartaric acid with acetal protected hydroxyl groups. It is worth noting that the dioxolane rings of dihydrazides can be loaded with different functionalities by simple choice of the ketone to be protected. The new functionalized macrocycles, which possess covalent reversible bonds, will be ideal candidates for different DCC applications.

The second task of work is to generate a DCL of the new macrocycles and to assess their molecular recognition ability to a selection of oligopeptides, which mimic bacterial cell wall structure. Generation of the DCL should be achieved by two parallel synthetic pathways. In a first crossover experiment the pure macrocycles will be mixed in the appropriate solvent, while in a second crossover experiment the dialdehyde building blocks along with the dihydrazides will be mixed. At equilibration, the composition of the DCLs obtained from the two synthetic routes should be almost identical. Addition of the guest oligopeptide should shift equilibration towards the most stable assembly of host and guest and allowing its amplification under thermodynamic control. The use of ESI-TOF/MS should provide direct screening of the composition of the DCL, while the observation of the molecular ion peaks corresponding to the host/guest complexes by ESI-MS and tandem MS should qualitatively confirm molecular recognition ability of the macrocycles. Molecular modeling simulations will be used to predict the energy-minimized structure of the most stable host/guest complex, thus providing valuable information about the nature of binding between them. Other objectives of thesis will focus on synthesis of modified versions of the macrocycles and assessment of their molecular recognition abilities towards chiral carboxylic acids and oligopeptides by ESI-MS and MS/MS.

Scope of Work

In this work the chemistry of trianglimine and tetra-carbohydrazide cyclophane macrocycles have been utilized to generate DCLs in attempts to develop new macrocyclic receptors with molecular recognition affinity to a selection of oligopeptides unique in bacteria. The difference between human and bacterial cells is that the former completely lack a cell wall, while the latter die without an intact cell wall. This makes bacterial cell wall a versatile target for developing new antibiotics. Bacteria make their cell wall from *N*-acetyl glucosamine and *N*-acetylmuramic acid in a series of cross linking steps called transglycosylation and transpeptidation. Penicillin, Bacitracin and Vancomycin act by causing disruption of the processes of cross linking and inhibition of the carrier required for moving the building blocks of the cell wall across the membrane. Vancomycin antibiotic binds D-Ala-D-Ala, which is an essential component forming bacterial cell wall. Bacteria accomplished a resistance to Vancomycin by replacing the section D-Ala-D-Ala with D-Ala-D-Lac.¹ The ability of Vancomycin to bind with D-Ala-D-Lac dramatically reduced as a consequence of the elimination of a one hydrogen bond as illustrated in Figure 3.1. DCC allows generation of structurally unique architectures, which cannot be obtained by conventional synthesis. Trianglimines possess six imine bonds making them ideal candidates for different DCC applications.² Trianglimines can be obtained in good quantities from commercially available starting materials with complete control of the size of the central hole of the macrocycles.^{3,4} The cavity of the macrocycle itself can function as a good binding motif, while the triangular side walls can be loaded with different functionalities, which can recognize and bind with biological targets of interest. Aromatic dialdehyde **2** underwent successfully [3+3]-cyclocondensation reaction with *trans*-(1*R*,2*R*)-1,2-diaminocyclohexane **3** to form a mixture of regioisomeric *C*₃-symmetrical **5** and non-symmetrical **6** trianglimines, which were separated by column chromatography (CC) in high purity, but unfortunately in low yields (4-37%).⁵ It is noteworthy that compound **2** is an example of non-symmetrical dialdehydes, which was synthesized using the Suzuki-coupling methodology of 4-bromo-2-substituted benzaldehyde and 4-formylphenyl boronic acid. Trianglimines underwent successfully dynamic exchange reactions with generation of a DCL of interesting triangular architectures.⁶ The major obstacles, however, were the low yields of the macrocycles and the equilibration of the regioisomers in solution. These obstacles would certainly render the assignment of the host, which forms the most stable complex with the oligopeptide targets. In order to improve the yields of the macrocycles and to

enhance their recognition ability, it was necessary to synthesize selectively the C_3 -symmetrical trianglimines. All attempts to synthesize C_3 -symmetrical biphenyl dialdehydes of the type **4** (Figure 3.2) did not succeed.

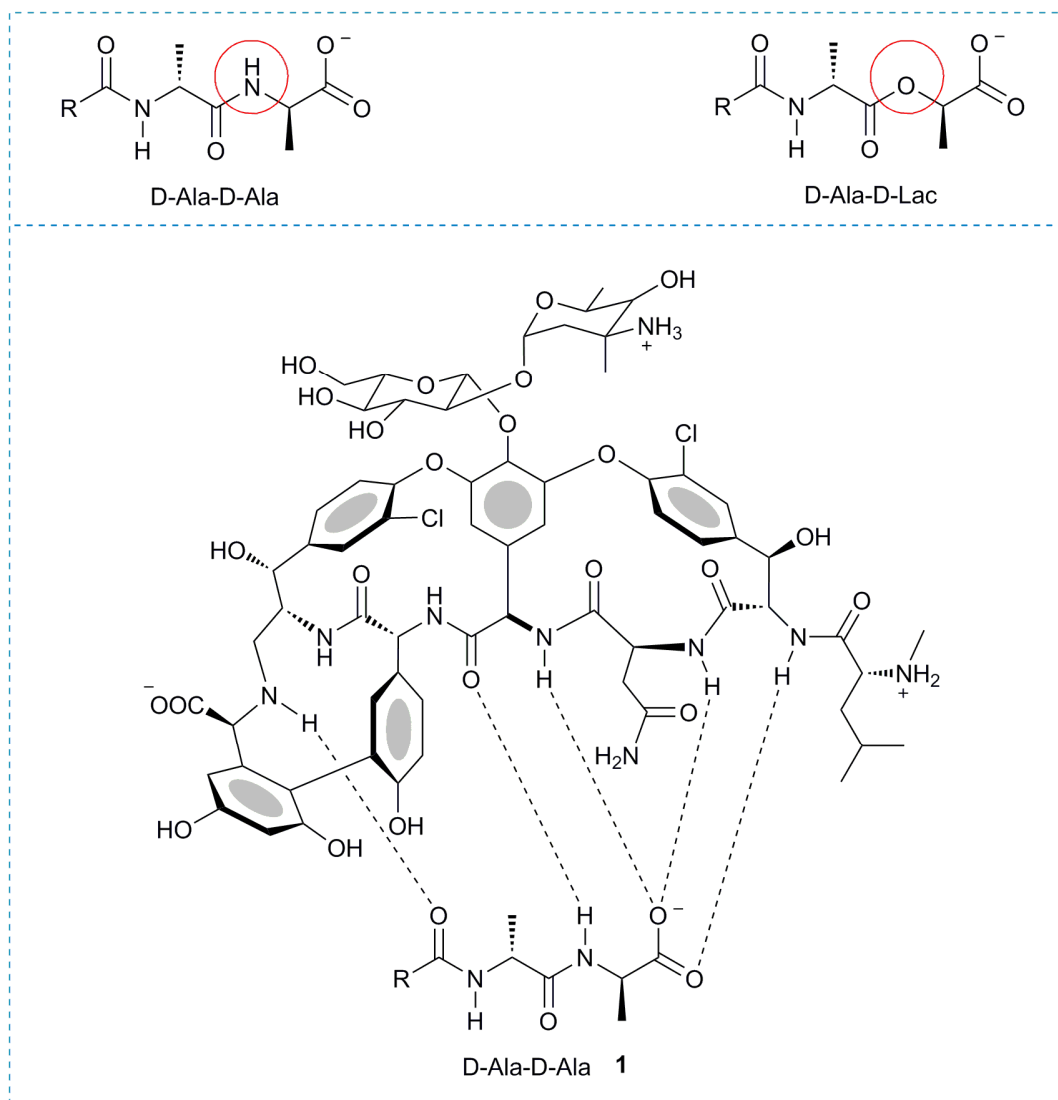


Figure 3.1 Molecular recognition of Vancomycin to D-Ala-D-Ala.

The basic structure of trianglimine macrocycles (*i.e.*, **7**) contains many attractive features such as the conformational bias of the (1*R*,2*R*)-1,2-diaminocyclohexane ring, the ability to introduce functionalities into the aromatic moieties, the chirality and most importantly the dynamic reversibility of the imine covalent bonds (Figure 3.3). An interesting idea, which came to mind was replacing the (1*R*,2*R*)-1,2-diaminocyclohexane units by dicarbohydrazides (*i.e.*, **8**), which

can be obtained from commercially available tartaric acid in both enantiomeric forms (*R* or *S*). Dihydrazides (*i.e.*, **8**) possess high reactivity in comparison with *trans*-(1*R*,2*R*)-diaminocyclohexane **3**. It is worth noting that the macrocycles obtained by reacting the protected dicarbohydrazides with aromatic dialdehydes in [2+2]-cyclocondensation reactions have not been previously reported in literature and constitute a novel class of structurally unique architectures with intriguing design.^{7,8}

The novel macrocycles obtained by this approach were named tetra-carbohydrazide cyclophanes. A comparison between trianglimine structure and the structure of the novel cyclophane macrocycles is shown in Figure 3.4. In addition to all attractive features present in trianglimine structure, tetra-carbohydrazide cyclophanes possess four carbonyl moieties, which can function as extra binding motifs (Figure 3.4). Tetra-carbohydrazide cyclophanes underwent successfully dynamic exchange in a mixture of DMF/MeOH and in presence of catalytic AcOH to form a DCL of macrocycles possessing mixed building blocks with different structures of the type shown in Figure 3.5.⁹

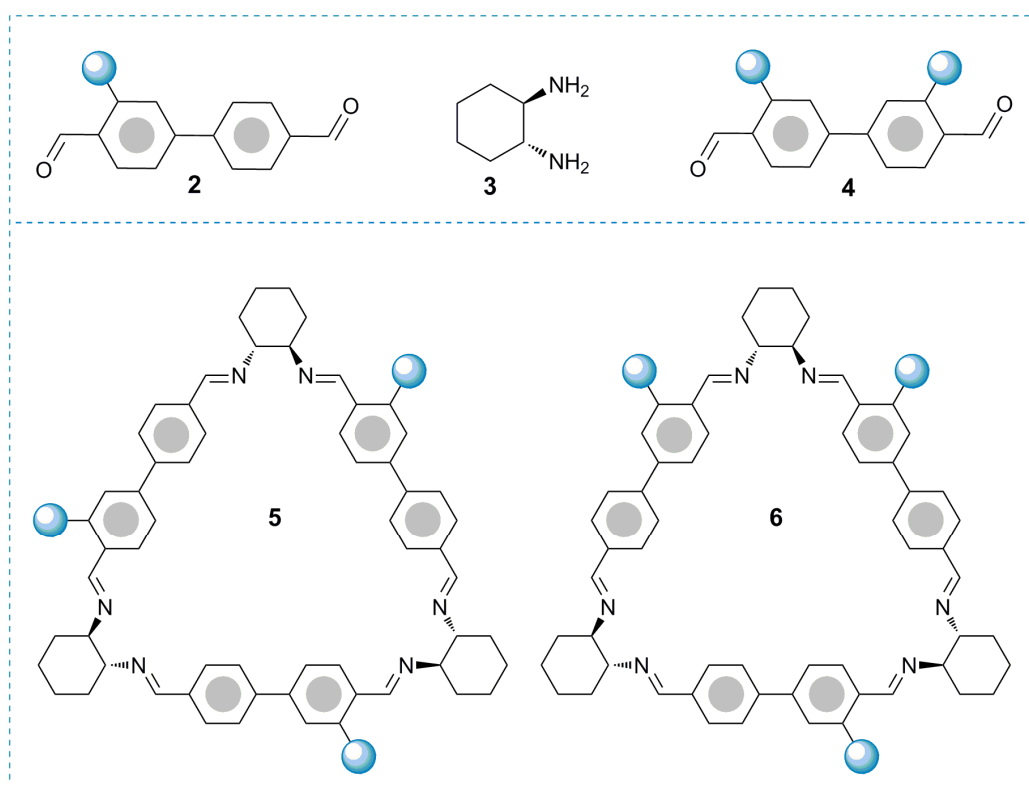


Figure 3.2 *C*₃-symmetrical **5** and non-symmetrical **6** trianglimines obtained from **2**.

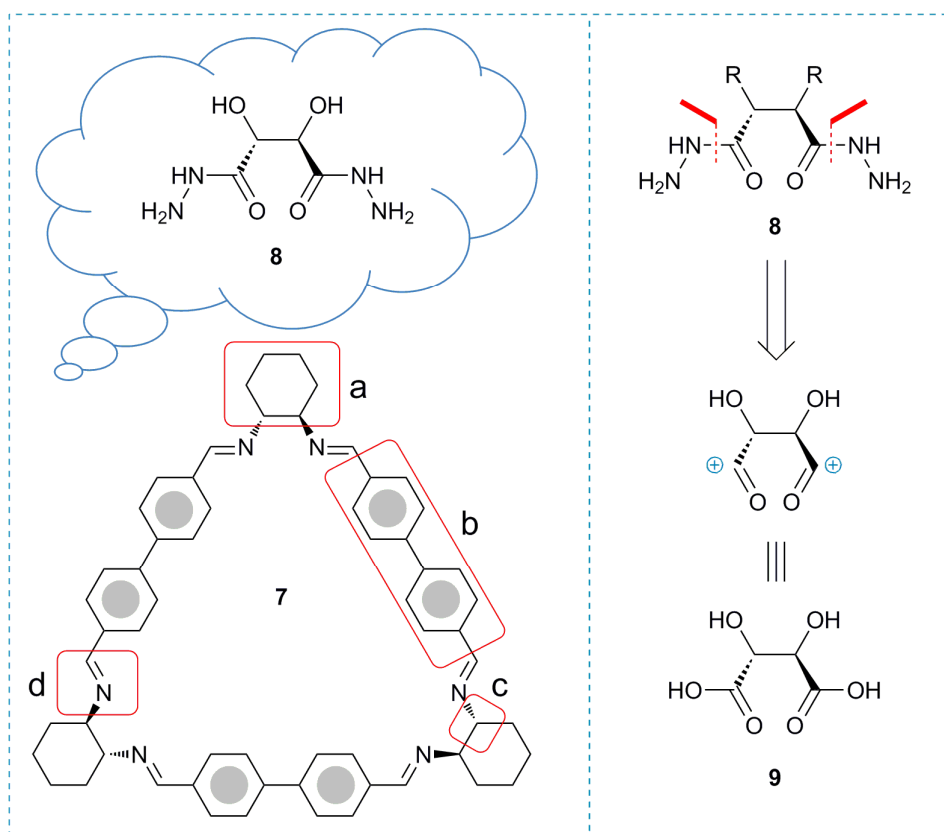


Figure 3.3 Modification of the core structure of trianglimine **7**.

Macrocycle **12** showed potential recognition in the gas phase to AcNH-L-Lys-D-Ala-D-Ala-Gly-COOH oligopeptide **11** as confirmed by ESI-TOF/MS. Molecular modeling simulation for the host/guest complex **12/11** is shown in Figure 3.5. It can be inferred from the lowest energy structure that the carbonyl group of the carbamate moiety (NCOOC_2H_5) in macrocycle **12** binds to the hydroxyl group (COOH) of the COOH terminal of Glycine in oligopeptide **11** via hydrogen bonding. Also, the amidic proton (NHCO) in macrocycle **12** binds with the amidic carbonyl (NHCO) of D-Alanine in peptide **11** via hydrogen bonding. Furthermore, the side chain of L-lysine is embedded within the cavity of the macrocycle.⁹

A modified and more flexible version of macrocycle **12** was synthesized by reacting dicarbohydrazides with aromatic diisocyanates. Macrocycle **13** constitutes a novel class of polyamide macrocycles, which has been named *terta*-(hydrazinecarboxamide) cyclophanes. Cyclophanes **13** showed excellent recognition affinity to a selection of chiral carboxylic acids oligopeptides in the gas phase.¹⁰

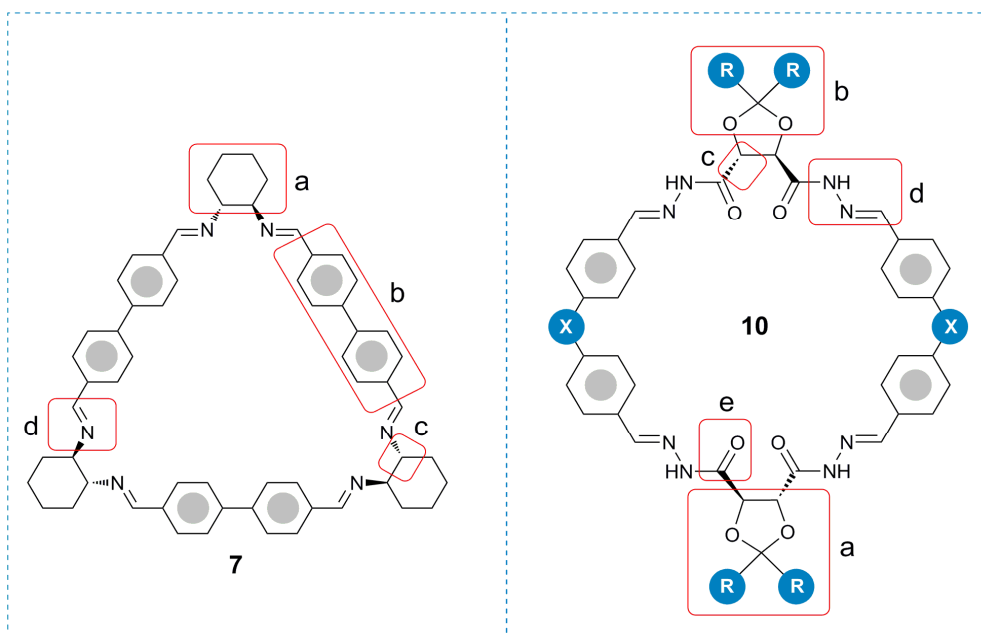


Figure 3.4 Structures of triaglimine **7** and tetra-carbohydrazide cyclophane **10**.

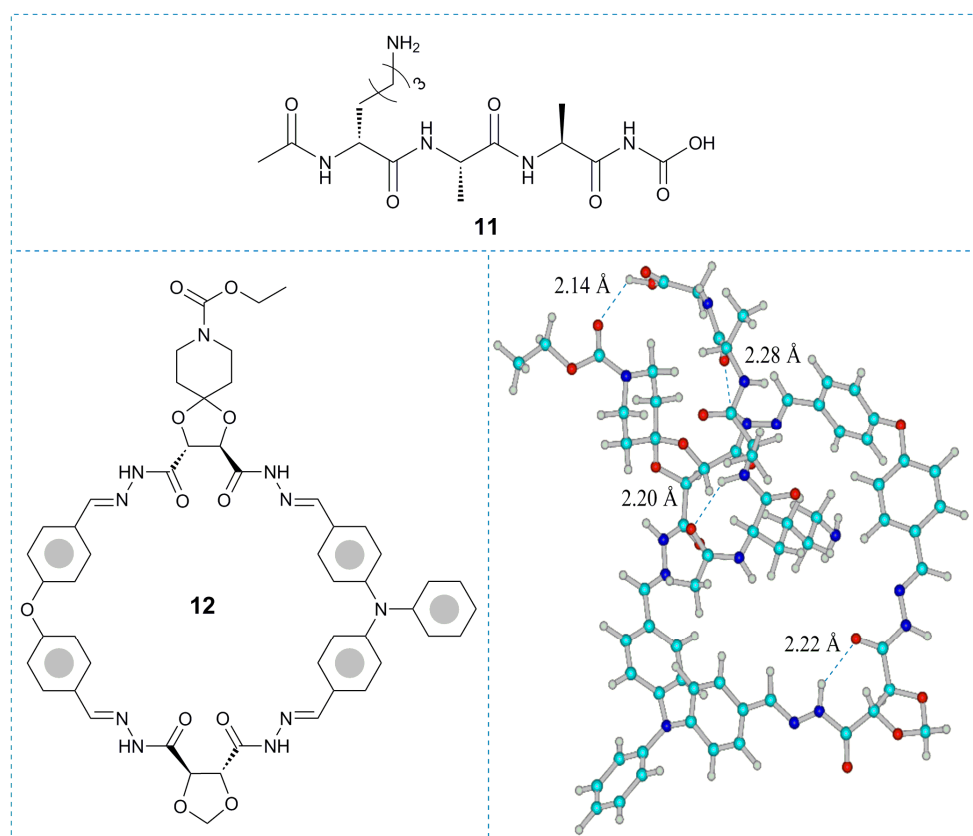


Figure 3.5 Computed structure for host/guest complex **12/11** at the MM+ level.

Terta-(hydrazinecarboxamide) cyclophanes (*i.e.*, **13**) possess flexible structures and unlike **10**, they cannot undergo dynamic exchange under normal condition, however in the presence of Lewis-acid catalysts, they might undergo catalytic transamidation.¹¹ The novel tetra-(hydrazinecarboxamide) cyclophanes **13** assume a conformation in which the NH moieties are *syn-anti* oriented, which has been confirmed by 2D-ROESY NMR. A new class of two-armed receptors (*i.e.*, **14**) was synthesized in extension to the synthetic strategy used in the preparation of the novel macrocycles **10** and **13**.¹² Receptor **14** showed unprecedented dual self-assembly and recognition in the gas phase with formation of structurally unique associations of hosts and guests. The NH moieties in **14** assume a *syn-syn* conformation, which is stabilized by inter- and intramolecular hydrogen bonds. Selective recognition to chiral carboxylic acids and oligopeptide guests has also been demonstrated.

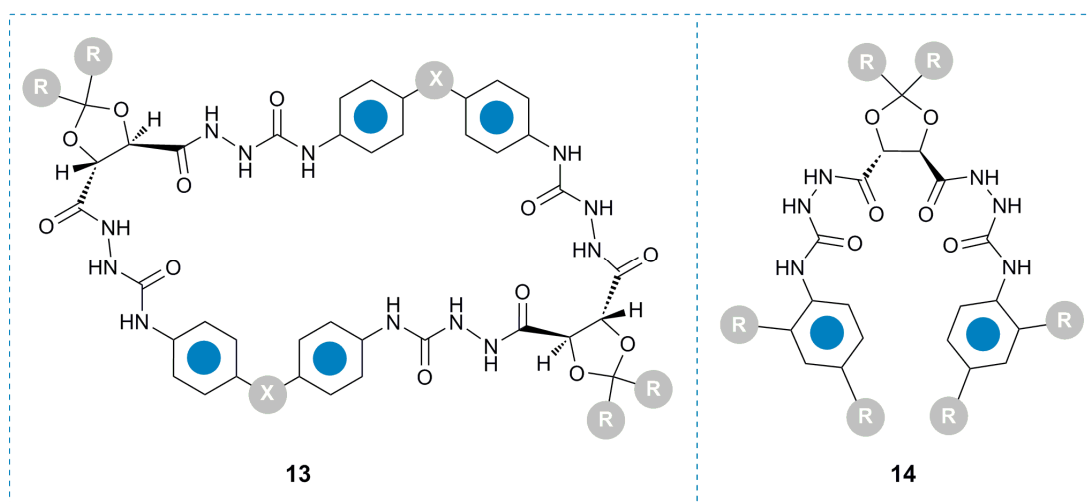


Figure 3.6 Macrocycle **13** and receptor **14** which bind with oligopeptides.

References

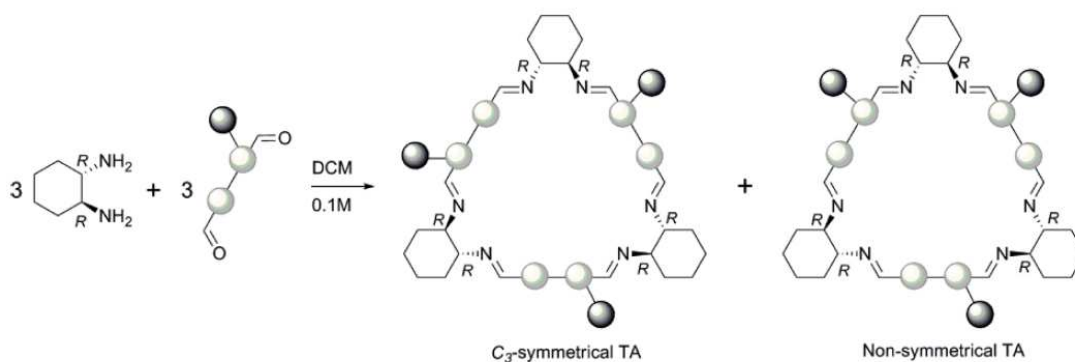
1. G. Wright, *Nat. Rev. Microbiol.*, **2007**, 5, 175.
2. A. González-Álvarez, I. Alfonso, F. López-Ortiz, Á. Aguirre, S. García-Granda, V. Gotor, *Eur. J. Org. Chem.*, **2004**, 1117.
3. N. Kuhnert, N. Burzlaff, C. Patel, A. López-Periago, *Org. Biomol. Chem.*, **2005**, 3, 1911.
4. N. Kuhnert, C. Straßnig, A. Lopez-Periago, *Tetrahedron: Asymm.*, **2002**, 13, 123.
5. H. Nour, M. Matei, B. Bassil, U. Kortz, N. Kuhnert, *Org. Biomol. Chem.*, **2011**, 9, 3258.
6. H. Nour, A. López-Periago, N. Kuhnert, *Rapid Commun. Mass Spectrom.*, **2012**, 26, 1070.
7. H. Nour, N. Hourani, N. Kuhnert, *Org. Biomol. Chem.*, **2012**, 10, 4381.
8. H. Nour, A. Golon, A. Le-Gresley, N. Kuhnert, *Chem. Eur. J.*, **2012**, submitted manuscript.
9. H. Nour, T. Islam, M. Fernández-Lahore, N. Kuhnert, *Rapid Commun. Mass Spectrom.*, **2012**, accepted manuscript.
10. H. Nour, A. Golon, T. Islam, M. Fernández-Lahore, N. Kuhnert, unpublished results.
11. S. E. Eldred, D. A. Stone, S. H. Gellman, S. S. Stahl, *J. Am. Chem. Soc.*, **2003**, 125, 3422.
12. H. Nour, A. Golon, T. Islam, M. Fernández-Lahore, N. Kuhnert, unpublished results.

Synthesis of tri-substituted biaryl based trianglimines: formation of C_3 -symmetrical and non-symmetrical regioisomers

Hany F. Nour, Marius F. Matei, Bassem S. Bassil, Ulrich Kortz and Nikolai Kuhnert*

Reproduced by permission of The Royal Society of Chemistry

<http://pubs.rsc.org/en/content/articlelanding/2011/ob/c0ob00944j>



Objectives of the work

The objective of this work is to synthesize highly functionalized trianglimine macrocycles, which can be used in the generation of DCLs. 4-Bromo-2-fluorobenzaldehyde reacted with secondary amines to form 2-functionalized aromatic monoaldehydes. The Suzuki-coupling reactions of 4-formylphenylboronic acid with the substituted monoaldehydes gave 2-functionalized-4,4'-biphenyldialdehydes, which underwent successfully [3+3]-cyclocondensation reactions with *trans*-(1*R*,2*R*)-1,2-diaminocyclohexane to give a mixture of regioisomeric trianglimine macrocycles. Separation of the regioisomers was a real challenge due to the ease of hydrolysis of the imine bonds. After several trials, the regioisomers were successfully separated on pretreated silica gel. ESI-TOF/MS was used to monitor the progress of the macrocyclization reactions and to determine the time at which all intermediates were almost consumed in formation of the macrocycles. The new trianglimines were successfully reduced with NaBH_4 in a mixture of THF/MeOH to the corresponding triangelamines in almost quantitative yields.

Synthesis of tri-substituted biaryl based trianglimines: formation of C_3 -symmetrical and non-symmetrical regioisomers†

Hany F. Nour, Marius F. Matei, Bassem S. Bassil, Ulrich Kortz and Nikolai Kuhnert*

Received 27th October 2010, Accepted 6th January 2011

DOI: 10.1039/c0ob00944j

2-Functionalised aromatic monoaldehydes were synthesised in good to excellent yields by reacting 4-bromo-2-fluorobenzaldehyde with different secondary amines and phenol. The Suzuki-coupling reaction of the newly functionalised aromatic monoaldehydes with 4-formylphenylboronic acid afforded the corresponding 2-functionalised-4,4'-biphenyldialdehydes in good yields (47–85%). The [3+3]-cyclocondensation reactions of the 2-functionalised-4,4'-biphenyldialdehydes with (1*R*,2*R*)-1,2-diaminocyclohexane afforded a mixture of regioisomeric C_3 -symmetrical and non-symmetrical trianglimines. Reduction of the C_3 -symmetrical and the non-symmetrical trianglimines with NaBH_4 in a mixture of THF and MeOH afforded the corresponding trianglamines in high yields.

Introduction

Trianglimines form a class of chiral non-racemic macrocycles that are formed in a [3+3]-cyclocondensation reaction between a chiral non-racemic diamine and an aromatic dicarboxaldehyde, in which six new imine bonds are formed in a single reaction. The first member of this class of macrocycles has been introduced by Gawroński a decade ago; more recently the compounds were named trianglimines by our group due to their unique triangular geometry.^{1–3} Hexa-amine macrocycles, which constitute reduced versions of their hexa-imine analogues are referred to as trianglamines.⁴ Trianglimines combine a series of features and characteristics that make them promising compounds for molecular recognition applications including sensing, chiral recognition, *etc.*, in many cases their potential is much superior if compared to their macrocyclic competitors such as calix-[n]-arenes,^{5–8} cyclodextrins,⁹ cucurbiturils^{10,11} or crown ethers.¹² Trianglimines are chiral, and unlike in cyclodextrin chemistry both enantiomers of any derivative are readily available in a pure form and have been reported.⁴ Trianglimines are obtained using a modular approach, in which two building blocks are reacted to form macrocyclic compounds with complete control over the size of the macrocycle,¹³ electronic properties of the macrocycle and functional groups included.¹⁴ These features make trianglimines in particular attractive for the molecular recognition of small and medium sized organic molecules with complementary

functionalities and complementary size to be included in the macrocyclic host by well-designed building blocks.

The [3+3]-cyclocondensation reaction is usually high yielding, with quantitative conversions not uncommon, at relatively high concentrations of the two building blocks. The formation of trianglimines is based on conformational bias rather than on a template effect or high dilution conditions, frequently used in other macrocyclic chemistry.¹ Despite these obviously attractive features of trianglimines, only few applications of trianglimines and their amine analogues in supramolecular chemistry have been reported. Gawroński and others have used trianglimines as organo-catalysts for asymmetric catalysis and they also reported the inclusion of solvent molecules into the trianglimine cavity.^{1,15,16} Hodacova¹⁷ reported on the binding of simple aromatic guests in the trianglimine cavity and finally we have reported on chiral recognition of trianglimines binding chiral carboxylic acids and amino acid derivatives.¹⁸ In most of these cases, binding constants were reported with the best values in the region of 10^4 M^{-1} . A second currently existing obstacle in trianglimine and trianglamine chemistry is the poor water solubility. For any attractive application in supramolecular chemistry, host molecules should have satisfactory solubilities in aqueous solution. The imines themselves are of course sensitive to hydrolysis and water stable trianglamines obtained so far, possess water solubilities at neutral pH in low μM region only. In order to overcome these obstacles, in particular unsatisfactory binding constants and water solubilities, novel trianglamine derivatives are urgently required, in which these properties are improved. The strategy to achieve this must include the incorporation of further substituents in one of the trianglimine building blocks that due to their polar nature enhance water solubility and that at the same time offer suitable complementary binding motifs, including salt bridges, hydrogen bond donors and acceptors or further aromatic

School of Engineering and Science, Jacobs University Bremen, P.O. Box 750 561, 28725 Bremen, Germany. E-mail: n.kuhnert@jacobs-university.de; Fax: +49 421 200 3229; Tel: +49 421 200 3120

† Electronic supplementary information (ESI) available: ^1H , ^{13}C NMR and ESI-MS spectra. CCDC reference number 779417. For ESI and crystallographic data in CIF or other electronic format see DOI: 10.1039/c0ob00944j

Table 1 Theoretical and experimental molecular weights for both the newly synthesised compounds and the assigned intermediates (ESI-MS, micrOTOF)

Compound / intermediate (Int.)	Molecular formula	Molecular weight (Calcd.)	Molecular weight (<i>m/z</i>) (Exp.)	Error [ppm]	Yield (%)	
6	C ₁₄ H ₁₇ BrN ₂ O ₃	340.0423	363.0400	M + Na ⁺	2.6	90
8	C ₁₅ H ₁₅ BrN ₂ O	318.0368	341.0367	M + Na ⁺	1.7	66
9	C ₁₂ H ₁₆ BrNO ₃	301.0314	324.0326	M + Na ⁺	4.2	94
11	C ₂₁ H ₂₂ N ₂ O ₄	366.1580	389.1554	M + Na ⁺	1.0	75
12	C ₂₀ H ₁₄ O ₃	302.0943	325.0820	M + Na ⁺	4.8	47
13	C ₂₂ H ₂₀ N ₂ O ₂	344.1525	367.1598	M + Na ⁺	2.0	85
14	C ₁₉ H ₂₁ NO ₄	327.1471	350.1356	M + Na ⁺	2.0	79
16	C ₈₁ H ₉₆ N ₁₂ O ₆	1332.7576	1333.7668	M + H ⁺	0.3	10
17	C ₇₅ H ₉₃ N ₉ O ₆	1215.7249	1216.7305	M + H ⁺	0.1	4
18	C ₇₈ H ₇₂ N ₆ O ₃	1140.5666	1163.5534	M + Na ⁺	4.0	22
19	C ₈₁ H ₉₆ N ₁₂ O ₆	1332.7576	1333.4865	M + H ⁺	0.3	35
20	C ₇₅ H ₉₃ N ₉ O ₆	1216.7322	1216.7292	M ⁺	2.4	31
21	C ₇₈ H ₇₂ N ₆ O ₃	1140.5666	1163.5545	M + Na ⁺	1.8	37
22	C ₈₄ H ₉₀ N ₁₂	1267.7482	1267.7439	M ⁺	3.4	11
23	C ₂₈ H ₃₂ N ₄ O	440.2576	441.2758	M + H ⁺	5.0	(Int.)
24	C ₅₀ H ₅₀ N ₆ O ₂	766.3995	767.4107	M + H ⁺	4.9	(Int.)
25	C ₅₆ H ₆₀ N ₈	844.4941	845.5072	M + H ⁺	2.8	(Int.)
26	C ₇₈ H ₈₄ N ₆ O ₃	1152.6605	1153.6665	M + H ⁺	1.8	>98
27	C ₈₁ H ₁₀₈ N ₁₂ O ₆	1344.8515	1345.8617	M + H ⁺	2.2	>98
28	C ₇₈ H ₈₄ N ₆ O ₃	1152.6605	1153.6658	M + H ⁺	1.7	>98
29	C ₇₅ H ₁₀₅ N ₉ O ₆	1227.8188	1228.8261	M + H ⁺	0.4	>98

groups for the binding of functionalised organic molecules. Within this contribution we present a new synthetic strategy for the introduction of such substituents into novel trianglimines and trianglamines. As core building blocks we have chosen substituted biaryl dicarboxaldehydes. We present a novel functionalisation approach, in which starting from a fluorinated aromatic aldehyde a nucleophilic aromatic substitution reaction introduces a suitable heteroatom substituent. Subsequent Suzuki-coupling methodology,¹⁹ based on our previous work, furnishes a substituted biaryl dialdehyde that serves as a building block for trianglimine synthesis.

Results and discussion

Aromatic nucleophilic substitution reactions of 4-bromo-2-fluorobenzaldehyde (**1**) with secondary amines in DMF have been reported by Nielsen *et al.*²⁰ We modified this method using alternative nucleophiles such as ethyl piperazine-1-carboxylate (**2**), phenol (**3**), *N*-methyl-2-(pyridin-2-yl)-ethanamine (**4**) and 2,2-dimethoxy-*N*-methylethanamine (**5**) in acetonitrile to afford the corresponding 2-functionalised monoaldehydes (**6–9**) (Scheme 1) in good to excellent yields (62–94%, Table 1). Compound (**7**) has already been reported in the literature.^{21–23}

The solid state structure of compound (**6**) based on single crystal X-ray diffraction is shown in Fig. 1. The Suzuki-coupling reaction¹⁹ of the 4-functionalised monoaldehydes (**6–9**) with 4-formylphenylboronic acid (**10**) afforded the newly functionalised 4,4'-biphenyldialdehydes (**11–14**) (Scheme 1) in good yields (47–85%). Compound (**12**) was isolated in low yield (26%) in the case where 0.9 mol% of tetrakis(triphenylphosphine)-palladium(0) was used as a catalyst. The yield for compound (**12**) was dramatically improved to (47%) by using 3.0 mol% of the catalyst. With the 2-substituted-4,4'-biphenyldialdehydes (**11–14**) in hand we investigated their behaviour in the [3+3]-cyclocondensation reaction. It is worth noting that compounds (**11–14**) constitute non-symmetrical dialdehyde building blocks leading potentially to regioisomeric macrocycles where the reactivity of such non-symmetrical building

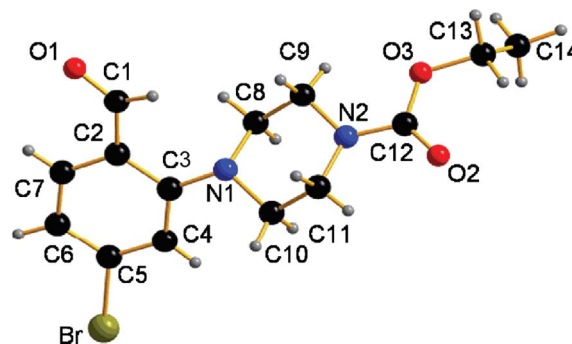
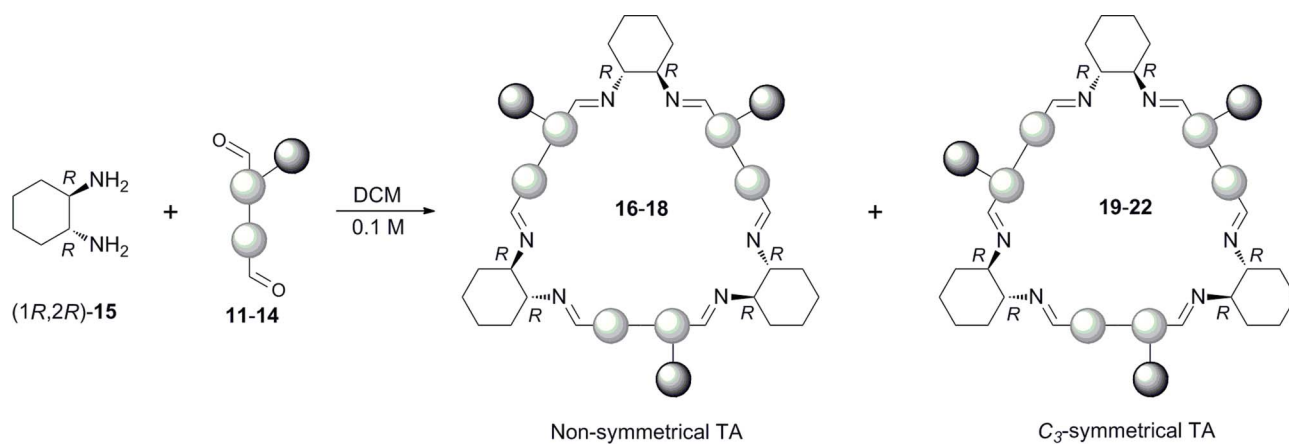
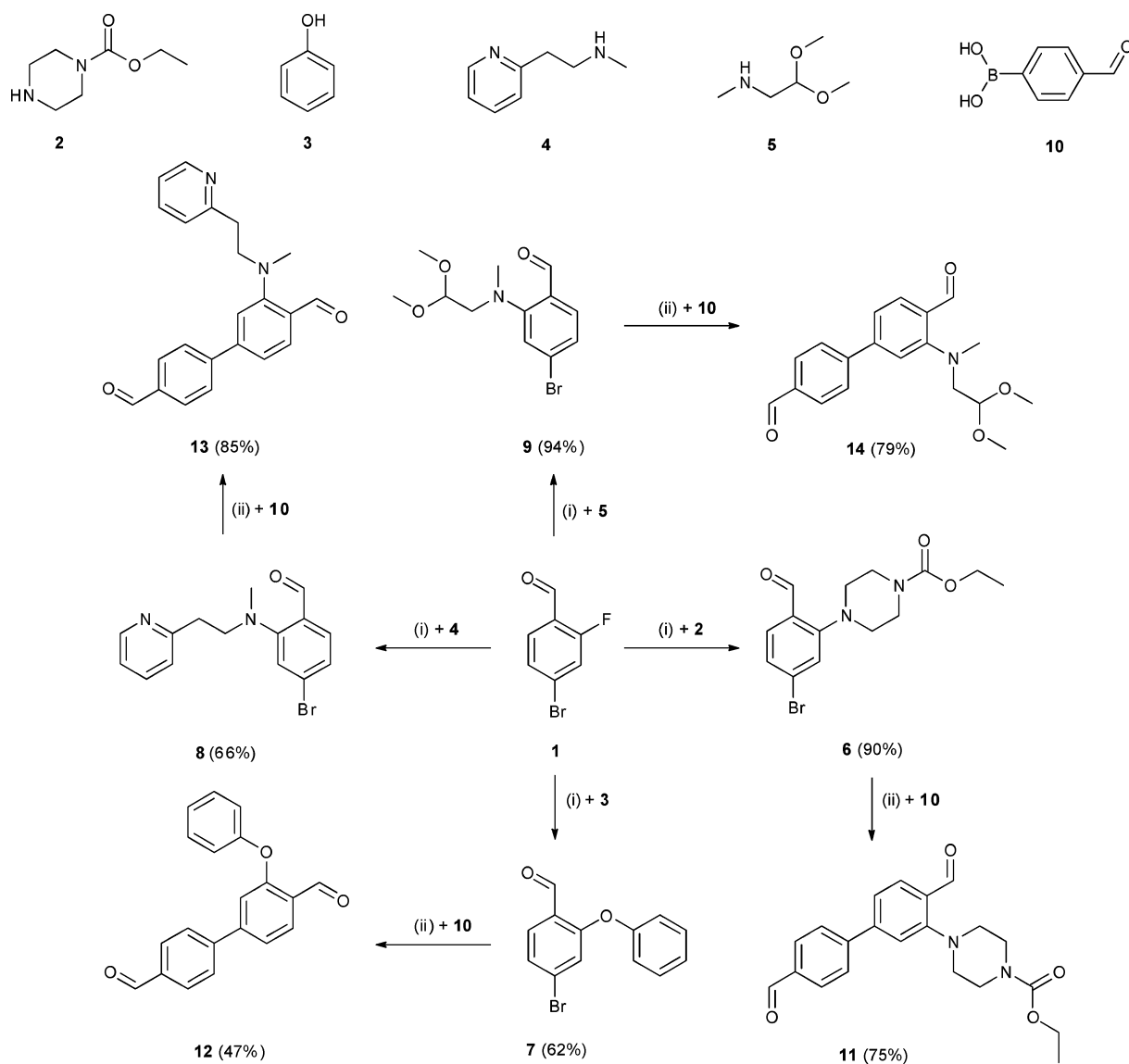


Fig. 1 Molecular structure of substituted monoaldehyde (**6**); thermal ellipsoids are drawn at 50% probability level. Selected bond lengths (Å) and angles (°) are given in the supplementary information.[†] Hydrogen atoms are shown as small grey balls.

blocks has never been investigated in trianglimine chemistry and forms an interesting topic. We have previously investigated non-symmetrical 2,5-aryl substituted dialdehydes, where no issue of regiochemistry arose, however, diastereomeric compounds with the aromatic ring acting as a stereogenic plane were formed.

Furthermore we have reported on the use of non-symmetrical biaryl dialdehydes, in which the [O=C–C_{Ar}–C_{Ar}–C=O] angle was smaller than 180° resulting in [2+2]-cyclocondensation products that form in excellent regioselectivities. Hence compounds (**11–14**) were reacted with (1*R*,2*R*)-1,2-diaminocyclohexane²⁴ (**15**) in dichloromethane to afford crude macrocyclic products in almost quantitative yields (**16–22**, Fig. 3) each containing mixtures of *C*₃-symmetrical trianglimines, non-symmetrical regioisomers along with some oligomers (Fig. 2 and 3). An accurate estimation of the regioselectivity was not possible due to signals overlapping in the ¹H-NMR spectra. However, a ratio of 1 : 1 for the formation of the *C*₃-symmetrical and the non-symmetrical regioisomers can be established from the crude integrals. *C*₃-symmetrical trianglimines (**16–18**) and their non-symmetrical regioisomers (**19–22**) could be separated using column chromatography on pretreated silica gel to give the individual regioisomers in high purity, although low



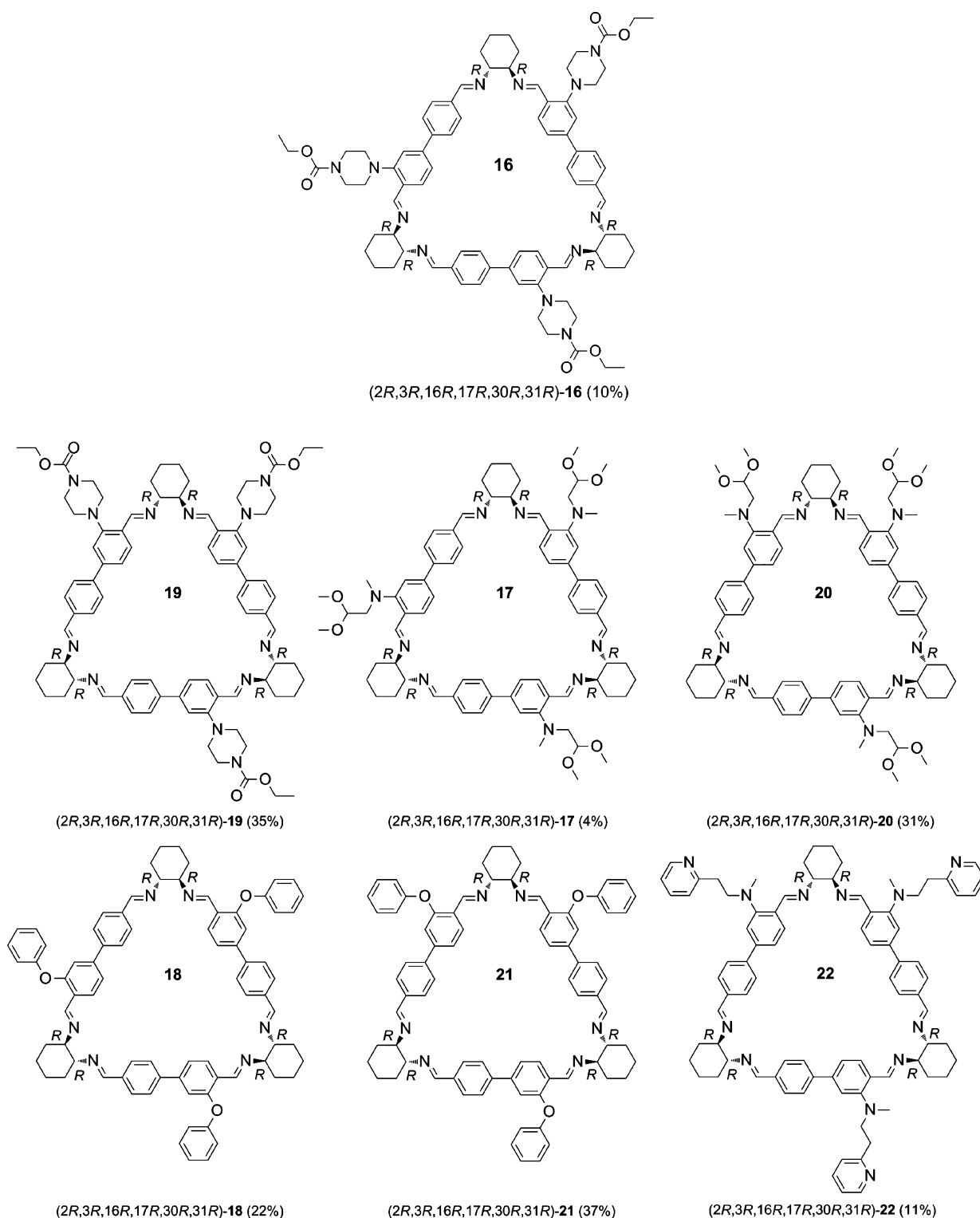


Fig. 3 C_3 -symmetrical (**16–18**) and the non-symmetrical (**19–22**) macrocyclisation products from the [3 + 3]-cyclocondensation reaction of (1*R*,2*R*)-1,2-diaminocyclohexane (**15**) with dialdehydes (**11–14**).

isolated yield. It is worth noting that in previous work due to their water sensitivity triallimines were always purified using crystallisation methods, whereas we give here for the first time in triallimine chemistry an experimental procedure allowing purification by column chromatography. ESI mass spectrum for

triallimine (**20**) showed two peaks at m/z 1216 and 1238 corresponding to $[M+H]^+$ and $[M+Na]^+$, respectively (Fig. 4). Fig. 5a represents the 1H -NMR spectrum for a crude mixture of triallimines (**17**) and (**20**) before being purified by column chromatography (CC). The number of signals corresponding to

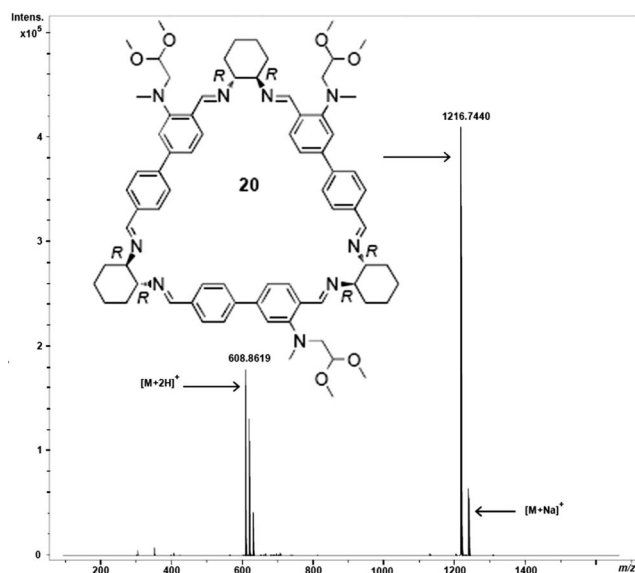


Fig. 4 ESI-MS spectrum for trianglimine (**20**) (microTOF, CH_2Cl_2 and MeOH).

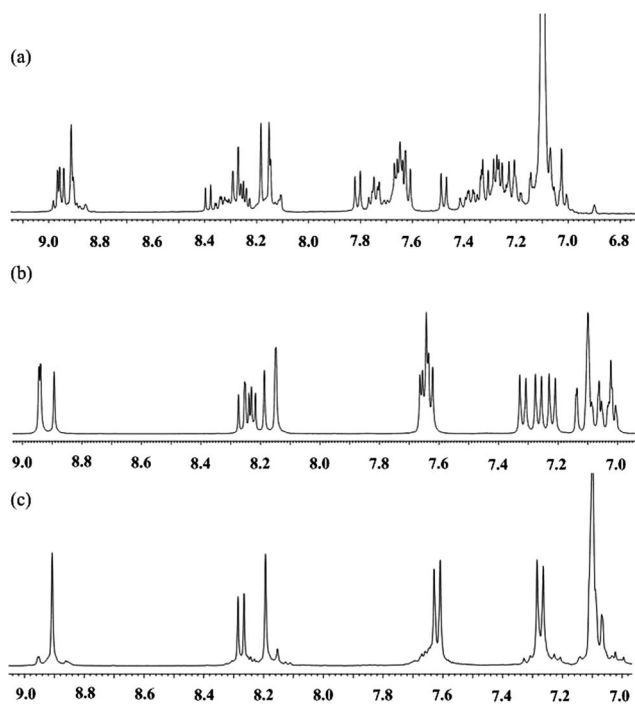


Fig. 5 Expanded ^1H -NMR spectra for (a) a crude mixture of trianglimines (**17**) and (**20**) before purification with CC, (b) the non-symmetrical trianglimine (**20**) after purification and (c) the C_3 -symmetrical trianglimine (**17**) after purification with CC (C_6D_6 , 400 MHz).

the azomethine protons for the C_3 -symmetrical trianglimine (**17**) should be two singlets and each signal should have an integration of three. For the non-symmetrical trianglimine (**20**), six different azomethine protons should be recognised. The presence of many signals in the region from δ 8.8 to 9 ppm indicates that the crude mixture contains more than one isomer. Fig. 5b and 5c represent the ^1H -NMR spectra for both the non-symmetrical trianglimine

(**20**) and its C_3 -symmetrical regioisomer (**17**), respectively. The ^1H -NMR spectrum for the non-symmetrical trianglimine (**20**) showed four singlets at δ 8.94, 8.93, 8.89 and 8.18 ppm. Each signal had an integration of one. It also showed a broad signal at δ 8.14 ppm with an integration of two corresponding to the six non-equivalent azomethine protons (Fig. 5b). On the other hand the ^1H -NMR spectrum for the C_3 -symmetrical trianglimine (**17**) showed two set of singlets at δ 8.90 and 8.19 ppm. Each signal had an integration of three corresponding to the six azomethine protons (Fig. 5c). Furthermore, the IR spectra for regioisomers (**17**) and (**20**) showed an intense absorption band at ν_{max} 1637 cm^{-1} corresponding to the imine functional groups. In addition, all the protons and carbons could be unambiguously assigned by ^1H - ^1H -COSY, ^1H - ^1H -ROESY, HMBC and HMQC 2D-experiments.

Monitoring the [3+3]-cyclocondensation reactions by direct infusion ESI-MS

Here, we report the use of the high resolution ESI-mass spectrometry as an efficient technique for monitoring the progress of the [3+3]-macrocyclisation reactions. (1*R*,2*R*)-1,2-Diaminocyclohexane (**15**) reacted with dialdehyde (**13**) in dichloromethane at 0.1 M concentration. The mixture was stirred at room temperature for 43 h. Aliquots were taken at different time intervals, diluted and methanol added to the solution before being directly infused to the ESI-TOF-MS. Fascinatingly a total of 15 different reaction intermediates could be detected at different intensities and their appearance and disappearance monitored over the cause of the reaction. This represents to our knowledge the largest number of reaction intermediates ever observed in a single chemical reaction. All intermediates could be assigned on the basis of their high resolution m/z values. This method does not only allow monitoring of the progress of the reaction, previously not possible by TLC due to the acidic nature of silica plates,²⁵ but provides an intriguing insight into mechanistic aspects of this unusual reaction. Intermediates (**23**) and (**24**) were for example detected along with both the [2+2]-macrocyclisation product (**25**) and the starting material (**13**) after 3 h from the start of the experiment (Fig. 6). Most of these intermediates were completely consumed in the construction of trianglimine (**22**) after 43 h (Fig. 7). A peak at m/z 845, corresponding to the [2+2]-cyclocondensation intermediate (**25**) was still observed after that time. We assumed that intermediates (**24**), (**25**) and the final product (**22**) are non-symmetric, but in fact the peaks appearing at m/z 767, 845 and 1267 can also be related to their symmetrical counterparts. Although the [3+3]-macrocyclisation reaction of dialdehyde (**13**) with (1*R*,2*R*)-1,2-diaminocyclohexane (**15**) had resulted in the formation of the non-symmetrical trianglimine (**22**) along with its C_3 -symmetrical regioisomer, we could not succeed in separating the C_3 -symmetrical regioisomer because its R_f value was very close to that of the non-symmetrical trianglimine (**22**). The chirality of the newly synthesised trianglimines was confirmed by circular dichroism (CD) spectra (Fig. 8). Trianglimines (**18**) and (**21**) have very similar UV absorption spectra with a slightly increased absorption for the non-symmetrical trianglimine (**21**). Large negative amplitudes were observed for the two regioisomers (**18**) and (**21**) at $\lambda \approx 300\text{ nm}$ indicating negative Cotton effects.

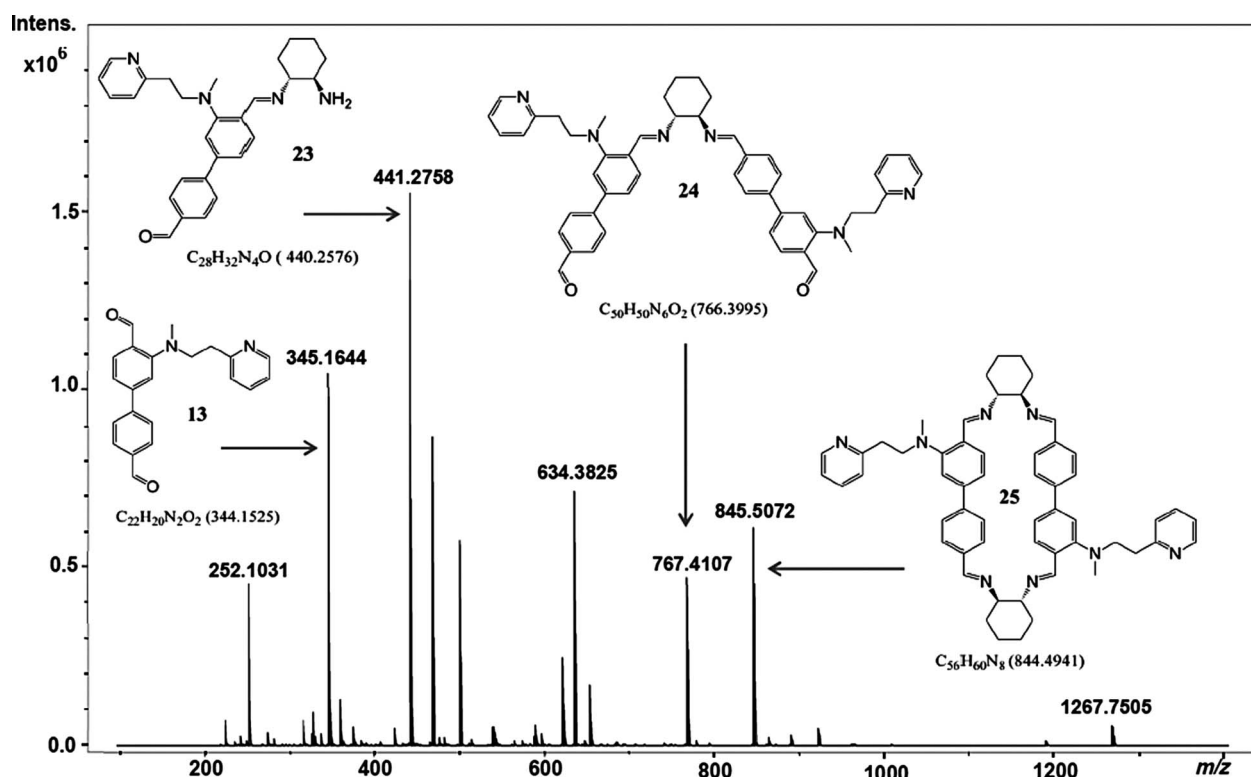


Fig. 6 ESI-MS spectrum for following up the [3+3]-macrocyclisation reaction of diamine (15) with dialdehyde (13) (microTOF, measured after 3 h from the start of the experiment in CH_2Cl_2 and MeOH).

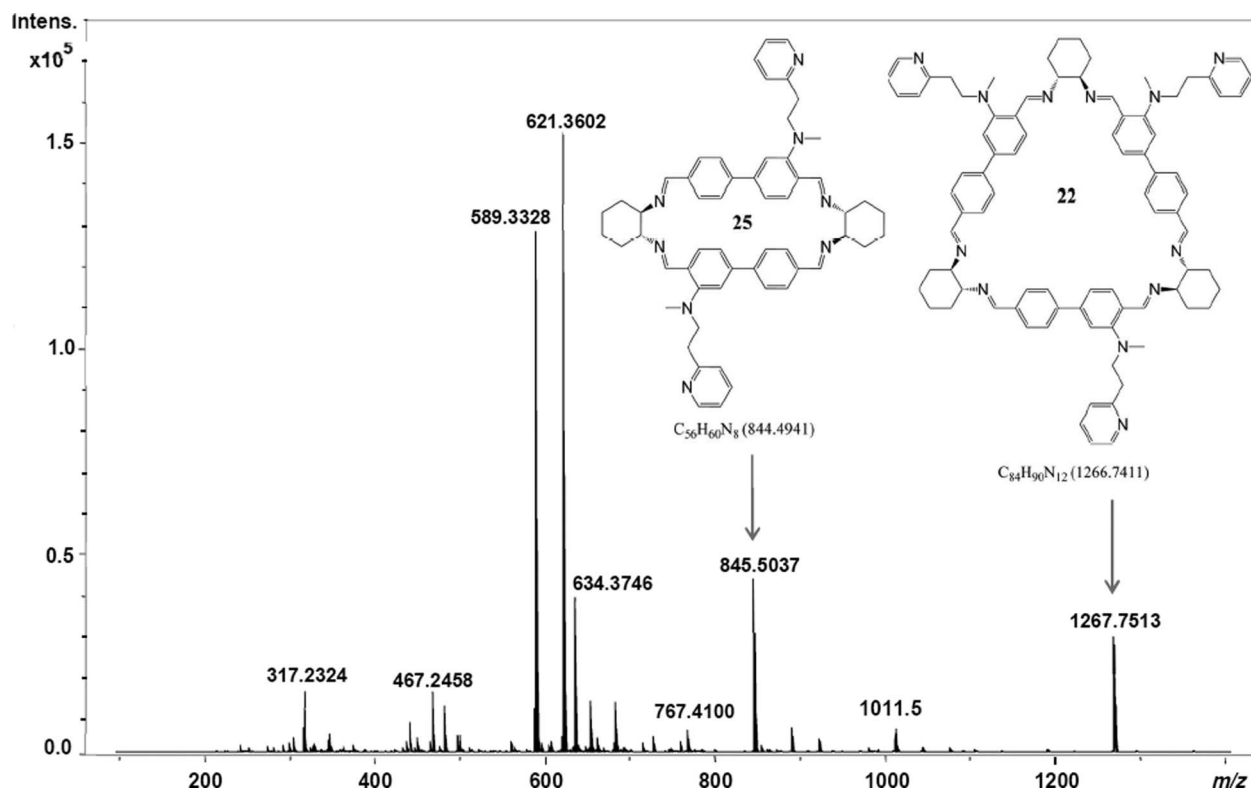


Fig. 7 ESI-MS spectrum for following up the [3+3]-macrocyclisation reaction of diamine (15) with dialdehyde (13) (microTOF, measured after 43 h from the start of the experiment in CH_2Cl_2 and MeOH).

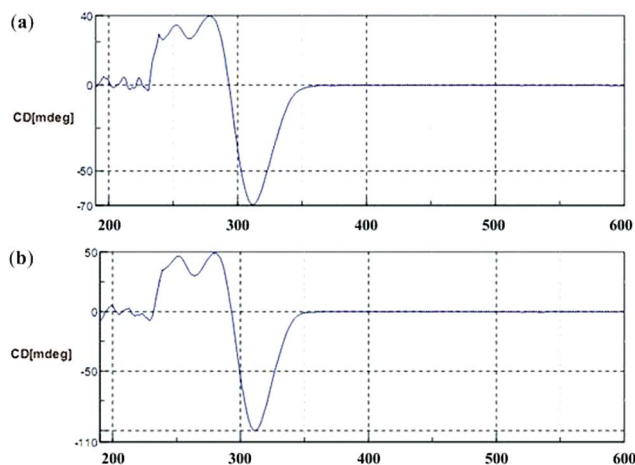


Fig. 8 CD spectra for (a) the C_3 -symmetrical triaglimine (**18**) and (b) the non-symmetrical regioisomer (**21**) in CHCl_3 .

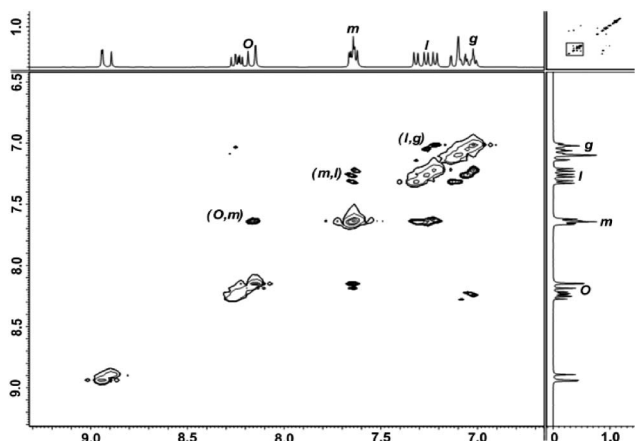


Fig. 9 2D-ROESY spectrum for triaglimine (**20**) showing through space interactions between the aromatic protons (CDCl_3 , 400 MHz).

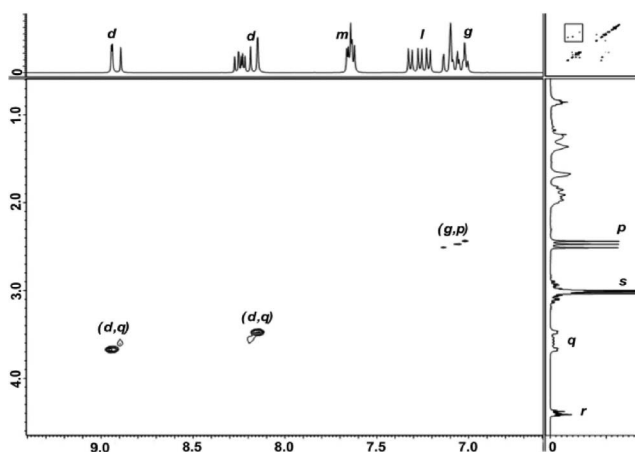


Fig. 10 2D-ROESY spectrum for triaglimine (**20**) showing through space interactions between aromatic and aliphatic protons (CDCl_3 , 400 MHz).

Regioisomers (**18**) and (**21**) can be distinguishable by their spectral fine structure between 250 and 280 nm.

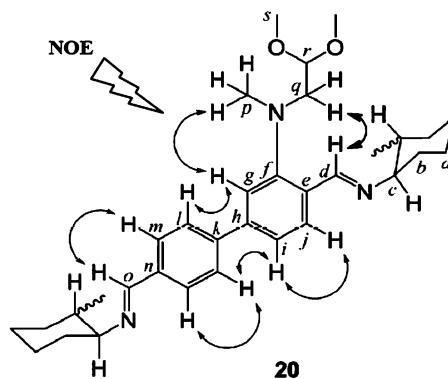


Fig. 11 Conformation structure of triaglimine (**20**).

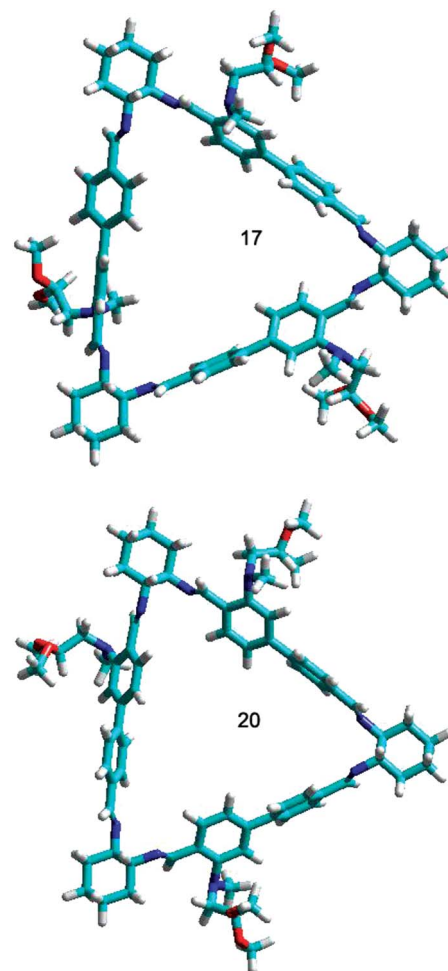
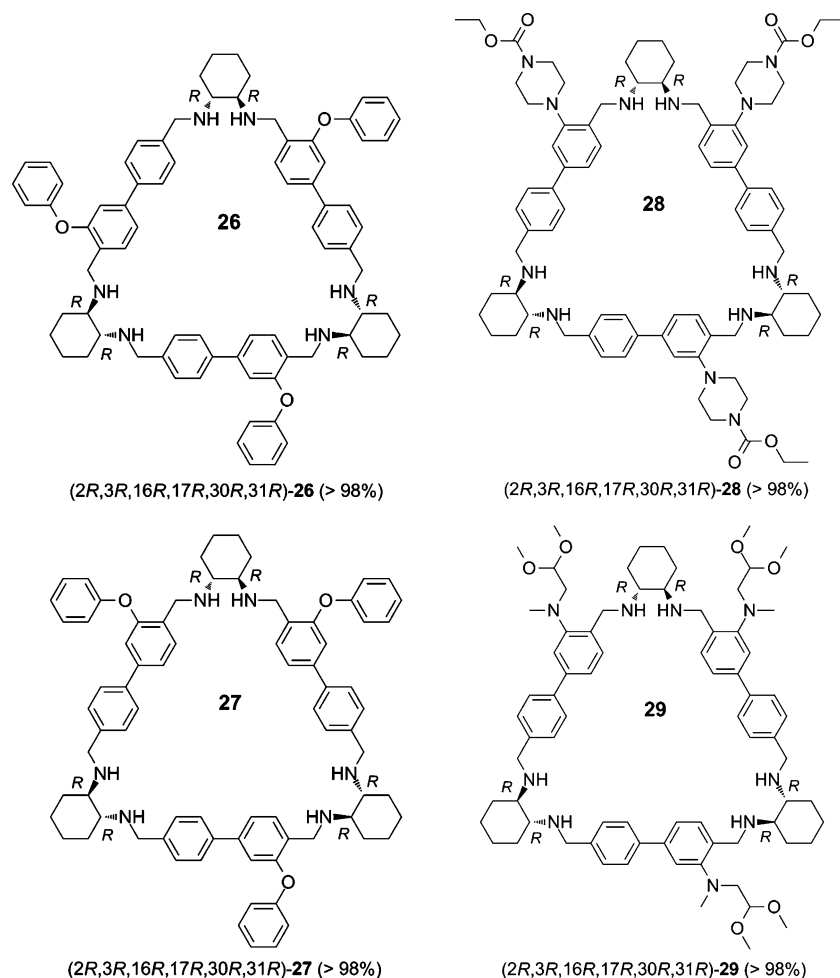


Fig. 12 Computed structures of triaglimines (**17**) and (**20**) using the Polak-Ribiere conjugate gradient with rms 0.007 Kcal/mol.

Equilibration of the C_3 -symmetrical triaglimine (**16**) with its non-symmetrical regioisomer (**19**)



Surprisingly, triaglimine (**16**) equilibrated with its non-symmetrical regioisomer (**19**) in the NMR tubes during the

Fig. 13 Reduced triallamines (**26–29**).

NMR measurements in the case where CDCl_3 was the solvent used. On attempts to elucidate the reason behind this equilibration, the ^1H -NMR measurements were carried out in different deuterated solvents, such as acetone- d_6 , CDCl_3 and C_6D_6 . Only C_3 -symmetrical triallamines equilibrated with their non-symmetrical regioisomers in CDCl_3 . This can be attributed to the slight acidity of CDCl_3 which facilitates the acid catalysed imine exchange reaction in addition to the fact that the non-symmetrical triallamine (**19**) is statistically favoured since the arrangements of the building blocks are three times more probable than that with triallamine (**16**). The ratio of the C_3 -symmetrical triallamine (**16**) to its non-symmetrical regioisomer (**19**) after six days of standing in CDCl_3 was estimated from the ^1H -NMR integrals and was found to be 58 to 42%, respectively. The ^1H -NMR spectrum for the non-symmetrical triallamine (**19**) showed a doublet signal at δ 6.93 ppm (ArH) and six different signals at δ 8.19, 8.20, 8.23, 8.43, 8.44 and 8.53 ppm corresponding to the imine protons (see supplementary information†). The ^1H -NMR spectrum for the C_3 -symmetrical triallamine (**16**) showed a set of two singlet signals at δ 8.23 and 8.50 ppm corresponding to the azomethine protons.

After six days of standing in CDCl_3 , the ^1H -NMR spectrum for the C_3 -symmetrical triallamine (**16**) showed a doublet signal at δ 6.93 ppm related to the non-symmetrical triallamine (**19**)

(ArH). It also showed many aldehydic signals in the region from δ 10.02 to 10.07 ppm and δ 10.32 to 10.36 ppm. The singlet signals appearing at δ 10.07 and 10.36 ppm are related to the two aldehydic protons of dialdehyde (**11**). In addition, all the assigned signals corresponding to the azomethine protons for both the C_3 -symmetrical triallamine (**16**) and its non-symmetrical regioisomer (**19**) were observed at δ 8.18, 8.20, 8.23, 8.43, 8.44, 8.50 and 8.53 ppm indicating clearly an equilibration between the two isomers.

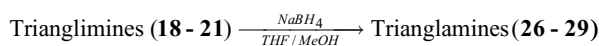
Conformational analysis for the non-symmetrical triallamine (**20**)

The two-dimensional ^1H - ^1H -ROESY experiments confirmed both the regiochemistry and the stereochemistry for all of the newly synthesised triallamines (e.g., triallamine **20**). The ^1H - ^1H -ROESY spectrum for compound (**20**) showed through space interactions between the methylene protons (*q*) and the azomethine proton (*d*) (Fig. 9–11). It can be concluded from the observed nOe effects that triallamine (**20**) adopts a conformation in solution in which the 2-biaryl substituent is placed *syn*- to the imine ($\text{HC}=\text{N}$) group and *anti*- to the nitrogen lone pairs. Structures of triallamines (**17**) and (**20**) were optimised with Hyperchem²⁶ software (Release 8.0) using MM+ molecular mechanics along with the semi-empirical molecular orbital PM3 method (Parametric Method 3,

Fig. 12).²⁷ The structures were minimised using the Polak–Ribiere conjugate gradient with rms 0.007 Kcal/mol. Reaching a gradient of 0.007 Kcal/mol took 28 h of calculations for the C_3 -symmetrical trianglimine (**17**) and 30 h for its non-symmetrical regioisomer (**20**). The total energies for trianglimines (**17**) and (**20**) were found to be exactly identical with a value of -497.56 a.u.

The results from the computational calculations were found to be in accordance with both the conformational structures suggested by the 2D-ROESY experiments and the previously reported X-ray data.²⁸

Reduction of trianglimines (18–21)



Trianglimines (**18–21**) were reduced by sodium borohydride (NaBH_4) in a mixture of THF and MeOH to the corresponding trianglamines (**26–29**) in excellent yields without needing further purification (Fig. 13). The $^1\text{H-NMR}$ spectrum for trianglamine (**27**) showed multiplet signals at δ 3.94–4.00 and 3.63–3.72 ($J = 13.2$) ppm corresponding to $-\text{CH}_A\text{CH}_B\text{N}$ and $-\text{CH}_A\text{CH}_B\text{N}$ in the AB spin system. It also showed a broad multiplet at δ 2.08–2.31 ppm with an integration of 18 corresponding to the twelve methylene protons ($-\text{CH}_2-$) of the cyclohexyl group and the six ($-\text{NH}-$) protons. On the other hand, the IR spectrum showed a broad absorption band at $\nu = 3286\text{ cm}^{-1}$ corresponding to the ($-\text{NH}-$) groups.

Conclusion

In conclusion, we have shown an efficient procedure for synthesising functionalised aromatic dialdehydes in excellent yields using nucleophilic aromatic substitution reactions along with the Suzuki-coupling methodology. The newly functionalised dialdehydes successfully underwent [3+3]-cyclocondensation reactions to give C_3 -symmetrical trianglimines along their non-symmetrical regioisomers, which were separated and purified efficiently using column chromatography. Computational calculations at the PM3 level showed great flexibility of the newly synthesised trianglimines due to the free rotations around the C_9-C_{10} , $C_{23}-C_{24}$ and $C_{37}-C_{38}$ single bonds. The C_3 -symmetrical trianglimines showed dynamic interchange to the non-symmetrical regioisomers in CDCl_3 during the NMR measurements. All the synthesised trianglimine and trianglamine regioisomers are enantiomerically pure and can serve as good receptors for different guests. Although the water solubility for the newly synthesised trianglamines was not enhanced in a satisfactory way by the introduction of the substituents chosen in this work, we still believe that a careful choice of the substituents which possess functional groups capable of forming hydrogen bonds or salt bridges can lead to a dramatic improvement in the solubility of this class of macrocycle, leading to potential applications. We showed that the ESI-MS instrument can be used as an efficient technique for monitoring the progress of the [3+3]-macrocyclisation reaction providing vital information about the reactive intermediates participating in the formation of the final product.

Experimental

Ethyl 4-(5-bromo-2-formylphenyl)-piperazine-1-carboxylate (**6**)

To a stirred solution of 4-bromo-2-fluorobenzaldehyde (**1**) (2.02 g, 10 mmol) in acetonitrile (20 mL), K_2CO_3 (4.07 g, 29.5 mmol) and ethyl *N*-piperazinecarboxylate (**2**) (2.2 mL, 14.79 mmol) was added. The mixture was stirred at 100°C for 48 h. The solvent was evaporated under vacuum. Water was added to the crude product and the aqueous phase was extracted with Et_2O ($3 \times 100\text{ mL}$). The combined organic phases were washed with H_2O , dried with Na_2SO_4 and evaporated under vacuum. The crude mixture was purified by column chromatography (petroleum ether : ethylacetate, 9 : 1, the polarity was increased gradually to 7 : 3 after receiving the first fraction of impurities) to give the title compound (**6**) as a yellow solid (3.06 g, 90%); mp $95-96^\circ\text{C}$; R_f (0.6, petroleum ether : ethylacetate, 7 : 3); IR $\nu_{\text{max}}/\text{cm}^{-1}$ 1686 (br, $\text{N}(\text{C}=\text{O})\text{O}$ and $\text{H}(\text{C}=\text{O})$); $^1\text{H-NMR}$ (400 MHz, CDCl_3) δ_H 10.20 (1H, s, CHO), 7.62 (1H, dd, $J = 8.2$, ArH), 7.24 (1H, d, $J = 8.2$, ArH), 7.19 (1H, s, ArH), 4.14 (2H, q, CH_2CH_3), 3.64 (4H, t, $J = 4.5$, CH_2N), 3.01 (4H, t, $J = 4.1$, CH_2N), 1.25 (3H, m, CH_2CH_3); $^{13}\text{C-NMR}$ (100 MHz, CDCl_3) δ_C 189.91, 155.78, 155.48, 132.00, 130.08, 127.46, 126.38, 122.76, 61.70, 53.57, 43.72, 14.74; MS (ESI-MS, microTOF) m/z (Calcd. 340.0423; exp. 363.0400, $\text{M} + \text{Na}^+$, 100%). A crystal structure was obtained and solved.¹⁹

4-Bromo-2-phenoxybenzaldehyde (**7**)

To a stirred solution of 4-bromo-2-fluorobenzaldehyde (**1**) (4.0 g, 19.7 mmol) in acetonitrile (20 mL), K_2CO_3 (8.18 g, 59.3 mmol) and phenol (**3**) (2.32 g, 24.7 mmol) was added. The mixture was stirred at 100°C for 48 h. The solvent was evaporated under vacuum. Water was added to the crude product and the aqueous phase was extracted with Et_2O ($3 \times 100\text{ mL}$). The combined organic phases were washed with H_2O , dried with Na_2SO_4 and evaporated under vacuum. The crude compound was purified by column chromatography (petroleum ether : ether, 9.7 : 0.3 mL) to give the title compound (**7**) as a pale yellow solid (3.68 g, 62%); mp $86-87^\circ\text{C}$; R_f (0.9, petroleum ether : ethylacetate, 7 : 3); IR $\nu_{\text{max}}/\text{cm}^{-1}$ 1676 ($\text{C}=\text{O}$); $^1\text{H-NMR}$ (400 MHz, CDCl_3) δ_H 10.46 (1H, s, CHO), 7.77 (1H, d, $J = 8.4$, ArH), 7.41 (2H, t, $J = 8.4$, ArH), 7.21–7.29 (2H, m, ArH), 7.08 (2H, d, $J = 8.4$, ArH), 6.99 (1H, s, ArH); $^{13}\text{C-NMR}$ (100 MHz, CDCl_3) δ_C 188.39, 160.51, 155.44, 130.46, 130.27, 129.69, 126.66, 125.44, 125.22, 121.09, 119.95; MS (APCI-MS, HCTultra) m/z (Calcd. 275.9; exp. 276.9, $\text{M} + \text{H}^+$, 100%).

4-Bromo-2-[methyl-(2-pyridin-2-yl)-ethylamino]-benzaldehyde (**8**)

To a stirred solution of 4-bromo-2-fluorobenzaldehyde (**1**) (4.0 g, 19.7 mmol) in acetonitrile (20 mL), K_2CO_3 (8.14 g, 59 mmol) and *N*-methyl-2-(pyridin-2-yl)-ethanamine (**4**) (2.7 mL, 19.8 mmol) was added. The mixture was stirred at 100°C for 48 h. The solvent was evaporated under vacuum. Water was added to the crude product and the aqueous phase was extracted with Et_2O ($3 \times 100\text{ mL}$). The combined organic phases were washed with H_2O , dried with Na_2SO_4 and evaporated under vacuum. The crude mixture was purified by column chromatography (petroleum ether : ethylacetate, 8 : 2) to give the title compound (**8**) as a yellow oil (4.43 g, 66%); R_f (0.17, petroleum ether : ethylacetate, 7 : 3); IR $\nu_{\text{max}}/\text{cm}^{-1}$ 1682 ($\text{C}=\text{O}$), 1580 ($\text{C}=\text{N}$); $^1\text{H-NMR}$ (400 MHz,

CDCl_3) δ_{H} 9.92 (1H, s, CHO), 8.41 (1H, m, ArH), 7.44–7.51 (2H, m, ArH), 7.12 (1H, s, ArH), 6.99–7.05 (3H, m, ArH), 3.51 (2H, m, CH_2N), 2.99 (2H, m, CH_2CH_2), 2.86 (3H, s, CH_3); ^{13}C -NMR (100 MHz, CDCl_3) δ_{C} 190.16, 158.98, 155.99, 149.45, 136.41, 131.66, 129.56, 126.76, 124.56, 123.30, 122.77, 121.58, 57.58, 42.40, 36.03; MS (ESI-MS, microTOF) m/z (Calcd. 318.0368; exp. 341.0367, M + Na^+ , 100%).

4-Bromo-2-[(2,2-dimethoxyethyl)-methylamino]-benzaldehyde (9)

To a stirred solution of 4-bromo-2-fluorobenzaldehyde (**1**) (4.0 g, 19.7 mmol) in acetonitrile (20 mL), K_2CO_3 (8.14 g, 59 mmol) and 1,1-dimethoxy-*N*-methylethanamine (**5**) (2.5 mL, 19.78 mmol) was added. The mixture was stirred at 100 °C for 48 h. The solvent was evaporated under vacuum. Water was added to the crude product and the aqueous phase was extracted with Et_2O (3 \times 100 mL). The combined organic phases were washed with H_2O , dried with Na_2SO_4 and evaporated under vacuum. The crude mixture was purified by column chromatography (petroleum ether was used as an eluent for the first fraction of impurities and then a mixture of petroleum ether and ethylacetate was used to get the target product, 7 : 3 mL) to give the title compound (**9**) as a yellow oil (5.66 g, 94%); R_f (0.67, petroleum ether : ethylacetate, 7 : 3); IR $\nu_{\text{max}}/\text{cm}^{-1}$ 1738 (C=O); ^1H -NMR (400 MHz, CDCl_3) δ_{H} 10.12 (1H, s, CHO), 7.54 (1H, d, $J = 8.2$, ArH), 7.21 (1H, s, ArH), 7.10 (1H, d, $J = 8.2$, ArH), 4.51 (1H, m, CH_2CH), 3.23–3.25 (8H, m, 2 -OCH₃, CH_2CH), 2.92 (3H, s, -NCH₃); ^{13}C -NMR (100 MHz, CDCl_3) δ_{C} 190.25, 156.02, 132.04, 129.60, 126.67, 124.72, 122.98, 102.41, 59.16, 53.72, 42.96; MS (ESI-MS, microTOF) m/z (Calcd. 301.0314; exp. 324.0326, M + Na^+ , 100%).

Ethyl 4-[4,4'-diformyl-(1,1'-biphenyl)-3-yl]-piperazine-1-carboxylate (11)

To a stirred solution of ethyl 4-(5-bromo-2-formylphenyl)-piperazine-1-carboxylate (**6**) (3.0 g, 8.82 mmol) in toluene (20 mL) under nitrogen atmosphere, $\text{Pd}(\text{PPh}_3)_4$ (0.4 g, 0.35 mmol, 3.0 mol%) and an aqueous solution of Na_2CO_3 (10 mL, 2 mol L⁻¹) was added. The mixture was stirred vigorously and then 4-formylphenylboronic acid (**10**) (1.32 g, 8.8 mmol) in 15 mL of ethanol was added. The mixture was refluxed overnight under vigorous stirring. The organic phase was extracted with Na_2CO_3 solution (2 \times 50 mL) and 10 mL brine. The organic phase was dried over MgSO_4 , filtered and the solvent was removed under vacuum. The crude product was purified by column chromatography (petroleum ether : ethylacetate, 8 : 2 mL) to give the title compound (**11**) as a yellow solid (2.43 g, 75%); mp 139–140 °C; R_f (0.28, petroleum ether : ethylacetate, 7 : 3); IR $\nu_{\text{max}}/\text{cm}^{-1}$ 1684 (br, N(C=O)O, H(C=O)); ^1H -NMR (400 MHz, CDCl_3) δ_{H} 10.36 (1H, s, CHO), 10.07 (1H, s, CHO), 7.97 (2H, d, $J = 8.2$, ArH), 7.92 (1H, d, $J = 7.7$, ArH), 7.74 (2H, d, $J = 7.7$, ArH), 7.40 (1H, dd, $J = 7.7$, ArH), 7.30 (1H, s, ArH), 4.17 (2H, q, CH_2CH_3), 3.71 (4H, m, CH_2N), 3.12 (4H, m, CH_2N), 1.28 (3H, m, CH_2CH_3); ^{13}C -NMR (100 MHz, CDCl_3) δ_{C} 191.76, 190.55, 155.63, 146.42, 145.91, 136.10, 131.35, 130.40, 128.37, 128.05, 122.23, 118.29, 61.72, 53.77, 43.88, 14.76; MS (ESI-MS, microTOF) m/z (Calcd. 366.1580; exp. 389.1554, M + Na^+ , 100%).

3-Phenoxybiphenyl-4,4'-dicarbaldehyde (12)

To a stirred solution of 4-bromo-2-phenoxybenzaldehyde (**7**) (3.0 g, 10.9 mmol) in toluene (20 mL) under nitrogen atmosphere, $\text{Pd}(\text{PPh}_3)_4$ (0.32 g, 0.28 mmol, 3.0 mol%) and an aqueous solution of Na_2CO_3 (10 mL, 2 mol L⁻¹) was added. The mixture was stirred vigorously and then 4-formylphenylboronic acid (**10**) (1.62 g, 10.8 mmol) in 15 mL ethanol was added. The mixture was refluxed overnight under vigorous stirring. The organic phase was extracted with Na_2CO_3 solution (2 \times 50 mL) and 10 mL brine. The organic phase was dried over MgSO_4 , filtered, and the solvent was removed under vacuum. The crude product was purified by column chromatography (petroleum ether : ethylacetate, 8 : 2 mL) to give the title compound (**12**) as a pale yellow solid (1.54 g, 47%); mp 100–101 °C; R_f (0.74, petroleum ether : ethylacetate, 7 : 3); IR $\nu_{\text{max}}/\text{cm}^{-1}$ 1733 (C=O); ^1H -NMR (400 MHz, CDCl_3) δ_{H} 10.52 (1H, s, CHO), 10.01 (1H, s, CHO), 8.01 (1H, d, $J = 7.7$, ArH), 7.90 (2H, d, $J = 7.7$, ArH), 7.63 (2H, d, $J = 7.7$, ArH), 7.38–7.44 (3H, m, ArH), 7.10–7.21 (4H, m, ArH); ^{13}C -NMR (100 MHz, CDCl_3) δ_{C} 191.66, 188.88, 160.35, 156.33, 147.21, 145.09, 136.19, 130.37, 130.09, 129.28, 127.97, 126.47, 124.68, 122.50, 119.44, 117.32; MS (ESI-MS, microTOF) m/z (Calcd. 302.0943; exp. 325.0820, M + Na^+ , 100%).

3-[Methyl-(2-pyridin-2-yl)-ethylamino]-1,1'-biphenyl-4,4'-dicarbaldehyde (13)

To a stirred solution of 4-bromo-2-[methyl-(2-pyridin-2-yl)-ethylamino]-benzaldehyde (**8**) (3.02 g, 9.49 mmol) in toluene (20 mL) under nitrogen atmosphere, $\text{Pd}(\text{PPh}_3)_4$ (0.33 g, 0.28 mmol, 3.0 mol%) and an aqueous solution of Na_2CO_3 (10 mL, 2 mol L⁻¹) was added. The mixture was stirred vigorously and then 4-formylphenylboronic acid (**10**) (1.56 g, 10.4 mmol) in 15 mL ethanol was added. The mixture was refluxed overnight under vigorous stirring. The organic phase was extracted with Na_2CO_3 solution (2 \times 50 mL) and 10 mL brine. The organic phase was dried over MgSO_4 , filtered and the solvent was removed under vacuum. The crude product was purified by column chromatography (petroleum ether : ethylacetate, 7 : 3 then the polarity was increased to 6 : 4) to give the title compound (**13**) as a yellow oil (2.8 g, 85%); R_f (0.28, petroleum ether : ethylacetate, 7 : 3); IR $\nu_{\text{max}}/\text{cm}^{-1}$ 1697 and 1676 (C=O), 1596 (C=N); ^1H -NMR (400 MHz, CDCl_3) δ_{H} 10.12 (1H, s, CHO), 10.05 (1H, s, CHO), 8.48 (1H, m, ArH), 7.95 (2H, d, $J = 8.2$, ArH), 7.83 (1H, d, $J = 8.2$, ArH), 7.74 (2H, d, $J = 8.2$, ArH), 7.53 (1H, ddd, $J = 7.7$, ArH), 7.30 (1H, s, ArH), 7.24–7.26 (1H, m, ArH), 7.06–7.10 (2H, m, ArH), 3.64 (2H, m, CH_2N), 3.10 (2H, m, CH_2CH_2), 3.01 (3H, s, CH_3N); ^{13}C -NMR (100 MHz, CDCl_3) δ_{C} 191.83, 190.91, 159.27, 155.83, 149.46, 146.27, 145.76, 136.50, 135.95, 131.05, 130.33, 128.05, 123.37, 121.58, 120.65, 118.68, 57.60, 42.97, 36.19; MS (ESI-MS, microTOF) m/z (Calcd. 344.1525; exp. 367.1598, M + Na^+ , 100%).

3-[(2,2-Dimethoxyethyl)-methylamino]-1,1'-biphenyl-4,4'-dicarbaldehyde (14)

To a stirred solution of 4-bromo-2-[(2,2-dimethoxyethyl)-methylamino]-benzaldehyde (**9**) (3.0 g, 9.9 mmol) in toluene (20 mL) under nitrogen atmosphere, $\text{Pd}(\text{PPh}_3)_4$ (0.35 g, 0.3 mmol, 3.0 mol%) and an aqueous solution of Na_2CO_3 (10 mL, 2 mol L⁻¹) was added. The mixture was stirred vigorously and then

4-formylphenylboronic acid (**10**) (1.49 g, 9.9 mmol) in 15 mL ethanol was added. The mixture was refluxed overnight under vigorous stirring. The organic phase was extracted with Na₂CO₃ solution (2 × 50 mL) and 10 mL brine. The organic phase was dried over MgSO₄, filtered, and the solvent was removed under vacuum. The crude product was purified by column chromatography (petroleum ether:ethylacetate, 9:1 mL) to give the title compound (**14**) as a yellow oil (2.58 g, 79%); R_f (0.37, petroleum ether:ethylacetate, 7:3); IR ν_{\max} /cm⁻¹ 1697, 1678 (C=O), ¹H-NMR (400 MHz, CDCl₃) δ_{H} 10.31 (1H, s, CHO), 10.06 (1H, s, CHO), 7.96 (2H, d, *J* = 8.2, ArH), 7.86 (1H, d, *J* = 7.7, ArH), 7.75 (2H, d, *J* = 7.7, ArH), 7.34 (1H, s, ArH), 7.29 (1H, d, *J* = 8.2, ArH); ¹³C-NMR (100 MHz, CDCl₃) δ_{C} 191.80, 190.96, 155.93, 146.21, 145.84, 135.99, 131.35, 130.35, 128.04, 127.79, 120.80, 118.90, 102.58, 59.20, 53.72, 43.46; MS (ESI-MS, microTOF) *m/z* (Calcd. 327.1471; exp. 350.1356, M + Na⁺, 100%).

(2R,3R,16R,17R,30R,31R)-(1,4,15,18,29,32)-Hexaza-(2,3:16,17:30,31)-tributano-(7,21,35)-tri-*N*-piprazinocarboxylate-(6,9:10,13:20,23:24,27:34,37:38,41)-hexa-etheno-(2H,3H,16H,17H,30H,31H)-hexahydro-[42]-annulene (16**)**

Dialdehyde (**11**) (1.15 g, 3.14 mmol) in dichloromethane (16 mL) was added to a solution of (1*R*,2*R*)-1,2-diaminocyclohexane (**15**) (540 mg, 4.74 mmol) in dichloromethane (16 mL). The mixture was stirred at room temperature for 72 h. The solvent was removed under vacuum. The crude mixture was purified by column chromatography (petroleum ether:ethylacetate:triethylamine, 7:2:1 mL) to give the title compound (**16**) as a yellow solid (140 mg, 10%); mp > 150 °C; IR ν_{\max} /cm⁻¹ 1687 (N(C=O)O), 1638 (C=N); ¹H-NMR (400 MHz, CDCl₃) δ_{H} 8.49 (3H, s, N=CH), 8.22 (3H, s, -N=CH), 7.80–7.85 (1H, m, ArH), 7.70 (2H, d, *J* = 8.2, ArH), 7.60 (6H, d, *J* = 8.2, ArH), 7.44 (6H, d, *J* = 8.2, ArH), 7.14–7.21 (4H, m, ArH), 7.05 (2H, s, ArH), 4.08–4.17 (6H, m, CH₂CH₃), 3.35–3.62 (18H, m, -NCH₂, HCN), 2.75–2.98 (12H, br, m, -NCH₂), 1.86 (18H, br, m, CH₂), 1.49 (6H, br, m, CH₂), 1.21–1.32 (9H, m, CH₃CH₂); ¹³C-NMR (100 MHz, CDCl₃) δ_{C} 160.35, 158.57, 155.54, 152.73, 142.82, 142.32, 135.56, 129.09, 128.54, 126.99, 121.93, 117.70, (74.83, 74.76), 61.49, 45.95, 44.95, 44.00, 32.76, 24.57, (14.94, 14.79); MS (ESI-MS, microTOF) *m/z* (Calcd. 1332.7576; exp. 1333.7668, M+H⁺, 100%).

(2R,3R,16R,17R,30R,31R)-(1,4,15,18,29,32)-Hexaza-(2,3:16,17:30,31)-tributano-(7,21,35)-tri-(2,2-dimethoxy-*N*-methylethanamino)-(6,9:10,13:20,23:24,27:34,37:38,41)-hexa-etheno-(2H,3H,16H,17H,30H,31H)-hexahydro-[42]-annulene (17**)**

Dialdehyde (**14**) (1.73 g, 5.29 mmol) in dichloromethane (26 mL) was added to a solution of (1*R*,2*R*)-1,2-diaminocyclohexane (**15**) (906 mg, 7.95 mmol) in dichloromethane (26 mL). The mixture was stirred at room temperature for 50 h. The crude product was purified by column chromatography (petroleum ether:ethylacetate:triethylamine, 8:1:1) to give the title compound (**17**) as a yellow solid (90 mg, 4%); mp > 115 °C; IR ν_{\max} /cm⁻¹ 1637 (C=N); ¹H-NMR (400 MHz, C₆D₆) δ_{H} 8.90 (3H, s, -N=CH), 8.27 (3H, d, *J* = 7.7, ArH), 8.19 (3H, s, -N=CH), 7.61 (6H, d, *J* = 8.7, ArH), 7.27 (6H, d, *J* = 8.2, ArH), 7.60–7.09 (6H,

m, ArH overlapping with C₆D₆ signals), 4.38 (3H, m, CH₂CH), 3.52–3.65 (6H, m, HCN), 2.91–3.10 (24, m, CH₃, -NCH₂), 2.48 (9H, s, CH₃), 1.83–2.00 (16H, br, m, CH₂), 1.66–1.69 (8H, br, m, CH₂); ¹³C-NMR (100 MHz, C₆D₆) δ_{C} 159.65, 158.34, 153.74, 142.47, 142.21, 135.97, 129.94, 128.79, 128.69, 126.87, 121.50, 119.07, 102.66, (75.31, 77.21) 58.00, (52.65, 52.61), 43.79, (33.38, 33.18), 24.74; MS (ESI-MS, microTOF) *m/z* (Calcd. 1215.7249; exp. 1216.7305, M + H⁺, 100%).

(2R,3R,16R,17R,30R,31R)-(1,4,15,18,29,32)-Hexaza-(2,3:16,17:30,31)-tributano-(7,21,35)-triphenoxy-(6,9:10,13:20,23:24,27:34,37:38,41)-hexa-etheno-(2H,3H,16H,17H,30H,31H)-hexahydro-[42]-annulene (18**)**

Dialdehyde (**12**) (1.2 g, 3.97 mmol) in dichloromethane (19.9 mL) was added to a solution of (1*R*,2*R*)-1,2-diaminocyclohexane (**15**) (679 mg, 5.96 mmol) in dichloromethane (19.9 mL). The mixture was stirred at room temperature for 8 h. The solvent was evaporated under vacuum. The crude mixture was purified by column chromatography (petroleum ether:diethylether:triethylamine, 5:4:1 mL) to give the title compound (**18**) as a pale yellow solid (344 mg, 22%); mp > 250 °C; IR ν_{\max} /cm⁻¹ 1637 (C=N); ¹H-NMR (400 MHz, CDCl₃) δ_{H} 8.51 (3H, s, -N=CH), 8.14 (3H, s, -N=CH), 7.93 (3H, d, *J* = 8.2, ArH), 7.52 (6H, d, *J* = 8.2, ArH), 7.35 (6H, d, *J* = 8.2, ArH), 7.20–7.28 (5H, m, ArH), 6.94–6.99 (8H, m, ArH), 6.66–6.80 (8H, m, ArH), 3.35 (6H, br, m, HCN), 1.83 (18H, br, m, CH₂), 1.46 (6H, br, m, CH₂); ¹³C-NMR (100 MHz, CDCl₃) δ_{C} 170.03, 160.59, 157.57, 156.49, 143.58, 141.12, 135.83, 129.80, 128.47, 127.88, 126.97, 126.83, 123.23, 122.35, 118.05, 117.61, (74.40, 74.13), 32.72, 24.52; MS (ESI-MS, microTOF) *m/z* (Calcd. 1140.5666; exp. 1140.5534, M⁺, 100%).

(2R,3R,16R,17R,30R,31R)-(1,4,15,18,29,32)-Hexaza-(2,3:16,17:30,31)-tributano-(7,21,40)-tri-*N*-piprazinocarboxylate-(6,9:10,13:20,23:24,27:34,37:38,41)-hexa-etheno-(2H,3H,16H,17H,30H,31H)-hexahydro-[42]-annulene (19**)**

Dialdehyde (**11**) (1.15 g, 3.14 mmol) in dichloromethane (16 mL) was added to a solution of (1*R*,2*R*)-1,2-diaminocyclohexane (**15**) (537 mg, 4.71 mmol) in dichloromethane (16 mL). The mixture was stirred at room temperature for 72 h. The solvent was removed under vacuum. The crude mixture was purified by column chromatography (petroleum ether:ethylacetate:triethylamine, 7:2:1 mL) to give the title compound (**19**) as a pale yellow solid (430 mg, 35%); mp > 200 °C; IR ν_{\max} /cm⁻¹ 1691 (N(C=O)O), 1638 (C=N); ¹H-NMR (400 MHz, CDCl₃) δ_{H} 8.53 (1H, s, -N=CH), 8.43 (1H, s, -N=CH), 8.42 (1H, s, -N=CH), 8.22 (1H, s, -N=CH), 8.19 (1H, s, -N=CH), 8.18 (1H, s, -N=CH), 7.83–7.86 (2H, m, ArH), 7.75 (1H, d, *J* = 8.2, ArH), 7.57–7.60 (6H, m, ArH), 7.42–7.45 (6H, m, ArH), 7.17–7.25 (3H, m, ArH), 7.06 (1H, s, ArH), 6.90–6.93 (2H, m, ArH), 4.12–4.18 (6H, m, CH₂CH₃), 3.72 (2H, br, m, CH₂N-), 3.50 (6H, br, m, HCN), 3.36–3.41 (10H, m, CH₂N-), 2.76 (4H, br, m, CH₂N-), 2.53 (4H, br, m, CH₂N-), 2.43 (4H, br, m, CH₂N-), 1.85 (18H, br, m, CH₂), 1.48 (6H, br, m, CH₂), 1.23–1.28 (9H, m, CH₂CH₃); ¹³C-NMR (100 MHz, CDCl₃) δ_{C} (160.59, 160.48, 160.27), (158.36, 157.86, 157.76), (155.54, 155.48, 155.42), (152.84, 153.68), (143.44, 143.22, 142.84), (142.38, 142.12), (135.63, 135.57, 135.46), (129.10,

128.98), (128.60, 128.51, 128.44), (128.41, 128.33, 128.27), (127.26, 127.14, 126.96), (122.11, 121.97), (118.18, 118.03, 117.82), (75.25, 75.14, 75.01, 74.82, 74.66, 74.38), (61.53, 61.50, 61.45), (52.53), (43.98), (32.98, 32.83, 32.73, 32.61), (24.60), (14.87, 14.82); MS (ESI-MS, micrOTOF) m/z (Calcd. 1332.7576; exp. 1333.4865, $M + H^+$, 100%).

(2R,3R,16R,17R,30R,31R)-(1,4,15,18,29,32)-Hexaza-(2,3:16,17:30,31)-tributano-(7,21,40)-tri-(2,2-dimethoxy-N-methylethanamino)-(6,9:10,13:20,23:24,27:34,37:38,41)-hexa-etheno-(2H,3H,16H,17H,30H,31H)-hexahydro-[42]-annulene (20)

Yellow solid (680 mg, 31%); mp > 125 °C; IR $\nu_{\max}/\text{cm}^{-1}$ 1637 (C=N); $^1\text{H-NMR}$ (400 MHz, C_6D_6) δ_{H} 8.94 (1H, s, -N=CH), 8.93 (1H, s, -N=CH), 8.89 (1H, s, -N=CH), 8.21–8.27 (3H, m, ArH), 8.18 (1H, s, -N=CH), 8.14 (2H, br, s, -N=CH), 7.62–7.66 (6H, m, ArH), 7.31 (2H, d, $J = 8.2$, ArH), 7.26 (2H, d, $J = 8.2$, ArH), (2H, d, $J = 8.2$, ArH), 7.00–7.13 (6H, m, ArH), 4.36–4.42 (3H, m, CH_2CH), 3.46–3.68 (6H, m, CH_2), 3.00–3.03 (24H, m, CH_3 , -NCH₂) 2.51 (3H, s, CH_3), 2.47 (3H, s, CH_3), 2.43 (3H, s, CH_3), 1.82–1.99 (12H, br, m, CH_2), 1.67 (6H, br, m, CH_2), 1.36 (6H, br, m, CH_2); $^{13}\text{C-NMR}$ (100 MHz, C_6D_6) δ_{C} (159.78, 159.69, 159.60), (158.42, 158.22, 158.17), (153.87, 153.82, 153.77), (142.43, 142.36, 142.31), (136.01, 135.88, 135.84), (130.00, 129.91), (128.88, 128.73, 128.58), (126.97, 126.86), (121.45), (119.25, 119.21, 119.11), (102.78, 102.69), (75.62, 75.57), (75.24), (74.76), (58.08, 58.04, 57.94), (52.77, 52.70, 52.61), (44.01, 43.95, 43.87), (33.34, 33.14), (24.74); MS (ESI-MS, micrOTOF) m/z (Calcd. 1215.7322; exp. 1216.7292, $M + H^+$, 100%).

(2R,3R,16R,17R,30R,31R)-(1,4,15,18,29,32)-Hexaza-(2,3:16,17:30,31)-tributano-(7,21,40)-triphenoxy-(6,9:10,13:20,23:24,27:34,37:38,41)-hexa-etheno-(2H,3H,16H,17H,30H,31H)-hexahydro-[42]-annulene (21)

Yellow solid (564 g, 37%); mp > 135 °C (decomposition); IR $\nu_{\max}/\text{cm}^{-1}$ 1637 (C=N); $^1\text{H-NMR}$ (400 MHz, CDCl_3) δ_{H} 8.57 (1H, s, -N=CH), 8.55 (1H, s, -N=CH), 8.54 (1H, s, -N=CH), 8.18 (1H, s, -N=CH), 8.15 (1H, s, -N=CH), 8.14 (1H, s, -N=CH), 7.94–7.97 (3H, m, ArH), 7.53–7.57 (6H, m, ArH), 7.34–7.42 (6H, m, ArH), 7.22–7.31 (6H, m, ArH), 6.99–7.11 (7H, m, ArH), 6.91 (1H, s, ArH), 6.75–6.86 (5H, m, ArH), 6.69 (2H, d, $J = 8.2$, ArH), 3.37 (6H, m, br, HCN), 1.85 (18H, m, br, CH_2), 1.47 (6H, m, br, CH_2); $^{13}\text{C-NMR}$ (100 MHz, CDCl_3) δ_{C} (160.62, 160.53), (157.78, 157.65, 157.45), (156.49), (143.63, 143.58), (141.23, 141.18), (135.93, 135.85, 135.78), (130.00, 129.95, 129.80), (128.54, 128.47), (128.23), (127.92), (127.17, 127.06), (126.86), (123.28, 123.19, 123.13), (122.51, 122.37, 122.26), (118.18), (117.70, 117.60), (74.45, 74.36, 74.32, 74.26, 74.20, 74.05), (32.78, 32.71), (24.57); MS (ESI-MS, micrOTOF) m/z (Calcd. 1140.5666; exp. 1163.5545, $M + \text{Na}^+$, 100%).

(2R,3R,16R,17R,30R,31R)-(1,4,15,18,29,32)-Hexaza-(2,3:16,17:30,31)-tributano-(7,21,40)-tri-[N-methyl-2-(pyridin-2-yl)-ethan-amino]-(6,9:10,13:20,23:24,27:34,37:38,41)-hexa-etheno-(2H,3H,16H,17H,30H,31H)-hexahydro-[42]-annulene (22)

Dicarbaldehyde (13) (2.3 g, 6.69 mmol) in dichloromethane (33.4 mL) was added to a solution of (1R,2R)-1,2-

diaminocyclohexane (15) (1.14 g, 10.03 mmol) in dichloromethane (33.4 mL). The mixture was stirred at room temperature for 96 h. The crude product was purified by column chromatography (petroleum ether:ethylacetate:triethylamine, 7:2:1) to give the title compound (22) as a yellow solid (310 mg, 11%); mp > 125 °C; IR $\nu_{\max}/\text{cm}^{-1}$ 1637; $^1\text{H-NMR}$ (400 MHz, C_6D_6) δ_{H} 8.66–8.69 (3H, br, m, -N=CH), 8.41–8.43 (3H, br, m, -N=CH), 8.14–8.26 (6H, m, ArH), 7.62–7.68 (6H, m, ArH), 7.24–7.28 (6H, m, ArH), 6.95–7.04 (9H, m, ArH), 6.58–6.71 (6H, m, ArH), 3.48–3.55 (6H, m, CH_2), 3.13–3.23 (6H, m, -NCH₂), 2.77–2.84 (6H, m, CH_2CH_2), 2.34–2.41 (9H, m, CH_3), 1.86–1.95 (12H, br, m, CH_2), 1.68 (6H, br, m, CH_2), 1.37 (6H, br, m, CH_2); $^{13}\text{C-NMR}$ (100 MHz, C_6D_6) δ_{C} (160.25), (159.83, 159.76, 159.67), (158.34, 158.20, 158.18), (153.65, 153.58, 153.50), (149.42), (142.49, 142.42), (135.87, 135.82, 135.79), (135.54, 135.50, 135.47), (130.16, 130.13, 130.09), (128.68, 128.63, 128.53), (127.06, 127.04, 126.96), (123.08, 122.97), (121.34), (120.85), (119.26, 119.18, 119.10), (75.61, 75.53), (75.34, 75.27), (74.80), (56.09), (43.27, 43.22, 43.19), (36.65, 36.63, 36.53), (33.36, 33.21, 33.16), (24.84, 24.78, 24.70); MS (ESI-MS, micrOTOF) m/z (Calcd. 1267.7482; exp. 1267.7439, M^+ , 100%).

(2R,3R,16R,17R,30R,31R)-(1,4,15,18,29,32)-Hexaza-(2,3:16,17:30,31)-tributano-(7,21,35)-triphenoxy-(6,9:10,13:20,23:24,27:34,37:38,41)-hexa-etheno-(1H,2H,3H,4H,5H,14H,15H,16H,17H,18H,19H,28H,29H,30H,31H,32H,33H,42H)-octadecahydro-[42]-annulene (26)

To a stirred solution of triaglimine (18) (125 mg, 0.11 mmol) in THF–MeOH (1:1, 20 mL) solid NaBH_4 (36.5 mg, 0.96 mmol) was gradually added and the solution was stirred for 5 h at room temperature. After removal of solvents the residue was extracted with CH_2Cl_2 and water. The organic extracts were dried over MgSO_4 , filtered and evaporated under reduced pressure to give the title compound (26) as a pale yellow solid (>98%) which required no further purification; mp > 180 °C; IR $\nu_{\max}/\text{cm}^{-1}$ 3289 (NH); $^1\text{H-NMR}$ (400 MHz, CDCl_3) δ_{H} 7.48 (8H, t, $J = 7.7$, ArH), 7.38 (8H, d, $J = 8.2$, ArH), 7.20–7.25 (8H, m, ArH), 7.14 (3H, s, ArH), 6.99 (3H, m, ArH), 6.92 (6H, d, $J = 7.7$, ArH), 3.94–3.98 (6H, m, AB system, - $\text{CH}_A\text{CH}_B\text{N}$), 3.63–3.74 (6H, m, AB system, $J = 12.8$, $\text{CH}_A\text{CH}_B\text{N}$), 2.18–2.34 (18H, m, CH_2 , -NH), 1.73 (6H, br, s, CHN-), 1.18–1.27 (6H, br, m, CH_2), 1.03–1.08 (6H, br, m, CH_2); $^{13}\text{C-NMR}$ (100 MHz, CDCl_3) δ_{C} 157.70, 155.18, 141.34, 140.42, 138.79, (130.97, 130.64), 129.87, 128.63, 126.98, 122.91, 122.44, (118.02, 117.78), (61.02, 60.97), 50.50, (31.52, 31.37), (25.22, 25.10); MS (ESI-MS, micrOTOF) m/z (Calcd. 1152.6605; exp. 1153.6665, $M + H^+$, 100%).

(2R,3R,16R,17R,30R,31R)-(1,4,15,18,29,32)-Hexaza-(2,3:16,17:30,31)-tributano-(7,21,40)-triphenoxy-(6,9:10,13:20,23:24,27:34,37:38,41)-hexa-etheno-(1H,2H,3H,4H,5H,14H,15H,16H,17H,18H,19H,28H,29H,30H,31H,32H,33H,42H)-octadecahydro-[42]-annulene (27)

To a stirred solution of triaglimine (21) (125 mg, 0.11 mmol) in THF–MeOH (1:1, 10 mL) solid NaBH_4 (36.5 mg, 0.96 mmol) was gradually added and the solution was stirred for 5 h at room temperature. After removal of solvents the residue was extracted with CH_2Cl_2 and water. The organic extracts were dried over

MgSO₄, filtered and evaporated under reduced pressure to give the title compound (**27**) as a pale yellow solid (>98%) which required no further purification; mp > 110 °C; IR $\nu_{\text{max}}/\text{cm}^{-1}$ 3286 (NH); ¹H-NMR (400 MHz, CDCl₃) δ_{H} 7.53 (2H, dd, $J = 7.7$, ArH), 7.46–7.49 (6H, m, ArH), 7.29–7.38 (12H, m, ArH), 7.20–7.25 (8H, m, ArH), 7.12–7.15 (3H, m, ArH), 6.97–7.02 (4H, m, ArH), 6.91–6.92 (6H, d, $J = 7.3$, ArH), 3.94–4.00 (6H, m, AB system, -CH_ACH_BN), 3.63–3.72 (6H, m, AB system, $J = 13.2$, -CH_ACH_BN), 2.08–2.31 (18H, m, CH₂, NH), 1.96–1.74 (6H, br, s, CHN), 1.26 (6H, br, m, CH₂), 1.05–1.07 (6H, br, m, CH₂); ¹³C-NMR (100 MHz, CDCl₃) δ_{C} (157.57, 157.54), (155.23, 155.20, 155.16), (141.49, 141.45, 141.39), (140.25), (138.81), (135.87), (130.96), (130.69), (129.87), (128.66, 128.49), (127.00, 127.03), (125.62), (122.96), (122.53, 122.47), (118.04, 118.02, 117.98), (117.72, 117.69, 117.61), (60.99, 60.92, 60.86, 60.81), (50.45), (31.43, 31.14, 31.02), (25.14, 25.02); MS (ESI-MS, micrOTOF) m/z (Calcd. 1152.6605; exp. 1153.6658, M+H⁺, 100%).

(2R,3R,16R,17R,30R,31R)-(1,4,15,18,29,32)-Hexaza-(2,3:16,17:30,31)-tributano-(7,21,40)-tri-*N*-piprazinocarboxylate-(6,9:10,13:20,23:24,27:34,37:38,41)-hexa-etheno-(1H,2H,3H,4H,5H,14H,15H,16H,17H,18H,19H,28H,29H,30H,31H,32H,33H,42H)-octadecahydro-[42]-annulene (28)

To a stirred solution of trianglimine (**19**) (111 mg, 0.083 mmol) in THF–MeOH (1:1, 10 mL) solid NaBH₄ (32 mg, 0.83 mmol) was gradually added and the solution was stirred for 5 h at room temperature. After removal of solvents the residue was extracted with CH₂Cl₂ and water. The organic extracts were dried over MgSO₄, filtered and evaporated under reduced pressure to give the title compound (**28**) as a pale yellow solid (>98%) which required no further purification; mp > 110 °C; IR $\nu_{\text{max}}/\text{cm}^{-1}$ 3293 (NH), 1686 (N(C=O)O); ¹H-NMR (400 MHz, CDCl₃) δ_{H} 7.50–7.56 (6H, m, ArH), 7.45 (2H, d, $J = 7.79$, ArH), 7.41 (3H, d, $J = 7.79$, ArH), 7.29–7.38 (7H, m, ArH), 7.27 (1H, s, ArH), 7.25 (3H, s, ArH), 3.96–4.71 (12H, m, AB system, $J = 13.28$, -CH_ACH_BN), 3.49–3.69 (18H, m, CH₂N, HCN), 2.90–2.95 (12H, br, m, CH₂N), 2.24–2.33 (12H, br, m, CH₂), 2.02 (6H, br, s, CH₂NH), 1.78 (6H, br, s, CH₂), 1.17–1.25 (15H, m, CH₃CH₂, CH₃CH₂); ¹³C-NMR (100 MHz, CDCl₃) δ_{C} (155.68, 155.65), (151.76, 151.72), (140.72), (140.19, 140.15, 140.07), (139.55, 139.53, 139.50), (134.79, 134.74), (130.61, 130.58, 130.48), (128.55), (127.09, 127.05, 127.02), (123.02), (121.39), (122.93), (118.84), (61.60, 61.53, 61.42), (61.14, 61.01, 60.94), (52.76), (50.66, 50.61, 50.58), (44.30), (31.53), (25.18), (14.77); MS (ESI-MS, micrOTOF) m/z (Calcd. 1344.8515; exp. 1345.8617, (ESI-MS, micrOTOF) m/z (Calcd. 1344.8515; exp. 1345.8617, M+H⁺, 100%).

(2R,3R,16R,17R,30R,31R)-(1,4,15,18,29,32)-Hexaza-(2,3:16,17:30,31)-tributano-(7,21,40)-tri-(2,2-dimethoxy-*N*-methylethanamino)-(6,9:10,13:20,23:24,27:34,37:38,41)-hexa-etheno-(1H,2H,3H,4H,5H,14H,15H,16H,17H,18H,19H,28H,29H,30H,31H,32H,33H,42H)-octadecahydro-[42]-annulene (29)

To a stirred solution of trianglimine (**20**) (207 mg, 0.17 mmol) in THF–MeOH (1:1, 10 mL) solid NaBH₄ (65 mg, 1.7 mmol) was gradually added and the solution was stirred for 5 h at room

temperature. After removal of solvents the residue was extracted with CH₂Cl₂ and water, the organic extracts were dried over MgSO₄, filtered and evaporated under reduced pressure to give the title compound (**29**) as a yellow oil (>98%) which required no further purification, ¹H-NMR (400 MHz, C₆D₆) δ_{H} 7.49–7.54 (8H, m, ArH), 7.37–7.40 (9H, m, ArH), 7.23–7.28 (1H, m, ArH), 7.09 (2H, s, ArH), 4.45–4.47 (3H, m, CH₂CH), 4.11–4.19 (3H, m, AB system, $J = 12.82$, -CH_ACH_BN), 3.76–3.87 (6H, m, HCN), 3.53–3.58 (3H, m, AB system, -CH_ACH_BN), 3.13–3.21 (6H, m, CH₂CH), 3.03 (18H, s, OCH₃), 2.64 (9H, s, NCH₃), 2.01–2.37 (18H, m, CH₂, NH), 1.56–1.62 (6H, m, CH₂), 1.24 (6H, br, s, CH₂); ¹³C-NMR (100 MHz, C₆D₆) δ_{C} (152.47), (140.59, 140.56, 140.50, 140.41), (140.08, 140.04, 140.00), (135.47), (130.57, 130.49), (128.65, 128.52), (127.15, 127.06), (125.55), (122.65, 122.53), (119.99, 119.92), (102.71), (77.65), (61.74), (60.97, 60.90), (58.04), (52.45), (43.53), (31.52, 31.36), (25.35, 25.17); MS (ESI-MS, micrOTOF) m/z (Calcd. 1227.8188; exp. 1228.8261, M⁺+H⁺, 100%).

Acknowledgements

Hany Nour deeply thanks the German Academic Exchange Service (DAAD) for giving him the opportunity to carry out his PhD project in Germany by granting him a full PhD scholarship in 2008. He also thanks Jacobs University Bremen for hosting the project. We thank Mrs Anja Müller for carrying out the MS measurements.

Notes and references

- 1 J. Gawroński, H. Kolbon, M. Kwit and A. Katrusiak, *J. Org. Chem.*, 2000, **65**, 5768.
- 2 N. Kuhnert, A. Lopez-Periago and G. Rossignolo, *Org. Biomol. Chem.*, 2005, **3**, 524.
- 3 N. Kuhnert, A. Lopez-Periago and G. Rossignolo, *Org. Biomol. Chem.*, 2003, **1**, 1157.
- 4 N. Kuhnert and A. Lopez-Periago, *Tetrahedron Lett.*, 2002, **43**, 3329.
- 5 C. Gutsche, *Calixarenes in Monographs in Supramolecular Chemistry*, ed. J. Stoddart, Royal Society of Chemistry, Cambridge, 1989.
- 6 Gutsche, *Calixarenes Revisited in Monographs in Supramolecular Chemistry*, ed. J. Stoddart, Royal Society of Chemistry, Cambridge, 1998.
- 7 V. Böhmer, *Angew. Chem., Int. Ed. Engl.*, 1995, **34**, 713.
- 8 A. Danil de Namor, R. Cleverley and M. Zapata-Ormachea, *Chem. Rev.*, 1998, **98**, 2495.
- 9 For cyclodextrins see special edition of Chemical Review, edition 5, 1998.
- 10 J. Kim, I. Jung, S. Kim, E. Lee, K. Kang, S. Sakamoto, K. Yamaguchi and K. Kim, *J. Am. Chem. Soc.*, 2000, **122**, 540.
- 11 S. Kim, I. Jung, E. Lee, J. Kim, S. Sakamoto, K. Yamaguchi and K. Kim, *Angew. Chem., Int. Ed.*, 2001, **40**, 2119.
- 12 C. Pederson, *J. Am. Chem. Soc.*, 1967, **89**, 7017.
- 13 N. Kuhnert, N. Burzlaff, C. Patel and A. Lopez-Periago, *Org. Biomol. Chem.*, 2005, **3**, 1911.
- 14 N. Kuhnert, A. Lopez-Periago and G. Rossignolo, *Org. Biomol. Chem.*, 2005, **3**, 524.
- 15 J. Gajewy, M. Kwit and J. Gawroński, *Adv. Synth. Catal.*, 2009, **351**, 1.
- 16 K. Tanaka and S. Hachiken, *Tetrahedron Lett.*, 2008, **49**, 2533.
- 17 M. Chadim, M. Budesinsky, J. Hodacova, J. Zavada and P. Junk, *Tetrahedron: Asymmetry*, 2001, **12**, 127.
- 18 N. Kuhnert, D. Marsh and D. Nicolau, *Tetrahedron: Asymmetry*, 2007, **18**, 1648.

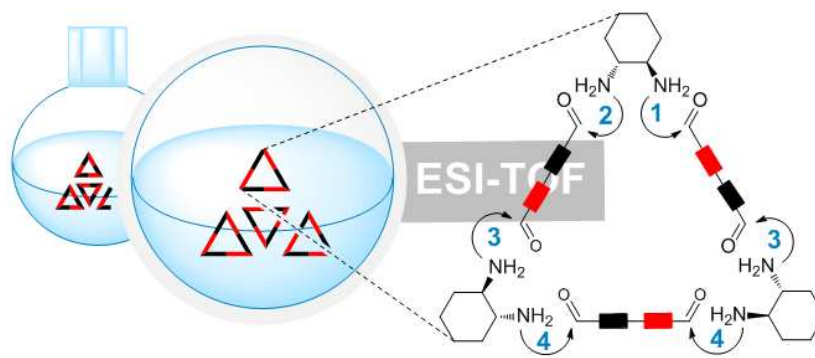
- 19 N. Miyaura and A. Suzuki, *Chem. Rev.*, 1995, **95**, 2457.
- 20 S. Nielsen, M. Larsen, T. Boesen, K. Schønning and H. Kromann, *J. Med. Chem.*, 2005, **48**, 2667.
- 21 Y. Yamaguchi, T. Yanase, S. Muto and A. Itai, *US Pat. Appl. Publ.*, 20090312315, 2009.
- 22 Y. Yamaguchi, T. Yanase, S. Muto and A. Itai, *US Pat. Appl. Publ.*, 2009125606, 2009.
- 23 K. Hattori, Y. Tomishita and M. Imanishi, *PCT Int. Appl.*, 2004002939, 2004.
- 24 H. Smith, J. Neegaard, E. Burrows and F. Chen, *J. Am. Chem. Soc.*, 1974, **96**, 2908.
- 25 M. Smith and J. March, in *Advanced Organic Chemistry: Reactions, Mechanisms and Structures*, John Wiley & Sons, Ltd., Chichester, UK, 5th edn, 2001, pp. 1177.
- 26 Molecular modeling was carried out using Hyperchem software (Release 8.0). Hypercube, Inc., 1115 NW 4th Street, Gainesville, FL 32601 USA. Trial, version from <http://www.hypercube.com>.
- 27 J. Stewart, *J. Comput. Chem.*, 1989, **10**(209), 221.
- 28 J. Cannadine, J. Corden, W. Errington, P. Moore and M. Wallbridge, *Acta Crystallogr., Sect. C: Cryst. Struct. Commun.*, 1996, **C52**, 1014.
- 29 G. Sheldrick, *Acta Crystallogr., Sect. A: Found. Crystallogr.*, 2008, **A64**, 112.

Probing the mechanism and dynamic reversibility of trianglimine formation using real-time electrospray ionization time-of-flight mass spectrometry

Hany F. Nour, Ana M. López-Periago and Nikolai Kuhnert*

Reproduced by permission of John Wiley and Sons

Copyright Clearance Center (CCC), License number, 2951290933234



Objectives of the work

The objective of this work is to study the mechanism of trianglimine formation in real-time using ESI-TOF/MS. Trianglimines were reported a decade ago and the mechanism of their formation was believed to proceed through a stepwise pathway; however, no intermediates were ever isolated or detected and characterized. The [3+3]-cyclocondensation reaction was monitored in real-time by ESI-TOF/MS. All reaction intermediates participating in the cyclocondensation reaction were observed and their structures were unambiguously assigned based on their high resolution m/z values. The dynamic reversibility of trianglimines was investigated by conducting two crossover experiments. In the first experiment two different trianglimines were mixed in DCM and stirred at room temperature. In the second experiment the dialdehyde building blocks forming the macrocycles were mixed in DCM along with *trans*-(1*R*,2*R*)-1,2-diaminocyclohexane and the reaction was stirred at room temperature. At equilibration and after 46 h, statistical mixtures, with almost similar composition, of mixed macrocycles and open chain intermediates were obtained from the two reaction pathways.

Rapid Commun. Mass Spectrom. 2012, 26, 1070–1080
(wileyonlinelibrary.com) DOI: 10.1002/rcm.6203

Probing the mechanism and dynamic reversibility of trianglimine formation using real-time electrospray ionization time-of-flight mass spectrometry

Hany F. Nour¹, Ana M. Lopez-Periago² and Nikolai Kuhnert^{1,2*}

¹School of Engineering and Science, Organic and Analytical Chemistry Laboratory, Jacobs University, 28759 Bremen, Germany

²Synthetic and Biological Organic Chemistry Laboratory, School of Biomolecular and Medical Science, The University of Surrey, Guildford GU2 7XH, UK

RATIONALE: The [3+3]-cyclocondensation reactions of chiral (1*R*,2*R*)-1,2-diaminocyclohexane with aromatic or aliphatic *bis*-aldehydes to form trianglimine macrocycles were reported a decade ago and were believed to proceed through a stepwise mechanistic pathway; however, no intermediates were ever isolated or detected and characterized.

METHODS: We investigated the mechanism of the [3+3]-cyclocondensation reaction using a selection of dialdehyde starting materials using real-time electrospray ionization time-of-flight mass spectrometry.

RESULTS: We observed up to a maximum of 16 reaction intermediates along the reaction pathway, more than for any other multistep reaction reported. We also probed the dynamic reversibility of trianglimines using selected small dynamic combinatorial libraries and showed that trianglimine formation is indeed fully reversible.

CONCLUSIONS: This study represents a significant contribution towards understanding the mechanism of trianglimine formation and its potential applicability can be extended to include other cascade reactions. Copyright © 2012 John Wiley & Sons, Ltd.

The synthesis of imine macrocycles relies in numerous cases on $[n+n]$ -cyclocondensation reactions of diamines and dialdehydes.^[1–4] In most cases, it involves preorganization of the building blocks with the aid of a template or non-covalent interactions to a predictable geometry.^[5–8] [3+3]-Cyclocondensation reactions have only been discovered in the last decade and promise a new approach for the synthesis of architecturally unique and exciting macrocyclic structures with potential applications.

Gawroński *et al.* have introduced an efficient synthetic strategy for the synthesis of large poly-imine *meta*- and *para*-cyclophane type macrocycles which were named trianglimines by our group due to their unique triangular structure.^[9,10]

Trianglimines form in quantitative yields without using a template and the reaction takes place under the influence of conformational bias imposed on the reactive intermediates.^[9] Hexamine macrocycles are referred to as trianglaminines and they constitute reduced version of trianglimines.^[9,10] Trianglaminines are readily synthesized in quantitative yields by reducing trianglimines with

sodium borohydride.^[9,10] We have shown that trianglimines can be obtained from almost any synthetically accessible aromatic dialdehyde with complete control of the size of the macrocycle and functionalities incorporated into the aromatic moiety.^[10–14] More importantly, we have demonstrated that trianglimines can be incorporated into more sophisticated structures such as catenanes and shown their promise in chiral recognition.^[15,16] Trianglimines are characterized by their structural diversity, ease of synthesis in quantitative yields and most importantly by their chirality, where both enantiomers of any derivative are readily available in a pure form.^[9–17] Recently, we reported a novel functionalization approach for the synthesis of regioisomeric C₃-symmetrical and non-symmetrical trianglimines.^[18] We showed also that ESI-TOF (electrospray ionization time-of-flight) mass spectrometry (MS) could be used as a sophisticated technique for monitoring the progress of the [3+3]-cyclocondensation reactions.^[18] ESI-MS has been used recently as a sophisticated tool for studying complex reaction mechanisms in real time in solution.^[19–22] Examples of such mechanistic work include the investigation of enzymatic reactions such as proteases, glycosidases or nucleases or cascade reactions in organocatalysis.^[23–27] In this contribution, we describe our efforts to utilize ESI-TOF MS to detect and to characterize the reactive intermediates participating in the formation of trianglimine macrocycles. We also studied dynamic reversibility of trianglimines in solution by ESI-TOF MS.

* Correspondence to: N. Kuhnert, School of Engineering and Science, Jacobs University, P.O. Box 750 561, 28725 Bremen, Germany.
E-mail: n.kuhnert@jacobs-university.de

EXPERIMENTAL

All the solvents and reagents used for the reactions were purchased from Sigma-Aldrich (Munich, Germany) or Applichem (Darmstadt, Germany) and were used as obtained. Solvents and reagents were used without further purification. Whenever possible the reactions were monitored by thin layer chromatography on aluminum-backed plates pre-coated with silica gel 60 (UV₂₅₄) (Macherey-Nagel, Düren, Germany). Column chromatography was carried out on dried silica gel 60 (0.040–0.063 mm) and triethylamine was used along with the eluting solvent under flash conditions.^[18] Compounds **1**, **4**, **5**, **19** and **31–33** (Figs. 1 and 6, and Scheme 4) were synthesized according to standard published procedures.^[9,18,28] Positive ion mode mass spectra of the samples dissolved either in MeOH (methanol) or in DCM (dichloromethane) were recorded on a ESI-TOF mass spectrometer (Bruker Daltonics, Bremen, Germany). Calibration was carried out using a 0.1 M solution of sodium formate in the enhanced quadratic mode prior to each experimental run. The results of the measurements were processed using Compass 1.3 data analysis software for a Bruker Daltonics micrOTOF TOF mass spectrometer. Nuclear magnetic resonance (NMR) spectra were recorded using a Bruker Avance 500 MHz spectrometer (Bruker BioSpin, Rheinstetten, Germany) and tetramethylsilane (TMS) was used as the internal reference standard. Molecular modeling calculations were carried out with HyperChem software (Release 8.0, trial version)^[29] using the semi-empirical optimization method PM3 (Parameterized Model number 3) along with the molecular mechanics force field MM+ method. A Polak-Ribiere algorithm was employed until the root-mean square (RMS) gradient was 0.01 kcal.mol⁻¹ or less. All calculations were carried out *in vacuo* and no influence of solvents was taken into account.^[29,30]

Monitoring the [3+3]-cyclocondensation reaction of terephthalaldehyde **2** with (1*R*,2*R*)-1,2-diaminocyclohexane **1**

Terephthalaldehyde **2** (1.85 g, 13.8 mmol) in DCM (11.5 mL) was added to a stirred solution of (1*R*,2*R*)-1,2-diaminocyclohexane **1** (1.58 g, 13.8 mmol) in DCM (7 mL). The mixture was

stirred at room temperature for 6 h. Aliquots (0.1 mL) were taken at defined time intervals, diluted with DCM (10 mL) and few drops of MeOH were added to the sample before it was infused into the ESI-TOF mass spectrometer.

Monitoring the [3+3]-cyclocondensation reaction of isophthalaldehyde **3** with (1*R*,2*R*)-1,2-diaminocyclohexane **1**

Isophthalaldehyde **3** (1.85 g, 13.8 mmol) in DCM (11.5 mL) was added to a stirred solution of (1*R*,2*R*)-1,2-diaminocyclohexane **1** (1.58 g, 13.8 mmol) in DCM (7 mL). The mixture was stirred at room temperature for 12 h. Aliquots (0.1 mL) were taken at defined time intervals, diluted with DCM (10 mL) and few drops of MeOH were added to the sample before it was infused into the ESI-TOF mass spectrometer.

Monitoring the [3+3]-cyclocondensation reaction of 3-phenoxybiphenyl-4,4'-dicarbaldehyde **19** with (1*R*,2*R*)-1,2-diaminocyclohexane **1**

3-Phenoxybiphenyl-4,4'-dicarbaldehyde **19** (600 mg, 1.98 mmol) in DCM (10 mL) was added to a stirred solution of (1*R*,2*R*)-1,2-diaminocyclohexane **1** (340 mg, 2.98 mmol) in DCM (10 mL). The mixture was stirred at room temperature for 8 h. Aliquots (0.1 mL) were taken at defined time intervals, diluted with DCM (10 mL) and a few drops of MeOH were added to the sample before it was infused into the ESI-TOF mass spectrometer.

Dynamic reversibility of trianglimines **31** and **32**

(a) Mixing equimolar quantities of trianglimines **31** and **32** in DCM

To a stirred solution of trianglimine **31** (20 mg, 17.5 μmol) in DCM (44 μL) was added trianglimine **32** (23.4 mg, 17.5 μmol) in DCM (44 μL). The mixture was stirred at room temperature for 46 h. Aliquots were taken at defined time intervals, diluted with DCM and a few drops of MeOH were added to the sample before it was infused into the ESI-TOF mass spectrometer.

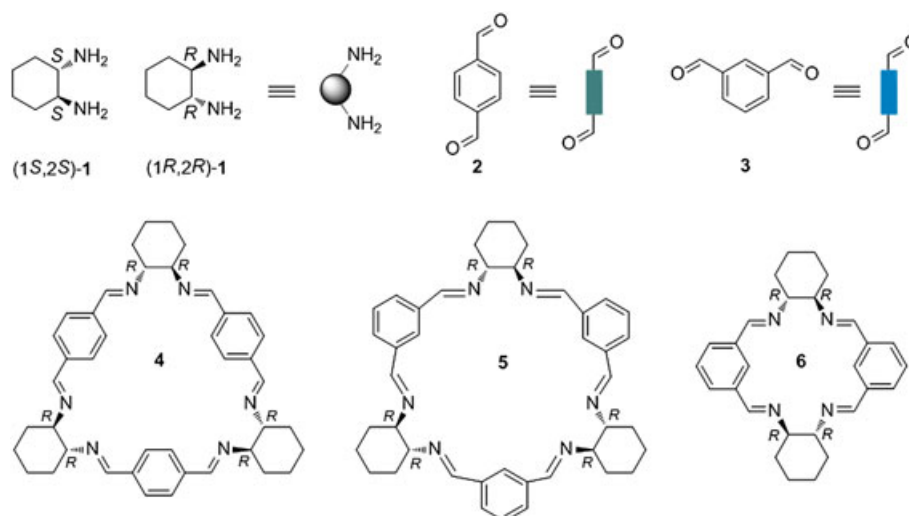


Figure 1. Products of the cyclocondensation reactions of (1*R*,2*R*)-1,2-diaminocyclohexane **1** with terephthalaldehyde **2** and isophthalaldehyde **3**.

(b) *Mixing equimolar quantities of dialdehydes 19 and 33 with (1R,2R)-1,2-diaminocyclohexane 1 in DCM*

To a stirred solution of (1R,2R)-1,2-diaminocyclohexane **1** (15.62 mg, 0.137 mmol) in DCM (182 μ L) were added 3-phenoxybiphenyl-4,4'-dicarbaldehyde **19** (18.12 mg, 0.06 mmol) in DCM (182 μ L) and ethyl 4-[4,4'-diformyl-(1,1'-biphenyl)-3-yl]-piperazine-1-carboxylate **33** (23.3 mg, 0.06 mmol) in DCM (182 μ L). The mixture was stirred at room temperature for 46 h. Aliquots were taken at defined time intervals and a few drops of MeOH were added to the sample before it was infused into the ESI-TOF mass spectrometer.

RESULTS AND DISCUSSION

The formation of trianglimines constitutes a complex multi-step reaction, in which six imine bonds are formed in a single one-pot reaction at relatively high concentrations of all reactants. Gawroński *et al.* reported that the reactions of (1R,2R)-1,2-diaminocyclohexane **1** with terephthaldehyde **2** and isophthaldehyde **3** resulted in clean formation of the corresponding trianglimines **4** and **5** after 2–3 h of stirring at room temperature (Fig. 1).^[9] We decided to study the mechanism of this reaction in detail taking advantage of the capability of ESI-MS in the positive ion mode to potentially detect all possible reaction intermediates. The reactions were conducted between **1** and **2** or **3** at a concentration of 0.1 M in DCM at room temperature. For MS

analysis, aliquots of the reaction mixture were taken at different time intervals, diluted to a concentration of 0.1 mM and directly infused into the ESI-TOF mass spectrometer.

Cyclocondensation mechanism of *trans*-(1R,2R)-1,2-diaminocyclohexane with terephthaldehyde and isophthaldehyde

By monitoring the reaction between (1R,2R)-1,2-diaminocyclohexane **1** and dialdehyde **2** and **3** in real time with ESI-TOF MS, a total of eleven different reaction intermediates could be detected by the appearance of their protonated pseudomolecular ions and their structures were assigned based on their high-resolution m/z values (Figs. 2 and 3). The reaction intermediates include a series of *mono*- to *penta*-imines **7–17** along with some long-chain higher polyimine oligomers (not shown in figures; for structures and ESI-TOF data, see Supplementary Information). In the course of the reaction the higher oligomers disappear at the expense of the final macrocyclization products. Interestingly, the relative intensity of the ions corresponding to the intermediates of the reaction with isophthaldehyde and terephthaldehyde are very different, suggesting that the mechanism of formation of the two geometrically distinct macrocycles is different. For terephthaldehyde **2** the intermediates with the two most intense signals correspond to *mono*-imine **7** and *bis*-imine **8** bearing two terminal amino moieties. In contrast, for isophthaldehyde **3** the *bis*-imine **14** with two

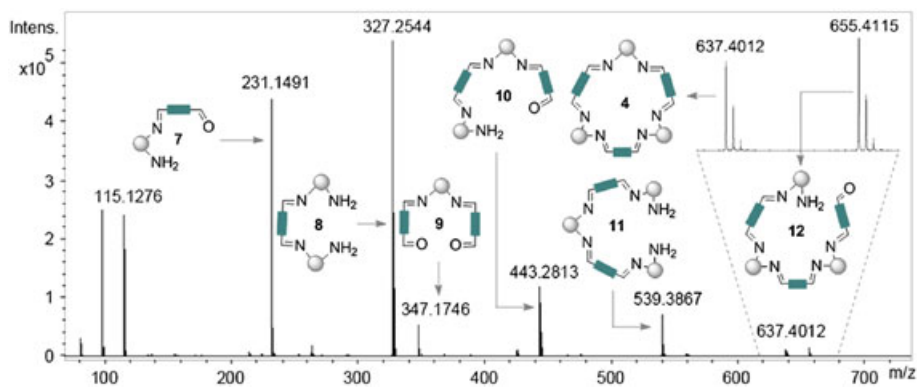


Figure 2. ESI-TOF mass spectrum in the positive ion mode recorded after 10 min from the start of the reaction of (1R,2R)-1,2-diaminocyclohexane **1** with terephthaldehyde **2**; the products were detected as $[M+H]^+$ ions.

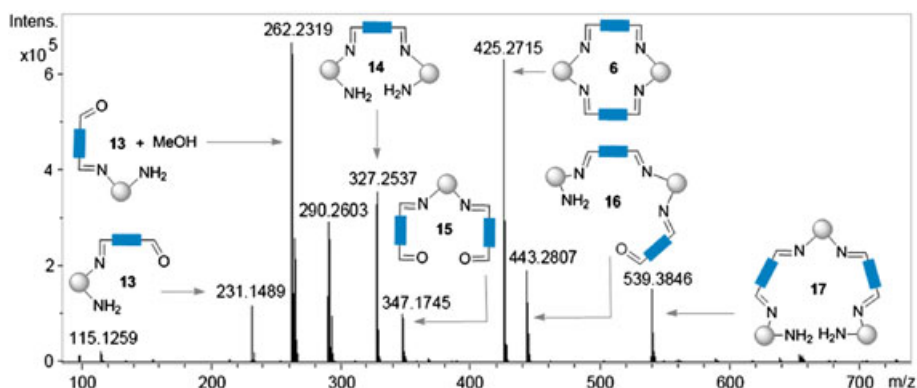
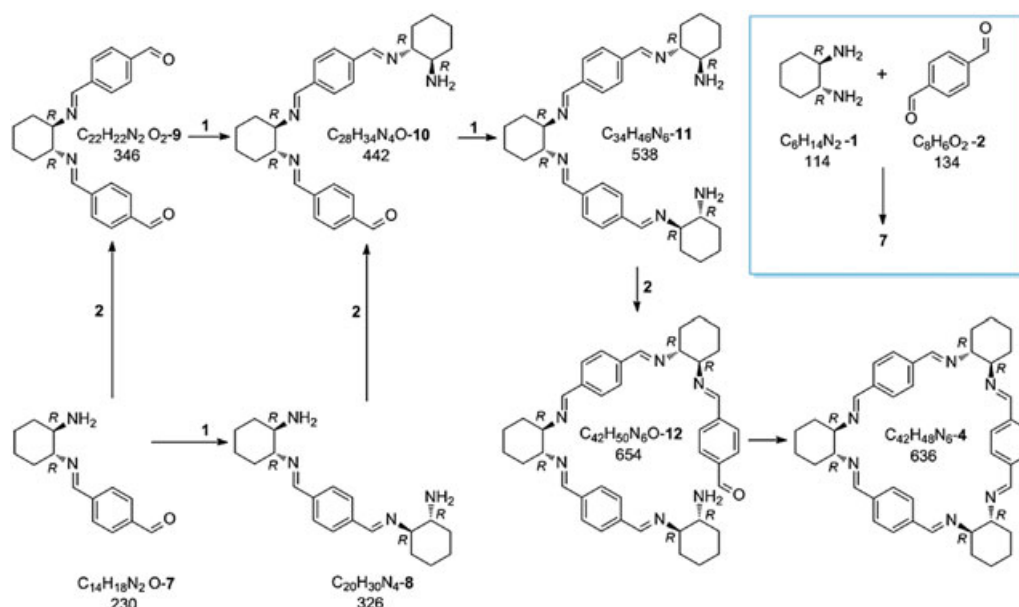


Figure 3. ESI-TOF mass spectrum in the positive ion mode recorded after 10 min from the start of the reaction of (1R,2R)-1,2-diaminocyclohexane **1** with isophthaldehyde **3**; the products were detected as $[M+H]^+$ ions.

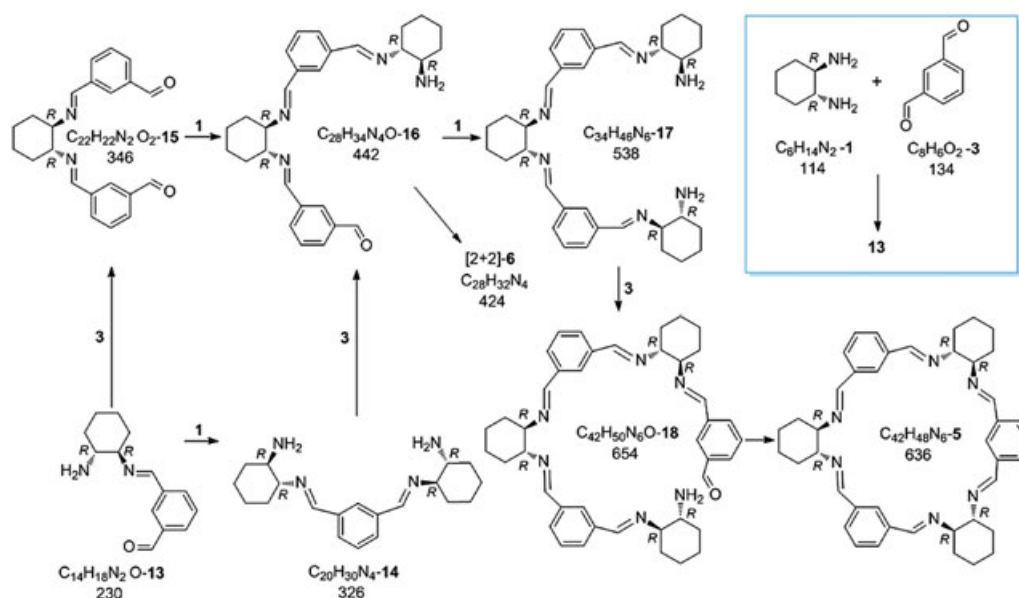
terminal amine moieties forms the major intermediate. Unusual *tri*-imine intermediates **10** and **16** bearing terminal amino and carbonyl moieties were observed as relatively stable and long-lived reaction intermediates in both cyclocondensation reactions. Furthermore, the [3+3]-cyclocondensation reaction of (1*R*,2*R*)-1,2-diaminocyclohexane **1** with terephthalaldehyde **2** proceeds *via* intermediates **7** to **12**, while with isophthalaldehyde **3** it proceeds *via* intermediates **13** to **18**. Most importantly, the analysis of trianglimines by ESI-MS shows considerable promise due to the ability of this technique to provide precise mass values, high-resolution and little or almost no fragmentations. ESI-MS can also be used as a useful reaction monitoring system, identifying the maximum yield and end-point of the reaction (see Supporting Information).

The reaction intermediates observed are shown in Schemes 1 and 2 and the observed masses and their assignments are shown in Tables 1 and 2. From the ESI-TOF MS data we can infer that the cyclocondensation reaction of (1*R*,2*R*)-1,2-diaminocyclohexane **1** with terephthalaldehyde **2** requires 6 h for completion, while with isophthalaldehyde **3** a mixture of [2+2]- and [3+3]-cyclocondensation products along with some minor impurities was observed after 12 h.

It is worth noting that the intensity of the peaks corresponding to the assigned intermediates can be plotted versus reaction time to provide a visual representation of the progress of the reaction (Figs. 4(a)–4(c)). It can be inferred that the relative intensity of the $[M+H]^+$ ion for trianglimine **4** increased with time and reached a maximum value after 2 h of the reaction



Scheme 1. Exact mechanism for the [3+3]-cyclocondensation reaction of terephthalaldehyde **2** to yield trianglimine **4** based on real-time ESI-TOF MS measurements.



Scheme 2. Exact mechanism for the [3+3]-cyclocondensation reaction of isophthalaldehyde **3** to yield trianglimine **5** based on ESI-TOF MS measurements.

Table 1. ESI-TOF MS data in the positive ion mode for the intermediates using terephthalaldehyde **2**, forming trianglimine **4**

Entry	Calcd. m/z	Measured m/z	Molecular formula	Error [ppm]
4	637.4013	637.4012	C ₄₂ H ₄₈ N ₆	0.2
7	231.1492	231.1491	C ₁₄ H ₁₈ N ₂ O	0.2
8	327.2543	327.2544	C ₂₀ H ₃₀ N ₄	−0.3
9	347.1754	347.1746	C ₂₂ H ₂₂ N ₂ O ₂	2.3
10	443.2805	443.2813	C ₂₈ H ₃₄ N ₄ O	−1.7
11	539.3857	539.3867	C ₃₄ H ₄₆ N ₆	−1.8
12	655.4119	655.4115	C ₄₂ H ₅₀ N ₆ O	0.6

Table 2. ESI-TOF mass spectrometry data in the positive ion mode for the intermediates using isophthalaldehyde **3**, forming trianglimine **5**

Entry	Calcd. m/z	Measured m/z	Molecular formula	Error [ppm]
6	425.2700	425.2715	C ₂₈ H ₃₂ N ₄	−3.7
13	231.1492	231.1489	C ₁₄ H ₁₈ N ₂ O	1.3
14	327.2543	327.2537	C ₂₀ H ₃₀ N ₄	2
15	347.1745	347.1745	C ₂₂ H ₂₂ N ₂ O ₂	2.7
16	443.2805	443.2807	C ₂₈ H ₃₄ N ₄ O	−0.4
17	539.3857	539.3846	C ₃₄ H ₄₆ N ₆	2
18*	655.4119	655.4114	C ₄₂ H ₅₀ N ₆ O	0.7

*Intermediate was detected after 30 min from the start of the reaction.

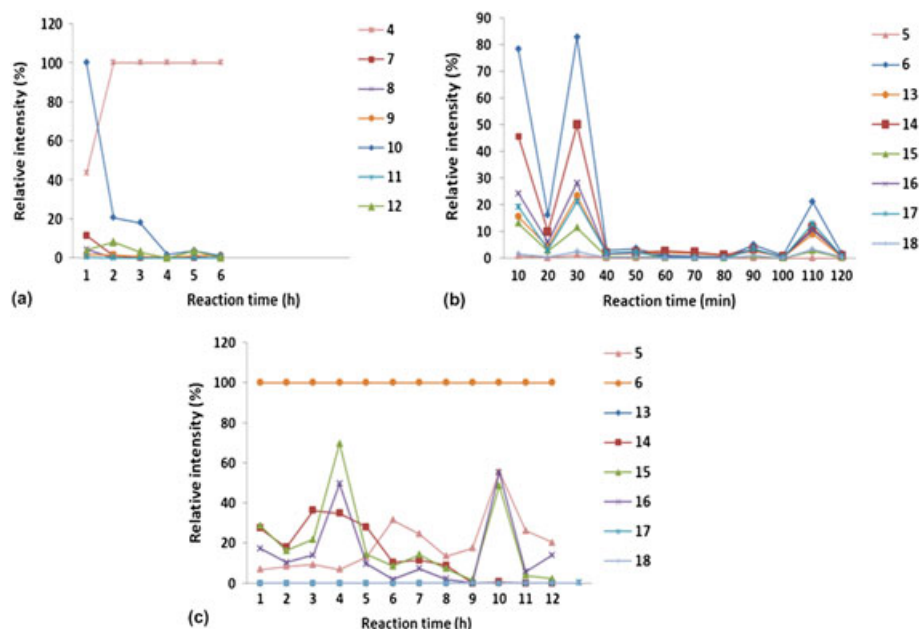


Figure 4. A plot of relative intensity for intermediates 7–18 versus reaction time (a) reaction of (1R,2R)-1,2-diaminocyclohexane **1** with terephthalaldehyde **2** (6 h), (b) reaction of (1R,2R)-1,2-diaminocyclohexane **1** with isophthalaldehyde **3** (2 h), and (c) reaction of (1R,2R)-1,2-diaminocyclohexane **1** with isophthalaldehyde **3** (12 h).

while the intensities for the rest of intermediates decreased. Furthermore, the peaks corresponding to all intermediates disappeared after 6 h.

In the case of isophthalaldehyde, the intensity of the peak corresponding to trianglimine **5** goes through a maximum value after 10 h and later decreases at the expense of the

smaller macrocycle **6**. This is in line with our earlier observations that in this case the [3+3]-macrocycle is the kinetic product of the reaction and the [2+2]-macrocycle appears as the thermodynamically stable product. In this particular case we could only obtain a maximum of 50% yield for the [3+3]-cyclocondensation product and not the reported quantitative

yield.^[9] Reviewing the literature evidence and our previous experience it can be concluded that when the two dialdehyde functionalities deviate from an ideal dihedral angle $O=C\cdots C=O$, the reaction can give two or more products. Obtaining the desired [3+3]-cyclocondensation macrocycle requires careful optimization of the reaction conditions such as concentration and time or alternatively the addition of a template as illustrated by González-Álvarez *et al.*^[31] and Saggiomo and Lünig,^[32] to achieve a maximum yield and high purity of the desired product, which should be the [2+2]- or [3+3]-macrocycle.

Stoichiometry dependence and NMR investigations

In order to gain more insight into the mechanism of the reaction we conducted the [3+3]-cyclocondensation reaction using different stoichiometries of (1*R*,2*R*)-1,2-diaminocyclohexane and terephthalaldehyde **2** or isophthalaldehyde **3**. In the case of terephthalaldehyde **2** we found that the macrocycle **4** was clearly

formed using a 1:1 stoichiometry and an excess of the dialdehyde (1:2 and 1:5). If an excess of the diamine component was used (2:1), the yield of the macrocycle was dramatically reduced and no macrocycle at all was obtained using higher excess (5:1) of the diamine **1**. Using isophthalaldehyde **3** the opposite results were observed. The macrocycle **5** was obtained using an excess of (1*R*,2*R*)-1,2-diaminocyclohexane **1** whereas reduced yields or no macrocycle were obtained using an excess of the dialdehyde component.

In order to gather more insight, to rationalize this unusual behavior and to identify the reaction intermediates we followed the reaction of **2** and **1** at 0.1 M in $CDCl_3$ with a 1:1 stoichiometry of the components by 1H -NMR, 1H - 1H -COSY and 1H - 1H -TOCSY NMR. For both reactions we recorded the 1H -NMR spectrum every 5 min for 2 h and the 2D spectra every 30 min for 2 h.

In case of the terephthalaldehyde **2** the signals of the two starting materials disappeared and after 10 min the first intermediate began to accumulate. After 20 min the signals

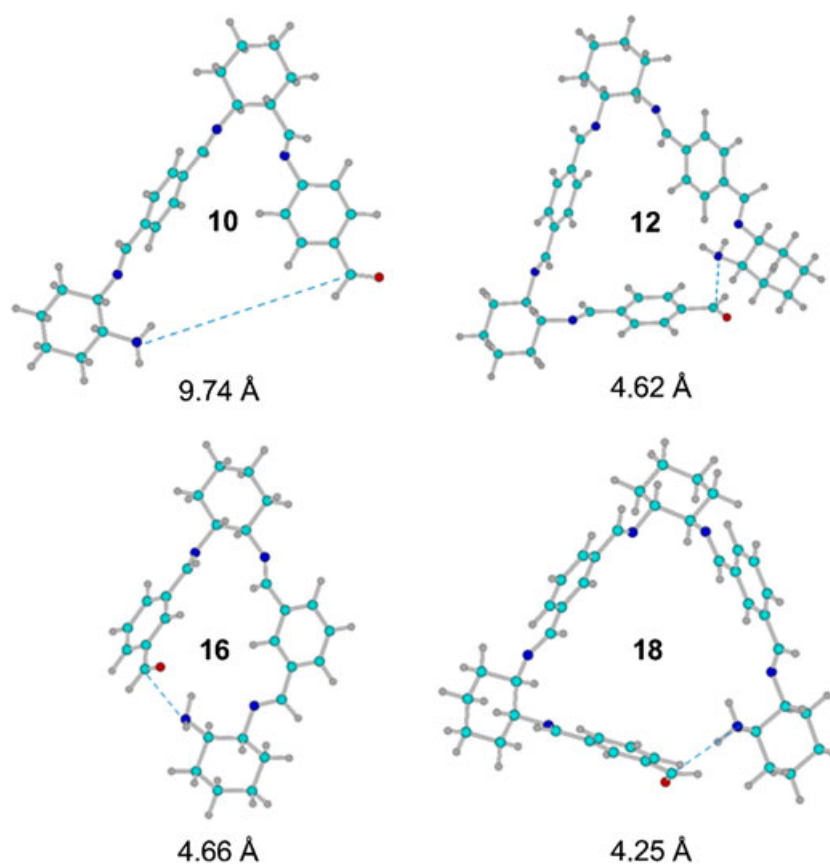


Figure 5. Computed structures for intermediates **10**, **12**, **16** and **18** at the PM3 level using a Polak-Ribiere conjugate gradient with rms <0.01 kcal.mol $^{-1}$.

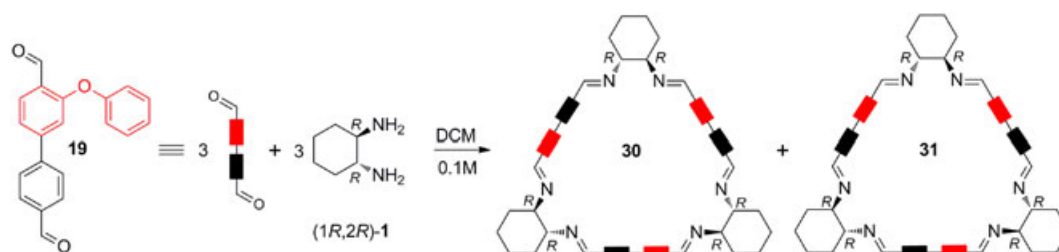
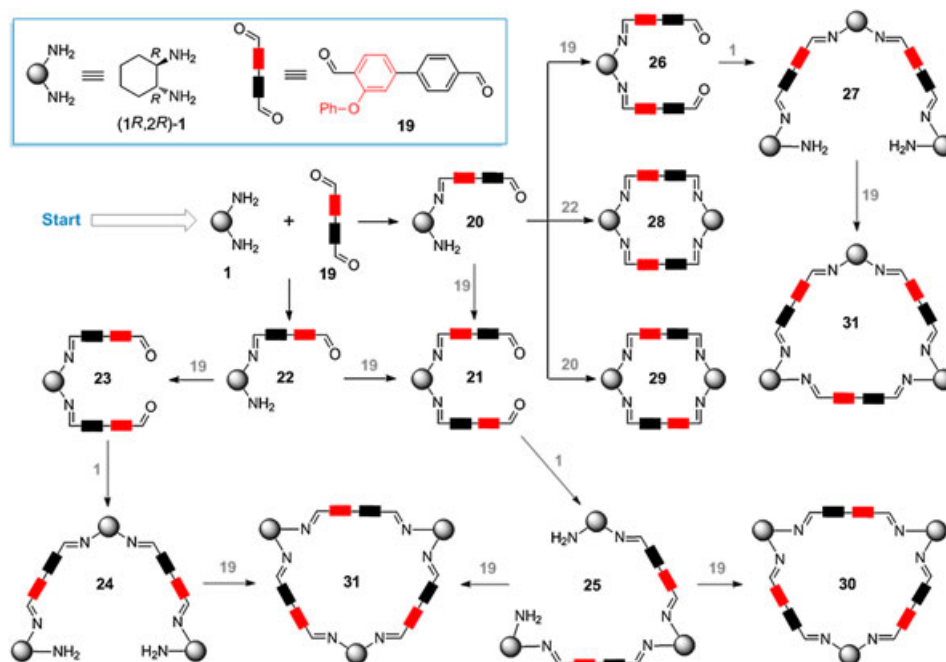


Figure 6. [3+3]-Cyclocondensation reaction of dialdehyde **19** with (1*R*,2*R*)-1,2-diaminocyclohexane **1**.



Scheme 3. Graphical representation illustrating the exact mechanism for the formation of triaglimines **30** and **31** based on ESI-TOF MS measurements.

Table 3. High-resolution ESI-TOF MS data in the positive ion mode for intermediates and compounds **20–29**

Entry	<i>m/z</i>	Measured <i>m/z</i>	Molecular formula	Error [ppm]
20, 22	399.2067	399.2048	C ₂₆ H ₂₆ N ₂ O ₂	4.8
21, 23, 26	683.2904	683.2869	C ₄₆ H ₃₈ N ₂ O ₄	5.2
28, 29	761.3850	761.3814	C ₅₂ H ₄₈ N ₄ O ₂	4.7
24, 25, 27	875.5007	875.4977	C ₅₈ H ₆₂ N ₆ O ₂	3.4
30, 31	1141.5666	1141.5707	C ₇₈ H ₇₂ N ₆ O ₃	3.5

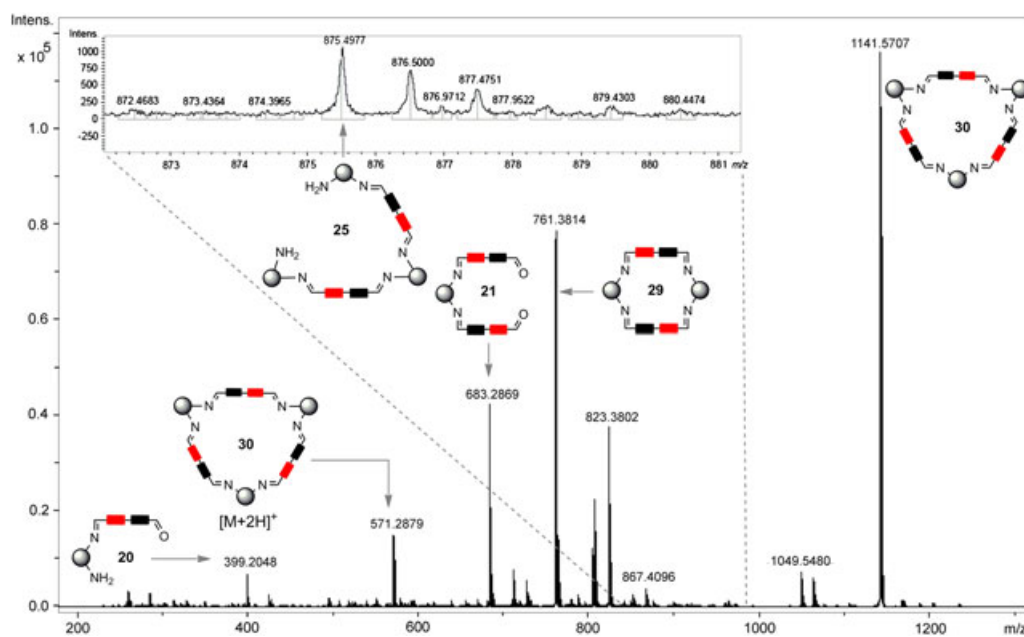


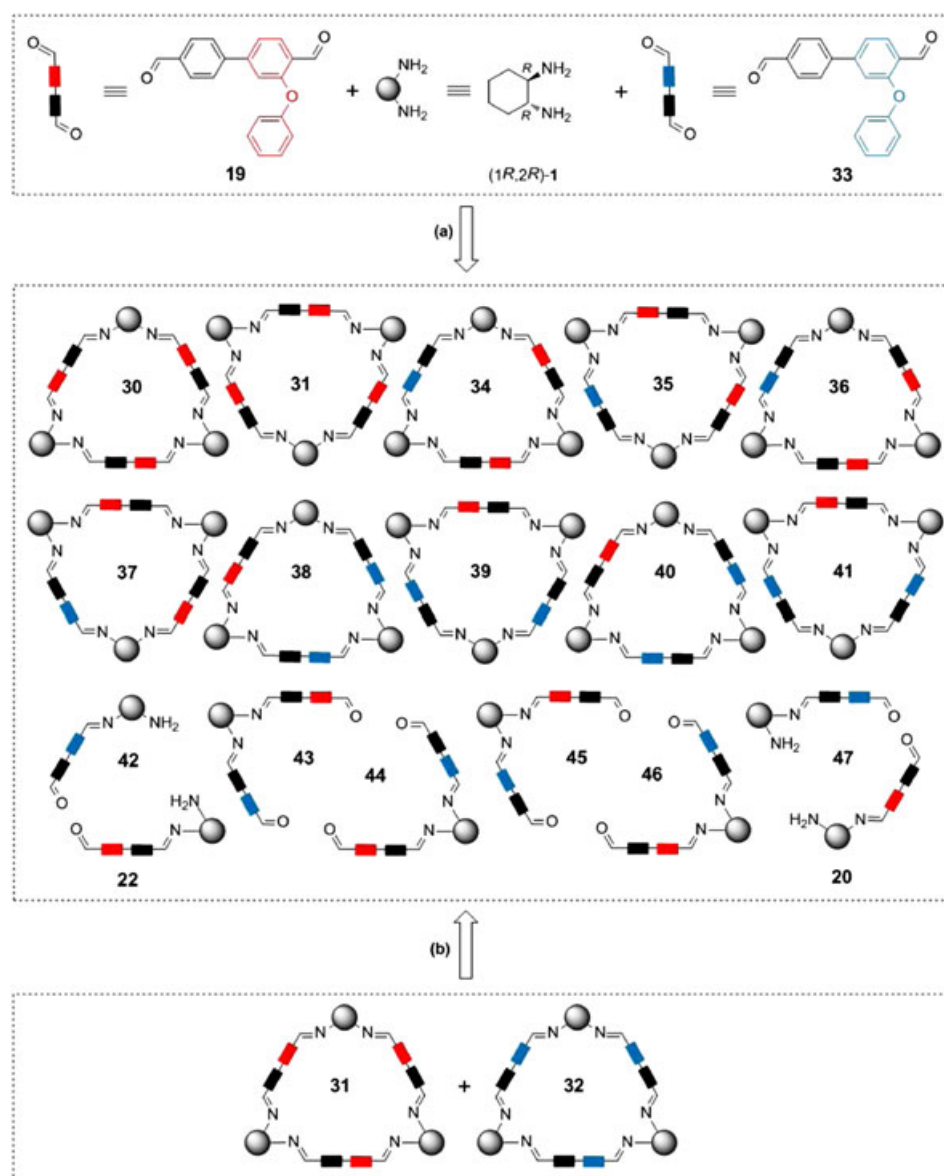
Figure 7. ESI-TOF mass spectrum in the positive ion mode for monitoring the reaction forming triaglimines **30** and **31**, spectrum recorded after 2 h from the start of the reaction.

corresponding to a second intermediate was clearly appearing at the expense of the first intermediate. After 20 min again the first signals of the macrocycle **4** were visible in the spectrum and could be clearly assigned. In addition to the starting materials, the final products and two defined intermediates, minor amounts of other material appeared in the spectrum that could not be assigned to a specific structure. The first intermediate showed a singlet signal in the aromatic region, a singlet signal corresponding to a $\text{CH}=\text{N}$ proton and two multiplet signals for protons next to nitrogen. The ^1H - ^1H -COSY NMR spectrum showed that these protons coupled to one another. From these data we assigned this intermediate to structure **7** which we observed in the ESI-MS experiment. The second intermediate showed three signals in the aromatic region, one singlet and one AB-quartet, two $\text{CH}=\text{N}$ singlets, one aldehyde singlet and a broad multiplet for the $\text{C}=\text{N}-\text{CH}$ protons. Integration of

the signals and data from ^1H - ^1H -COSY and ^1H - ^1H -TOCSY spectra allowed us to assign this intermediate to compound **9**.

Computational studies

It was argued earlier that trianglimines are the kinetic products of the cyclocondensation reaction. Gawroński *et al.* pointed out that the course of the reaction, leading to cyclocondensation, was governed by conformational constraints imposed on the structural components of the reactive intermediates.^[9] We performed molecular modelling calculations using HyperChem software (Release 8) at the PM3 level to further investigate the effect of conformational bias on the final ring closure step.^[29,30] The distances through space between the nucleophilic amino and the electrophilic carbonyl groups in intermediates **10**, **12**, **16** and **18** are good indicators for the ease of ring closure and formation of macrocycles



Scheme 4. Graphical representation showing dynamic exchange between (a) trianglimines **31** and **32** and (b) dialdehydes **19**, **33** and (1R,2R)-1,2-diaminocyclohexane **1**.

4, 5 and 6. The closer the nucleophilic amino and the electrophilic carbonyl groups are in space the more rapidly ring closure will occur. The lowest energy conformations for intermediates **10**, **12**, **16** and **18** are shown in Fig. 5. It can be concluded from the computational calculations that the nucleophilic and electrophilic groups in intermediates **12** and **18** are located 4.62 and 4.25 Å apart in space. This certainly allows facile ring closure due to conformational bias. Furthermore, the formation of the [2+2]-cyclocondensation macrocycle **6** is in complete agreement with the computed structure **16** in which the reactive sites are 4.66 Å separated. Unlike the case with intermediate **16**, intermediate **10** cannot cyclocondense to the corresponding [2+2]-macrocycle because, in terephthalaldehyde, the dihedral angle $O=C\cdots C=O$ biases intermediate **10** to a conformation in which the reactive nucleophilic and electrophilic sites are separated by 9.74 Å. This distance does not permit cyclocondensation to the [2+2]-macrocycle but it rather permits further condensation with one molecule of (1*R*,2*R*)-1,2-diaminocyclohexane **1** and another molecule of terephthalaldehyde **2** to form trianglimine **4**.

Similar to the [3+3]-cyclocondensation reactions of (1*R*,2*R*)-1,2-diaminocyclohexane **1** with tere- **2** and isophthalaldehyde **3** which constitute symmetrical dialdehyde building blocks, the cyclocondensation reaction of (1*R*,2*R*)-1,2-diaminocyclohexane **1** with non-symmetrical dialdehydes was investigated. The reaction was monitored as described with tere- **2** and isophthalaldehyde **3** using ESI-TOF MS. Interestingly, a total of ten different intermediates were detected and their structures were assigned based on their high-resolution *m/z* values. To the best of our knowledge, the detection and structural assignment of ten reaction intermediates in a one single reaction have not previously been reported, illustrating the power of mass spectrometry in mechanistic studies of multistep and cascade reactions. Recently, we reported the synthesis of 3-phenoxybiphenyl-4,4'-dicarbaldehyde **19** from the corresponding 4-bromo-2-fluorobenzaldehyde *via* nucleophilic aromatic

substitution reaction with phenol followed by Suzuki coupling with 4-formylphenylboronic acid.^[18] It is worth noting that 3-phenoxybiphenyl-4,4'-dicarbaldehyde **19** constitutes a non-symmetrical dialdehyde building block and its reaction with (1*R*,2*R*)-1,2-diaminocyclohexane **1** has resulted in the formation of a mixture of regioisomeric C₃-symmetrical **30** and non-symmetrical **31** trianglimines as shown in Fig. 6.^[18]

The mechanism of the [3+3]-cyclocondensation reaction was studied and confirmed by ESI-TOF MS (Scheme 3). A solution of 3-phenoxybiphenyl-4,4'-dicarbaldehyde **19** in DCM was stirred at room temperature with (1*R*,2*R*)-1,2-diaminocyclohexane **1** at 0.1 M for 8 h. Aliquots were taken every 2 h, diluted with DCM and a few drops of MeOH were added before it was directly infused into the ESI-TOF mass spectrometer. Intermediates **20**–**29** were detected and assigned based on their high-resolution *m/z* values (Table 3). Figure 7 shows the ESI-TOF mass spectra for all the intermediates which were detected 2 h after the start of the reaction.

Dynamic reversibility of trianglimine formation

Should the cyclocondensation reaction be fully reversible as suggested by the reversible nature of the imine bond (C=N) formation, the design of dynamic combinatorial libraries would be feasible.^[33] Ultimate proof of reversibility has been defined by Sanders and co-workers.^[34–43] Here reversibility is demonstrated by reaching the same equilibrium composition of a mixture from different starting points of the reaction system. For this reason we undertook a series of crossover experiments. In a first series we mixed two sets of the non-symmetrical trisubstituted trianglimines **31** and **32** in DCM and the reaction was monitored with ESI-TOF MS (Scheme 4).

Trianglimines **31** and **32** were synthesized following our strategy from non-symmetrical dialdehyde building blocks.^[18] The two macrocycles were mixed together in DCM

Table 4. ESI-TOF MS data in the positive ion mode for the products of imine exchange reactions

Entry	Calcd. <i>m/z</i>	Measured <i>m/z</i>	Molecular formula	Error [ppm]
20 , 22 ^a	399.2067	399.2063	C ₂₆ H ₂₆ N ₂ O ₂	1
30 , 31 ^a	1141.5666	1141.5629	C ₇₈ H ₇₂ N ₆ O ₃	3.2
32 ^a	1333.7576	1333.7542	C ₈₁ H ₉₆ N ₁₂ O ₆	2.5
42 , 47 ^a	463.2704	463.2723	C ₂₇ H ₃₄ N ₄ O ₃	4.1
20 , 22 ^b	399.2067	399.2046	C ₂₆ H ₂₆ N ₂ O ₂	5.2
42 , 47 ^b	463.2704	463.2688	C ₂₇ H ₃₄ N ₄ O ₃	4.6
20 , 22 ^c	399.2067	399.2060	C ₂₆ H ₂₆ N ₂ O ₂	1.6
30 , 31 ^c	1141.5666	1141.5680	C ₇₈ H ₇₂ N ₆ O ₃	–1.2
34 – 37 ^c	1205.6303	1205.6242	C ₇₉ H ₈₀ N ₈ O ₄	5
38 – 41 ^c	1269.6939	1269.6941	C ₈₀ H ₈₈ N ₁₀ O ₅	–0.1
42 , 47 ^c	463.2704	463.2693	C ₂₇ H ₃₄ N ₄ O ₃	2.6
43 – 46 ^c	747.3541	747.3510	C ₄₇ H ₄₆ N ₄ O ₅	4.1
20 , 22 ^d	399.2067	399.2067	C ₂₆ H ₂₆ N ₂ O ₂	4.8
30 , 31 ^d	1141.5666	1141.5658	C ₇₈ H ₇₂ N ₆ O ₃	0.7
34 – 37 ^d	1205.6303	1205.6249	C ₇₉ H ₈₀ N ₈ O ₄	4.4
38 – 41 ^d	1269.6939	1269.6923	C ₈₀ H ₈₈ N ₁₀ O ₅	1.2
42 , 47 ^d	463.2704	463.2695	C ₂₇ H ₃₄ N ₄ O ₃	1.8
43 – 46 ^d	747.3541	747.3501	C ₄₇ H ₄₆ N ₄ O ₅	5

^aDynamic reversibility of trianglimines **31** and **32** (3 h); ^bdynamic reversibility of compounds **1**, **19** and **33** (3 h); ^cdynamic reversibility of trianglimines **31** and **32** (46 h); ^ddynamic reversibility of compounds **1**, **19** and **33** (46 h).

and stirred at room temperature for 48 h. Aliquots were taken at defined time intervals, diluted with DCM and directly infused into the ESI-TOF mass spectrometer. After 46 h a statistical mixture of ten trianglimines **30**, **31** and **34–41** in addition to uncyclized intermediates **20**, **22** and **42–47** was detected and the structures of all the compounds were assigned.

In a second crossover experiment we mixed (1*R*,2*R*)-1,2-diaminocyclohexane **1** with dialdehydes **19** and **33** which constitute the building blocks for the constructed macrocycles **31** and **32**, respectively. ESI-TOF MS data for the products of imine exchange are shown in Table 4. The reaction was monitored as previously described.

After 46 h of stirring at room temperature, the reaction reached the point of equilibrium at which a statistical mixture of macrocycles and uncyclized intermediates was detected. These experiments clearly demonstrated the reversibility of the process and showed that trianglimines obtained from non-symmetrical dialdehyde building blocks are the products of kinetic control. It is worth noting that although imine formation is known to be reversible, this work is to the best of our knowledge the first example in which kinetic control has been clearly demonstrated for imine-only macrocycles.

CONCLUSIONS

We have shown for the first time that a complex multistep macrocyclization reaction can be monitored using real-time ESI-TOF MS, identifying an unprecedented number of 16 reaction intermediates. The [3+3]-cyclocondensation reaction between (1*R*,2*R*)-1,2-diaminocyclohexane **1** and terephthalaldehyde **2** or isophthalaldehyde **3** proceeds *via* a stepwise cyclocondensation reaction mechanism, in which definite intermediates accumulate during the reaction. All the intermediates participating in the macrocyclization reaction were detected by ESI-TOF MS and identified according to their high-resolution *m/z* values. The information about the stable reaction intermediates will allow us to rationally design new [3+3]-cyclocondensation strategies and further exploits this fascinating reaction, in which six chemical bonds form in a single reaction. We confirmed the dynamic reversibility of trianglimines and we hope that this work will open up new applications of trianglimines in the field of dynamic combinatorial libraries, leading potentially to the synthesis of selective chiral hosts for different organic compounds.

SUPPORTING INFORMATION

Additional supporting information may be found in the online version of this article.

Acknowledgements

Hany Nour deeply thanks the German Academic Exchange Service (DAAD) for financial support and Jacobs University for hosting his PhD project. We thank Ms Svetlana Gracheva and Mr Julien Sauveplain for further experiments and Mrs Anja Müller for technical assistance with mass spectrometry measurements.

REFERENCES

- [1] J. Jiang, M. MacLachlan. Unsymmetrical triangular Schiff-base macrocycles with cone conformations. *Org. Lett.* **2010**, *12*, 1020.
- [2] M. Grigoras, L. Vacareanu, T. Ivan, G. Ailiesei. Triphenylamine-based rhombimine macrocycles with solution interconvertible conformation. *Org. Biomol. Chem.* **2010**, *8*, 3638.
- [3] A. Gallant, M. Yun, M. Sauer, C. Yeung, M. MacLachlan. Tautomerization in naphthalenediimines: a keto-enamine Schiff-base macrocycle. *Org. Lett.* **2005**, *7*, 4827.
- [4] J. Hui, M. MacLachlan. [6+6] Schiff-base macrocycles with 12 imines: giant analogues of cyclohexane. *Chem. Commun.* **2006**, 2480.
- [5] M. Formica, V. Fusi, L. Giorgi, M. Micheloni, P. Palma, R. Pontellini. A template synthesis of polyamine macrocycles containing the 1,1'-bis-(2-phenol) function. *Eur. J. Org. Chem.* **2002**, *3*, 402.
- [6] A. González-Álvarez, I. Alfonso, F. Lopez-Ortiz, A. Aguirre, S. Garcia-Granda, V. Gotor. Selective host amplification from a dynamic combinatorial library of oligoimines for the synthesis of different optically active polyazamacrocycles. *Eur. J. Org. Chem.* **2004**, *5*, 1117.
- [7] L. Wang, G.-T. Wang, X. Zhao, X.-K. Jiang, Z.-T. Li. Hydrogen bonding-directed quantitative self-assembly of cyclotri-*veratrylene* capsules and their encapsulation of C₆₀ and C₇₀. *J. Org. Chem.* **2011**, *76*, 3531.
- [8] B.-Y. Lu, G.-J. Sun, J.-B. Lin, X.-K. Jiang, X. Zhao, Z.-T. Li. Hydrogen-bonded benzylidenebenzohydrazide macrocycles and oligomers: testing the robust capacity of an amide chain in promoting the formation of vesicles. *Tetrahedron Lett.* **2010**, *51*, 3830.
- [9] J. Gawroński, H. Kołbon, M. Kwit, A. Katrusiak. Designing large triangular chiral macrocycles: efficient [3+3] diamine-dialdehyde condensations based on conformational bias. *J. Org. Chem.* **2000**, *65*, 5768.
- [10] N. Kuhnert, A. Lopez-Periago. Synthesis of novel chiral non-racemic substituted trianglimine and trianglamine macrocycles. *Tetrahedron Lett.* **2002**, *43*, 3329.
- [11] N. Kuhnert, A. Lopez-Periago, G. Rossignolo. The synthesis and conformation of oxygenated trianglimine macrocycles. *Org. Biomol. Chem.* **2005**, *3*, 524.
- [12] N. Kuhnert, G. Rossignolo, A. Lopez-Periago. The synthesis of trianglimines: on the scope and limitations of the [3+3] cyclocondensation reaction between (1*R*,2*R*)-diaminocyclohexane and aromatic dicarboxaldehydes. *Org. Biomol. Chem.* **2003**, *1*, 1157.
- [13] N. Kuhnert, C. Straßnig, A. Lopez-Periago. Synthesis of novel enantiomerically pure trianglimine and trianglamine macrocycles. *Tetrahedron: Asymmetry* **2002**, *13*, 123.
- [14] N. Kuhnert, C. Patel, F. Jami. Synthesis of chiral non-racemic polyimine macrocycles from cyclocondensation reactions of biaryl and terphenyl based dicarboxaldehydes and (1*R*,2*R*)-diaminocyclohexane. *Tetrahedron Lett.* **2005**, *46*, 7575.
- [15] N. Kuhnert, B. Tang. Synthesis of diastereomeric trianglamine- β -cyclodextrin-[2]-catenanes. *Tetrahedron Lett.* **2006**, *47*, 2985.
- [16] N. Kuhnert, D. Marsh, D. Nicolau. The application of quasi-enantiomeric trianglamine macrocycles as chiral probes for anion recognition in ion trap ESI mass spectrometry. *Tetrahedron: Asymmetry* **2007**, *18*, 1648.
- [17] M. Chadim, M. Buděšínský, J. Hodačová, J. Závada, P. Junk. [3+3]-Cyclocondensation of the enantiopure and racemic forms of *trans*-1,2-diaminocyclohexane with terephthalaldehyde. Formation of diastereomeric molecular triangles and their stereoselective solid-state stacking into microporous chiral columns. *Tetrahedron: Asymmetry* **2001**, *12*, 127.

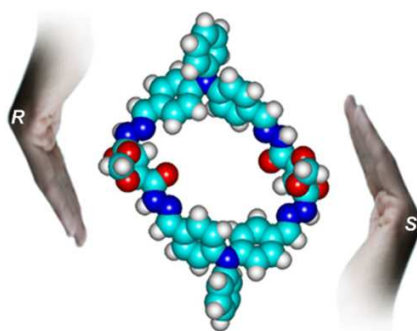
- [18] H. Nour, M. Matei, B. Bassil, U. Kortz, N. Kuhnert. Synthesis of tri-substituted biaryl based trianglimines: formation of C₃-symmetrical and non-symmetrical regioisomers. *Org. Biomol. Chem.* **2011**, 9, 3258.
- [19] L. Santos, L. Knaack, J. Metzger. Investigation of chemical reactions in solution using API-MS. *Int. J. Mass Spectrom.* **2005**, 246, 84.
- [20] A. Sabino, A. Machado, C. Correia, M. Eberlin. Probing the mechanism of the Heck reaction with arene diazonium salts by electrospray mass and tandem mass spectrometry. *Angew. Chem. Int. Ed.* **2004**, 43, 2514.
- [21] L. Santos, C. Pavam, W. Almeida, F. Coelho, M. Eberlin. Probing the mechanism of the Baylis–Hillman reaction by electrospray ionization mass and tandem mass spectrometry. *Angew. Chem. Int. Ed.* **2004**, 43, 4330.
- [22] F. Moura, M. Araujo, I. Dalmazio, T. Alves, L. Santos, M. Eberlin, R. Augusti, R. Lago. Investigation of reaction mechanisms by electrospray ionization mass spectrometry: characterization of intermediates in the degradation of phenol by a novel iron/magnetite/hydrogen peroxide heterogeneous oxidation system. *Rapid Commun. Mass Spectrom.* **2006**, 20, 1859.
- [23] R. van den Heuvel, S. Gato, C. Versluis, P. Gerbaux, C. Kleanthous, A. Heck. Real-time monitoring of enzymatic DNA hydrolysis by electrospray ionization mass spectrometry. *Nucleic Acids Res.* **2005**, 33, e96.
- [24] N. Denhart, T. Letzel. Mass spectrometric real-time monitoring of enzymatic glycosidic hydrolysis, enzymatic inhibition and enzyme complexes. *Anal. Bioanal. Chem.* **2006**, 386, 689.
- [25] G. Ghale, N. Kuhnert, W. Nau. Monitoring stepwise proteolytic degradation of peptides by supramolecular domino tandem assays and mass spectrometry for trypsin and leucine aminopeptidase. *Nat. Prod. Commun.* **2012**, in press.
- [26] V. Oleg, O. Alexander, G. Sergei. Chiral ionic liquid/ESI-MS methodology as an efficient tool for the study of transformations of supported organocatalysts: deactivation pathways of Jorgensen-Hayashi-type catalysts in asymmetric Michael reactions. *Chem. Eur. J.* **2011**, 17, 6109.
- [27] S. Wolfgang, P. Handayani, J. Zhou, B. List. Characterization of key intermediates in a complex organocatalytic cascade reaction using mass spectrometry. *Angew. Chem. Int. Ed.* **2009**, 48, 1463.
- [28] H. Smith, J. Neegaard, E. Burrows, F. Chen. Optically active amines. XVI. Exciton chirality method applied to the salicylidenimino chromophore. Salicylidenimino chirality rule. *J. Am. Chem. Soc.* **1974**, 96, 2908.
- [29] Release 8.0. Hypercube, Inc., 1115 NW 4th Street, Gainesville, FL 32601, USA. Available: <http://www.hypercube.com>.
- [30] J. Stewart. Optimization of parameters for semiempirical methods. II. Applications. *J. Comput. Chem.* **1989**, 10, 221.
- [31] A. González-Álvarez, I. Alfonso, V. Gotor. Highly diastereoselective amplification from a dynamic combinatorial library of macrocyclic oligoimines. *Chem. Commun.* **2006**, 2224.
- [32] V. Saggiomo, U. Lüning. Remarkable stability of imino macrocycles in water. *Eur. J. Org. Chem.* **2008**, 2008, 4329.
- [33] N. Kuhnert, A. Le-Gresley. The synthesis of static and dynamic combinatorial libraries using deep cavity tetraformyl calix[4]arenes. *Tetrahedron Lett.* **2005**, 46, 2059.
- [34] R. Furlan, G. Cousins, J. Sanders. Molecular amplification in a dynamic combinatorial library using non-covalent interactions. *Chem. Commun.* **2000**, 1761.
- [35] S. Otto, R. Furlan, J. Sanders. Dynamic combinatorial libraries of macrocyclic disulfides in water. *J. Am. Chem. Soc.* **2000**, 122, 12063.
- [36] G. Cousins, R. Furlan, Y.-F. Ng, J. Redman, J. Sanders. Identification and isolation of a receptor for N-methyl alkylammonium salts: molecular amplification in a pseudo-peptide dynamic combinatorial library. *Angew. Chem. Int. Ed.* **2001**, 40, 423.
- [37] R. Furlan, Y.-F. Ng, G. Cousins, J. Redman, J. Sanders. Molecular amplification in a dynamic system by ammonium cations. *Tetrahedron* **2002**, 58, 771.
- [38] S. Otto, R. Furlan, J. Sanders. Selection and amplification of hosts from dynamic combinatorial libraries of macrocyclic disulfides. *Science* **2002**, 297, 590.
- [39] P. Corbett, S. Otto, J. Sanders. What are the limits to the size of effective dynamic combinatorial libraries? *Org. Lett.* **2004**, 6, 1825.
- [40] M. Simpson, M. Pittelkow, S. Watson, J. Sanders. Dynamic combinatorial chemistry with hydrazones: chocolate-based building blocks and libraries. *Org. Biomol. Chem.* **2010**, 8, 1181.
- [41] H. Au-Yeung, G. Pantoş, J. Sanders. Dynamic combinatorial donor-acceptor catenanes in water: access to unconventional and unexpected structures. *J. Org. Chem.* **2011**, 76, 1257.
- [42] J. Liu, K. West, C. Bondy, J. Sanders. Dynamic combinatorial libraries of hydrazone-linked pseudo-peptides: dependence of diversity on building block structure and chirality. *Org. Biomol. Chem.* **2007**, 5, 778.
- [43] M. Simpson, M. Pittelkow, S. Watson, J. Sanders. Dynamic combinatorial chemistry with hydrazones: chocolate-based building blocks and libraries. *Org. Biomol. Chem.* **2010**, 8, 1173.

Synthesis of novel enantiomerically pure tetra-carbohydrazide cyclophane macrocycles

Hany F. Nour, Nadim Hourani and Nikolai Kuhnert*

Reproduced by permission of The Royal Society of Chemistry

<http://pubs.rsc.org/en/content/articlelanding/2012/OB/C2OB25171J>



Objectives of the work

Trianglimines were synthesized in high purity; however the yields of the macrocycles were low. In addition, the regioisomeric macrocycles equilibrated with one another in the NMR tube during measurements. Equilibration of the regioisomers was only observed in case where CDCl_3 was the deuterated solvent used. It was accordingly necessary to improve the yields of trianglimines by avoiding formation of the regioisomers. All attempts to synthesize symmetrically functionalized dialdehyde building blocks did not succeed. Replacing the diaminocyclohexane unit in trianglimine was an objective towards the synthesis of symmetrical macrocycles. The ring which replaces diaminocyclohexane should be chiral and should possess the attractive conformational bias feature of diaminocyclohexane. Also, it should be easily loaded with different functionalities. A ring with all these features can be obtained by protecting ketones with the vicinal hydroxyl groups of commercially available (+)-diethyl L-tartrate or (–)-diethyl D-tartrate. Molecular modeling at the MM+ level showed that dihydrazides obtained by this approach can undergo macrocyclization reactions. The new dihydrazides reacted with aromatic dialdehydes in [2+2]-cyclocondensation reactions to form a novel class of chiral non-racemic macrocycles which were named tetra-carbohydrazide cyclophanes.

Synthesis of novel enantiomerically pure tetra-carbohydrazide cyclophane macrocycles†

Hany F. Nour, Nadim Hourani and Nikolai Kuhnert*

Received 22nd January 2012, Accepted 3rd April 2012

DOI: 10.1039/c2ob25171j

A total of twelve novel enantiomerically pure tetra-carbohydrazide cyclophane macrocycles have been synthesised in quantitative yields by reacting chiral (4*R*,5*R*)- and (4*S*,5*S*)-1,3-dioxolane-4,5-dicarbohydrazides with aromatic bis-aldehydes in a [2 + 2]-cyclocondensation reaction. The compounds show a dynamic behaviour in solution, which has been rationalized in terms of an unprecedented conformational interconversion between two conformers one stabilised by intramolecular hydrogen bonding and π - π stacking interactions.

Introduction

In recent years supramolecular chemistry has emerged as one of the most actively pursued fields of the chemical sciences. Its implications now reach from the basis of molecular recognition in natural systems such as protein substrate interactions to exciting new applications in chemical technology and material sciences.^{1–9} Molecular recognition of metal cations using non-natural receptors has reached a high level of maturity and sophistication and as a consequence is successfully applied on an industrial scale.^{10–12} Molecular recognition of anions using non-natural receptors is making rapid progress,¹³ whereas molecular recognition of small to medium sized organic molecules is somehow lingering behind mainly due to the complexity of the scientific challenge.^{9,10} However, a diverse number of potentially useful applications of molecular recognition of small organic molecules using synthetic receptors have been suggested and are actively pursued. Among the most promising applications of molecular recognition are the binding and remediation of environmental toxins from soil, water and food and the binding and removal of undesired trace by-products from the bulk manufacturing of fine chemicals, which all require good water solubility of the supramolecular host.¹⁴ Moreover, chiral recognition and resolution of enantiomers, the development of sensors and biosensors and finally the design, development and synthesis of nano-gadgets and molecular machines form exciting challenges for supramolecular chemistry for the next decade.^{8,9} The

majority of supramolecular systems employ synthetic macrocyclic compounds as host molecules.

Certain classes of macrocyclic molecules have dominated the field including calix[*n*]arenes, cyclodextrins, crown-ethers and cucurbiturils. These macrocycles were characterised by synthetic methods making them easily available in large quantities, functional groups allowing simple transformations to access more sophisticated structures with elaborate binding motifs, good water solubility for cyclodextrins and cucurbiturils and their ability to bind a large variety of important guest molecules.

In the search for an ideal class of macrocycle, we have reported on numerous occasions on the synthesis of trianglimine macrocycles, obtained through a [3 + 3]-cyclocondensation reaction.^{1,2,15–20} These macrocycles fulfil, from a synthetic point of view, all the requirements for an ideal macrocycle. Since the compounds are available in a simple synthetic procedure in almost quantitative yields from versatile building blocks, purification is simple, the structure of building blocks can be largely varied to allow a modular assembly of compounds with tunable sizes and ample functionalities and finally they are enantiomerically pure and are accessible in both enantiomeric forms.

Despite all of these synthetic advantages, we have failed in the last decade to obtain trianglimine derivatives showing good solubility in polar solvents and additionally reported binding constants have on no occasion exceeded the mM range. For this reason we decided to redesign the synthetic approach we successfully employed in trianglimine chemistry to obtain novel macrocycles with improved properties. Maintaining the attractive concept of conformationally biased macrocyclisations in [*n* + *n*]-cyclocondensation reactions, we searched for suitable novel chiral building blocks that allow incorporation of ample functionality into the macrocycle combined with improved solubility properties. Work by Sanders and co-workers have demonstrated on numerous occasions that the combination of hydrazides with reactive carbonyl compounds allow an efficient construction of

School of Engineering and Science, Organic and Analytical Chemistry Laboratory, Jacobs University Bremen, Campus ring 1, P. O. Box. 750 561, 28725 Bremen, Germany. E-mail: n.kuhnert@jacobs-university.de, h.nour@jacobs-university.de; Fax: (+)49 421 200 3229

†Electronic supplementary information (ESI) available: ¹H NMR, ¹³C NMR, ESI- and APCI-MS, proposed fragmentation mechanisms of the novel macrocycles. See DOI: 10.1039/c2ob25171j

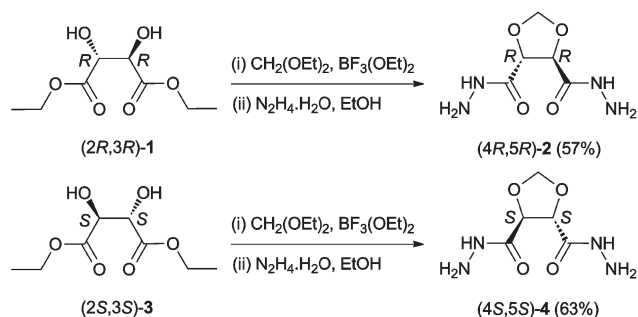
multifunctional macrocyclic structures.^{21,22} Adapting this approach to the synthesis of novel macrocycles by $[n+n]$ -cyclocondensation, meant that we investigated the reaction between a selection of chiral dihydrazides with aromatic dicarbonyl compounds. In this contribution we report on the successful synthesis of novel chiral tetra-carbohydrazide cyclophane macrocycles based on dihydrazides obtained from tartaric acid and a selection of aromatic dialdehydes.

Results and discussion

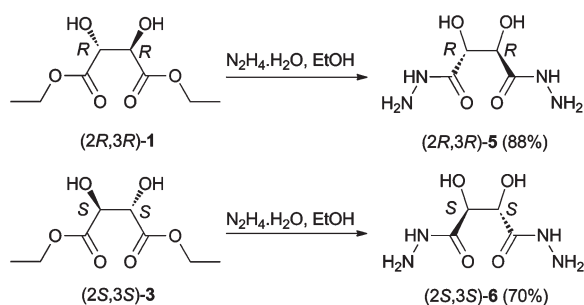
For the modular assembly of chiral macrocycles we decided to investigate dihydrazides based on tartaric acid, offering the advantage that both enantiomeric forms of a macrocycle will be accessible. Our approach towards the synthesis of dihydrazide building blocks involves protection of the *vicinal* hydroxyl groups of commercially available (+)-diethyl L-tartrate (**1**) and (–)-diethyl D-tartrate (**2**) with diethoxymethane in the presence of the Lewis acid catalyst $\text{BF}_3(\text{OEt})_2$.²³

In situ condensation of the protected diesters with hydrazine monohydrate in absolute ethanol afforded the corresponding (4*R*,5*R*)-1,3-dioxolane-4,5-dicarbohydrazide (**2**) and (4*S*,5*S*)-1,3-dioxolane-4,5-dicarbohydrazide (**4**), which serve as the building blocks for the novel macrocycles (Scheme 1).

Similarly, chiral dihydroxy (2*R*,3*R*)-hydrazide (**5**) and (2*S*,3*S*)-hydrazide (**6**) were synthesised by reacting (+)-diethyl L-tartrate (**1**) and (–)-diethyl D-tartrate (**3**) with hydrazine mono-hydrate in absolute ethanol (Scheme 2).²⁴ Structures of hydrazides (**2**), (**4**), (**5**) and (**6**), were fully characterised using various spectroscopic techniques. ¹H NMR spectrum for (*i.e.*, dicarbohydrazide **2**) showed broad signals at δ 9.42, 5.04, 4.41 and 4.32 ppm corresponding to (NH), (CH), (CH₂) and (NH₂), respectively.



Scheme 1 Synthetic route to chiral hydrazides (**2**) and (**4**).



Scheme 2 Synthetic route to chiral hydrazides (**5**) and (**6**).

¹³C NMR spectrum showed three signals at δ 168.0, 96.8 and 77.2 ppm corresponding to (C=O), (CH₂) and (CH), respectively.

FT-IR (Fourier transform infrared spectroscopy) spectrum showed strong absorption band at ν 1667 cm^{-1} corresponding to the stretching vibration of the ν C=O. It showed also weak absorption bands at ν 3191 and 3320 cm^{-1} corresponding to the hydrazide NH moieties. ESI-TOF (electrospray ionization time-of-flight) mass spectrum showed the expected pseudo molecular ion peak at 403.1277 Da as the sodium adduct of two molecules of the hydrazide ($2\text{M} + \text{Na}^+$).

It is worth noting that the novel dicarbohydrazides adopt conformations in which the carbonyl groups assume *anti*-orientation to each other.²⁵ These conformations are stabilised by strong $n \rightarrow \pi^*$ interaction and intramolecular hydrogen bonding as suggested by computational calculations (Fig. 1). Consequently, the dicarbohydrazides become good candidates for macrocyclisation based on conformational bias, rather than polymerisation.

Next we turned out attention to the macrocyclisation reaction of the obtained dihydrazides **2**, **4**, **5** and **6** with a selection of aromatic dialdehydes. The $[2+2]$ -cyclocondensation reaction was optimised in terms of stoichiometries and concentration of the reactants. The common strategies for the synthesis of macrocycles involve either using external template to assist the macrocyclisation process or applying high dilution conditions to avoid polymerisation.^{26–29} We conducted the $[2+2]$ -cyclocondensation reaction in CH_2Cl_2 at 0.1 and 0.01 M. After 24 h we noticed that, the macrocyclic product neither form by stirring at room temperature nor by refluxing. However, some intermediates were detected by ESI-TOF mass spectrometry which existed in equilibrium over the course of the reaction (see ESI†). Following our strategy, the $[2+2]$ -cyclocondensation reaction took place efficiently in MeOH at relatively high concentration of the reactants (0.05 M or less) under reflux for 7 h in the presence of few drops of AcOH as a catalyst. The $[3+3]$ - and $[4+4]$ -cyclocondensation products were observed along with the $[2+2]$ -macrocyclisation products were observed along with the $[2+2]$ -macrocyclisation under high dilution conditions (1 M), however the $[2+2]$ -macrocyclisation was the predominant product. We also found that, the $[2+2]$ -macrocyclisation forms selectively in analytically pure form in case where a slightly excess of the dicarbohydrazide was used (*i.e.*, 1.2 to 1 M).

(4*R*,5*R*)-1,3-Dioxolane-4,5-dicarbohydrazide (**2**) reacted with isophthalaldehyde, terephthalaldehyde, 4,4'-diformylbiphenyl, 4-(4-formylphenoxy)-benzaldehyde and 4,4'-diformyltriphenylamine

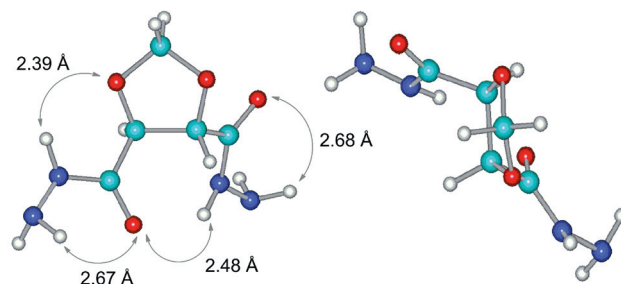
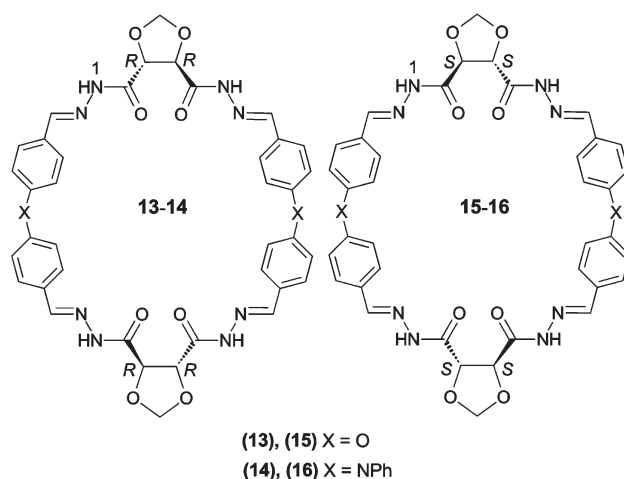


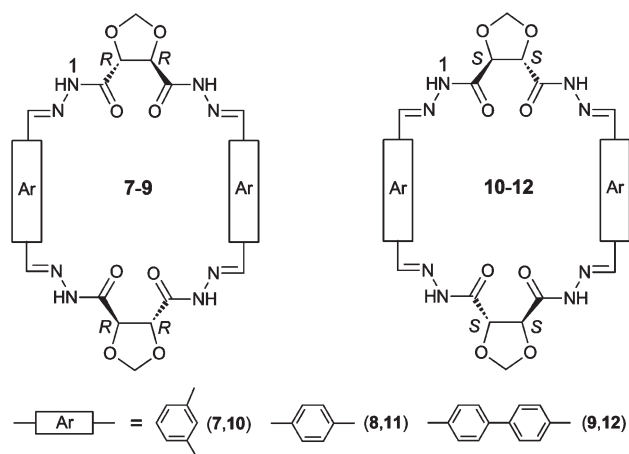
Fig. 1 Bird's-eye view for the computed structure of chiral dihydrazides (**2**) and (**4**). Structures were energy minimised using AM1 method and a Polak–Ribiere conjugate gradient with rms < 0.01 kcal. mol^{–1}.

to afford the corresponding [2 + 2]-cyclocondensation products (7–9), (13) and (14) in quantitative yields which were sufficiently pure as judged by ^1H NMR and ESI-TOF mass spectra (Schemes 3 and 4). Similarly, macrocycles (10–12), (15) and (16) were synthesised according to the above mentioned procedure from (4*S*,5*S*)-1,3-dioxolane-4,5-dicarbohydrazide (4) (Schemes 3 and 4).

Structures of the novel macrocycles were fully assigned on the basis of ^1H NMR, ^{13}C NMR, 2D-NMR, VT-(variable temperature) NMR, CD-spectroscopy, ESI- or APCI-TOF (atmospheric pressure chemical ionisation) and FT-IR. APCI-TOF mass spectrum for macrocycle (10) showed the expected molecular ion peak ($M + \text{Na}^+$) at 599.1599 Da (Fig. 2, see ESI† for ESI-mass spectra and fragmentation mechanisms). High resolution TOF-mass spectrometry data are given in Table 1. FT-IR spectrum for macrocycle (10) showed the presence of a strong absorption band at ν 1680 cm^{-1} corresponding to the stretching vibration of the ν C=O and ν C=N. ^1H NMR spectra for the novel macrocycles at ambient temperature in both $\text{DMSO}-d_6$ and $\text{DMF}-d_7$ showed broad signals suggesting conformational flexibility in



Scheme 4 [2 + 2]-Cyclocondensation products (13–16).



Scheme 3 [2 + 2]-Cyclocondensation products (7–12).

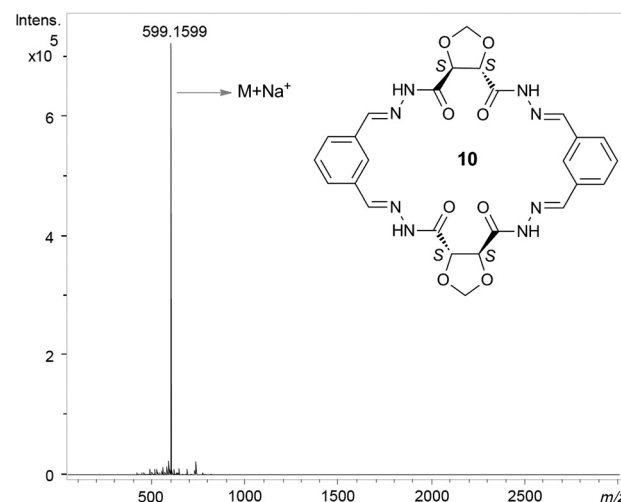


Fig. 2 APCI-TOF mass spectrum for macrocycle (10), from DMSO.

Table 1 High resolution TOF-mass data for the novel chiral macrocycles and isolated yields

Compound	Molecular formula		m/z	Meas. m/z	Error (ppm)	Yield (%)
2	$\text{C}_{10}\text{H}_{20}\text{N}_8\text{NaO}_8$	$2M + \text{Na}^+$	403.1296	403.1277	4.7	57
4	$\text{C}_{10}\text{H}_{20}\text{N}_8\text{NaO}_8$	$2M + \text{Na}^+$	403.1296	403.1276	5.1	63
5	$\text{C}_8\text{H}_{20}\text{N}_8\text{NaO}_8$	$2M + \text{Na}^+$	379.1296	379.1285	3.1	88
6	$\text{C}_8\text{H}_{20}\text{N}_8\text{NaO}_8$	$2M + \text{Na}^+$	379.1296	379.1281	4	70
7	$\text{C}_{26}\text{H}_{24}\text{N}_8\text{NaO}_8$	$M + \text{Na}^+$	599.1609	599.1596	2.3	99
8	$\text{C}_{26}\text{H}_{25}\text{N}_8\text{O}_8$	$M + \text{H}^+$	577.1790	577.1782	1.4	99
9	$\text{C}_{38}\text{H}_{33}\text{N}_8\text{O}_8$	$M + \text{H}^+$	729.2475	729.2508	4.5	98
10	$\text{C}_{26}\text{H}_{24}\text{N}_8\text{NaO}_8$	$M + \text{Na}^+$	599.1609	599.1599	1.7	99
11	$\text{C}_{26}\text{H}_{25}\text{N}_8\text{O}_8$	$M + \text{H}^+$	577.1429	577.1450	3.6	99
12	$\text{C}_{38}\text{H}_{31}\text{N}_8\text{O}_8$	$M - \text{H}^+$	^b	727 ^b	^{a,b}	97
13	$\text{C}_{38}\text{H}_{33}\text{N}_8\text{O}_{10}$	$M + \text{H}^+$	761.2314	761.2292	2.9	99
14	$\text{C}_{50}\text{H}_{42}\text{N}_{10}\text{NaO}_8$	$M + \text{Na}^+$	933.3079	933.3048	3.4	99
15	$\text{C}_{38}\text{H}_{32}\text{N}_8\text{NaO}_{10}$	$M + \text{Na}^+$	783.2134	783.2113	2.6	98
16	$\text{C}_{50}\text{H}_{43}\text{N}_{10}\text{O}_8$	$M + \text{H}^+$	911.3260	911.3292	−3.5	99
17	$\text{C}_{24}\text{H}_{25}\text{N}_8\text{O}_8$	$M + \text{H}^+$	553.1844	553.1816	5	99
18	$\text{C}_{24}\text{H}_{25}\text{N}_8\text{O}_8$	$M + \text{H}^+$	553.1941	553.1954	−2.3	99

^a Error value could not be estimated due to poor solubility and hence low peak intensity. ^b APCI-MS².

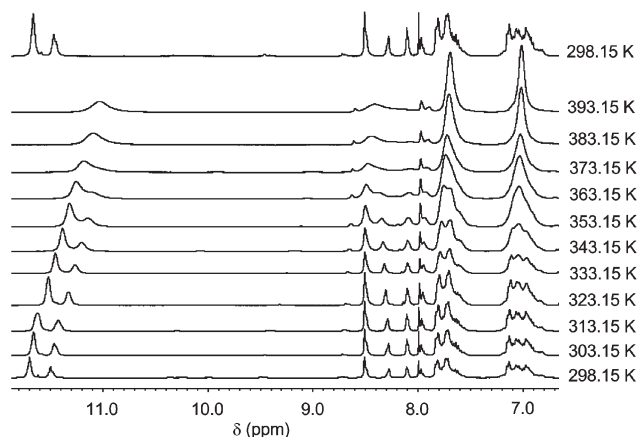


Fig. 3 Variable temperature ^1H NMR spectra for compound (**13**), 400 MHz, DMF-d_7 .

solution. ^1H NMR spectrum for macrocycle (**13**) in DMSO-d_6 showed a broad signal at δ 11.66 ppm with an integration of four ($4 \times \text{NH}$). It showed also four broad singlets at δ 8.34, 8.06, 7.93 and a signal at 7.71 ppm overlapping with the aromatic protons corresponding to four non-equivalent azomethine protons (see Fig. 3). In DMF-d_7 the signal corresponding to the (NH) protons splits into two broad signals appearing at δ 11.70 and 11.54 ppm, each signal integrated with two ($4 \times \text{NH}$). In addition, four broad signals appeared at δ 8.51, 8.28, 8.12 and 7.97 ppm corresponding to four non-symmetrical azomethine protons.

In order to characterise the behaviour of the novel macrocycles in solution, we performed VT-NMR studies for macrocycles (**13**) and (**14**). VT-NMR was performed from 303 to 393 K in DMF-d_7 . The two broad signals appearing at δ 11.70 and 11.54 ppm corresponding to the four (NH) protons coalesced at 383 K to a broad singlet appearing at δ 11.10 ppm (Fig. 3). Cooling the NMR to 298 K yields the same spectrum as first recorded illustrating the reversibility of the process.

We suggest that two distinct conformational isomers could result from intramolecular hydrogen bonding interactions ($-\text{NH}\cdots\text{O}=\text{C}$), whose interconversion involved fast exchange during the ^1H NMR time scale and resulted in reducing the solubility of the macrocycles in common organic solvents and water.

VT-NMR spectra for macrocycle (**14**) is available with the ESI.[†] The change in chemical shifts in response to changing temperature can be graphically represented by plotting the values of chemical shift (δ in ppm) versus temperature ($^\circ\text{C}$) as shown in Fig. 4.

It can be inferred that a intramolecular hydrogen bond breaks upon heating, resulting in upfield shift of the associated (NH) protons. Our hypothesis of conformational isomers was further supported by 2D-NMR experiments. The 2D-ROESY spectrum for macrocycle (**14**) showed through space interactions between two (NH) protons with two azomethine protons ($\text{HC}=\text{N}$) and two methine protons (CH) (Fig. 5 and 6).

The other (NH) protons interacted through space with two azomethine protons ($\text{HC}=\text{N}$), while no interactions were observed with methine protons.

In order to further understand the nature of the intramolecular hydrogen bonding, we performed several molecular modelling

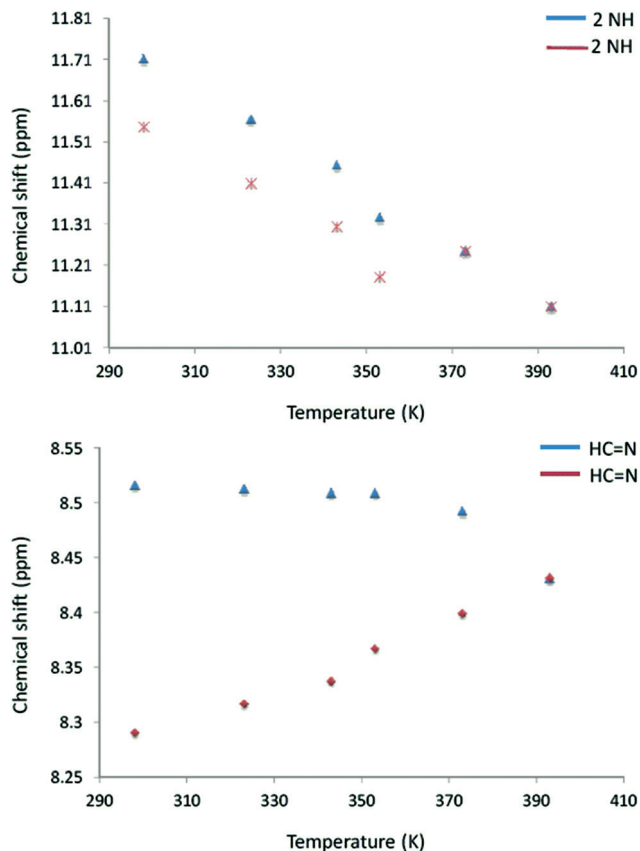


Fig. 4 Graphical representation for the change of chemical shift in response to increasing temperature.

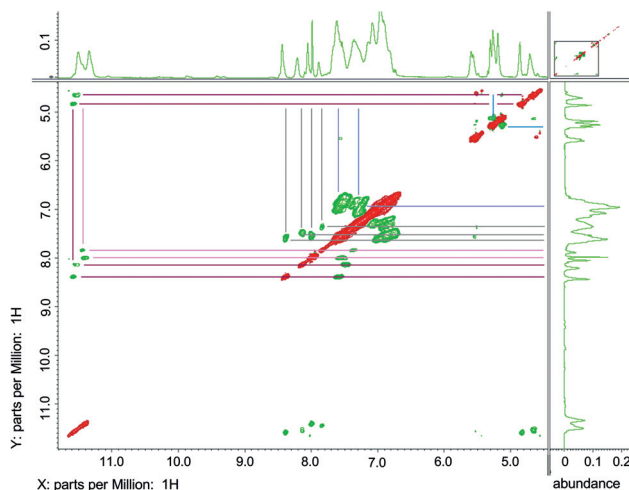


Fig. 5 2D-ROESY spectrum for macrocycle (**14**), 400 MHz, DMF-d_7 .

based studies. Data from 2D-ROESY experiments were used for subsequent structure modelling calculations. Structures of the novel macrocycles (*i.e.*, macrocycle **14**) were optimised using HyperChem software (Release 8).

The molecular structures were optimised at the AMBER (assisted model building with energy refinement) and PM3 (parameterised model number 3) levels using the Polak–Ribiere algorithm until the root mean square (RMS) gradient was

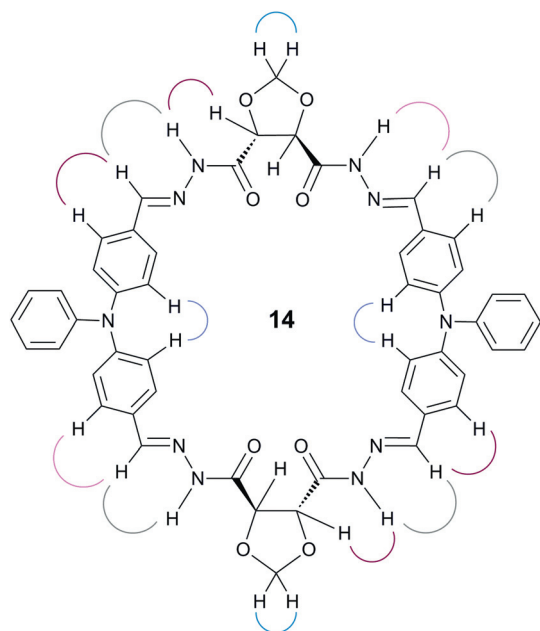


Fig. 6 2D-ROESY interactions for macrocycle (14).

0.01 kcal. mol⁻¹ or less. The results of molecular modelling are in good agreement with the structures suggested by 2D-ROESY experiment and confirm the presence of intramolecular hydrogen bonding interactions (Fig. 7).

In solution, macrocycle (14) can assume a minimum energy conformation (14b) which comprises intramolecular hydrogen bonding and π - π stacking interactions. Upon heating (14b) rapid interconversion to the more symmetric conformation (14a) occurs measurable on the NMR time scale.

Next, we turned our attention to assessing the reactivity of the unprotected dicarbohydrazides towards the [2 + 2]-cyclocondensation reaction. (2*R*,3*R*)-hydrazide (5) and (2*S*,3*S*)-hydrazide (6) reacted with terephthalaldehyde in methanol (<0.05 M) in the presence of a few drops of catalytic AcOH to form highly C₂-symmetrical [2 + 2]-cyclocondensation products (17) and (18) as judged by the ¹H and ¹³C NMR spectra (Fig. 8).

This indicated the presence of only one conformer in solution. ¹H NMR spectrum for macrocycle (17) showed a broad signal at δ 11.27 ppm (4 \times NH). It also showed broad signals at δ 8.44 ppm corresponding to four azomethine protons (4 \times HC=N). APCI-TOF mass data for macrocycles (17) and (18) are shown in Table 1. 2D-ROESY spectrum showed through space interactions between (NH), (HC=N) and (OH) protons (see ESI†). In an attempt to investigate and to explain the behaviour of the non-protected macrocycles in solution, we performed molecular modelling studies at the MM+ (molecular mechanics) level based on data from 2D-ROESY experiments. Molecular modelling showed that macrocycle (17) adopts a conformation in which all azomethine protons (HC=N) are *anti*-oriented. The free hydroxyl groups can form concerted intramolecular hydrogen bonding with the carbonyl groups to yield symmetrical and stable conformers (Fig. 9).

Distances (Å) between some selected atoms based on molecular modelling calculations for macrocycles (13) and (14) are shown in Table 2.

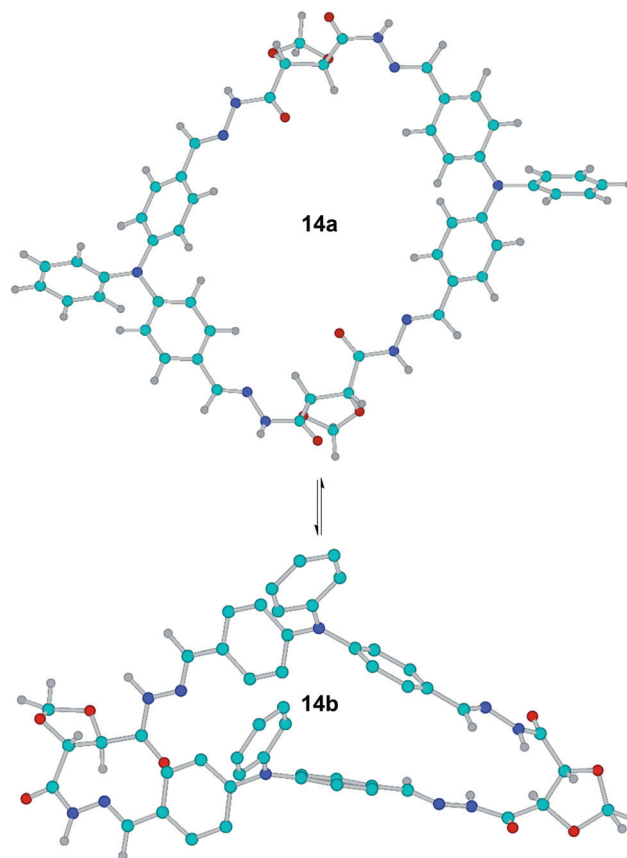


Fig. 7 Computed structures for macrocycle (14) at the PM3 and AMBER levels. A Polak–Ribiere conjugate gradient with rms < 0.01 kcal.mol⁻¹ was used. Some hydrogen atoms were omitted for clarity.

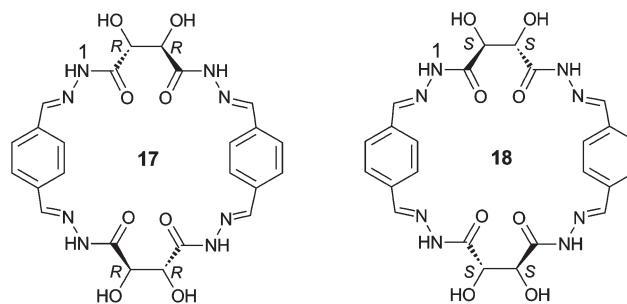


Fig. 8 [2 + 2]-cyclocondensation products (17) and (18).

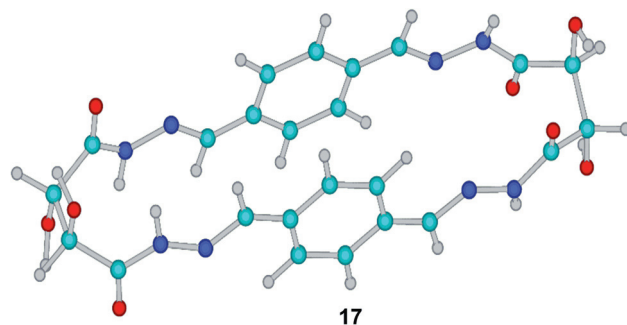


Fig. 9 Computed structure for macrocycle (17).

Table 2 Distances (Å) between some selected atoms for macrocycles (13) and (14)

Atoms	Macrocycle (13) (Å)	Macrocycle (14a) (Å)	Macrocycle (14b) (Å)
C2–C21	11.83	11.12	16.64
C3–C22	14.02	13.51	17.14
C4–C23	13.56	13.45	15.77
C5–C24	15.56	15.43	13.45
N6–N25	15.90	16.04	12.21
N7–N26	14.02	14.29	10.18
C8–C27	14.99	15.43	9.31
C9–C28	13.79	14.40	7.33
C12–C31	13.25	14.18	6.60
X13–X32	14.09	14.94	5.28
C14–C33	12.51	13.27	6.29
C17–C36	11.49	11.70	9.84
C18–C37	12.06	12.00	12.00
N19–N38	11.59	10.55	13.15
N20–N1	12.42	11.92	15.27

The chirality of the novel macrocycles and their precursors was confirmed by CD-spectroscopy as shown in Fig. 10. *All-R* macrocycle (14) shows for example a positive Cotton effect with a zero intercept at around 370 nm, whereas its enantiomeric counterpart *all-S* (16) shows a negative Cotton effect. Similar to trianglimines the observed Cotton effect is a consequence of the interaction of the two aromatic chromophores within the macrocycle.

Conclusion

In summary, we have synthesised a novel class of chiral non-racemic tetra-carbohydrazide macrocycles starting from commercially available diethyl tartrates. After conversion of the chiral building block to a dihydrazide, reaction with aromatic dialdehydes yielded the novel macrocycles. The macrocyclisation reaction takes place at relatively high concentration of the reactants in MeOH (<0.05 M) to afford, presumably under conformational bias, selectivity the [2 + 2]-cyclocondensation products. Macrocycle is available in both enantiomeric forms. VT-NMR along with 2D-NMR experiments confirmed the presence of a dynamic behaviour in solution, which has been rationalized in terms of an unprecedented conformational interconversion between two conformers one stabilised by intramolecular hydrogen bonding and π - π stacking interactions. Further work aimed at assessing molecular recognition of the novel macrocycles in DMF and enhancing solubility in other organic solvents is under investigation and will be published in due course.

Experimental

All the reagents used for the reactions were purchased from Sigma-Aldrich, Applichem or Flucka (Germany) and were used as obtained. Whenever possible the reactions were monitored by thin layer chromatography (TLC). TLC was performed on Macherey–Nagel aluminium-backed plates pre-coated with silica gel 60 (UV₂₅₄). Column chromatography was carried out on silica gel 60 (0.040–0.063 mm) under flash conditions. Melting points were determined in open capillaries using a Buechl

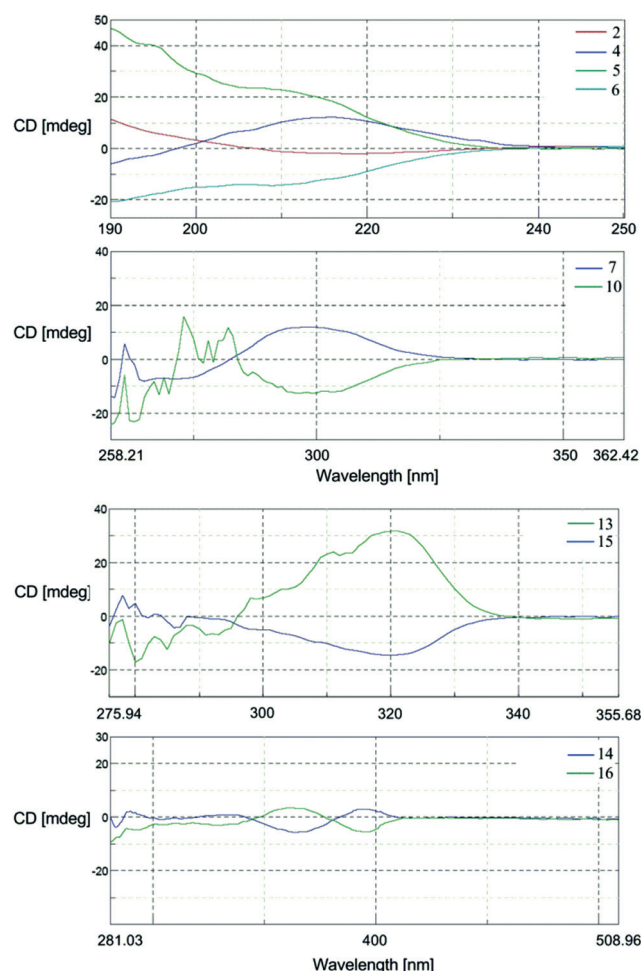


Fig. 10 CD-spectra for chiral hydrazides (2,4–6) in water and [2 + 2]-cyclocondensation products (7,10 and 13–16) in DMSO.

B-545 melting point apparatus and are not corrected. Infrared spectra were determined using a Vector-33 Bruker FT-IR spectrometer.

The samples were measured directly as solids or oils; ν_{max} values were expressed in cm^{-1} and were given for the main absorption bands. ^1H NMR and ^{13}C NMR spectra were acquired on a JEOL ECX-400 spectrometer operating at 400 MHz for ^1H NMR and 100 MHz for ^{13}C NMR in DMSO- d_6 , D_2O , CDCl_3 or DMF- d_7 using a 5 mm probe. The chemical shifts (δ) are reported in parts per million and were referenced to the residual solvent peak. The following abbreviations are used: s, singlet; m, multiplet; br, broad signal. Mass spectra were recorded using HCTultra and ESI- or APCI-TOF Bruker Daltonics mass spectrometers and samples were dissolved in DMSO, DMF and acetonitrile or water using the positive and negative electrospray ionisation modes. Calibration was carried out using a 0.1 M solution of sodium formate in the enhanced quadratic mode prior to each experimental run. The results of measurements were processed using Compass 1.3 data analysis software for a Bruker Daltonics time-of-flight mass spectrometer (microTOF). Molecular modelling calculations were carried out with Hyperchem software (Release 8.0) at the AM1, PM3, AMBER and MM+ levels *in vacuo* and no influence of solvents was taken into

account in these calculations.^{30,31} 4,4'-Biphenyl dicarboxaldehyde was synthesised according to the literature.³² Circular Dichroism measurements were carried out using Jasco-J-810 Spectropolarimeter in H₂O and DMSO. We could not measure the ¹³C-spectrum for macrocycles (**9**) due to its poor solubility in DMSO-d₆. All products were suitable for use without further purification.

(4*R*,5*R*)-1,3-dioxolane-4,5-dicarbohydrazide (**2**)

To a stirred solution of (+)-diethyl L-tartrate (17.8 mL, 71.70 mmol) in isopropyl acetate (100 mL) were added diethoxymethane (12.1 mL, 96.86 mmol) and boron trifluoride diethyl etherate (23.8 mL, 192.84 mmol), and the mixture was refluxed for 7 h. The reaction mixture was carefully quenched with saturated aqueous sodium bicarbonate and the layers were separated. The water phase was extracted with isopropyl acetate (2 × 100 mL) and the combined organic layers were dried with sodium sulfate, filtered and evaporated under reduced pressure. The crude mixture (21.9 g) was dissolved without further purification in ethanol (100 mL) and hydrazine monohydrate (6.8 mL, 213.44 mmol) was added. The reaction mixture was refluxed for 7 h. The precipitate was filtered off, washed with ethanol and diethyl ether to give the title compound (**2**) as a white solid (11.58 g, 57%); mp 210–211 °C; IR $\nu_{\max}/\text{cm}^{-1}$ 3320, 3191 (NH), 1667 (C=O); ¹H NMR (400 MHz, DMSO-d₆) δ_{H} 9.42 (2H, brs, NH), 5.04 (2H, brs, CH), 4.41 (2H, brs, CH₂), 4.32 (4H, brs, NH₂); ¹³C NMR (100 MHz, DMSO-d₆) δ_{C} 168.0, 96.8, 77.2; MS (ESI-MS, H₂O, HCTultra) m/z (Calcd 190.1; exp. 212.8, M + Na⁺, 100%), (Calcd 190.1; exp. 402.9, 2M + Na⁺, 74%), (HRMS, ESI-TOF, H₂O) m/z (Calcd 403.1296; meas. 403.1277, 2M + Na⁺).

(4*S*,5*S*)-1,3-dioxolane-4,5-dicarbohydrazide (**4**)

To a stirred solution of (–)-diethyl D-tartrate (17.8 mL, 71.70 mmol) in isopropyl acetate (100 mL) were added diethoxymethane (12.1 mL, 96.86 mmol) and boron trifluoride diethyl etherate (23.8 mL, 192.84 mmol), and the mixture was refluxed for 7 h. The reaction mixture was quenched with saturated aqueous sodium bicarbonate and the layers were separated. The water phase was extracted with isopropyl acetate (2 × 100 mL), and the combined organic layers were dried with sodium sulfate, filtered and evaporated under reduced pressure. The crude mixture (22.63 g) was dissolved without further purification in ethanol (100 mL) and hydrazine monohydrate (6.5 mL, 207.6 mmol) was added to the reaction mixture. The reaction mixture was refluxed for 7 h. The precipitate was filtered off, washed with ethanol and diethyl ether to give the title compound (**4**) as a white solid (13.11 g, 63%); mp 209–210 °C; IR $\nu_{\max}/\text{cm}^{-1}$ 3320, 3193 (NH), 1667 (C=O); ¹H NMR (400 MHz, DMSO-d₆) δ_{H} 9.41 (2H, brs, NH), 5.04 (2H, brs, CH), 4.41 (2H, brs, CH₂), 4.31 (4H, brs, NH₂); ¹³C NMR (100 MHz, DMSO-d₆) δ_{C} 168.0, 96.8, 77.2; MS (ESI-MS, H₂O, HCTultra) m/z (Calcd 190.1; exp. 212.8, M + Na⁺, 100%), (Calcd 190.1; exp. 402.9, 2M + Na⁺, 67%), (HRMS, ESI-TOF, H₂O) m/z (Calcd 403.1296; meas. 403.1276, 2M + Na⁺).

(2*R*,3*R*)-2,3-Dihydroxydicarbohydrazide (**5**)

Hydrazine monohydrate (3.1 mL, 116.8 mmol) was added to a stirred solution of (+)-diethyl L-tartrate (5 mL, 29.2 mmol) in ethanol (40 mL). The mixture was refluxed for 7 h. The precipitate was filtered off, washed with methanol, diethyl ether and dried to give the title compound (**5**) as a white solid (4.61 g, 88%); mp 208–209 °C; IR $\nu_{\max}/\text{cm}^{-1}$ 3408, 3354, 3309 and 3286 (OH and NH), 1661 (C=O); ¹H NMR (400 MHz, DMSO-d₆) δ_{H} 8.75 (2H, brs, NH), 5.34 (2H, brs, CH), 4.21 (6H, brs, NH₂ and OH); ¹³C NMR (100 MHz, DMSO-d₆) δ_{C} 171.0, 72.7; MS (ESI-MS, H₂O, HCTultra) m/z (Calcd 178.1; exp. 200.7, M + Na⁺, 100%), (HRMS, ESI-TOF, H₂O) m/z (Calcd 379.1296; meas. 379.1285, 2M + Na⁺).

(2*S*,3*S*)-2,3-Dihydroxydicarbohydrazide (**6**)

Hydrazine monohydrate (3.1 mL, 116.8 mmol) was added to a stirred solution of (–)-diethyl D-tartrate (5 mL, 29.2 mmol) in ethanol (40 mL). The mixture was refluxed for 7 h. The precipitate was filtered off, washed with methanol, diethyl ether and dried to give the title compound (**6**) as a white solid (3.64 g, 70%); mp 208–209 °C; IR $\nu_{\max}/\text{cm}^{-1}$ 3408, 3354, 3309 and 3286 (OH and NH), 1659 (C=O); ¹H NMR (400 MHz, D₂O) δ_{H} 4.64 and 4.46 (2H, brs, CH); ¹³C NMR (100 MHz, D₂O) δ_{C} 171.8, 71.9; MS (ESI-MS, H₂O, HCTultra) m/z (Calcd 178.1; exp. 200.7, M + Na⁺, 100%), (HRMS, ESI-TOF, H₂O) m/z (Calcd 379.1296; meas. 379.1281, 2M + Na⁺).

General procedure for the synthesis of tetra-carbohydrazide macrocycles (**7**–**18**)

Dicarbohydrazide (**2**), (**4**), (**5**) or (**6**) (1.2 mmol) and the corresponding dialdehyde (1 mmol) were mixed in MeOH (<0.05 M) and two drops of catalytic AcOH were added. The reaction mixture was refluxed for 7 h. The precipitate which form was filtered off, washed with water, chloroform and dried to give the corresponding macrocycle in a quantitative yield.

(3*R*,4*R*,16*R*,17*R*)-Tetra-carbohydrazide cyclophane (**7**)

Prepared from (4*R*,5*R*)-1,3-dioxolane-4,5-dicarbohydrazide (**2**) and isophthalaldehyde as a white solid precipitate (99%); mp > 315 °C (decomp.); IR $\nu_{\max}/\text{cm}^{-1}$ 3218 (NH), 1681 (C=O, C=N); ¹H NMR (400 MHz, DMSO-d₆) δ_{H} 11.78 (4H, brs, NH), 8.40–8.19 (2H, m, CH=N), 8.08–7.96 (2H, m, CH=N), 7.88–7.12 (8H, m, ArH), 5.45 (2H, brs, CH), 5.23–5.08 (4H, m, CH₂), 4.78 (1H, brs, CH), 4.52 (1H, brs, CH); ¹³C NMR (100 MHz, DMSO-d₆) δ_{C} 170.4, 165.8, 148.9, 144.5, 134.7, 129.7, 97.2, 77.5; MS (ESI-MS, DMF and ACN, HCTultra) m/z (Calcd 576.2; exp. 599.1, M + Na⁺, 100%), (HRMS, APCI-TOF, DMSO) m/z (Calcd 599.1609; meas. 599.1596, M + Na⁺).

(3*R*,4*R*,17*R*,18*R*)-Tetra-carbohydrazide cyclophane (**8**)

Prepared from (4*R*,5*R*)-1,3-dioxolane-4,5-dicarbohydrazide (**2**) and terephthalaldehyde as a pale yellow solid precipitate (99%); mp > 345 °C (decomp.); IR $\nu_{\max}/\text{cm}^{-1}$ 3206 (NH), 1672 (C=O,

C=N); ^1H NMR (400 MHz, DMSO- d_6) δ_{H} 11.77 (4H, brs, NH), 8.35 (1H, brs, CH=N), 7.95–7.87 (2H, m, CH=N), 7.74–7.11 (9H, m, CH=N and ArH), 5.38 (2H, brs, CH), 5.20–4.99 (4H, m, CH₂), 4.76 (1H, brs, CH), 4.49 (1H, brs, CH); ^{13}C NMR (100 MHz, DMSO- d_6) δ_{C} 170.5, 165.7, 148.9, 144.4, 134.3, 128.0, 97.5, 77.3; MS (ESI-MS, DMF and ACN, HCTultra) m/z (Calcd 576.2; exp. 577.1, M + H⁺, 100%), (HRMS, APCI-TOF, DMSO) m/z (Calcd 577.1790; meas. 577.1782, M + H⁺).

(3R,4R,21R,22R)-Tetra-carbohydrazide cyclophane (9)

Prepared from (4R,5R)-1,3-dioxolane-4,5-dicarbohydrazide (**2**) and 4,4'-diformylbiphenyl as a yellow solid precipitate (98%); mp > 340 °C (decomp.); IR $\nu_{\text{max}}/\text{cm}^{-1}$ 3211 (NH), 1672 (C=O, C=N); ^1H NMR (400 MHz, DMSO- d_6) δ_{H} 11.72 (4H, brs, NH), 7.94 (2H, brs, CH=N), 7.79–7.05 (18H, m, CH=N and ArH), 5.38–5.02 (6H, m, CH and CH₂), 4.48 (1H, brs, CH), 4.33 (1H, brs, CH); MS (ESI-MS, DMSO, HCTultra) m/z (Calcd 728.2; exp. 729.2, M + H⁺, APCI-MS², 100%), (HRMS, APCI-TOF, DMSO) m/z (Calcd 729.2475; meas. 729.2508, M + H⁺).

(3S,4S,16S,17S)-Tetra-carbohydrazide cyclophane (10)

Prepared from (4S,5S)-1,3-dioxolane-4,5-dicarbohydrazide (**4**) and isophthalaldehyde as a white solid precipitate (99%); mp > 323 °C (decomp.); IR $\nu_{\text{max}}/\text{cm}^{-1}$ 3223 (NH), 1680 (C=O, C=N); ^1H NMR (400 MHz, DMSO- d_6) δ_{H} 11.78 (4H, brs, NH), 8.40 (1H, brs, CH=N), 8.07–7.96 (2H, m, CH=N), 7.88–7.14 (9H, m, CH=N and ArH), 5.46–5.40 (2H, m, CH), 5.23–5.08 (4H, m, CH₂), 4.86–4.79 (1H, brs, CH), 4.52 (1H, brs, CH); ^{13}C NMR (100 MHz, DMSO- d_6) δ_{C} 170.4, 165.8, 148.9, 144.5, 134.4, 129.7, 97.3, 77.5; MS (ESI-MS, DMF and ACN, HCTultra) m/z (Calcd 576.2; exp. 599.1, M + Na⁺, 100%), (HRMS, APCI-TOF, DMSO) m/z (Calcd 599.1609; meas. 599.1599, M + Na⁺).

(3S,4S,17S,18S)-Tetra-carbohydrazide cyclophane (11)

Prepared from (4S,5S)-1,3-dioxolane-4,5-dicarbohydrazide (**4**) and terephthalaldehyde as a pale yellow solid precipitate (99%); mp > 346 °C (decomp.); IR $\nu_{\text{max}}/\text{cm}^{-1}$ 3206 (NH), 1671 (C=O, C=N); ^1H NMR (400 MHz, DMSO- d_6) δ_{H} 11.77 (2H, brs, NH), 11.62 (2H, brs, NH), 8.36 (1H, brs, CH=N), 7.92–7.87 (2H, m, CH=N), 7.80–7.18 (9H, m, CH=N and ArH), 5.37–5.00 (6H, m, CH and CH₂), 4.76 (1H, brs, CH), 4.22 (1H, brs, CH); ^{13}C NMR (100 MHz, DMSO- d_6) δ_{C} 170.7, 165.4, 146.1, 144.2, 135.3, 128.0, 97.0, 77.8; MS (ESI-MS, DMF and ACN, HCTultra) m/z (Calcd 576.2; exp. 577.1, M + H⁺, 100%), (HRMS, APCI-TOF, DMSO) m/z (Calcd 577.1429; meas. 577.1450, M + H⁺).

(3S,4S,21S,22S)-Tetra-carbohydrazide cyclophane (12)

Prepared from (4S,5S)-1,3-dioxolane-4,5-dicarbohydrazide (**4**) and 4,4'-diformylbiphenyl as a yellow solid precipitate (97%); mp > 340 °C (decomp.); IR $\nu_{\text{max}}/\text{cm}^{-1}$ 3210 (NH), 1673 (C=O,

C=N); ^1H NMR (400 MHz, DMSO- d_6) δ_{H} 11.72 (4H, brs, NH), 8.39 (1H, brs, CH=N), 7.94 (2H, brs, CH=N), 7.79–7.04 (17H, m, CH=N and ArH), 5.38 (2H, brs, CH), 5.19–5.02 (4H, m, CH₂), 4.75–4.32 (2H, m, CH); MS (APCI-MS², DMSO, HCTultra) m/z (Calcd 728.2; exp. 729.2, M + H⁺, 100%), (Calcd 728.2; exp. 727.2, M – H⁺, 100%).

(3R,4R,22R,23R)-Tetra-carbohydrazide cyclophane (13)

Prepared from (4R,5R)-1,3-dioxolane-4,5-dicarbohydrazide (**2**) and 4-(4-formylphenoxy)benzaldehyde as a white solid precipitate (99%); mp > 315 °C (decomp.); IR $\nu_{\text{max}}/\text{cm}^{-1}$ 3220 (NH), 1681 (C=O, C=N); ^1H NMR (400 MHz, DMSO- d_6) δ_{H} 11.66 (4H, brs, NH), 8.34 (1H, brs, CH=N), 8.06 (1H, brs, CH=N), 7.93 (1H, brs, CH=N), 7.71–7.43 (9H, m, CH=N and ArH), 7.09–6.65 (8H, m, ArH), 5.42 (2H, brs, CH), 5.42–5.10 (4H, brs, CH₂), 4.75 (1H, brs, CH), 4.54 (1H, brs, CH); ^1H NMR (400 MHz, DMF- d_7) δ_{H} 11.70 (2H, brs, NH), 11.54 (2H, brs, NH), 8.51 (1H, brs, CH=N), 8.28 (1H, brs, CH=N), 8.12 (1H, brs, CH=N), 8.00–7.94 (1H, m, CH=N), 7.76 (7H, m, ArH), 7.57 (1H, brs, ArH), 7.14–6.83 (8H, m, ArH), 5.65 (1H, brs, CH), 5.59 (1H, brs, CH), 5.35–5.23 (4H, m, CH₂), 4.90 (1H, brs, CH), 4.78 (1H, brs, CH); ^{13}C NMR (100 MHz, DMSO- d_6) 170.3, 165.6, 157.7, 148.8, 144.4, 129.7, 119.5, 97.2, 77.5; ^{13}C NMR (100 MHz, DMF- d_7) 170.2, 165.7, 158.4, 148.6, 144.2, 129.4, 119.2, 97.4, 78.0; MS (ESI-MS, DMF and ACN, HCTultra) m/z (Calcd 760.2; exp. 761.3, M + H⁺, 100%), (HRMS, APCI-TOF, DMSO) m/z (Calcd 761.2314; meas. 761.2292, M + H⁺).

(3R,4R,22R,23R)-Tetra-carbohydrazide cyclophane (14)

Prepared from (4R,5R)-1,3-dioxolane-4,5-dicarbohydrazide (**2**) and 4,4'-diformyltriphenylamine as a yellow solid precipitate (99%); mp > 224 °C (decomp.); IR $\nu_{\text{max}}/\text{cm}^{-1}$ 3214 (NH), 1681 (C=O, C=N); ^1H NMR (400 MHz, DMF- d_7) δ_{H} 11.38 (2H, brs, NH), 11.22 (2H, brs, NH), 8.20 (1H, brs, CH=N), 7.92 (1H, brs, CH=N), 7.80 (1H, brs, CH=N), 7.74 (1H, brs, CH=N), 7.49–7.22 (6H, m, ArH), 7.22–6.98 (6H, m, ArH), 6.91–6.77 (6H, m, ArH), 6.77–6.49 (8H, m, ArH); 5.32 (2H, brs, CH), 5.06–4.94 (4H, m, CH₂), 4.62 (1H, brs, CH), 4.46 (1H, brs, CH); ^{13}C NMR (100 MHz, DMSO- d_6) 170.3, 165.4, 148.3, 146.3, 144.4, 130.4, 129.1, 126.0, 125.2, 123.5, 97.1, 77.5; MS (ESI-MS, DMF and ACN, HCTultra) m/z (Calcd 910.3; exp. 911.5, M + H⁺, 100%), (HRMS, APCI-TOF, DMSO) m/z (Calcd 933.3079; meas. 933.3048, M + Na⁺).

(3S,4S,22S,23S)-Tetra-carbohydrazide cyclophane (15)

Prepared from (4S,5S)-1,3-dioxolane-4,5-dicarbohydrazide (**4**) and 4-(4-formylphenoxy)benzaldehyde as a white solid precipitate (98%); mp > 305 °C (decomp.); IR $\nu_{\text{max}}/\text{cm}^{-1}$ 3219 (NH), 1681 (C=O, C=N); ^1H NMR (400 MHz, DMSO- d_6) δ_{H} 11.65 (4H, brs, NH), 8.35 (1H, brs, CH=N), 8.07 (1H, brs, CH=N), 7.93 (1H, brs, CH=N), 7.71–7.52 (8H, m, CH=N and ArH), 7.43 (1H, brs, ArH) 7.10–6.66 (8H, m, ArH), 5.42 (2H, brs, CH), 5.22–5.05 (4H, brs, CH₂), 4.75 (1H, brs, CH), 4.54 (1H, brs, CH); ^{13}C NMR (100 MHz, DMSO- d_6) 170.3, 165.6, 157.7,

148.8, 144.4, 129.7, 119.5, 97.2, 77.5; MS (ESI-MS, DMF and ACN, HCTultra) m/z (Calcd 760.2; exp. 761.3, $M + H^+$, 100%), (HRMS, APCI-TOF, DMSO) m/z (Calcd 783.2134; meas. 783.2113, $M + Na^+$).

(3*S*,4*S*,22*S*,23*S*)-Tetra-carbohydrazide cyclophane (16)

Prepared from (4*S*,5*S*)-1,3-dioxolane-4,5-dicarbohydrazide (**4**) and 4,4'-diformyltriphenylamine as a yellow solid precipitate (99%); mp > 220 °C (decomp.); IR $\nu_{\max}/\text{cm}^{-1}$ 3214 (NH), 1681 (C=O, C=N); ^1H NMR (400 MHz, DMSO- d_6) δ_{H} 11.59 (4H, brs, NH), 8.28 (1H, brs, CH=N), 7.96 (1H, brs, CH=N), 7.85 (1H, brs, CH=N), 7.67–7.57 (2H, m, CH=N, ArH), 7.46–7.28 (7H, m, ArH), 7.22–6.96 (8H, m, ArH), 6.94–6.56 (10H, m, ArH), 5.35 (2H, brs, CH), 5.19–5.05 (4H, m, CH₂), 4.71 (1H, brs, CH), 4.45 (1H, brs, CH); ^{13}C NMR (100 MHz, DMSO- d_6) 170.3, 165.4, 148.3, 146.3, 144.3, 130.4, 129.1, 126.1, 125.1, 123.5, 97.1, 77.5; MS (ESI-MS, DMF and ACN, HCTultra) m/z (Calcd 910.3; exp. 911.5, $M + H^+$, 100%), (HRMS, APCI-TOF, DMSO) m/z (Calcd 911.3260; meas. 911.3292, $M + H^+$).

(3*R*,4*R*,17*R*,18*R*)-Tetra-carbohydrazide cyclophane (17)

Prepared from (2*R*,3*R*)-2,3-dihydroxy dicarbohydrazide (**5**) and terephthaldehyde as a white solid precipitate, (99%); mp > 295 °C (decomp.); IR $\nu_{\max}/\text{cm}^{-1}$ 3268 (broad absorption band, OH and NH), 1668 (C=O, C=N); ^1H NMR (400 MHz, DMSO- d_6) δ_{H} 11.27 (4H, brs, NH), 8.44 (4H, brs, CH=N), 7.70 (8H, brs, ArH) 5.91 (4H, brs, OH), 4.49 (4H, brs, CH); ^{13}C NMR (100 MHz, DMSO- d_6) δ_{C} 168.9, 147.6, 136.2, 127.9, 73.4; MS (APCI-MS², DMSO, HCTultra) m/z (Calcd 552.2; exp. 553.0, $M + H^+$, 100%), (Calcd 552.2; exp. 551, $M - H^+$, 100%), (HRMS, APCI-TOF, DMSO) m/z (Calcd 553.1844; meas. 553.1816, $M + H^+$).

(3*S*,4*S*,17*S*,18*S*)-Tetra-carbohydrazide cyclophane (18)

Prepared from (2*S*,3*S*)-2,3-dihydroxy dicarbohydrazide (**6**) and terephthaldehyde as a pale yellow solid precipitate, (99%); mp > 295 °C (decomp.); IR $\nu_{\max}/\text{cm}^{-1}$ 3263 (broad absorption band, OH and NH), 1667 (C=O, C=N); ^1H NMR (400 MHz, DMSO- d_6) δ_{H} 11.27 (4H, brs, NH), 8.43 (4H, brs, CH=N), 7.70 (8H, brs, ArH) 5.94 (4H, brs, OH), 4.49 (4H, brs, CH); ^{13}C NMR (100 MHz, DMSO- d_6) δ_{C} 169.0, 147.7, 136.2, 127.9, 73.4; MS (APCI-MS², DMSO, HCTultra) m/z (Calcd 552.2; exp. 553.0, $M + H^+$, 100%), (Calcd 552.2; exp. 550.9, $M - H^+$, 100%), (HRMS, APCI-TOF, DMSO) m/z (Calcd 553.1941; meas. 553.1954, $M + H^+$).

Acknowledgements

Financial support from Deutscher Akademischer Austausch Dienst (DAAD) is gratefully acknowledged. We thank Mr

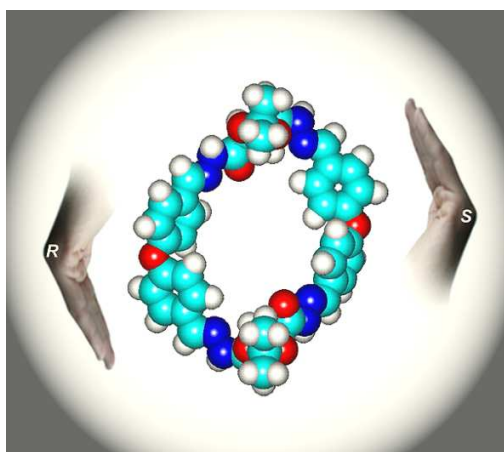
Indrajit Ghosh for assistant with Circular Dichroism measurements and Mrs Anja Müller for excellent technical assistant.

Notes and references

- 1 N. Kuhnert, G. Rossignolo and A. Lopez-Periago, *Org. Biomol. Chem.*, 2003, **1**, 1157.
- 2 N. Kuhnert, C. Patel and F. Jami, *Tetrahedron Lett.*, 2005, **46**, 7575.
- 3 M. Florea and W. Nau, *Angew. Chem., Int. Ed.*, 2011, **50**, 9338.
- 4 N. Saleh, M. Meetani, L. Al-Kaabi, I. Ghosh and W. Nau, *Supramol. Chem.*, 2011, **23**, 654.
- 5 C. Carvalho, V. Uzunova, J. da Silva, W. Nau and U. Pischel, *Chem. Commun.*, 2011, **47**, 8793.
- 6 A. Koner, I. Ghosh, N. Saleh and W. Nau, *Can. J. Chem.*, 2011, **89**, 139.
- 7 A. Koner, C. Márquez, M. Dickman and W. Nau, *Angew. Chem.*, 2011, **123**, 567.
- 8 H.-J. Schneider and A. Yatsimirsky, *Principles and Applications of Supramolecular Chemistry*, Wiley & Sons, Chichester, 1st ed., 2000.
- 9 J. Steed and J. Atwood, *Supramolecular Chemistry*, Wiley & Sons, Chichester, 1st ed., 2000.
- 10 G. Gokel and Y. Inoue, *Cation Binding by Macrocycles*, Marcel Dekker, New York and Basel, 1990.
- 11 A. Danil de Namor, R. Cleverley and M. Zapata-Ormachea, *Chem. Rev.*, 1998, **98**, 2495.
- 12 P. Beer, P. Gale and A. Philip, *Angew. Chem., Int. Ed.*, 2001, **40**, 486.
- 13 V. Balzani, A. Credi, F. Raymo and J. Stoddart, *Angew. Chem., Int. Ed.*, 2000, **39**, 3348.
- 14 N. Kuhnert and A. Le-Gresley, *Org. Biomol. Chem.*, 2005, **3**, 2175.
- 15 N. Kuhnert and A. Lopez-Periago, *Tetrahedron Lett.*, 2002, **43**, 3329.
- 16 N. Kuhnert, A. Lopez-Periago and G. Rossignolo, *Org. Biomol. Chem.*, 2005, **3**, 524.
- 17 N. Kuhnert, C. Straßnig and A. Lopez-Periago, *Tetrahedron: Asymmetry*, 2002, **13**, 123.
- 18 N. Kuhnert and B. Tang, *Tetrahedron Lett.*, 2006, **47**, 2985.
- 19 N. Kuhnert, D. Marsh and D. Nicolau, *Tetrahedron: Asymmetry*, 2007, **18**, 1648.
- 20 H. Nour, M. Matei, B. Bassil, U. Kortz and N. Kuhnert, *Org. Biomol. Chem.*, 2011, **9**, 3258.
- 21 G. Cousins, S.-A. Poulsen and J. Sanders, *Chem. Commun.*, 1999 (16), 1575.
- 22 J. Liu, K. West, C. Bondy and J. Sanders, *Org. Biomol. Chem.*, 2007, **5**, 778.
- 23 A. Dahlgren, J. Brånalt, I. Kvarnström, I. Nilsson, D. Musile and B. Samuelsson, *Bioorg. Med. Chem.*, 2002, **10**, 1567.
- 24 K. Vercruysse, D. Marecak, J. Marecek and G. Prestwich, *Bioconjugate Chem.*, 1997, **8**, 686.
- 25 C. Jakobsche, A. Choudhary, S. Miller and R. Raines, *J. Am. Chem. Soc.*, 2010, **132**, 6651.
- 26 M. Formica, V. Fusi, L. Giorgi, M. Micheloni, P. Palma and R. Pontellini, *Eur. J. Org. Chem.*, 2002, 402.
- 27 A. González-Álvarez, I. Alfonso, F. Lopez-Ortiz, A. Aguirre, S. Garcia-Granda and V. Gotor, *Eur. J. Org. Chem.*, 2004, 1117.
- 28 L. Wang, G.-T. Wang, X. Zhao, X.-K. Jiang and Z.-T. Li, *J. Org. Chem.*, 2011, **76**, 3531.
- 29 B.-Y. Lu, G.-J. Sun, J.-B. Lin, X.-K. Jiang, X. Zhao and Z.-T. Li, *Tetrahedron Lett.*, 2010, **51**, 3830.
- 30 *Molecular Modeling was Carried out Using HyperChem Software (Release 8.0)*. Hypercube, Inc., 1115 NW 4th Street, Gainesville, FL 32601, USA. Trial, version from <http://www.hypercube.com>
- 31 J. Stewart, *J. Comput. Chem.*, 1989, **10**, 221.
- 32 M. Kozáková, M. Buděšínský and J. Hodačová, *Synth. Commun.*, 2005, **35**, 161.

Novel synthesis of enantiomerically pure dioxaspiro[4.5]decane tetra-carbohydrazide cyclophane macrocycles

Hany F. Nour, Agnieszka Golon, Adam Le-Gresley and Nikolai Kuhnert*



Objectives of the work

After successful synthesis of the novel tetra-carbohydrazide cyclophanes, the second objective was introducing functionalities into the macrocyclic framework. As previously mentioned, tetra-carbohydrazide cyclophanes possess two aromatic side walls, which are connected together by dihydrazide dioxolane rings. Introducing functionalities into the aromatic side walls and keeping the size of the macrocycle large is difficult to be achieved. The dioxolane ring can be loaded with different functionalities by simple replacement of the basic methylene group. 1,1-Dimethoxycyclohexane reacted with (+)-diethyl L-tartrate and (–)-diethyl D-tartrate followed by *in situ* condensation with hydrazine monohydrate to give 1,4-dioxaspiro[4.5]decane-2,3-dicarbohydrazides. Similarly, commercially available (4*R*,5*R*)- and (4*S*,5*S*)-dimethyl-2,2-dimethyl-1,3-dioxolane-4,5-dicarboxylate reacted with hydrazine monohydrate to give the corresponding dihydrazides. The novel dihydrazides showed interesting self-assembly in the gas phase with formation of structurally unique associations of macrocycles. They underwent successfully [2+2]-cyclocondensation reactions with 4-(4-formylphenoxy)-benzaldehyde and 4,4'-diformyltriphenylamine to form eight novel functionalized tetra-carbohydrazide cyclophanes in almost quantitative yields. It is worth noting that the solubility of the new macrocycles in organic solvents (*i.e.*, DMF) has been dramatically improved after functionalization making them suitable for dynamic combinatorial chemistry (DCC) applications.

Novel synthesis of enantiomerically pure dioxaspiro[4.5]decane tetra-carbohydrazide cyclophane macrocycles

Hany F. Nour,^[a] Agnieszka Golon,^[a] Adam Le-Gresley,^[b] and Nikolai Kuhnert*^[a]

Abstract: This paper describes a novel highly efficient synthetic approach to substituted enantiomerically pure tetra-carbohydrazide cyclophane macrocycles in [2+2]-cyclocondensation reactions of aromatic dialdehydes and substituted chiral dihydrazides. The novel macrocycles were obtained in quantitative yields at relatively high concentration of the reactants without using external templates or dehydrating agents. Self-

assembly of the dihydrazide building blocks in the gas phase to dimeric, trimeric and tetrameric macrocycles mediated by intramolecular hydrogen bonding was recognised by ESI-TOF MS. The compounds show a dynamic behaviour in solution, which has been rationalized in terms of an unprecedented conformational interconversion between two conformers one stabilised by intramolecular hydrogen bonding and

π - π stacking interactions. Structures of the novel macrocycles were fully assigned and characterised by different spectroscopic techniques, such as ¹H-NMR, ¹³C-NMR, FT-IR, and ESI- or APCI-TOF mass spectrometry.

Keywords: tetra-carbohydrazide cyclophane • [2+2]-cyclocondensation • macrocycle • self-assembly • dicarbohydrazide

Introduction

Over the past few decades supramolecular chemistry has been considered a stupendous field of endeavours. Macrocycles obtained in [n+n]-cyclocondensation reactions have attracted considerable and growing attention due to their relative ease of synthesis and potential applications in molecular recognition.^{1–8} Unlike calix[n]arenes,^{9,10} cyclodextrins,¹¹ cucurbiturils^{12,13} and crown ethers,¹⁴ macrocycles with reversible bond formation are of particular interest for different supramolecular and dynamic combinatorial library applications (DCL).¹ Inspired by the work initially done by Gawróński *et al.*,¹⁵ we reported on significant extensions for the synthesis of chiral trianglimine macrocycles having different chemical functionalities and variable cavity sizes.^{16–23} We recently investigated the mechanism and dynamic reversibility of trianglimine formation in solution using real-time ESI-TOF mass spectrometry and proved that trianglimine formation is indeed fully reversible.²⁴ Trianglimines formed in [3+3]-cyclocondensation reactions showed their promise in supramolecular chemistry as organo-catalysts and chiral hosts for carboxylic and amino acid derivatives.^{22,25}

However their low solubility in water or organic solvents is still a current obstacle. In addition, their reported binding constants with organic guests did not exceed the mM concentration range. To this end, there is a growing demand for synthesizing new supramolecular architectures, which combine structure diversity, ease of preparation, recognition capability and most importantly sufficient solubility in water and organic solvents. Improving the solubility can be achieved by introducing polar functionalities into the macrocyclic structure. In an attempt to synthesize novel macrocycles with improved solubility, the reactivity of substituted dihydrazides, obtained from tartaric acid, to [2+2]-cyclocondensation reactions with aromatic *bis*-aldehydes was assessed. In this study the efficiency of the [2+2]-cyclocondensation reaction to form *spiro*-tetracarbohydrazide cyclophane macrocycles is demonstrated.

Results and Discussion

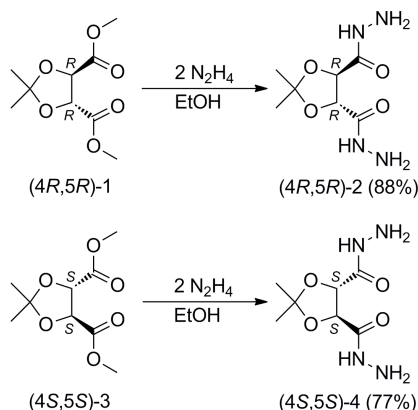
In continuation to our work with tetracarbohydrazide cyclophane macrocycles,²⁴ we report in this paper a novel highly efficient synthetic approach for preparing multigram quantities of substituted enantiomerically pure tetracarbohydrazide macrocycles based on [2+2]-cyclocondensation reactions of chiral dicarbohydrazides and aromatic *bis*-aldehydes. Strategies for the synthesis of macrocycles involve either applying high dilution conditions to prevent polymerization or using a template, which acts by gathering the reactants to a given predictable geometry.^{26–30} Synthesis of macrocycles at relatively high concentration of the reactants, is uncommon and favour formation of polymeric or undesired by-products. The novel macrocycles described here were quantitatively synthesized at 88–99% yield in a one-pot [2+2]-cyclocondensation reaction in which four new bonds form without using dehydrating agents or external templates.

[a] Prof. Dr. Nikolai Kuhnert, Hany F. Nour, Agnieszka Golon
Organic and Analytical Chemistry Department
School of Engineering and Science, Jacobs University Bremen
Campus ring 1, P. O. Box. 750 561, 28725 Bremen, Germany, Tel: +49
421 200 3120, Fax: (+) 49 421 200 3229.
E-mail: n.kuhnert@jacobs-university.de.

[b] Dr. Adam Le Gresley
Pharmacy and Chemistry
Faculty of Science, Engineering and Computing, Kingston University, UK

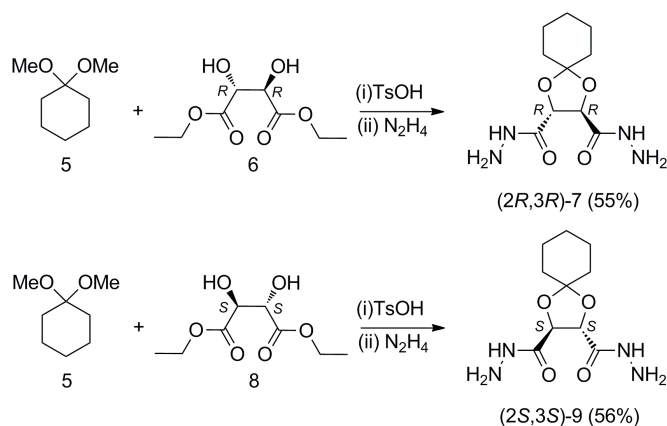
Supporting information for this article (ESI- and APCI-MS, ¹H-NMR, ¹³C-NMR and proposed fragmentation mechanisms) is available on the WWW under <http://www.chemeurj.org/> or from the author.

(4*R*,5*R*)- and (4*S*,5*S*)-dimethyl-2,2-dimethyl-1,3-dioxolane-4,5-dicarboxylate **1** and **3** reacted with hydrazine hydrate in absolute ethanol to afford the corresponding dicarbohydrazides **2** and **4** in good yields (Scheme 1).



Scheme 1. Synthetic route to chiral dicarbohydrazides **2** and **4**.

Similarly, chiral dihydrazides **7** and **9** were prepared from (+)-diethyl L-tartrate **6** and (–)-diethyl D-tartrate **8**, respectively by reacting with 1,1-dimethoxycyclohexane **5** as shown in Scheme 2. Structures of dicarbohydrazides **2**, **4**, **7** and **9**, which constitute the building blocks of the novel macrocycles, were fully elucidated using various spectroscopic techniques.



Scheme 2. Synthetic route to chiral dicarbohydrazides **7** and **9**.

^1H -NMR spectrum for (*i.e.*, dicarbohydrazide **2**) showed broad signals at δ 9.3, 4.4, 4.2 and 1.3 ppm corresponding to (NH), (CH), (NH_2) and (CH_3), respectively. ^{13}C -NMR spectrum showed four signals at δ 167.8, 112.2, 77.2 and 26.6 ppm corresponding to (C=O), quaternary C-atom, (CH) and (CH_3), respectively. FT-IR spectrum showed a strong absorption band at $\tilde{\nu}$ 1660 cm^{-1} corresponding to the stretching vibration of the carbonyl group. It showed also weak absorption bands at $\tilde{\nu}$ 3316 cm^{-1} corresponding to the primary and secondary amino moieties. ESI-TOF MS showed the expected pseudo-molecular ion peak at 241.0900 Da ($\text{M}+\text{Na}^+$). Molecular modeling at the MM+ level showed that the novel dicarbohydrazides adopt conformations in which the carbonyl groups are *anti*-oriented to each other. These conformations are stabilised by strong $n \rightarrow \pi^*$ interaction and intramolecular hydrogen bonding ($\text{C}=\text{O} \cdots \text{HN}$) (Figure 1).³¹

We next examined the behaviour of the novel dicarbohydrazides towards the cyclocondensation reaction with aromatic dialdehydes.

The reaction conditions were tuned in terms of stoichiometries and concentration of the reactants to form selectively the [2+2]-macrocycles.³²

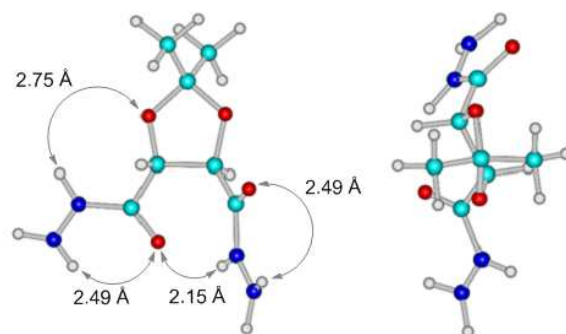


Figure 1. Bird's-eye view for the computed structure of chiral dicarbohydrazides **2** and **4** using MM+ method and a Polak-Ribiere conjugate gradient with rms < 0.01 Kcal.mol^{-1} .

The novel hydrazides showed fascinating molecular self-assembly in the gas phase as confirmed by ESI-TOF MS (See supporting information and table 1). Dicarbohydrazides **2**, **4**, **7** and **9** assembled to hydrogen-bonded dimeric, sodium adduct of dimeric and trimeric macrocycles. Protonated molecular ions $[\text{M}+\text{H}]^+$ for tetrameric macrocycles were observed only with dicarbohydrazides **7** and **9**. Molecular modeling studies at the MM+ and AMBER force fields were conducted to simulate such interesting interactions. Energy-minimised structures are shown in Figure 2. To the best of our knowledge self-assembly of four molecules in the gas phase has not been reported yet.

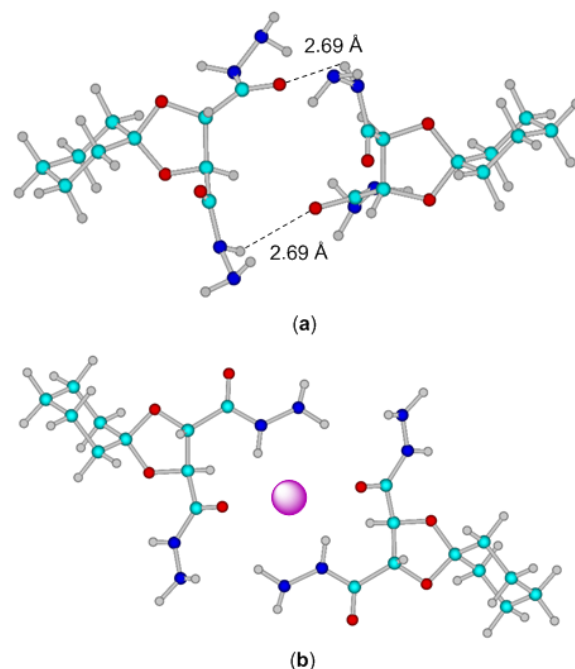


Figure 2. Molecular modeling simulation for self-assembly of chiral dicarbohydrazides **7** and **9** using MM+, AMBER force field methods and a Polak-Ribiere conjugate gradient with rms < 0.01 Kcal.mol^{-1} . (a) Self-assembled two molecules of **7** or **9** and (b) macrocycle (a) hosting Na^+ ion.

(4*R*,5*R*)- and (4*S*,5*S*)-2,2-dimethyl-1,3-dioxolane-4,5-dicarbohydrazide **2** and **4** reacted with 4-(4-formylphenoxy)-benzaldehyde and 4,4'-diformyltriphenylamine to yield macrocycles **10–13** in quantitative yields 94–99%. Spiro-macrocycles **14–17** were synthesized as similar way as previously described from (2*R*,3*R*)- and (2*S*,3*S*)-1,4-dioxaspiro[4.5]decane-2,3-dicarbohydrazide **7** and **9** (Scheme 3).

Structures of the novel macrocycles were fully assigned using various spectroscopic techniques and the chirality was confirmed by CD-spectroscopy. APCI-TOF MS for macrocycle **13** showed the expected molecular ion peak ($M+Na^+$) at 989.3752 Da (Figure 3). FT-IR spectrum showed a strong absorption band at $\tilde{\nu}$ 1681 cm^{-1} corresponding to the stretching vibration of the ν C=O and ν C=N.

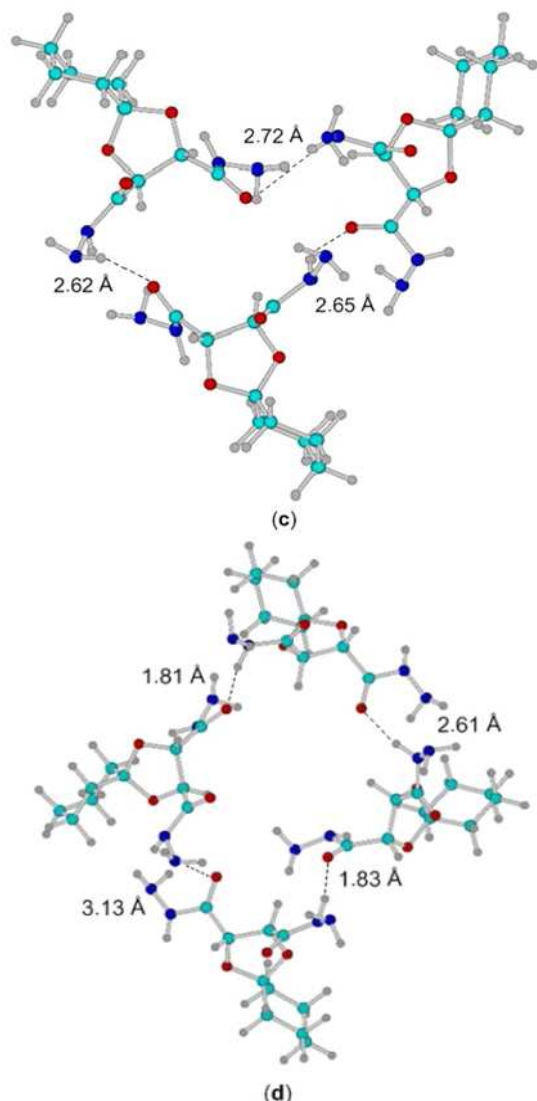
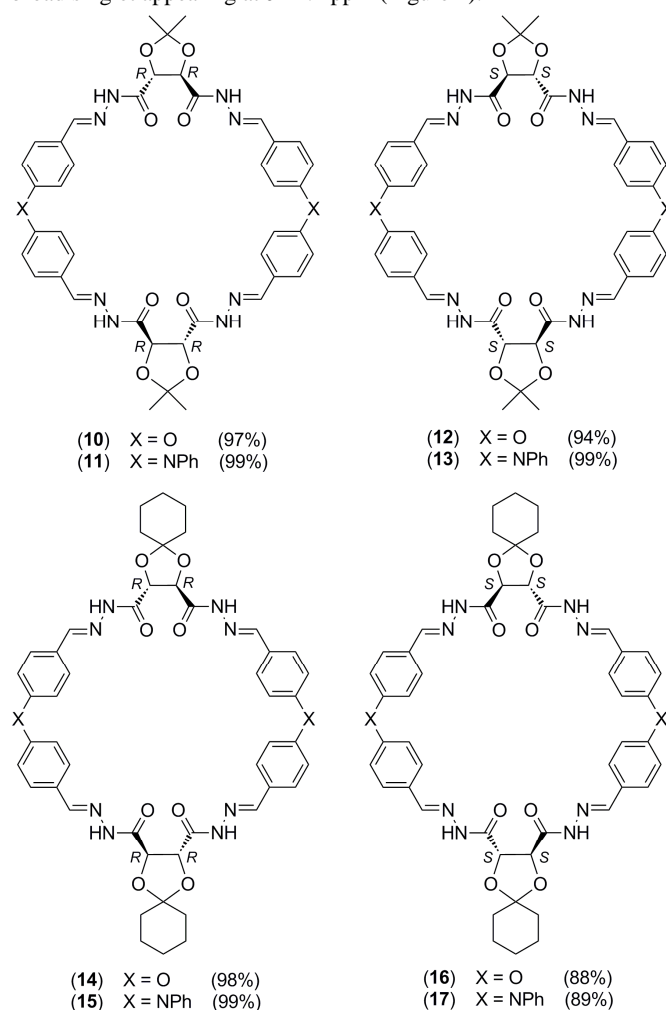


Figure 2. Continued, (c) self-assembled three molecules of **7** or **9** and (d) self-assembled four molecules of **7** or **9**.

^1H -NMR spectra for the novel macrocycles at ambient temperature in DMSO-d_6 and DMF-d_7 showed broad signals suggesting conformational flexibility in solution. ^1H -NMR spectrum (*i.e.*, for macrocycle **10**) in DMSO-d_6 showed a broad signal at δ 11.5–11.6 ppm with an integration of four ($4 \times \text{NH}$). It showed also four broad singlets at δ 8.3, 8.0, 7.9 and a signal at 7.5–7.7 ppm overlapping with the aromatic protons corresponding to four non-equivalent azomethine protons ($4 \times \text{HC=N}$). In DMF-d_7 , the signal corresponding to the (NH) group splits into two broad signals appearing at δ 11.4 and 11.6 ppm, each signal integrated with two ($4 \times \text{NH}$). In addition, four broad signals appeared at δ 8.5, 8.2, 8.1 and 7.9 ppm corresponding to four non-symmetrical azomethine protons ($4 \times \text{HC=N}$). In order to characterise the behaviour of the novel macrocycles in solution, we performed VT-NMR study for macrocycle **10**. VT-NMR was performed from 303 to 393 K in

DMF-d_7 . The two broad signals appearing at δ 11.4 and 11.6 ppm corresponding to the four (NH) protons coalesced at 373 K to a broad singlet appearing at δ 11.1 ppm (Figure 4).



Scheme 3. [2+2]-Cyclocondensation products **10–17**.

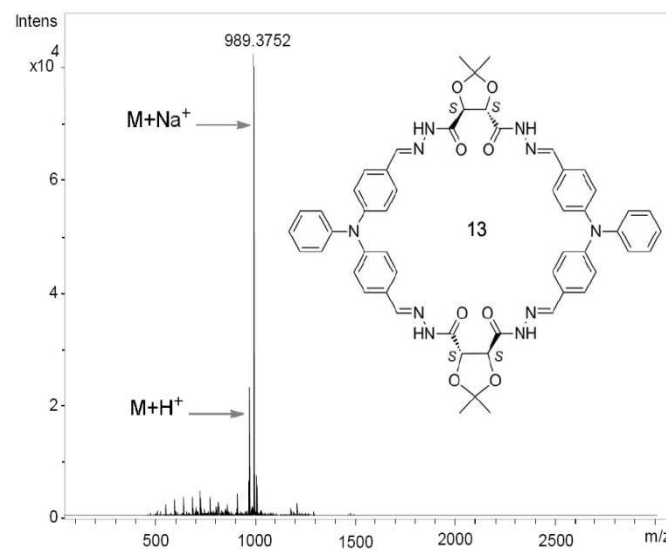


Figure 3. APCI-TOF MS spectrum for macrocycle **13** (from DMSO).

Cooling the NMR to 298 K yields the same spectrum as first recorded, which illustrate the reversibility of the process. We suggest

that two distinct conformational isomers could result from intramolecular hydrogen bonding ($C=O\cdots HN$) and π - π stacking interactions.

Table 1. ESI- and APCI-TOF MS data for the novel macrocycles

Cpd	Molecular Formula	Calcd. m/z	Meas. m/z	Error (ppm)	Yield (%)
2	$C_7H_{14}N_4O_4$	241.0907	241.0900	3.0	88
4	$C_7H_{14}N_4O_4$	241.0907	241.0900	3.1	77
7	$C_{20}H_{36}N_8O_8$	539.2548	539.2572	- 4.4	55
9 ^[a]	$C_{20}H_{36}N_8O_8$	539.2545	539.2550	- 0.3	56
10	$C_{42}H_{40}N_8O_{10}$	839.2760	839.2795	- 4.3	97
11	$C_{34}H_{50}N_{10}O_8$	989.3705	989.3668	3.8	99
12	$C_{42}H_{40}N_8O_{10}$	839.2760	839.2744	1.9	94
13	$C_{54}H_{50}N_{10}O_8$	989.3933	989.3752	- 4.8	99
14	$C_{48}H_{48}N_8O_{10}$	897.3566	897.3526	4.5	98
15	$C_{60}H_{58}N_{10}O_8$	1047.4512	1047.4521	- 0.9	99
16	$C_{48}H_{48}N_8O_{10}$	897.3566	897.3539	3.0	88
17	$C_{60}H_{58}N_{10}O_8$	1047.4512	1047.4509	0.3	89
9 ^[b]	$C_{20}H_{36}N_8O_8$	517.2729	517.2706	4.3	-
9 ^[c]	$C_{30}H_{54}N_{12}O_{12}$	775.4057	775.4022	4.5	-
9 ^[d]	$C_{40}H_{72}N_{16}O_{16}$	1033.5385	1033.5420	- 3.4	-

[a], [b], [c] and [d] are self-assembled macrocycles (a-d).

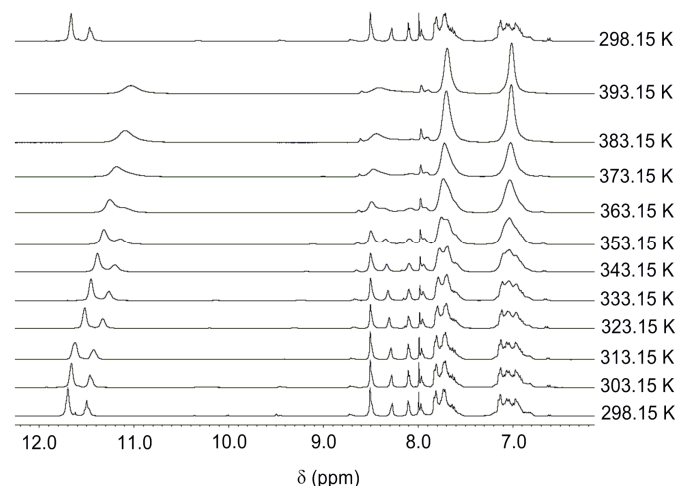


Figure 4. Stacked 1H -NMR spectra for macrocycle **10** showing changes in δ in response to increased temperature, 400 MHz in $DMF-d_7$.

The change in chemical shifts in response to increased temperature can be graphically visualised by plotting the values of chemical shift (δ in ppm) versus temperature (K) as shown in figure 5. It can be inferred that intramolecular hydrogen bonds break upon heating, resulting in upfield shift of the associated (NH) protons.

Our hypothesis of conformational isomers is further supported by 2D-NMR experiments. 2D-ROESY spectrum for macrocycle **10** showed through space interactions of two (NH) protons with two azomethine protons ($HC=N$) and two methine protons (See supporting information). The other (NH) protons showed through space interactions only with two azomethine protons ($HC=N$), while no interactions were observed with methine protons. In order to further understand the nature of the intramolecular hydrogen bonding, we performed several molecular modeling studies. Data from 2D-ROESY experiments were used for subsequent structure modeling

calculations. Structures of the novel macrocycles (*i.e.*, macrocycle **10**) were energy minimised using HyperChem software (Release 8.0) as shown in Figure 6.³³

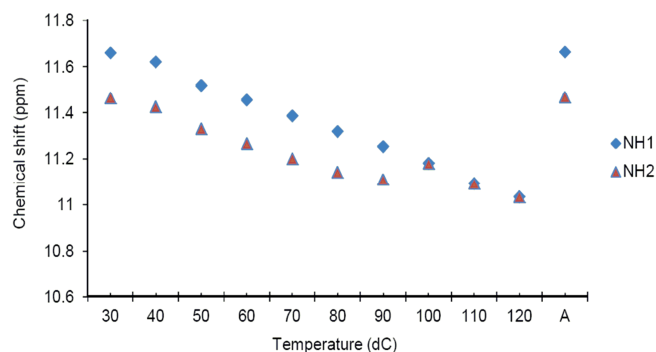


Figure 5. Graphical representation showing changes of chemical shift in response to increased temperature, (A) 1H -NMR spectrum was recorded at ambient temperature after cooling the sample.

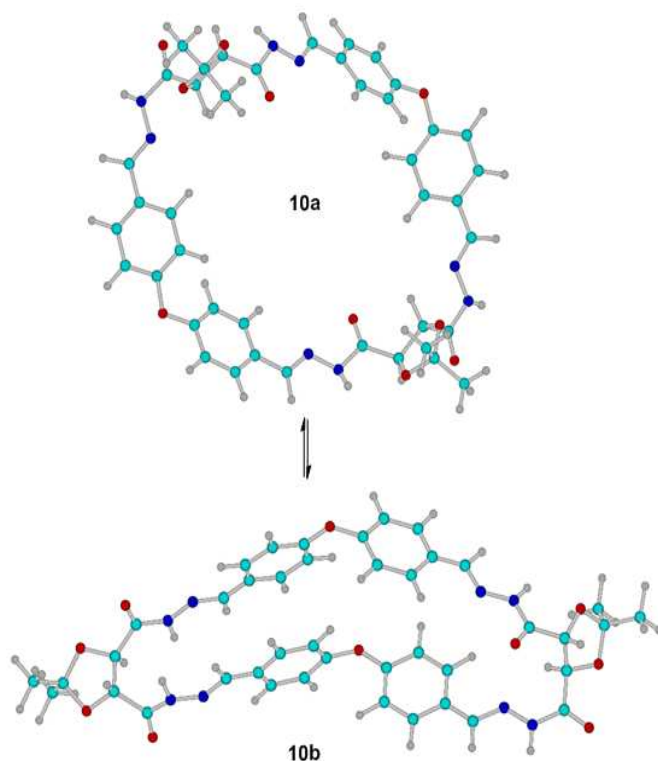


Figure 6. Computed structures for macrocycle **10** at the AMBER and PM3 levels using a Polak-Ribiere conjugate gradient with rms < 0.01 Kcal.mol⁻¹.

The molecular structures were optimised at the AMBER and PM3 levels using the Polak-Ribiere algorithm until the root-mean square (RMS) gradient was 0.01 Kcal.mol⁻¹ or less. The results of molecular modeling are in good agreement with the data from 2D-ROESY experiments. In solution, macrocycle **10** assumes conformation **10b** which is highly stabilised by intramolecular hydrogen bonding and π - π stacking interactions. The chirality of the novel macrocycles and their precursors was confirmed by CD-spectroscopy as shown in figure 6. *All-R* macrocycle **11** shows for example a positive Cotton effect with a zero intercept at around 370 nm, whereas its enantiomeric counterpart *all-S* **13** shows a negative Cotton effect. Similar to trianglimines the observed Cotton effect is a consequence of the interaction of the two aromatic chromophores

within the macrocycle (Figure 7).

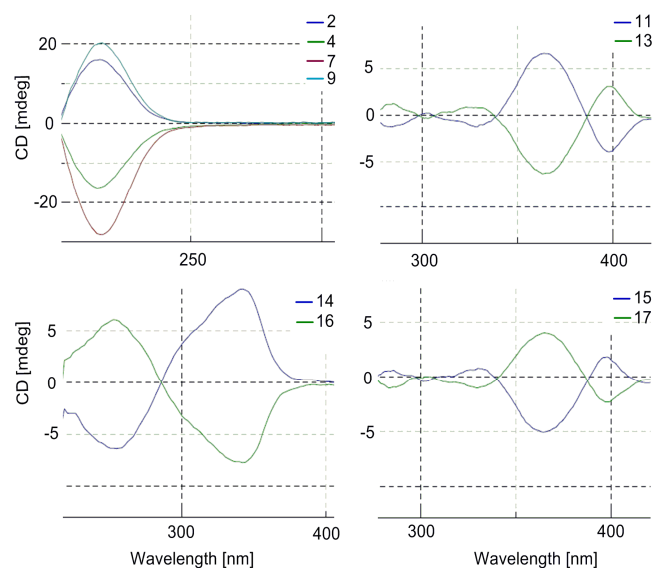


Figure 7. Circular Dichroism spectra for the novel macrocycles and their precursors.

Conclusion

In summary, we have developed a versatile methodology for the synthesis of a novel class of chiral non-racemic tetra-carbohydrazone cyclophane macrocycles. Both (*R*) and (*S*) enantiomers can be readily synthesised in short reaction steps, high purity and quantitative yields. The novel macrocycles can be functionalized by simple choice of the target ketone or diketal to be protected. This can lead to the synthesis of supramolecular architectures with fascinating structures and improved solubility. In addition, the dicarbohydrazone precursors showed interesting molecular self-assembly in the gas phase to form hydrogen bonded macrocycles, which has been confirmed by ESI-TOF MS. Further studies aimed at assessing the molecular recognition properties of the novel macrocycles are under investigation.

Experimental Section

All the reagents used for the reactions were purchased from Sigma-Aldrich, Applchem or Flucka (Germany) and were used as obtained. Whenever possible the reactions were monitored by thin layer chromatography (TLC). TLC was performed on Macherey-Nagel aluminium-backed plates pre-coated with silica gel 60 (UV₂₅₄). Melting points were determined in open capillaries using a Buechl B-545 melting point apparatus and are not corrected. Infrared spectra were determined using a Vector-33 Bruker FT-IR spectrometer. The samples were measured directly as solids or oils; $\tilde{\nu}_{\text{max}}$ values were expressed in cm^{-1} and were given for the main absorption bands. ^1H -NMR and ^{13}C -NMR spectra were acquired on a JEOL ECX-400 spectrometer operating at 400 MHz for ^1H -NMR and 100 MHz for ^{13}C -NMR in [D₆]DMSO or [D₇]DMF using a 5 mm probe. The chemical shifts (δ) are reported in parts per million and were referenced to the residual solvent peak. The following abbreviations are used: s, singlet; m, multiplet; br, broad signal. Mass spectra were recorded using Bruker HCTultra and high resolution Bruker Daltonics microTOF instruments from DMSO, DMF and acetonitrile or water using the positive electrospray ionisation ESI- and APCI-MS modes. Calibration was carried out using a 0.1 M solution of sodium formate in the enhanced quadratic mode prior to each experimental run. The results of measurements were processed using Compass 1.3 data analysis software for a Bruker Daltonics time-of-flight mass spectrometer (microTOF). Molecular modeling was carried out with HyperChem

(Release 8.0) software using PM3, AMBER and MM+ methods and no influence of solvents was taken into account in the calculations.^{33,34} Circular Dichroism (CD) measurements were carried out using Jasco-J-810 Spectropolarimeter in H₂O and DMSO.

(4*R*,5*R*)-2,2-dimethyl-1,3-dioxolane-4,5-dicarbohydrazone 2: To a stirred solution of (4*R*,5*R*)-dimethyl-2,2-dimethyl-1,3-dioxolane-4,5-dicarboxylate **1** (4.76 g, 21.83 mmol) in absolute ethanol (20 mL) was added hydrazine monohydrate (2.3 mL, 72.76 mmol) and the mixture was refluxed for 12 h. The solvent was evaporated under vacuum and the resulting oil was partitioned between ethyl acetate and water (10 mL). To the water phase was added ethanol (200 mL) and anhydrous Na₂SO₄. The solvent was filtered off and evaporated under vacuum to afford the title product as a white gummy material (4.21 g, 88%). ^1H NMR (400 MHz, [D₆]DMSO, 25 °C, TMS): δ = 9.3 (brs, 2H; NH), 4.4 (brs, 2H; CH), 4.2 (brs, 4H; NH₂), 1.3 ppm (s, 6H; CH₃); ^{13}C NMR (100 MHz, [D₆]DMSO, 25 °C, TMS): δ = 167.8, 112.2, 77.2, 26.6 ppm; FT-IR: $\tilde{\nu}$ = 3316 (NH and NH₂), 1660 cm^{-1} (C[dbond]O); HRMS (ESI-): m/z calcd. for [C₇H₁₄N₄O₄+ Na⁺]: 241.0907 [M+ Na⁺]; found: 241.0900.

(4*S*,5*S*)-2,2-dimethyl-1,3-dioxolane-4,5-dicarbohydrazone 4: To a stirred solution of (4*S*,5*S*)-dimethyl-2,2-dimethyl-1,3-dioxolane-4,5-dicarboxylate **3** (5.8 g, 26.60 mmol) in absolute ethanol (20 mL) was added hydrazine monohydrate (2.8 mL, 88.68 mmol) and the mixture was refluxed for 12 h. The solvent was evaporated under vacuum and the resulting oil was partitioned between ethyl acetate and water (10 mL). To the water phase was added ethanol (200 mL) and anhydrous Na₂SO₄. The solvent was filtered off and evaporated under vacuum to afford the title product as a white gummy material (4.50 g, 77%). ^1H NMR (400 MHz, [D₆]DMSO, 25 °C, TMS): δ = 9.3 (brs, 2H; NH), 4.4 (brs, 2H; CH), 4.3 (brs, 4H; NH₂), 1.3 ppm (s, 6H; CH₃); ^{13}C NMR (100 MHz, [D₆]DMSO, 25 °C, TMS): δ = 167.8, 112.2, 77.2, 26.6 ppm; FT-IR: $\tilde{\nu}$ = 3316 (NH and NH₂), 1660 cm^{-1} (C[dbond]O); HRMS (ESI-): m/z calcd. for [C₇H₁₄N₄O₄+Na⁺]: 241.0907 [M+ Na⁺]; found: 241.0900.

(2*R*,3*R*)-1,4-dioxaspiro-[4.5]-decane-2,3-dicarbohydrazone 7: To a stirred solution of (+)-diethyl L-tartrate (7.5 mL, 44 mmol) in toluene (150 mL) were added 1,1-dimethoxycyclohexane (10 mL, 65.8 mmol) and PTSA (103 mg, 0.54 mmol). The flask was fitted with a Soxhlet extractor, reflux condenser and a thimble containing freshly activated 4 Å molecular sieves (15 g). The mixture was refluxed for 7h, during which the thimble was recharged with fresh molecular sieves twice. The reaction mixture was neutralised with anhydrous sodium bicarbonate and the suspension was filtered off. The solvent was evaporated under vacuum and the residue was partitioned between ethyl acetate and water, washed with saturated sodium bicarbonate (70 mL), brine (70 mL) and dried with Na₂SO₄. The solvent was filtered off and evaporated under vacuum. The crude oil (11.17 g) was dissolved without further purification in absolute ethanol (50 mL) and hydrazine monohydrate was added (4.4 mL, 140 mmol). The mixture was refluxed for 7 h and the solvent was evaporated under vacuum. The residue was dissolved in water (10 mL) and extracted with ethyl acetate (3×50 mL). The water extract was dissolved in ethanol (200 mL), dried with Na₂SO₄ and evaporated under vacuum to afford the title product as pale yellow gummy material (5.58 g, 55%). ^1H NMR (400 MHz, [D₆]DMSO, 25 °C, TMS): δ = 9.2 (brs, 2H; NH), 4.4 (brs, 2H; CH), 4.3 (brs, 4H; NH₂), 1.4-1.5 (m, 8H; CH₂), 1.2 ppm (m, 2H; CH₂); ^{13}C NMR (100 MHz, [D₆]DMSO, 25 °C, TMS): δ = 167.9, 112.9, 76.9, 35.7, 24.9, 23.8 ppm; FT-IR: $\tilde{\nu}$ = 3313 (NH and NH₂), 1666 cm^{-1} (C[dbond]O); HRMS (ESI-): m/z calcd. for [C₁₀H₁₈N₄O₄+Na⁺]: 281.1220 [M+ Na⁺]; found: 281.1231.

(2*S*,3*S*)-1,4-dioxaspiro-[4.5]-decane-2,3-dicarbohydrazone 9: To a stirred solution of (-)-diethyl D-tartrate (7.5 mL, 44 mmol) in toluene (150 mL) were added 1,1-dimethoxycyclohexane (10 mL, 65.8 mmol) and PTSA (103 mg, 0.54 mmol). The flask was fitted with a Soxhlet extractor, reflux condenser and a thimble containing freshly activated 4 Å molecular sieves (15 g). The mixture was refluxed for 7h, during which

the thimble was recharged with fresh molecular sieves twice. The reaction mixture was neutralised with anhydrous sodium hydrogen carbonate and the suspension was filtered off. The solvent was evaporated under vacuum and the residue was partitioned between ethyl acetate and water, washed with saturated sodium bicarbonate (70 mL), brine (70 mL) and dried with Na₂SO₄. The solvent was filtered off and evaporated under vacuum. The crude oil (11.42 g) was dissolved without further purification in absolute ethanol (50 mL) and hydrazine monohydrate was added (6.3 mL, 201 mmol). The mixture was refluxed for 7 h and the solvent was evaporated under vacuum. The residue was dissolved in water (10 mL) and extracted with ethylacetate (3×50 mL). The water extract was dissolved in ethanol (200 mL), dried with Na₂SO₄ and evaporated under vacuum to afford the title product as pale yellow gummy material (5.97 g, 56%). ¹H NMR (400 MHz, [D₆]DMSO, 25 °C, TMS): δ = 9.3 (brs, 2H; NH), 4.4 (brs, 2H; CH), 4.0 (brs, 4H; NH₂), 1.4-1.6 (m, 8H; CH₂), 1.2-1.3 ppm (m, 2H; CH₂); ¹³C NMR (100 MHz, [D₆]DMSO, 25 °C, TMS): δ = 167.8, 112.8, 76.9, 35.8, 25.0, 23.8 ppm; FT-IR: $\tilde{\nu}$ = 3316 (NH and NH₂), 1666 cm⁻¹ (C[dbond]O); HRMS (ESI-): m/z calcd. for [C₁₀H₁₈N₄O₄+Na⁺]: 539.2545 [2M+ Na⁺]; found: 539.2550.

General procedures for the synthesis of tetra-carbohydrazide cyclophanes 10-17:

To a stirred solution of dicarbohydrazide **2**, **4**, **7** or **9** (1.2 mmol) and the corresponding dialdehyde (1 mmol) in MeOH (< 0.05 M) was added two drops of AcOH. The reaction mixture was refluxed for 7 h. The precipitate was filtered off, washed with water, chloroform and dried to give the corresponding macrocycle in a quantitative yield.

(3R,4R,16R,17R)-Tetra-carbohydrazide cyclophane 10: Prepared from (4R,5R)-dimethyl-2,2-dimethyl-1,3-dioxolane-4,5-dicarboxylate **2** and 4-(4-formylphenoxy)-benzaldehyde as a white precipitate (97%). M.p. > 310 °C. ¹H NMR (400 MHz, [D₆]DMSO, 25 °C, TMS): δ = 11.5-11.6 (m, 4H; NH), 8.3 (brs, 1H; CH=N), 8.0 (brs, 1H; CH=N), 7.9 (brs, 1H; CH=N), 7.5-7.7 (m, 9H; CH=N and ArH), 6.6-7.0 (m, 8H; ArH), 5.4 (brs, 2H; CH), 4.7 (brs, 1H; CH), 4.5 (brs, 1H; CH), 1.40-1.45 ppm (m, 12H; CH₃); ¹H NMR (400 MHz, [D₇]DMF, 25 °C, TMS): δ = 11.6 (brs, 2H; NH), 11.5 (brs, 2H; NH), 8.5 (brs, 1H; CH=N), 8.2 (brs, 1H; CH=N), 8.1 (brs, 1H; CH=N), 7.9 (brs, 1H; CH=N), 7.5-7.8 (m, 8H; ArH), 6.8-7.1 (m, 8H; ArH), 5.6 (brs, 2H; CH), 4.9 (brs, 1H; CH), 4.8 (brs, 1H; CH), 1.4-1.5 ppm (m, 12H; CH₃); ¹³C NMR (100 MHz, [D₇]DMF, 25 °C, TMS): δ = 170.5, 165.8, 158.4, 148.4, 144.2, 129.5, 119.2, 113.0, 77.8, 25.9 ppm; FT-IR: $\tilde{\nu}$ = 3208 (NH and NH₂), 1681 cm⁻¹ (C[dbond]O and C[dbond]N); HRMS (APCI-): m/z calcd. for [C₄₂H₄₀N₈O₁₀+Na⁺]: 839.2760 [M+ Na⁺]; found: 839.2795.

(3R,4R,16R,17R)-Tetra-carbohydrazide cyclophane 11: Prepared from (4R,5R)-dimethyl-2,2-dimethyl-1,3-dioxolane-4,5-dicarboxylate **2** and 4,4'-diformyltriphenylamine as a yellow precipitate (99%). M.p. > 325 °C. ¹H NMR (400 MHz, [D₆]DMSO, 25 °C, TMS): δ = 11.5 (brs, 4H; NH), 8.2 (brs, 1H; CH=N), 7.9 (brs, 1H; CH=N), 7.8 (brs, 1H; CH=N), 7.5 (brs, 1H; CH=N), 7.2-7.4 (m, 8H; ArH), 6.8-7.0 (m, 8H; ArH), 6.5-6.8 (m, 10H; ArH), 5.4 (brs, 2H; CH), 4.7 (brs, 1H; CH), 4.5 (brs, 1H; CH), 1.3-1.4 ppm (m, 12H; CH₃); ¹³C NMR (100 MHz, [D₆]DMSO, 25 °C, TMS): δ = 170.6, 165.3, 148.7, 146.5, 144.4, 130.4, 129.1, 126.2, 123.2, 112.8, 77.5, 26.6 ppm; FT-IR: $\tilde{\nu}$ = 3212 (NH and NH₂), 1681 cm⁻¹ (C[dbond]O and C[dbond]N); HRMS (APCI-): m/z calcd. for [C₅₄H₅₀N₁₀O₈+Na⁺]: 989.3705 [M+ Na⁺]; found: 989.3668.

(3S,4S,16S,17S)-Tetra-carbohydrazide cyclophane 12: Prepared from (4S,5S)-dimethyl-2,2-dimethyl-1,3-dioxolane-4,5-dicarboxylate **4** and 4-(4-formylphenoxy)-benzaldehyde as a white precipitate (94%). M.p. > 300 °C. ¹H NMR (400 MHz, [D₆]DMSO, 25 °C, TMS): δ = 11.6 (m, 4H; NH), 8.3 (brs, 1H; CH=N), 8.0 (brs, 1H; CH=N), 7.9 (brs, 1H; CH=N), 7.5-7.7 (m, 9H; CH=N and ArH), 6.6-7.0 (m, 8H; ArH), 5.4 (brs, 2H; CH), 4.7 (brs, 1H; CH), 4.5 (brs, 1H; CH), 1.3-1.4 ppm (m, 12H; CH₃); ¹³C NMR (100 MHz, [D₆]DMSO, 25 °C, TMS): δ = 170.6, 165.5, 158.2, 148.5, 144.3, 129.7, 119.4, 112.9, 77.5, 26.6 ppm; FT-IR: $\tilde{\nu}$ = 3211 (NH and NH₂), 1681 cm⁻¹ (C[dbond]O and C[dbond]N); HRMS (APCI-): m/z calcd. for [C₄₂H₄₀N₈O₁₀+Na⁺]: 839.2760 [M+ Na⁺]; found: 839.2744.

(3S,4S,16S,17S)-Tetra-carbohydrazide cyclophane 13: Prepared from (4S,5S)-dimethyl-2,2-dimethyl-1,3-dioxolane-4,5-dicarboxylate **4** and 4,4'-diformyltriphenylamine as a yellow precipitate (99%). M.p. > 325 °C. ¹H NMR (400 MHz, [D₆]DMSO, 25 °C, TMS): δ = 11.5 (brs, 4H; NH), 8.2 (brs, 1H; CH=N), 7.9 (brs, 1H; CH=N), 7.8 (brs, 1H; CH=N), 7.5 (brs, 1H; CH=N), 7.2-7.4 (m, 8H; ArH), 7.0-7.2 (m, 8H; ArH), 6.5-6.8 (m, 10H; ArH), 5.4 (brs, 2H; CH), 4.7 (brs, 1H; CH), 4.5 (brs, 1H; CH), 1.3-1.4 ppm (m, 12H; CH₃); ¹³C NMR (100 MHz, [D₆]DMSO, 25 °C, TMS): δ = 170.6, 165.3, 148.7, 146.3, 144.4, 130.4, 129.1, 126.1, 123.5, 112.9, 77.5, 26.6 ppm; FT-IR: $\tilde{\nu}$ = 3212 (NH and NH₂), 1681 cm⁻¹ (C[dbond]O and C[dbond]N); HRMS (APCI-): m/z calcd. for [C₅₄H₅₀N₁₀O₈+Na⁺]: 989.3933 [M+ Na⁺]; found: 989.3752.

(3R,4R,16R,17R)-Tetra-carbohydrazide cyclophane 14: Prepared from (2R,3R)-1,4-dioxaspiro-[4.5]-decane-2,3-dicarbohydrazide **7** and 4-(4-formylphenoxy)-benzaldehyde as a white precipitate (98%). M.p. > 320 °C. ¹H NMR (400 MHz, [D₆]DMSO, 25 °C, TMS): δ = 11.6 (m, 4H; NH), 8.3 (brs, 1H; CH=N), 8.0 (brs, 1H; CH=N), 7.8 (brs, 1H; CH=N), 7.4-7.7 (m, 9H; CH=N and ArH), 6.6-7.0 (m, 8H; ArH), 5.4 (brs, 2H; CH), 4.7 (brs, 1H; CH), 4.5 (brs, 1H; CH), 1.6 (brs, 8H; CH₂), 1.5 (brs, 8H; CH₂), 1.3 (brs, 4H; CH₂); ¹³C NMR (100 MHz, [D₆]DMSO, 25 °C, TMS): δ = 170.8, 165.7, 158.2, 148.5, 144.2, 129.9, 119.4, 113.5, 77.2, 35.8, 25.0, 23.8 ppm; FT-IR: $\tilde{\nu}$ = 3206 (NH and NH₂), 1681 cm⁻¹ (C[dbond]O and C[dbond]N); HRMS (APCI-): m/z calcd. for [C₄₈H₄₈N₈O₁₀+H⁺]: 897.3566 [M+ H⁺]; found: 897.3526.

(3R,4R,16R,17R)-Tetra-carbohydrazide cyclophane 15: Prepared from (2R,3R)-1,4-dioxaspiro-[4.5]-decane-2,3-dicarbohydrazide **7** and 4,4'-diformyltriphenylamine as a yellow precipitate (99%). M.p. > 310 °C. ¹H NMR (400 MHz, [D₆]DMSO, 25 °C, TMS): δ = 11.5 (m, 4H; NH), 8.2 (brs, 1H; CH=N), 7.9 (brs, 1H; CH=N), 7.8 (brs, 1H; CH=N), 7.5 (brs, 1H; CH=N), 7.2-7.4 (m, 8H; ArH), 7.0-7.1 (m, 8H; ArH), 6.5-6.7 (m, 10H; ArH), 5.4 (brs, 2H; CH), 4.7 (brs, 1H; CH), 4.5 (brs, 1H; CH), 1.6 (brs, 8H; CH₂), 1.5 (brs, 8H; CH₂), 1.3 (brs, 4H; CH₂); ¹³C NMR (100 MHz, [D₆]DMSO, 25 °C, TMS): δ = 170.9, 165.5, 146.3, 144.3, 130.4, 129.1, 126.2, 123.5, 113.4, 77.2, 35.9, 25.0, 24.0 ppm; FT-IR: $\tilde{\nu}$ = 3218 (NH and NH₂), 1681 cm⁻¹ (C[dbond]O and C[dbond]N); HRMS (APCI-): m/z calcd. for [C₆₀H₅₈N₁₀O₈+H⁺]: 1047.4512 [M+ H⁺]; found: 1047.4521.

(3S,4S,16S,17S)-Tetra-carbohydrazide cyclophane 16: Prepared from (2S,3S)-1,4-dioxaspiro-[4.5]-decane-2,3-dicarbohydrazide **9** and 4-(4-formylphenoxy)-benzaldehyde as a white precipitate (88%). M.p. > 310 °C. ¹H NMR (400 MHz, [D₆]DMSO, 25 °C, TMS): δ = 11.6 (m, 4H; NH), 8.3 (brs, 1H; CH=N), 8.0 (brs, 1H; CH=N), 7.8 (brs, 2H; CH=N), 7.4-7.7 (m, 8H; ArH), 6.6-7.0 (m, 8H; ArH), 5.4 (brs, 2H; CH), 4.7 (brs, 1H; CH), 4.5 (brs, 1H; CH), 1.6 (brs, 8H; CH₂), 1.5 (brs, 8H; CH₂), 1.3 (brs, 4H; CH₂); ¹³C NMR (100 MHz, [D₆]DMSO, 25 °C, TMS): δ = 170.8, 165.6, 158.2, 148.5, 144.2, 129.7, 119.4, 113.5, 77.2, 35.9, 25.0, 24.0 ppm; FT-IR: $\tilde{\nu}$ = 3220 (NH and NH₂), 1682 cm⁻¹ (C[dbond]O and C[dbond]N); HRMS (APCI-): m/z calcd. for [C₄₈H₄₈N₈O₁₀+H⁺]: 897.3566 [M+ H⁺]; found: 897.3539.

(3S,4S,16S,17S)-Tetra-carbohydrazide cyclophane 17: Prepared from (2S,3S)-1,4-dioxaspiro-[4.5]-decane-2,3-dicarbohydrazide **9** and 4,4'-diformyltriphenylamine as a yellow precipitate (89%). M.p. > 310 °C. ¹H NMR (400 MHz, [D₆]DMSO, 25 °C, TMS): δ = 11.5 (m, 4H; NH), 8.2 (brs, 1H; CH=N), 7.9 (brs, 1H; CH=N), 7.8 (brs, 1H; CH=N), 7.5 (brs, 1H; CH=N), 7.2-7.4 (m, 8H; ArH), 6.9-7.1 (m, 8H; ArH), 6.5-6.9 (m, 10H; ArH), 5.4 (brs, 2H; CH), 4.7 (brs, 1H; CH), 4.5 (brs, 1H; CH), 1.6 (brs, 8H; CH₂), 1.5 (brs, 8H; CH₂), 1.3 (brs, 4H; CH₂); ¹³C NMR (100 MHz, [D₆]DMSO, 25 °C, TMS): δ = 170.9, 165.4, 146.5, 144.2, 130.4, 128.8, 126.0, 123.4, 113.4, 77.2, 35.8, 25.0, 24.0 ppm; FT-IR: $\tilde{\nu}$ = 3210 (NH and NH₂), 1681 cm⁻¹ (C[dbond]O and C[dbond]N); HRMS (APCI-): m/z calcd. for [C₆₀H₅₈N₁₀O₈+H⁺]: 1047.4512 [M+ H⁺]; found: 1047.4509.

Acknowledgment

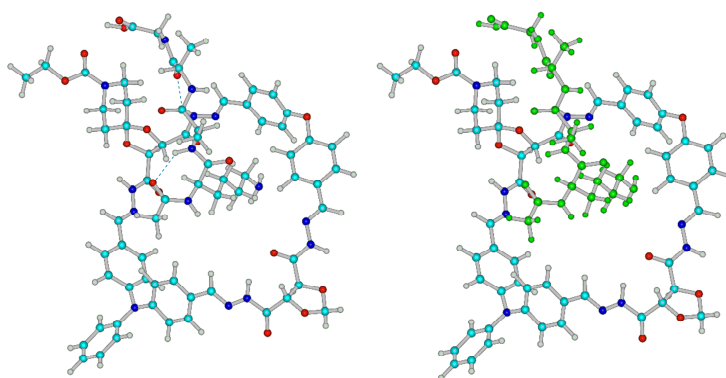
Hany Nour deeply thanks the financial support from Deutscher

Akademischer Austausch Dienst (DAAD) under the PhD fellowship program and Jacobs University for excellent facilities.

- [1] J. Klein, V. Saggiomo, L. Reck, U. Lüning, J. Sanders, *Org. Biomol. Chem.* **2012**, *10*, 60.
- [2] M. Kumar, R. Mahajan, V. Sharma (nee Bhallla), H. Singh, N. Sharma, I. Kaur, *Tetrahedron Lett.* **2001**, *42*, 5315.
- [3] M. Kumar, V. Sharma (nee Bhallla), J. Nagendra Babua, *Tetrahedron* **2003**, *59*, 3267.
- [4] J. Jiang, M. J. MacLachlan, *Chem. Commun.* **2009**, 5695.
- [5] S. Akine, F. Utsuno, T. Nabeshima, *Chem. Commun.* **2010**, *46*, 1029.
- [6] S. Katsiaouni, S. Dechert, C. Brückner, F. Meyer, *Chem. Commun.* **2007**, 951.
- [7] E. Katayev, N. Boev, V. Khrustalev, Y. Ustynyuk, I. Tananaev, J. Sessler, *J. Org. Chem.* **2007**, *72*, 2886.
- [8] S. Akine, D. Hashimoto, T. Saiki, T. Nabeshima, *Tetrahedron Lett.* **2004**, *45*, 4225.
- [9] V. Böhmer, *Angew. Chem. Int. Ed. Engl.* **1995**, *34*, 713.
- [10] A. Danil de Namor, R. Cleverley, M. Chem. Rev. **1998**, *98*, 2495.
- [11] For cyclodextrins see special edition of Chemical Review, edition 5, **1998**.
- [12] J. Kim, I. Jung, S. Kim, E. Lee, J. Kang, S. Sakamoto, K. Yamaguchi, K. Kim, *J. Am. Chem. Soc.* **2000**, *122*, 540.
- [13] S. Kim, I. Jung, E. Lee, J. Kim, S. Sakamoto, K. Yamaguchi, K. Kim, *Angew. Chem. Int. Ed. Engl.* **2001**, *40*, 2119.
- [14] C. Pederson, *J. Am. Chem. Soc.* **1967**, *89*, 7017.
- [15] J. Gawroński, H. Kolbon, M. Kwit, A. Katrusiak, *J. Org. Chem.* **2000**, *65*, 5768.
- [16] N. Kuhnert, A. Lopez-Periago, *Tetrahedron Lett.* **2002**, *43*, 3329.
- [17] N. Kuhnert, A. Lopez-Periago, G. Rossignolo, *Org. Biomol. Chem.* **2005**, *3*, 524.
- [18] N. Kuhnert, G. Rossignolo, A. Lopez-Periago, *Org. Biomol. Chem.* **2003**, *1*, 1157.
- [19] N. Kuhnert, C. Straßnig, A. Lopez-Periago, *Tetrahedron: Asymm.* **2002**, *13*, 123.
- [20] N. Kuhnert, C. Patel, F. Jami, *Tetrahedron Lett.* **2005**, *46*, 7575.
- [21] N. Kuhnert, B. Tang, *Tetrahedron Lett.* **2006**, *47*, 2985.
- [22] N. Kuhnert, D. Marsh, D. Nicolau, *Tetrahedron: Asymm.* **2007**, *18*, 1648.
- [23] H. Nour, M. Matei, B. Bassil, U. Kortz, N. Kuhnert, *Org. Biomol. Chem.* **2011**, *9*, 3258.
- [24] H. Nour, A. Lopez-Periago, N. Kuhnert, *Rapid Comm. Mass Spectrom.* **2012**, *accepted manuscript*.
- [25] K. Tanaka, S. Hachiken, *Tetrahedron Lett.* **2008**, *49*, 2533.
- [26] C. Jakobsche, A. Choudhary, S. Miller, R. Raines, *J. Am. Chem. Soc.* **2010**, *132*, 6651.
- [27] M. Formica, V. Fusi, L. Giorgi, M. Micheloni, P. Palma, R. Pontellini, *Eur. J. Org. Chem.* **2002**, *3*, 402.
- [28] A. González-Álvarez, I. Alfonso, F. Lopez-Ortiz, A. Aguirre, S. Garcia-Granda, V. Gotor, *Eur. J. Org. Chem.* **2004**, *5*, 1117.
- [29] L. Wang, G.-T. Wang, X. Zhao, X.-K. Jiang, Z.-T. Li, *J. Org. Chem.* **2011**, *76*, 3531.
- [30] B.-Y. Lu, G.-J. Sun, J.-B. Lin, X.-K. Jiang, X. Zhao, Z.-T. Li, *Tetrahedron Lett.* **2010**, *51*, 3830.
- [31] C. Jakobsche, A. Choudhary, S. Miller, R. Raines, *J. Am. Chem. Soc.* **2010**, *132*, 6651.
- [32] H. Nour, N. Hourani, N. Kuhnert, *Org. Biomol. Chem.* **2012**, *submitted manuscript*.
- [33] Molecular modelling was carried out using HyperChem software (Release 8.0). Hypercube, Inc., 1115 NW 4th Street, Gainesville, FL 32601 USA. Trial version from <http://www.hypercube.com>
- [34] J. Stewart., *J. Comput. Chem.* **1989**, *10*, 221.

Probing the dynamic reversibility and generation of dynamic combinatorial libraries in the presence of bacterial model oligopeptides as templating guests of tetra-carbohydrazide macrocycles using electrospray mass spectrometry

Hany F. Nour, Tuhidul Islam, Marcelo Fernández-Lahore and Nikolai Kuhnert*



Objectives of the work

Functionalized tetra-carbohydrazide cyclophanes were successfully synthesized in excellent yields following the previously discussed approaches. The first objective of this work is to confirm the dynamic reversibility of the novel macrocycles. Two crossover experiments were conducted in order to prove the dynamic reversibility of tetra-carbohydrazide cyclophanes. In the first crossover experiment, three different pure macrocycles were mixed in a mixture of DMF/MeOH in presence of catalytic AcOH and the reaction was refluxed. In the second crossover experiment, the macrocyclic precursors were mixed in a mixture of DMF/MeOH in presence of catalytic AcOH and the reaction was refluxed. After eight days of reflux, the reaction reached the point of equilibrium, at which an almost identical statistical mixture of macrocycles was obtained. The second objective is to generate a DCL of tetra-carbohydrazide cyclophanes in which the members possess more polar functionalities. Introducing such functionalities is expected to reinforce binding with biological guests. A DCL of eight highly functionalized cyclophane macrocycles was generated in solution by mixing two different dihydrazides with two different dialdehydes. The composition of the DCL was screened by ESI-TOF/MS and the molecular ion peaks for all expected members were observed and assigned based on their high resolution m/z values. Three members in the dynamic library showed recognition in the gas phase to a selection of oligopeptides which mimic bacterial cell wall structure.

Probing the dynamic reversibility and generation of dynamic combinatorial libraries in the presence of bacterial model oligopeptides as templating guests of tetra-carbohydrazide macrocycles using electrospray mass spectrometry

Hany F. Nour^{1,2}, Tuhidul Islam¹, Marcelo Fernández-Lahore¹ and Nikolai Kuhnert^{1*}

¹School of Engineering and Science, Centre for Nano and Functional Materials (NanoFun), Jacobs University, 28759 Bremen, Germany

²National Research Centre, Department of Photochemistry, El Behoose Street, P.O. Box 12622, Dokki, Cairo, Egypt

RATIONALE: Over the past few decades, bacterial resistance against antibiotics has emerged as a real threat to human health. Accordingly, there is an urgent demand to develop innovative strategies for discovering new antibiotics. We present the first application of tetra-carbohydrazide cyclophane macrocycles in dynamic combinatorial chemistry (DCC) and molecular recognition as chiral hosts binding oligopeptides, which mimic bacterial cell wall. This study introduces an innovative application of electrospray ionisation time-of-flight mass spectrometry (ESI-TOF MS) to oligopeptides recognition using DCC.

METHODS: A small dynamic library composed of 8 functionalised macrocycles has been generated in solution and all members were characterised by ESI-TOF MS. We also probed the dynamic reversibility and mechanism of formation of tetra-carbohydrazide cyclophanes in real-time using ESI-TOF MS.

RESULTS: Dynamic reversibility of tetra-carbohydrazide cyclophanes is favored under thermodynamic control. The mechanism of formation of tetra-carbohydrazide cyclophanes involves key dialdehyde intermediates which have been detected and assigned according to their high resolution m/z values. Three members of the dynamic library bind efficiently in the gas phase to a selection of oligopeptides, unique to bacteria allowing observation of host-guest complex ions in the gas phase.

CONCLUSIONS: We probed the mechanism of the [2+2]-cyclocondensation reaction forming library members, proved dynamic reversibility of tetra-carbohydrazide cyclophanes and showed that complex ions formed between library members and guests can be observed in the gas phase, allowing the solution of an important problem of biological interest.

*Correspondence to: N. Kuhnert, School of Engineering and Science, Jacobs University, P.O. Box 750 561, D-28725 Bremen, Germany, Fax: +49 421 200 3229, Tel: +49 421 200 3120. E-mail: n.kuhnert@jacobs-university.de

INTRODUCTION

No single class of drugs has improved public health and the quality of life more dramatically than antibiotics. Before the introduction of sulfonamides in the 1930s, β -lactam antibiotics in the 1940s and tetracyclins, aminoglycosides and macrolides in the 1950s, one in three deaths worldwide was attributed to a bacterial infection.^[1] Antibiotics clearly represent medicinal chemistry's ultimate benefit to mankind. Although the success of antibiotics has led to a temporary victory over bacterial infection there should be little reason for complacency. Many bacterial strains have accomplished a fight back through the development of resistance against many antibiotics only introduced less than 50 years ago. Both mutations and more importantly the efficient and rapid exchange of genetic information between bacteria have resulted in multi-drug resistant strains that spread through hospitals at an alarming rate. Currently antibiotic management with stringent policies of "reserve antibiotics" have prevented a humanitarian disaster, but it is clearly evident that there is an urgent need for novel antibiotics, ideally comprising completely different chemical structures and possibly new mechanisms of action as compared to the classical compounds. The development of novel antibiotics should be viewed as a race against time due to the adaptability of bacterial strains. A statement of the World Health Organisation (WHO) predicts that by 2020, 30 % of all bacterial infections cannot be successfully treated because of resistance.^[2] While the major pharmaceutical companies have committed themselves to the development of novel antibiotics their strategy relies on traditional medicinal chemistry involving the screening of large numbers of compounds either of natural or synthetic origin and depends on serendipity and the quality and structural diversity of the compound libraries available. A new and radical approach towards the development of novel antibiotics is highly desirable. This approach should take the adaptability of bacteria into account and should be rapid and flexible and therefore able to react in a short period of time towards the threat posed by drug resistance.

The principle of evolutionary chemistry, using dynamic combinatorial libraries (DCLs) would be such an option, proposed and developed by Sanders and Lehn.^[3-10] It relies on the basic principle that a number of building blocks bind *via* non-covalent interactions to a given guest molecule. Reversible bond formation between the individual building blocks assembles a stable receptor (macrocyclic or open chained) around the chosen target. The Le-Chatelier principle will drive the

reaction towards the thermodynamically most stable assembly of host and guest and allows its isolation. In a series of seminal papers Sanders has demonstrated the viability of the concept.^[5-9] In this contribution, we aim to develop a novel antibiotic compound using DCC using real-time mass spectrometry to monitor the DCL.^[11-14] As a biological target mimic, we have chosen a peptide sequence unique for bacteria in the synthesis of their cell walls. A bacterial cell wall obtains mechanic stability by cross linking carbohydrate co-polymer chains build from *N*-acetyl glucosamine and muraminic acid with peptide bridges to form murein. β -Lactam antibiotics inhibit this process by inhibition of the transpeptidase enzyme carrying out the cross linking,^[15] while Vancomycin binds specifically to the interpeptide sequence.^[16]

The compounds to be developed here should share the same biological activity and mechanism as Vancomycin being selected to bind to the specific amino acid sequence of the interpeptide linkage. In terms of DCL building blocks we have chosen aromatic dialdehydes in combination with dihydrazides based on tartaric acid. We have shown that dialdehydes in combination with diamines are able to form triaglimine macrocycles allowing large variability in the dialdehyde building block.^[17-25] Recently, we have shown that using real-time mass spectrometry, we could detect all intermediates in a DCL formation along with probing the dynamic reversibility of the process.^[25] In a further contribution we have shown that diamines can be replaced by dihydrazides allowing increased versatility in building block selection with dihydrazides bearing useful functionalities, facilitating molecular recognition and enhancing solubility in polar solvents.^[26,27] When analysing a DCL by mass spectrometry, the most important question arising is whether the members amplified and selected in DCL are observable as individual compounds or as complex ions formed from host and guest. The majority of DCL studies using MS (Mass spectrometry) as a prime analytical tool have reported the detection of the DCL host compounds rather than supramolecular complex ions, with a notable exception published by Poulsen using a peptide library.^[28] The ability to detect intact complex ions is of particular importance for two reasons. Firstly, the positive observation of a complex ion is evidence that the chosen guest molecule amplifies the host rather than any other building block present in the library. Secondly, modern tandem MS techniques using energy resolved mass spectrometry would allow in principle to screen the binding energy between each individual host-guest system during the MS experiment.

EXPERIMENTAL

All the solvents and reagents used for the reactions were purchased from Sigma-Aldrich (Munich, Germany) or Applichem (Darmstadt, Germany) and were used as obtained. Solvents and reagents were used without further purification. Whenever possible the reactions were monitored by thin layer chromatography on aluminum-backed plates pre-coated with silica gel 60 (UV₂₅₄) (Macherey-Nagel, Düren, Germany). Preloaded wang resin, *N,N*-diisopropylethylamine (DIEA), *O*-(Benzotriazol-1-yl)-hydroxybenzotriazole (HOBt), *N,N,N',N'*-tetramethyl-uranium hexafluorophosphate (HBTU), 1-Fmoc (9-fluorenylmethoxycarbonyl)amino acid derivatives, dimethylformamide (DMF), *N*-methylpyrrolidone (NMP), trifluoroacetic acid (TFA), 1,2-ethanedithiol (EDT) and other chemicals required for peptide synthesis were bought from Iris Biotech GmbH (Marktredwitz, Germany). Peptides were synthesised with standard solid phase peptide synthesis technique and it was carried out on an automated peptide synthesiser (ABI-433A, Applied Biosystems, Foster city, USA). Fmoc protected preloaded resin was used to grow peptide chain on it. In detail, deprotection of the *N*-terminal of resin bound amino acid was performed by 20% piperidine in NMP and the *C*-terminal of other protected amino acid was activated using HBTU/HOBt/DIEA (1:1:2) in DMF for coupling with the free *N*-terminal of the resin bound amino acid. A mixture of 82.5% TFA, 5% phenol, 5% water, 5% thioanisol and 2.5% EDT was used to separate the peptide from resin as well as to remove the side chain protecting groups. Subsequently, the peptide was isolated through precipitation in cold (-20 °C) diethyl ether and lyophilised by Christ freeze dryers (Martin Christ Gefriertrocknungsanlagen GmbH, Osterode am Harz, Germany).

Peptides were purified by high performance liquid chromatography (HPLC) and analysed by high resolution mass spectrometry (HRMS). Compounds **1** and **4-7** (Scheme 1) were synthesised following our synthetic procedure.^[26,27] Mass spectra of the samples dissolved in DMF and acetonitrile (ACN) were acquired by a high resolution (exceeding 15000 FWHM) micrOTOF Focus mass spectrometer equipped with an electrospray ionisation (ESI) source in the positive ion mode (Bruker Daltonics, Bremen, Germany). Calibration was carried out using a 0.1 M solution of sodium formate in the enhanced quadratic mode prior to each experimental run. Samples were directly infused into the ESI-TOF mass spectrometer. The results of the measurements were processed using Compass 1.3 data analysis software for a Bruker Daltonics

microTOF TOF mass spectrometer. Molecular modeling calculations were carried out with HyperChem software (Release 8.0, trial version from <http://www.hypercube.com>, USA)^[29] using Austin Model 1 (AM1) method. A Polak-Ribiere algorithm was employed until the root-mean square (RMS) gradient was 0.01 kcal.mol⁻¹. All calculations were carried out in vacuo and no influence of solvents was taken into account.^[30]

(2*R*,3*R*)-Ethyl 2,3-di(hydrazinecarbonyl)1,4-dioxaspiro[4.5]decane-8-carboxylate **26**

To a stirred solution of (+)-diethyl L-tartrate **24** (5.7 mL, 33.29 mmol) in ethyl acetate (20 mL) were added ethyl 4-oxopiperidine-1-carboxylate **25** (5 mL, 33.19 mmol) and boron trifluoride etherate (17 mL, 82.97 mmol). The mixture was refluxed for 7 h, cooled to room temperature, carefully quenched with saturated sodium bicarbonate solution (100 mL), extracted with water, dried with sodium sulfate, filtered off and evaporated in vacuum. The crude oil (10.29 g) was dissolved without further purification in absolute ethanol (40 mL) and hydrazine monohydrate was added (3 mL). The mixture was refluxed for 7 h. The solvent was evaporated in vacuum; the residue was dissolved in water (10 mL) and extracted with ethyl acetate (3×100 mL). The water extract was dissolved in ethanol (200 mL), dried and evaporated in vacuum to give compound **26** as a yellow gummy material (4.36 g, 13.17 mmol) in 46 % yield. ¹H NMR (400 MHz, [D₆]DMSO, 300 K): δ = 1.3 (t, J = 7.3, CH₃, 3H), 1.5-1.7 (m, CH₂, 4H), 3.3-3.4 (m, CH₂, 4H), 3.9-4.0 (q, J = 7.3, CH₂, 2H), 3.4 (brs, NH₂, 4H), 4.4 (brs, CH, 2H), 9.3 (brs, NH, 2H) ppm. ¹³C NMR (100 MHz, [D₆]DMSO, 300 K): δ = 15.0, 35.4, 41.8, 61.3, 77.2, 110.9, 155.0, 167.6 ppm; FT-IR: $\tilde{\nu}$ = 3309 (NH and NH₂), 1668 cm⁻¹ (C[dbond]O); HRMS (ESI, negative ion mode): Calcd. for [C₁₂H₂₁N₅O₆-H⁺]: 330.1436; found 330.1419, (Error, -5.0 ppm).

Dynamic reversibility of tetra-carbohydrazide cyclophane macrocycles

*(a) Refluxing compounds **1**, **2**, **3** and **4** in DMF/MeOH*

(2*R*,3*R*)-1,4-Dioxaspiro[4.5]decane-2,3-dicarbohydrazide **1** (100 mg, 0.39 mmol), (4*R*,5*R*)-1,3-dioxolane-4,5-dicarbohydrazide **4** (147.3 mg, 0.78 mmol), 4-(4-formylphenoxy)benzaldehyde **2** (175.2 mg, 0.78 mmol) and 4,4'-diformyltriphenylamine **3** (116.67 mg, 0.39 mmol) were mixed in 5 mL MeOH and 5 mL DMF, 50 μ L of catalytic AcOH were added and the mixture was refluxed for 192 h. Aliquot was taken and 5 μ L of DMF was added. Sample was well sonicated, diluted with ACN and infused into the ESI-TOF mass spectrometer in the positive ion mode.

(b) Refluxing macrocycles 5, 6 and 7 in DMF/MeOH

Tetra-carbohydrazide cyclophanes **5** (100 mg, 0.132 mmol), **6** (119.74 mg, 0.132 mmol) and **7** (117.9 mg, 0.132 mmol) were mixed in 5 mL MeOH and 5 mL DMF, 50 μ L of catalytic AcOH were added and the mixture was refluxed for 192 h. Aliquot was taken and 5 μ L of DMF was added. Sample was well sonicated, diluted with ACN and infused into the ESI-TOF mass spectrometer in the positive ion mode.

Generation of a dynamic library from dialdehyde and dihydrazide precursors 26, 2-4

(2*R*,3*R*)-Ethyl 2,3-di(hydrazinecarbonyl)1,4-dioxo-8-azaspiro[4.5]decane-8-carboxylate **26** (150 mg, 0.45 mmol), (4*R*,5*R*)-1,3-dioxolane-4,5-dicarbohydrazide **4** (172.2 mg, 0.90 mmol), 4-(4-formylphenoxy)benzaldehyde **2** (204.83 mg, 0.90 mmol) and 4,4'-diformyltriphenylamine **3** (136.4 mg, 0.45 mmol) were mixed in 4 mL MeOH and 4 mL DMF, 50 μ L of catalytic AcOH were added and the mixture was refluxed for 48 h. Aliquot was taken and 5 μ L of DMF was added. Sample was well sonicated, diluted with ACN and infused into the ESI-TOF MS in the negative ion mode.

Molecular recognition of library members 27-34 to oligopeptides 37-39

After generation of the dynamic library, 3 aliquots were taken. To each aliquot, 5 μ L of DMF, 1 mL of ACN and 5 μ L of water were added and samples were well sonicated. Oligopeptides **37**, **38** and **39** were added and samples were infused into the ESI-TOF MS in the positive ion mode.

RESULTS AND DISCUSSION

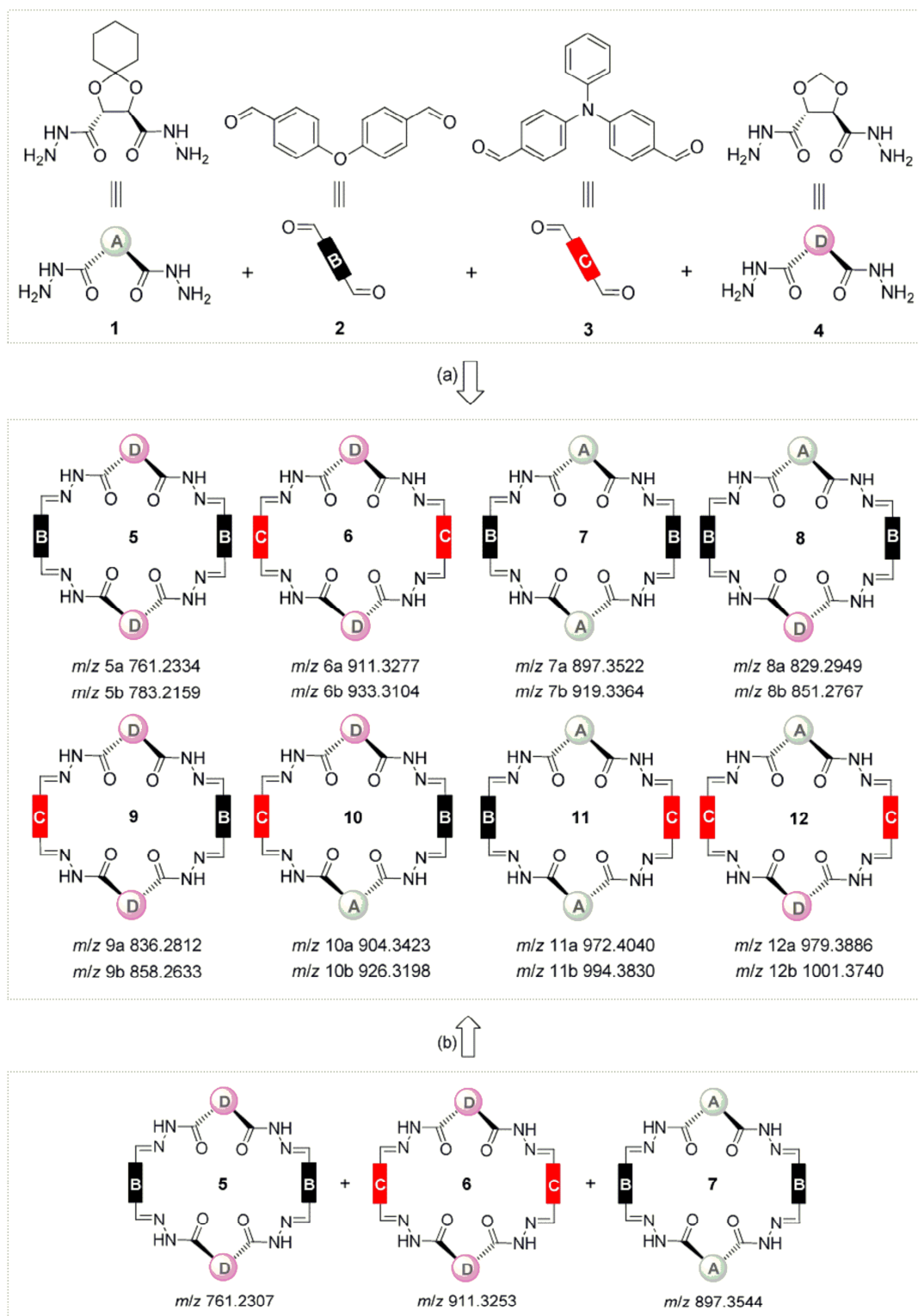
Tetra-carbohydrazide cyclophanes form a new class of chiral enantiomerically pure macrocycles, which have recently been synthesised in our laboratory using [2+2]-cyclocondensation reactions of chiral (4*R*,5*R*)- and (4*S*,5*S*)-1,3-dioxolane-4,5-dicarbohydrazides and aromatic dialdehydes.^[26,27] The macrocycles show a dynamic behaviour in solution, which has been rationalized in terms of an unprecedented conformational interconversion between two conformers, one stabilised by intramolecular hydrogen bonding and π - π stacking interactions. Both (*R*) and (*S*) enantiomers are readily available and can be obtained in almost quantitative yields. The cyclocondensation reaction takes place at relatively high concentration of reactants under conformational bias of dicarbohydrazides without addition of an external template or applying

high dilution conditions. In continuation to our work with tetra-carbohydrazide cyclophanes, we decided to study the dynamic reversibility of the macrocycles and the mechanism of the [2+2]-cyclocondensation reaction. We also decided to assess the molecular recognition ability of tetra-carbohydrazide cyclophanes to a selection of oligopeptides unique in bacteria by ESI-TOF MS, offering an innovative approach to the discovery of novel compounds with antibiotic activity.

Dynamic reversibility of tetra-carbohydrazide cyclophanes

Unlike conventional chemistry, dynamic combinatorial chemistry (DCC) is the field, in which building blocks assemble to larger structures *via* reversibly formed covalent bonds. In DCC, library members undergo continuous exchange until they reach an equilibration point, at which a statistical mixture of all possible species has formed. Addition of an external trigger, usually a guest molecule of interest, shifts equilibration to the most stable host guest complex and allows its amplification. Despite its interesting features, only few applications of DCC in drug discovery were reported.^[31-34] Analysis of library members by ESI-MS shows considerable promise due to the ability of this technique to provide precise mass values, high resolution and little or almost no fragmentations. To realize DCCs, firstly the full reversibility of the reaction employed must be demonstrated. Dynamic reversibility of tetra-carbohydrazide cyclophane formation was therefore demonstrated by obtaining the same equilibrium composition of a mixture from two different starting points of the reaction.

In a first crossover experiment, the macrocyclic precursors **1-4** were mixed in a mixture of DMF/MeOH in presence of catalytic AcOH and the reaction was refluxed (path *a*). In a second crossover experiment, we mixed equimolar amounts of macrocycles **5-7** in a mixture of DMF/MeOH in presence of catalytic AcOH and the reaction was refluxed (path *b*). After eight days the reaction reached the point of equilibrium, at which an almost identical statistical mixture of macrocycles was obtained (Scheme 1). The macrocyclic library members appear in the mass spectrum as both protonated and sodiated ions. ESI-TOF MS data for the products of carbohydrazide exchange are shown in Table 1. (For ESI-TOF MS spectra at equilibration, see Supporting Information). It is worth noting that the intensity of the peaks corresponding to the characterised macrocycles can be plotted versus reaction time to provide a visual representation of the composition of the dynamic library over the course of the reaction time as shown in Figure 1a and 1b.



Scheme 1. Graphical representation showing dynamic exchange between (a) dicarbohydrazides and dialdehydes **1-4** (b) tetra-carbohydrazides **5-7**.

Table 1. High resolution ESI-TOF MS data in the positive ion mode for the products of carbohydrazide exchange reactions, products appeared as (M+H)⁺, path *a*) and (M+Na)⁺, path *b*) ions

Entry	Measured <i>m/z</i>		Molecular Formula	Theoretical <i>m/z</i>	Error [ppm]
5^{a,b}	761.2334 ^a	[M+H] ⁺	C ₃₈ H ₃₂ N ₈ O ₁₀	761.2314 ^a	-2.6
	783.2159 ^b	[M+Na] ⁺		783.2134 ^b	-3.2
6^{a,b}	911.3277 ^a	[M+H] ⁺	C ₅₀ H ₄₂ N ₁₀ O ₈	911.3260 ^a	-1.9
	933.3104 ^b	[M+Na] ⁺		933.3079 ^b	-2.6
7^{a,b}	897.3522 ^a	[M+H] ⁺	C ₄₈ H ₄₈ N ₈ O ₁₀	897.3566 ^a	4.9
	919.3364 ^b	[M+Na] ⁺		919.3386 ^b	2.3
8^{a,b}	829.2949 ^a	[M+H] ⁺	C ₄₃ H ₄₀ N ₈ O ₁₀	829.2940 ^a	-1.1
	851.2767 ^b	[M+Na] ⁺		851.2760 ^b	-0.9
9^{a,b}	836.2812 ^a	[M+H] ⁺	C ₄₄ H ₃₇ N ₉ O ₉	836.2787 ^a	-3.0
	858.2633 ^b	[M+Na] ⁺		858.2606 ^b	-3.1
10^{a,b}	904.3423 ^a	[M+H] ⁺	C ₄₉ H ₄₅ N ₉ O ₉	904.3413 ^a	-1.1
	926.3198 ^b	[M+Na] ⁺		926.3232 ^b	3.7
11^{a,b}	972.4040 ^a	[M+H] ⁺	C ₅₄ H ₅₃ N ₉ O ₉	972.4039 ^a	-0.1
	994.3830 ^b	[M+Na] ⁺		994.3858 ^b	2.8
12^{a,b}	979.3886 ^a	[M+H] ⁺	C ₅₅ H ₅₀ N ₁₀ O ₈	979.3886 ^a	0.0
	1001.3740 ^b	[M+Na] ⁺		1001.3705 ^b	-3.5

^aRefluxing macrocycles **5-7**, spectrum recorded after 8 days in the positive ion mode. ^bRefluxing building block precursors **1-4**, spectrum recorded after 8 days in the positive ion mode.

After 144 h of refluxing tetra-carbohydrazide cyclophanes **5-7** in a mixture of DMF/MeOH and in the presence of 5 µL of AcOH, the reaction did not reach the equilibrium point. Addition of an excess of AcOH (45 µL) was vital to facilitate the exchange process and to drive the reaction to equilibration. In the final equilibrium composition, the molecular ions of macrocycles **5** and **8-10** possess high peak intensities in comparison with those corresponding to macrocycles **6, 7, 11** and **12**. The peak intensities for all macrocycles obtained *via* path (*a*) remain steady over the course of the reaction and did not change by prolonged refluxing. This suggested that equilibration point can be easily reached only after 48 h of refluxing *via* path (*a*). Interestingly, a total of 11 different reaction intermediates were detected after 2 h of refluxing tetra-carbohydrazide cyclophane macrocycles **5-7** and their precursors **1-4**.

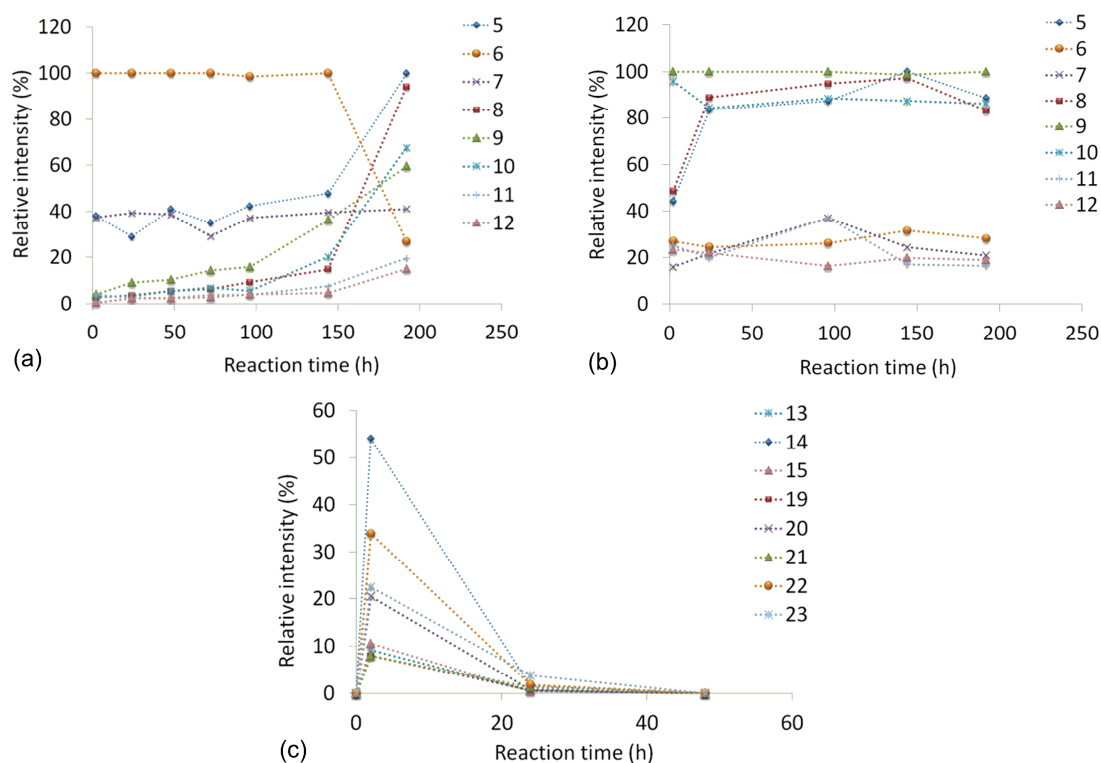


Figure 1. A plot of relative intensity *versus* reaction time showing the composition of the generated dynamic library (a) refluxing tetra-carbohydrazide cyclophanes **5-7**, (b) refluxing dihydrazide and dialdehyde precursors **1-4** and (c) intermediates detected after 2 h of refluxing dihydrazide and dialdehyde precursors **1-4**, products were detected as (M+H⁺) or (M+Na⁺) ions.

All intermediates later disappeared at the expense of the formation of the final [2+2]-cyclocondensation products (Figs. 1, 2 and table 2). The observation of 11 different reaction intermediates demonstrates the unique versatility of mass spectrometry in the detection of reactive species and screening of amplified members in a dynamic library.^[25] Structures and MS data for intermediates **13-23** are shown in Figure 2 and Table 2. The change of intensities of molecular ions for selected intermediates is shown in Figure 1c.

Mechanism of the [2+2]-cyclocondensation reaction forming library members 5-12

It is worth noting that the mechanism of formation of library members **5-12**, which were generated in solution *via* path (a) involves for (*i.e.*, macrocycle **5**) condensation of two equivalents of the dialdehyde **2** with one equivalent of dicarbohydrazide **4** to form intermediate **19** with two terminal aldehyde moieties (Fig. 3).

Table 2. High resolution ESI-TOF MS data in the positive ion mode for the intermediates which were detected after 2 h *via* paths (a) and (b), products appeared as (M+H)⁺, paths a and b) ions

Intermediate	Measured <i>m/z</i>		Molecular Formula	Theoretical <i>m/z</i>	Error [ppm]
13 ^{a,b}	399.1285 ^a	[M+H] ⁺	C ₁₉ H ₁₈ N ₄ O ₆	399.1299	3.5
	399.1304 ^b	[M+H] ⁺		399.1299	1.3
14 ^{a,b}	474.1759 ^a	[M+H] ⁺	C ₂₅ H ₂₃ N ₅ O ₅	474.1772	2.8
	474.1769 ^b	[M+H] ⁺		474.1772	0.7
15 ^{a,b}	467.1910 ^a	[M+H] ⁺	C ₂₄ H ₂₆ N ₄ O ₆	467.1925	3.2
	467.1916 ^b	[M+H] ⁺		467.1925	1.9
16 ^{a,b}	571.1903 ^a	[M+H] ⁺	C ₂₄ H ₂₆ N ₈ O ₉	571.1896	-1.2
	571.1879 ^b	[M+H] ⁺		571.1896	3.0
17 ^{a,b}	646.2388 ^a	[M+H] ⁺	C ₃₀ H ₃₁ N ₉ O ₈	646.2368	-3.0
	646.2356 ^b	[M+H] ⁺		646.2368	1.9
18 ^{a,b}	707.3144 ^a	[M+H] ⁺	C ₃₄ H ₄₂ N ₈ O ₉	707.3148	0.5
	707.3135 ^b	[M+H] ⁺		707.3148	-0.1
19 ^{a,b}	607.1806 ^a	[M+H] ⁺	C ₃₃ H ₂₆ N ₄ O ₈	607.1823	2.9
	607.1824 ^b	[M+H] ⁺		607.1823	-0.1
20 ^{a,b}	757.2752 ^a	[M+H] ⁺	C ₄₅ H ₃₆ N ₆ O ₆	757.2769	2.3
	757.2761 ^b	[M+H] ⁺		757.2769	1.1
21 ^{a,b}	675.2440 ^a	[M+H] ⁺	C ₃₈ H ₃₄ N ₄ O ₈	675.2449	1.3
	675.2435 ^b	[M+H] ⁺		675.2449	2.1
22 ^{a,b}	682.2280 ^a	[M+H] ⁺	C ₃₉ H ₃₁ N ₅ O ₇	682.2296	2.4
	682.2272 ^b	[M+H] ⁺		682.2296	3.6
23 ^{a,b}	750.2888 ^a	[M+H] ⁺	C ₄₄ H ₃₉ N ₅ O ₇	750.2922	4.5
	750.2924 ^b	[M+H] ⁺		750.2922	-0.3

^a Intermediates were detected after 2 h of refluxing dialdehyde and dihydrazide building block precursors **1-4**,

^b Intermediates were detected after 2 h of refluxing macrocycles **5-7**.

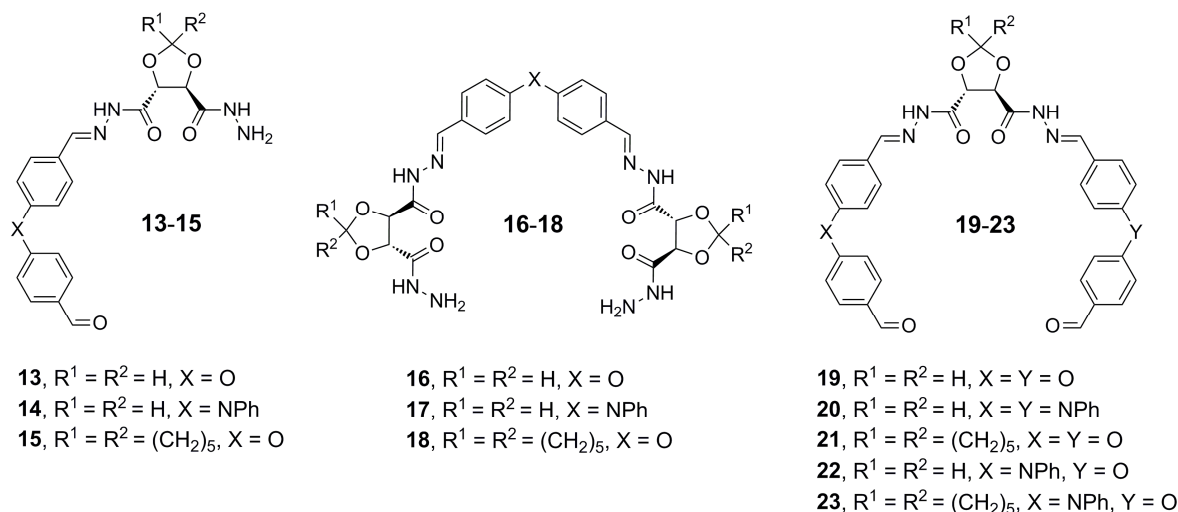


Figure 2. Intermediates detected after 2 h of refluxing dihydrazide and dialdehyde precursors **1-4** in DMF/MeOH.

In contrast, formation of library members **5-12** *via* path (b) for (*i.e.*, macrocycle **5**) requires partial hydrolysis to intermediate **16** with two hydrazide terminals. In general, molecular ions of intermediates **16-18** (Fig. 2) possess low peak intensities when they form *via* path (a) and high peak intensities in case of formation *via* path (b). For intermediates **19-21** (Fig. 2), the opposite case was observed.

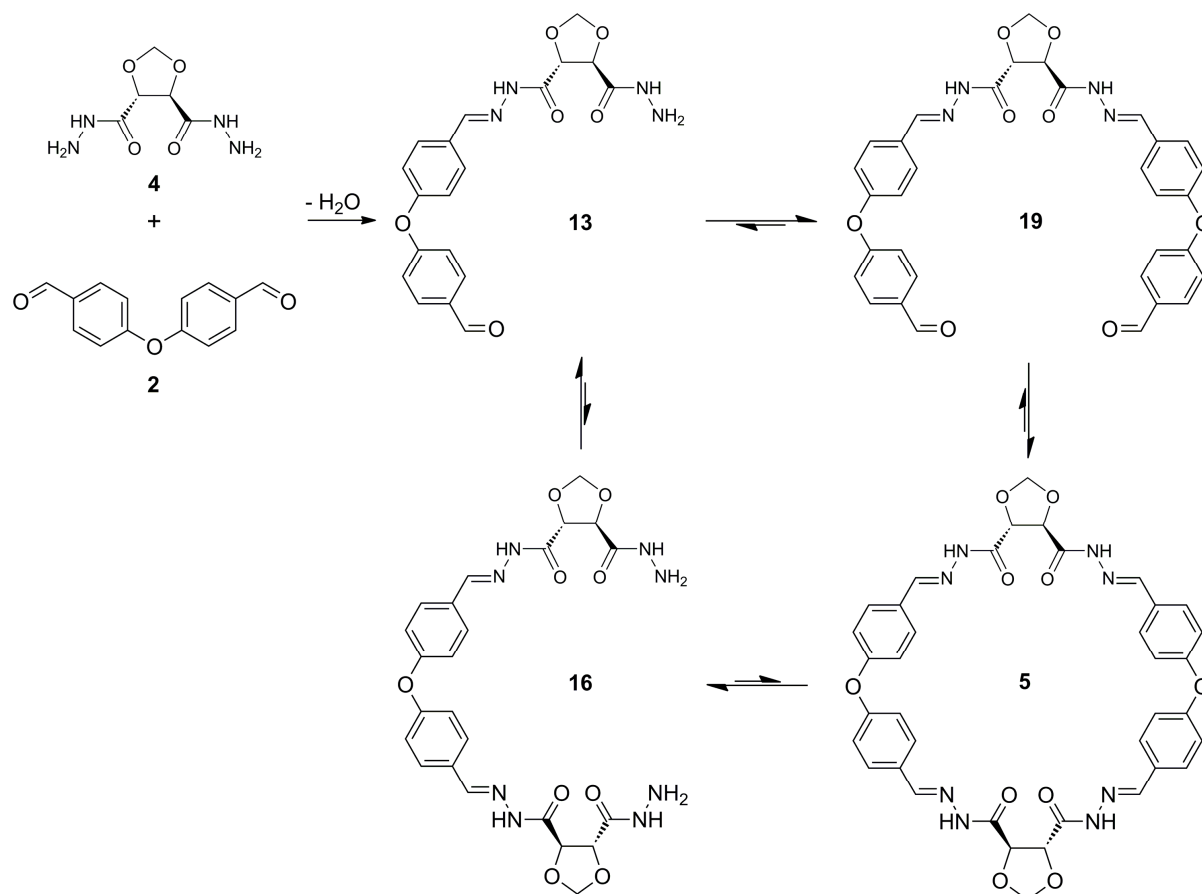


Figure 3. Proposed mechanism for the formation and exchange of tetra-carbohydrazide **5**.

Generation of a dynamic library of tetra-carbohydrazide cyclophanes with polar functionalities

After successfully probing the dynamic reversibility of tetra-carbohydrazide cyclophanes, we decided to generate a dynamic library in solution, in which some members possess polar functionalities to facilitate non-covalent interactions in the presence of a guest molecule. We followed path (a) for the generation of library members taking advantage of the shorter reaction

time. A functionalised chiral dihydrazide **26** was synthesised by reacting (+)-diethyl L-tartrate **24** with ethyl 4-oxopiperidine-1-carboxylate **25** in the presence of the Lewis acid catalyst $\text{BF}_3(\text{OEt})_2$.^[35] *In situ* condensation of the protected diesters with hydrazine monohydrate in absolute ethanol afforded the corresponding dicarbohydrazide **26** (Fig. 4).

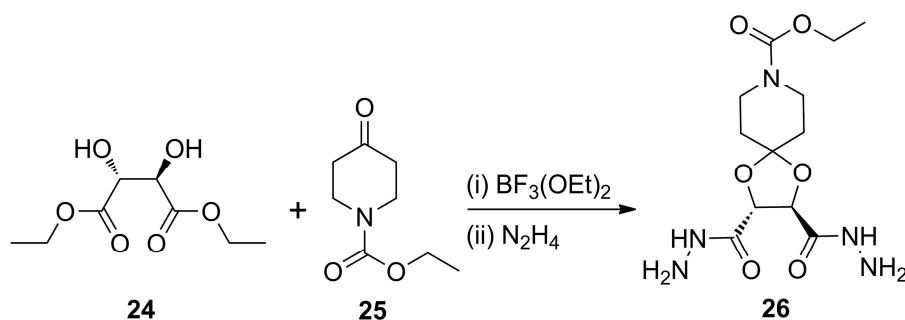


Figure 4. Synthetic route to chiral hydrazide **26**.

For the modular assembly of chiral macrocycles, (2*R*,3*R*)-ethyl 2,3-di(hydrazinecarbonyl)1,4-dioxo-8-azaspiro[4.5]decane-8-carboxylate **26**, (4*R*,5*R*)-1,3-dioxolane-4,5-dicarbohydrazide **4**, 4-(4-formylphenoxy)benzaldehyde **2** and 4,4'-diformyltriphenylamine **3** were refluxed in a mixture of DMF/MeOH in presence of catalytic AcOH (Fig. 5). After 24 h of reflux, 8 different macrocycles were detected and assigned by ESI-TOF MS in the negative ion mode according to their high resolution m/z values (Figs. 5 and 6). Peaks appearing at m/z 804.2512 and 729.2058 are fragments of macrocycles **30** and **33**, respectively (Figs. 6 and 7). High resolution m/z values for members of the dynamic library **27-34** are shown in table 3. Next, we turned our attention to assess the molecular recognition ability of library members **27-34** to oligopeptides. For molecular recognition, AcNH-D-Ala-D-Glu-L-Lys-D-Ala-D-Ala-Gly-COOH **37**, AcNH-D-Glu-L-Lys-D-Ala-D-Ala-Gly-COOH **38** and AcNH-L-Lys-D-Ala-D-Ala-Gly-COOH **39** were chosen and synthesised using solid phase peptide synthesis using the Fmoc method. The purity and identity of oligopeptides **37-39** were assessed by HPLC-tandem MS (Fig. 8). Tetra-carbohydrazide cyclophanes **27**, **33** and **34** are C_2 -symmetric, whereas **28-32** are non-symmetric. Macrocycle **32** has a unique and fascinating structure since the four building blocks forming it are all different. In comparison with other spectroscopic tools, mass spectrometry is the only technique which can provide vital information about the chemical composition of the library members based on high resolution m/z values.

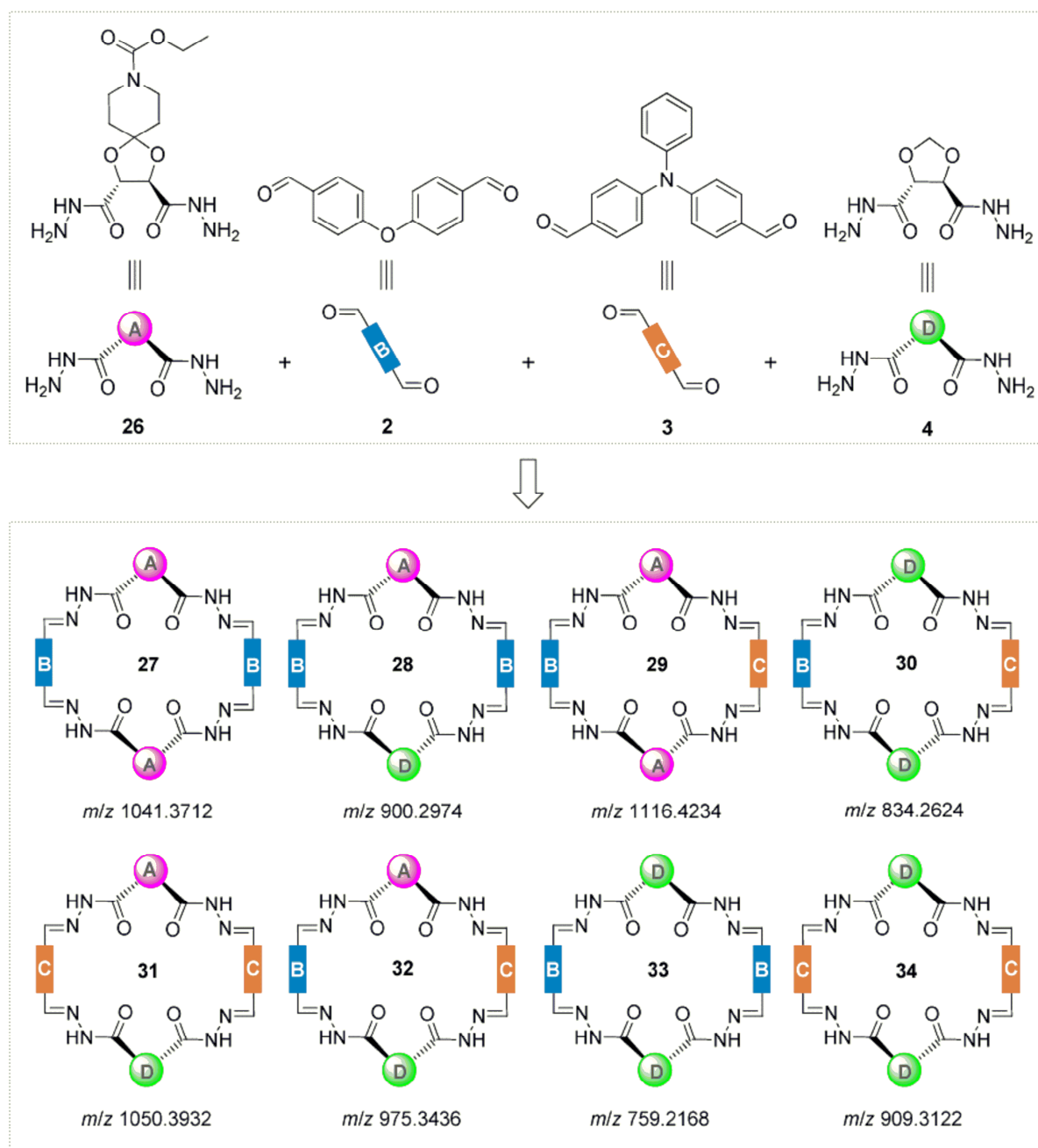


Figure 5. Generated dynamic library of macrocycles **27-34**.

After generation of the dynamic library members, aliquot was taken from solution, 5 μL of DMF was added, sample was well sonicated, and oligopeptide (**37**, **38** or **39**) was added. Sample was diluted with ACN, well sonicated and directly infused into the ESI-TOF mass spectrometer in the positive ion mode.

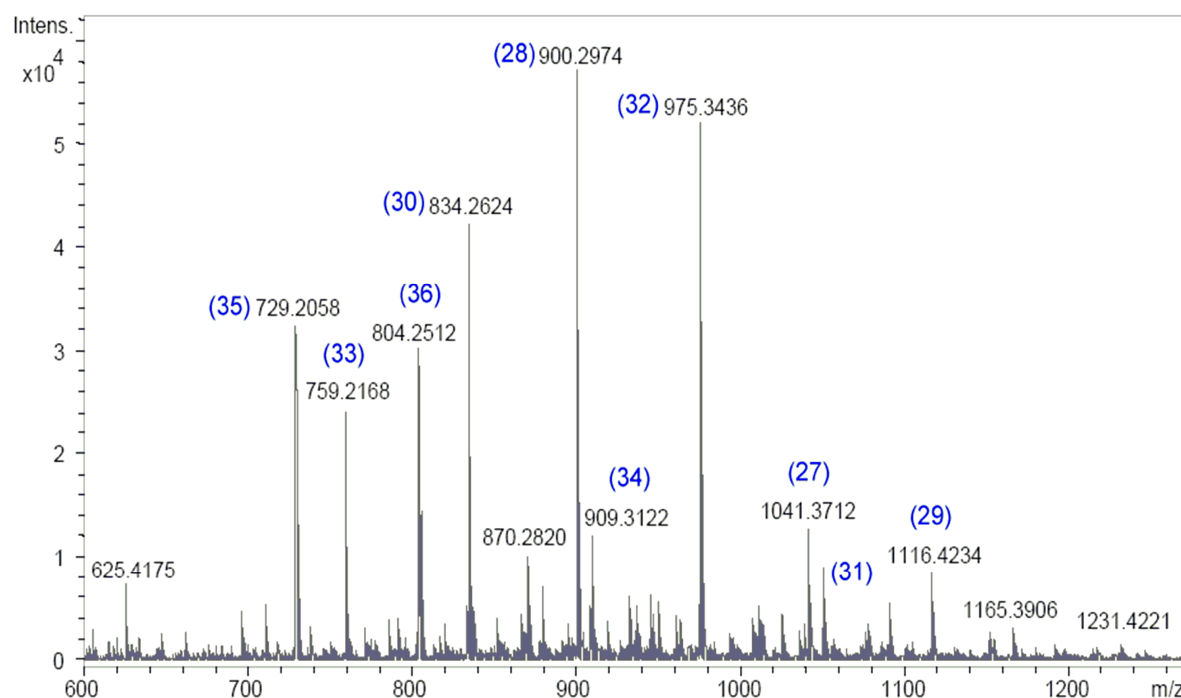


Figure 6. ESI-TOF mass spectrum for library members **27-34** in the negative ion mode.

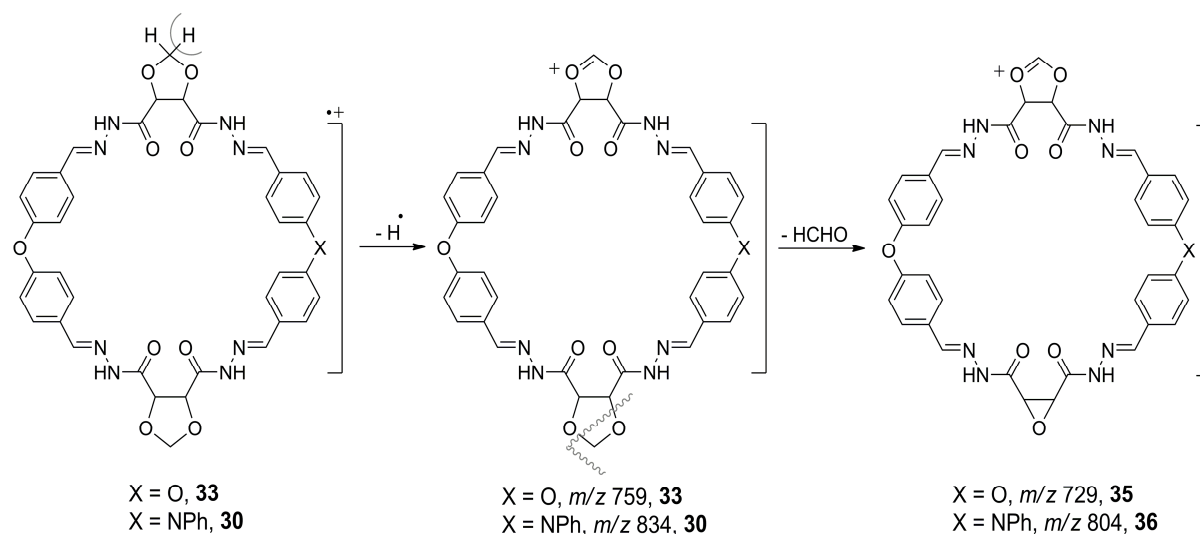


Figure 7. Proposed fragmentation mechanism for macrocycles **30** and **33**.

Macrocycles **28**, **30**, **32** and **33** showed recognition to oligopeptides **37-39** in the gas phase. Figure 10 shows ESI-TOF mass spectrum for recognition of AcNH-L-Lys-D-Ala-D-Ala-Gly-COOH **39** with macrocycles **28**, **30** and **32**. The host/guest complex with the highest peak intensity referred to macrocycle **32** binding oligopeptide **39** (Fig. 10). All attempts to amplify

macrocycle **32** from the dynamic library did not succeed. High resolution m/z values for the assigned host/guest complexes are shown in table 4. Tandem ESI-MS spectrum for host/guest complex **42** (m/z 1364.5635) is shown in Figure 11, which demonstrates the identity of the observed ion as a host guest complex ion.

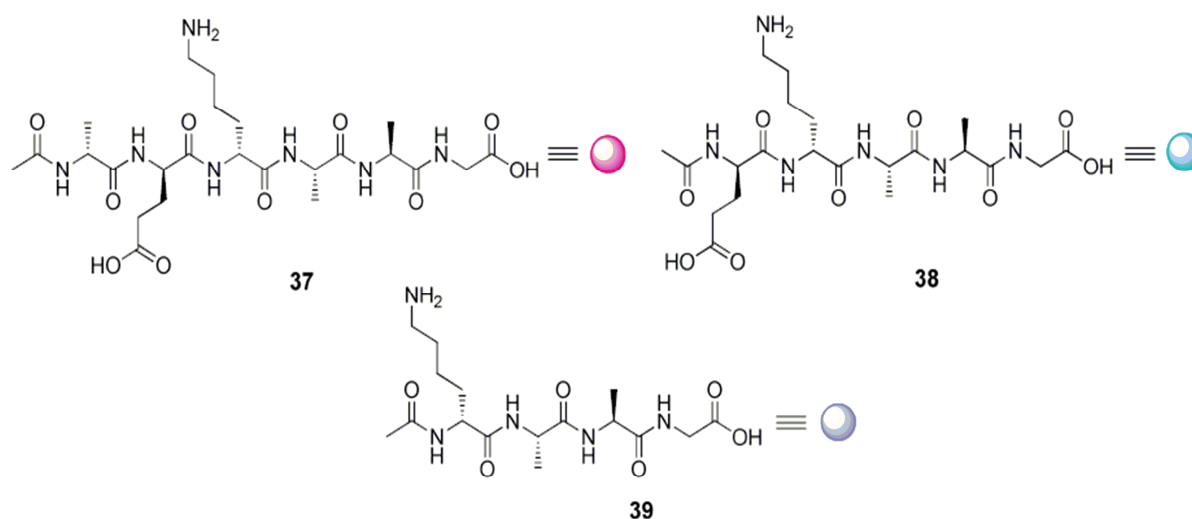


Figure 8. Oligopeptides **37-39** which mimic bacterial cell wall.

Table 3. High resolution ESI-TOF MS data in the negative ion mode for library members **27-34**, products appeared as $[M-H]^-$ ions

Entry	Measured m/z		Molecular Formula	Theoretical m/z	Peak intensity (%)	Error [ppm]
27	1041.3712	$[M-H]^-$	$C_{52}H_{54}N_{10}O_{14}$	1041.3748	22.82	3.4
28	900.2974	$[M-H]^-$	$C_{45}H_{43}N_9O_{12}$	900.2958	100	-1.7
29	1116.4234	$[M-H]^-$	$C_{58}H_{59}N_{11}O_{13}$	1116.4221	13.32	-1.1
30	834.2624	$[M-H]^-$	$C_{44}H_{37}N_9O_9$	834.2641	75.86	2.1
31	1050.3932	$[M-H]^-$	$C_{57}H_{53}N_{11}O_{10}$	1050.3904	15.86	-2.6
32	975.3436	$[M-H]^-$	$C_{51}H_{48}N_{10}O_{11}$	975.3431	91.35	-0.5
33	759.2168	$[M-H]^-$	$C_{38}H_{32}N_8O_{10}$	759.2169	43.07	0
34	909.3122	$[M-H]^-$	$C_{50}H_{42}N_{10}O_8$	909.3114	20.16	-0.8
35	729.2058	<i>a</i>	$C_{37}H_{29}N_8O_9$	729.2063	56.00	0.7
36	804.2512	<i>b</i>	$C_{43}H_{34}N_9O_8$	804.2536	52.00	3.0

^{a,b} Fragments of macrocycles **33** and **30**.

Computational studies

In order to further understand the nature of the host/guest interactions, we performed molecular modeling simulation for host/guest complex **42** at the Austin Model 1 (AM1 level) using HyperChem software (Release 8.0) (Fig. 9).^[29,30] It can be inferred from the minimised energy structure that the carbonyl group of the carbamate moiety (NCOOC₂H₅) in macrocycle **32** binds the hydroxyl group (COOH) of the COOH terminal Glycine in oligopeptide **39** *via* hydrogen bonding. Also, the amidic proton (NHCO) in macrocycle **32** binds the amidic carbonyl (NHCO) of D-Alanine in peptide **39** through hydrogen bonding. Furthermore, the side chain of L-lysine is embedded within the cavity of the macrocycle. This forms a stable host/guest complex and suggests that macrocycle **32** can show promising antibacterial activity.

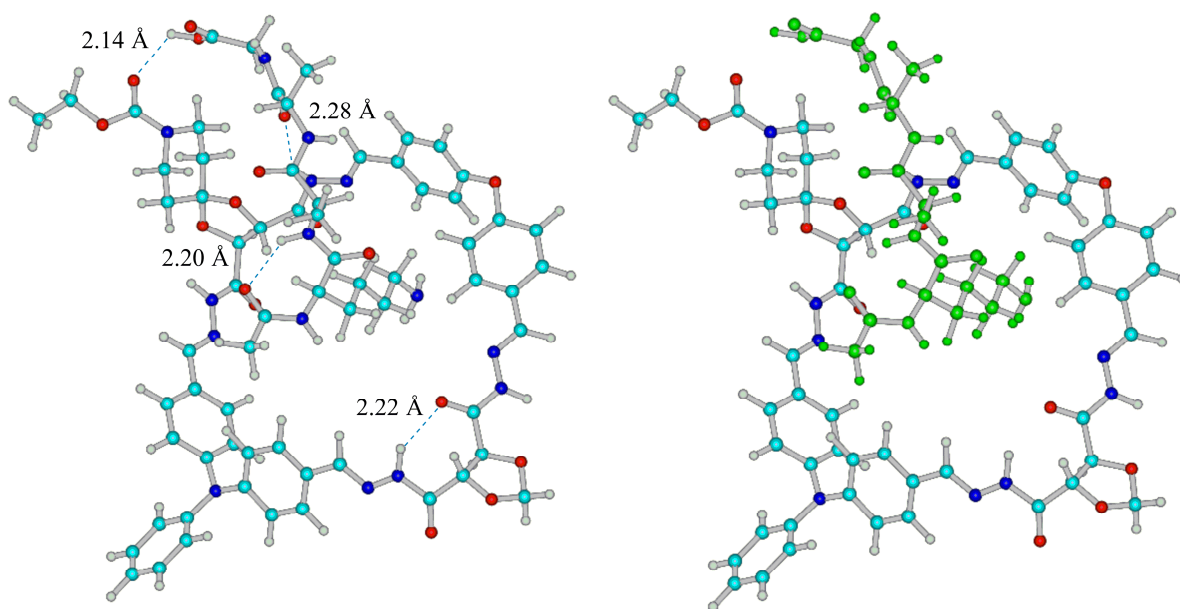


Figure 9. Computed structure for host/guest complex **42** at the AM1 level using a Polak-Ribiere conjugate gradient with rms < 0.01 kcal.mol⁻¹.

CONCLUSIONS

ESI-TOF MS is an enormously versatile technique for studying non-covalent interactions and providing vital information about the reactive reaction intermediates, which cannot be obtained from other analytical instruments. Tetra-carbohydrazide cyclophane **32** forms a stable host/guest complex with oligopeptide **39**.

The polar carbamate group participates efficiently in strengthening the binding interactions in the formed complex **42**. In addition to improving water solubility, introducing polar functionalities and isolation of the macrocycle, which binds preferentially to oligopeptides can lead to discovery of a novel macrocycle which can function as an antibiotic. We probed the dynamic reversibility of tetra-carbohydrazide cyclophanes and proved that they were fully reversible under thermodynamic control. We hope that this new class of macrocycles will find wide applications in drug discovery using DCC.

Table 4. High resolution ESI-TOF MS data in the positive ion mode for library members hosting oligopeptides, products appeared as $[M+H]^+$ ions

Host/Guest complex	Measured m/z		Molecular Formula	Theoretical m/z	Error [ppm]
28/37	1489.6005	$[M+H]^+$	$C_{69}H_{84}N_{16}O_{22}$	1489.6019	0.9
30/37	1423.5649	$[M+H]^+$	$C_{68}H_{78}N_{16}O_{19}$	1423.5702	3.7
32/37	1564.6445	$[M+H]^+$	$C_{75}H_{89}N_{17}O_{21}$	1564.6492	3.0
33/37	1348.5243	$[M+H]^+$	$C_{62}H_{73}N_{15}O_{20}$	1348.5229	-1.0
28/38	1418.5591	$[M+H]^+$	$C_{66}H_{79}N_{15}O_{21}$	1418.5648	4.0
30/38	1352.5285	$[M+H]^+$	$C_{65}H_{73}N_{15}O_{18}$	1352.5331	3.4
32/38	1493.6091	$[M+H]^+$	$C_{72}H_{84}N_{16}O_{20}$	1493.6121	2.0
40	1223.4929	$[M+H]^+$	$C_{60}H_{66}N_{14}O_{15}$	1223.4905	-2.0
41	1289.5235	$[M+H]^+$	$C_{61}H_{72}N_{14}O_{18}$	1289.5222	-1.0
42	1364.5635	$[M+H]^+$	$C_{67}H_{77}N_{15}O_{17}$	1364.5695	4.4
43	1162.6380	$[M+H]^+$	$C_{48}H_{87}N_{15}O_{18}$	1162.6426	4.0
44	1549.8487	$[M+H]^+$	$C_{64}H_{116}N_{20}O_{24}$	1549.8544	3.7

Acknowledgements

Hany Nour deeply thanks Deutscher Akademischer Austauschdienst (DAAD) for financial support and Jacobs University for excellent facilities.

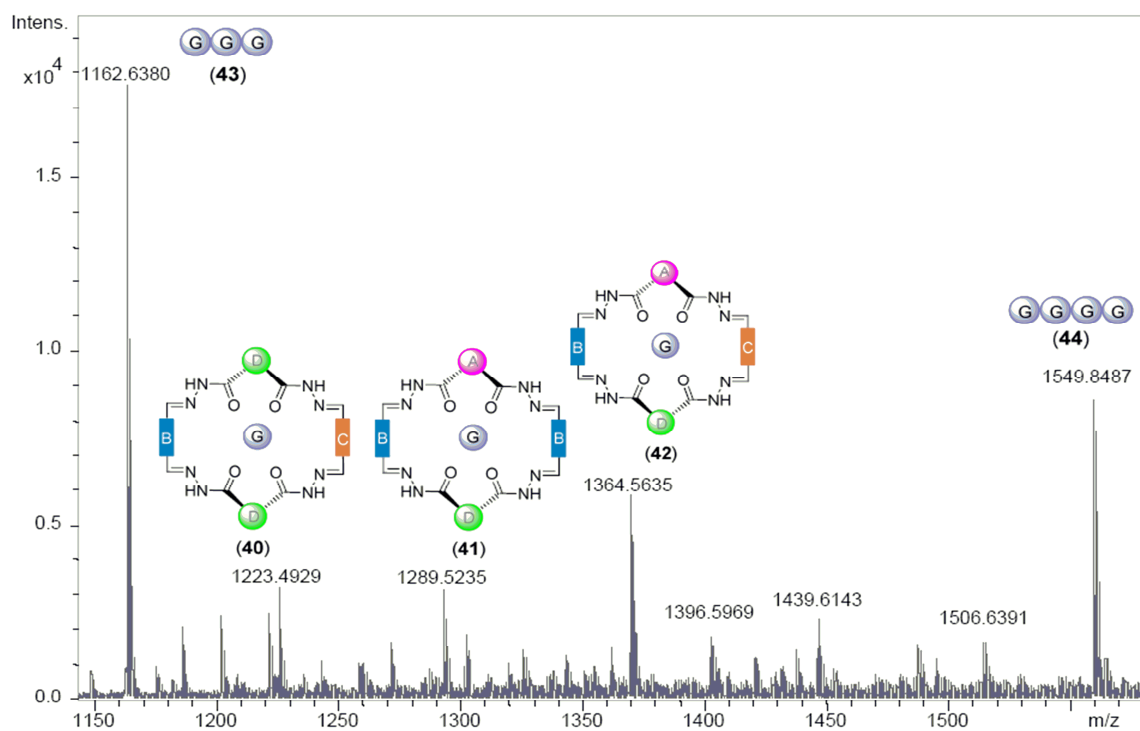


Figure 10. ESI-TOF mass spectrum for host/guest complexes **40-42** in the positive ion mode.

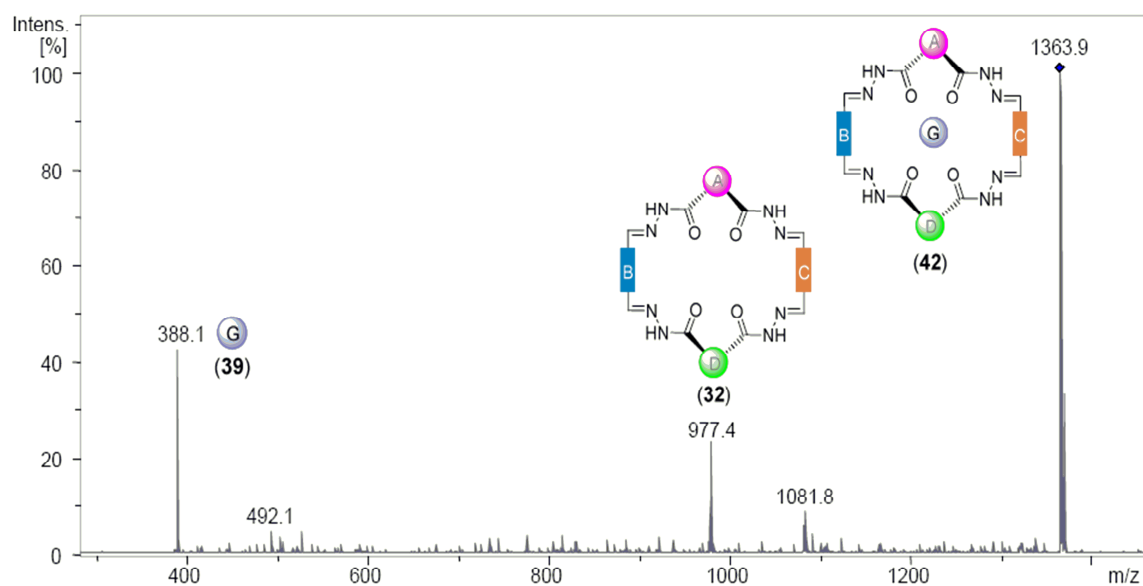


Figure 11. Tandem ESI mass spectrum for host/guest complex **42** (m/z 1364.5635) in the positive ion mode.

REFERENCES

- [1] A. Koch. Bacterial wall as target for attack: Past, present, and future research. *Clin. Microbiol. Rev.* **2003**, *16*, 673.

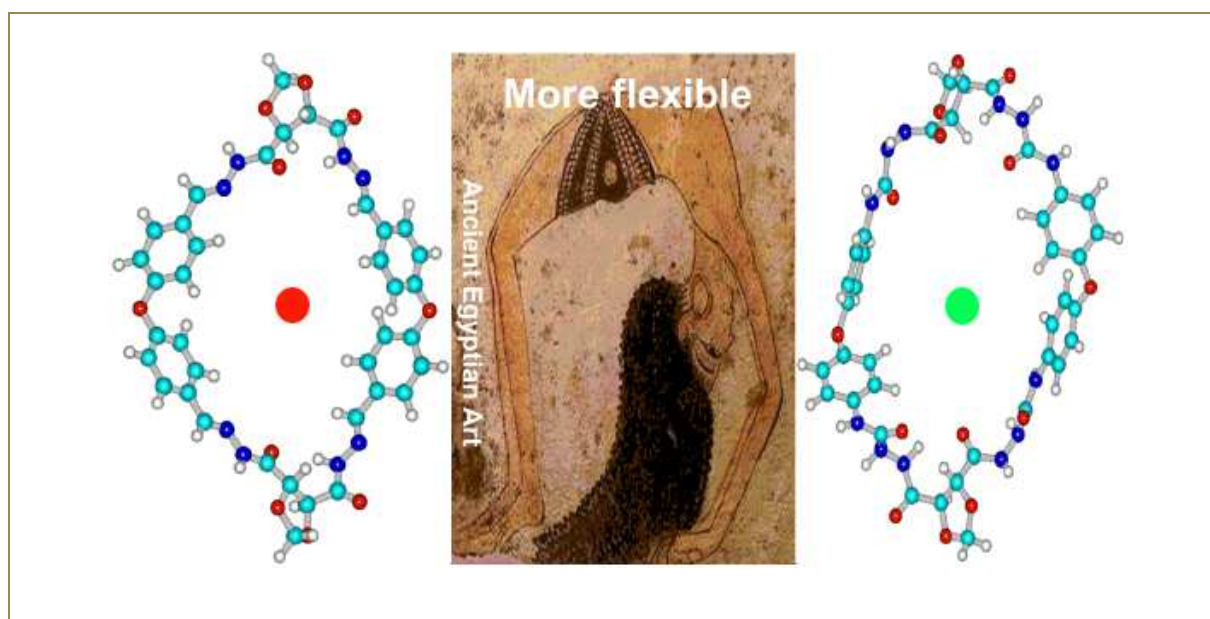
- [2] WHO World health report **2003**. <http://www.who.int/whr/en/>
- [3] J. -M. Lehn, A. V. Eliseev. Dynamic combinatorial chemistry. *Science* **2001**, 291, 2331.
- [4] J. -M. Lehn. Dynamic combinatorial chemistry and virtual combinatorial libraries. *Chem. Eur. J.* **1999**, 5, 2455.
- [5] G. Cousins, S. Poulsen, J. Sanders. Dynamic combinatorial libraries of pseudo-peptide hydrazone macrocycles. *Chem. Comm.* **1999**, 1575.
- [6] G. Cousins, R. Furlan, Y. Ng, J. Sanders. Identification and isolation of a receptor for *N*-methyl alkylammonium salts: Molecular amplification in a pseudo-peptide dynamic combinatorial library. *Angew. Chem. Int. Ed.* **2001**, 40, 423.
- [7] E. Stulz, Y. Ng, S. Scott, J. Sanders. Amplification of a cyclic mixed-metalloporphyrin tetramer from a dynamic combinatorial library through orthogonal metal coordination. *Chem. Comm.* **2002**, 524.
- [8] R. Furlan, Y. Ng, S. Otto, J. Sanders. A new cyclic pseudopeptide receptor for Li⁺ from a dynamic combinatorial library. *J. Am. Chem. Soc.* **2001**, 123, 8876.
- [9] S. Otto, R. Furlan, J. Sanders. Selection and amplification of hosts from dynamic combinatorial libraries of macrocyclic disulfides. *Science* **2002**, 297, 590.
- [10] T. Bunyapaiboonsri, O. Ramstrom, S. Lohmann, J. -M. Lehn, L. Peng, M. Goeldner. Dynamic deconvolution of a pre-equilibrated: Dynamic combinatorial library of acetylcholinesterase inhibitors. *ChemBiochem.* **2001**, 2, 438.
- [11] S.-A. Poulsen. Direct screening of a dynamic combinatorial library using mass spectrometry. *J. Am. Chem. Soc. Mass Spectrom.* **2006**, 17, 1074.
- [12] H. Schiltz, M.-K. Chung, S. Lee, M. Gagné. The effect of gas-phase reactions on the quantitation of cyclic hydrazone libraries by electrospray ionization (ESI) mass spectrometry. *Org. Biomol. Chem.* **2008**, 6, 3597.
- [13] B. Liénard, R. Hüting, P. Lassaux, M. Galleni, J.-M. Frère, C. Schofield. Dynamic combinatorial mass spectrometry leads to metallo- β -lactamase inhibitors. *J. Med. Chem.* **2008**, 51, 684.
- [14] S.-A. Poulsen, P. Gates, G. Cousins, J. Sanders. Electrospray ionisation Fourier-transform ion cyclotron resonance mass spectrometry of dynamic combinatorial libraries. *Rapid Comm. Mass Spectrom.* **2000**, 14, 44.
- [15] C. Hubschwerlen. β -lactam antibiotics. *Comprehensive Medicinal Chemistry II* **2006**, 7, 479.
- [16] Y. Nitnai, T. Kikuchi, K. Kakoi, S. Hanamaki, I. Fujisawa, K. Aoki. Crystal structures of the complexes between Vancomycin and cell-wall precursor analogs. *J. Mol. Biol.* **2009**, 385, 1422.

- [17] N. Kuhnert, A. Lopez-Periago. Synthesis of novel chiral non-racemic substituted trianglimine and trianglamine macrocycles. *Tetrahedron Lett.* **2002**, 43, 3329.
- [18] N. Kuhnert, A. Lopez-Periago, G. Rossignolo. The synthesis and conformation of oxygenated trianglimine macrocycles. *Org. Biomol. Chem.* **2005**, 3, 524.
- [19] N. Kuhnert, G. Rossignolo, A. Lopez-Periago. The synthesis of trianglimines: on the scope and limitations of the [3+3]-cyclocondensation reaction between (1*R*,2*R*)-diaminocyclohexane and aromatic dicarboxaldehydes. *Org. Biomol. Chem.* **2003**, 1, 1157.
- [20] N. Kuhnert, C. Straßnig, A. Lopez-Periago. Synthesis of novel enantiomerically pure trianglimine and trianglamine macrocycles. *Tetrahedron: Asymmetry* **2002**, 13, 123.
- [21] N. Kuhnert, C. Patel, F. Jami. Synthesis of chiral non-racemic polyimine macrocycles from cyclocondensation reactions of biaryl and terphenyl based dicarboxaldehydes and (1*R*,2*R*)-diaminocyclohexane. *Tetrahedron Lett.* **2005**, 46, 7575.
- [22] N. Kuhnert, B. Tang. Synthesis of diastereomeric trianglamine- β -cyclodextrin-[2]-catenanes. *Tetrahedron Lett.* **2006**, 47, 2985.
- [23] N. Kuhnert, D. Marsh, D. Nicolau. The application of quasienantiomeric trianglamine macrocycles as chiral probes for anion recognition in ion trap ESI mass spectrometry. *Tetrahedron: Asymmetry* **2007**, 18, 1648.
- [24] H. Nour, M. Matei, B. Bassil, U. Kortz, N. Kuhnert. Synthesis of tri-substituted biaryl based trianglimines: formation of C_3 -symmetrical and non-symmetrical regioisomers. *Org. Biomol. Chem.* **2011**, 9, 3258.
- [25] H. Nour, A. Lopez-Periago, N. Kuhnert. Probing the mechanism and dynamic reversibility of trianglimine formation using real-time electrospray ionization time-of-flight mass spectrometry. *Rapid Comm. Mass Spectrom.* **2012**, 26, 1070.
- [26] H. Nour, N. Hourani, N. Kuhnert. Synthesis of novel enantiomerically pure tetracarbohydrazide cyclophane macrocycles. *Org. Biomol. Chem.* **2012**, 10, 4381.
- [27] H. Nour, A. Golon, A. Le Gresley, N. Kuhnert. Novel synthesis of enantiomerically pure dioxaspiro[4.5]decane tetra-carbohydrazide cyclophane macrocycles. *Chem. Eur. J.* **2012**, submitted manuscript.
- [28] S.-A. Poulsen. Direct screening of a dynamic combinatorial library using mass spectrometry. *J. Am. Soc. Mass. Spectrom.*, **2006**, 17, 1074.
- [29] Release 8.0. Hypercube, Inc., 1115NW 4th Street, Gainesville, FL 32601, USA. Available: <http://www.hypercube.com>.
- [30] J. Stewart. Optimization of parameters for semiempirical methods. II. Applications. *J. Comput. Chem.* **1989**, 10, 221.
- [31] Z. Ziora, N. Wimmer, R. New, I. Toth. Design and synthesis of lipopeptides and lipopeptidomimetics as novel potential drugs. *Peptide Sci.* **2010**, 47, 214.

- [32] B. Lienard, N. Selevsek, N. Oldham, C. Schofield. Combined mass spectrometry and dynamic chemistry approach to identify metalloenzyme inhibitors. *ChemMedChem*. **2007**, 2, 175.
- [33] S.-A. Poulsen, L. Bornaghi. Fragment-based drug discovery of carbonic anhydrase II inhibitors by dynamic combinatorial chemistry utilizing alkene cross metathesis. *Bioorg. Med. Chem.* **2006**, 14, 3275.
- [34] T. Bunyapaiboonsri, H. Ramstroem, O. Ramstroem, J. Haiech, J.-M. Lehn. Generation of bis-cationic heterocyclic inhibitors of bacillus subtilis HPr Kinase/Phosphatase from a ditopic dynamic combinatorial library. *J. Med. Chem.* **2003**, 46, 5803.
- [35] A. Dahlgren, J. Brånalt, I. Kvarnström, I. Nilsson, D. Musilc, B. Samuelsson. Synthesis of potential thrombin inhibitors. Incorporation of tartaric acid templates as P2 proline mimetics. *Bioorg. Med. Chem.* **2002**, 10, 1567.

Synthesis and ESI-MS Complexation Studies of Novel Chiral Tetra-(hydrazinecarboxamide) cyclophane Macrocycles

Hany F. Nour, Agnieszka Golon, Tuhidul Islam, Marcelo Fernández-Lahore, and Nikolai Kuhnert*



Objectives of the work

The objective of this work is to synthesize a modified and more flexible version of tetra-carbohydrazide cyclophanes to enhance the recognition ability of the macrocycles. The new dicarbohydrazides reacted with 4,4'-oxybis-(phenylisocyanate) and *bis*-(4-isocyanatophenyl)-methane in anhydrous THF in a [2+2]-cyclocondensation reaction to form polyamide cyclophane macrocycles. The compounds obtained by this approach constitute a novel class of macrocycles, which were named tetra-(hydrazinecarboxamide) cyclophanes. The *NH* moieties in the novel macrocycles assume a *syn-anti* conformation as confirmed by 2D-ROESY NMR and molecular modeling calculations at the MM+ level. ESI-TOF/MS and MS/MS were used to qualitatively assess the molecular recognition ability of the novel macrocycles to a selection of oligopeptides and chiral carboxylic acids. The results showed enhanced recognition affinity of the novel tetra-(hydrazinecarboxamide) cyclophanes to chiral carboxylic acids and oligopeptides in comparison with their tetra-carbohydrazide cyclophane analogs.

Synthesis and ESI-MS Complexation Studies of Novel Chiral Tetra-(hydrazine-carboxamide) cyclophane Macrocycles

Hany F. Nour,^[a,b] Agnieszka Golon,^[a] Tuhidul Islam,^[a] Marcelo Fernández-Lahore,^[a] and Nikolai Kuhnert^{*[a]}

Keywords: Macrocycles / Cyclophane / ESI-TOF MS / Dicarbohydrazides / Diisocyanates

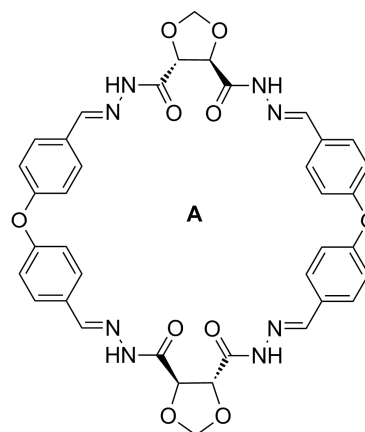
We report the synthesis of novel C_2 -symmetric chiral polyamide macrocycles, derived from chiral dioxolane dicarbohydrazides and aromatic diisocyanates. The new macrocycles form in [2+2]-cyclocondensation reactions in almost quantitative yields under conformational bias of dicarbohydrazides. The reactions took place in anhydrous THF at relatively high concentration of reactants without addition of external templates or applying high dilution conditions.

The novel macrocycles showed potential recognition affinity in the gas phase to a selection of chiral carboxylic acids and oligopeptides. Structures of the novel macrocycles were fully characterised by various spectroscopic techniques such as FT IR, ^1H NMR, ^{13}C NMR, 2D ROESY NMR, 2D HMBC, 2D HMQC, DEPT-135, CD spectroscopy and molecular recognition was investigated by ESI-TOF/MS and tandem MS.

Introduction

The development of novel macrocyclic receptors with high affinity to recognise wide variety of guests of different sizes is a current challenge in supramolecular chemistry. Yet molecular recognition demonstrated by any macrocycle towards a certain guest is reckoned on its versatile design and its possession of interacting functional groups. For an example, the urea functional group has played for more than two decades a predominant role in supramolecular chemistry, in particular in the field of anion recognition.^{1,2} In 1992 Wilcox observed that urea derivatives were able to interact strongly with phosphonates, sulfates and carboxylates in non-polar solvents by forming a stable 1:1 complex held together by two parallel N-H-O hydrogen bonds.³ Further research showed that the design of naturally occurring anion transporters is based on the interaction of amide N-H bonds with anion oxygen functionalities, stimulating further interest into the field of urea based anion receptor chemistry, which has recently been reviewed by Amendola *et al.*⁴ In particular urea based structures have been elaborated into powerful synthetic receptors in analytical chemistry based on changes of their fluorescent properties, with compounds having more than a single urea binding motif. The majority of receptors developed are until now based on open chain structures with only few macrocyclic compounds reported e.g. by Böhmer *et al.*, despite the fact that macrocyclic receptors offer clear advantages in molecular recognition based on conformational restriction and entropically favourable binding contributions.⁵ Macrocycles obtained in $[n+n]$ -cyclocondensation reactions have attracted considerable attention due to their ease of synthesis in large quantities and their unique molecular architectures.

We reported in many occasions the synthesis of trianglimine and trianglamine macrocycles under conformational bias of (1*R*, 2*R*)- and (1*S*, 2*S*)-1,2-diaminocyclohexane in [3+3]-cyclocondensation reactions.⁶⁻¹⁴ Moreover, we have recently reported on a new class of enantiomerically pure tetra-carbohydrazide cyclophane macrocycles, which have at the same time been reported by Gawroński and co-workers based on chiral tartaric acid dihydrazides, obtained in a chemoselective [2+2]-cyclocondensation reaction with aromatic dialdehydes.¹⁵⁻¹⁷ An example for tetra-carbohydrazide cyclophane macrocycles is **A**.



The [2+2]-cyclocondensation reaction takes place at relatively high concentration of the reactants under conformational bias of dicarbohydrazides without addition of external templates or applying high dilution conditions. We recently reported the first application of tetra-carbohydrazide cyclophane macrocycles in DCC (Dynamic combinatorial chemistry) as chiral hosts binding efficiently in the gas phase to oligopeptides of biological interest.¹⁸ In this contribution, we decided to investigate the reactivity of chiral tartaric acid based dihydrazides with aromatic diisocyanates, which would yield six novel macrocyclic compounds with a hydrazido urea as a potential binding motif. The recognition affinity of the novel macrocycles obtained by this approach to chiral carboxylic acids and oligopeptides is demonstrated using high resolution mass spectrometry (ESI-TOF) and tandem MS.

[a] Centre of Nano and Functional Materials (NanoFun), Jacobs University Bremen, Campus Ring 1, 28759 Bremen, Germany.

*Correspondence to: N. Kuhnert, email: n.kuhnert@jacobs-university.de

Fax: +49 421 200-3229, Tel: +49 421 200-3120.

[b] Department of Photochemistry, National Research Centre, El-Beheose street, P.O.Box 12622, Dokki, Egypt.

Results and Discussion

Dicarbohydrazides **1-3** were synthesised from commercially available (+)-diethyl L-tartrate according to literature (Figure 1).¹⁵⁻¹⁶ Then they underwent successfully and selectively [2+2]-cyclocondensation reactions with 4,4'-oxybis-(phenylisocyanate) **4a** and bis-(4-isocyanatophenyl)-methane **4b** in anhydrous THF to afford tetra-(hydrazinecarboxamide) cyclophanes **5-10** in excellent yields (Figure 2). The [2+2]-cyclocondensation products **5-10** form in almost quantitative yields and high purity at a stoichiometry of 1.1:1 of dihydrazides and diisocyanates. Structures of the novel macrocycles were fully assigned and characterised by various spectroscopic techniques such as ¹H NMR, ¹³C NMR, FT IR, 2D ROESY NMR, 2D HMBC, 2D HMQC, DEPT-135 and chirality was confirmed by CD spectroscopy (Circular Dichroism). ¹H NMR spectrum for (*i.e.*, macrocycle **7**) in DMSO-d₆ showed three broad signals at δ 10.02, 8.68 and 8.15 ppm corresponding to 12 NH protons (Figure 3).

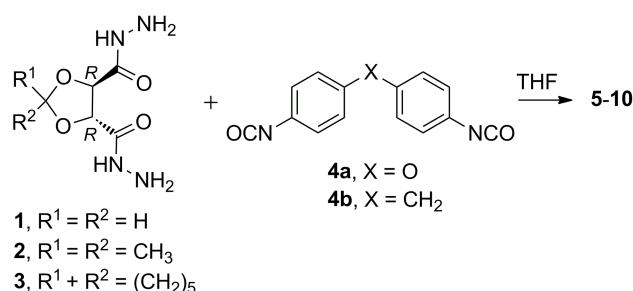


Figure 1 [2+2]-cyclocondensation reaction of dicarbohydrazides **1-3** with diisocyanates **4a** and **4b** in anhydrous THF.

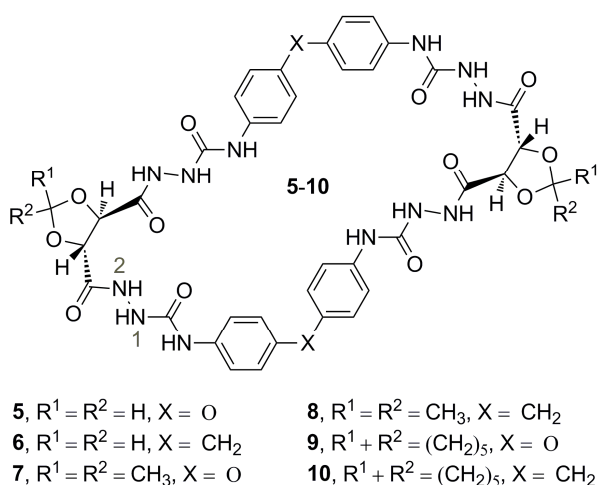


Figure 2 [2+2]-cyclocondensation products **5-10**.

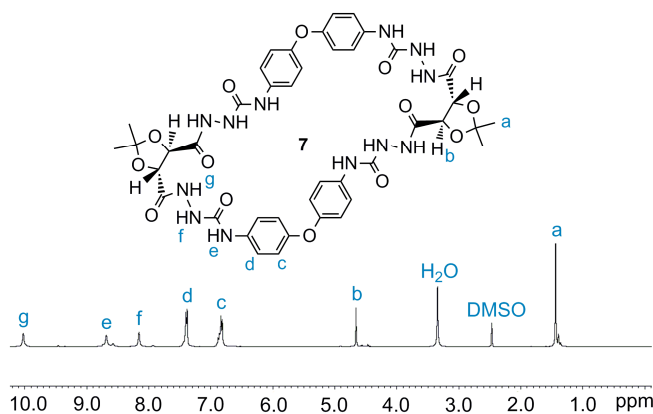


Figure 3 ¹H NMR spectrum for macrocycle **7**, 400 MHz, DMSO-d₆.

FT IR spectrum showed a strong absorption band at $\tilde{\nu}$ 1670 cm⁻¹ corresponding to the stretching vibration of the $\tilde{\nu}$ C=O. It showed also weak absorption band at $\tilde{\nu}$ 3298 cm⁻¹ for NH moieties. ESI-TOF mass spectrum (Electrospray ionisation time of flight) showed the expected pseudo-molecular ion peak at m/z 941.3173 [M+H⁺]. High resolution ESI-TOF/MS data for the novel macrocycles are shown in table 1. Tandem ESI-MS and proposed fragmentation mechanisms of the novel macrocycles are shown with supporting information.

Table 1. HRMS (ESI-TOF, +MS) data for macrocycles **5-10**

Entry	Molecular Formula	Calcd. m/z	Meas. m/z	Error [ppm]	Yield [%]
5 ^[a]	C ₃₈ H ₃₆ N ₁₂ O ₁₄	885.2544	885.2547	0.3	94
6 ^[b]	C ₄₀ H ₄₀ N ₁₂ O ₁₂	903.2781	903.2799	-2.0	99
7 ^[a]	C ₄₂ H ₄₄ N ₁₂ O ₁₄	941.3150	941.3173	2.4	89
8 ^[b]	C ₄₄ H ₄₈ N ₁₂ O ₁₂	959.3407	959.3439	-3.4	90
9 ^[b]	C ₄₈ H ₅₂ N ₁₂ O ₁₄	1043.3631	1043.3618	-1.2	97
10 ^[b]	C ₅₀ H ₅₆ N ₁₂ O ₁₂	1039.4033	1039.4066	-3.1	99

[a] Product ion appeared as [M+H⁺], [b] Product ion appeared as [M+Na⁺]

Molecular Modeling and Conformational Analysis

The novel tetra-(hydrazinecarboxamide) cyclophanes (*i.e.*, **5**) assume a conformation in which the NH moieties are *syn-anti* oriented (Figure 4, conformer **5a**). 2D ROESY spectrum showed through space interactions between H^d and H^e, while no interactions were observed for H^c and H^d or H^c and H^e which suggested a *syn-anti* conformer (Figure 5). Data from 2D ROESY NMR were used for subsequent structure modeling calculations. Structure of macrocycle **5** was optimised using HyperChem software (Release 8.0) at the MM+ level (Molecular mechanics).^{19,20} The molecular structure was optimised using the Polak-Ribiere algorithm till the RMS (Root mean square) gradient was 0.01 Kcal.mol⁻¹. Molecular modeling calculations for macrocycle **5** suggested conformer **5a** as the lowest-energy structure. Conformer **5b** appeared to be the least stable with the highest-energy due to the electrostatic repulsion between the carbonyl groups C=O (6)-(9), C=O (21)-(24), C=O (27)-(30) and C=O (3)-(42). Macrocycles **5-10** form under conformational bias of the reacting dicarbohydrazide and diisocyanate components. We envisage that the macrocycles form in a stepwise reaction in which the final intermediates are conformationally biased to form selectively [2+2]-cyclocondensation products rather than formation of higher oligomers. We performed molecular modeling simulations at the MM+ level to investigate the effect of conformational bias on the final ring closure step. The closer the nucleophilic hydrazide and the electrophilic isocyanate moieties are in space, the more rapidly the ring closure will occur to form the macrocycles. Molecular modeling suggested a distance of 3.59 Å between the reactive sites in intermediate **B** which permits facile ring closure under conformational bias (Figure 6). Molecular modeling also suggested formation of intramolecular hydrogen bonds between NH...O=C (2)-(6) and NH...O=C (23)-(27) which further stabilize and bias intermediate **B** towards formation of macrocycle **5**.

Investigation of Molecular Recognition by ESI-MS

ESI-MS has been widely used as a soft ionisation tool for studying weak non-covalent interactions in the gas phase.²¹⁻²⁵ The

ability of the technique to provide precise mass values, high resolution and little or almost no fragmentations make it an indispensable tool in supramolecular analysis. After successful synthesis and characterisation of tetra-(hydrazinecarboxamide) cyclophanes **5-10**, we decided to carry out a preliminary qualitative assessment of their recognition ability in the gas phase to a wide variety of chiral carboxylic acids, amino acids and oligopeptides of biological interest (Scheme 1). Macrocycles **7** and **8** were chosen for the complexation study. ESI-TOF/MS was used to provide information about high resolution m/z values of the screened host/guest complexes, while tandem MS was used for further confirmation of complexation by means of fragmentation.

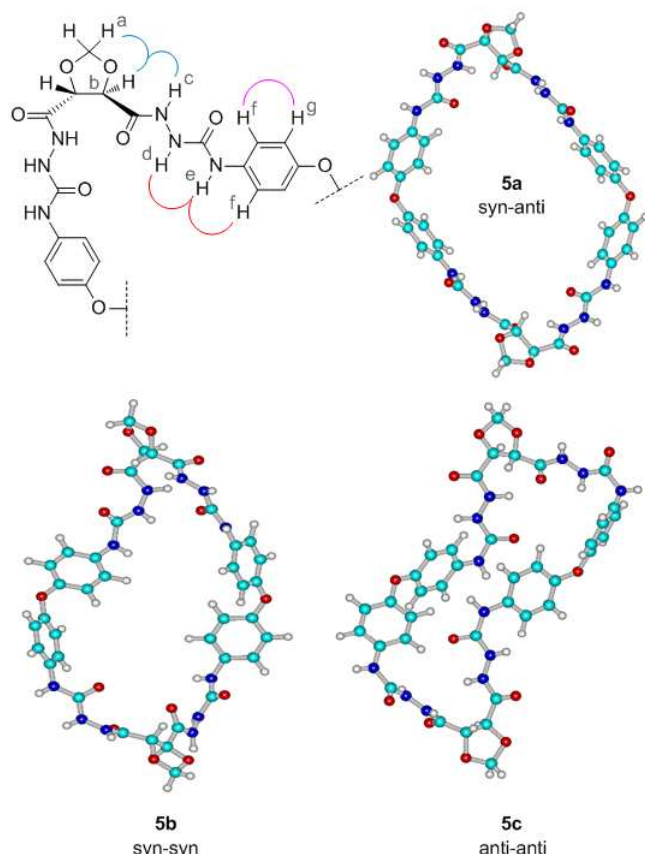


Figure 4. Computed structures and conformation of tetra-(hydrazinecarboxamide) cyclophanes **5** at the MM+ level. A Polak-Ribiere conjugate gradient with rms < 0.01 Kcal.mol⁻¹ was used.

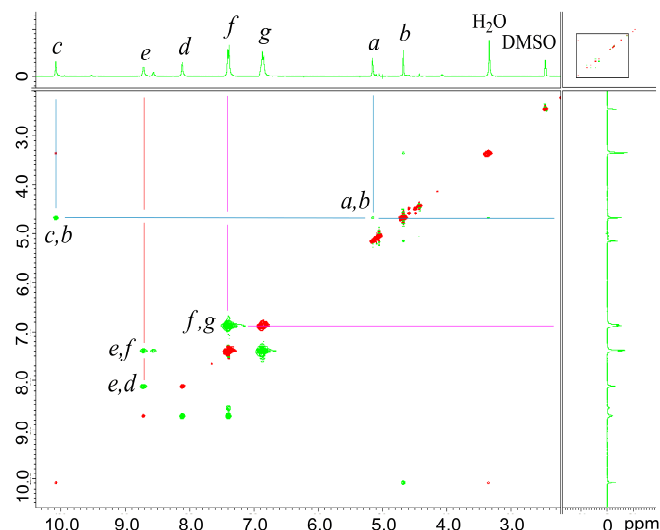


Figure 5. 2D ROESY spectrum for macrocycle **5**.

Oligopeptides AcNH-D-Ala-D-Glu-L-Lys-D-Ala-D-Ala-Gly-COOH **15**, AcNH-D-Glu-L-Lys-D-Ala-D-Ala-Gly-COOH **16** and AcNH-L-Lys-D-Ala-D-Ala-Gly-COOH **17** which mimic bacterial cell wall structure were chosen for the recognition study and were synthesised using solid phase peptide syntheses using the Fmoc method. The purity and identity of **15-17** were assessed by HPLC-tandem MS. Equimolar quantities of host **7** or **8** and guests **11-17** were used. To the host/guest mixture 5 μ L of DMF (*N,N*-dimethylformamide) and H₂O were added, sample was diluted with 1 mL of ACN (Acetonitrile) and well sonicated prior to direct injection into the ESI-TOF mass spectrometer. It can be inferred that macrocycles **7** and **8** showed promising recognition affinity in the gas phase to the chosen guests **11-17**. A stoichiometry of 1:1 host/guest complex was observed by ESI-MS which did not change by adding more equivalents of the guest molecules. As a general observation we found that the peak intensity of the screened host/guest complex increases by increasing the number of carboxylic motifs (COOH) in the guest molecule. Thus, host/guest complex **7/13** showed higher peak intensity in comparison with **7/11**. Also, guests **11** and **13** showed the highest peak intensities in comparison with the rest of the screened compounds shown in Scheme 1. At a competitive level, host **7** binds preferentially to guest **13** in a mixture of **7** with guests **11** and **13**. ESI-TOF/MS and tandem MS for host/guest complex **7/13** are shown in Figure 7.

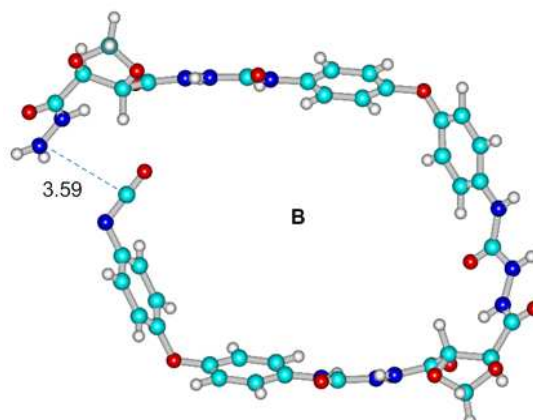
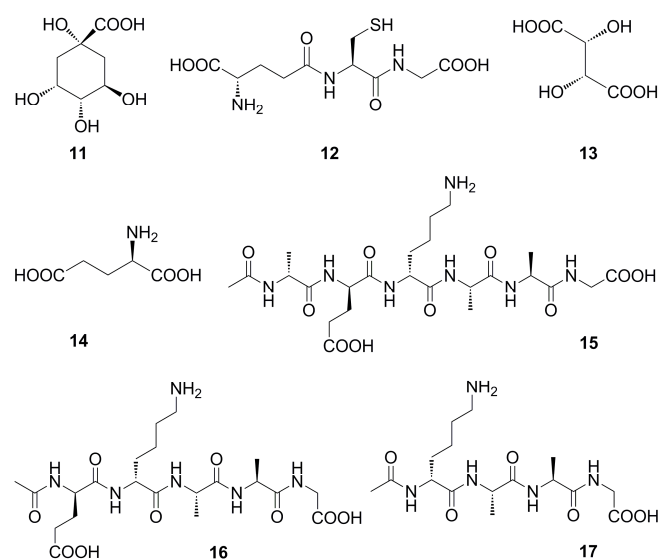


Figure 6. Computed structure for intermediate **B** at the MM+ level. A Polak-Ribiere conjugate gradient with rms < 0.01 Kcal.mol⁻¹ was used.



Scheme 1. Chiral guests **11-17** which have been recognised in the gas phase by hosts **7** and **8**.

Figure 7a showed a pseudo-molecular ion peak at m/z 941.3173 $[M+H]^+$ corresponding to the free host molecule **7**. ESI-TOF/MS for an equimolar mixture of macrocycle **7** and L-(+)-tartaric acid **13** showed a peak at m/z 1089.3192 for the host/guest complex **7/13** with almost disappearance of the peak corresponding to the free macrocycle **7** (Figure 7b). Tandem ESI-MS spectrum for complex **7/13** in the negative ion mode produced a base peak appearing at m/z 939.3 as shown in Figure 7c. High resolution ESI-MS data for host/guest complexes **7/11-17** and **8/11-17** are shown in Table 2 (For proposed fragmentation mechanisms and tandem MS spectra of the novel macrocycles, see supporting information).

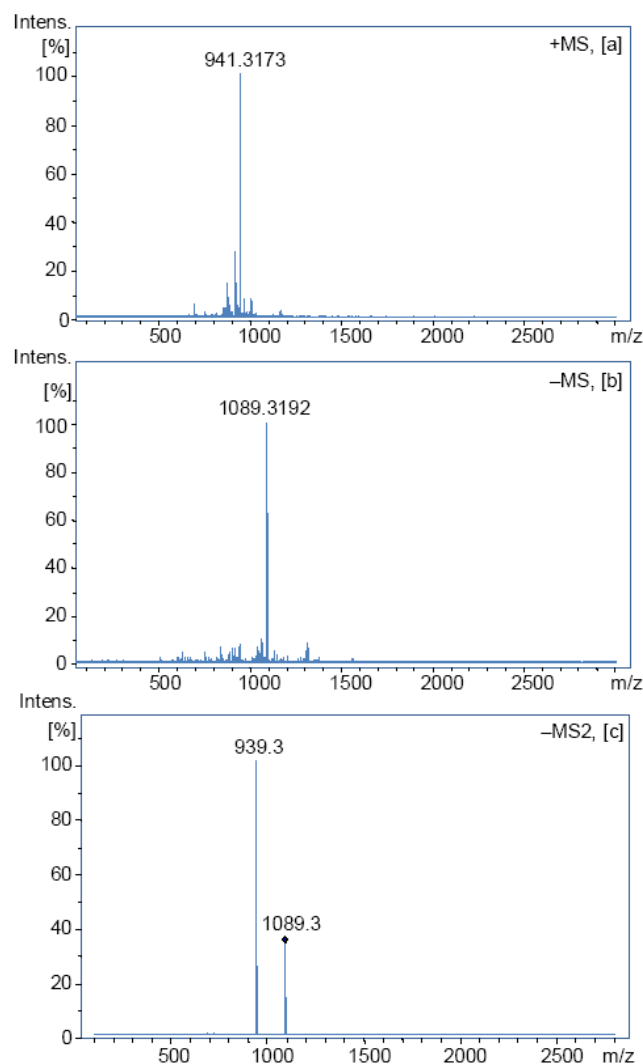


Figure 7. (a) ESI-TOF/MS for free macrocycle **7** $[M+H]^+$, (b) ESI-TOF/MS for host/guest complex **7/13** $[M-H]^-$ and (c) tandem ESI-MS for host/guest complex **7/13** $[M-H]^-$

The chirality of the novel macrocycles was confirmed by CD spectroscopy. The new macrocycles (*i.e.*, **6**) showed moderate Cotton effect at ~ 240 – 260 nm as consequence of the interaction of the aromatic chromophores within the macrocycle (Figure 8).

Conclusions

In summary, six novel tetra-(hydrazinecarboxamide) cyclophane macrocycles were synthesised in almost quantitative yields by reacting dicarbohydrazides obtained from commercially available

tartaric acid with 4,4'-oxybis-(phenylisocyanate) and *bis*-(4-isocyanatophenyl)-methane. Both *R* and *S* enantiomers can be readily available in a one pot [2+2]-cyclocondensation reaction. The *NH* moieties of the novel macrocycles assume *syn-anti* conformation as demonstrated and confirmed by 2D ROESY NMR.

Table 2. HRMS (ESI-TOF) for host/guest complexes **7/11-17** and **8/11-17**

Entry	Molecular Formula		Calcd. m/z	Meas. m/z	Error [ppm]
7/11	$C_{49}H_{56}N_{12}O_{20}$	$[M-H]^-$	1131.3634	1131.3661	2.4
7/12	$C_{52}H_{61}N_{15}O_{20}S$	$[M-H]^-$	1246.3845	1246.3865	1.6
7/13	$C_{46}H_{50}N_{12}O_{20}$	$[M-H]^-$	1089.3170	1089.3192	2.0
7/14	$C_{47}H_{53}N_{13}O_{18}$	$[M-H]^-$	1086.3527	1086.3559	2.9
7/15	$C_{66}H_{85}N_{19}O_{24}$	$[M+H]^+$	1528.6029	1528.6088	3.8
7/16	$C_{63}H_{80}N_{18}O_{23}$	$[M+H]^+$	1457.5774	1457.5716	-3.9
7/17	$C_{58}H_{73}N_{17}O_{20}$	$[M+H]^+$	1328.5262	1328.5291	2.2
8/11	$C_{51}H_{60}N_{12}O_{18}$	$[M-H]^-$	1127.4076	1127.4118	-3.8
8/12	$C_{54}H_{65}N_{15}O_{18}S$	$[M-H]^-$	1242.4280	1242.4255	2.0
8/13	$C_{48}H_{54}N_{12}O_{18}$	$[M-H]^-$	1085.3606	1085.3575	2.9
8/14	$C_{49}H_{57}N_{13}O_{16}$	$[M-H]^-$	1082.3973	1082.3966	0.7
8/15	$C_{68}H_{89}N_{19}O_{22}$	$[M+H]^+$	1524.6502	1524.6476	1.7
8/16	$C_{65}H_{84}N_{18}O_{21}$	$[M+H]^+$	1453.6131	1453.6167	-2.5
8/17	$C_{60}H_{77}N_{17}O_{18}$	$[M+H]^+$	1324.5705	1324.5750	-3.4

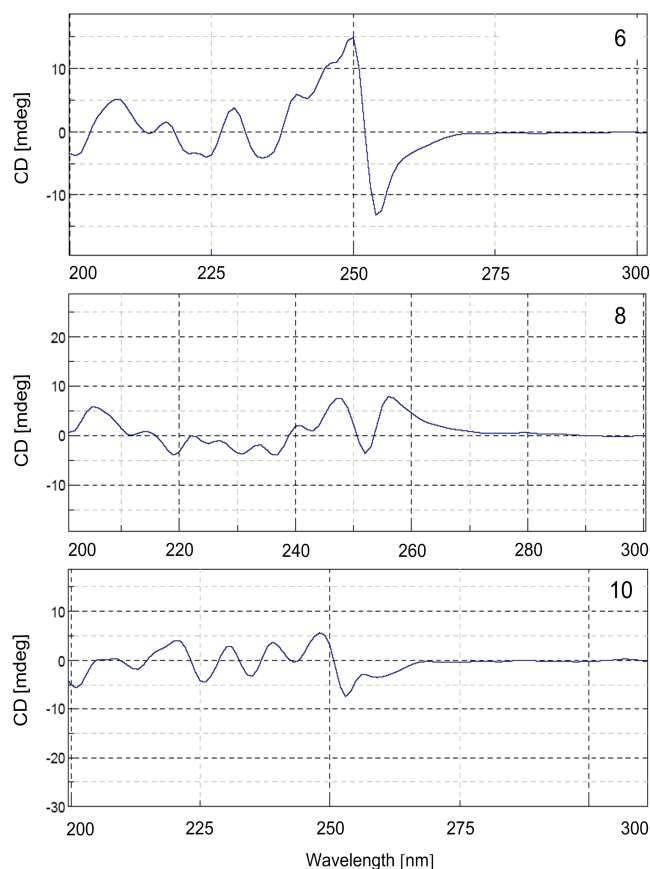


Figure 8. CD spectra for macrocycles **6**, **8** and **10**, from DMSO.

The dioxolane ring can be loaded with various functionalities by simple choice of the ketone to be protected. A preliminary ESI-MS study showed that the new macrocycles can efficiently recognise various guests of small or large sizes making them ideal receptors for different supramolecular applications. Further quantitative work

aimed at assessing molecular recognition ability of the novel macrocycles in solution is under investigation.

Experimental Section

All the reagents used for the reactions were purchased from Sigma-Aldrich, Applichem or Flucka (Germany) and were used as obtained. Whenever possible the reactions were monitored by thin layer chromatography (TLC). TLC was performed on Macherey-Nagel aluminium-backed plates pre-coated with silica gel 60 (UV₂₅₄). Melting points were determined in open capillaries using a Buechl B-545 melting point apparatus and are not corrected. Infrared spectra were determined using a Vector-33 Bruker FT IR spectrometer. The samples were measured directly as solids or oils; ν_{max} values were expressed in cm^{-1} and were given for the main absorption bands. ^1H , ^{13}C and 2D NMR spectra were acquired on a JEOL ECX-400 spectrometer operating at 400 MHz for ^1H NMR and 100 MHz for ^{13}C NMR in DMSO- d_6 using a 5 mm probe. The chemical shifts (δ) are reported in parts per million and were referenced to the residual solvent peak. The following abbreviations are used: s, singlet; m, multiplet; br, broad signal. Mass spectra were recorded using HCTultra and ESI-TOF Bruker Daltonics mass spectrometers and samples were dissolved in DMF, acetonitrile and water using the positive or negative electrospray ionisation modes. Calibration was carried out using a 0.1 M solution of sodium formate in the enhanced quadratic mode prior to each experimental run. The results of measurements were processed using Compass 1.3 data analysis software for a Bruker Daltonics time of flight mass spectrometer (microTOF). Preloaded wang resin, *N,N*-diisopropylethylamine (DIEA), *O*-(benzotriazol-1-yl)-hydroxybenzotriazole (HOBt), *N,N,N',N'*-tetramethyluranyl hexafluorophosphate (HBTU), 9-fluorenylmethoxycarbonyl-amino acid derivatives (1-Fmoc), DMF, *N*-methylpyrrolidone (NMP), trifluoroacetic acid (TFA), 1,2-ethanedithiol (EDT) and other chemicals required for peptide synthesis were bought from Iris Biotech GmbH (Marktredwitz, Germany). Peptides were synthesized with standard solid phase peptide synthesis technique and it was carried out on an automated peptide synthesizer (ABI-433A, Applied Biosystems, Foster city, USA). Fmoc protected preloaded resin was used to grow peptide chain on it. In detail, deprotection of the *N*-terminal of resin bound amino acid was performed by 20% piperidine in NMP and the *C*-terminal of other protected amino acid was activated using HBTU/ HOBt/DIEA (1:1:2) in DMF for coupling with the free *N*-terminal of the resin bound amino acid. A mixture of 82.5% TFA, 5% phenol, 5% water, 5% thioanisole and 2.5% EDT was used to separate the peptide from resin as well as to remove the side chain protecting groups. Subsequently, the peptide was isolated through precipitation in cold (-20°C) diethyl ether and lyophilized by Christ freeze dryers (Martin Christ Gefriertrocknungsanlagen GmbH, Osterode am Harz, Germany). Peptides were purified by high performance liquid chromatography (HPLC) and analyzed by HRMS. Molecular modeling calculations were carried out with HyperChem software (Release 8.0) at the MM+ levels in vacuo and no influence of solvents was taken into account in the calculations. Circular Dichroism measurements were performed using Jasco-J-810 Spectropolarimeter in DMSO.

(4*R*,5*R*,25*R*,26*R*)-Tetra-(hydrazinecarboxamide) cyclophane 5

To a stirred solution of 4,4'-oxybis-(phenylisocyanate) **4a** (500 mg, 1.98 mmol) in anhydrous THF (5 mL) were added (4*R*,5*R*)-1,3-dioxolane-4,5-dicarbohydrazide **1** (396 mg, 2.08 mmol) and 4 mL

anhydrous THF. The mixture was stirred at room temperature for 24 h. The white precipitate was filtered off, washed successively with water, MeOH and dried to yield 830 mg of the titled compound (94%). M.p. $> 260^\circ\text{C}$ (decomp.). IR $\tilde{\nu} = 3283$ (NH), 1676 (C=O) cm^{-1} . ^1H NMR (400 MHz, DMSO- d_6): $\delta = 10.07$ (4H, brs, NH), 8.71 (3H, brs, NH), 8.56 (1H, brs, NH), 8.11 (4H, brs, NH), 7.39 (8H, d, $J = 8.7$, ArH), 6.85 (8H, d, $J = 8.7$, ArH), 5.15 (4H, brs, CH_2), 4.67 (4H, brs, CH) ppm. ^{13}C NMR (100 MHz, DMSO- d_6): $\delta = 169.3$ (CO), 155.6 (CO), 152.4 (C), 135.4 (C), 120.6 (CH), 119.1 (CH), 97.0 (CH_2), 77.2 (CH) ppm. HRMS (ESI-TOF+, DMF/ACN): m/z calcd. for $\text{C}_{38}\text{H}_{36}\text{N}_{12}\text{O}_{14}$ [$\text{M}+\text{H}^+$] 885.2544; found 885.2547.

(4*R*,5*R*,25*R*,26*R*)-Tetra-(hydrazinecarboxamide) cyclophane 6

To a stirred solution of *bis*-(4-isocyanatophenyl)-methane **4b** (500 mg, 2 mmol) in THF (5 mL) were added (4*R*,5*R*)-1,3-dioxolane-4,5-dicarbohydrazide **1** (399 mg, 2.1 mmol) and 4 mL THF. The mixture was stirred at room temperature for 24 h. The white precipitate was filtered off, washed successively with water, diethyl ether and dried to yield 875 mg of the titled compound (99%). M.p. $> 260^\circ\text{C}$ (decomp.). IR $\tilde{\nu} = 3274$ (NH), 1683 (C=O) cm^{-1} . ^1H NMR (400 MHz, DMSO- d_6): $\delta = 10.05$ (4H, brs, NH), 8.64 (4H, brs, NH), 8.07 (4H, brs, NH), 7.31 (8H, d, $J = 8.2$, ArH), 7.03 (8H, d, $J = 8.2$, ArH), 5.14 (4H, brs, CH_2), 4.65 (4H, brs, CH), 3.74 (4H, brs, CH_2) ppm. ^{13}C NMR (100 MHz, DMSO- d_6): $\delta = 169.2$ (CO), 155.5 (CO), 137.9 (C), 135.6 (C), 129.3 (CH), 119.2 (CH), 97.0 (CH_2), 77.2 (CH) ppm. HRMS (ESI-TOF+, DMF/ACN): m/z calcd. for $\text{C}_{40}\text{H}_{40}\text{N}_{12}\text{O}_{12}$ [$\text{M}+\text{Na}^+$] 903.2781; found 903.2799.

(4*R*,5*R*,25*R*,26*R*)-Tetra-(hydrazinecarboxamide) cyclophane 7

To a stirred solution of 4,4'-oxybis-(phenylisocyanate) **4a** (500 mg, 1.98 mmol) in anhydrous THF (5 mL) were added (4*R*,5*R*)-2,2-dimethyl-1,3-dioxolane-4,5-dicarbohydrazide **2** (454 mg, 2.08 mmol) and 4 mL anhydrous THF. The mixture was stirred at room temperature for 24 h. The white precipitate was filtered off, washed successively with water, MeOH and dried to yield 820 mg of the titled compound (89%). M.p. $> 240^\circ\text{C}$ (decomp.). IR $\tilde{\nu} = 3298$ (NH), 1670 (C=O) cm^{-1} . ^1H NMR (400 MHz, DMSO- d_6): $\delta = 10.02$ (4H, brs, NH), 8.68 (4H, brs, NH), 8.15 (4H, brs, NH), 7.39 (8H, d, $J = 8.7$, ArH), 6.82 (8H, d, $J = 8.7$, ArH), 4.65 (4H, brs, CH), 1.43 (12H, s, CH_3) ppm. ^{13}C NMR (100 MHz, DMSO- d_6): $\delta = 169.4$ (CO), 155.6 (CO), 152.4 (C), 135.4 (C), 120.6 (CH), 119.2 (CH), 113.1 (C), 77.2 (CH), 26.7 (CH_3) ppm. HRMS (ESI-TOF+, DMF/ACN): m/z calcd. for $\text{C}_{42}\text{H}_{44}\text{N}_{12}\text{O}_{14}$ [$\text{M}+\text{H}^+$] 941.3150; found 941.3173.

(4*R*,5*R*,25*R*,26*R*)-Tetra-(hydrazinecarboxamide) cyclophane 8

To a stirred solution of *bis*-(4-isocyanatophenyl)-methane **4b** (500 mg, 2 mmol) in THF (5 mL) were added (4*R*,5*R*)-2,2-dimethyl-1,3-dioxolane-4,5-dicarbohydrazide **2** (458 mg, 2.1 mmol) and 4 mL anhydrous THF. The mixture was stirred at room temperature for 24 h. The white precipitate was filtered off, washed successively with water, diethyl ether and dried to yield 850 mg of the titled compound (90%). M.p. $> 230^\circ\text{C}$ (decomp.). IR $\tilde{\nu} = 3267$ (NH), 1668 (C=O) cm^{-1} . ^1H NMR (400 MHz, DMSO- d_6): $\delta = 10.01$ (4H, brs, NH), 8.61 (4H, brs, NH), 8.11 (4H, brs, NH), 7.31 (8H, d, $J = 8.2$, ArH), 7.00 (8H, d, $J = 7.7$, ArH), 4.63 (4H, brs, CH), 3.72 (4H, brs, CH_2), 1.43 (12H, s, CH_3) ppm. ^{13}C NMR (100 MHz, DMSO- d_6): $\delta = 169.3$ (CO), 155.5 (CO), 137.9 (C), 135.6 (C), 129.2 (CH), 119.2 (CH), 113.1 (C), 77.2 (CH), 26.7 (CH_3) ppm, signal for CH_2 overlapped with signals of DMSO- d_6 (For DEPT-135 spectrum, see supporting information). HRMS (ESI-TOF+,

DMF/ACN): m/z calcd. for $C_{44}H_{48}N_{12}O_{12}$ $[M+H]^+$ 959.3407; found 959.3439.

(4R,5R,25R,26R)-Tetra-(hydrazinecarboxamide) cyclophane 9

To a stirred solution of 4,4'-oxybis-(phenylisocyanate) **4a** (500 mg, 1.98 mmol) in anhydrous THF (5 mL) were added (2R,3R)-1,4-dioxaspiro-[4.5]-decane-2,3-dicarbohydrazide **3** (538 mg, 2.08 mmol) and 4 mL anhydrous THF. The mixture was stirred at room temperature for 24 h. The white precipitate was filtered off, washed successively with water, MeOH and dried to yield 980 mg of the titled compound (97%). M.p. > 240 °C (decomp.). IR $\tilde{\nu}$ = 3298 (NH), 1669 (C=O) cm^{-1} . 1H NMR (400 MHz, DMSO- d_6): δ = 9.99 (4H, brs, NH), 8.68 (4H, brs, NH), 8.16 (4H, brs, NH), 8.39 (8H, d, J = 8.24, ArH), 8.82 (8H, d, J = 8.7, ArH), 4.66 (4H, brs, CH), 1.71-1.51 (16H, m, CH_2), 1.33 (4H, m, CH_2) ppm. ^{13}C NMR (100 MHz, DMSO- d_6): δ = 169.4 (CO), 155.6 (CO), 152.4 (C), 135.4 (C), 120.8 (CH), 119.1 (CH), 113.7 (C), 76.9 (CH), 25.6 (CH_2), 25.0 (CH_2), 23.8 (CH_2) ppm. HRMS (ESI-TOF+, DMF/ACN): m/z calcd. for $C_{48}H_{52}N_{12}O_{14}$ $[M+Na]^+$ 1043.3631; found 1043.3618.

(4R,5R,25R,26R)-Tetra-(hydrazinecarboxamide) cyclophane 10

To a stirred solution of bis-(4-isocyanatophenyl)-methane **4b** (500 mg, 2 mmol) in THF (5 mL) were added (2R,3R)-1,4-dioxaspiro-[4.5]-decane-2,3-dicarbohydrazide **3** (542 mg, 2.1 mmol) and 4 mL anhydrous THF. The mixture was stirred at room temperature for 24 h. The white precipitate was filtered off, washed successively with water, diethyl ether and dried to yield 1.0 g of the titled compound (99%). M.p. > 245 °C (decomp.). IR $\tilde{\nu}$ = 3297 (NH), 1674 (C=O) cm^{-1} . 1H NMR (400 MHz, DMSO- d_6): δ = 9.98 (4H, brs, NH), 8.62 (4H, brs, NH), 8.12 (4H, brs, NH), 7.37 (8H, d, J = 8.2, ArH), 7.00 (8H, d, J = 8.2, ArH), 4.63 (4H, brs, CH), 3.71 (4H, brs, CH_2), 1.70-1.57 (12H, m, CH_2), 1.54-1.50 (4H, m, CH_2), 1.32 (4H, m, CH_2) ppm. ^{13}C NMR (100 MHz, DMSO- d_6): δ = 169.4 (CO), 155.5 (CO), 137.9 (C), 135.6 (C), 129.2 (CH), 119.2 (CH), 113.7 (C), 76.9 (CH), 35.8 (CH_2), 25.0 (CH_2), 23.8 (CH_2) ppm, signal for CH_2 overlapped with signals of DMSO- d_6 . HRMS (ESI-TOF+, DMF/ACN): m/z calcd. for $C_{50}H_{56}N_{12}O_{12}$ $[M+Na]^+$ 1039.4033; found 1039.4066.

Supporting Information (see footnote on the first page of this article): 1H NMR, ^{13}C NMR, 2D ROESY NMR, 2D HMBC, 2D HMQC, DEPT-135, ESI-TOF/MS for host/guest complexes, tandem MS and proposed fragmentation mechanisms of the novel macrocycles.

Acknowledgments

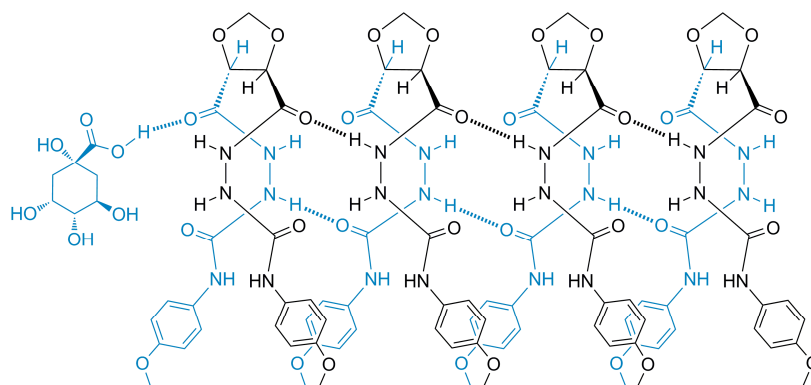
H. Nour thanks Deutscher Akademischer Austausch Dienst (DAAD) for financial support and Jacobs University for excellent facilities.

- [1] J. Steed, *Chem. Soc. Rev.* **2010**, 39, 3686.
- [2] Y.-J. Li, L. Xu, W.-L. Yang, H.-B. Liu, S.-W. Lai, C.-M. Che, Y.-L. Li, *Chem. Eur. J.* **2012**, 18, 4782.
- [3] P. Smith, M. Reddington, C. Wilcox, *Tetrahedron Lett.* **1992**, 33, 6085.
- [4] V. Amendola, L. Fabbrizzi, L. Mosca, *Chem. Soc. Rev.* **2010**, 39, 3889.
- [5] V. Böhmer, D. Meshcheryakov, F. Arnaud-Neu, M. Bolte, V. Hubscher-Bruder, E. Jobin, I. Thondorf, S. Werner, *Org. Biomol. Chem.* **2008**, 6, 1004.
- [6] N. Kuhnert, G. Rossignolo, A. Lopez-Periago, *Org. Biomol. Chem.* **2003**, 1, 1157.
- [7] N. Kuhnert, C. Patel, F. Jami, *Tetrahedron Lett.* **2005**, 46, 7575.
- [8] N. Kuhnert, A. Lopez-Periago, *Tetrahedron Lett.* **2002**, 43, 3329.

- [9] N. Kuhnert, A. Lopez-Periago, G. Rossignolo, *Org. Biomol. Chem.* **2005**, 3, 524.
- [10] N. Kuhnert, C. Straßnig, A. Lopez-Periago, *Tetrahedron: Asymm.* **2002**, 13, 123.
- [11] N. Kuhnert, B. Tang, *Tetrahedron Lett.* **2006**, 47, 2985.
- [12] N. Kuhnert, D. Marsh, D. Nicolau, *Tetrahedron: Asymm.* **2007**, 18, 1648.
- [13] H. Nour, M. Matei, B. Bassil, U. Kortz, N. Kuhnert, *Org. Biomol. Chem.* **2011**, 9, 3258.
- [14] H. Nour, A. Lopez-Periago, N. Kuhnert, *Rapid Comm. Mass Spectrom.* **2012**, 26, 1070.
- [15] H. Nour, N. Hourani, Nikolai Kuhnert, *Org. Biomol. Chem.* **2012**, 10, 4381.
- [16] H. Nour, A. Golon, A. Le Gresley, Nikolai Kuhnert, *Chem. Eur. J.* **2012**, submitted manuscript.
- [17] P. Skowronek, M. Kunciewicz, M. Brzostowska, A. Janiak, U. Rychlewska, J. Gawroński, *Tetrahedron: Asymm.* **2012**, 23, 300.
- [18] H. Nour, T. Islam, M. Fernández-Lahore, N. Kuhnert, *Rapid Comm. Mass Spectrom.* **2012**, submitted manuscript.
- [19] Molecular modelling was carried out using HyperChem software (Release 8.0). Hypercube, Inc., 1115 NW 4th Street, Gainesville, FL 32601 USA. Trial, version from <http://www.hypercube.com>
- [20] J. Stewart, *J. Comput. Chem.* **1989**, 10, 221.
- [21] P. Sarni-Manchado, V. Cheynier, *Rapid Comm. Mass Spectrom.* **2002**, 37, 609.
- [22] S. Banerjee, S. Mazumdar, *J. Mass Spectrom.* **2010**, 45, 1212.
- [23] Z. Yu, M. Cui, C. Yan, F. Song, Z. Liu, S. Liu, **2007**, 21, 683.
- [24] M. L. Colgrave, J. L. Beck, M. M. Sheil, M. S. Searle, *Chem. Commun.* **2002**, 556.
- [25] M. Guo, S. Zhang, F. Song, D. Wang, Z. Liu, S. Liu, *J. Mass Spectrom.* **2003**, 38, 723.

Synthesis, self-assembly and ESI-MS complexation studies of novel chiral bis-*N*-substituted-hydrazinecarboxamide receptors

Hany F. Nour, Agnieszka Golon, Tuhidul Islam, Marcelo Fernández-Lahore and Nikolai Kuhnert*



Objectives of the work

In continuing attempts to enhance the molecular recognition ability of the new tetra-carbohydrazide cyclophane macrocycles, a novel class of tetra-(hydrazinecarboxamide) cyclophanes was successfully synthesized in [2+2]-cyclocondensation reactions. Molecular modeling at the MM+ level predicted that a two-armed receptor with a structure simulating the structural framework of tetra-(hydrazinecarboxamide) cyclophanes should possess enhanced recognition ability and higher degree of flexibility. The objective of this work is accordingly to synthesize a novel class of two-armed receptors and to assess their molecular recognition ability to chiral carboxylic acids and oligopeptides. Dioxolane dihydrazides reacted with aromatic isocyanates in anhydrous THF to give bis-*N*-substituted-hydrazinecarboxamide receptors. Unlike in tetra-(hydrazinecarboxamide) cyclophanes, the *NH* moieties in the novel receptors assume a *syn/syn* conformation. The novel receptors showed unprecedented dual self-assembly and molecular recognition in the gas phase to the oligopeptide guests. ESI-TOF/MS and tandem MS were used to reveal the nature of associations formed between hosts and guests. The novel receptors showed selective recognition to the chosen guests in the gas phase, which has been confirmed by ESI-TOF/MS and tandem MS/MS.



Synthesis, self-assembly and ESI-MS complexation studies of novel chiral bis-*N*-substituted-hydrazinecarboxamide receptors

Hany F. Nour^{a,b}, Agnieszka Golon^a, Tuhidul Islam^a, Marcelo Fernández-Lahore^a and Nikolai Kuhnert^{a,*}

^aSchool of Engineering and Science, Centre for Nano and Functional Materials (NanoFun), Jacobs University, 28759 Bremen, Germany.

^bNational Research Centre, Department of Photochemistry, El Behoose Street, P.O. Box 12622, Dokki, Cairo, Egypt.

ARTICLE INFO

Article history:

Received

Received in revised form

Accepted

Available online

Keywords:

Hydrazinecarboxamide

Receptors

Self-assembly

ESI mass spectrometry

Dicarbohydrazides

ABSTRACT

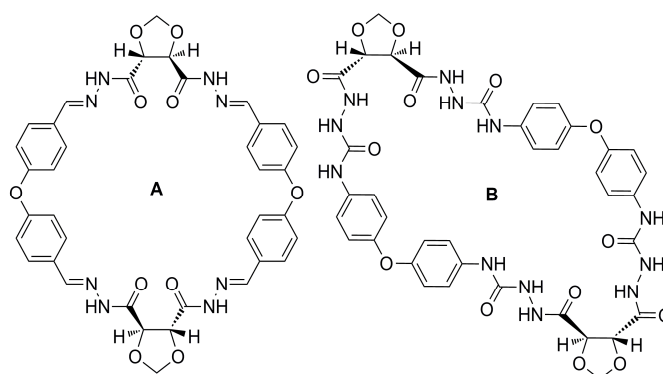
A total of seven novel bis-*N*-substituted-hydrazinecarboxamide two-armed molecular receptors were synthesized in good to excellent yields by reacting chiral dicarbohydrazides obtained from commercially available tartaric acid with aromatic isocyanates. Unlike tetra-carbohydrazide and tetra-(hydrazinecarboxamide) cyclophane macrocycles, which have recently been synthesized in our laboratory, the new receptors showed a remarkable degree of flexibility. The novel receptors showed efficient selective recognition ability in the gas phase to a selection of chiral carboxylic acids and oligopeptides with formation of structurally unique self-assembled host/guest complexes as confirmed by ESI-TOF and tandem MS. Structures of the novel receptors were fully assigned by various spectroscopic techniques such as ¹H NMR, ¹³C NMR, ESI-TOF/MS, tandem MS, 2D ROESY NMR and CD spectroscopy.

2012 Elsevier Ltd. All rights reserved.

1. Introduction

Over the past few decades, the synthesis of new artificial receptors has attracted considerable attention in supramolecular chemistry.^{1–7} Molecular tweezers form a class of acyclic receptors bearing *n*-number of arms which bind a target guest molecule.⁸ A central spacer unit connects the sidewalls of the tweezer and can be either flexible or rigid. The size of the spacer unit determines the shape and cavity of the tweezer. Symmetrical tweezers bear similar arms, while non-symmetrical tweezers possess different arms.^{3,7,9–13} The first version of molecular tweezers recognizing aromatic guests *via* π - π stacking interactions was developed by Whitlock and Zimmerman.^{8,14–16} Following this work, many structurally unique tweezers were synthesized and showed their promise in binding neutral and charged guests.^{1–7} Molecular recognition of synthetic receptors to carboxylic and amino acids is of particular interest to supramolecular chemists due to their biological, industrial and environmental concern. An ideal receptor should have adequate solubility and should incorporate functionalities into its structural framework in order to promote its recognition ability. Both hydrogen bonding and π - π stacking interactions play significant roles in stabilizing and strengthening the binding interactions of tweezer/guest complexes. Although many receptors which bind carboxylic acids are reported in literature, only few examples such as diketopiperazine are known

for peptide recognition.^{7,17–26} Recently, we have described the synthesis of a novel class of cyclophane-*type* macrocycles **A** and **B** in almost quantitative yields.^{27–29} We showed that the macrocycles can be obtained in both enantiomeric forms (*R* or *S*) by reacting chiral dicarbohydrazides obtained from diethyl tartrate with aromatic dialdehydes and diisocyanates in [2+2]-cyclocondensation reactions.



Parallel to our work with cyclophanes **A** and **B**, Gawroński *et al.* reported the synthesis of a tetra-carbohydrazide cyclophane macrocycle derived from (4*R*,5*R*)-2,2-dimethyl-1,3-dioxolane-4,5-dicarbohydrazide and terephthalaldehyde.³⁰ Macrocycle **A** possesses four amide and four imine moieties making it suitable for different applications in DCC (dynamic combinatorial chemistry), while macrocycle **B** has more functionalities and higher degree of flexibility.^{27–29,31}

*Correspondence to: N. Kuhnert, email: n.kuhnert@jacobs-university.de; Tel.: +49-421-200-3120; Fax: +49-421-200-3229.

Similar to the case of triallimine chemistry, macrocycles **A** and **B** form under conformational *bias* of dicarbohydrazides.³²⁻⁴⁰

2. Results and discussion

2.1. Synthesis and molecular modeling

In continuation to our work with cyclophane macrocycles **A** and **B**, we decided to synthesize a class of two-armed receptors which simulates the structural framework of macrocycle **B**. Receptors with such structural features are expected to be more flexible and to show improved molecular recognition abilities. Two-armed receptors **7-13** were synthesized from chiral dicarbohydrazides **1-3** by reacting with substituted aromatic isocyanate **4-6** in anhydrous THF (Fig. 1). The sidewalls of the receptors are made of amide moieties, which function as the receptor binding motifs, while dioxolane rings constitute the spacer units. The recognition affinity of the novel receptors in the gas phase to a selection of chiral carboxylic acids and oligopeptides is demonstrated by using electrospray ionization time of flight mass spectrometry (ESI-TOF/MS) and tandem MS. Structures of the novel receptors were fully assigned by various spectroscopic techniques such as FT IR, ¹H NMR, ¹³C NMR, 2D ROESY, Circular Dichroism spectroscopy (CD), ESI-TOF/MS and MS/MS.

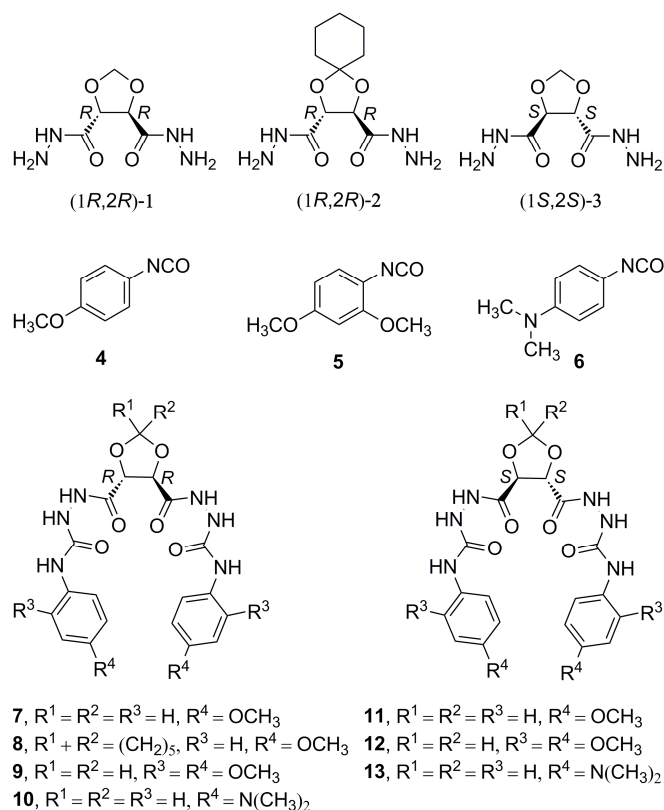


Fig. 1 Two-armed receptors **7-13**, which were synthesized from chiral dicarbohydrazides **1-3** and substituted aromatic isocyanates **4-6**.

¹H NMR spectrum for (*i.e.*, chiral receptor **7**) showed three broad signals at 10.05, 8.54 and 8.04 ppm corresponding to the amide NH protons. FT IR spectrum showed a strong absorption band at ν 1689 cm⁻¹ corresponding to the stretching vibration of the ν C=O. ESI-TOF/MS showed the expected pseudo-molecular ion peak at m/z 487.1588 [M-H]⁻ in the negative ion mode. High resolution mass spectrometry (HRMS) data for the new receptors are shown in table 1. 2D ROESY spectrum for receptor **7** (Fig. 2) showed through space interactions between H^d-H^c and H^d-H^e, which suggests a *syn/syn* conformation of the NH moieties. Unlike receptor **7**, the NH moieties in macrocycle **B** assume a *syn/anti* conformation.²⁹ Data from 2D ROESY NMR were used

for subsequent structure modeling calculations. Structure of receptor **7** was energy-minimized using HyperChem software (Release 8.0) at the Austin Model 1 level (AM1).^{41,42} Molecular modeling calculations are in good agreement with data from 2D ROESY NMR and suggests a spiral-like structure for receptor **7** in which the NH moieties are *syn/syn* oriented. Structures of receptors **7-13** are stabilized by intramolecular hydrogen bonds as shown in Figure 3.

Table 1. High resolution ESI-TOF/MS data for receptors **7-13**

Entry	Molecular formula	Calcd. m/z	^a Meas. m/z	Error [ppm]	Yield %
7	C ₂₁ H ₂₄ N ₆ O ₈	487.1583	487.1588	-1.0	78
8	C ₂₆ H ₃₂ N ₆ O ₈	555.2209	555.2224	-2.8	74
9	C ₂₃ H ₂₈ N ₆ O ₁₀	547.1794	547.1782	2.2	93
10	C ₂₃ H ₃₀ N ₈ O ₆	513.2216	513.2240	-4.8	89
11	C ₂₁ H ₂₄ N ₆ O ₈	487.1583	487.1570	2.7	96
12	C ₂₃ H ₂₈ N ₆ O ₁₀	547.1794	547.1799	-1.0	99
13	C ₂₃ H ₃₀ N ₈ O ₆	513.2216	513.2233	-3.5	93

^aProduct ions appeared as [M-H]⁻

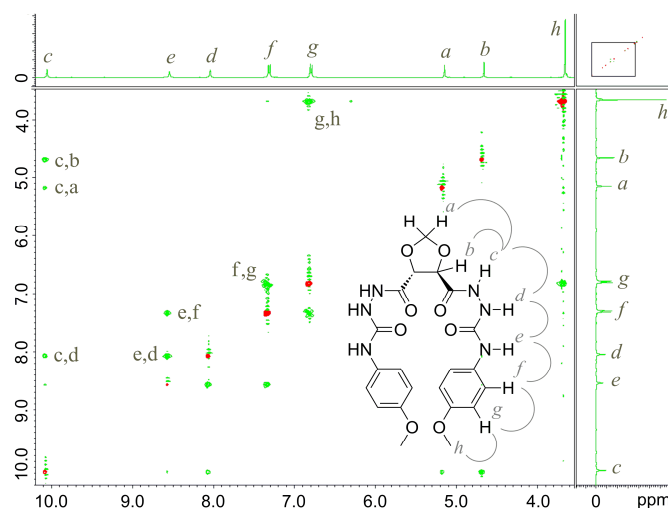


Fig. 2 2D ROESY NMR spectrum for receptor **7** (DMSO-d₆).

2.2. Molecular recognition and self-assembly in the gas phase

Electrospray ionization (ESI-MS) has been widely used as a versatile soft ionization method in studying weak non-covalent interactions and molecular recognition in the gas phase.⁴³⁻⁴⁵ The ability of the technique to provide precise mass values, high resolution and little or almost no fragmentations make it an indispensable tool in supramolecular analysis. Recently, we reported on the use of ESI-TOF/MS in probing the mechanism of triallimine formation in real-time and studying dynamic reversibility and molecular recognition of tetra-carbohydrazide cyclophanes in the gas phase to oligopeptides.^{31,46} Two-armed receptor **7** showed interesting molecular self-assembly both in solution and in the gas phase to form dimeric, trimeric and tetrameric supramolecular associations. Molecular self-assembly has been confirmed in solution by variable temperature NMR (VT NMR) and in the gas phase by ESI-TOF and tandem MS. VT NMR was performed from 313 to 413 K in DMSO-d₆. A downfield in chemical shift (δ) for NH^c, NH^e and NH^d, with increasing temperature, has been observed (Fig. 4). The decrease in δ is an indication of breaking inter- and intramolecular hydrogen bonding interactions (NH...O=C) for the associated receptor molecules. Cooling the NMR to 298 K yields the same spectrum as first recorded as a consequent of re-establishment of the hydrogen bonds. Tandem

ESI-MS for self-assembled associations of receptor **7** are shown in Figure 5a-d. ESI-TOF/MS (Fig. 5a) showed four peaks at m/z 511, 999, 1487 and 1976 corresponding to the sodiated pseudo-molecular ion peaks of the free receptor **7**, dimeric, trimeric and tetrameric self-assembled associations, respectively. Molecular modeling at the Molecular mechanics level (MM+) suggested that the receptor molecules are lined up in a queue-like structure and bind together by intermolecular hydrogen bonds (See supporting information). Proposed structure and fragmentation mechanisms of the self-assembled associations of receptor **7** are shown in Figure 6. Receptor **7** showed unique dual self-assembly and recognition in the gas phase with formation of 1:1, 1:2, 1:3 and 2:1 stoichiometries complexation with guests **14-20** (Scheme 1 and table 2). Tandem ESI-MS for host/guest complex **7/14** showed a peak at m/z 1168.3 corresponding to two assembled molecules of host **7** and a one molecule of guest **14** (Fig. 7). It yields upon fragmentation three peaks at m/z 487.0, 679.1 and 975.2, which confirms self-assembly and recognition in the order shown in Figure 8. ESI-TOF/MS and tandem ESI-MS for host/guest complexes **7/14-20** are shown with supporting information.

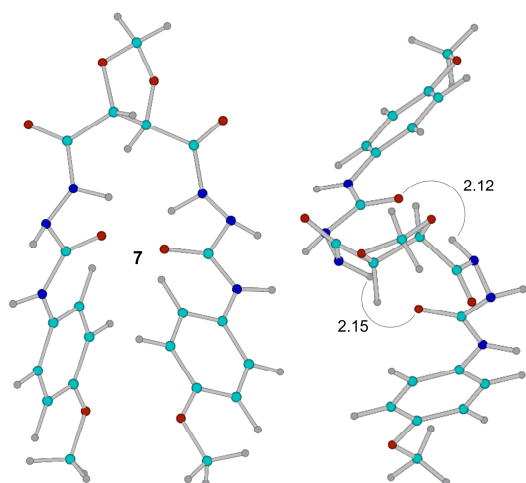


Fig. 3 Computed structure for receptor **7** at the AM1 level. A Polak-Ribiere conjugate gradient with rms < 0.01 Kcal.mol⁻¹ was used.

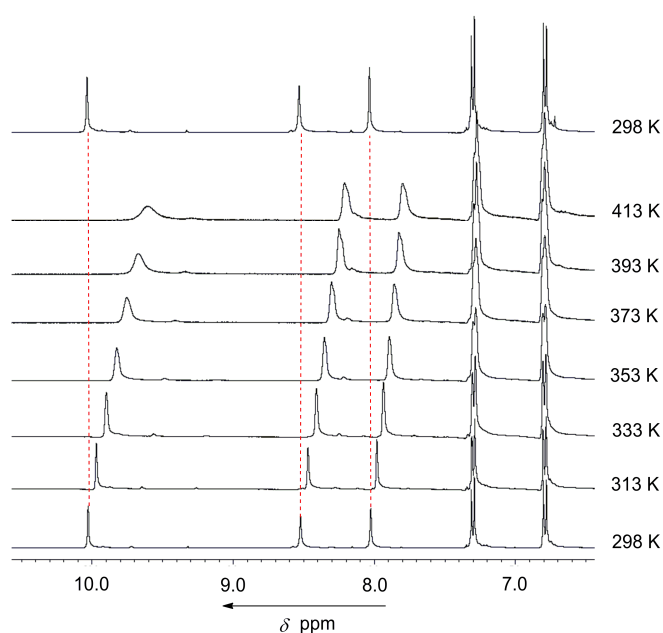


Fig. 4 Stacked VT NMR spectra for receptor **7** (400 MHz, DMSO-d₆, 298-413 K).

Receptor **7** showed potential recognition in the gas phase to AcNH-D-Ala-D-Glu-L-Lys-D-Ala-D-Ala-Gly-COOH **18**, AcNH-D-Glu-L-Lys-D-Ala-D-Ala-Gly-COOH **19** and AcNH-L-Lys-D-Ala-D-Ala-Gly-COOH **20** with free terminal carboxylic moieties. High resolution ESI-TOF/MS and tandem MS for host/guest complexes **7/18-20** are shown with supporting information.

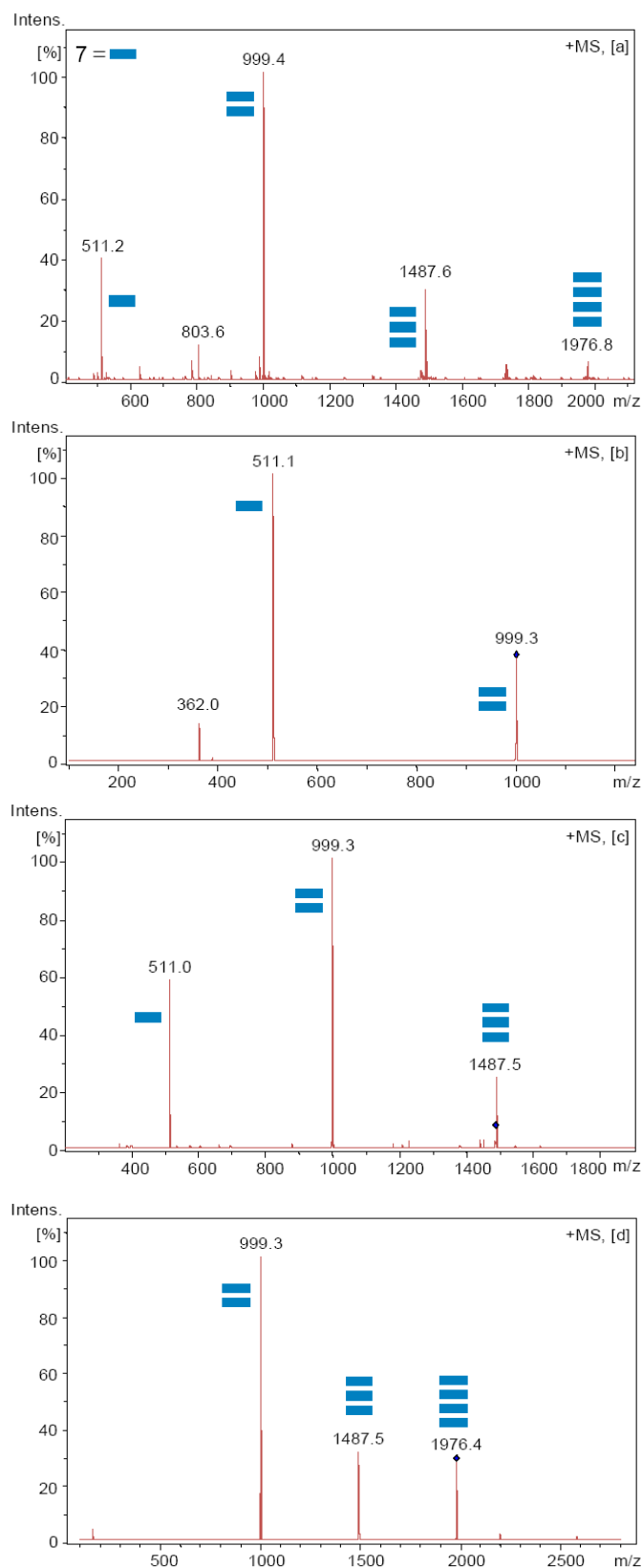


Fig. 5 Self-assembled associations of receptor **7**, (a) ESI-TOF/MS in the positive ion mode, (b-d) tandem ESI-MS for the self-assembled molecules in the positive ion mode. Products appeared as $[M + Na^+]$ ions.

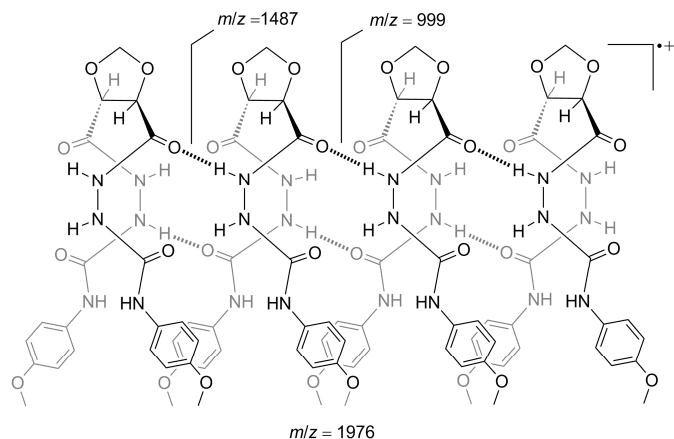
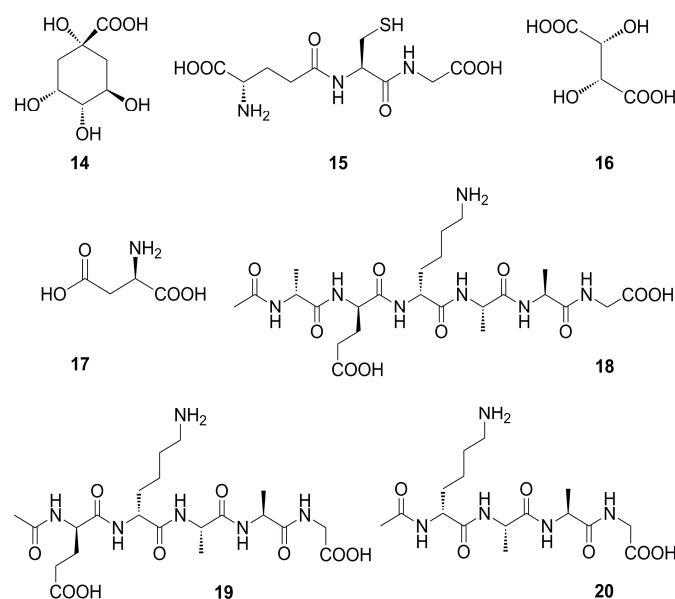


Fig. 6 Proposed structure and fragmentation mechanisms for self-assembled four molecules of receptor **7**.



Scheme 1 Chiral guests **14–20**, which bind with receptor **7** in the gas phase.

Table 2. ESI-TOF/MS data for host/guest complexes **7/14–20**

Host/Guest	Molecular Formula	Calcd. m/z	Meas. m/z	Error [ppm]
7/14^a	C ₂₈ H ₃₆ N ₆ O ₁₄	679.2217	679.2248	−4.6
7/14^b	C ₄₉ H ₆₀ N ₁₂ O ₂₂	1167.3872	1167.3888	−1.3
7/14^c	C ₇₀ H ₈₄ N ₁₈ O ₃₀	1655.5528	1655.5529	−0.1
7/15^a	C ₃₁ H ₄₃ N ₉ O ₁₄ S	796.2566	796.2573	−0.8
7/15^b	C ₅₂ H ₆₇ N ₁₅ O ₂₂ S	1284.4222	1284.4226	−0.3
7/16^a	C ₂₅ H ₃₀ N ₆ O ₁₄	637.1747	637.1777	−4.6
7/16^b	C ₄₆ H ₅₄ N ₁₂ O ₂₂	1125.3403	1125.3447	−3.9
7/16^c	C ₆₇ H ₇₈ N ₁₈ O ₃₀	1613.5058	1613.5082	−1.5
7/17^a	C ₂₅ H ₃₁ N ₇ O ₁₂	620.1958	620.1976	−2.9
7/18^a	C ₄₅ H ₆₇ N ₁₃ O ₁₈	1076.4643	1076.4673	−2.8
7/19^a	C ₄₂ H ₆₂ N ₁₂ O ₁₇	1005.4272	1005.4289	−1.7
7/19^b	C ₆₃ H ₈₆ N ₁₈ O ₂₅	1493.5928	1493.5875	3.6
7/20^a	C ₃₇ H ₅₅ N ₁₁ O ₁₄	876.3846	876.3864	−2.0
7/20^d	C ₅₃ H ₈₄ N ₁₆ O ₂₀	1263.5964	1263.5964	0

^aProducts appeared as (a) $[(M^H + M^G) - H]^-$, (b) $[(2M^H + M^G) - H]^-$, (c) $[(3M^H + M^G) - H]^-$ and (d) $[(M^H + 2M^G) - H]^-$ ions in the negative ion mode.

Receptor **7** showed enhanced recognition ability in the gas phase to guests **14–20** in comparison with macrocycle **B** due to its high flexibility (For comparative ESI-TOF/MS for **7** and **B**, see supporting information). Evaluation of the selective recognition behavior of receptors **7–10** to oligopeptides **18–20** has been investigated by ESI-TOF/MS and tandem MS. Four competitive experiments were conducted for equimolar mixtures of receptors (**7, 9**), (**7, 10**) and (**7, 9** and **10**) with oligopeptides **18–20** (Table 3 and Fig. 9a–c). Mass peaks of 1:1, 1:2 and 2:1 stoichiometries of host/guest complexes were observed. ESI-TOF/MS for a mixture of **7, 9** and **18** showed a peak with highest intensity at m/z 1136.4 corresponding to complex **9/18**. A peak with highest intensity at m/z 1102.5 was assigned to **10/18** in a mixture of **7, 10** and **18** (Fig. 9a and 9b).

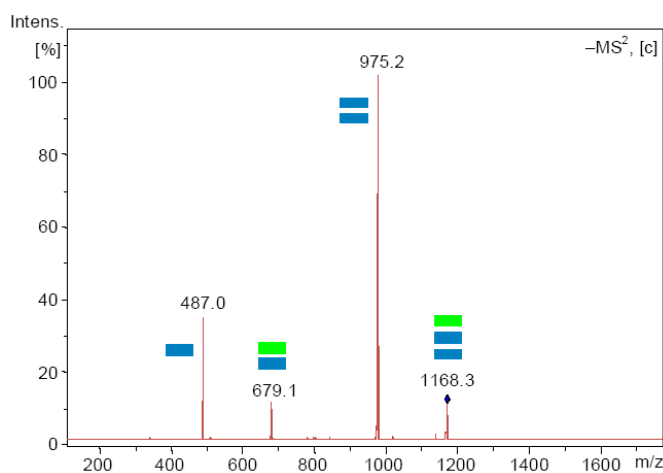
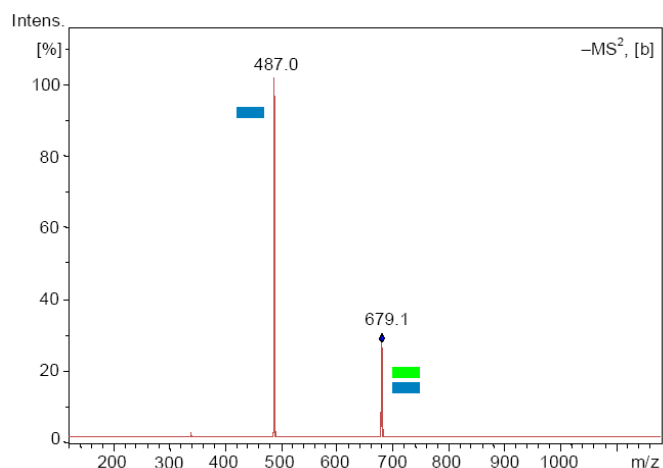
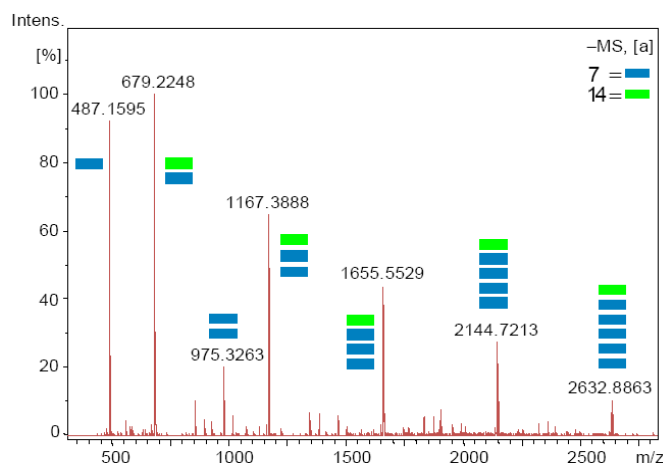
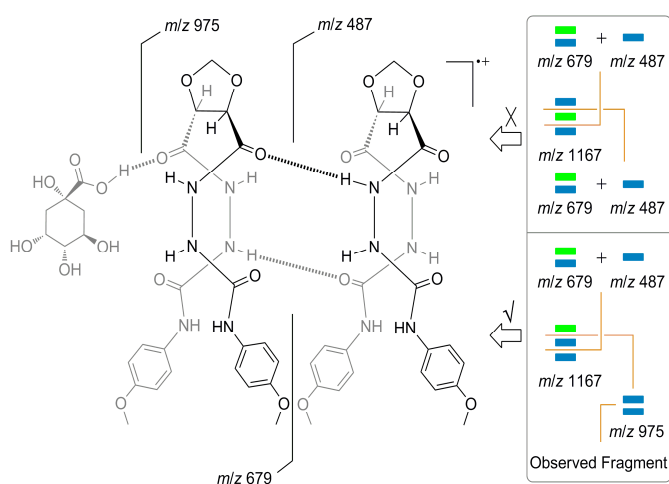


Fig. 7 Self-assembled host-guest complex **7/14**, (a) ESI-TOF/MS in the negative ion mode, (b, c) tandem ESI-MS for assembled associations of **7/14**. Products appeared as $[M - H]^-$ ions.

Table 3. ESI-TOF/MS data for selective recognition of receptors **7-10** to oligopeptide **18**

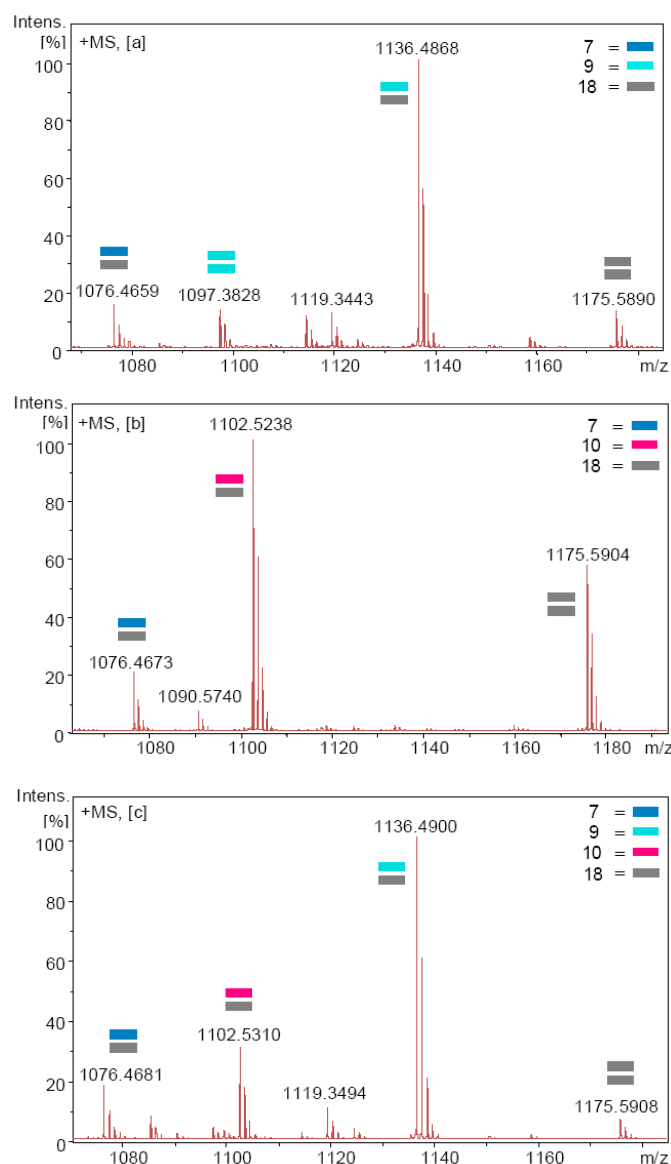
Hosts/guest	Molecular Formula	^a Product Ions	Calcd. <i>m/z</i>	Meas. <i>m/z</i>	Error [ppm]
(7 and 9)/18	C ₄₅ H ₆₅ N ₁₃ O ₁₈	[(M ⁷ + M ¹⁸) + H] ⁺	1076.4643	1076.4659	-1.5
	C ₄₆ H ₅₆ N ₁₂ O ₂₀	[(2M ⁹) + H] ⁺	1097.3807	1097.3828	-1.9
	C ₄₇ H ₆₉ N ₁₃ O ₂₀	[(M ⁹ + M ¹⁸) + H] ⁺	1136.4855	1136.4868	-1.2
	C ₄₈ H ₈₂ N ₁₄ O ₂₀	[2M ¹⁸ + H] ⁺	1175.5903	1175.5890	1.0
	C ₇₀ H ₉₇ N ₁₉ O ₃₀	[2M ⁹ + M ¹⁸ + H] ⁺	1684.6721	1684.6755	-2.0
(7 and 10)/18	C ₄₅ H ₆₅ N ₁₃ O ₁₈	[(M ⁷ + M ¹⁸) + H] ⁺	1076.4673	1076.4643	-2.7
	C ₄₈ H ₈₂ N ₁₄ O ₂₀	[2M ¹⁸ + H] ⁺	1175.5904	1175.5903	-0.1
	C ₄₇ H ₇₁ N ₁₅ O ₁₆	[(M ¹⁰ + M ¹⁸) + H] ⁺	1102.5238	1102.5276	3.4
(7, 9 and 10)/18	C ₄₅ H ₆₅ N ₁₃ O ₁₈	[(M ⁷ + M ¹⁸) + H] ⁺	1076.4681	1076.4643	-3.5
	C ₄₇ H ₆₉ N ₁₃ O ₂₀	[(M ⁹ + M ¹⁸) + H] ⁺	1136.4855	1136.4900	-4.0
	C ₄₇ H ₇₁ N ₁₅ O ₁₆	[(M ¹⁰ + M ¹⁸) + H] ⁺	1102.5310	1102.5276	-3.1
	C ₄₈ H ₈₂ N ₁₄ O ₂₀	[2M ¹⁸ + H] ⁺	1175.5908	1175.5903	-0.5
	C ₇₀ H ₉₉ N ₂₁ O ₂₆	[(M ⁹ + M ¹⁰ + M ¹⁸) + H] ⁺	1650.7193	1650.7143	3.1
	C ₇₀ H ₉₇ N ₁₉ O ₃₀	[(2M ⁹ + M ¹⁸) + H] ⁺	1684.6791	1684.6721	-4.1

^aESI-TOF/MS recorded in the positive ion mode.**Fig. 8** Proposed structure and fragmentation mechanisms for host/guest complex **7/14**.

The ESI-MS data indicate that receptors **9** and **10** in competitions with **7** bind best to guest **18**. Figure 9c shows preference binding of receptor **9** to oligopeptide **18** in a mixture of **7**, **9**, **10** and **18**. Introducing polar functionalities into the structural framework of the receptors improves their molecular recognition and binding abilities. ESI mass spectra for higher mass complexes of hosts and guests are available with supporting information. The chirality of the novel receptors **7-13** was confirmed by CD spectroscopy (Fig. 10). CD spectrum for (*i.e.*, receptor **7**) showed bisignate Cotton effect with a negative sign at ≈ 250 nm and a positive sign at ≈ 255 nm, which indicates a strong excitation coupling between chromophores. Also, receptor (*4R,5R*)-**7** showed greater molar ellipticity than (*4S,5S*)-**11**.

3. Conclusion

In summary, we have synthesized a novel class of chiral non-racemic two-armed receptors as potential hosts for selective recognition of oligopeptides in the gas phase. The new receptors assume a *syn/syn* conformation and showed unique self-assembly and molecular recognition in the gas phase. Both intermolecular hydrogen bonding and π - π stacking interactions participate efficiently in stabilizing the host/host and host/guest assemblies.

**Fig. 9** ESI-TOF/MS for selective recognition of receptors **7-10** to oligopeptide **18**, (a) **7/9/18**, (b) **7/10/18** (c) **7/9/10/18** in the positive ion mode.

The newly synthesized receptors showed a remarkable degree of flexibility in comparison with macrocycles **A** or **B**. In addition they are chiral and can be obtained in almost quantitative yields as analytically and enantiomerically pure products. This study is a preliminary assessment of the recognition ability of the novel receptors to oligopeptides in the gas phase and further quantitative work aimed at assessing recognition in solution is under investigation and will be published in due course.

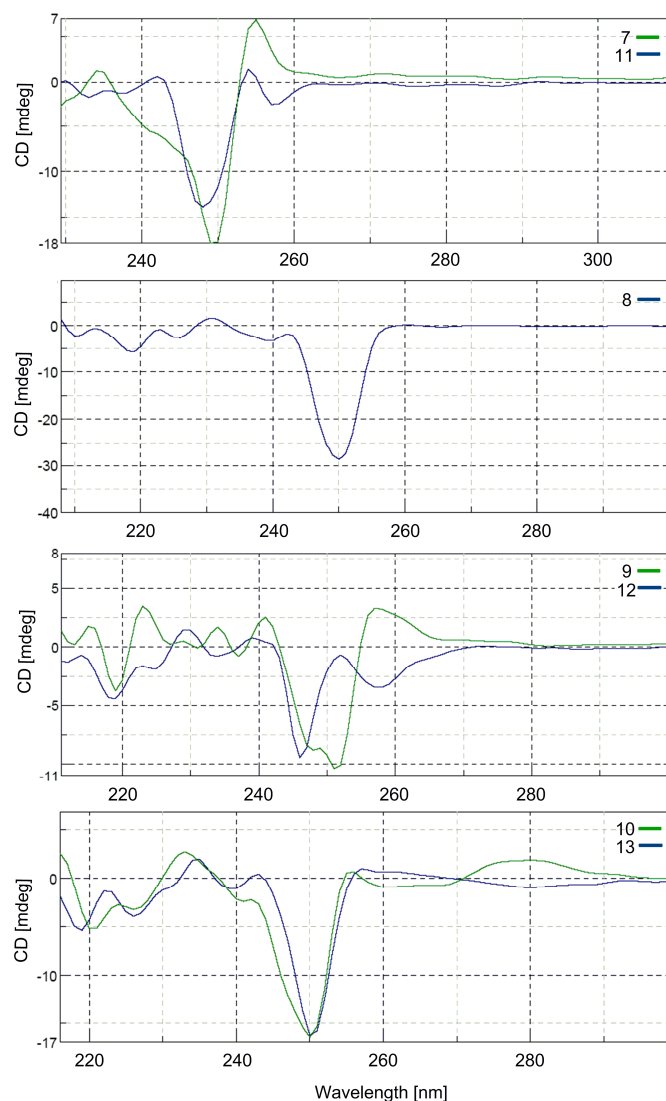


Fig. 10 CD spectra for chiral receptors 7-13, spectra recorded in DMSO.

4. Experimental section

All the reagents used for the reactions were purchased from Sigma-Aldrich, Applichem or Flucka (Germany) and were used as obtained. Whenever possible the reactions were monitored by thin layer chromatography (TLC). TLC was performed on Macherey-Nagel aluminium backed plates pre-coated with silica gel 60 (UV₂₅₄). Melting points were determined in open capillaries using a Buechl B-545 melting point apparatus and are not corrected. Infrared spectra were determined using a Vector-33 Bruker FT IR spectrometer. The samples were measured directly as solids or oils; ν_{\max} values were expressed in cm^{-1} and were given for the main absorption bands. ^1H NMR, ^{13}C NMR and 2D ROESY spectra were acquired on a JEOL ECX-400

spectrometer operating at 400 MHz for ^1H -NMR and 100 MHz for ^{13}C -NMR in DMSO- d_6 using a 5 mm probe. The chemical shifts (δ) are reported in parts per million and were referenced to the residual solvent peak. The following abbreviations are used: s, singlet; m, multiplet; br, broad signal. Mass spectra were recorded using HCTultra and ESI-TOF Bruker Daltonics mass spectrometers and samples were dissolved in DMF, acetonitrile and water using the positive and negative electrospray ionization modes. Calibration was carried out using a 0.1 M solution of sodium formate in the enhanced quadratic mode prior to each experimental run. The results of measurements were processed using Compass 1.3 data analysis software for a Bruker Daltonics time of flight mass spectrometer (microTOF). Molecular modeling calculations were carried out with HyperChem software (Release 8.0) at the MM+ levels in vacuo and no influence of solvents was taken into account in these calculations.^{41,42} Circular Dichroism measurements were carried out using Jasco-J-810 Spectropolarimeter in H₂O and DMSO. Preloaded wang resin, *N,N*-diisopropylethylamine (DIEA), *O*-(benzotriazol-1-yl)-hydroxybenzotriazole (HOBt), *N,N,N',N'*-tetramethyluranyl hexafluorophosphate (HBTU), 9-fluorenylmethoxycarbonyl-amino acid derivatives (1-Fmoc), DMF, *N*-methylpyrrolidone (NMP), trifluoroacetic acid (TFA), 1,2-ethanedithiol (EDT) and other chemicals required for peptide synthesis were bought from Iris Biotech GmbH (Marktredwitz, Germany). Peptides were synthesized with standard solid phase peptide synthesis technique and it was carried out on an automated peptide synthesizer (ABI-433A, Applied Biosystems, Foster city, USA). Fmoc protected preloaded resin was used to grow peptide chain on it. In detail, deprotection of the *N*-terminal of resin bound amino acid was performed by 20% piperidine in NMP and the *C*-terminal of other protected amino acid was activated using HBTU/HOBt/DIEA (1:1:2) in DMF for coupling with the free *N*-terminal of the resin bound amino acid. A mixture of 82.5% TFA, 5% phenol, 5% water, 5% thioanisole and 2.5% EDT was used to separate the peptide from resin as well as to remove the side chain protecting groups. Subsequently, the peptide was isolated through precipitation in cold (-20°C) diethyl ether and lyophilized by Christ freeze dryers (Martin Christ Gefriertrocknungsanlagen GmbH, Osterode am Harz, Germany). Peptides were purified by high performance liquid chromatography (HPLC) and analyzed by HRMS. Dicarbohydrazides **1-3** were synthesized according to literature.^{27,28}

General procedure for preparation of chiral receptors 7-13

To a stirred solution of the corresponding aryl isocyanates **4-6** (2 mmol) in anhydrous THF (6 mL) were added dicarbohydrazides **3-5** (1.1 mmol) in anhydrous THF (6 mL). The mixture was stirred at room temperature for 24 h. The solid was filtered off, washed successively with water, diethyl ether and dried to give chiral dioxolane receptors **7-13**.

4.1. 2,2'-[(4*R*,5*R*)-1,3-dioxolane-4,5-dicarbonyl]-bis-(*N*-(4-methoxyphenyl) hydrazinecarboxamide) **7**

Prepared from (4*R*,5*R*)-1,3-dioxolane-4,5-dicarbohydrazide **1** and 4-methoxyphenyl isocyanate **4** (740.0 mg, 78%) as a white solid precipitate (m.p. 227-228); n_{\max} (solid) 3271, 1689 cm^{-1} ; d_{H} (400 MHz DMSO- d_6) 10.05 (2H, brs, NHCO), 8.54 (2H, brs, NHCO), 8.04 (2H, brs, NHCO), 7.31 (4H, d, J 8.7 Hz, ArH), 6.79 (4H, d, J 9.1 Hz, ArH), 5.14 (2H, brs, OCH_2), 4.65 (2H, brs, CHCO), 3.65

(6H, brs, OMe); d_C (100 MHz, DMSO- d_6) 169.3, 155.7, 155.0, 133.0, 120.8, 114.3, 97.0, 77.2, 55.6; m/z 487.0 (40, MH^+), 337.8 (100%); HRMS: MH^+ , found 487.1588. $C_{21}H_{24}N_6O_8$ requires 487.1583.

4.2. 2,2'-[(4*R*,5*R*)-1,4-dioxaspiro-[4.5]-decane-2,3-dicarbonyl]-bis-(*N*-(4-methoxyphenyl) hydrazinecarboxamide] **8**

Prepared from (2*R*,3*R*)-1,4-dioxaspiro-[4.5]-decane-2,3-di-carbohydrazide **2** and 4-methoxyphenyl isocyanate **4** (800.0 mg, 74%). After 24 h or stirring at room temperature, water was added and the solid was filtered off as a white solid precipitate (m.p. > 140 °C); n_{max} (solid) 3294, 1681 cm^{-1} ; d_H (400 MHz DMSO- d_6) 9.99 (2H, brs, $NHCO$), 8.51 (2H, brs, $NHCO$), 8.09 (2H, brs, $NHCO$), 7.32 (4H, d, J 9.1 Hz, ArH), 6.76 (4H, d, J 8.7 Hz, ArH), 4.63 (2H, brs, $CHCO$), 3.64 (6H, brs, OMe), 1.73-1.55 (6H, m, CH_2), 1.53-1.49 (2H, m, CH_2), 1.33 (2H, m, CH_2); d_C (100 MHz, DMSO- d_6) 169.6, 156.1, 155.1, 132.8, 121.0, 114.4, 113.4, 76.8, 55.5, 36.0, 25.5, 25.2, 24.1; m/z 555.0 (52, MH^+), 405.9 (100%); HRMS: MH^+ , found 555.2224. $C_{26}H_{32}N_6O_8$ requires 555.2209.

4.3. 2,2'-[(4*R*,5*R*)-1,3-dioxolane-4,5-dicarbonyl]-bis-(*N*-(2,4-dimethoxyphenyl) hydrazinecarboxamide] **9**

Prepared from (4*R*,5*R*)-1,3-dioxolane-4,5-dicarbohydrazide **1** and 2,4-dimethoxyphenyl isocyanate **5** (711.0 mg, 93%) as a white solid precipitate (m.p. > 190 °C); n_{max} (solid) 3299, 1685 cm^{-1} ; d_H (400 MHz DMSO- d_6) 10.11 (2H, brs, $NHCO$), 8.48 (2H, brs, $NHCO$), 7.88 (2H, brs, $NHCO$), 7.79 (2H, d, J 8.7 Hz, ArH), 6.56 (2H, s, ArH), 6.42 (2H, dd, J 6.4 Hz, ArH), 5.16 (2H, brs, OCH_3), 4.63 (2H, brs, $CHCO$), 3.79 (6H, brs, OMe), 3.68 (6H, brs, OMe); d_C (100 MHz, DMSO- d_6) 169.1, 155.6, 155.4, 149.7, 122.0, 120.1, 104.6, 99.2, 97.0, 77.1, 56.3, 55.7; m/z 547.0 (66, MH^+), 367.9 (100%); HRMS: MH^+ , found 547.1782. $C_{23}H_{28}N_6O_{10}$ requires 547.1794.

4.4. 2,2'-[(4*R*,5*R*)-1,3-dioxolane-4,5-dicarbonyl]-bis-(*N*-(4-dimethylamino) hydrazinecarboxamide] **10**

Prepared from (4*R*,5*R*)-1,3-dioxolane-4,5-dicarbohydrazide **1** and 4-dimethylaminophenyl isocyanate **6** (705.0 mg, 89%) as a violet solid precipitate (m.p. > 200 °C); n_{max} (solid) 3263, 1688 cm^{-1} ; d_H (400 MHz DMSO- d_6) 10.04 (2H, brs, $NHCO$), 8.37 (2H, brs, $NHCO$), 7.95 (2H, brs, $NHCO$), 7.21 (4H, d, J 9.1 Hz, ArH), 6.62 (4H, d, J 9.1 Hz, ArH), 5.14 (2H, brs, OCH_3), 4.65 (2H, brs, $CHCO$), 2.77 (12H, brs, NMe); d_C (100 MHz, DMSO- d_6) 169.2, 155.8, 147.0, 129.7, 121.0, 113.5, 97.0, 77.2, 41.2; m/z 513.0 (70, MH^+), 350.9 (100%); HRMS: MH^+ , found 513.2240. $C_{23}H_{30}N_8O_6$ requires 513.2216.

4.5. 2,2'-[(4*S*,5*S*)-1,3-dioxolane-4,5-dicarbonyl]-bis-(*N*-(4-methoxyphenyl) hydrazinecarboxamide] **11**

Prepared from (4*S*,5*S*)-1,3-dioxolane-4,5-dicarbohydrazide **3** and 4-methoxyphenyl isocyanate **4** (910.0 mg, 96%) as a pale yellow solid precipitate (m.p. 224-225 °C); n_{max} (solid) 3260, 1681 cm^{-1} ; d_H (400 MHz DMSO- d_6) 10.05 (2H, brs, $NHCO$), 8.54 (2H, brs, $NHCO$), 8.04 (2H, brs, $NHCO$), 7.31 (4H, d, J 9.1 Hz, ArH), 6.79 (4H, d, J 9.1 Hz, ArH), 5.15 (2H, brs, OCH_3), 4.66 (2H, brs, $CHCO$), 3.65 (6H, brs, OMe); d_C (100 MHz, DMSO- d_6) 169.3, 155.7, 155.0, 133.0, 120.9, 114.3, 97.0, 77.2, 55.6; m/z 486.9 (100, MH^+), 337.9 (19%); HRMS: MH^+ , found 487.1570. $C_{21}H_{24}N_6O_8$ requires 487.1583.

4.6. 2,2'-[(4*S*,5*S*)-1,3-dioxolane-4,5-dicarbonyl] -bis-(*N*-(2,4-dimethoxyphenyl) hydrazinecarboxamide] **12**

Prepared from (4*S*,5*S*)-1,3-dioxolane-4,5-dicarbohydrazide **3** and 2,4-dimethoxyphenyl isocyanate **5** (735.0 mg, 99%) as a pale yellow solid precipitate (m.p. > 190 °C); n_{max} (solid) 3297, 1696

cm^{-1} ; d_H (400 MHz DMSO- d_6) 10.13 (2H, brs, $NHCO$), 8.50 (2H, brs, $NHCO$), 7.90 (2H, brs, $NHCO$), 7.90 (2H, d, J 8.7 Hz, ArH), 6.57 (2H, s, ArH), 6.42 (2H, dd, J 6.4 Hz, ArH), 5.18 (2H, brs, OCH_3), 4.66 (2H, brs, $CHCO$), 3.79 (6H, brs, OMe), 3.68 (6H, brs, OMe); d_C (100 MHz, DMSO- d_6) 169.2, 155.6, 155.4, 149.7, 121.9, 120.2, 104.6, 99.2, 97.1, 77.2, 56.2, 55.7; m/z 547.0 (39, MH^+), 367.9 (100%); HRMS: MH^+ , found 547.1799. $C_{23}H_{28}N_6O_{10}$ requires 547.1794.

4.7. 2,2'-[(4*S*,5*S*)-1,3-dioxolane-4,5-dicarbonyl]-bis-(*N*-(4-dimethylamino) hydrazinecarboxamide] **13**

Prepared from (4*S*,5*S*)-1,3-dioxolane-4,5-dicarbohydrazide **3** and 4-dimethylaminophenyl isocyanate **6** (740.0 mg, 93%) as a violet solid precipitate (m.p. > 210 °C); n_{max} (solid) 3256, 1688 cm^{-1} ; d_H (400 MHz DMSO- d_6) 10.04 (2H, brs, $NHCO$), 8.37 (2H, brs, $NHCO$), 7.95 (2H, brs, $NHCO$), 7.21 (4H, d, J 9.1 Hz, ArH), 6.61 (4H, d, J 9.1 Hz, ArH), 5.14 (2H, brs, OCH_3), 4.64 (2H, brs, $CHCO$), 2.76 (12H, brs, NMe); d_C (100 MHz, DMSO- d_6) 169.3, 155.8, 147.0, 129.7, 121.0, 113.5, 97.0, 77.2, 41.2; m/z 513.1 (31, MH^+), 350.9 (100%); HRMS: MH^+ , found 513.2233. $C_{23}H_{30}N_8O_6$ requires 513.2216.

Acknowledgments

H. Nour deeply thanks Deutscher Akademischer Austausch Dienst (DAAD) for financial support and Jacobs University for excellent facilities.

References and notes

- Bogaschenko, T. Y.; Lyapunov, A. Y.; Kikot', L. S.; Mazepa, A. V.; Botoshansky, M. M.; Fonari, M. S.; Kirichenko, T. I. *Tetrahedron* **2012**, *68*, 4757.
- Xie, T.-Z.; Guo, C.; Yu, S.-Y.; Pan, Y.-J. *Angew. Chem. Int. Ed.* **2012**, *51*, 1177.
- Kuchelmeister, H. Y.; Schmuck, C. *Chem. Eur. J.* **2011**, *17*, 5311.
- Zhu, Z.; Cardin, C. J.; Gan, Y.; Colquhoun, H. M. *Nat. Chem.* **2010**, *2*, 653.
- Nishiuchi, T.; Kuwatani, Y.; Nishinaga, T.; Iyoda, M. *Chem. Eur. J.* **2009**, *15*, 6838.
- Hayashi, N.; Ujihara, T. *Tetrahedron* **2009**, *65*, 8209.
- Wennemers, H.; Nold, M. C.; Conza, M. M.; Kulicke, K. J.; Neuburger, M. *Chem. Eur. J.* **2003**, *9*, 442.
- Chen, C.-W.; Whitlock, H. W. *J. Am. Chem. Soc.* **1978**, *100*, 4921.
- Vicente, A. I.; Caio, J. M.; Sardinha J.; Moiteiro, C.; Delgado, R.; Félix, V. *Tetrahedron* **2012**, *68*, 670.
- Barnhill, D. K.; Sargent, A. L.; Allen, W. E. *Tetrahedron* **2005**, *61*, 8366.
- Ishi-i, T.; Crego-Calama, M.; Timmerman, P.; Reinhoudt, D. N.; Shinkai, S. *Angew. Chem. Int. Ed.* **2002**, *41*, 1924.
- Kuchelmeister, H. Y.; Schmuck, C. *Eur. J. Org. Chem.* **2009**, 4480.
- Liu, S.-Y.; He, Y.-B.; Wu, J.-L.; Wei, L.-H.; Qin, H.-J.; Meng, L.-Z.; Hu, L. *Org. Biomol. Chem.* **2004**, *2*, 1582.
- Zimmerman, S. C.; VanZyl, C. M. *J. Am. Chem. Soc.* **1987**, *109*, 7894.
- Zimmerman, S. C.; Wu, W. *J. Am. Chem. Soc.* **1989**, *111*, 8054.
- Zimmerman, S. C. In *Topics in Current Chemistry*; SpringerLink: **1993**, Vol. 165/1993, 71-102, DOI: 10.1007/BFb0111281.
- Iorio, E. J.; Still W. C. *Bioorg. Med. Chem. Lett.* **1996**, *6*, 2673.
- Iorio, E. J.; Still W. C. *Bioorg. Med. Chem. Lett.* **1999**, *9*, 2145.
- Chen, X.; Du, D.-M.; Hua, W.-T. *Tetrahedron: Asymmetry* **2003**, *14*, 999.
- Shepherd, J.; Gale, T.; Jensen, K. B.; Kilburn, J. D. *Chem. Eur. J.* **2006**, *12*, 713.
- Braxmeier, T.; Demarcus, M.; Fessmann, T.; McAteer, S.; Kilburn, J. D. *Chem. Eur. J.* **2001**, *7*, 1889.
- Nestler, H. P. *Mol. Divers.* **1996**, *2*, 35.
- Conza, M.; Wennemers, H. *J. Org. Chem.* **2002**, *67*, 2696.
- Wennemers, H.; Bernard, J. *Org. Lett.* **2007**, *9*, 4284.
- Wennemers, H.; Krattiger, P. *Synlett* **2005**, *4*, 706.
- Bernard, J.; Wennemers, H. *Org. Lett.* **2007**, *9*, 4283.

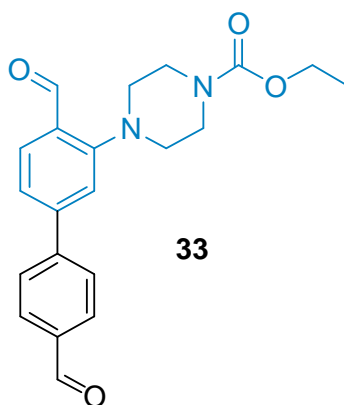
27. Nour, H. F.; Hourani, N.; Kuhnert, N.; *Org. Biomol. Chem.* **2012**, *10*, 4381.
28. Nour, H. F.; Golon, A.; Le Gresley, A.; Kuhnert, N. *Chem. Eur. J.* **2012**, *submitted manuscript*.
29. Nour, H. F.; Golon, A.; Islam, T.; Fernández-Lahore, M.; Kuhnert, N. *Unpublished results*.
30. Skowronek, P.; Kunciewicz, M.; Brzostowska, M.; Janiak, A.; Rychlewska, U.; Gawroński, J. *Tetrahedron: Asymm.* **2012**, *23*, 300.
31. Nour, H. F.; Islam, T.; Fernández-Lahore, M.; Kuhnert, N. *Rapid Comm. Mass. Spectrom.* **2012**, *accepted manuscript*.
32. Gawroński, J.; Kolbon, H.; Kwit, M.; Katrusiak, A. *J. Org. Chem.* **2000**, *65*, 5768.
33. Kuhnert, N.; Rossignolo, G.; Lopez-Periago, A. *Org. Biomol. Chem.* **2003**, *1*, 1157.
34. Kuhnert, N.; Patel, C.; Jami, F. *Tetrahedron Lett.* **2005**, *46*, 7575.
35. Kuhnert, N.; Lopez-Periago, A. *Tetrahedron Lett.* **2002**, *43*, 3329.
36. Kuhnert, N.; Lopez-Periago, A.; Rossignolo, G. *Org. Biomol. Chem.* **2005**, *3*, 524.
37. Kuhnert, N.; Straßnig, C.; Lopez-Periago, A. *Tetrahedron: Asymm.* **2002**, *13*, 123.
38. Kuhnert, N.; Tang, B. *Tetrahedron Lett.* **2006**, *47*, 2985.
39. Kuhnert, N.; Marsh, D.; Nicolau, D. *Tetrahedron: Asymm.* **2007**, *18*, 1648.
40. Nour, H. F.; Matei, M. F.; Bassil, B.; Kortz, U.; Kuhnert, N. *Org. Biomol. Chem.* **2011**, *9*, 3258.
41. Molecular modeling was carried out using HyperChem software (Release 8.0). Hypercube, Inc., 1115 NW 4th Street, Gainesville, FL 32601 USA. Trial, version from <http://www.hypercube.com>
42. Stewart, J. J. *Comput. Chem.* **1989**, *10*, 221.
43. Alfonso, I.; Bolte, M.; Bru, M.; Burguete, M. I.; Luis, S. V.; Vicent, C. *Org. Biomol. Chem.* **2010**, *8*, 1329.
44. Schug, K.; Fryčák, P.; Maier, N. M.; Lindner, W. *Anal. Chem.* **2005**, *77*, 3660.
45. Arakawa, R.; Kobayashi, M.; Fukuo, T.; Shiraiwa, T. *Rapid Comm. Mass. Spectrom.* **2001**, *15*, 685.
46. Nour, H. F.; Lopez-Periago, A.; Kuhnert, N. *Rapid Comm. Mass. Spectrom.* **2012**, *26*, 1070.

Conclusion

In conclusion *trans*-(1*R*,2*R*)-1,2-diaminocyclohexane reacted with non-symmetrical dialdehydes to form a mixture of C_3 -symmetrical and non-symmetrical trianglimine macrocycles. Trianglimine regioisomers were efficiently separated by CC and underwent successfully dynamic exchange reactions. The mechanism of trianglimine formation was investigated by ESI-TOF/MS. A number of unprecedented reaction intermediates were detected and assigned based on their high resolution m/z values. The new trianglimines were obtained as sufficiently pure products, but unfortunately in low yields. Attempts to improve the yields of the macrocycles by synthesizing one of the regioisomers did not succeed. It was thereby essential to replace the *trans*-(1*R*,2*R*)-1,2-diaminocyclohexane unit in trianglimine structure by another ring to which different functionalities can be introduced. The attractive features of diaminocyclohexane, which are chirality and conformational bias, should be kept. Tartaric acid dihydrazides with acetal protected hydroxyl groups were the alternative units to *trans*-(1*R*,2*R*)-1,2-diaminocyclohexane. The new dihydrazides underwent successfully [2+2]-cyclocondensation reactions to form a novel class of chiral non-racemic macrocycles, which were named tetra-carbohydrazide cyclophanes. The novel cyclophane macrocycles were obtained in almost quantitative yields without need of external templates or high dilution conditions. Both enantiomeric forms of the macrocycles (*R* or *S*) can be readily available. Tetra-carbohydrazide cyclophanes underwent successfully dynamic exchange with generation of a small dynamic library of eight macrocycles. Structures of library members were assigned and characterized based on their high resolution m/z values. Three members from the dynamic library showed molecular recognition in the gas phase to a selection of oligopeptides, which mimic bacterial cell wall. The [2+2]-cyclocondensation reactions of dihydrazides with aromatic diisocyanates afforded a new class of polyamide macrocycles, which were named tetra-(hydrazinecarboxamide) cyclophanes. The novel polyamide cyclophanes possess more flexible structure in comparison with tetra-carbohydrazide cyclophanes. They showed enhanced molecular recognition in the gas phase to oligopeptides and chiral carboxylic acids. In attempts to improve the recognition ability of the novel cyclophane macrocycles, a new series of open chain hydrazinecarboxamide receptors were successfully synthesized in excellent yields. The novel receptors constitute a new class of two-armed compounds, which showed, in the gas phase, unprecedented dual self-assembly and recognition to oligopeptides. Selective recognition of the novel receptors to peptides was observed by ESI-TOF/MS.

Appendix

Appendix | Compound **33**, paper 2, has the corrected structure shown below



Supplementary Information:

Synthesis of Tri-substituted Biaryl Based Trianglimines: Formation of C₃-symmetrical and Non-symmetrical Regioisomers

Hany F. Nour, Marius F. Matei, Bassem S. Bassil, Ulrich Kortz and Nikolai Kuhnert*

School of Engineering and Science, Jacobs University Bremen, P.O. Box 750 561, 28725 Bremen, Germany.

Experimental

All the reagents used for the reactions were purchased from Sigma-Aldrich or Applichem and were used as obtained. Whenever possible the reactions were monitored by thin layer chromatography (TLC). TLC was performed on Macherey-Nagel aluminium-backed plates pre-coated with silica gel 60 (UV₂₅₄). Column chromatography was carried out on silica gel 60 (0.040-0.063 mm) under flash conditions. For the separation and purification of the newly synthesised trianglimines, silica gel was activated before using by heating at 120 °C in the oven for 2 hours and triethylamine was used in combination with the solvent system during the elution process. Melting points were determined in open capillaries using a Stuart SMP3 capillary melting point apparatus and are not corrected. Infrared spectra were determined using a Vector-33 Bruker FT-IR spectrometer. The samples were measured as liquids and they were dissolved either in EtOAc or CHCl₃ during the measurement; ν_{\max} values were expressed in cm⁻¹ and were given for the main absorption bands. ¹H-NMR and ¹³C-NMR spectra were acquired on a JEOL ECX-400 spectrometer operating at 400 MHz for ¹H-NMR and 100 MHz for ¹³C-NMR at room temperature in CDCl₃, C₆D₆ or C₃D₆O using a 5 mm probe. The chemical shifts (δ) are reported in parts per million and were referenced to the residual solvent peak. The coupling constants (J) are quoted in hertz. The following abbreviations are used: s, singlet; d, doublet; dd, doublet of doublets; ddd, doublet of doublet of doublets; t, triplet; m, multiplet; br, broad signal. Mass spectra were recorded using both a Bruker HCTultra and a high resolution Bruker Daltonics micrOTOF instruments from methanol or dichloromethane solutions using the positive electrospray ionization ESI-MS and APCI-MS modes. Molecular modelling was carried out with Hyperchem (release 8.0) software using both PM3 and MM+ methods and no influence of solvents was taken into account in these calculations.^{24,25} Circular Dichroism (CD) measurements were carried out using Jasco-J-810 Spectropolarimeter in CHCl₃.

X-ray Crystallography: A single crystal of compound (**6**) was mounted in a Hampton cryoloop for indexing and intensity data collection at 173(2) K. Data was collected on a Bruker X8 APEX II CCD single crystal diffractometer with κ geometry and graphite monochromated Mo-K α radiation (λ = 0.71073 Å). Data collection, unit cell determination, intensity data integration, routine correction for Lorentz effects, polarization effects and multiscan absorption correction were performed using the APEX2 software package.²⁷ The structure was solved and refined using the SHELXTL software package.^{29,30} Direct methods were used to solve the structures and to locate the heavy atoms. The remaining atoms were found from successive Fourier synthesis. Heavy atoms (C, N, O, Br) were refined anisotropically, whereas the (H) atoms were refined isotropically.

CCDC reference number is 779417. Crystallographic data can be obtained free of charge from the Cambridge centre *via*: www.ccdc.cam.ac.uk/data_request/cif.

Diamine (**15**) was synthesised according to the published procedure.²⁴ All the synthesised compounds were fully characterised by different spectroscopical experiments.

* **Corresponding Author:**

Fax: +49 421 200 3229; Tel: +49 421 200 3120; E-mail: n.kuhnert@jacobs-university.de

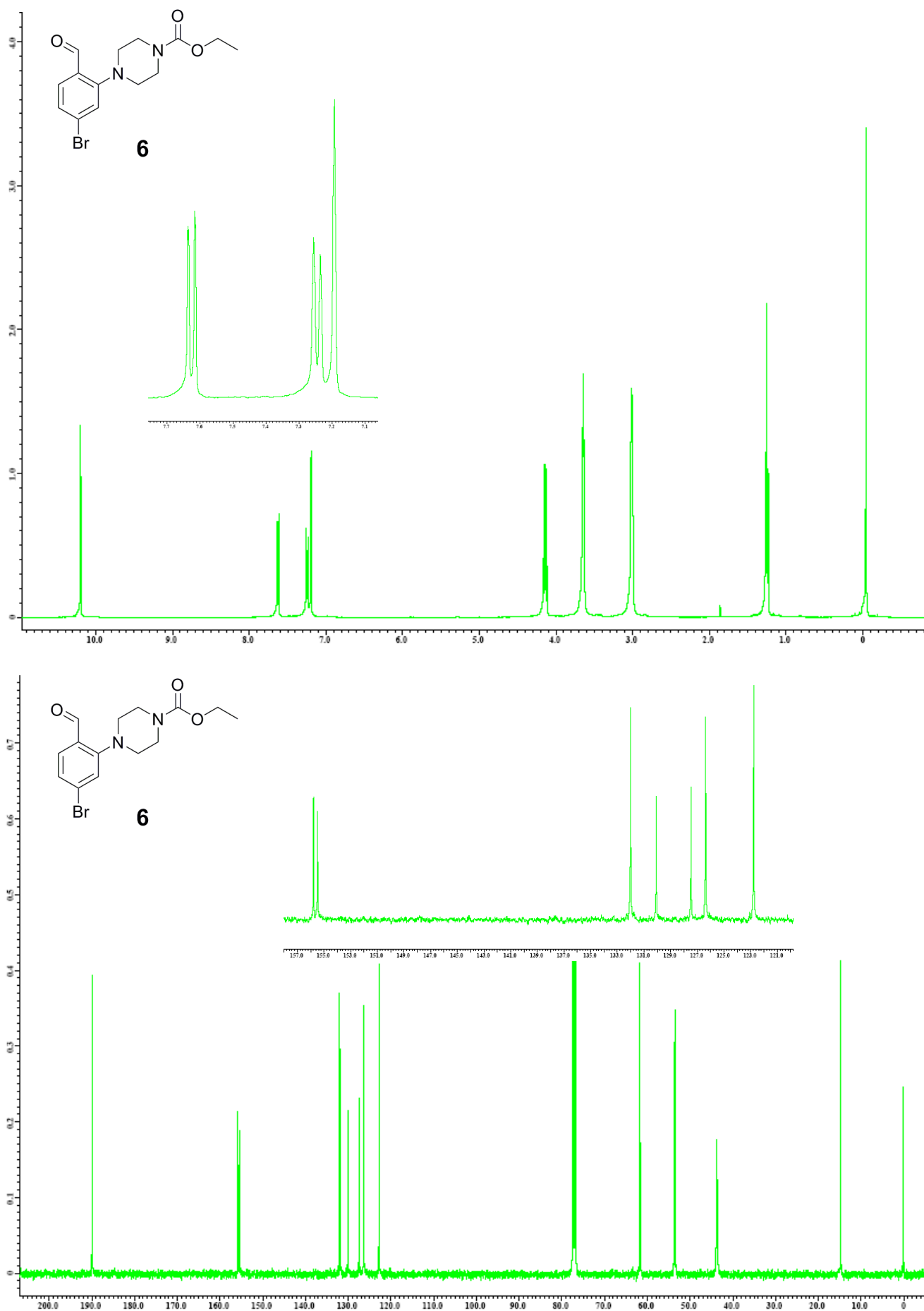


Figure 1: ¹H and ¹³C NMR spectra for the substituted monoaldehyde (**6**) in (CDCl₃, 400 MHz for ¹H-NMR and 100 MHz for ¹³C-NMR).

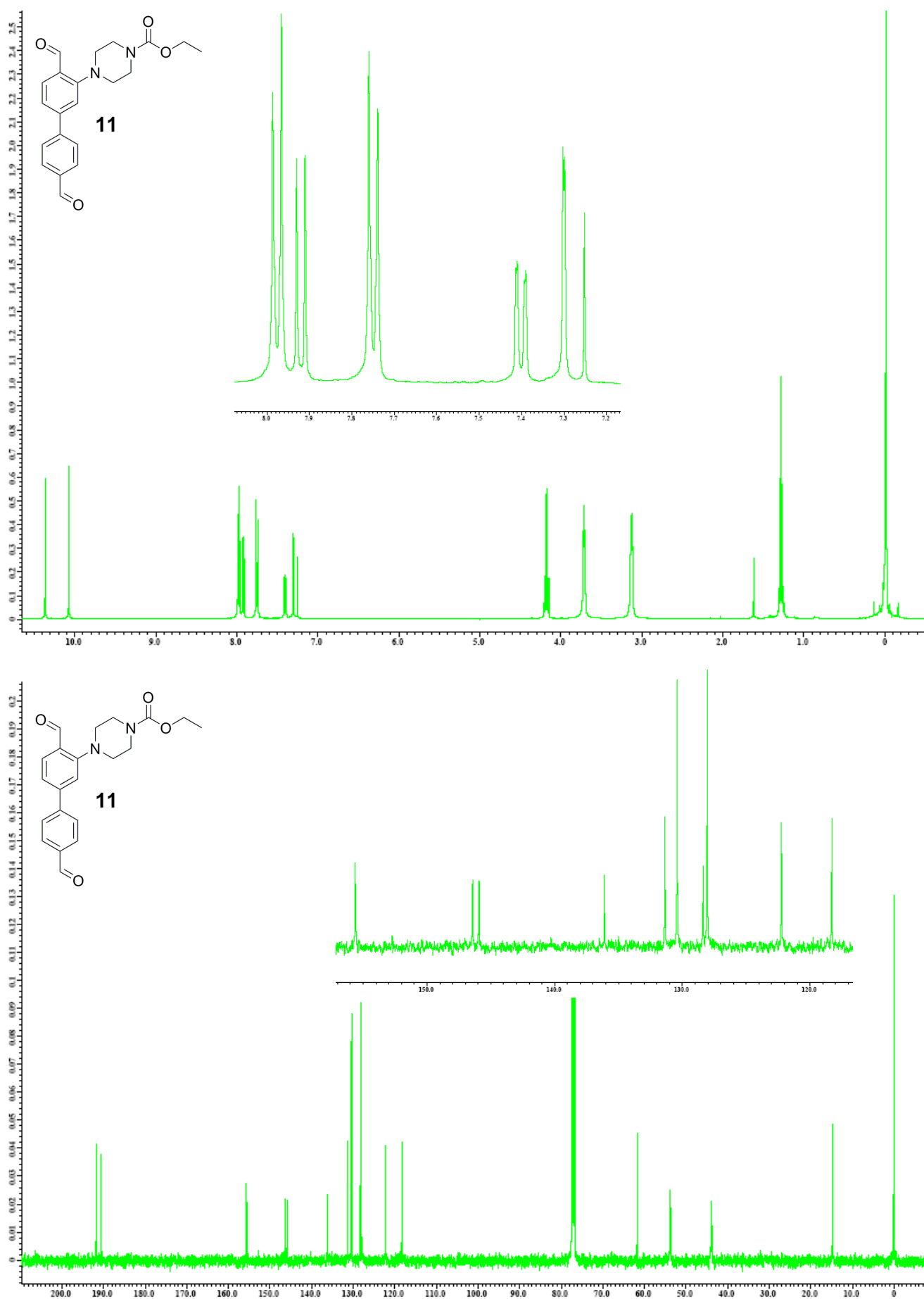


Figure 2: ¹H and ¹³C NMR spectra for the substituted dialdehyde (**11**) in (CDCl₃, 400 MHz for ¹H-NMR and 100 MHz for ¹³C-NMR).

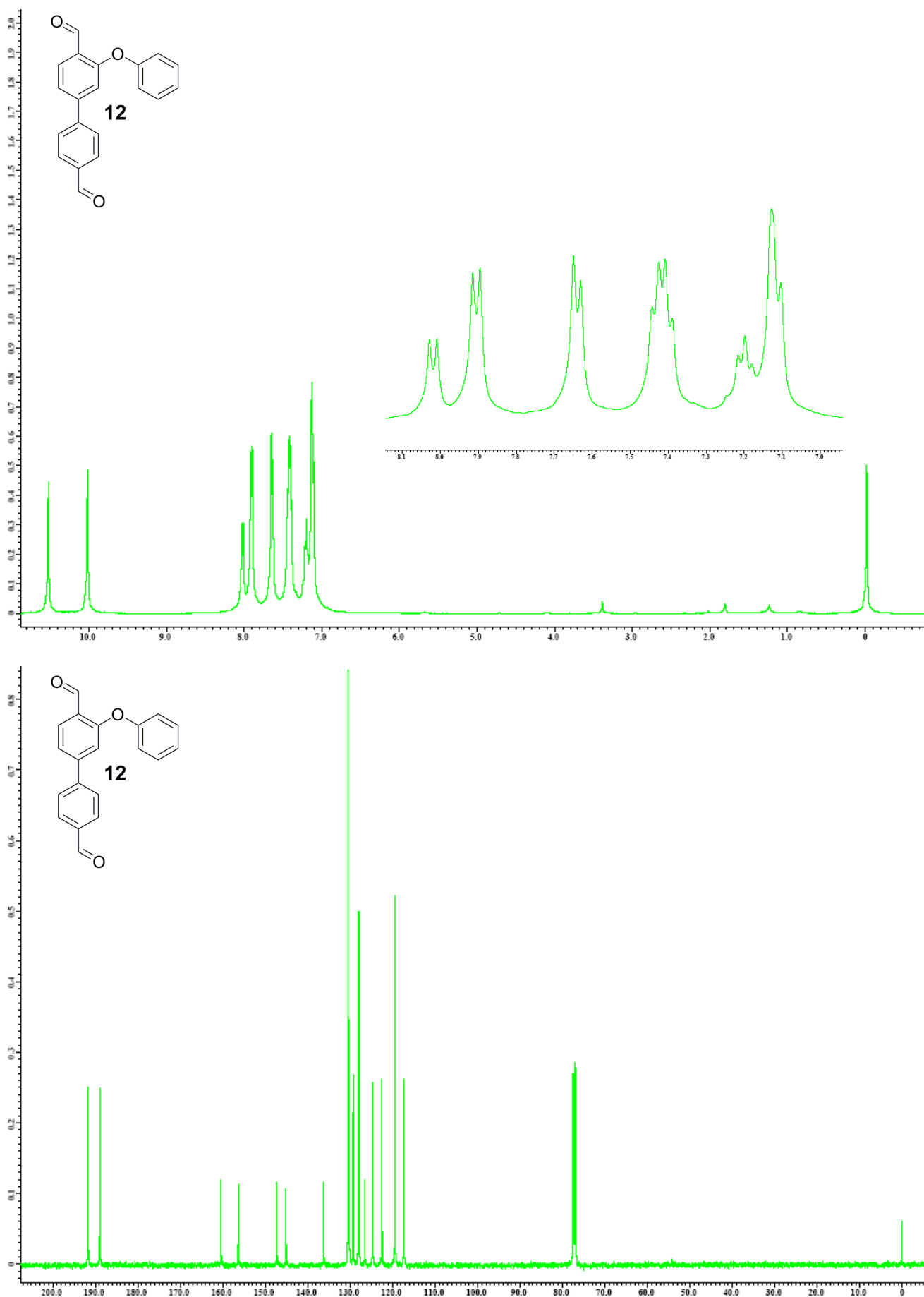


Figure 3: ¹H and ¹³C NMR spectra for the substituted dialdehyde (12) in (CDCl₃, 400 MHz for ¹H-NMR and 100 MHz for ¹³C-NMR).

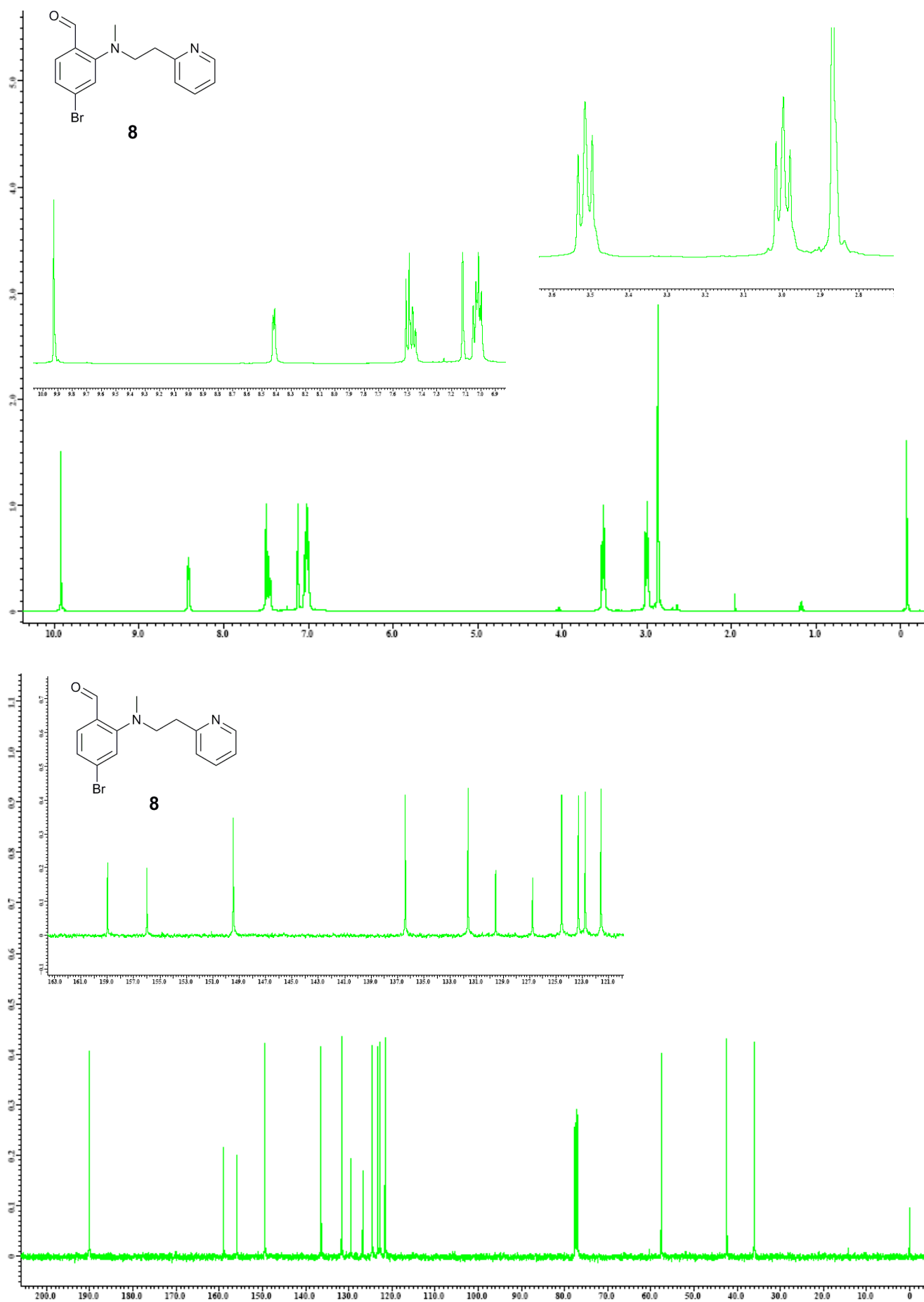


Figure 4: ^1H and ^{13}C NMR spectra for the substituted monoaldehyde (**8**) in (CDCl_3 , 400 MHz for ^1H -NMR and 100 MHz for ^{13}C -NMR).

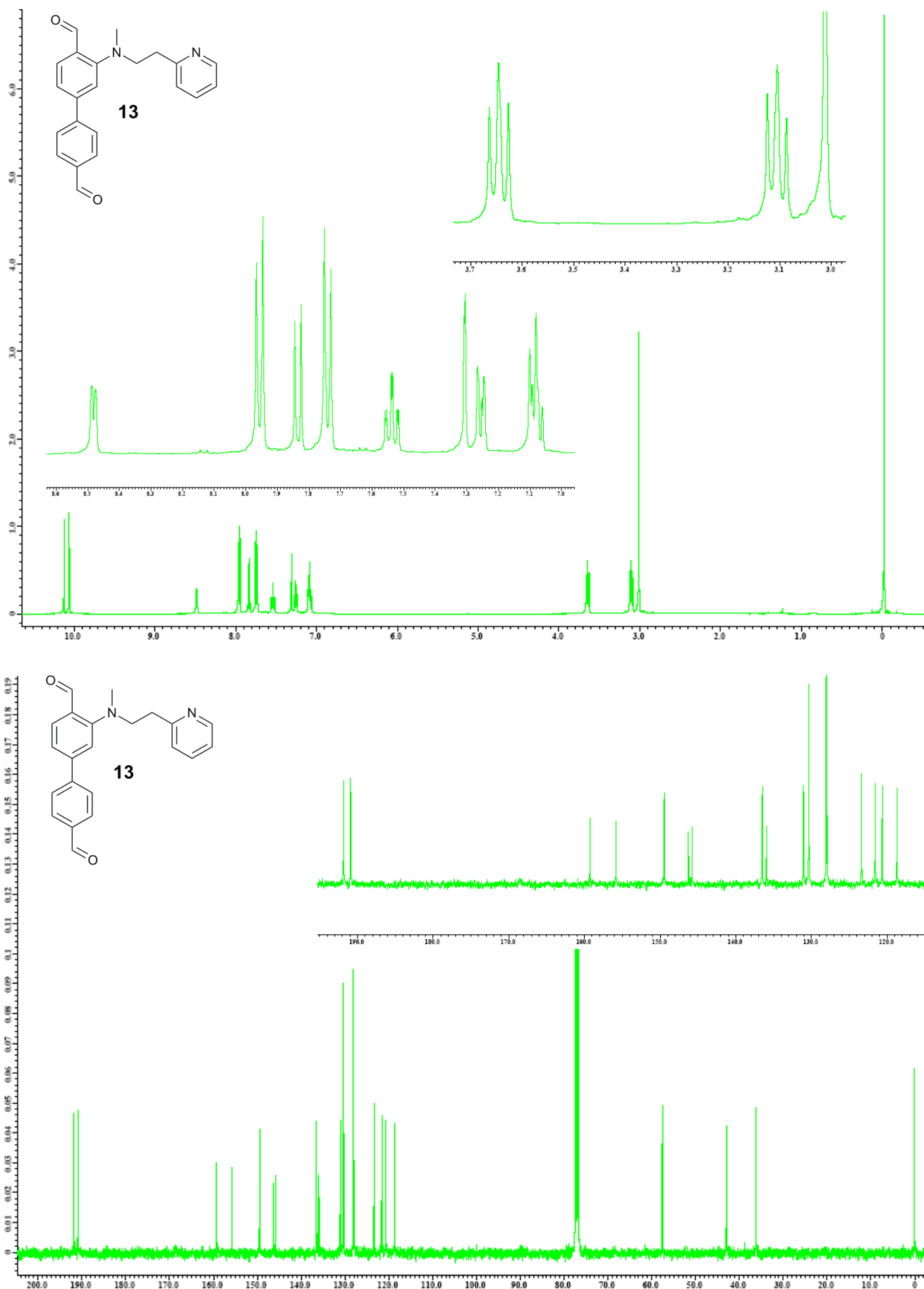


Figure 5: ^1H and ^{13}C NMR spectra for the substituted dialdehyde (**13**) in CDCl_3 , 400 MHz for ^1H -NMR and 100 MHz for ^{13}C -NMR).

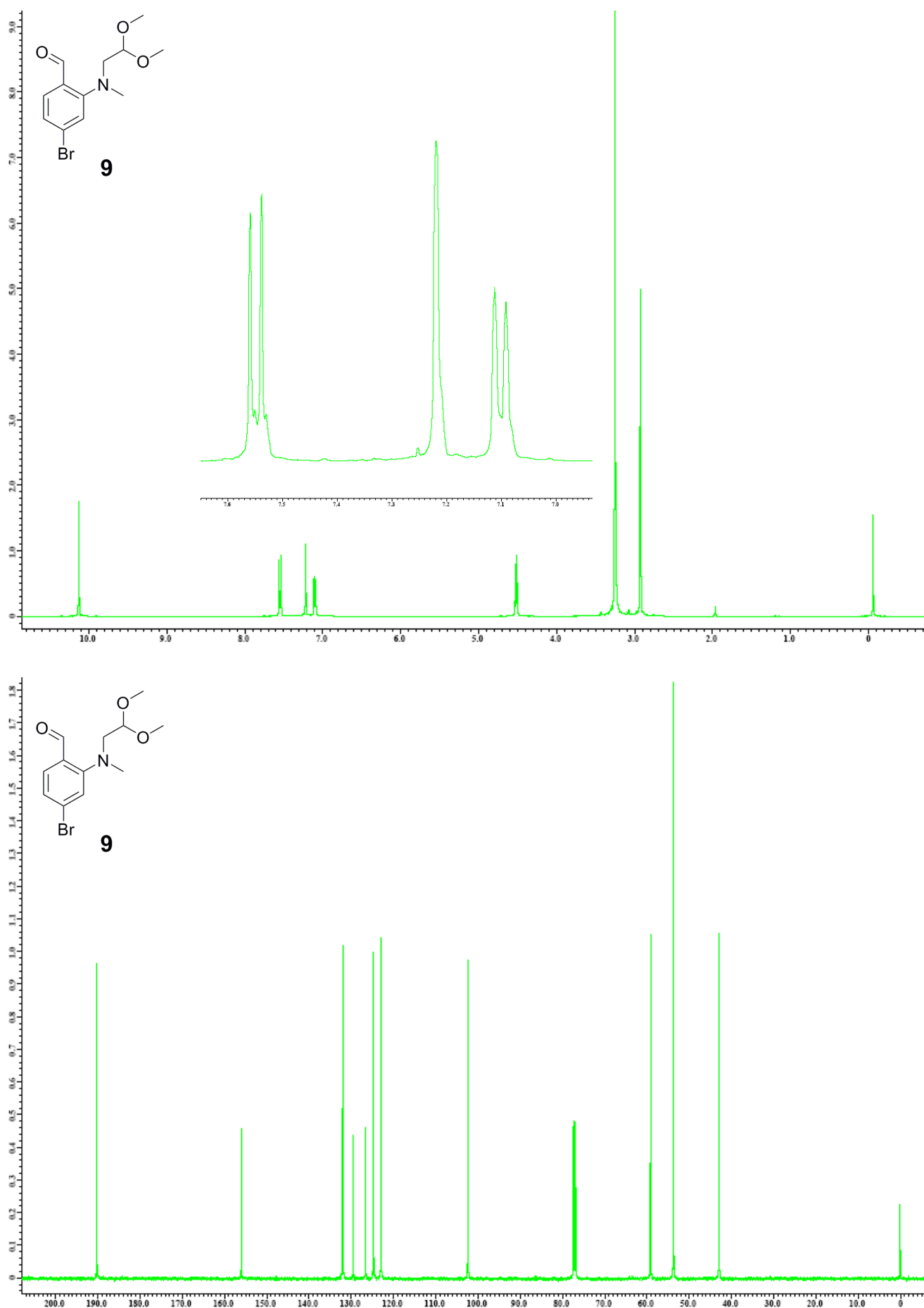


Figure 6: ¹H and ¹³C NMR spectra for the substituted monoaldehyde (**9**) in (CDCl₃, 400 MHz for ¹H-NMR and 100 MHz for ¹³C-NMR).

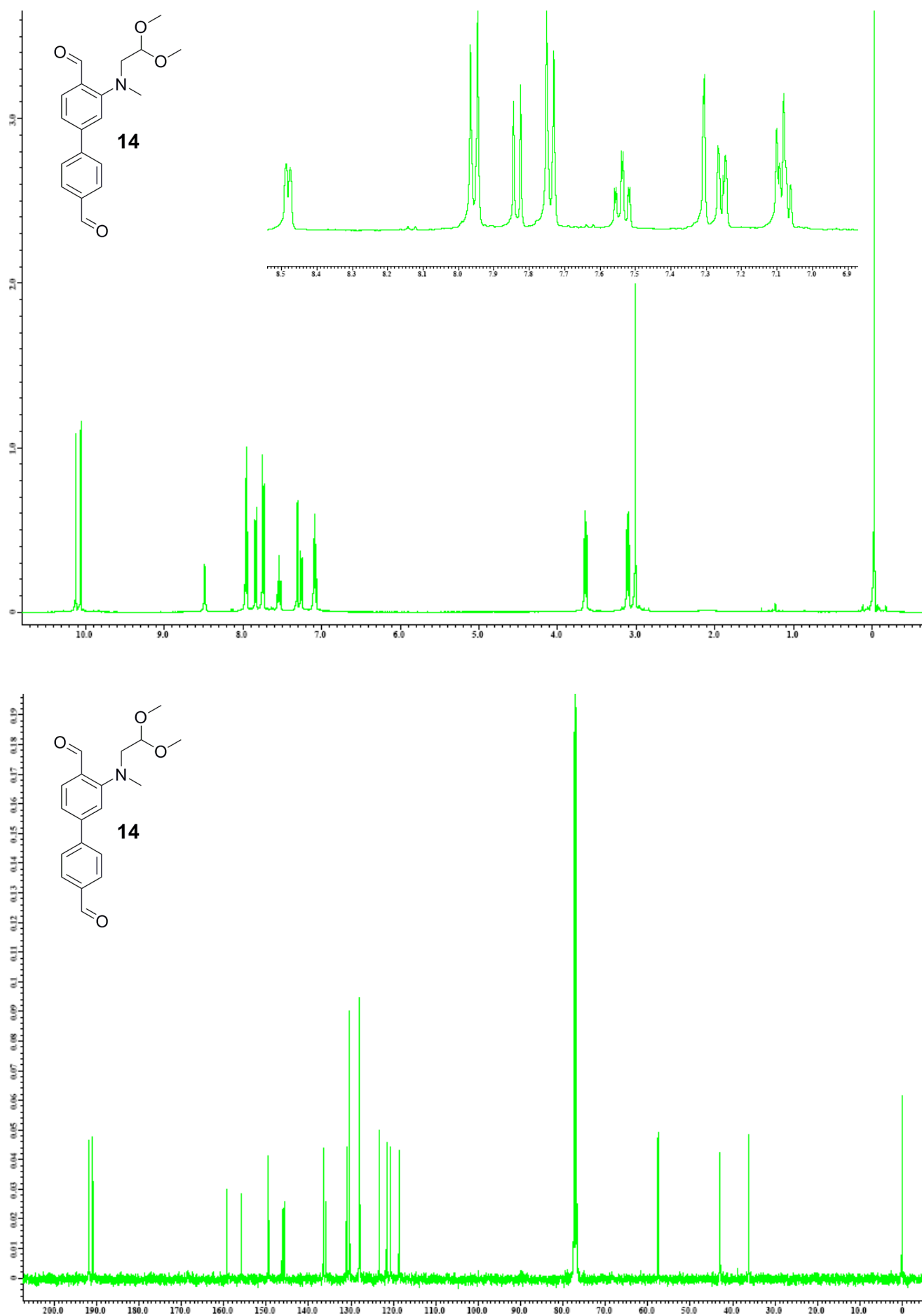


Figure 7: ^1H and ^{13}C NMR spectra for the substituted dialdehyde (**14**) in CDCl_3 , 400 MHz for ^1H -NMR and 100 MHz for ^{13}C -NMR).

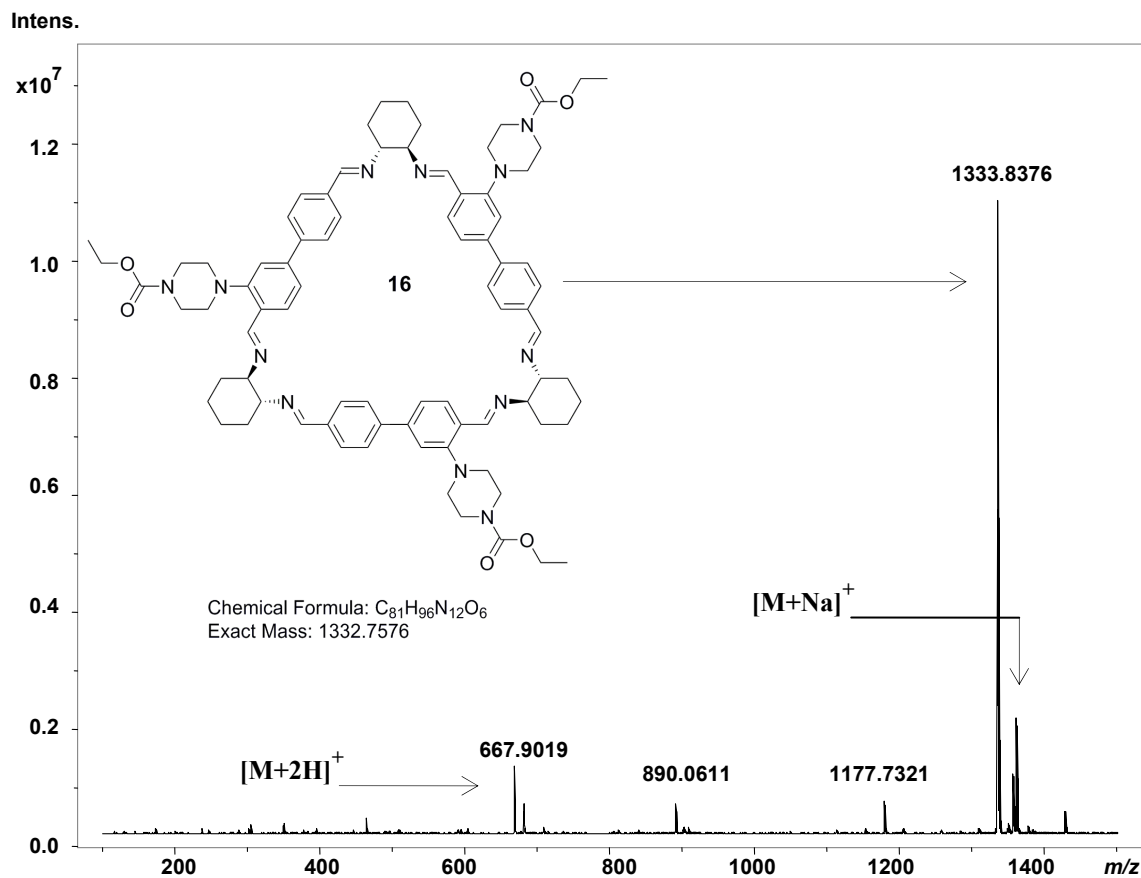
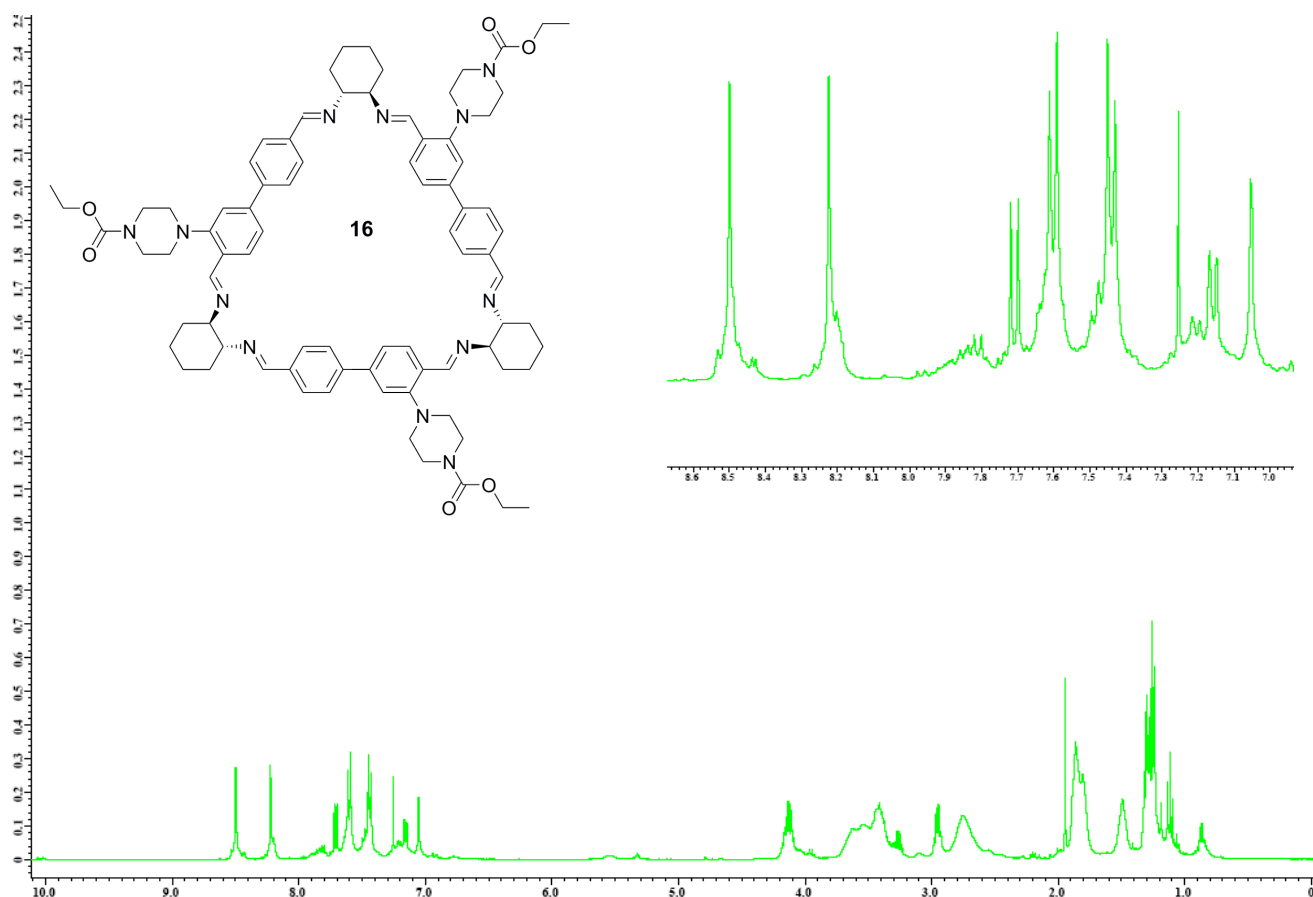


Figure 8: ¹H-NMR and ESI-MS spectra for the C₃-symmetrical triazoline (**16**) (¹H-NMR, CDCl₃, 400 MHz).

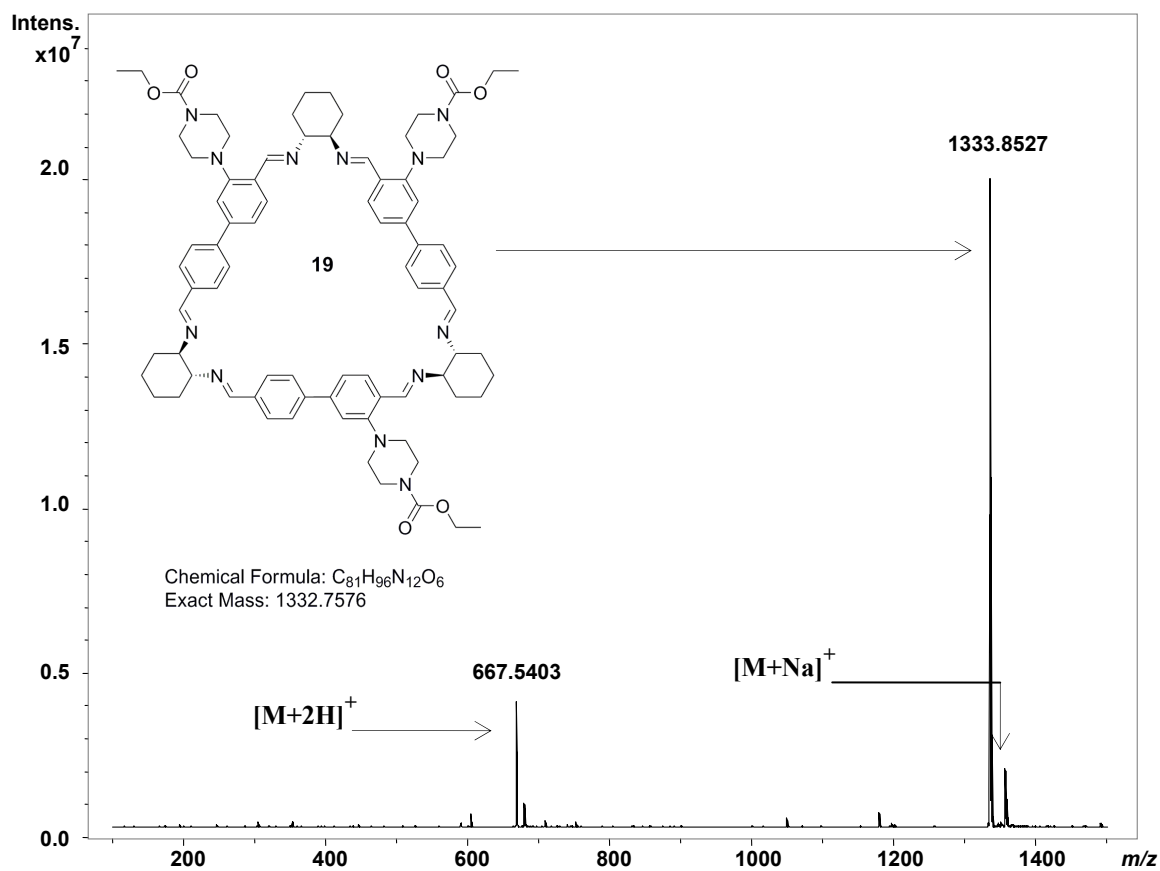
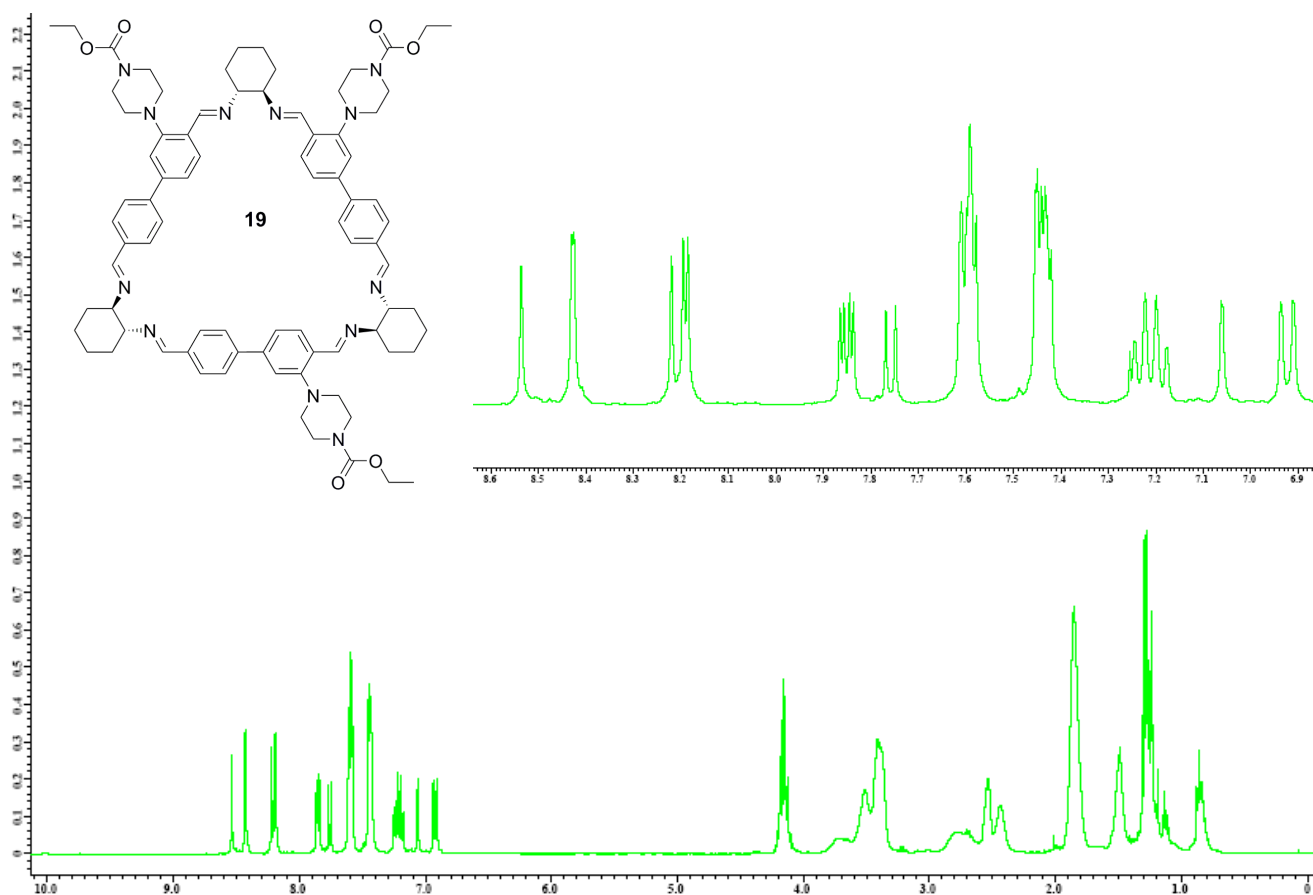


Figure 9: 1H -NMR and ESI-MS spectra for the non-symmetrical trianglimine (**19**) (1H -NMR, $CDCl_3$, 400 MHz).

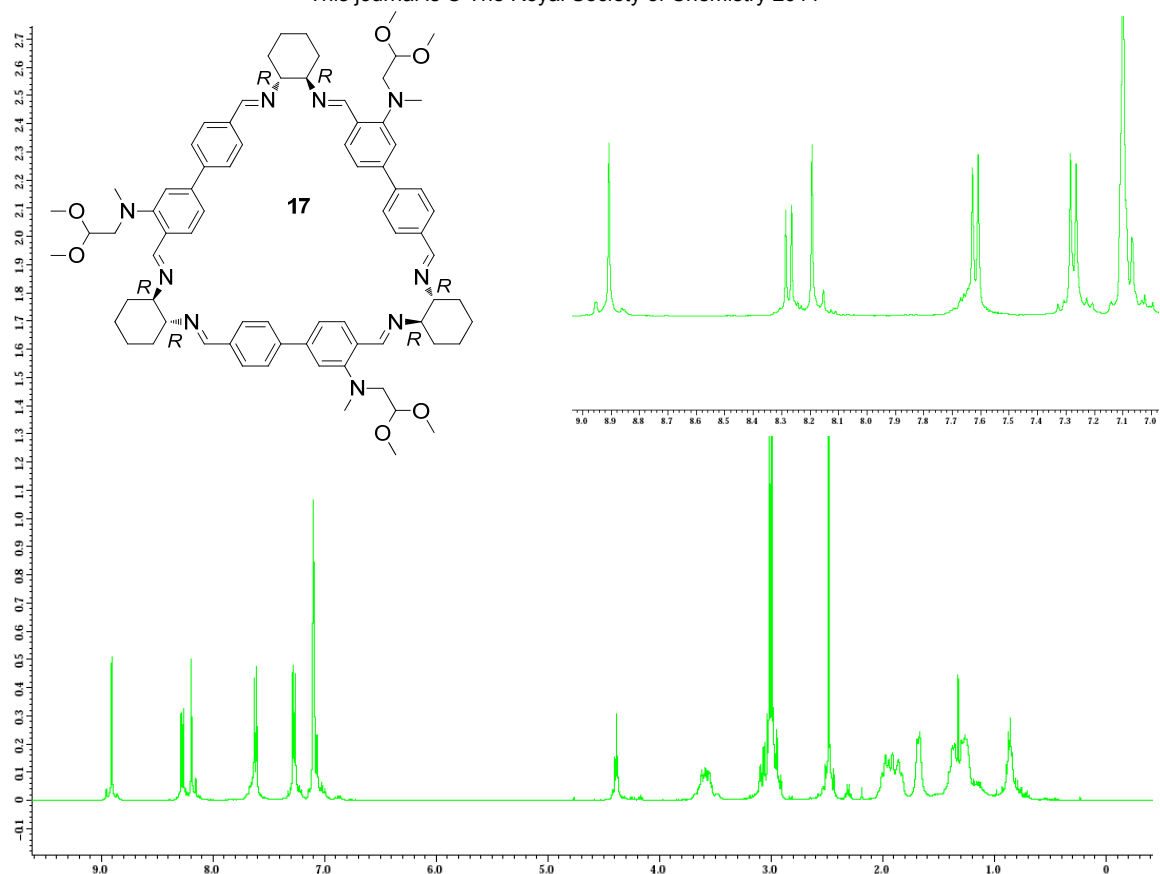


Figure 10: ^1H -NMR spectrum for the C_3 -symmetrical trianglimine (17) (^1H -NMR, C_6D_6 , 400 MHz).

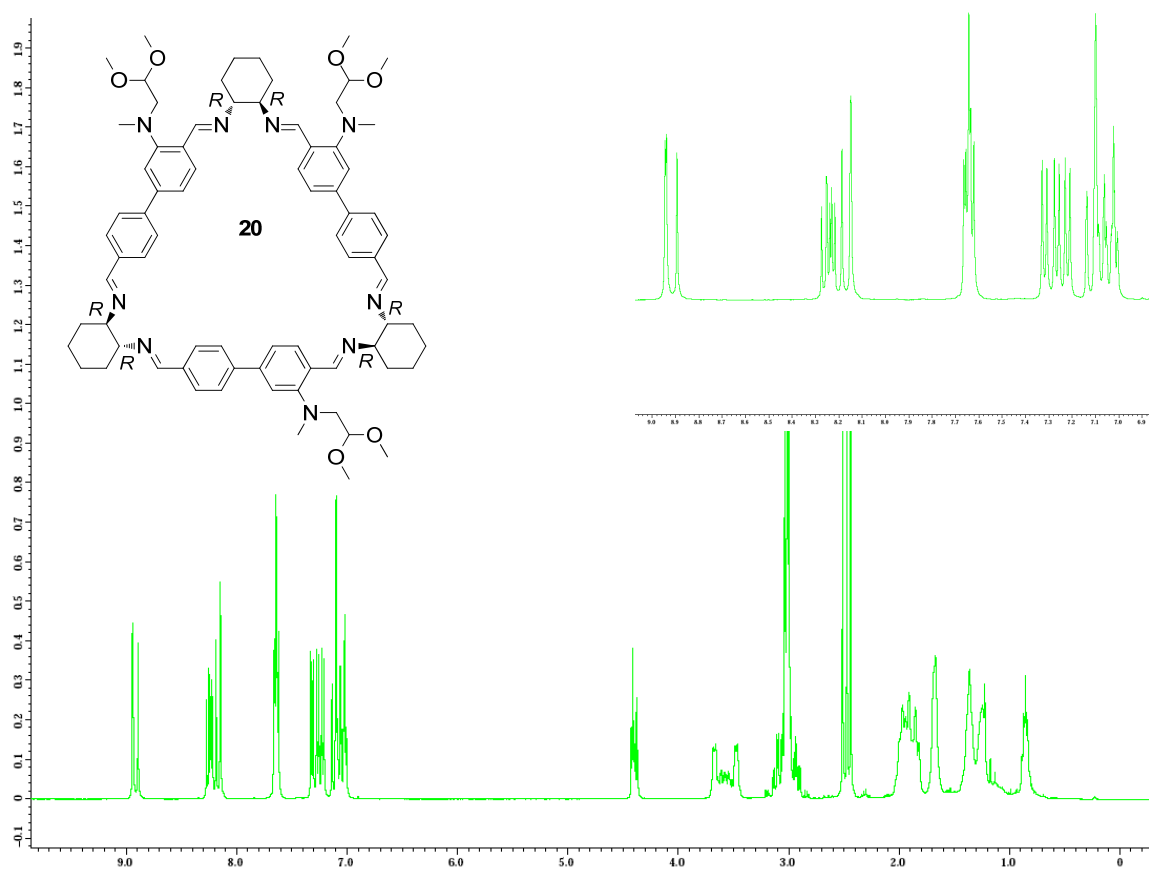


Figure 11: ^1H -NMR spectrum for the non-symmetrical trianglimine (20) (^1H -NMR, C_6D_6 , 400 MHz).

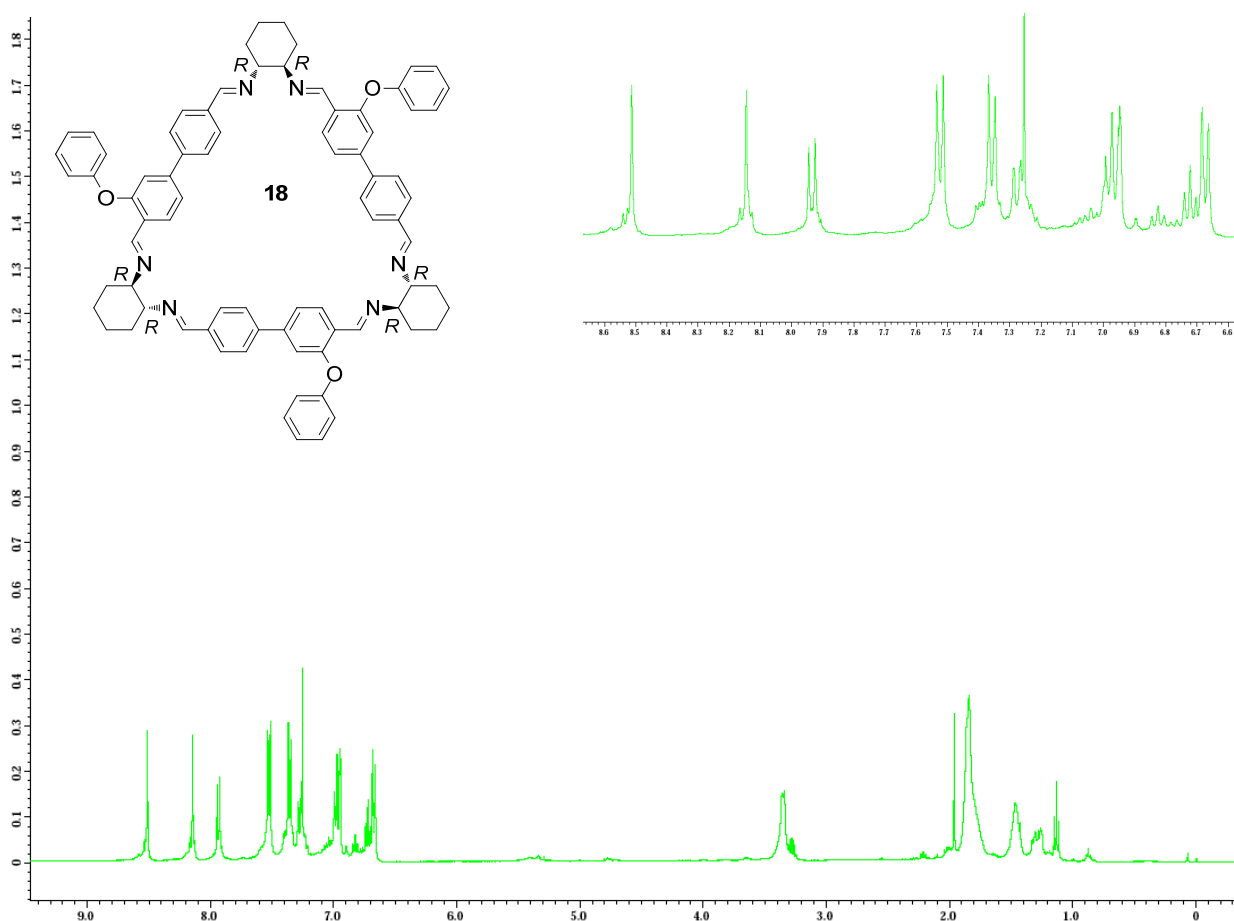


Figure 12: ^1H -NMR spectrum for the C_3 -symmetrical trianglimine (**18**) (^1H -NMR, CDCl_3 , 400 MHz).

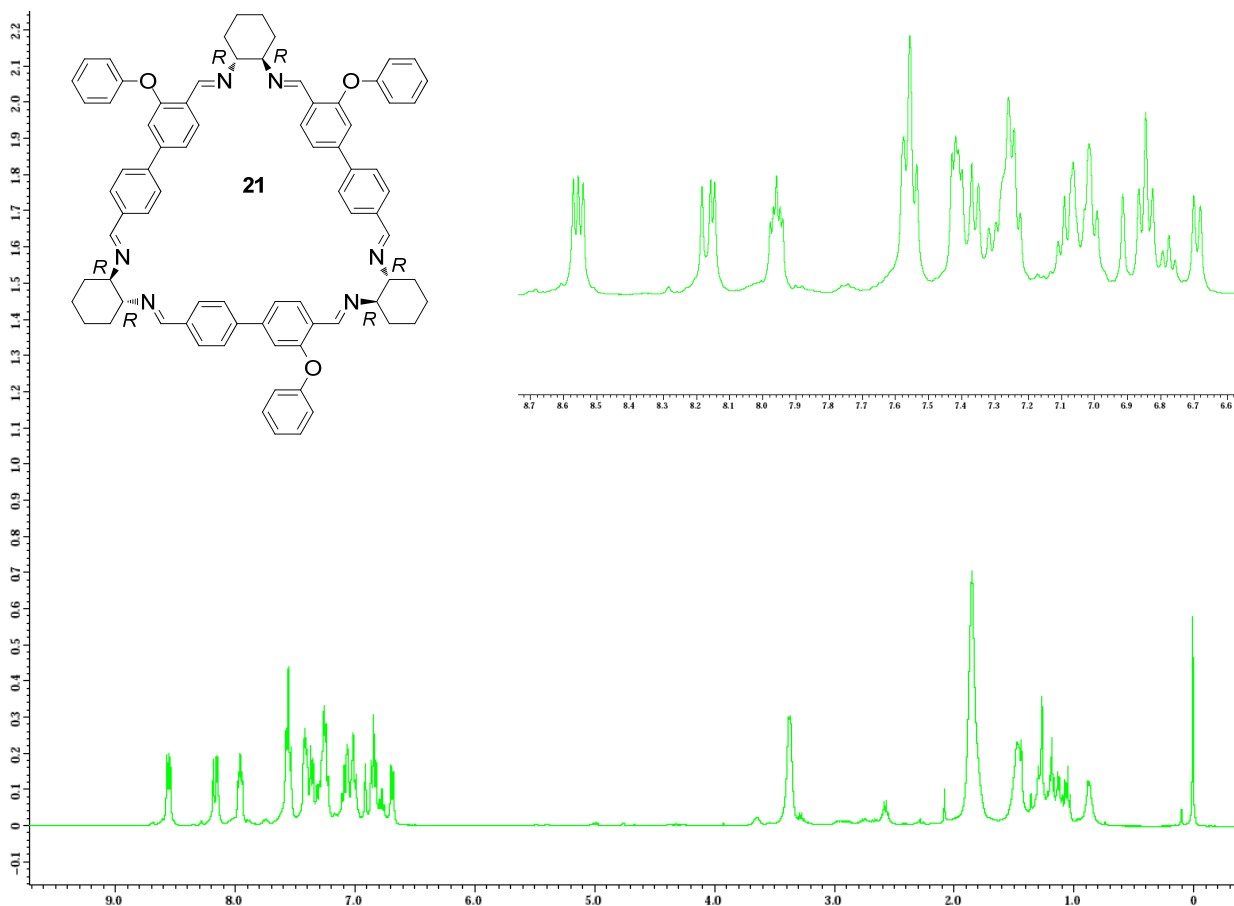


Figure 13: ^1H -NMR spectrum for the non-symmetrical trianglimine (**21**) (^1H -NMR, C_6D_6 , 400 MHz).

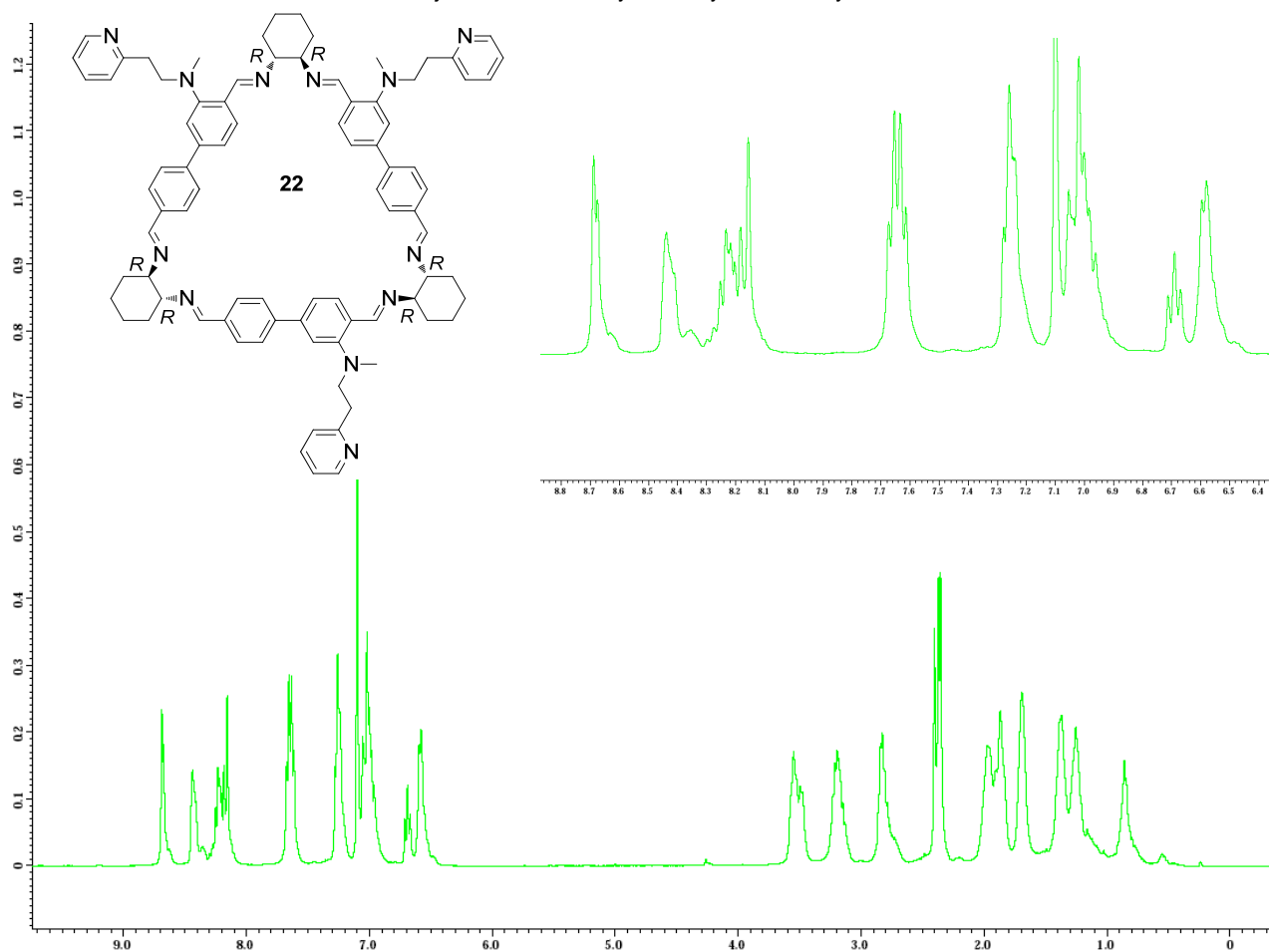


Figure 14: ^1H -NMR spectrum for the non-symmetrical trianglimine (**22**) (^1H -NMR, C_6D_6 , 400 MHz).

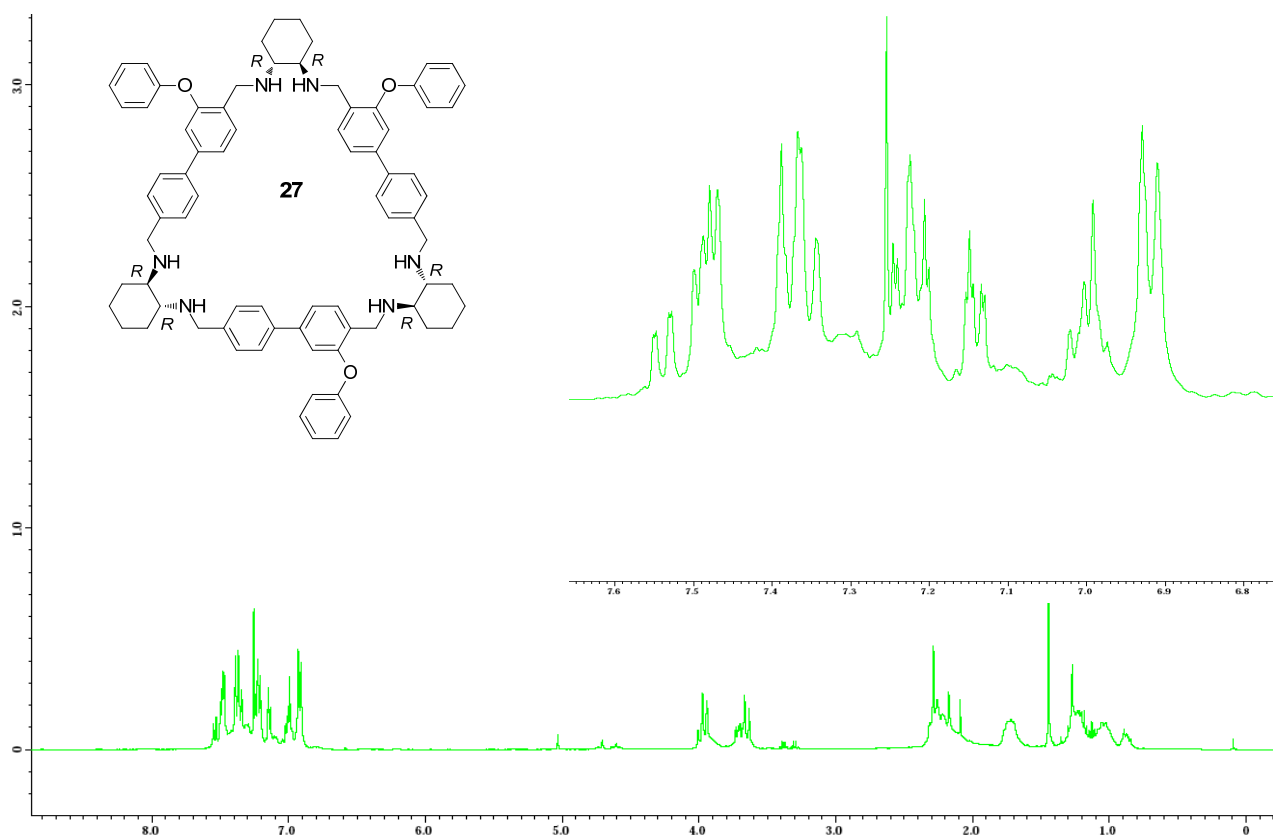


Figure 15: ^1H -NMR spectrum for the non-symmetrical trianglimine (**27**) (^1H -NMR, CDCl_3 , 400 MHz).

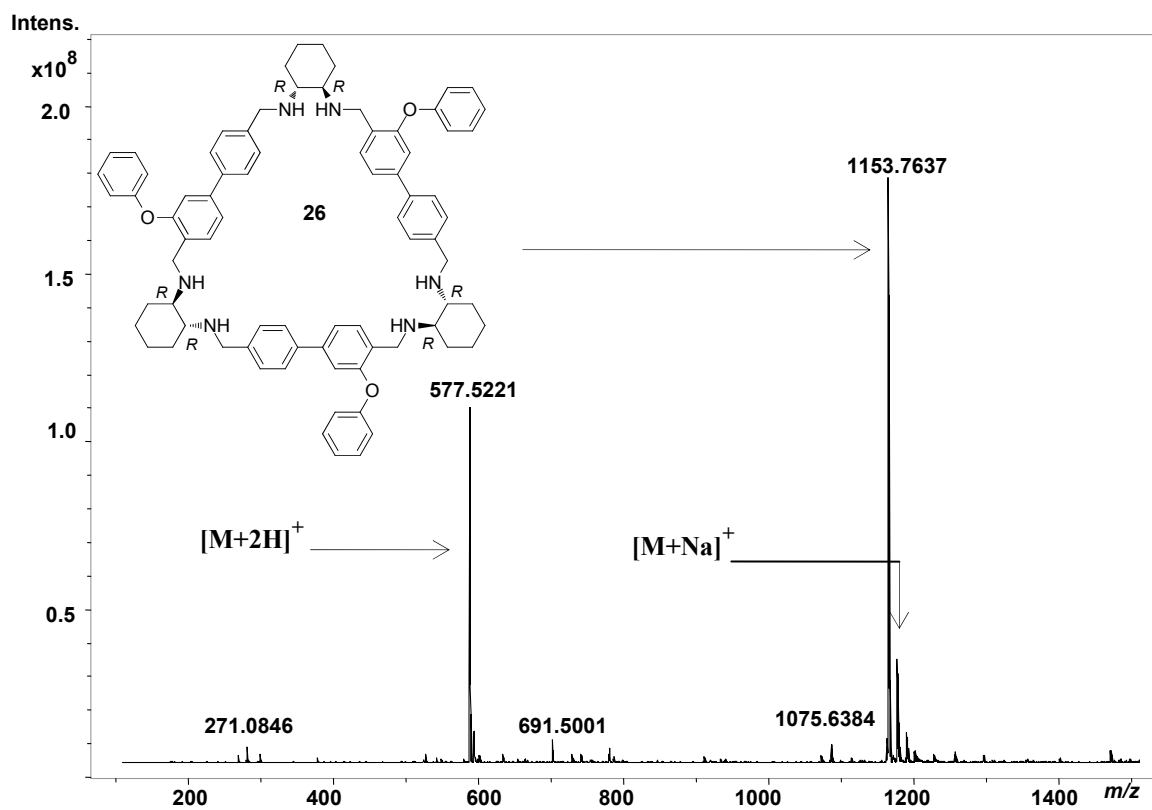
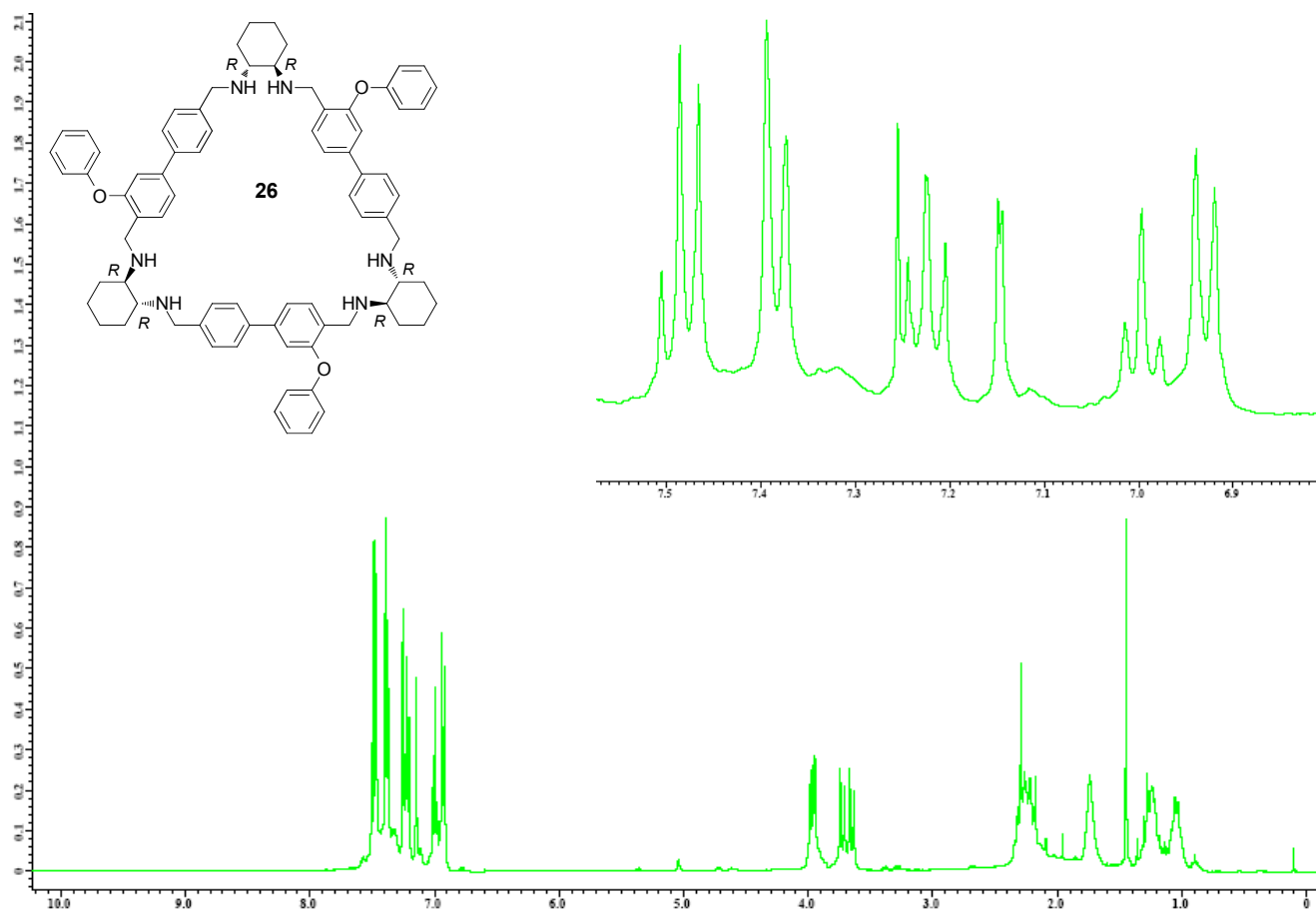


Figure 16: $^1\text{H-NMR}$ and ESI-MS spectra for the C_3 -symmetrical triamine (**26**) ($^1\text{H-NMR}$, CD₆, 400 MHz).

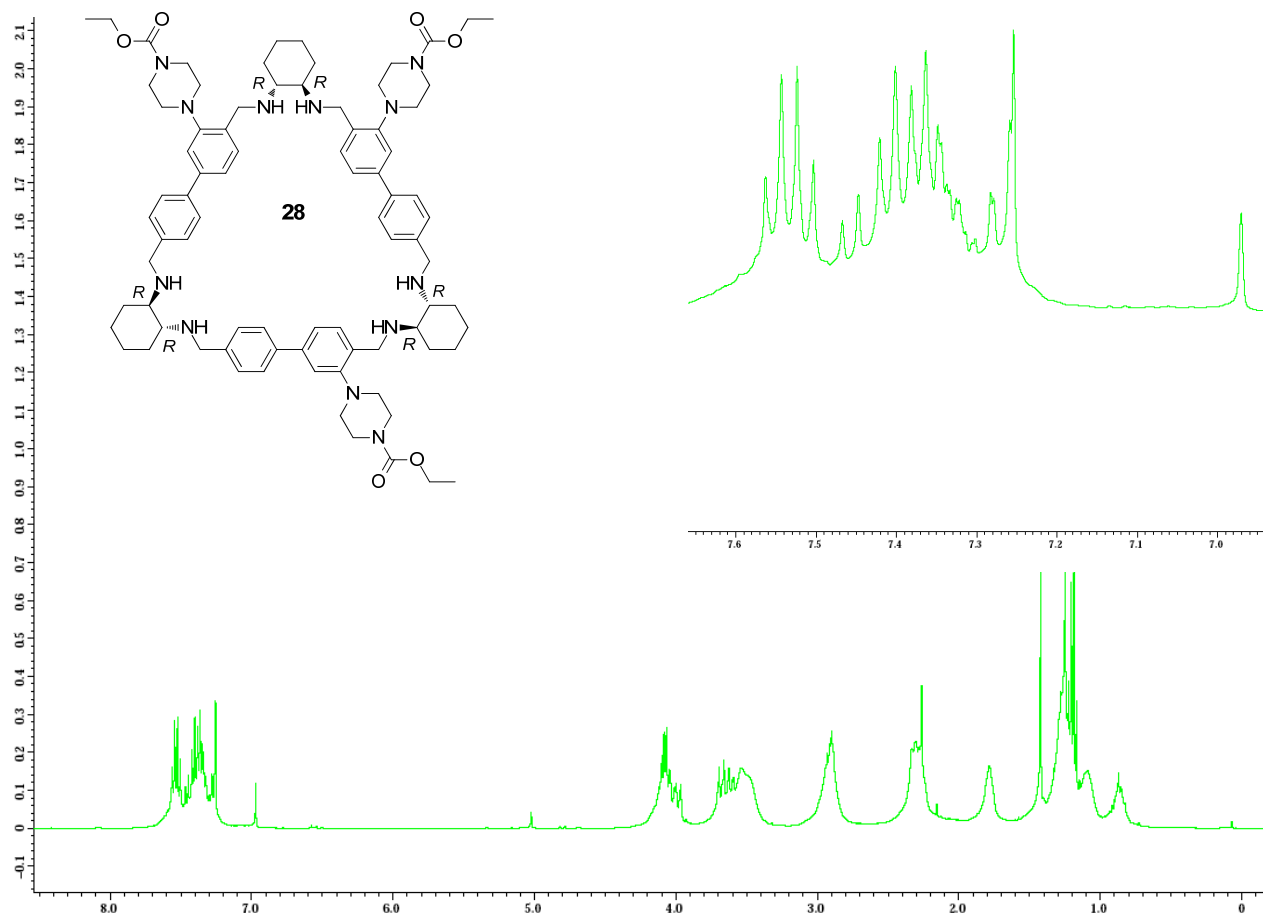


Figure 17: ^1H -NMR spectrum for the non-symmetrical trianglamine (**28**) (^1H -NMR, CDCl_3 , 400 MHz).

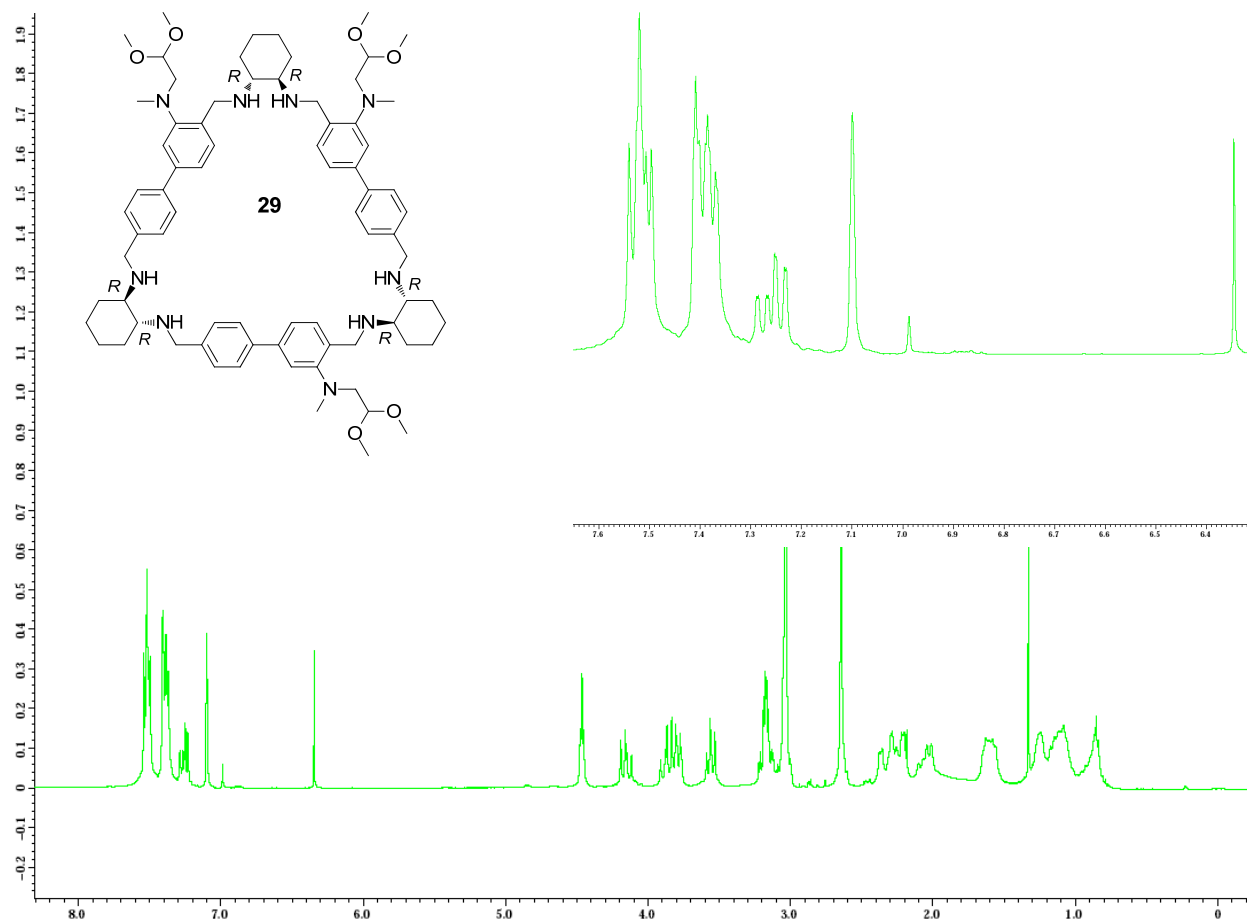


Figure 18: ^1H -NMR spectrum for the non-symmetrical trianglamine (**29**) (^1H -NMR, C_6D_6 , 400 MHz).

Computed structures for trianglimines **18** and **21**

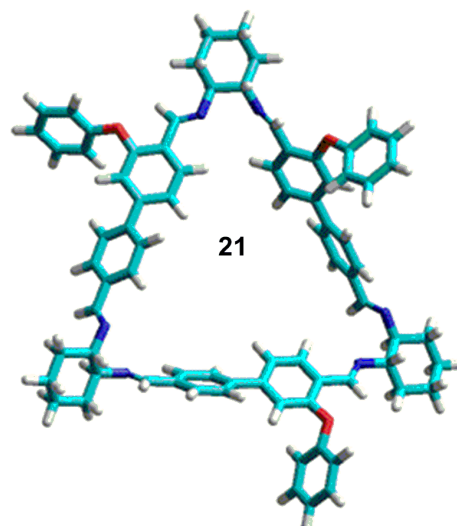
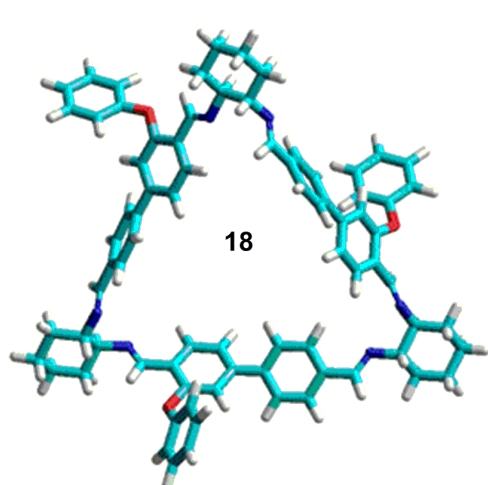
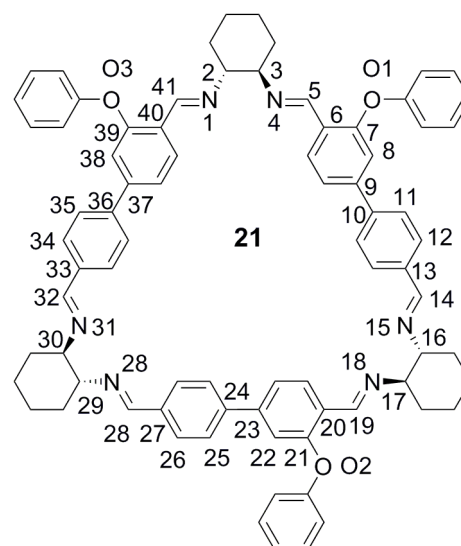


Table 1 Some selected bond lengths and angles for trianglimines **18** and **21**.

PM3 ^a	PM3 ^b	X-ray ²⁸	Bond / Angel (Å, °)
1.46	1.46	1.45	C41-C42
1.46	1.47	1.44	C05-C06
1.29	1.29	1.29	N01-C42
1.29	1.29	1.27	N04-C05
1.47	1.47	1.46	N04-C03
1.47	1.47	1.47	N01-C02
1.54	1.54	1.52	C02-C03
1.38	1.38	1.34	O01-C07
—	1.38	1.34	O03-C41
120.71	120.94	118.70	C05-N04-C03
121.25	120.91	119.40	C42-N01-C02
120.39	120.51	123.02	N04-C05-C06
120.89	120.54	122.60	N01-C42-C41
109.00	109.68	110.20	N04-C03-C02
109.07	109.26	108.90	N01-C02-C03
115.47	115.93	120.10	O01-C07-C06



Computed values of the bond lengths and angles for trianglimines **18**^a and **21**^b using the Polak-Ribiere conjugate gradient with rms 0.1 Kcal/mol.

Table 2 Crystallographic data for the substituted monoaldehyde (**6**)

Formula	C ₂₈ H ₃₄ Br ₂ N ₄ O ₆	Z	2	Selected bond lengths (Å) and angles (°)	
fw/g mol ⁻¹	682.41	D _c /g cm ⁻³	3.191	O(1)-C(1) 1.206(1) C(1)-C(2) 1.475(1) C(5)-Br 1.898(1) C(3)-N(1) 1.415(1) C(12)-N(2) 1.365(1) C(3)-N(1)-C(8) 115.810(4) C(3)-N(1)-C(10) 117.271(7) C(12)-N(2)-C(9) 123.382(7) C(12)-N(2)-C(11) 117.503(4) N(2)-C(12)-O(3) 110.899(4) C(12)-O(3)-C(13) 116.706(4)	
Crystal system	Triclinic	μ/mm ⁻¹	5.806		
Space group	P $\bar{1}$	Reflections:			
a/Å	7.8543(6)	Collected	38893		
b/Å	9.3193(7)	Unique (R _{int})	2900 (0.0569)		
c/Å	10.5343(6)	Observed [I > 2σ(I)]	2631		
α(°)	95.589(4)	Parameters	804		
β(°)	110.786(2)	R(F) ^a [I > 2σ(I)]	0.0274		
χ(°)	95.620(4)	wR(F ²) ^b (all data)	0.0840		
V/Å ³	710.15(9)	GoF	1.003		

$$^a R = \sum ||F_o| - |F_c|| / \sum |F_o| \quad ^b R_w = [\sum w(F_o^2 - F_c^2)^2 / \sum w(F_o^2)]^{1/2}.$$

Equilibration of the C_3 -symmetrical trianglimine (16) with its non-symmetrical regioisomer (19)

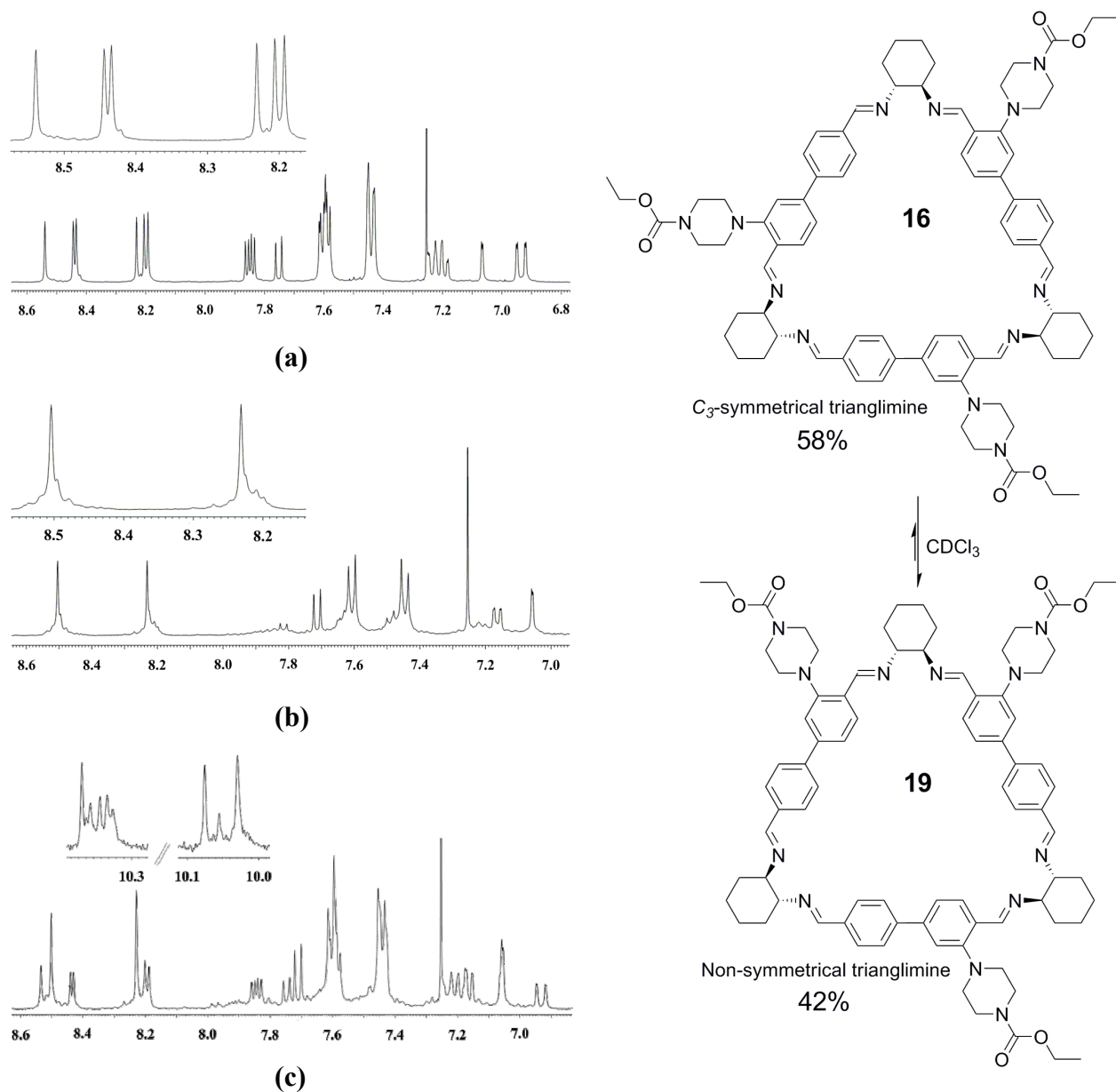


Figure 19: Expanded region of ^1H -NMR spectra for (a) trianglimine (19), (b) trianglimine (16), and (c) trianglimine (16) after 6 days of standing in CDCl_3 (CDCl_3 , 400 MHz).

Probing the mechanism and dynamic reversibility of trianglimine formation using real time electrospray ionization time-of-flight mass spectrometry

Hany F. Nour,¹ Ana M. Lopez-Periago² and Nikolai Kuhnert.^{1,2*}

¹School of Engineering and Science, Organic and Analytical Chemistry Laboratory, Jacobs University, 28759 Bremen, Germany. ²Synthetic and Biological Organic Chemistry Laboratory, School of Biomolecular and Medical Science, The University of Surrey, Guildford GU2 7XH, UK.

**Correspondence to:* Prof. Dr Nikolai Kuhnert, School of Engineering and Science, Jacobs University, P. O. Box 750 561, 2872 Bremen, Germany, E-mail: n.kuhnert@jacobs-university.de, Fax: +49 421 200 3229, Tel: +49 421 200 3120.

Monitoring the [3+3]-cyclocondensation reaction of terephthalaldehyde **2** with (1*R*,2*R*)-1,2-diaminocyclohexane **1**, product ions appeared as $[M+H]^+$

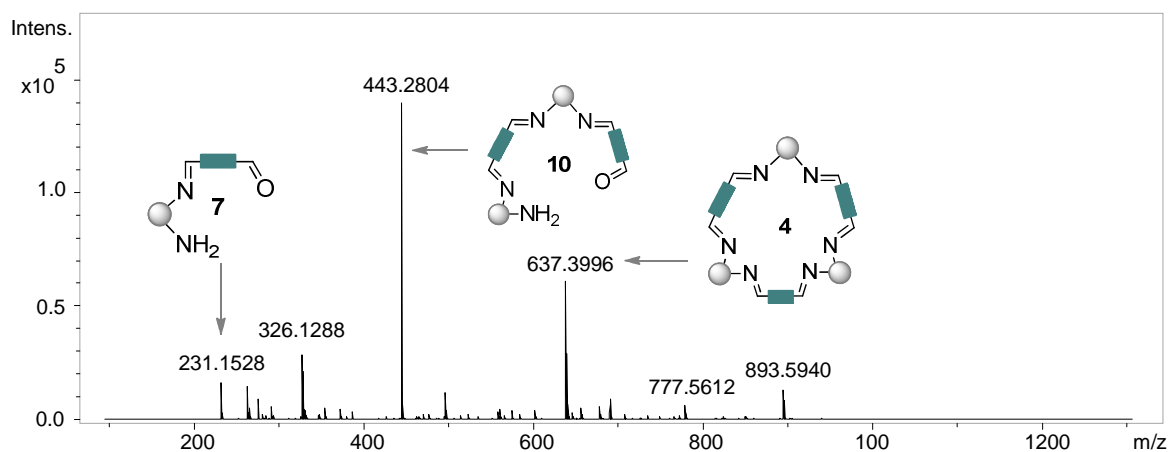


Figure 1. Mass spectrum recorded in the positive ion mode after 1 h.

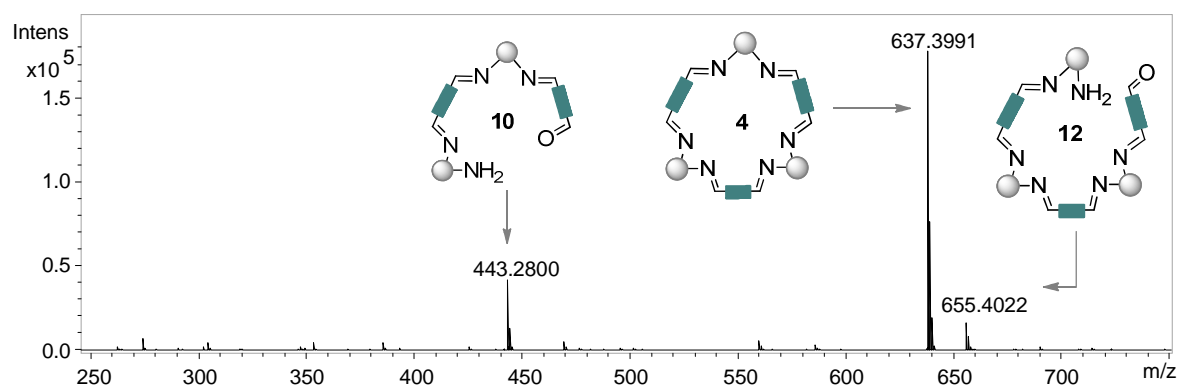


Figure 2. Mass spectrum recorded in the positive ion mode after 2 h.

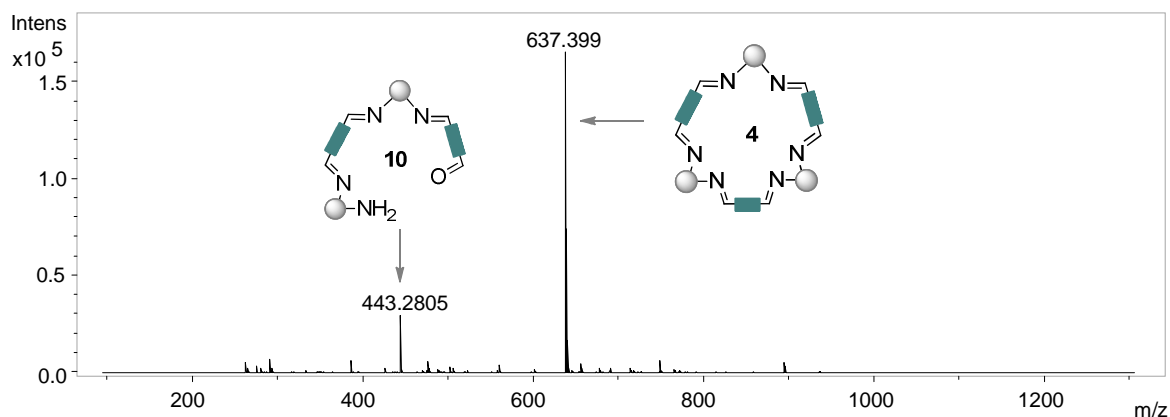


Figure 3. Mass spectrum recorded in the positive ion mode after 3 h.

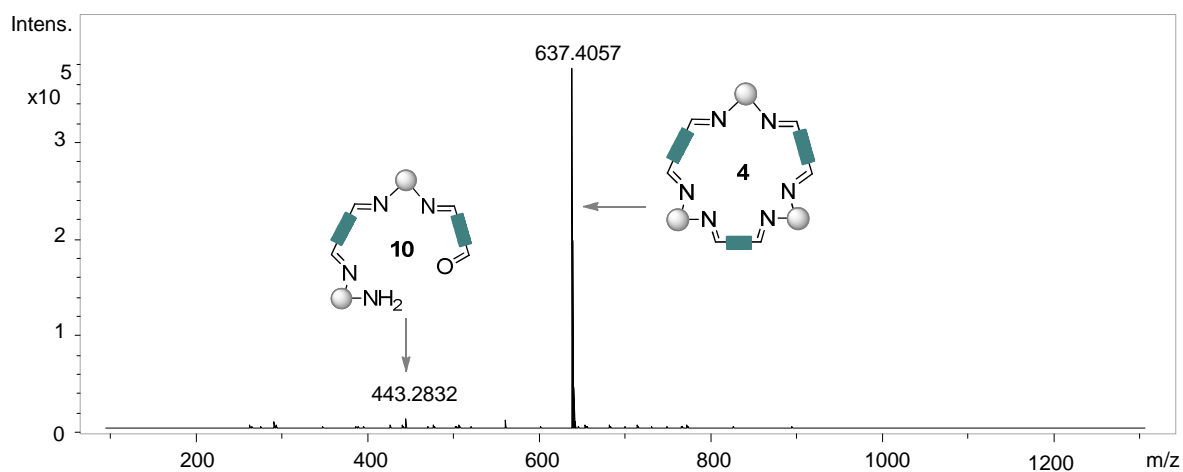


Figure 4. Mass spectrum recorded in the positive ion mode after 4 h.

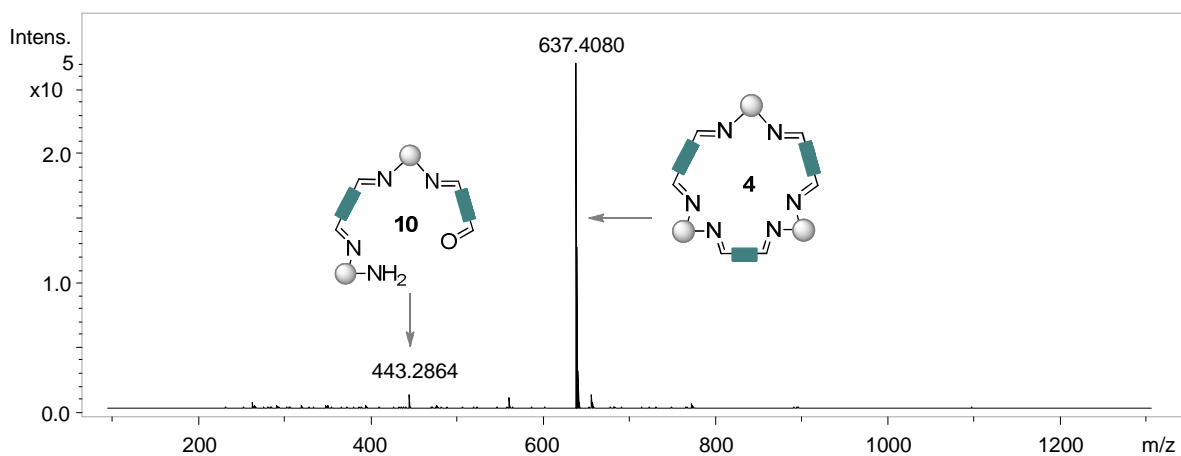


Figure 5. Mass spectrum recorded in the positive ion mode after 5 h.

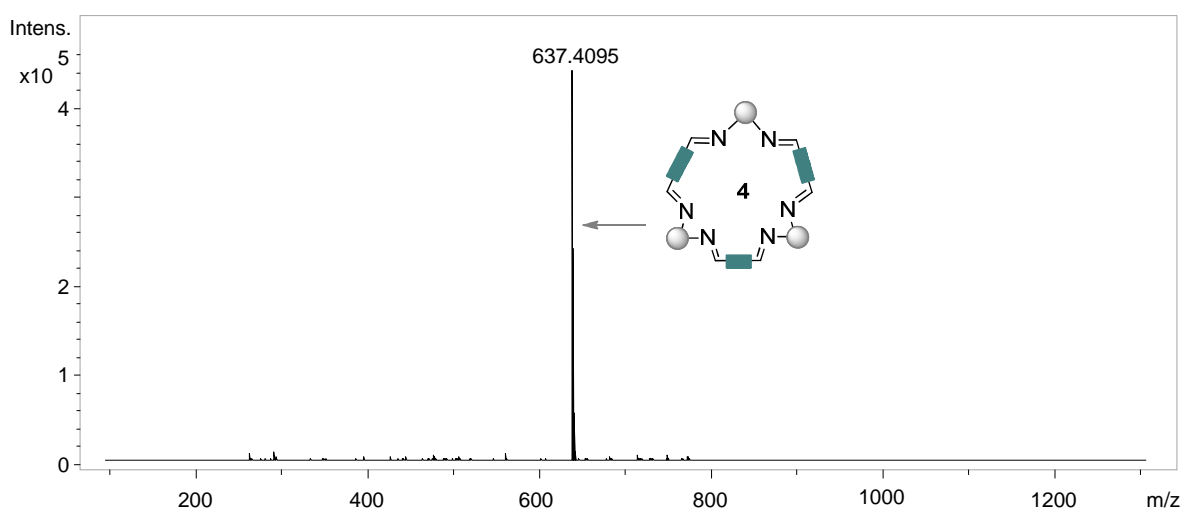


Figure 6. Mass spectrum recorded in the positive ion mode after 6 h.

Monitoring the cyclocondensation reaction of isophthalaldehyde **3** with (1*R*,2*R*)-1,2-diaminocyclohexane **1**, product ions appeared as $[M+H]^+$

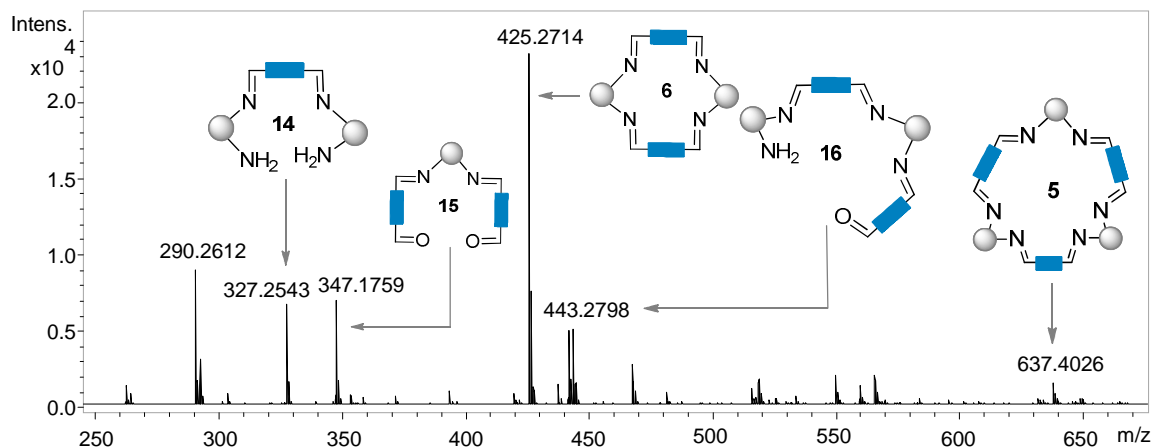


Figure 7. Mass spectrum recorded in the positive ion mode after 1 h.

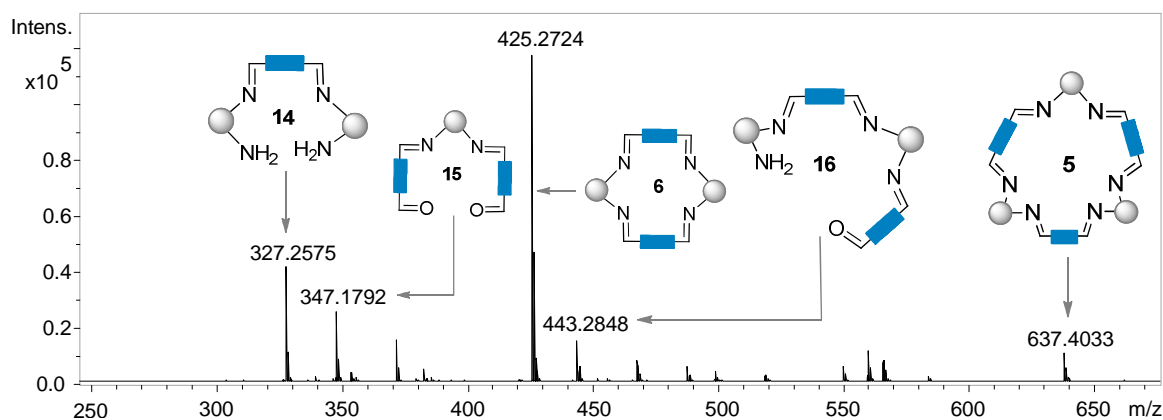


Figure 8. Mass spectrum recorded in the positive ion mode after 3 h.

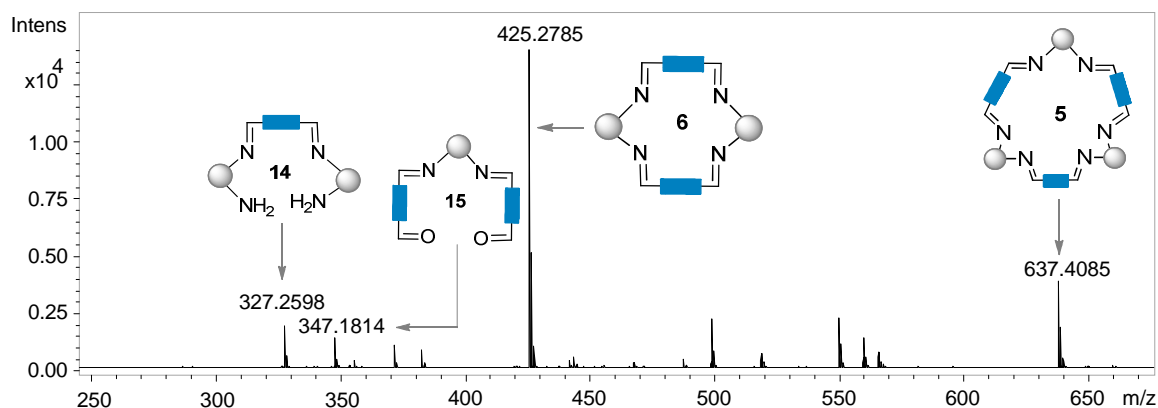


Figure 9. Mass spectrum recorded in the positive ion mode after 6 h.

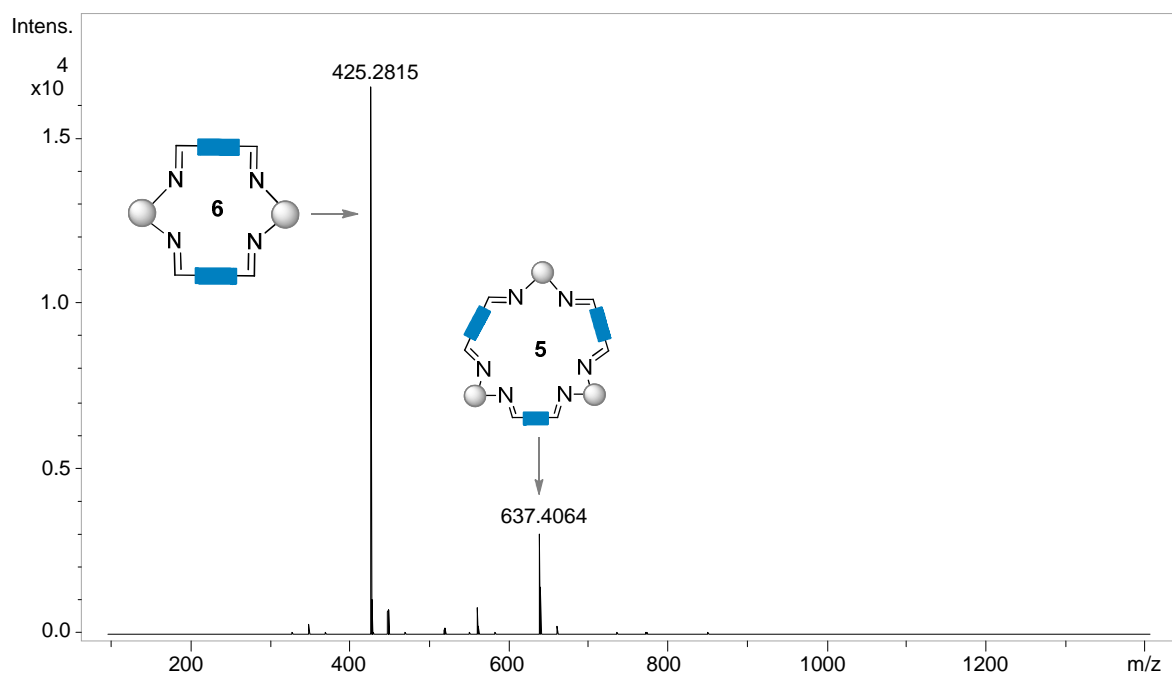


Figure 10. Mass spectrum recorded in the positive ion mode after 9 h.

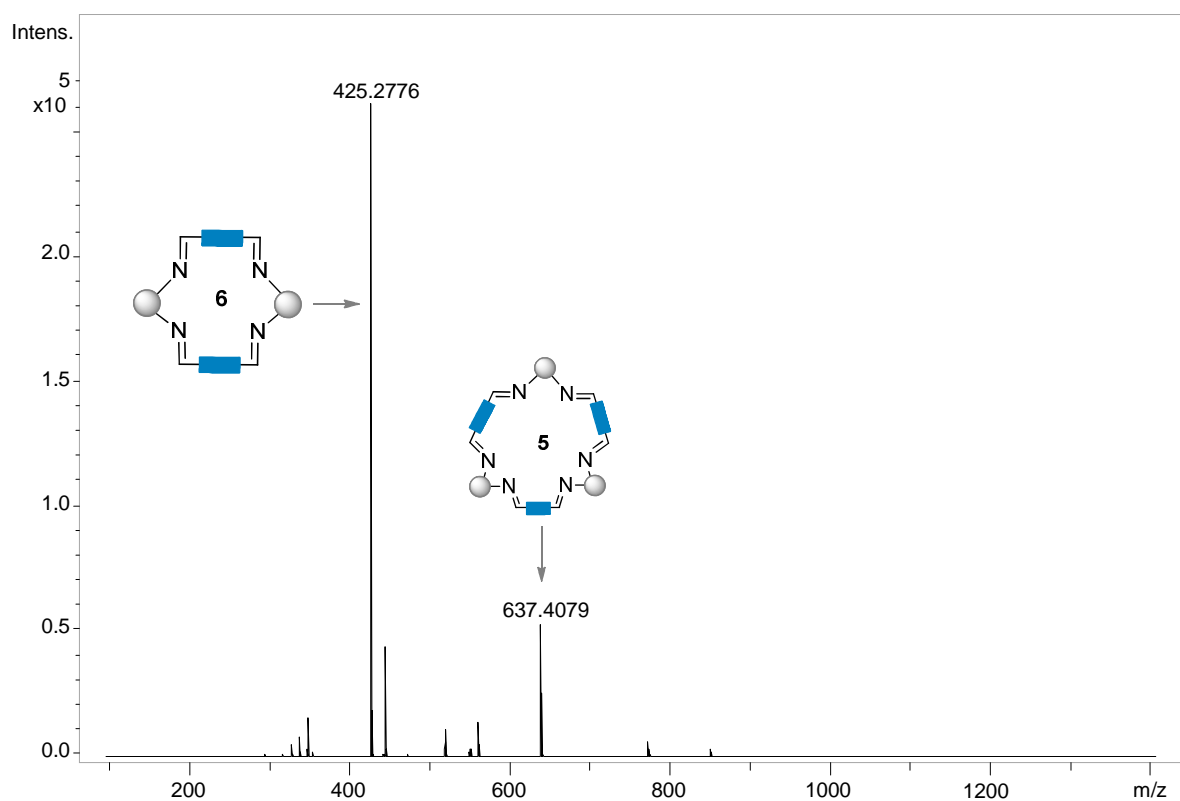


Figure 11. Mass spectrum recorded in the positive ion mode after 12 h.

Product ions appeared as $[M+H]^+$

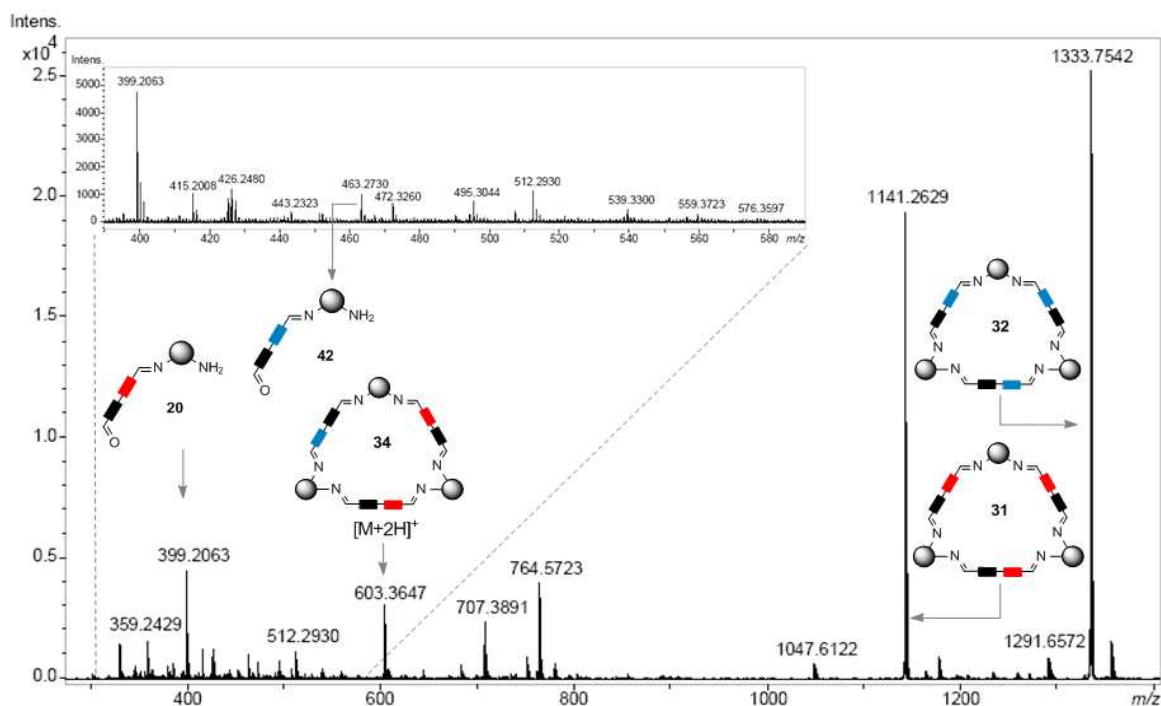


Figure 12. ESI-TOF mass spectrum showing the products resulting from mixing triaglimine **31** and **32** in DCM, mass spectrum recorded after 3 hours from the start of the reaction.

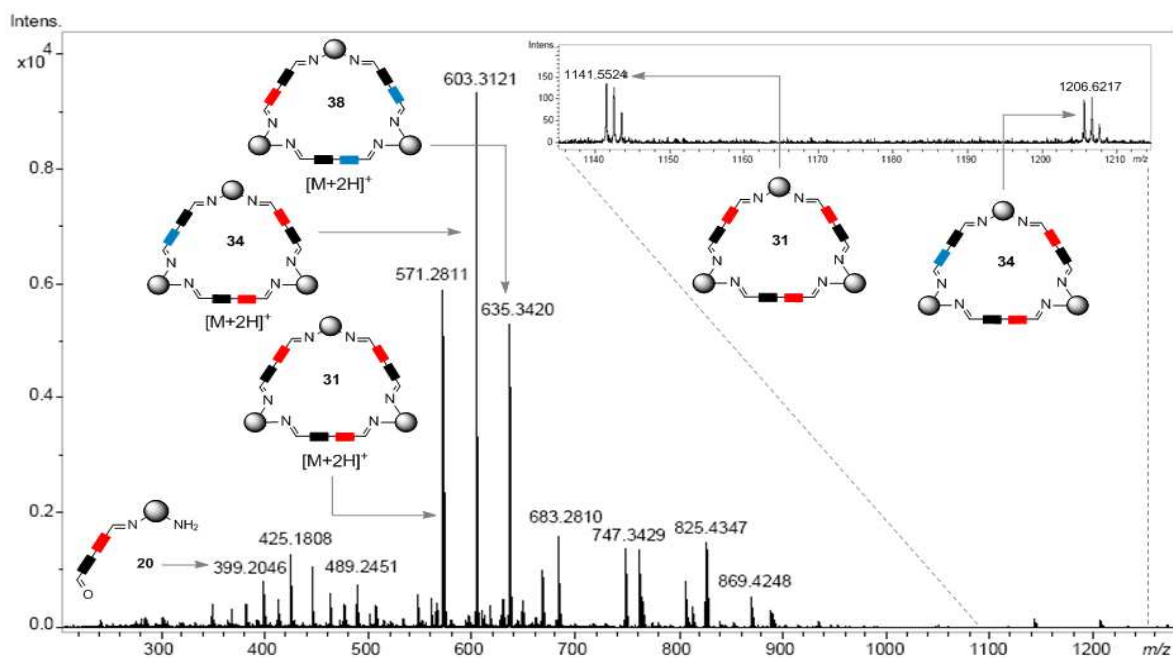


Figure 13. ESI-TOF mass spectrum showing the products resulting from mixing compounds **1**, **19** and **33** in DCM, mass spectrum recorded after 3 hours from the start of the reaction.

Product ions appeared as $[M+H]^+$

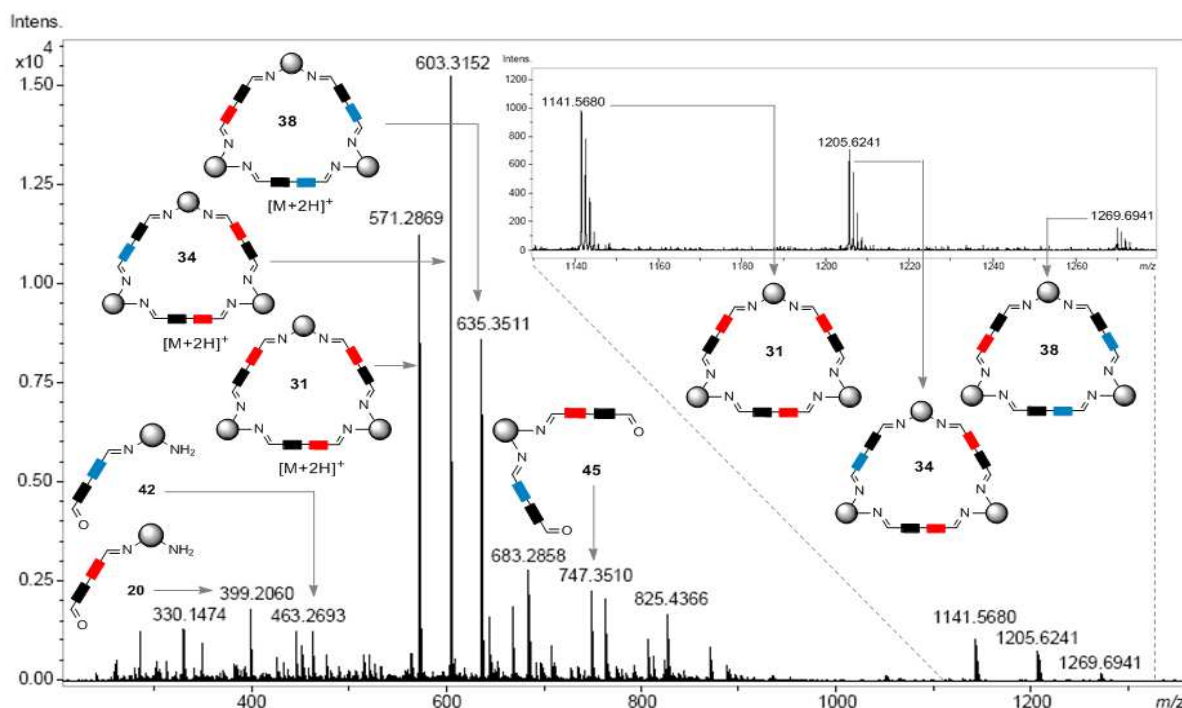


Figure 14. ESI-TOF mass spectrum showing the products resulting from mixing trianglimine **31** and **32** in DCM, mass spectrum recorded after 46 hours from the start of the reaction.

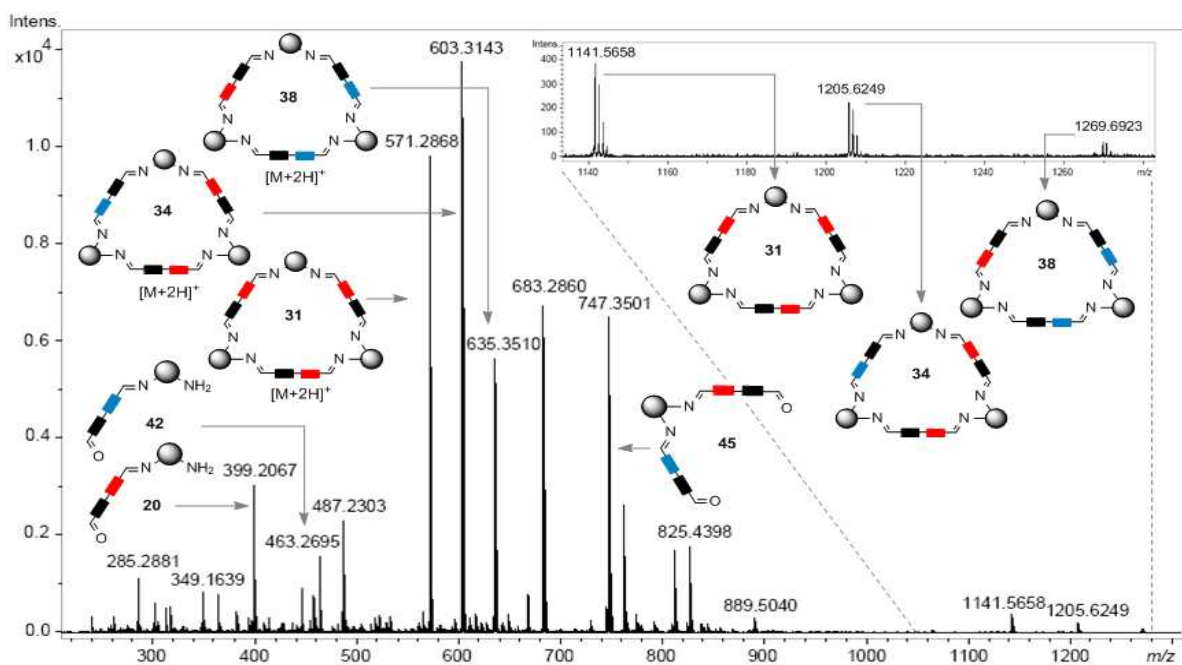
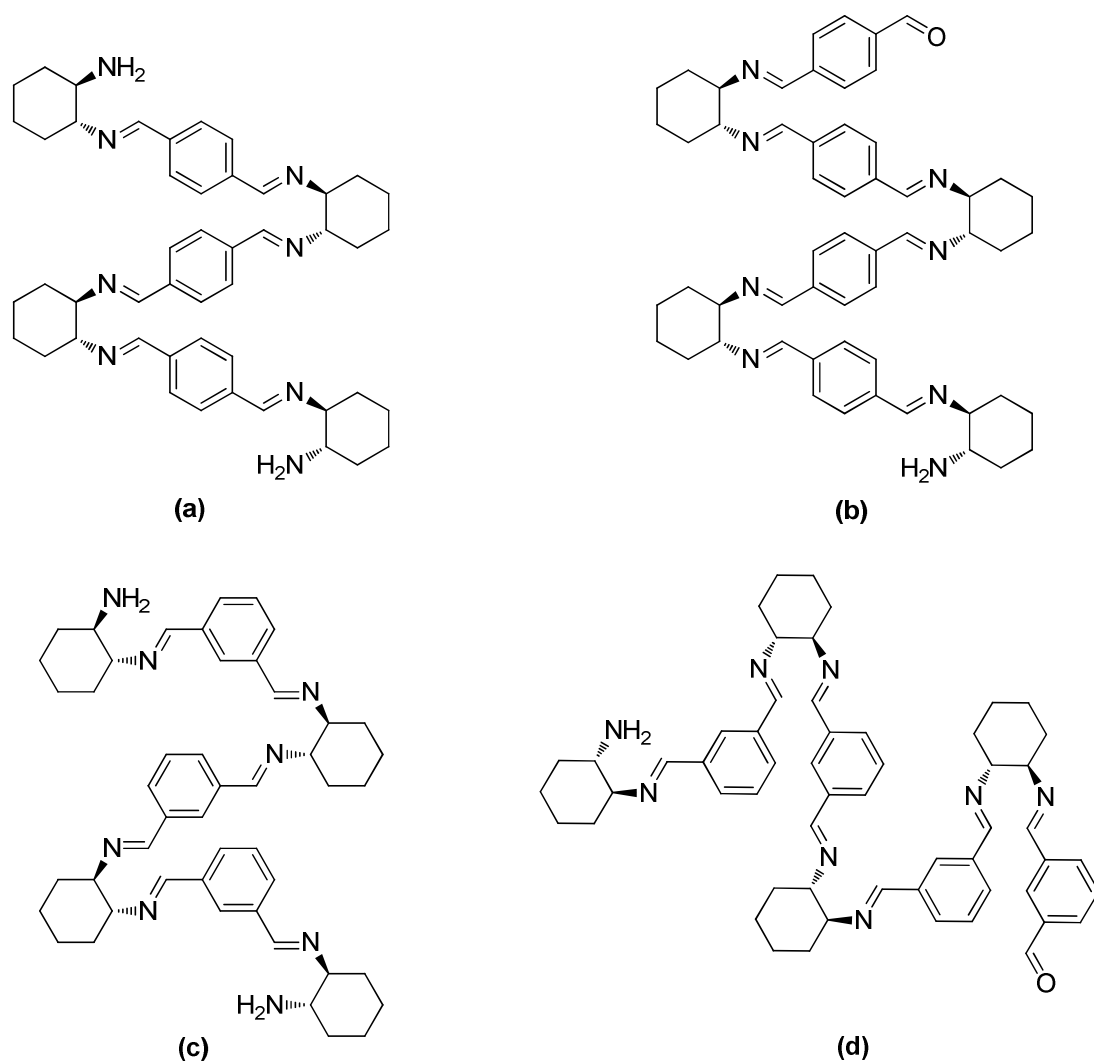


Figure 15. ESI-TOF mass spectrum showing the products resulting from mixing compounds **1**, **19** and **33** in DCM, mass spectrum recorded after 46 hours from the start of the reaction.



Scheme 1. Assigned higher oligomers which were detected by ESI-TOF mass spectrometry after 10 minutes from the start of the cyclocondensation reaction.

Table 1. ESI-TOF mass spectrometry data for the open chain oligomers (a-d)

Entry	Calcd. m/z	Measured m/z	Molecular formula		Error [ppm]
a	751.5135	751.5170	$C_{48}H_{63}N_8$	$M+H^+$	4.7
b	867.5390	867.5432	$C_{56}H_{67}N_8O$	$M+H^+$	4.8
c	751.5143	751.5170	$C_{48}H_{63}N_8$	$M+H^+$	3.6
d	867.5469	867.5432	$C_{56}H_{67}N_8O$	$M+H^+$	- 4.2

Product ions appeared as $[M+H]^+$

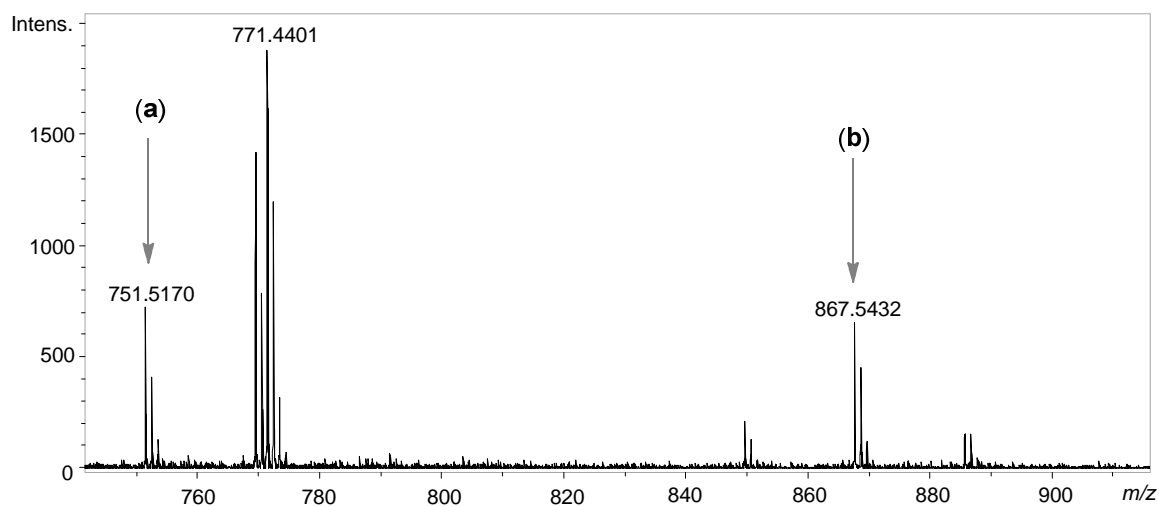


Figure 16. ESI-TOF mass spectrum showing higher oligomers formed in the [3+3]-cyclocondensation reaction of (1*R*,2*R*)-1,2-diaminocyclohexane **1** and terephthalaldehyde **2**, mass spectrum recorded after 10 minutes from the start of the reaction from DCM and MeOH.

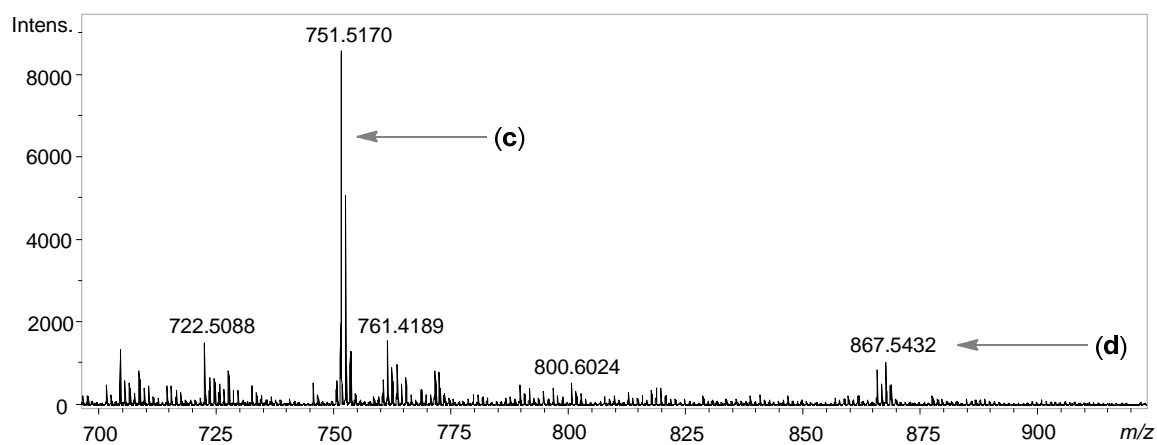


Figure 17. ESI-TOF mass spectrum showing higher oligomers formed in the [3+3]-cyclocondensation reaction of (1*R*,2*R*)-1,2-diaminocyclohexane **1** and isophthalaldehyde **3**, mass spectrum recorded after 10 minutes from the start of the reaction from DCM and MeOH.

Supplementary Information:

Synthesis of novel enantiomerically pure tetra-carbohydrazide cyclophane macrocycles

Hany F. Nour, Nadim Hourani and Nikolai Kuhnert*

School of Engineering and Science, Jacobs University Bremen, P.O. Box 750 561, 28725 Bremen, Germany.

****Corresponding Author:***

1. Prof. Dr Nikolai Kuhnert, Organic and Analytical Chemistry Laboratory, School of Engineering and Science, Jacobs University, P. O. Box. 750 561, 28725 Bremen, Germany, Fax: +49 421 200 3229, Tel: +49 421 200 3120, *E-mail:* n.kuhnert@jacobs-university.de
2. Hany F. Nour, Jacobs University Bremen, Germany, *E-mail:* h.nour@jacobs-university.de

List of figures and schemes:

	Page
Figure 1. ¹ H-NMR spectrum for (4 <i>R</i> ,5 <i>R</i>)-1,3-dioxolane-4,5-dicarbohydrazide (2).....	5
Figure 2. ¹³ C-NMR spectrum for (4 <i>R</i> ,5 <i>R</i>)-1,3-dioxolane-4,5-dicarbohydrazide (2).....	5
Figure 3. ESI-MS spectrum for (4 <i>R</i> ,5 <i>R</i>)-1,3-dioxolane-4,5-dicarbohydrazide (2).....	6
Figure 4. Tandem ESI-MS ² spectrum for (4 <i>R</i> ,5 <i>R</i>)-1,3-dioxolane-4,5-dicarbohydrazide (2).....	6
Figure 5. ¹ H-NMR spectrum for (4 <i>S</i> ,5 <i>S</i>)-1,3-dioxolane-4,5-dicarbohydrazide (4).....	6
Figure 6. ¹³ C-NMR spectrum for (4 <i>S</i> ,5 <i>S</i>)-1,3-dioxolane-4,5-dicarbohydrazide (4).....	7
Figure 7. ESI-MS spectrum for (4 <i>S</i> ,5 <i>S</i>)-1,3-dioxolane-4,5-dicarbohydrazide (4).....	7
Figure 8. Tandem ESI-MS ² spectrum for (4 <i>S</i> ,5 <i>S</i>)-1,3-dioxolane-4,5-dicarbohydrazide (4).....	7
Figure 9. ¹ H-NMR spectrum for (2 <i>R</i> ,3 <i>R</i>)-2,3-dihydroxy dicarbohydrazide (5).....	8
Figure 10. ¹³ C-NMR spectrum for (2 <i>R</i> ,3 <i>R</i>)-2,3-dihydroxy dicarbohydrazide (5).....	8
Figure 11. ESI-MS spectrum for (2 <i>R</i> ,3 <i>R</i>)- 2,3-dihydroxy dicarbohydrazide (5).....	9
Figure 12. Tandem ESI-MS ² spectrum for (2 <i>R</i> ,3 <i>R</i>)-2,3-dihydroxy dicarbohydrazide (5).....	9
Scheme 1. Proposed fragmentation mechanism for (2 <i>R</i> ,3 <i>R</i>)-2,3-dihydroxy dicarbohydrazide (5).....	9
Figure 13. ¹ H-NMR spectrum for (2 <i>S</i> ,3 <i>S</i>)- 2,3-dihydroxy dicarbohydrazide (6).....	10
Figure 14. ¹³ C-NMR spectrum for (2 <i>S</i> ,3 <i>S</i>)- 2,3-dihydroxy dicarbohydrazide (6).....	10
Figure 15. ESI-MS spectrum for (2 <i>S</i> ,3 <i>S</i>)-2,3-dihydroxy dicarbohydrazide (6).....	11
Figure 16. Tandem ESI-MS ² spectrum for (2 <i>S</i> ,3 <i>S</i>)- 2,3-dihydroxy dicarbohydrazide (6).....	11
Scheme 2. Proposed fragmentation mechanism for (2 <i>S</i> ,3 <i>S</i>)- 2,3-dihydroxy dicarbohydrazide (6).....	11
Optimisation of the [2+2]-cyclocondensation reaction	
• Figure 17. APCI-TOF MS for macrocycle 7 (ratio of hydrazide to dialdehyde is 2:1).....	12
• Figure 18. APCI-TOF MS for macrocycle 7 (ratio of hydrazide to dialdehyde is 1:2).....	12
• Figure 19. APCI-TOF MS for macrocycle 7 (ratio of hydrazide to dialdehyde is 1:1).....	13
• Figure 20. APCI-TOF MS for macrocycle 7 (ratio of hydrazide to dialdehyde is 1.2:1).....	13
Figure 21. ¹ H-NMR spectrum for macrocycle (7).....	14
Figure 22. ESI-MS spectrum for macrocycle (7).....	14
Figure 23. Tandem ESI-MS ² spectrum for macrocycle (7).....	14
Figure 24. ¹ H-NMR spectrum for macrocycle (8).....	15
Figure 25. ESI-MS spectrum for macrocycle (8).....	15
Figure 26. Tandem ESI-MS ² spectrum for macrocycle (8).....	15
Scheme 3. Proposed fragmentation mechanism for macrocycle (8).....	16
Figure 27. APCI-MS ² spectrum for macrocycle (9).....	16
Figure 28. APCI-MS ² spectrum for macrocycle (9).....	17
Figure 29. ¹ H-NMR spectrum for macrocycle (9).....	17
Figure 30. Tandem APCI-MS ² spectrum for macrocycle (9).....	17

Scheme 4. Proposed fragmentation mechanism for macrocycle (9).....	18
Figure 31. Tandem ESI-MS ² spectrum for macrocycle (9).....	19
Scheme 5. Proposed fragmentation mechanism for macrocycle (9).....	19
Figure 32. ¹ H-NMR spectrum for macrocycle (13).....	20
Figure 33. ESI-MS spectrum for macrocycle (13).....	20
Figure 34. Tandem ESI-MS ² spectrum for macrocycle (13).....	20
Scheme 6. Proposed fragmentation mechanism macrocycle (13).....	21
Figure 35. ¹ H-NMR spectrum for macrocycle (14).....	21
Figure 36. ESI-MS spectrum for macrocycle (14).....	22
Figure 37. Tandem ESI-MS ² spectrum for macrocycle (14).....	22
Scheme 7. Proposed fragmentation mechanism for macrocycle (14).....	22
Figure 38. ¹ H-NMR spectrum for macrocycle (17).....	23
Figure 39. ¹ H-NMR spectrum for macrocycle (17).....	23
Figure 40. ¹ H-NMR spectrum for macrocycle (17).....	24
Figure 41. APCI-MS ² spectrum for macrocycle (17).....	24
Figure 42. APCI-MS ² spectrum for macrocycle (17).....	24
Figure 43. Tandem APCI-MS ² spectrum for macrocycle (17).....	25
Scheme 8. Proposed fragmentation mechanism for macrocycle (17).....	25
Figure 44. Tandem APCI-MS ² spectrum for macrocycle (17).....	25
Scheme 9. Proposed fragmentation mechanism for macrocycle (17).....	26
Figure 45. ¹ H-NMR spectrum for macrocycle (10).....	26
Figure 46. ESI-MS spectrum for macrocycle (10).....	27
Figure 47. Tandem ESI-MS ² spectrum for macrocycle (10).....	27
Figure 48. ¹ H-NMR spectrum for macrocycle (11).....	27
Figure 49. APCI-MS spectrum for macrocycle (11).....	28
Figure 50. Tandem ESI-MS ² spectrum for macrocycle (11).....	28
Scheme 10. Proposed fragmentation mechanism for macrocycle (11).....	29
Figure 51. APCI-MS ² spectrum for macrocycle (12).....	29
Figure 52. Tandem APCI-MS ² spectrum for macrocycle (12).....	30
Figure 53. ¹ H-NMR spectrum for macrocycle (12).....	30
Figure 54. APCI-MS ² spectrum for macrocycle (12).....	30
Scheme 11. Proposed fragmentation mechanism for macrocycle (12).....	31
Figure 55. Tandem APCI-MS ² spectrum for macrocycle (12).....	32
Scheme 12. Proposed fragmentation mechanism for macrocycle (12).....	32
Figure 56. ¹ H-NMR spectrum for macrocycle (15).....	33
Figure 57. ESI-MS spectrum for macrocycle (15).....	33
Figure 58. Tandem ESI-MS ² spectrum for macrocycle (15).....	33

Scheme 13. Proposed fragmentation mechanism for macrocycle (15).....	34
Figure 59. APCI-MS spectrum for macrocycle (16).....	34
Figure 60. Tandem APCI-MS ² spectrum for macrocycle (16).....	34
Scheme 14. Proposed fragmentation mechanism for macrocycle (16).....	35
Figure 61. ¹ H-NMR spectrum for macrocycle (16).....	35
Figure 62. APCI-MS ² spectrum for macrocycle (18).....	36
Figure 63. Tandem APCI-MS ² spectrum for macrocycle (18).....	36
Scheme 15. Proposed fragmentation mechanism for macrocycle (17).....	36
Figure 64. APCI-MS ² spectrum for macrocycle (18).....	37
Figure 65. Tandem APCI-MS ² spectrum for macrocycle (18).....	37
Scheme 16. Proposed fragmentation mechanism for macrocycle (18).....	37
Figure 66. ¹ H-NMR spectrum for macrocycle (18).....	38
Figure 67. Stacked ¹ H-NMR spectra for macrocycle (14).....	38
Figure 68. 2D-ROESY spectrum for macrocycle (17).....	39
Figure 69. Through space interactions of different protons for macrocycle (17).....	39
Molecular modelling data for the computed structure (14a).....	40
Molecular modelling data for the computed structure (14b).....	42

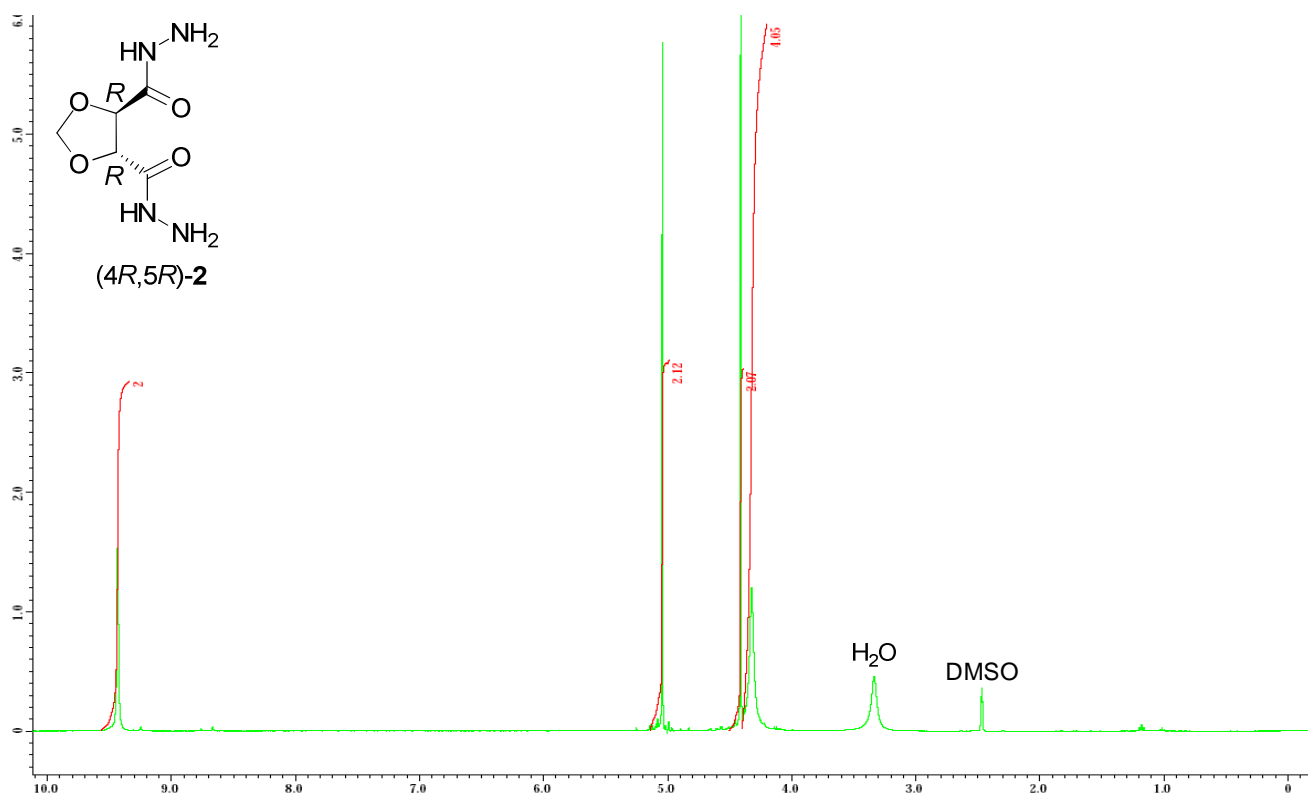


Figure 1. ¹H-NMR spectrum for (4*R*,5*R*)-1,3-dioxolane-4,5-dicarbohydrazide (**2**), DMSO-d₆, 400 MHz.

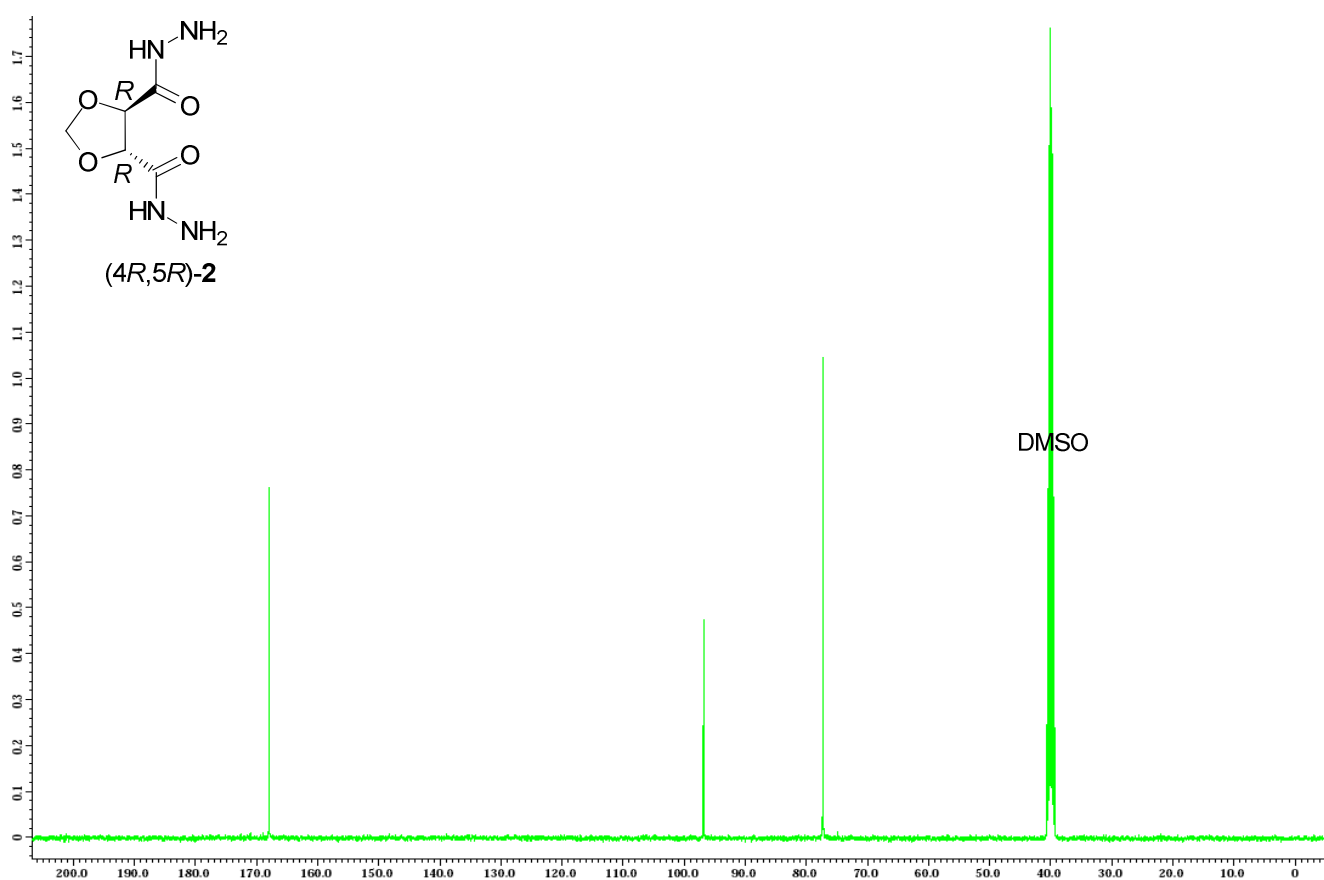


Figure 2. ¹³C-NMR spectrum for (4*R*,5*R*)-1,3-dioxolane-4,5-dicarbohydrazide (**2**), DMSO-d₆, 100 MHz.

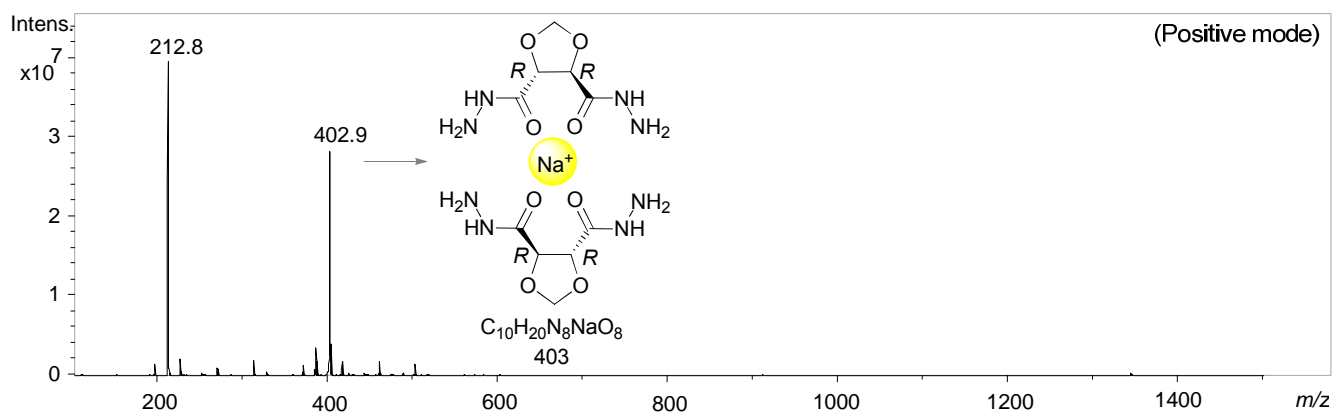


Figure 3. ESI-MS spectrum for (4R,5R)-1,3-dioxolane-4,5-dicarbohydrazide (**2**) from H₂O.

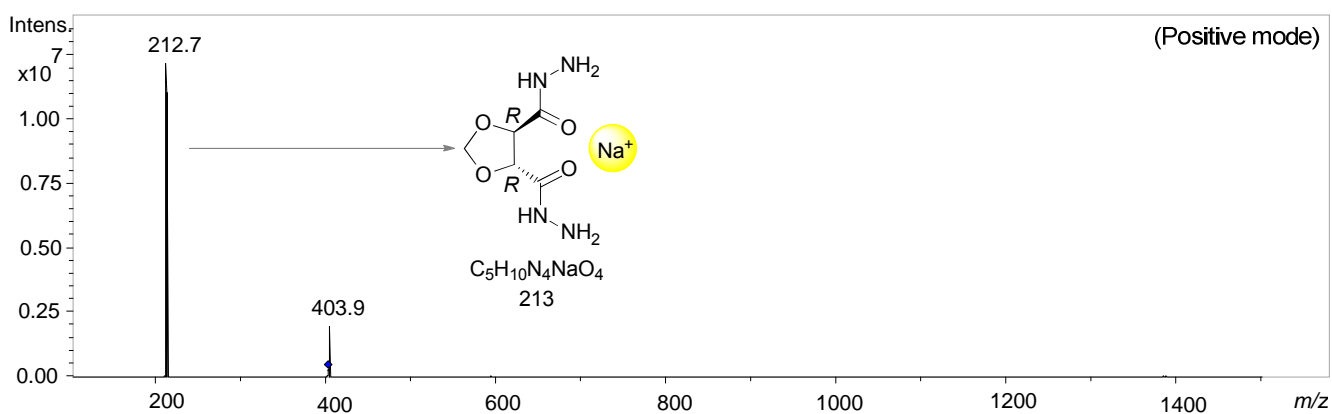


Figure 4. Tandem ESI-MS² spectrum for (4R,5R)-1,3-dioxolane-4,5-dicarbohydrazide (**2**) from H₂O.

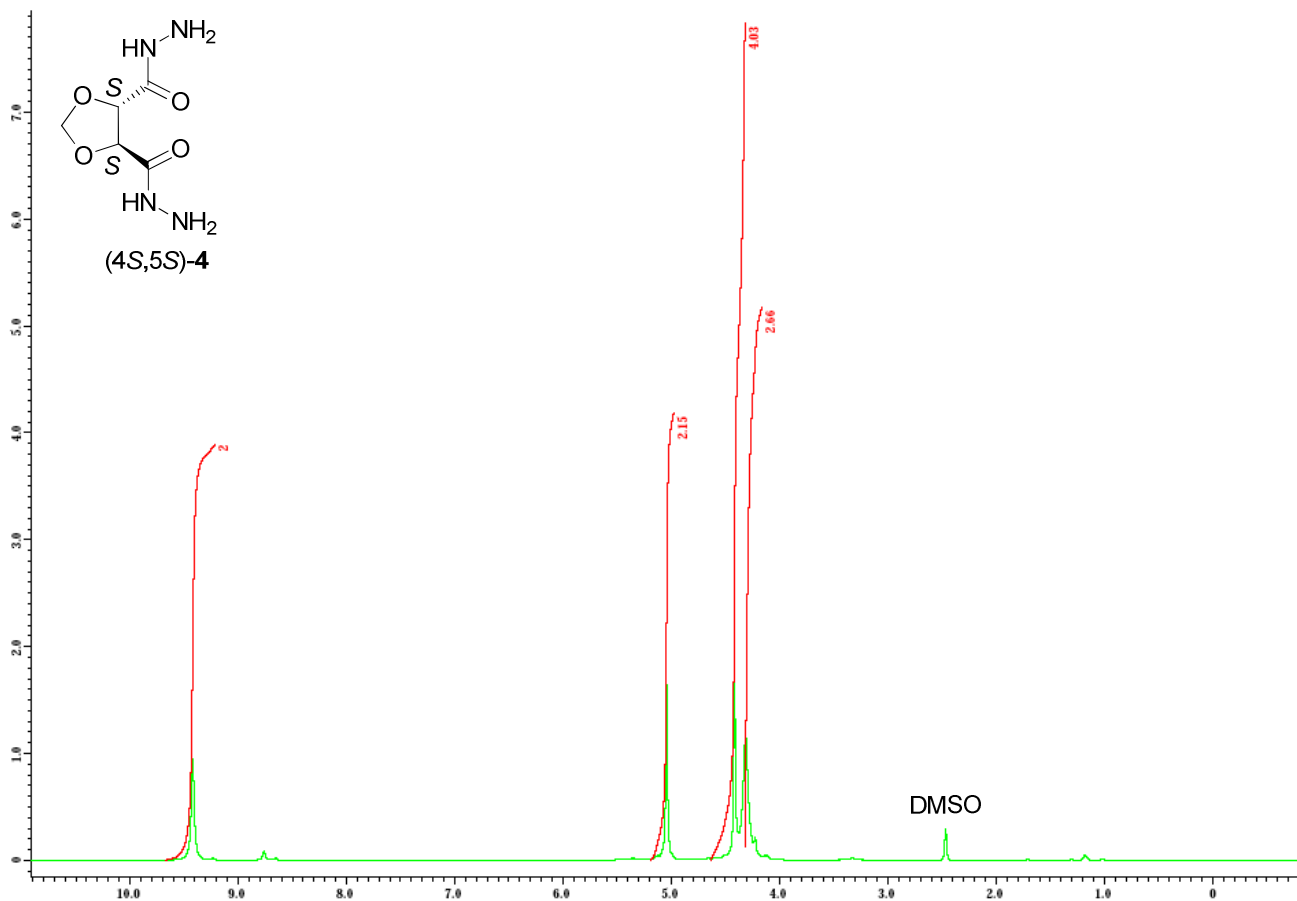


Figure 5. ¹H-NMR spectrum for (4S,5S)-1,3-dioxolane-4,5-dicarbohydrazide (**4**), DMSO-d₆, 400 MHz.

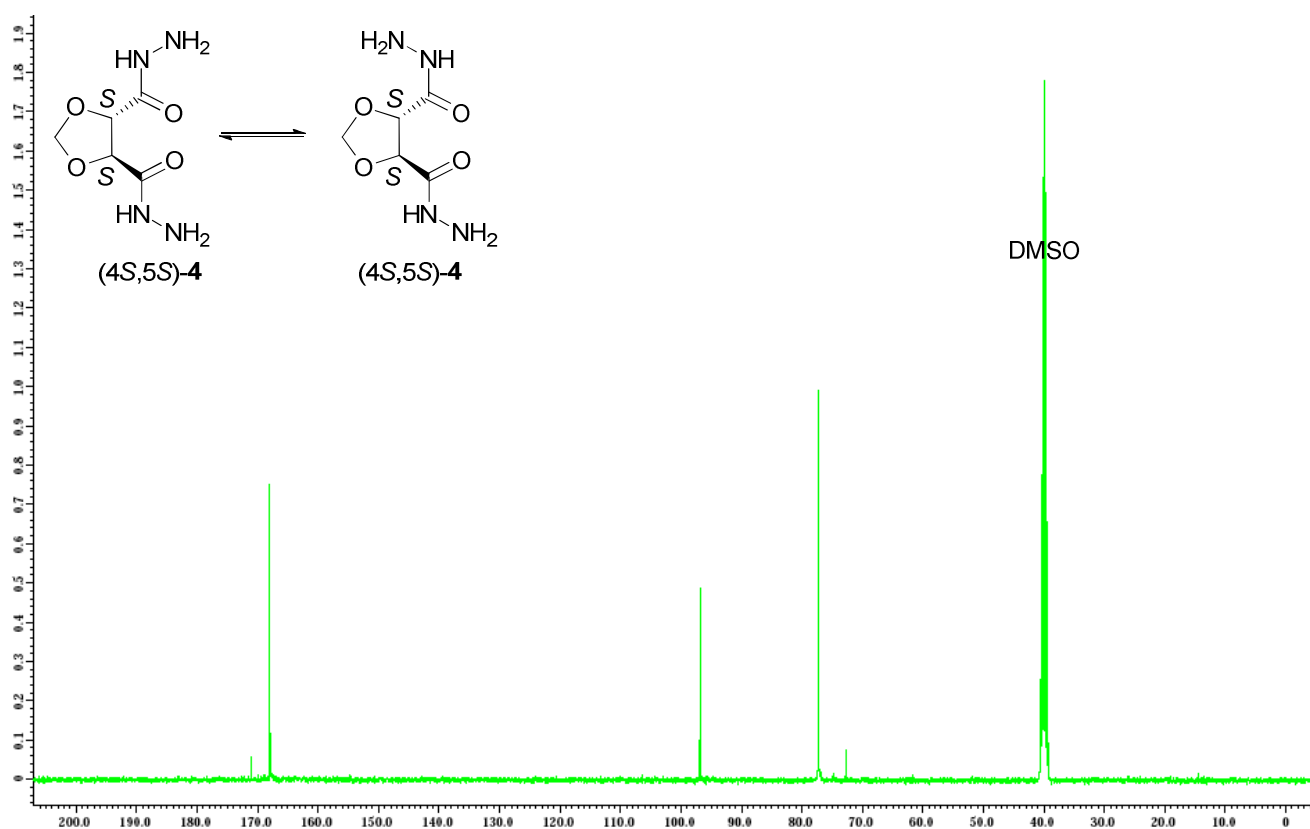


Figure 6. ^{13}C -NMR spectrum for (4*S*,5*S*)-1,3-dioxolane-4,5-dicarbohydrazide (**4**), DMSO-d_6 , 100 MHz.

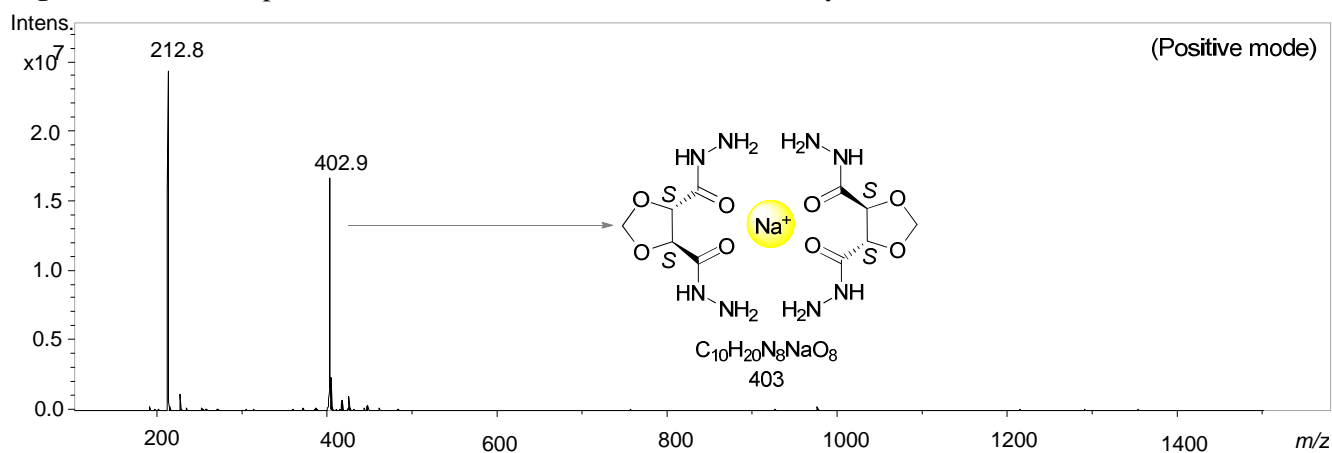


Figure 7. ESI-MS spectrum for (4*S*,5*S*)-1,3-dioxolane-4,5-dicarbohydrazide (**4**) from H_2O .

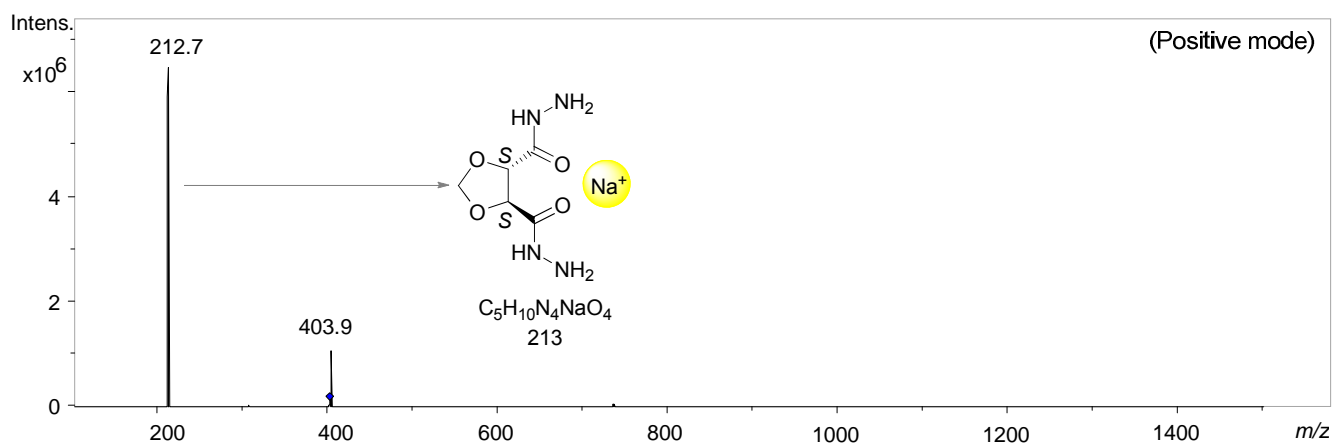


Figure 8. Tandem ESI-MS² spectrum for (4*S*,5*S*)-1,3-dioxolane-4,5-dicarbohydrazide (**4**) from H_2O .

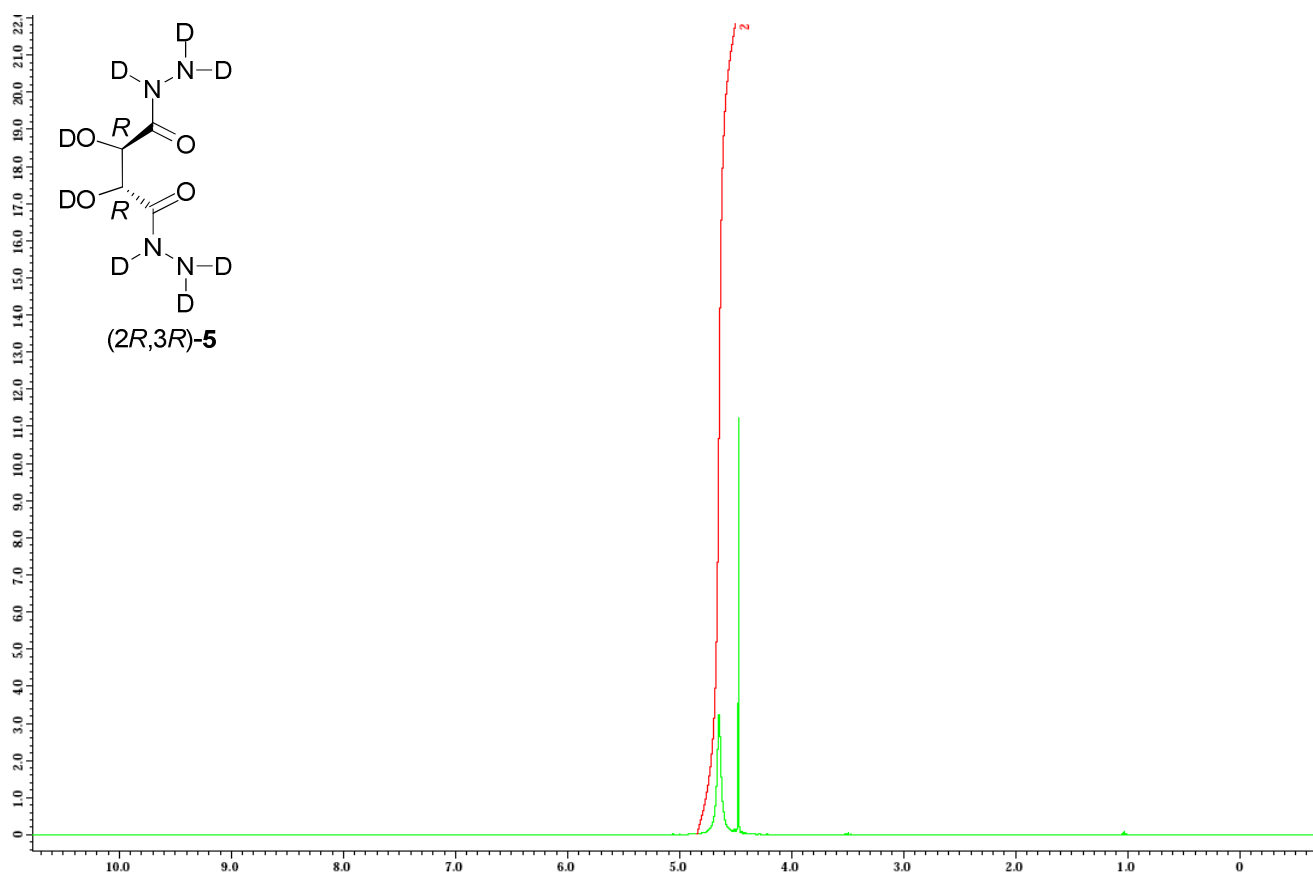


Figure 9. ¹H-NMR spectrum for (2*R*,3*R*)-2,3-dihydroxy dicarbohydrazide (**5**), D₂O, 400 MHz.

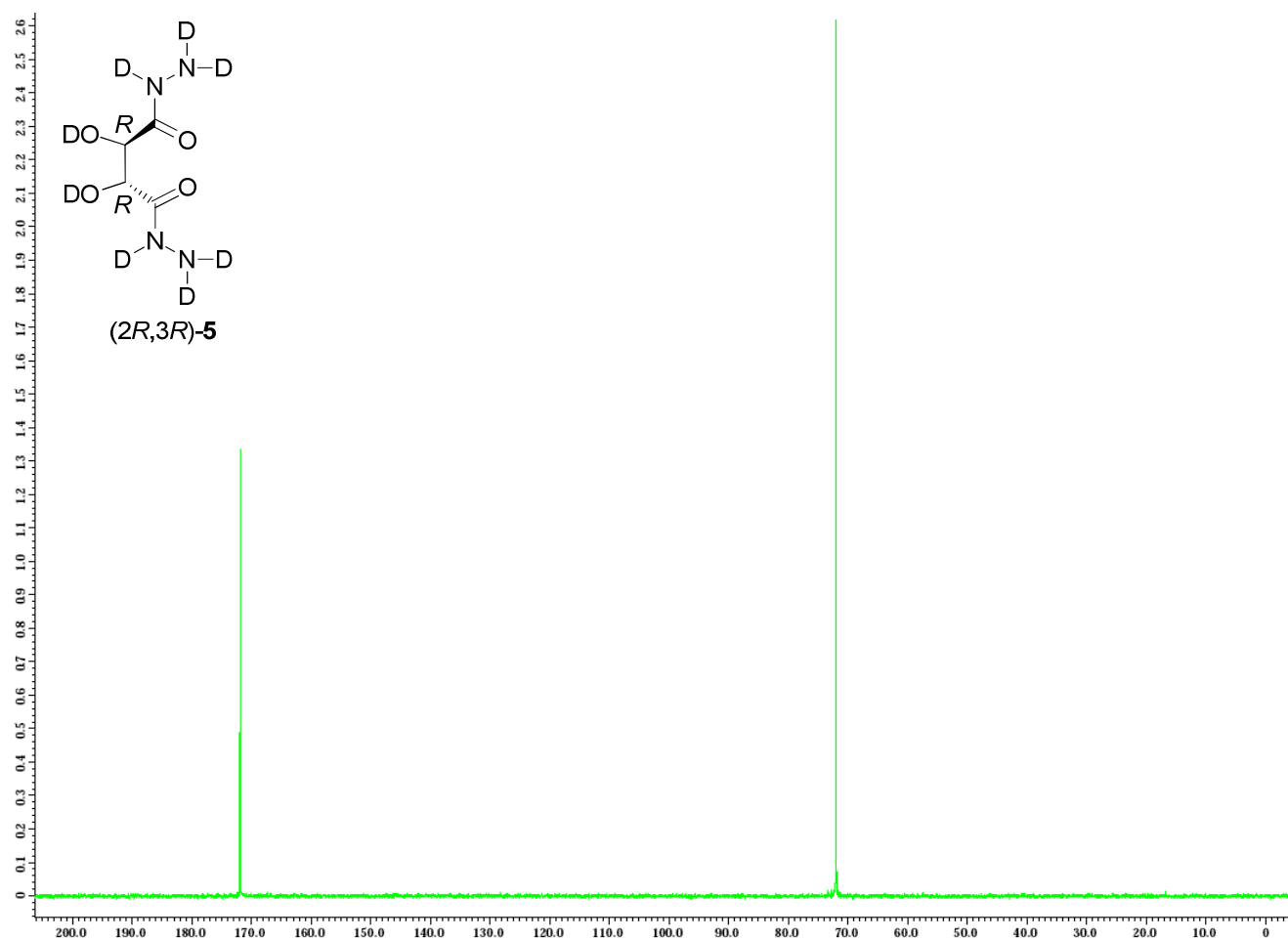


Figure 10. ¹³C-NMR spectrum for (2*R*,3*R*)-2,3-dihydroxy dicarbohydrazide (**5**), D₂O, 100 MHz.

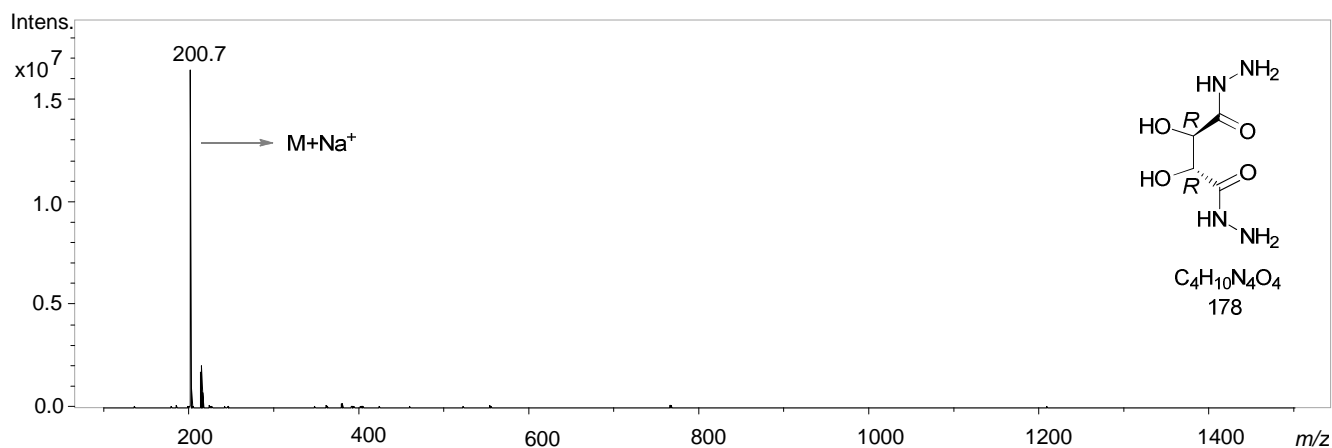


Figure 11. ESI-MS spectrum for (2*R*,3*R*)- 2,3-dihydroxy dicarbohydrazide (**5**) from H₂O (Positive mode).

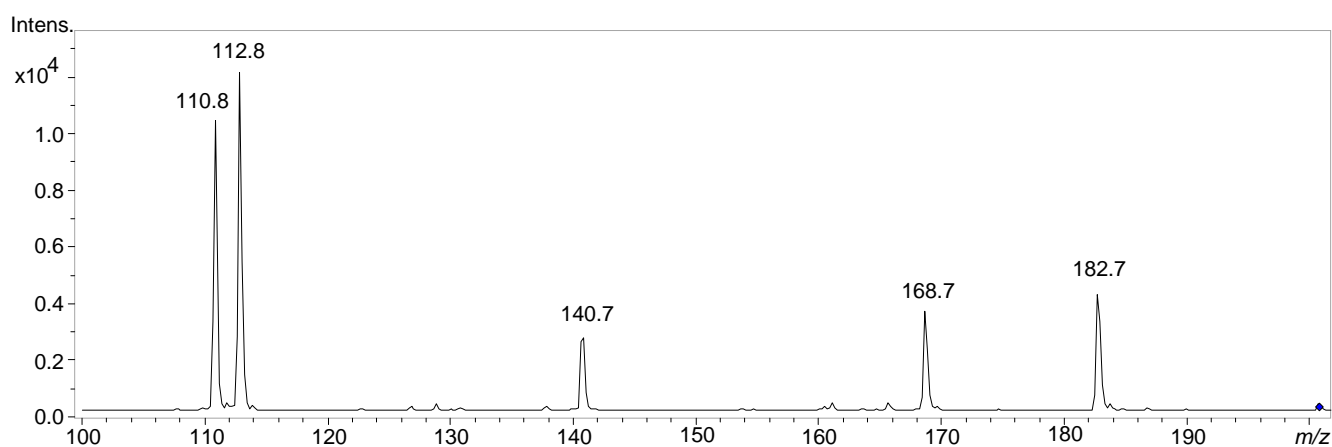
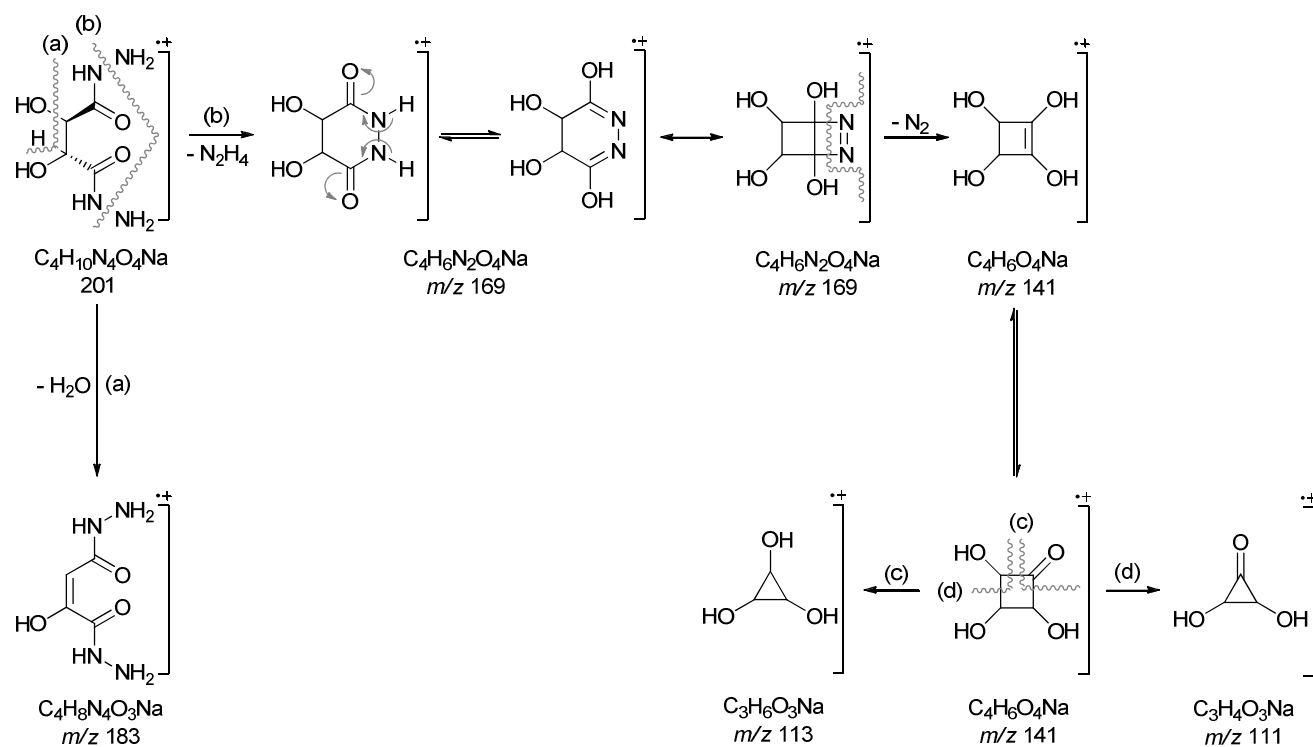


Figure 12. Tandem ESI-MS² spectrum for (2*R*,3*R*)-2,3-dihydroxy dicarbohydrazide (**5**) from H₂O (Positive mode).



Scheme 1. Proposed fragmentation mechanism for (2*R*,3*R*)-2,3-dihydroxy dicarbohydrazide (**5**).

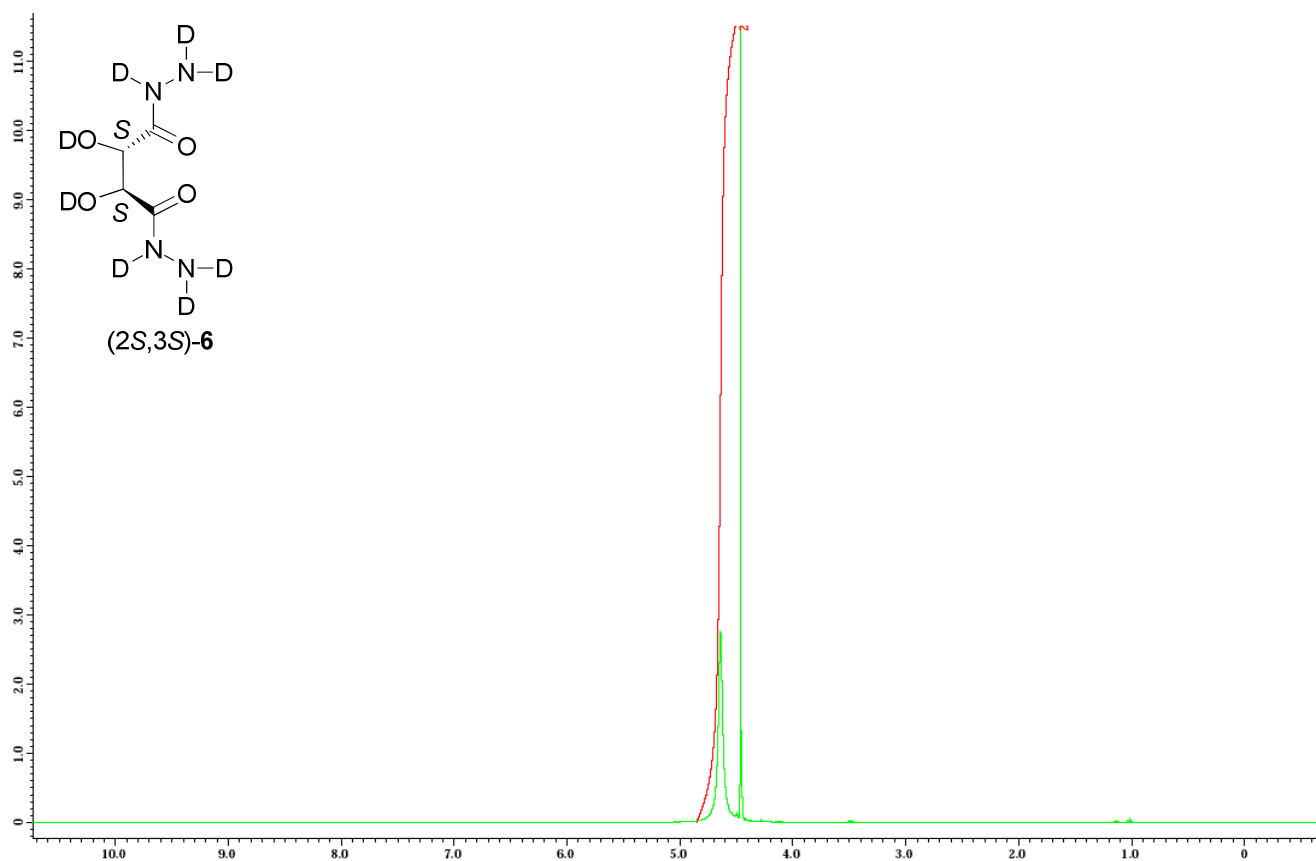


Figure 13. ^1H -NMR spectrum for (2*S*,3*S*)- 2,3-dihydroxy dicarbohydrazide (**6**), D_2O , 400 MHz.

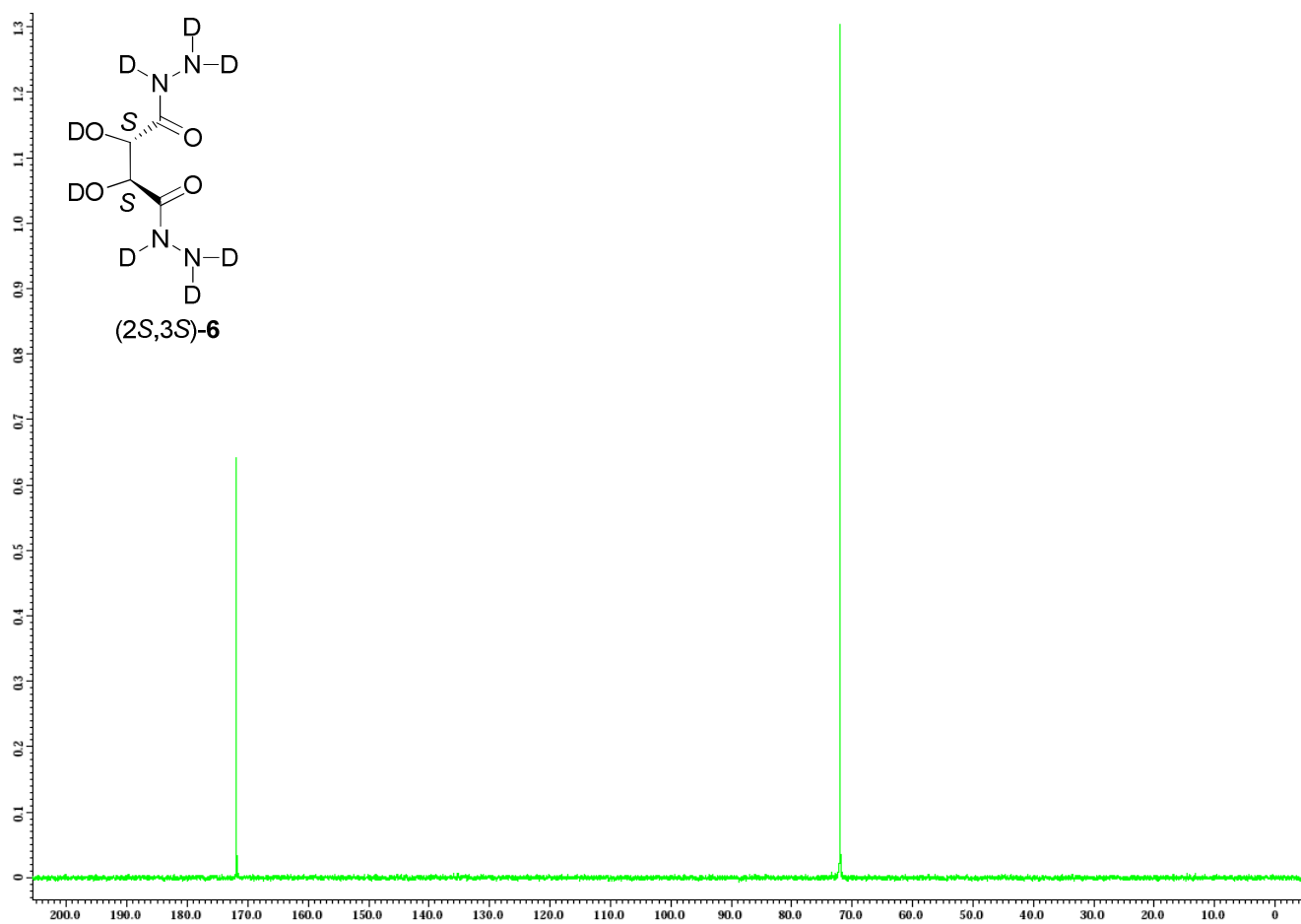


Figure 14. ^{13}C -NMR spectrum for (2*S*,3*S*)- 2,3-dihydroxy dicarbohydrazide (**6**), D_2O , 100 MHz.

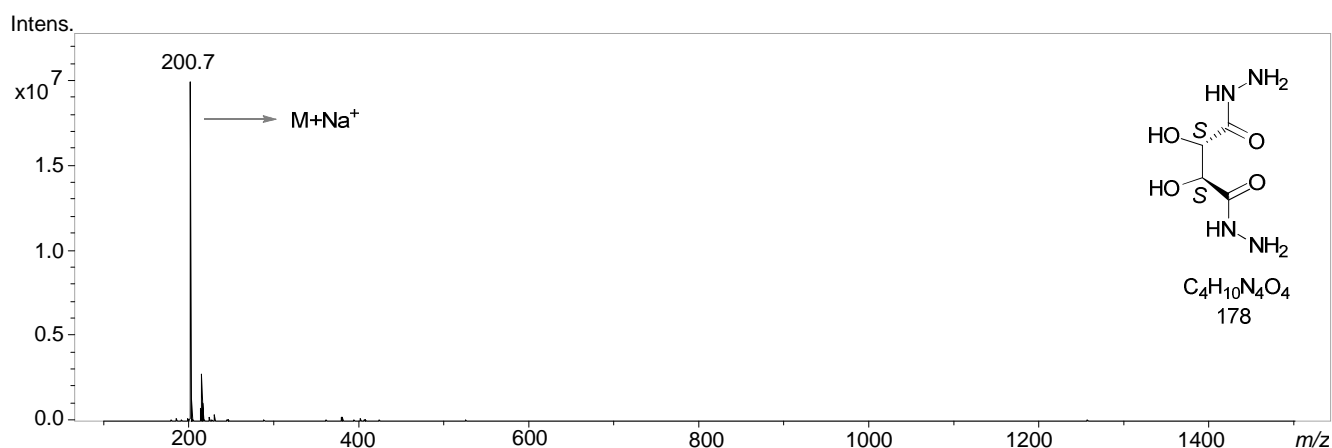


Figure 15. ESI-MS spectrum for (2S,3S)-2,3-dihydroxy dicarbohydrazide (6) from H₂O (Positive mode).

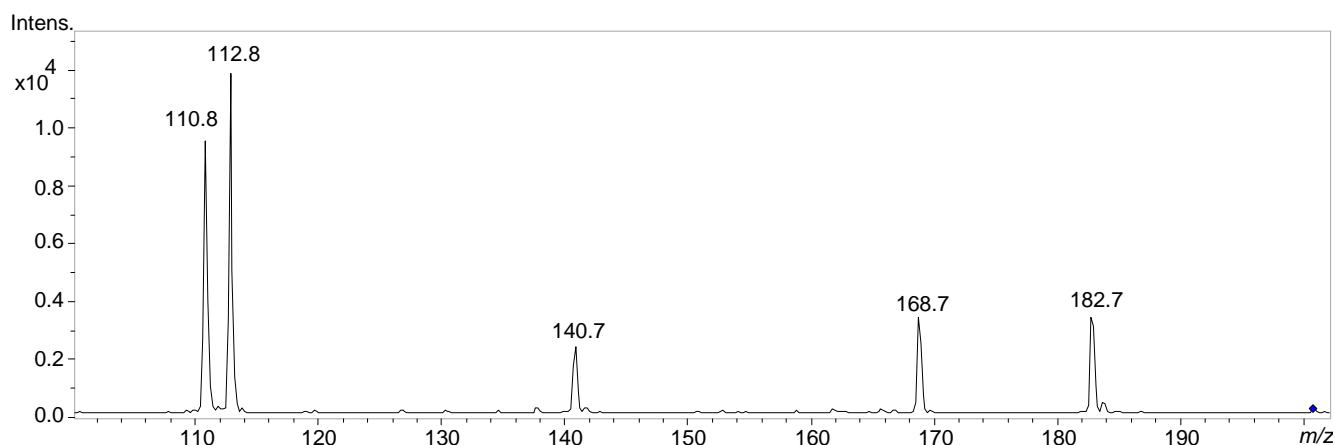
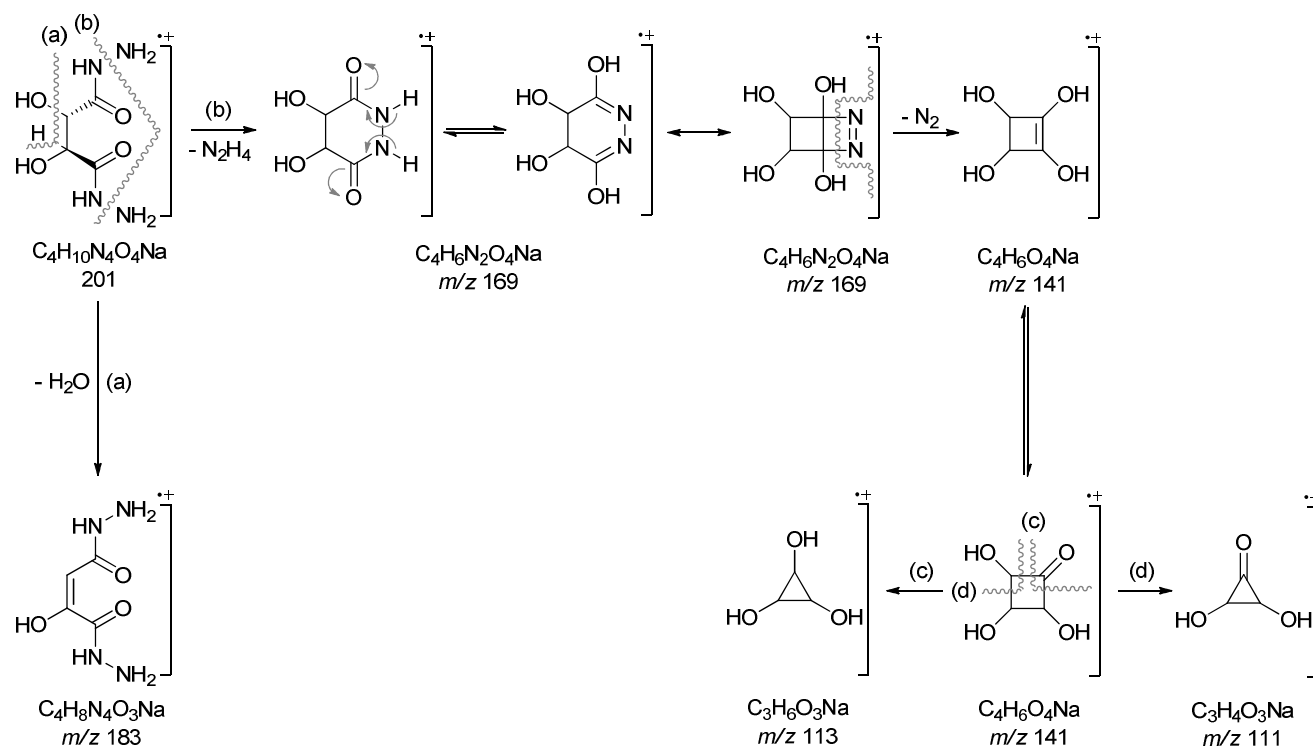


Figure 16. Tandem ESI-MS² spectrum for (2S,3S)-2,3-dihydroxy dicarbohydrazide (6) from H₂O (Positive mode).



Scheme 2. Proposed fragmentation mechanism for (2S,3S)- 2,3-dihydroxy dicarbohydrazide (6).

Optimisation of the [2+2]-cyclocondensation reaction

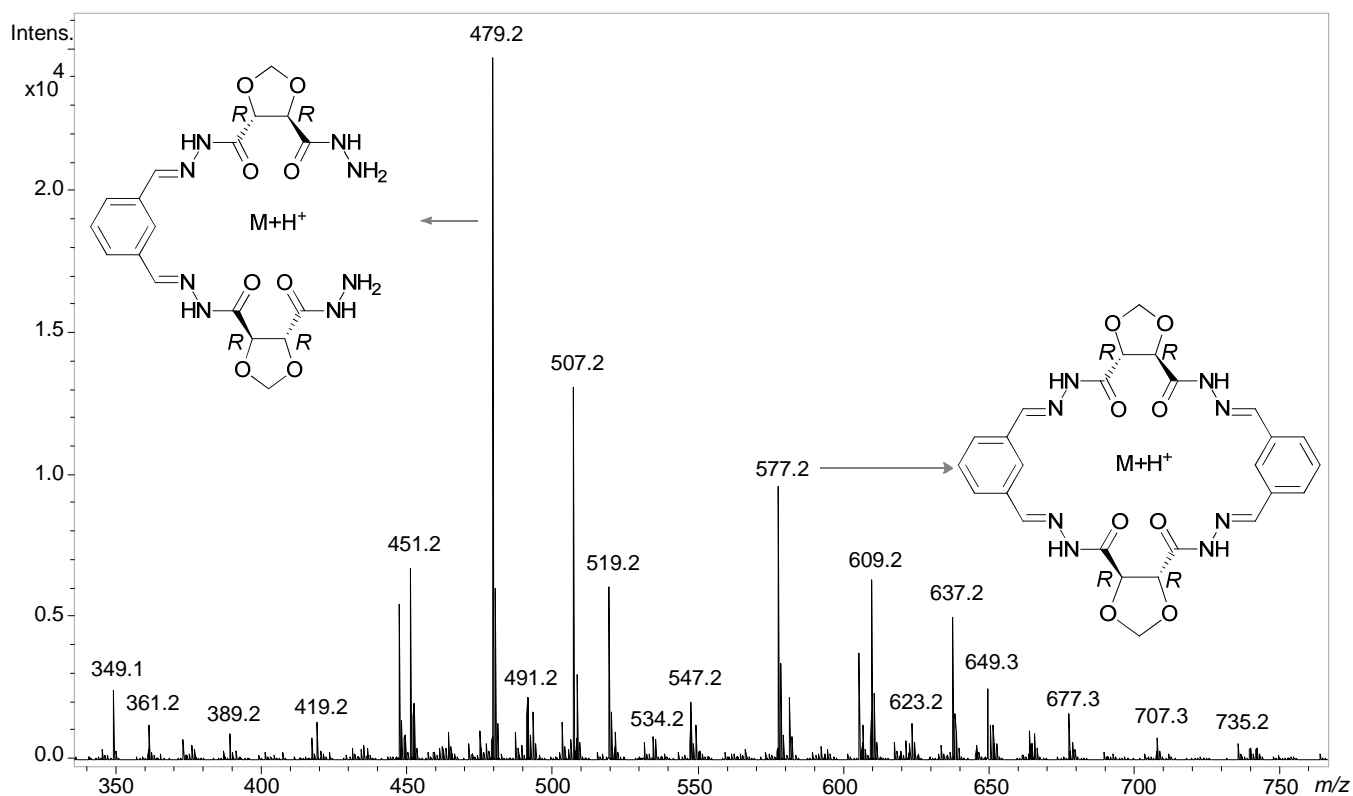


Figure 17. APCI-TOF MS from DMSO (macrocycle **7**, reaction was conducted in DMF in the presence of few drops of AcOH, ratio of hydrazide to dialdehyde is 2:1, positive mode).

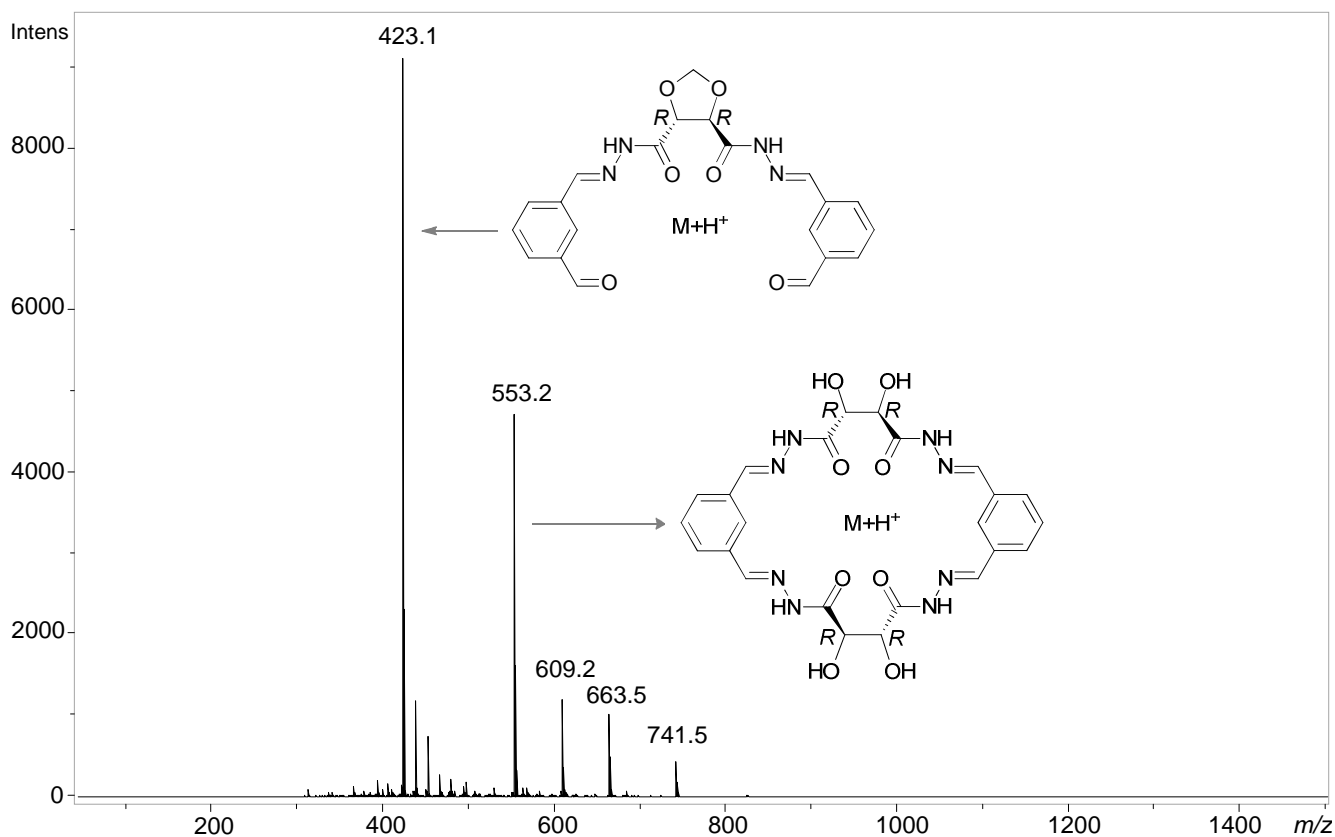


Figure 18. APCI-TOF MS from DMSO (macrocycle **7**, reaction was conducted in DMF in the presence of few drops of AcOH, ratio of hydrazide to dialdehyde is 1:2, positive mode).

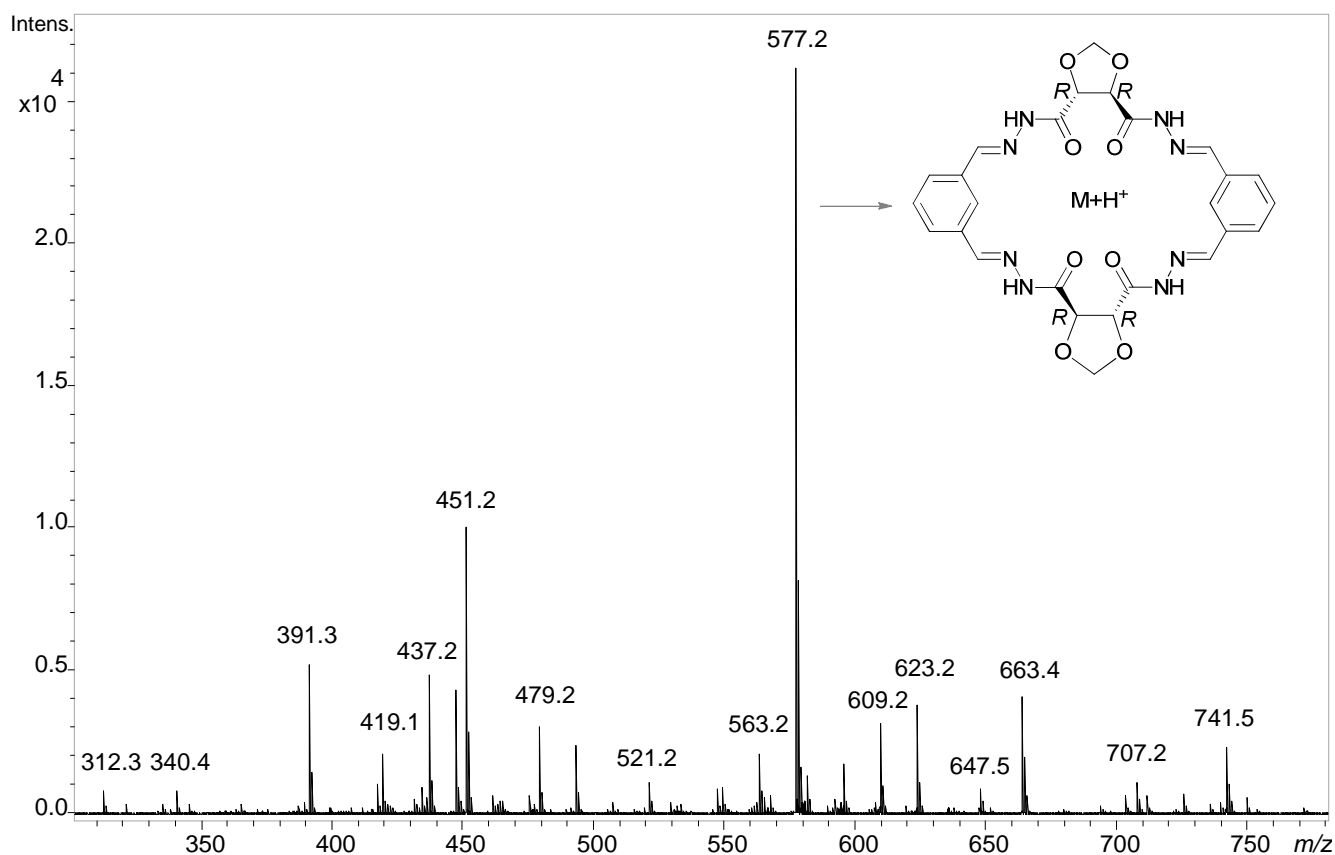


Figure 19. APCI-TOF MS from DMSO (macrocycle **7**, reaction was conducted in MeOH in the presence of few drops of AcOH, ratio of hydrazide to dialdehyde is 1:1, positive mode).

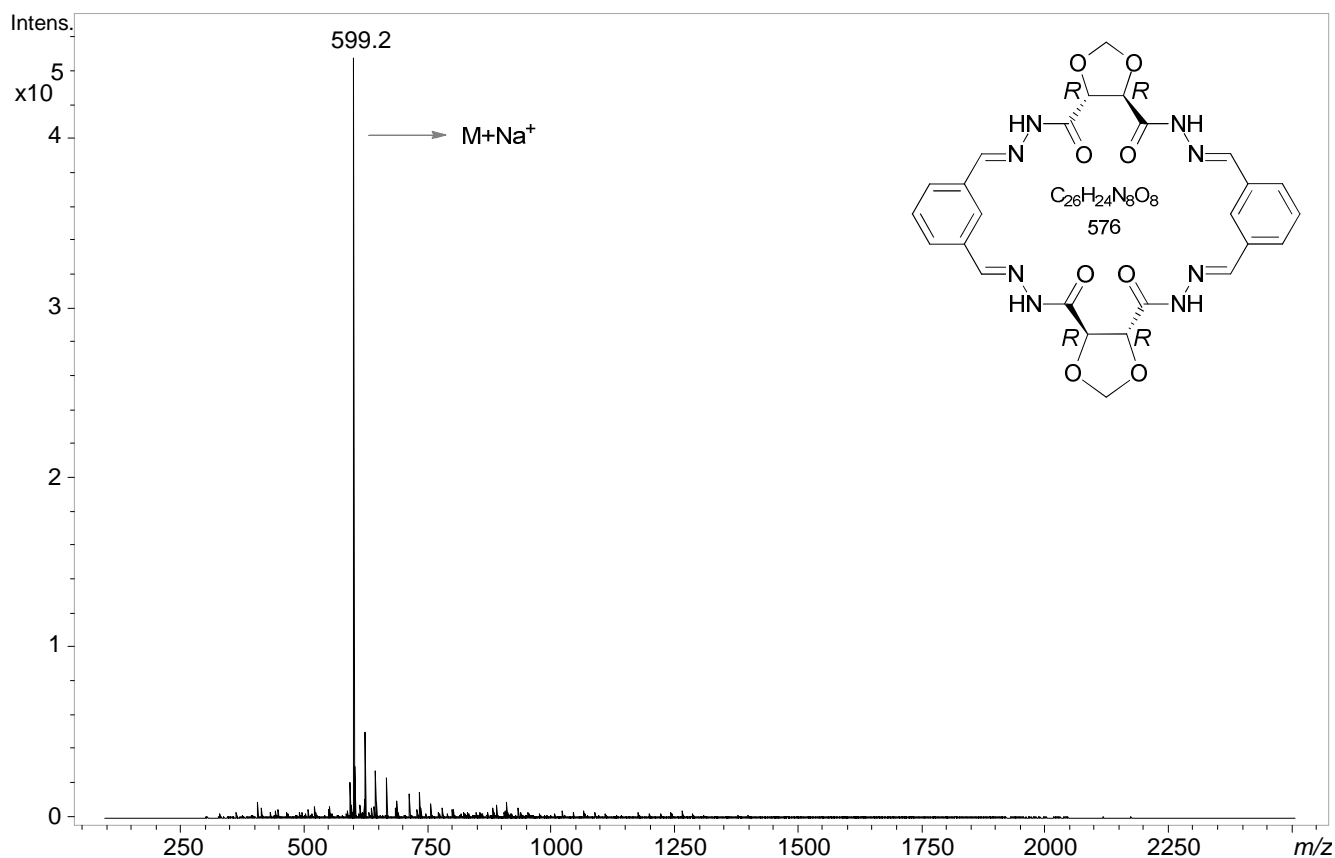


Figure 20. APCI-TOF MS from DMSO (macrocycle **7**, reaction was conducted in MeOH in the presence of few drops of AcOH, ratio of hydrazide to dialdehyde is 1.2:1, positive mode).

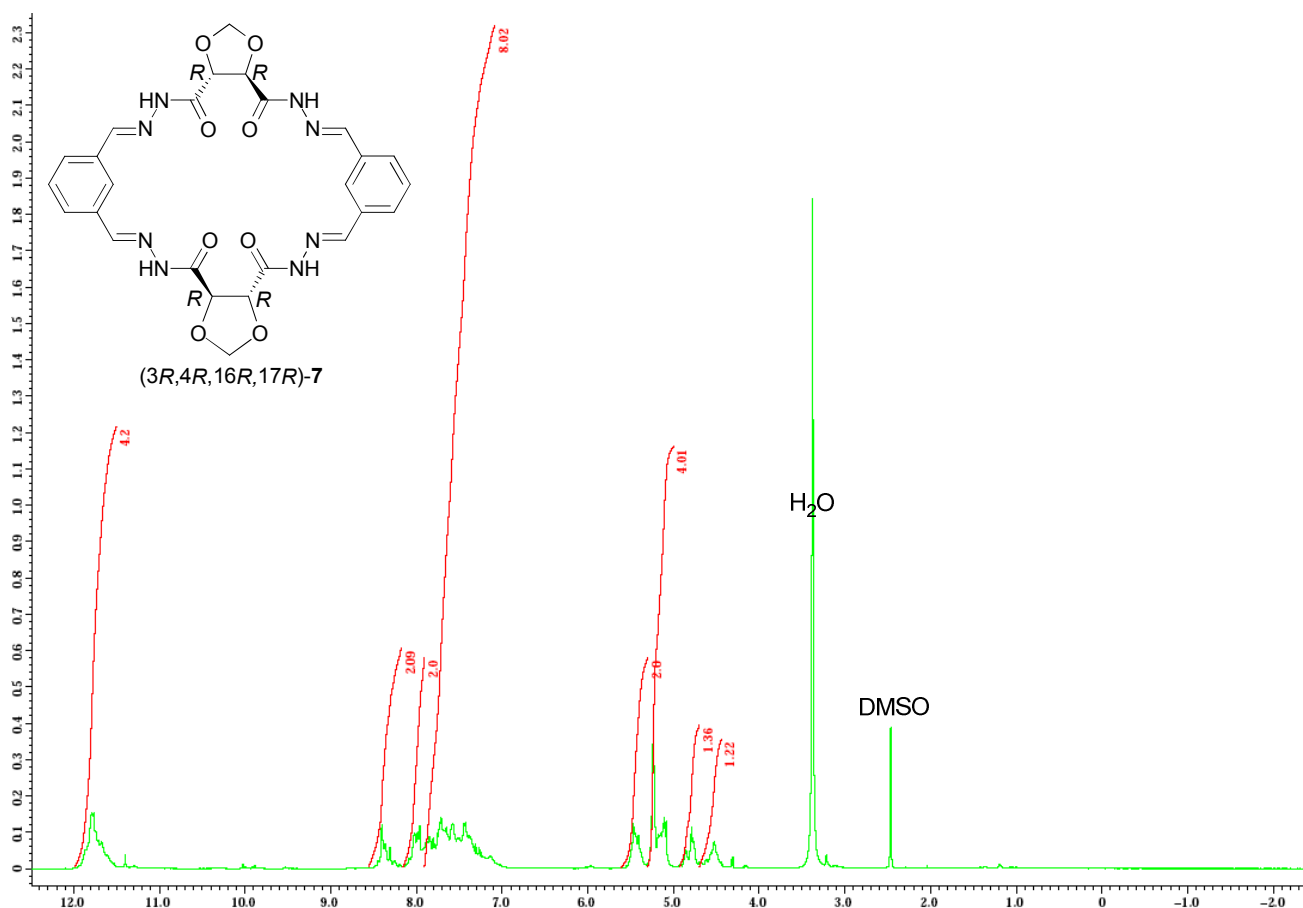


Figure 21. ^1H -NMR spectrum for macrocycle (**7**), DMSO-d_6 , 400 MHz.

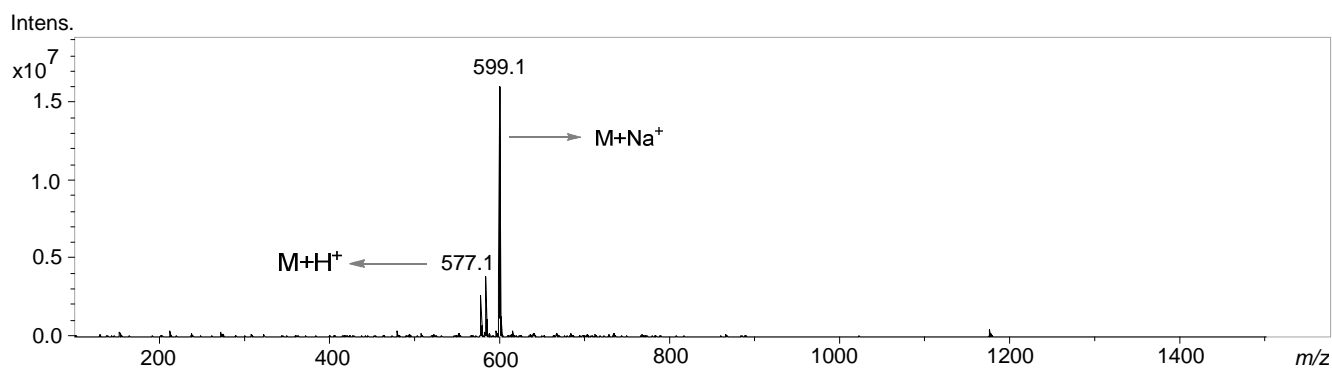


Figure 22. ESI-MS spectrum for macrocycle (**7**) from DMF and ACN (Positive mode).

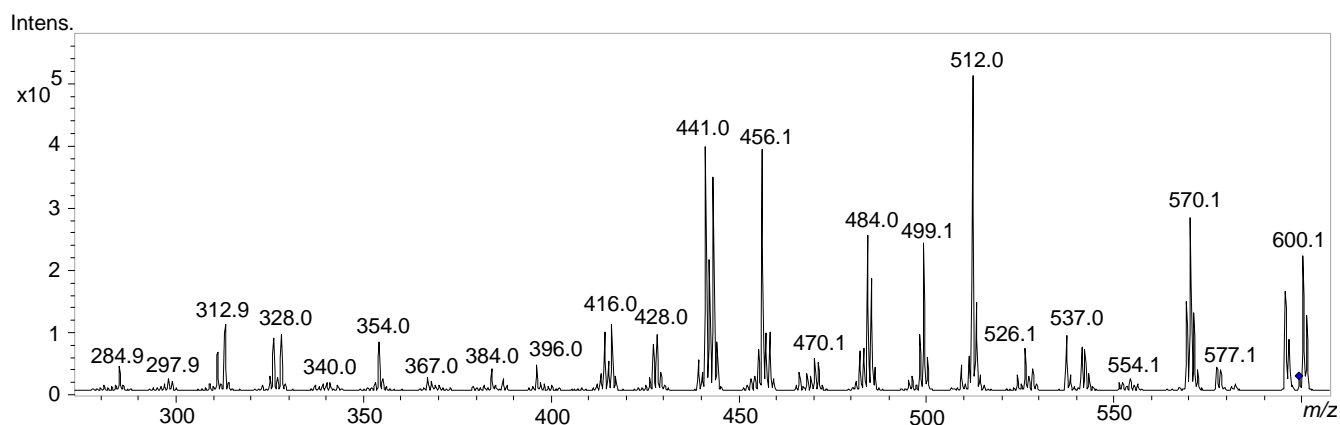


Figure 23. Tandem ESI-MS² spectrum for macrocycle (**7**) from DMF and ACN (Positive mode).

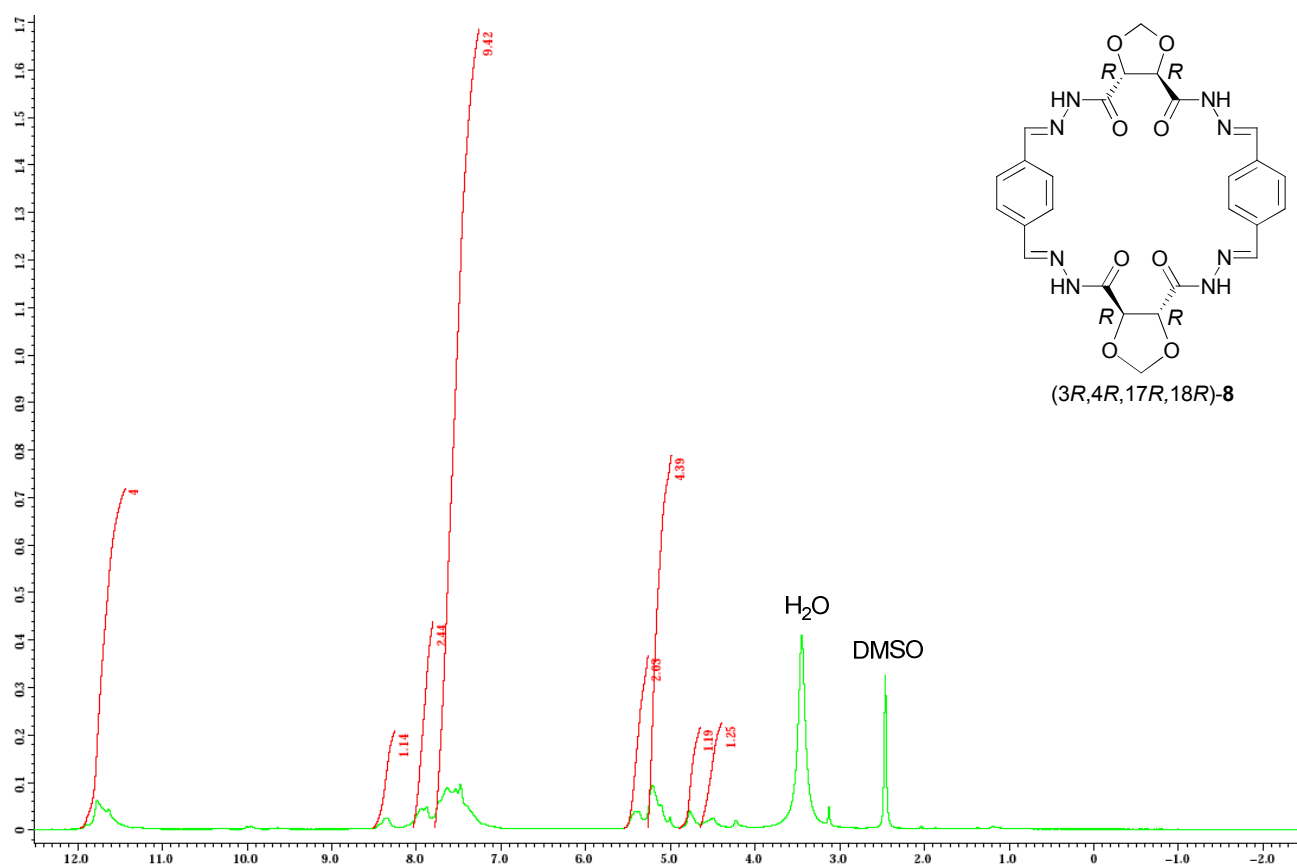


Figure 24. ¹H-NMR spectrum for macrocycle (**8**), DMSO-d₆, 400 MHz.

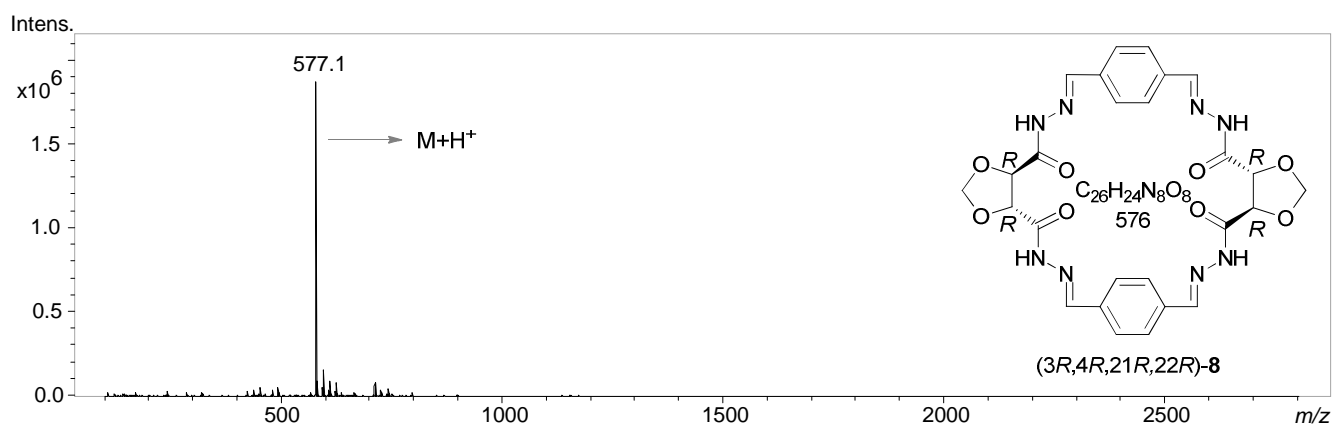


Figure 25. ESI-MS spectrum for macrocycle (**8**) from DMF and ACN (Positive mode).

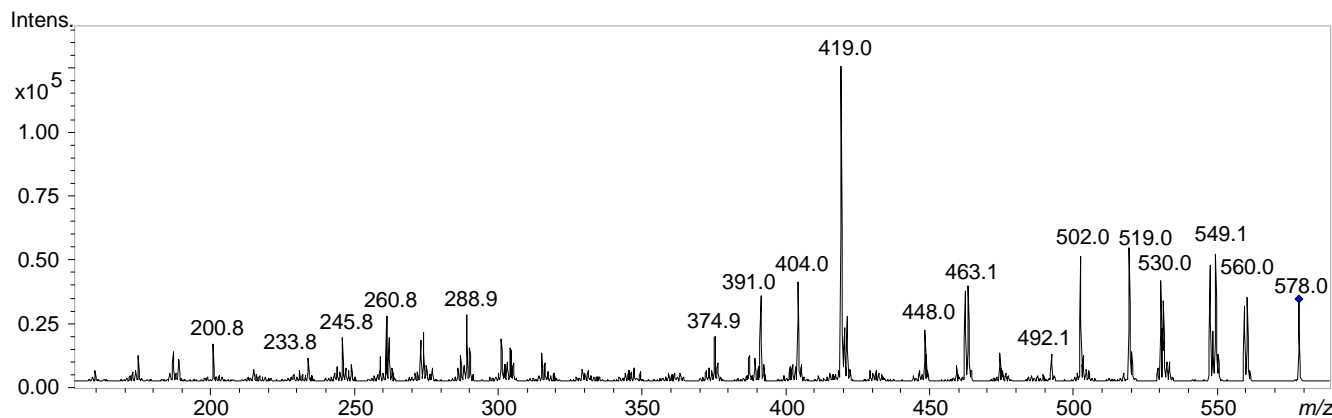
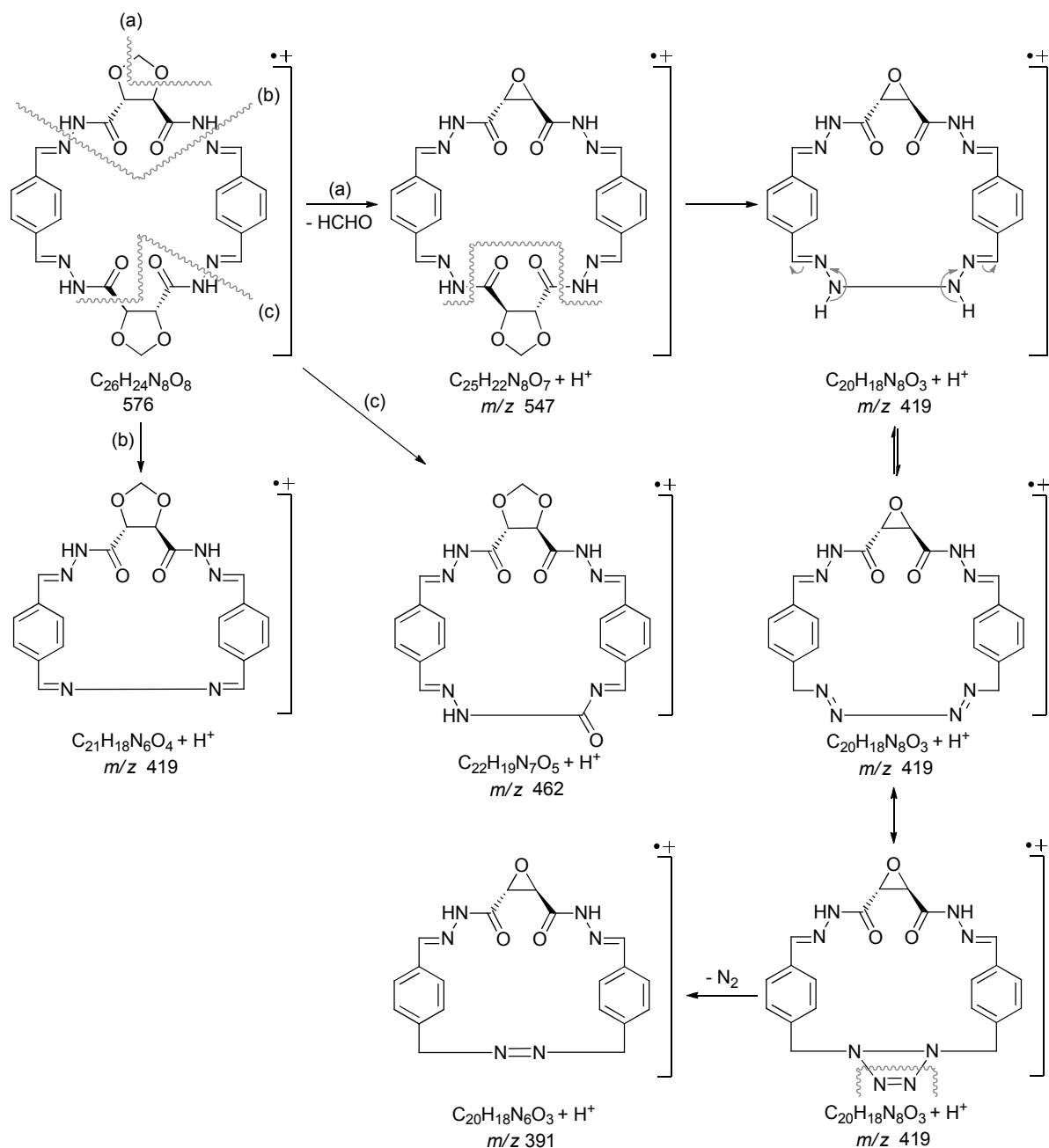


Figure 26. Tandem ESI-MS² spectrum for macrocycle (**8**) from DMF and ACN (Positive mode).



Scheme 3. Proposed fragmentation mechanism for macrocycle (**8**).

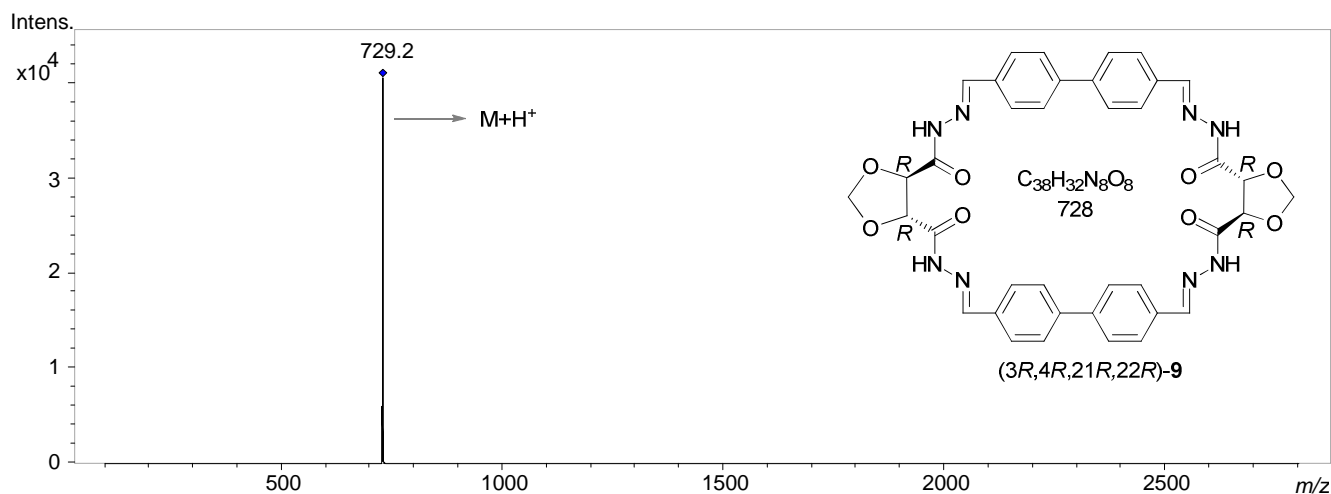
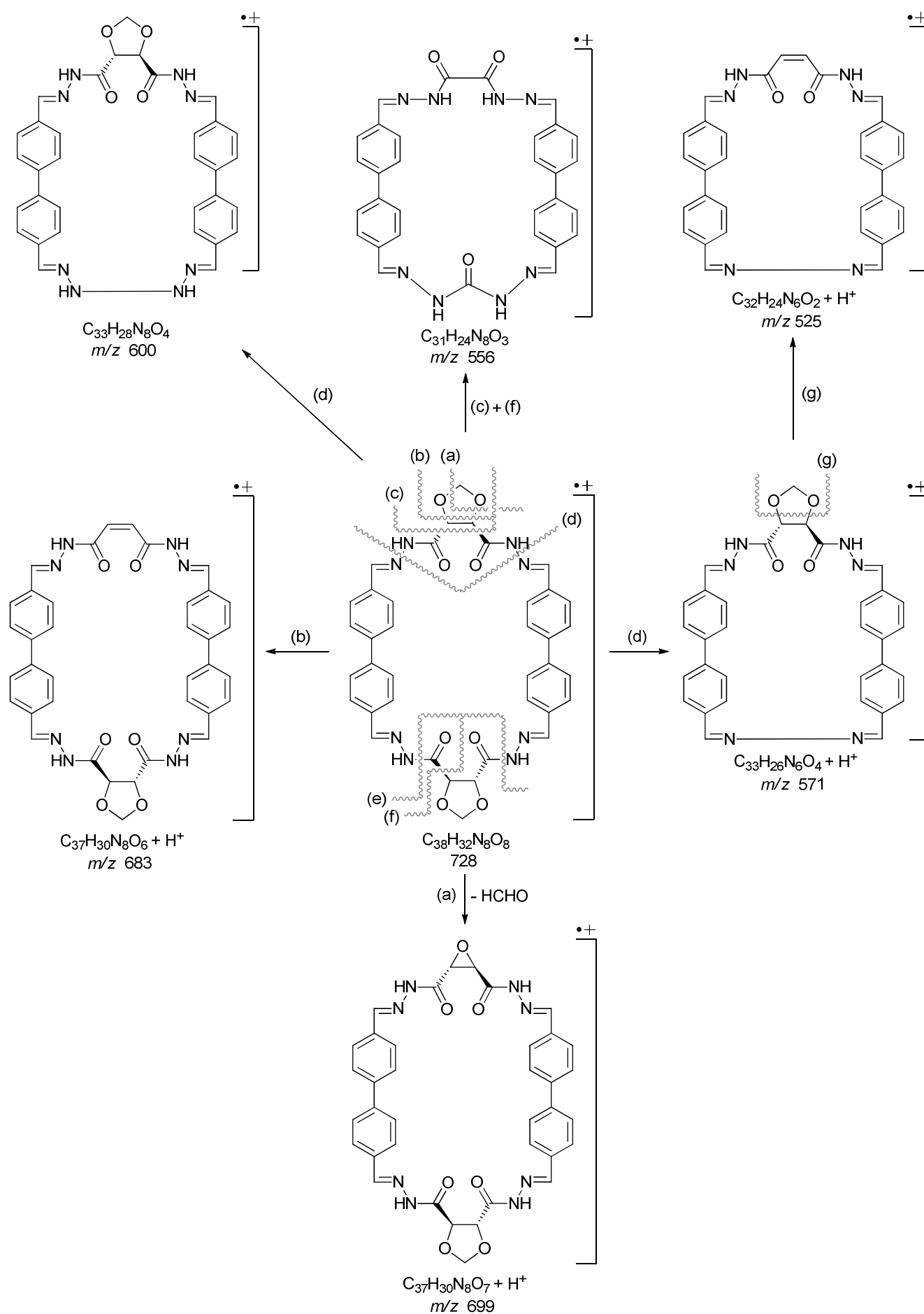


Figure 27. APCI-MS² spectrum for macrocycle (**9**), DMSO (Positive mode).



Scheme 4. Proposed fragmentation mechanism for macrocycle (9).

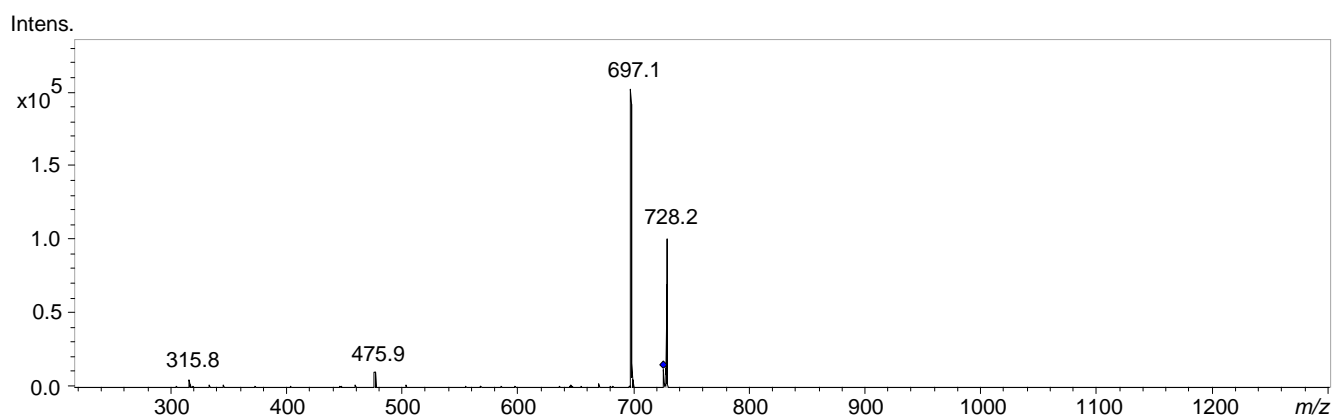
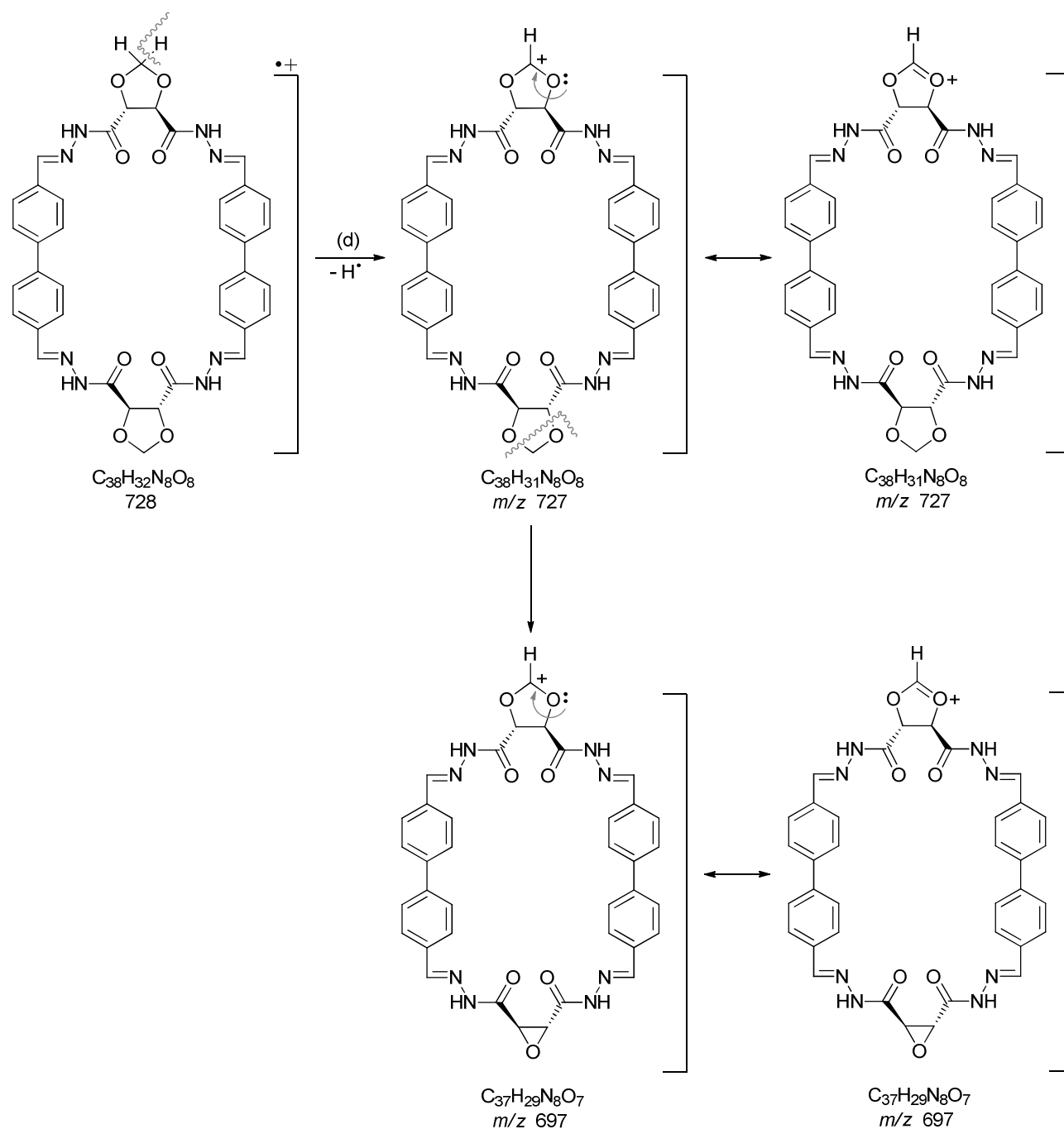


Figure 31. Tandem ESI-MS² spectrum for macrocycle (**9**) from DMSO (negative mode).



Scheme 5. Proposed fragmentation mechanism for macrocycle (**9**).

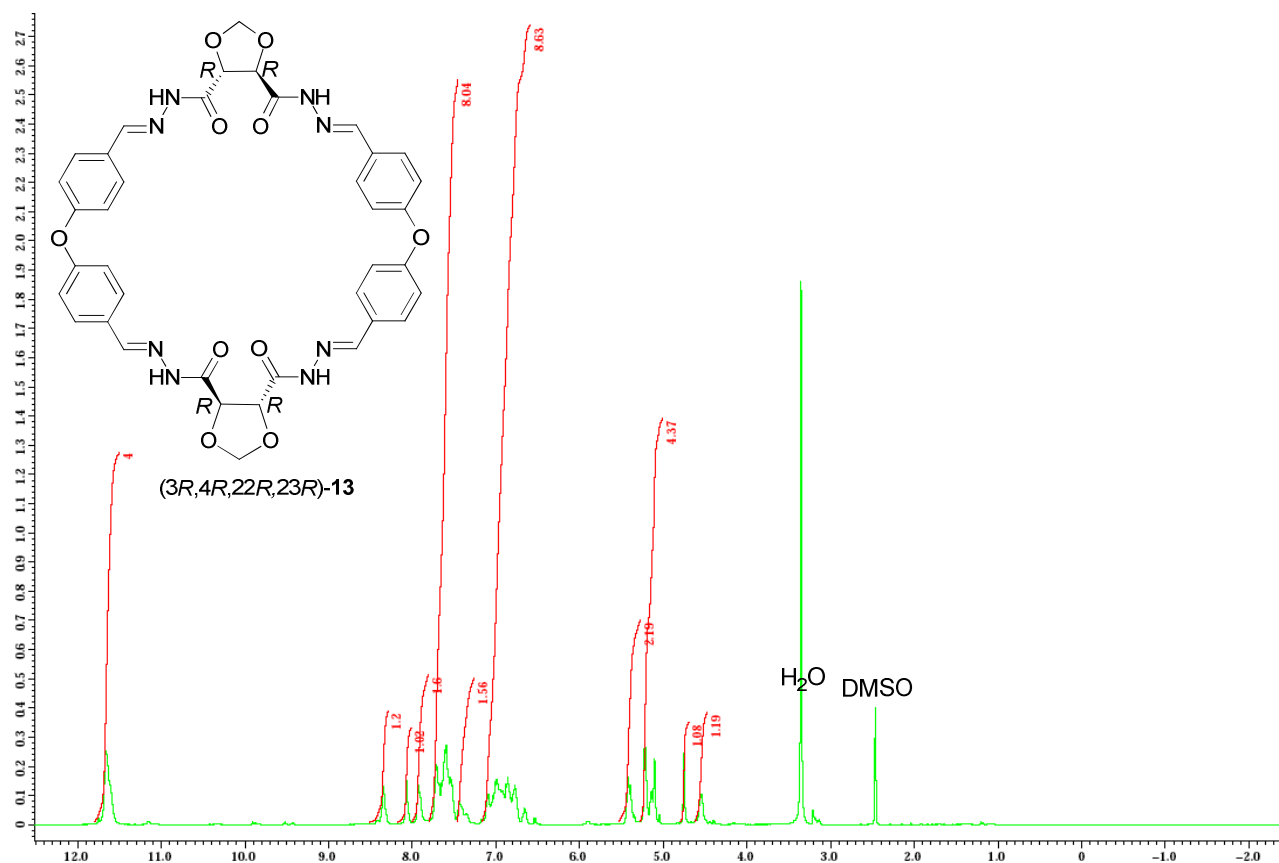


Figure 32. ^1H -NMR spectrum for macrocycle (**13**), DMSO-d_6 , 400 MHz.

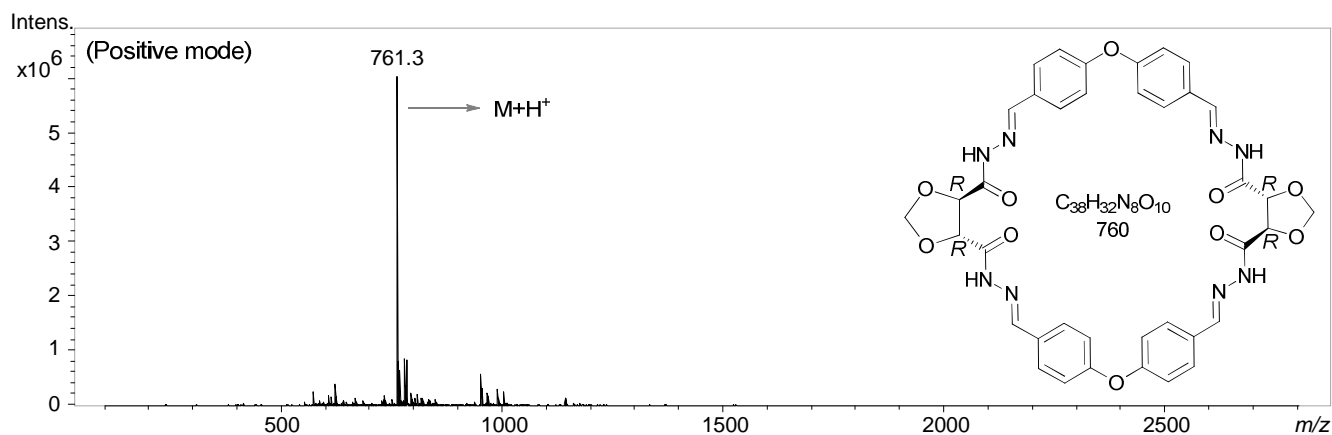


Figure 33. ESI-MS spectrum for macrocycle (**13**) from DMF and ACN.

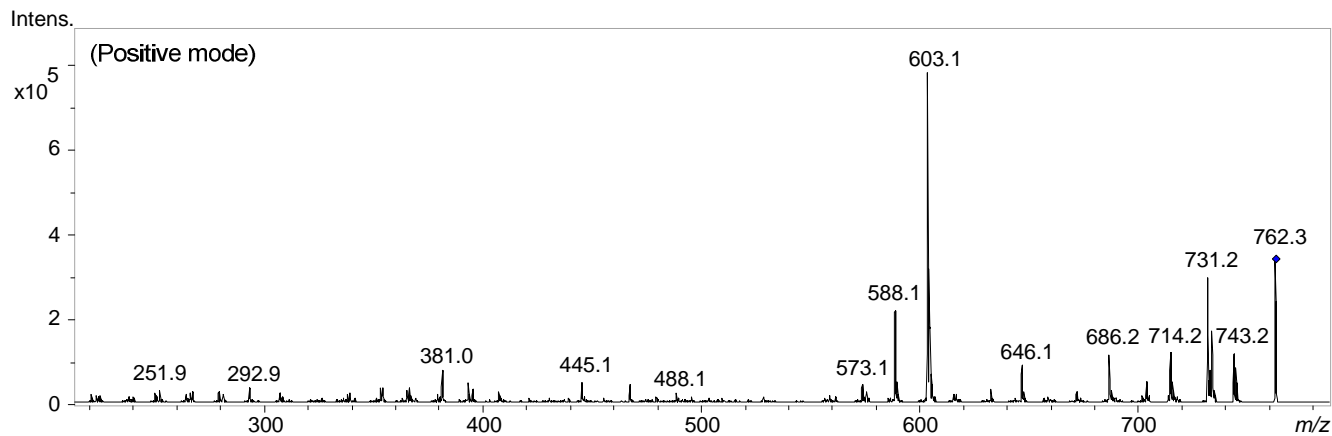
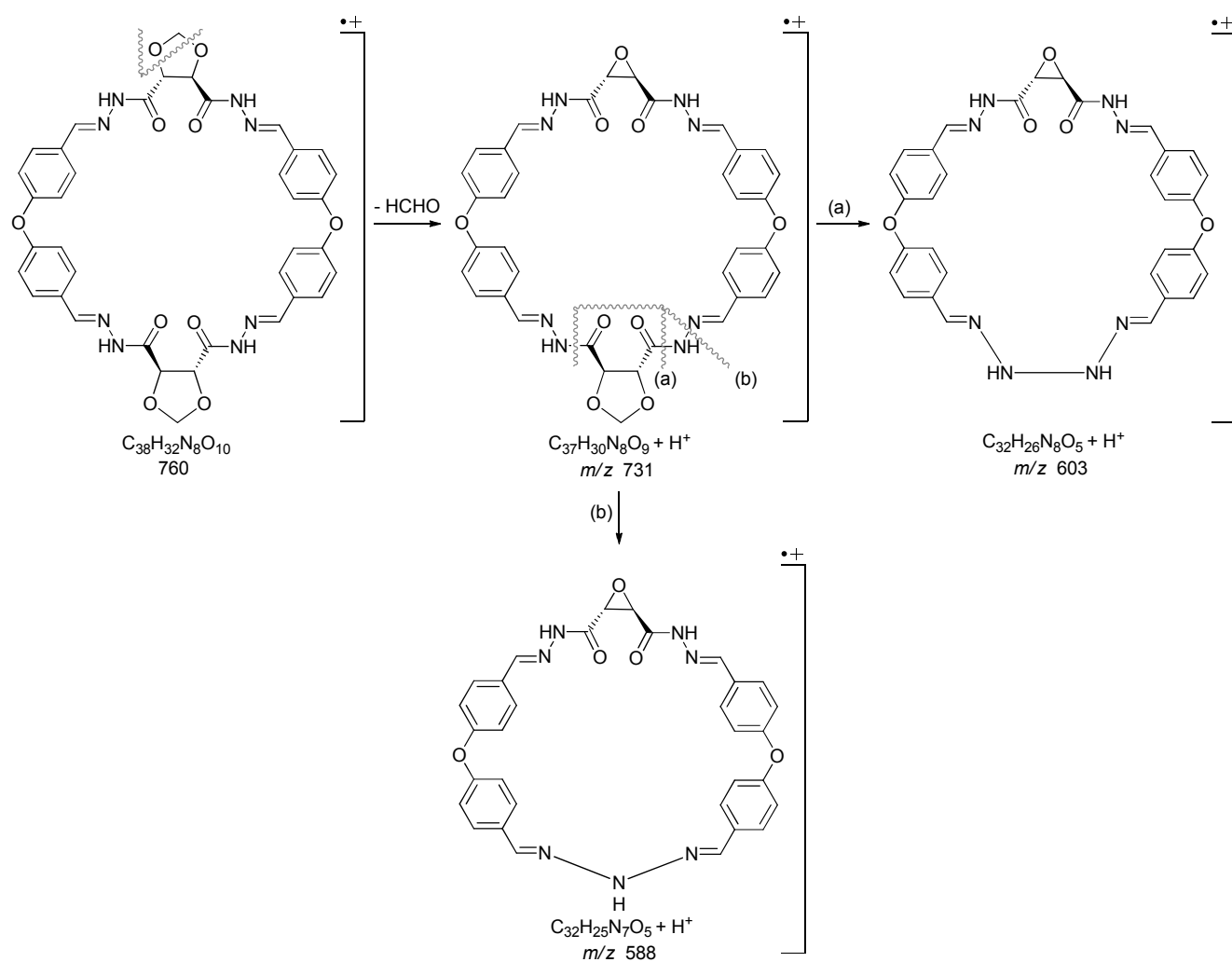


Figure 34. Tandem ESI-MS² spectrum for macrocycle (**13**) from DMF and ACN.



Scheme 6. Proposed fragmentation mechanism for macrocycle (**13**).

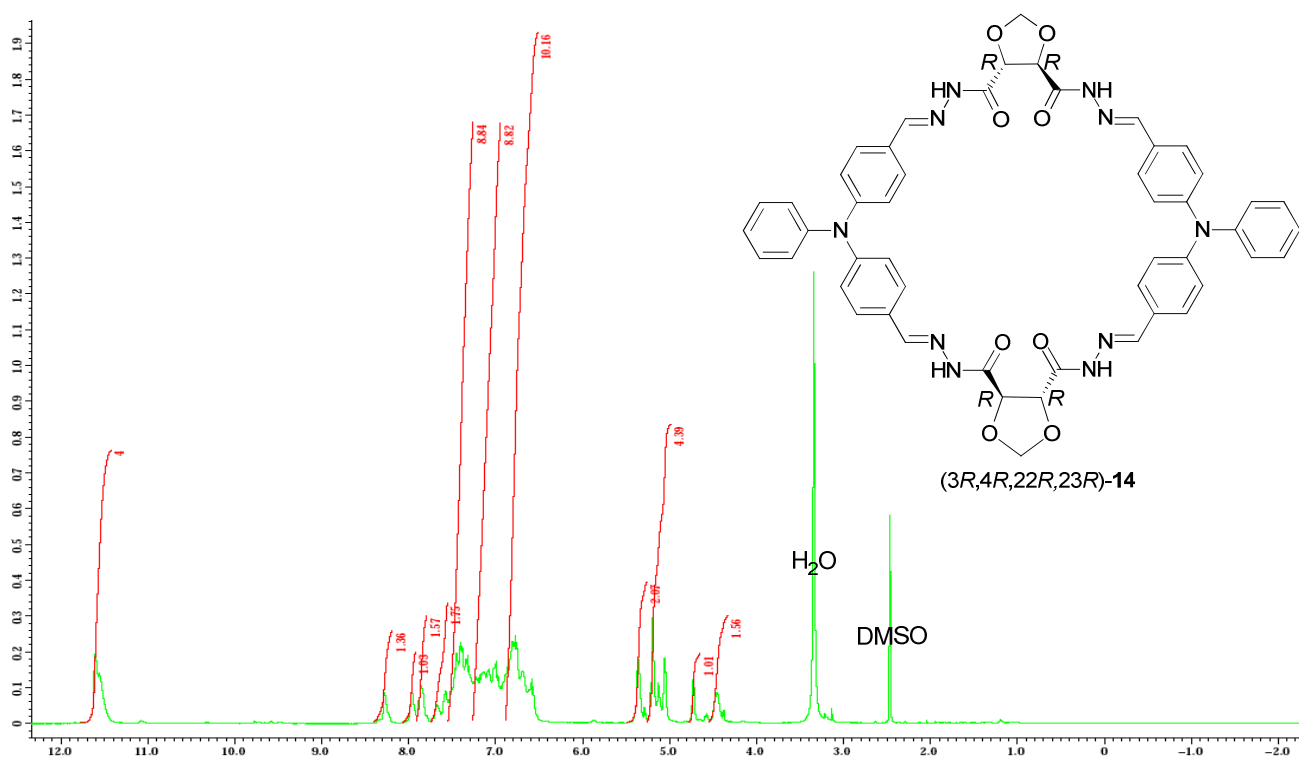


Figure 35. ^1H -NMR spectrum for macrocycle (**14**), DMSO-d_6 , 400 MHz.

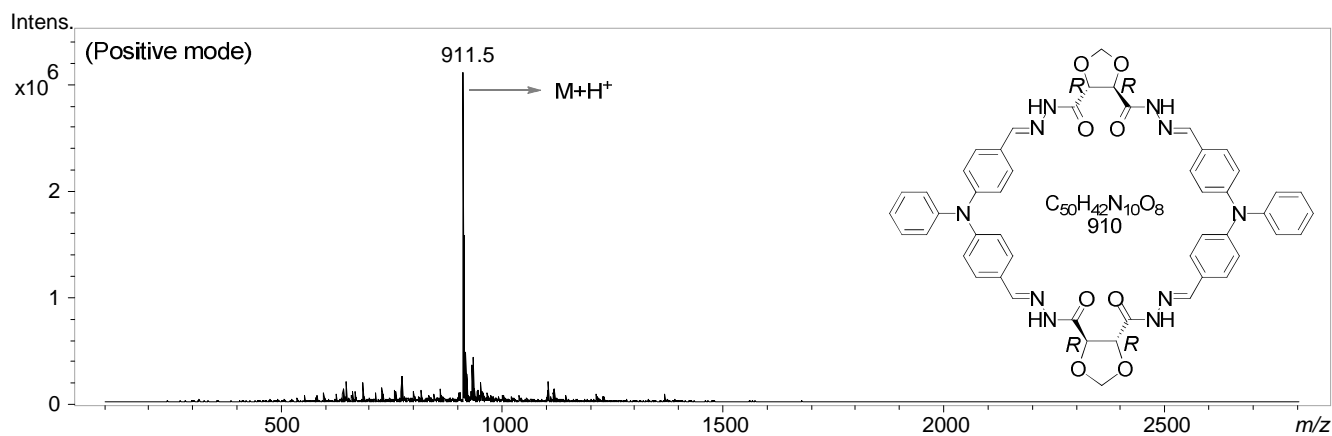


Figure 36. ESI-MS spectrum for macrocycle (14) from DMF and ACN.

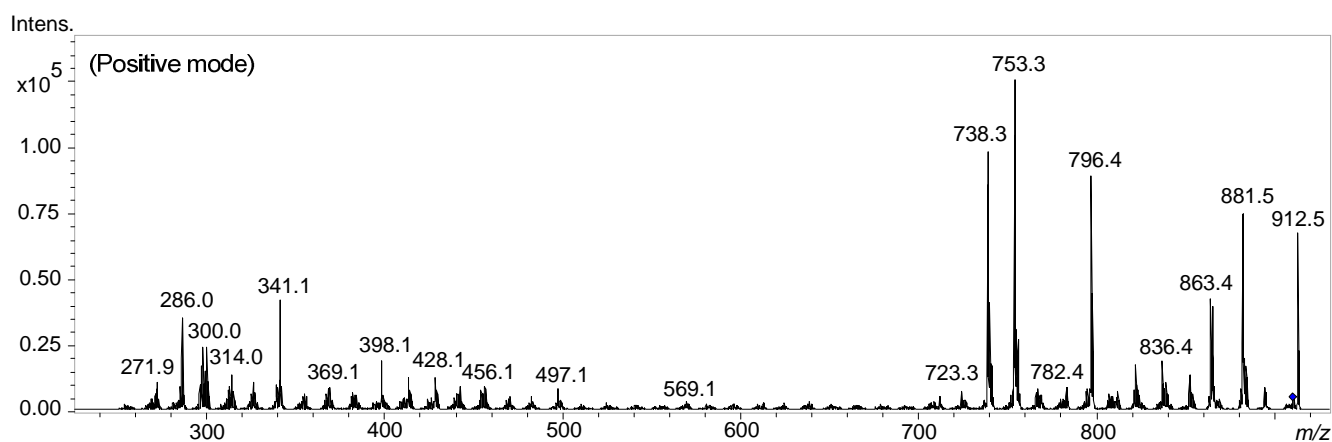
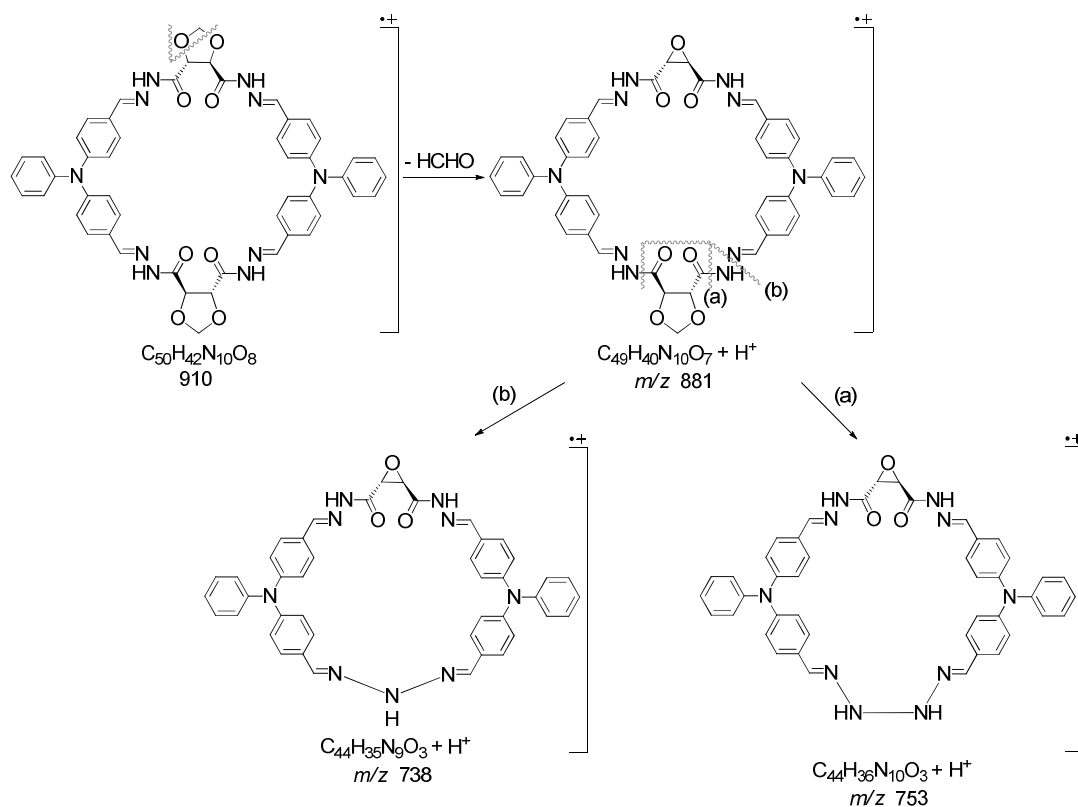


Figure 37. Tandem ESI-MS² spectrum for macrocycle (14) from DMF and ACN.



Scheme 7. Proposed fragmentation mechanism for macrocycle (14).

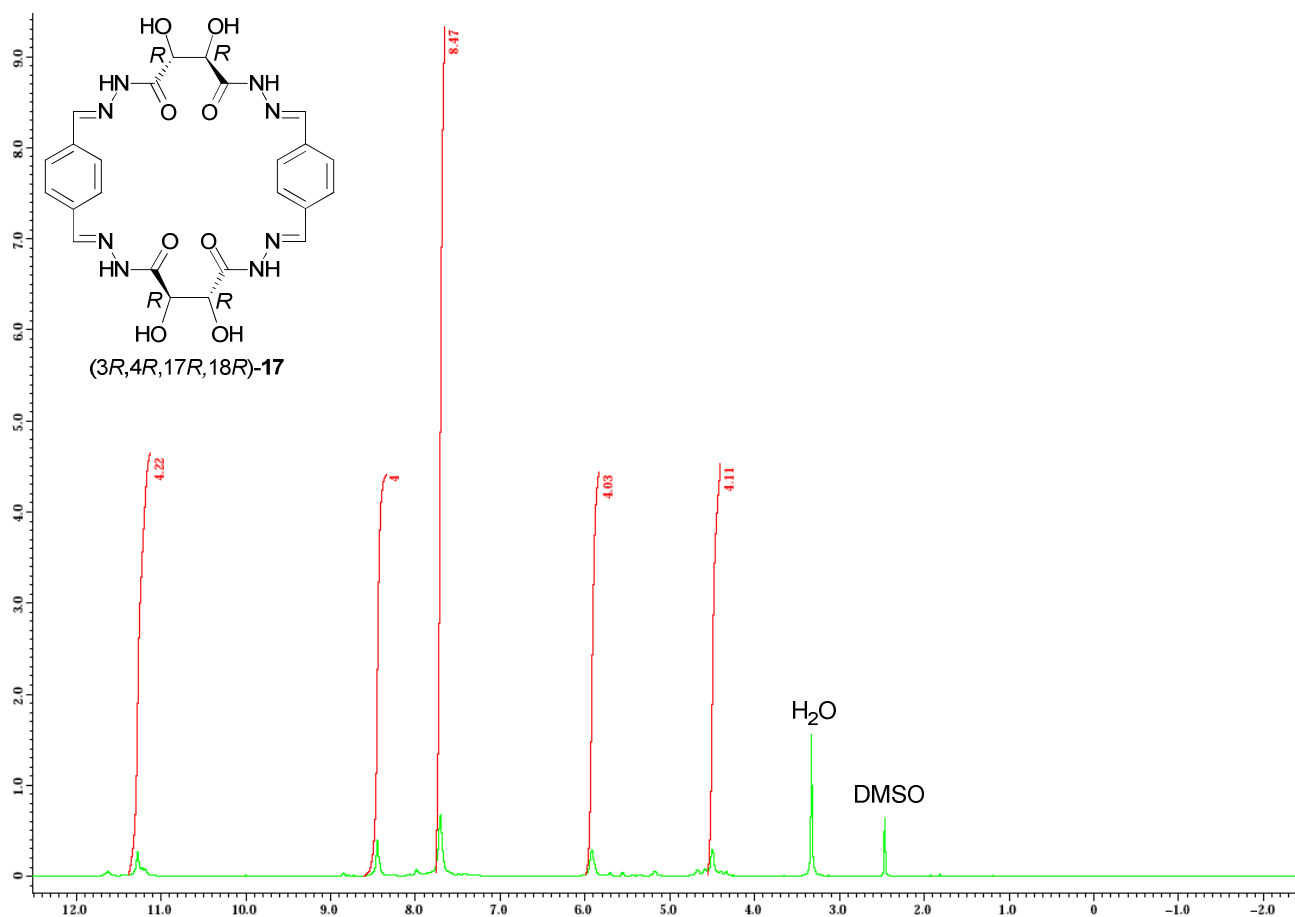


Figure 38. ¹H-NMR spectrum for macrocycle (17), DMSO-d₆, 400 MHz.

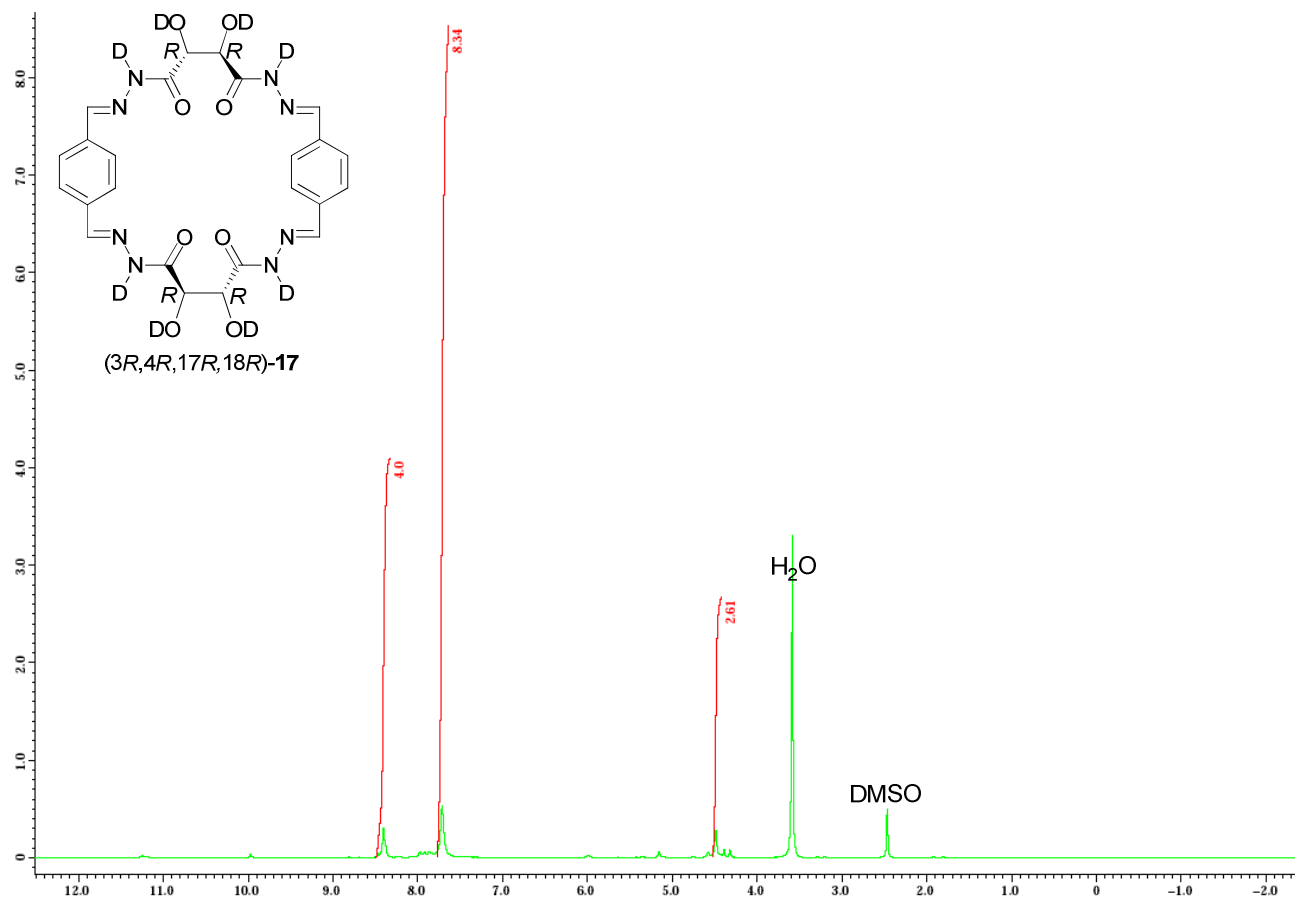


Figure 39. ¹H-NMR spectrum for macrocycle (17), DMSO-d₆ and D₂O, 400 MHz.

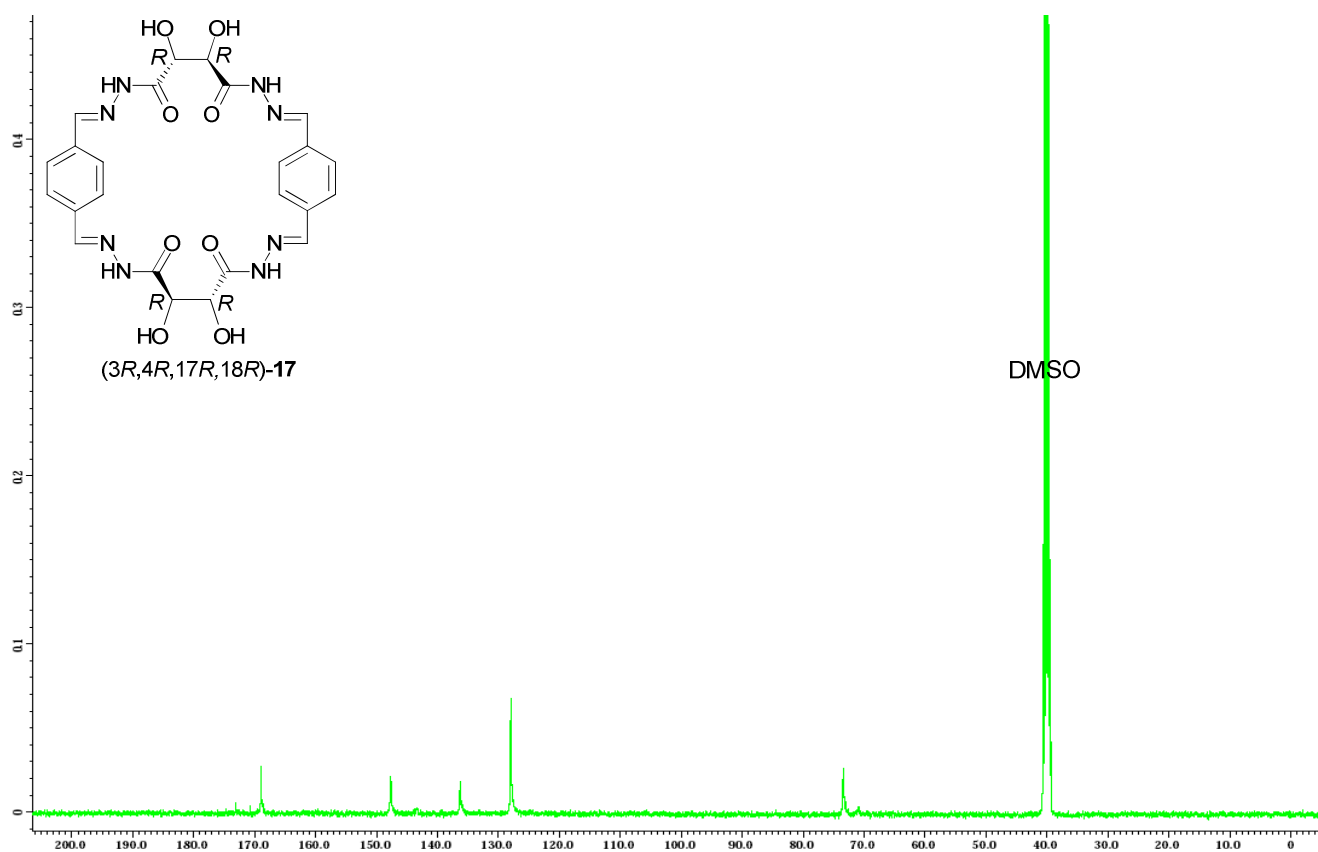


Figure 40. ^{13}C -NMR spectrum for macrocycle (17), DMSO- d_6 , 100 MHz.

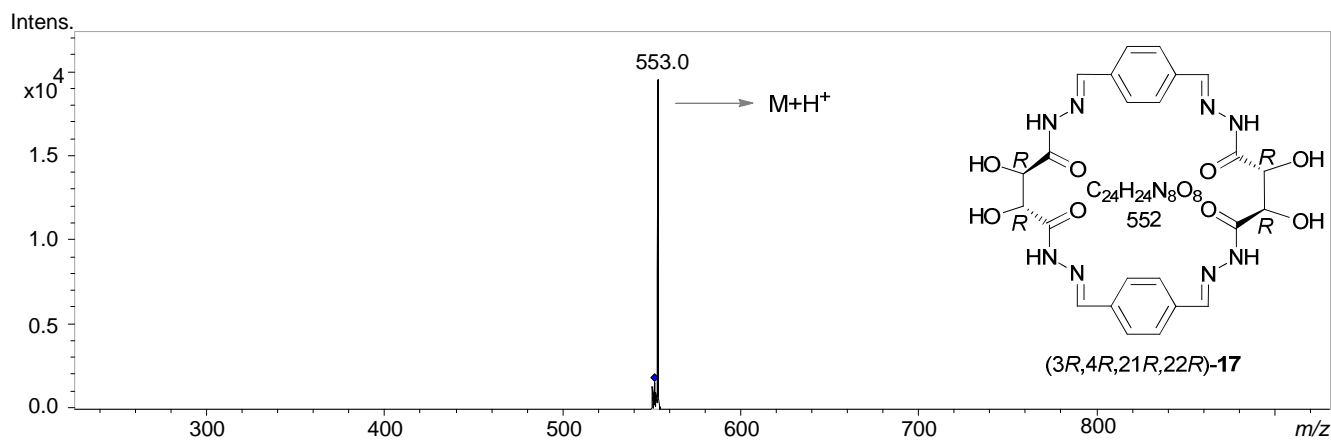


Figure 41. APCI- MS^2 spectrum for macrocycle (17), DMSO (positive mode).

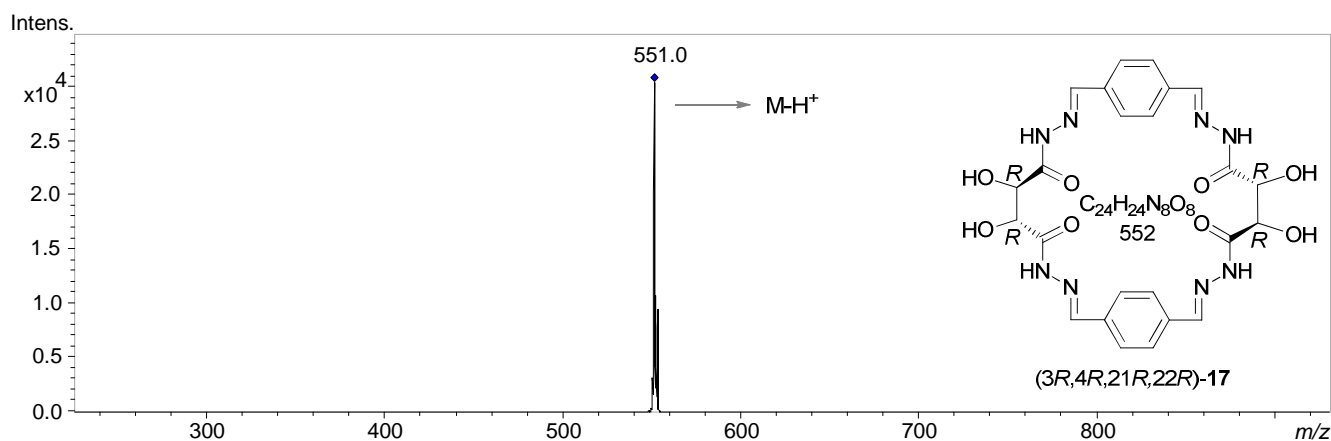


Figure 42. APCI- MS^2 spectrum for macrocycle (17), DMSO (negative mode).

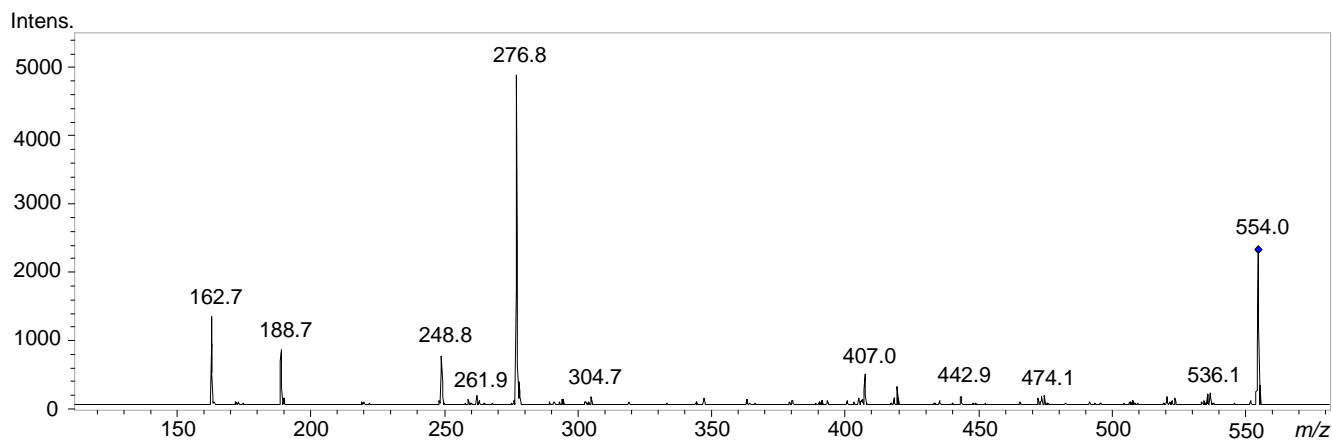
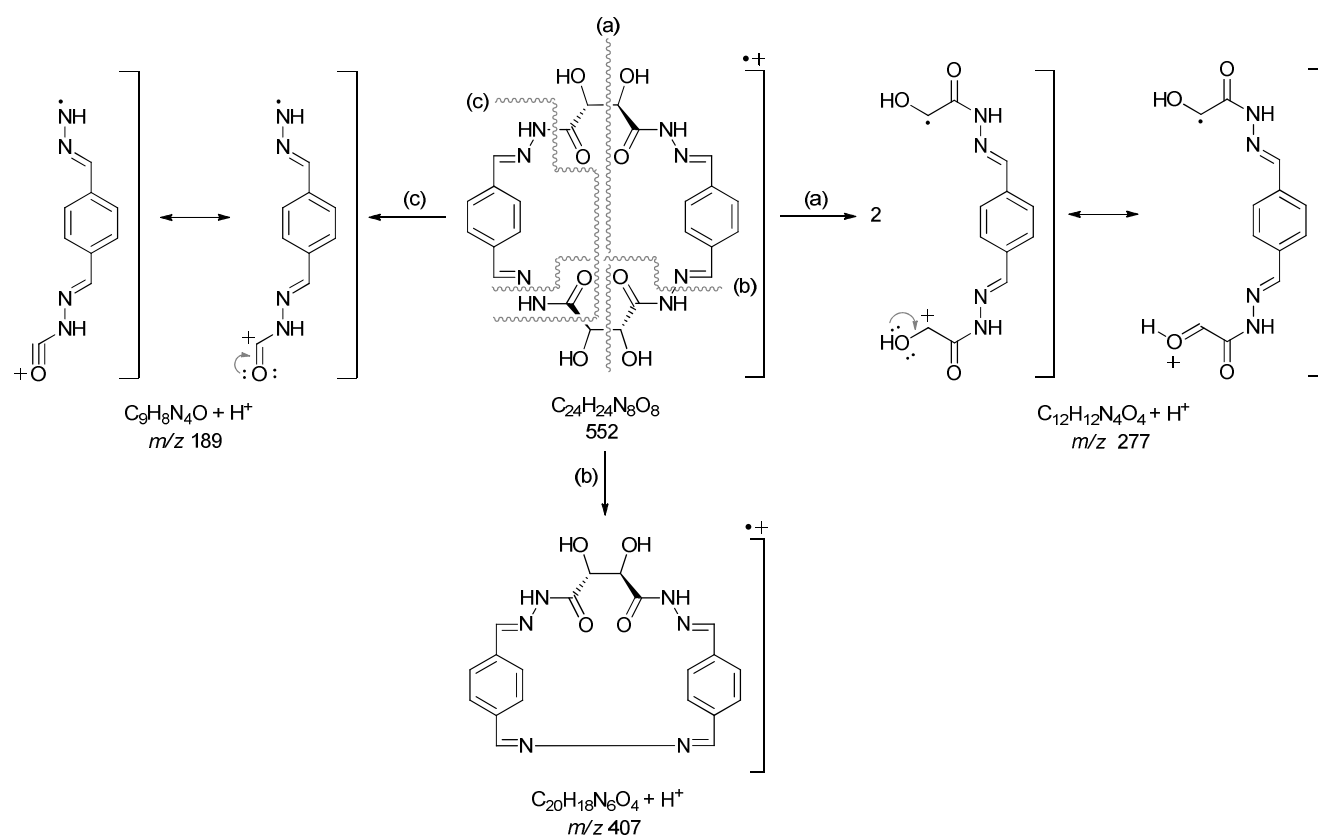


Figure 43. Tandem APCI-MS² spectrum for macrocycle (17), DMSO (positive mode).



Scheme 8. Proposed fragmentation mechanism for macrocycle (17).

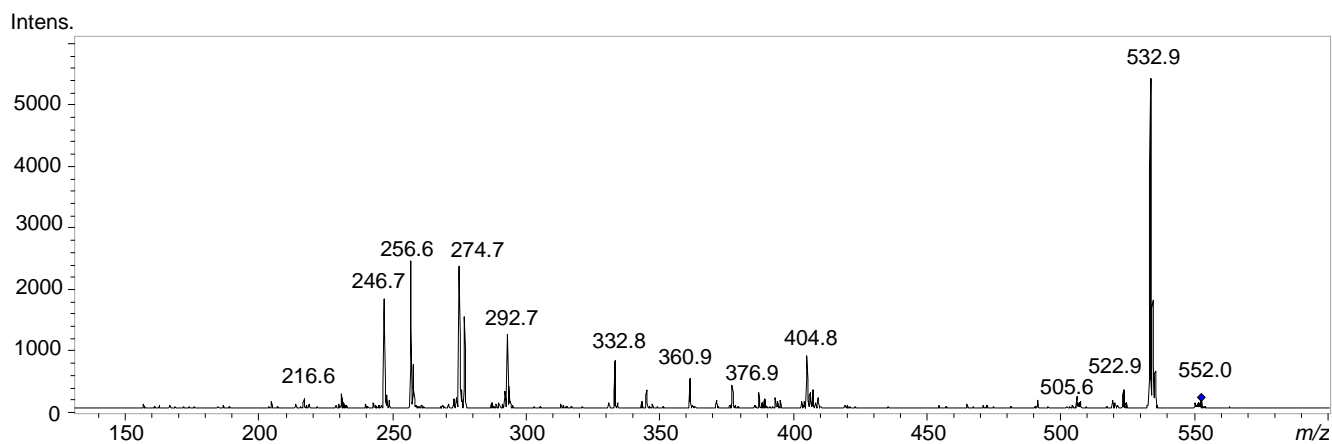
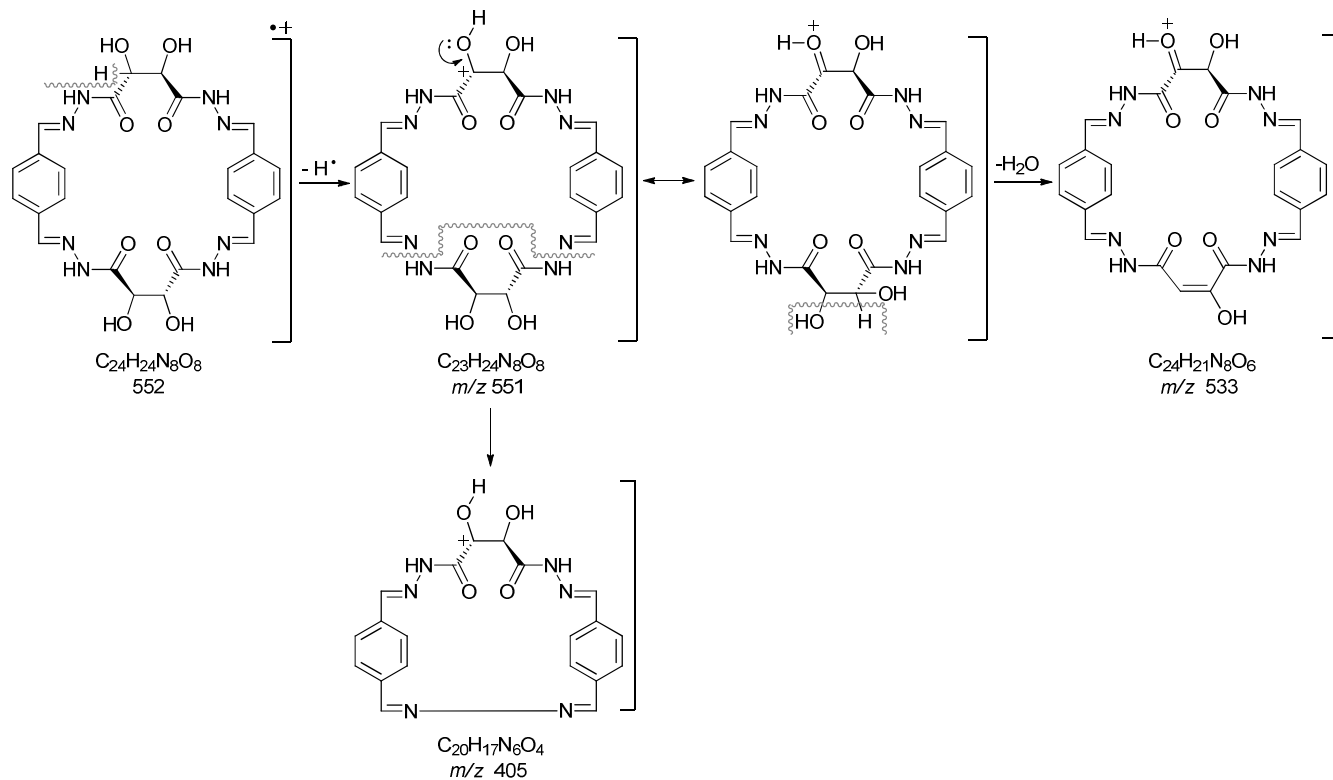


Figure 44. Tandem APCI-MS² spectrum for macrocycle (17), DMSO (negative mode).



Scheme 9. Proposed fragmentation mechanism for macrocycle (**17**).

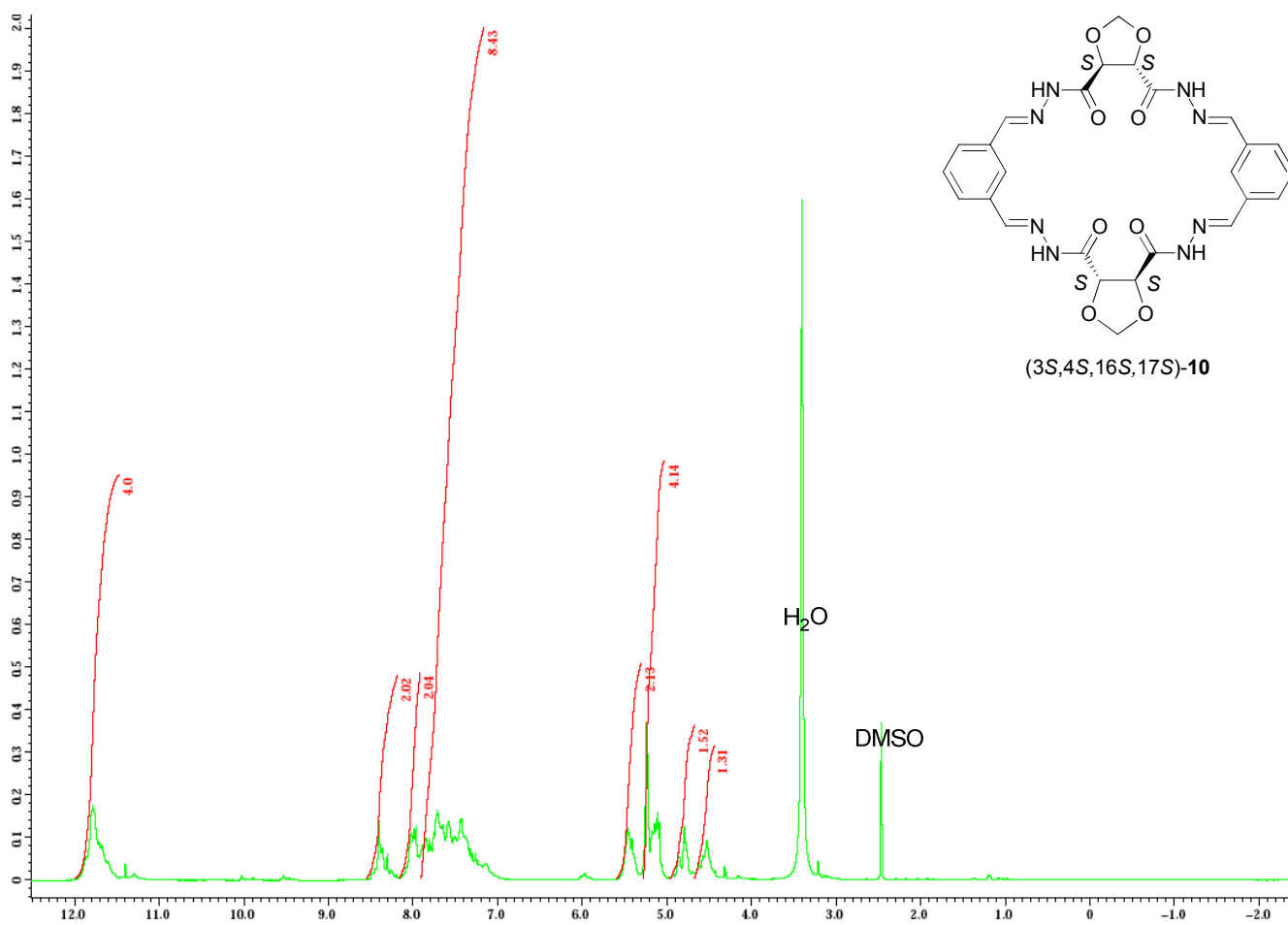


Figure 45. ^1H -NMR spectrum for macrocycle (**10**), DMSO-d_6 , 400 MHz.

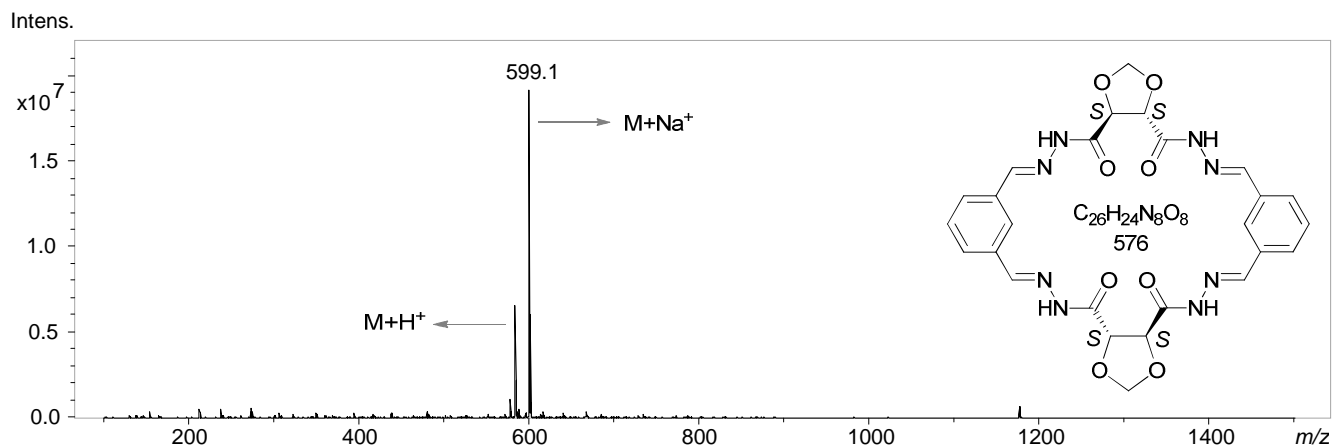


Figure 46. ESI-MS spectrum for macrocycle (10) from DMF and ACN (positive mode).

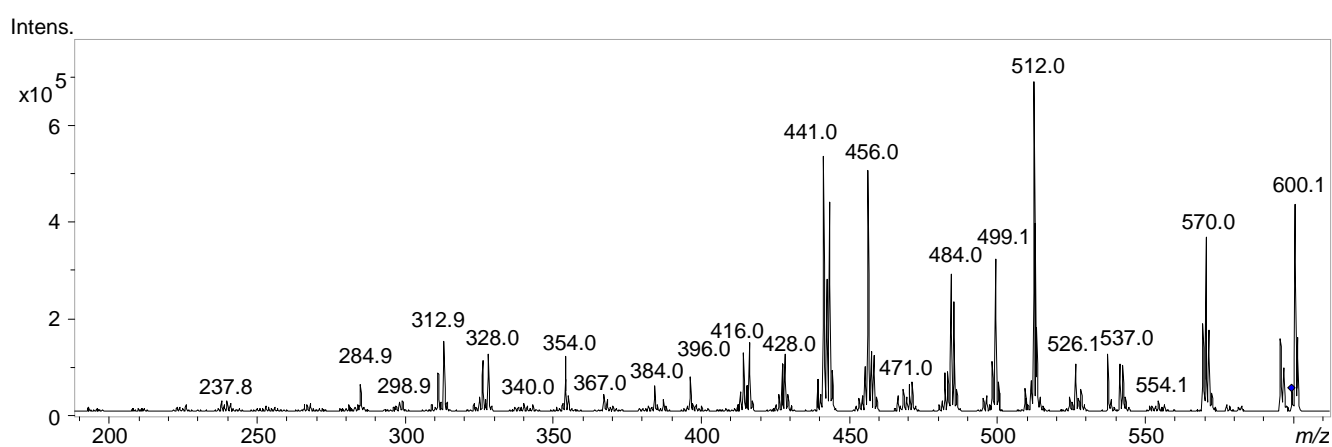


Figure 47. Tandem ESI-MS² spectrum for macrocycle (10) from DMF and ACN (positive mode).

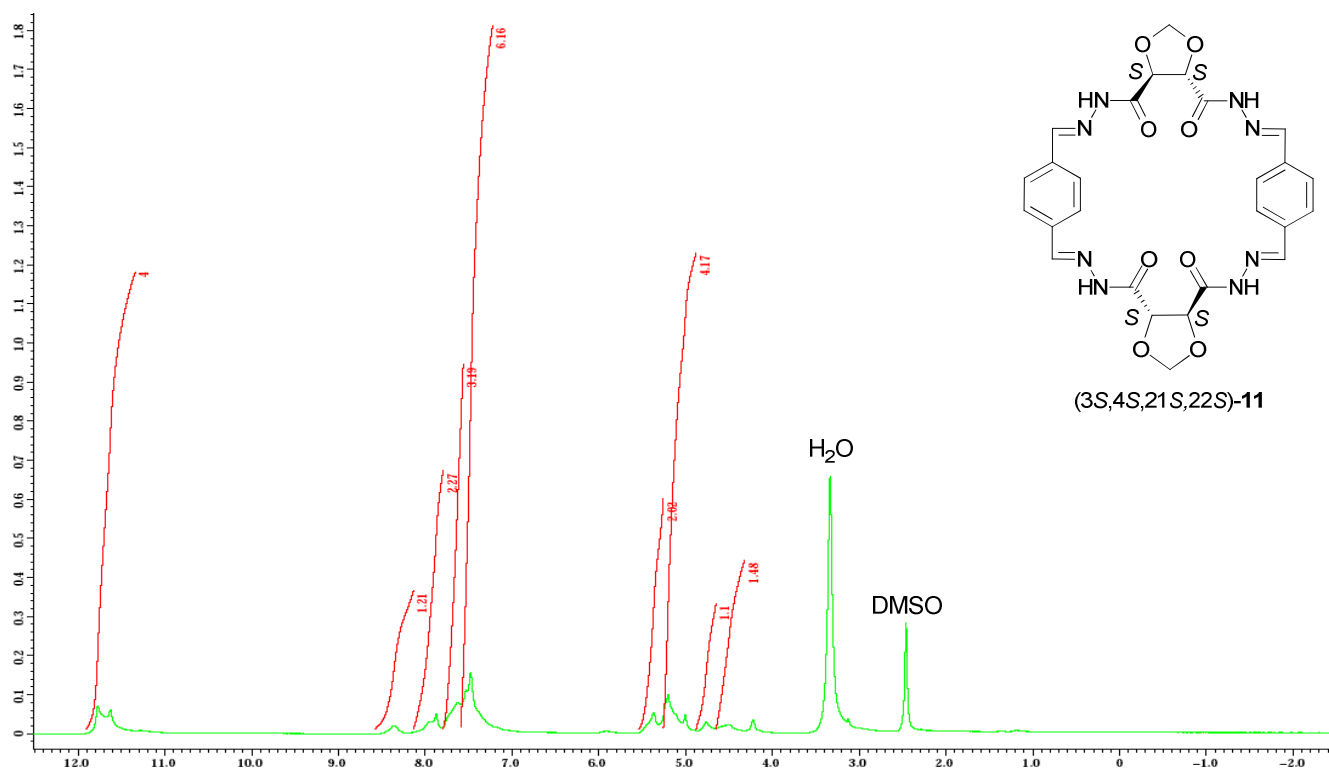


Figure 48. ¹H-NMR spectrum for macrocycle (11), DMSO- d_6 , 400 MHz.

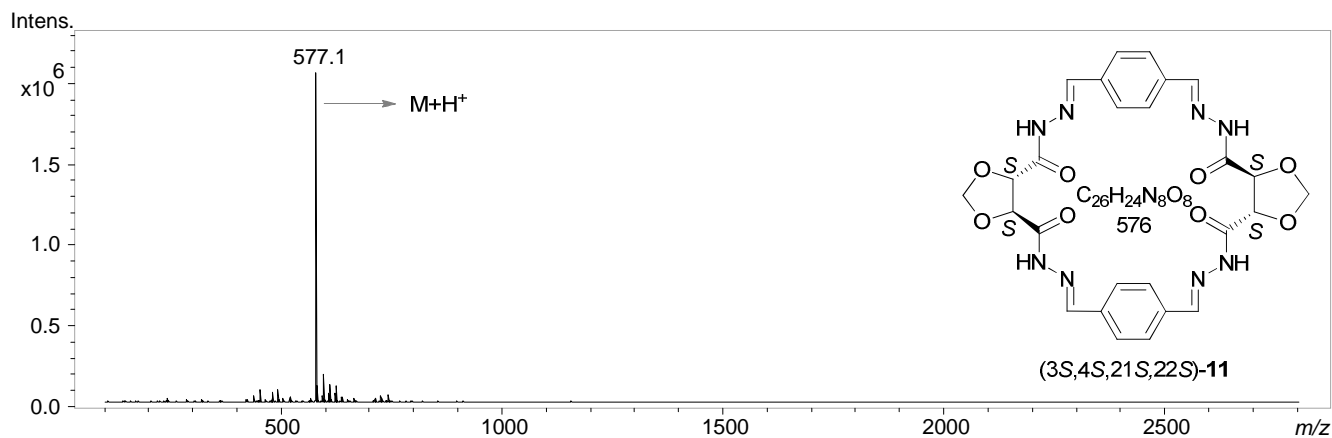


Figure 49. APCI-MS spectrum for macrocycle (11) from DMF and ACN (positive mode).

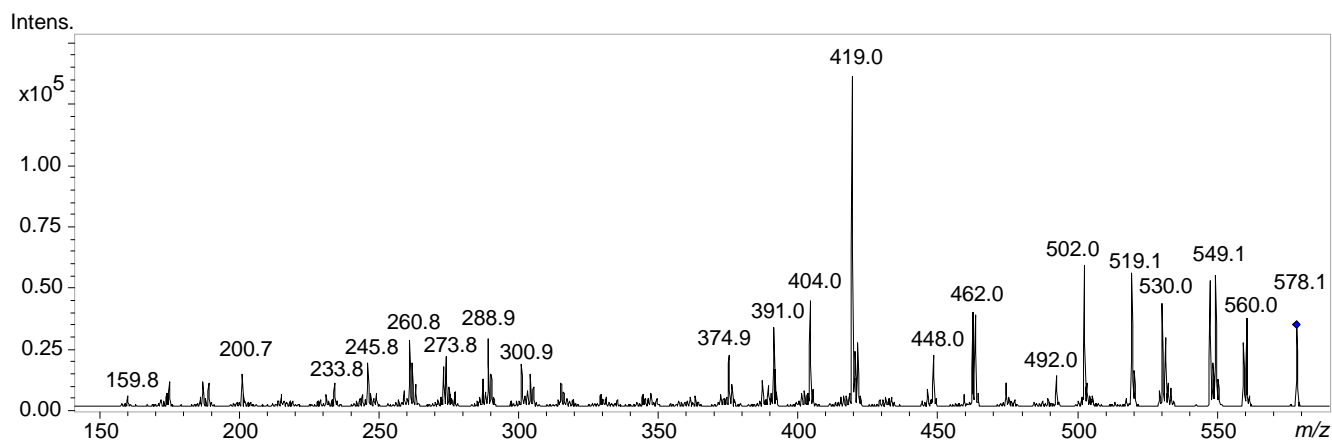
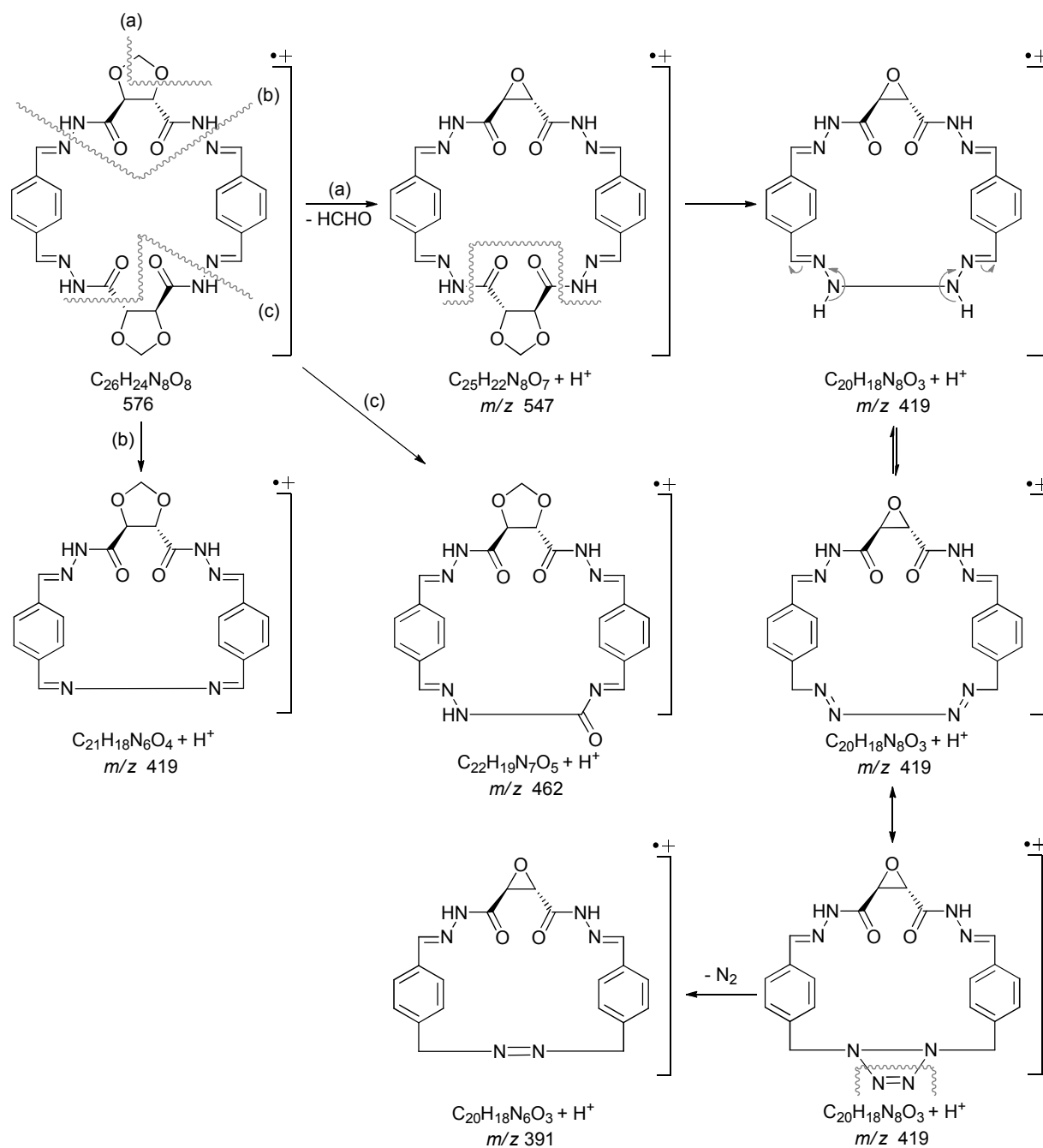


Figure 50. Tandem ESI-MS² spectrum for macrocycle (11) from DMF and ACN (positive mode).



Scheme 10. Proposed fragmentation mechanism for macrocycle (**11**).

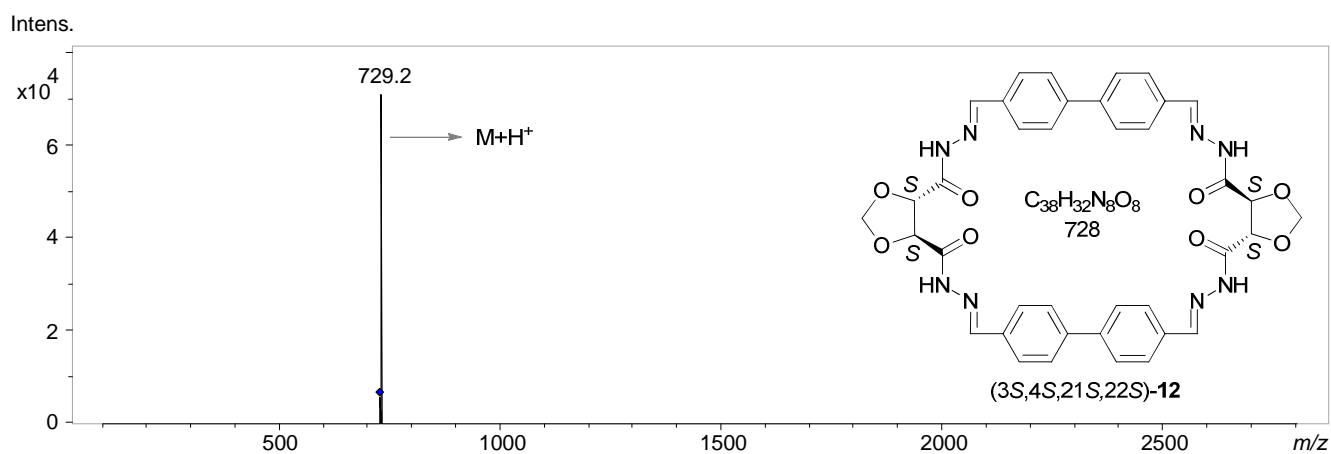


Figure 51. APCI-MS² spectrum for macrocycle (**12**) from DMSO (positive mode).

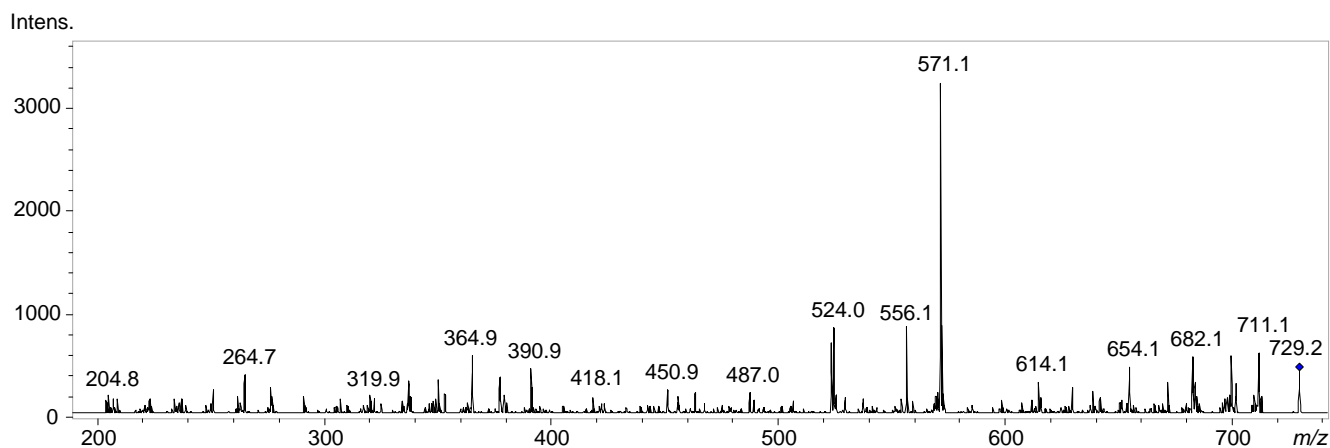


Figure 52. Tandem APCI-MS² spectrum for macrocycle (**12**) from DMSO (positive mode).

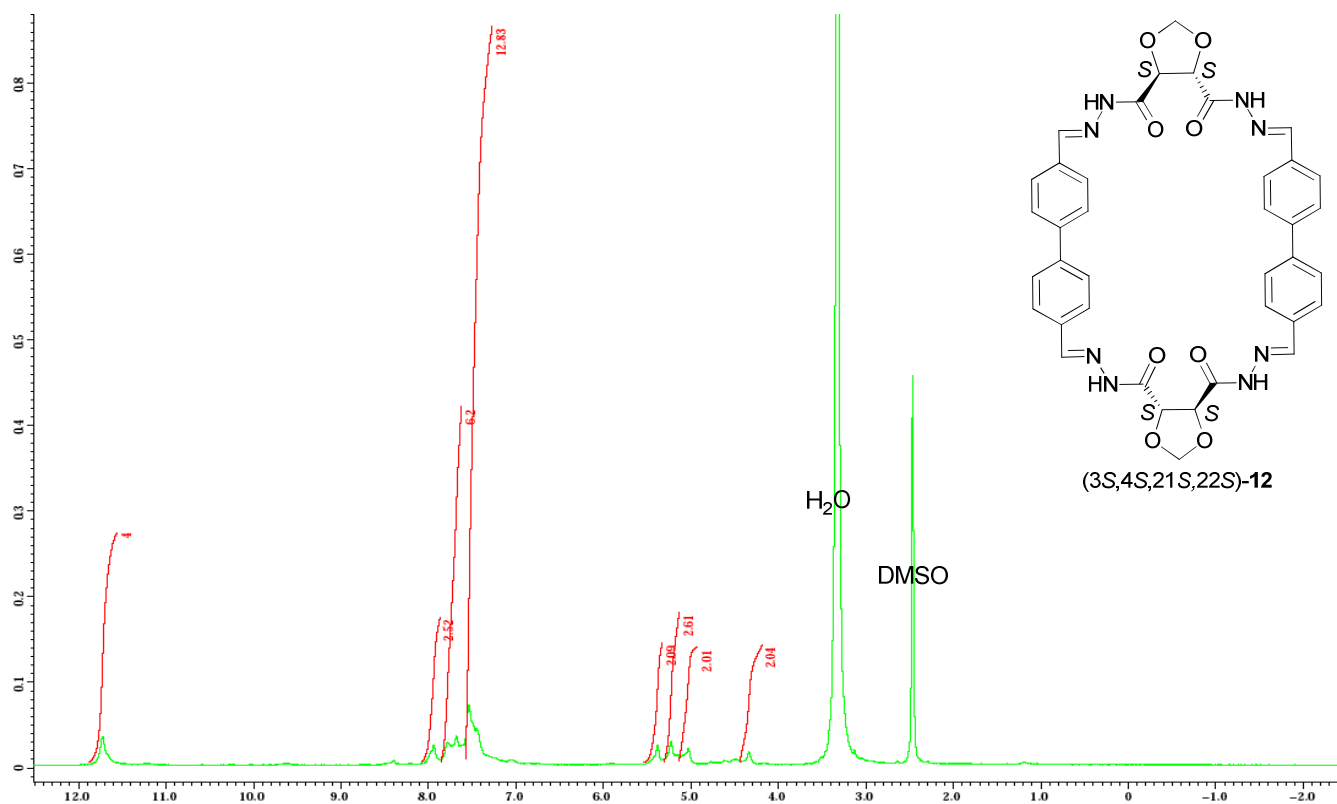


Figure 53. ¹H-NMR spectrum for macrocycle (**12**), DMSO-d₆, 400 MHz.

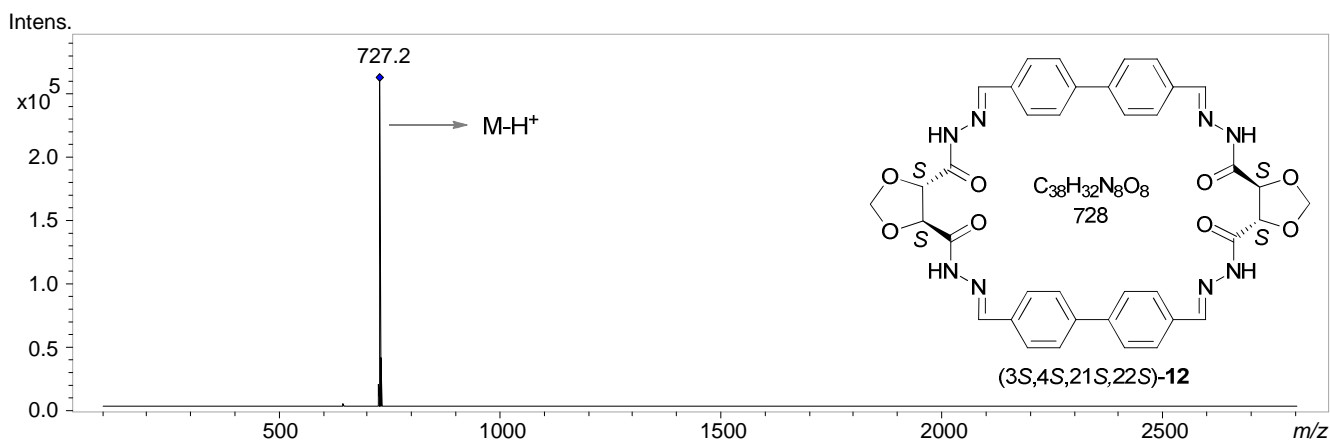
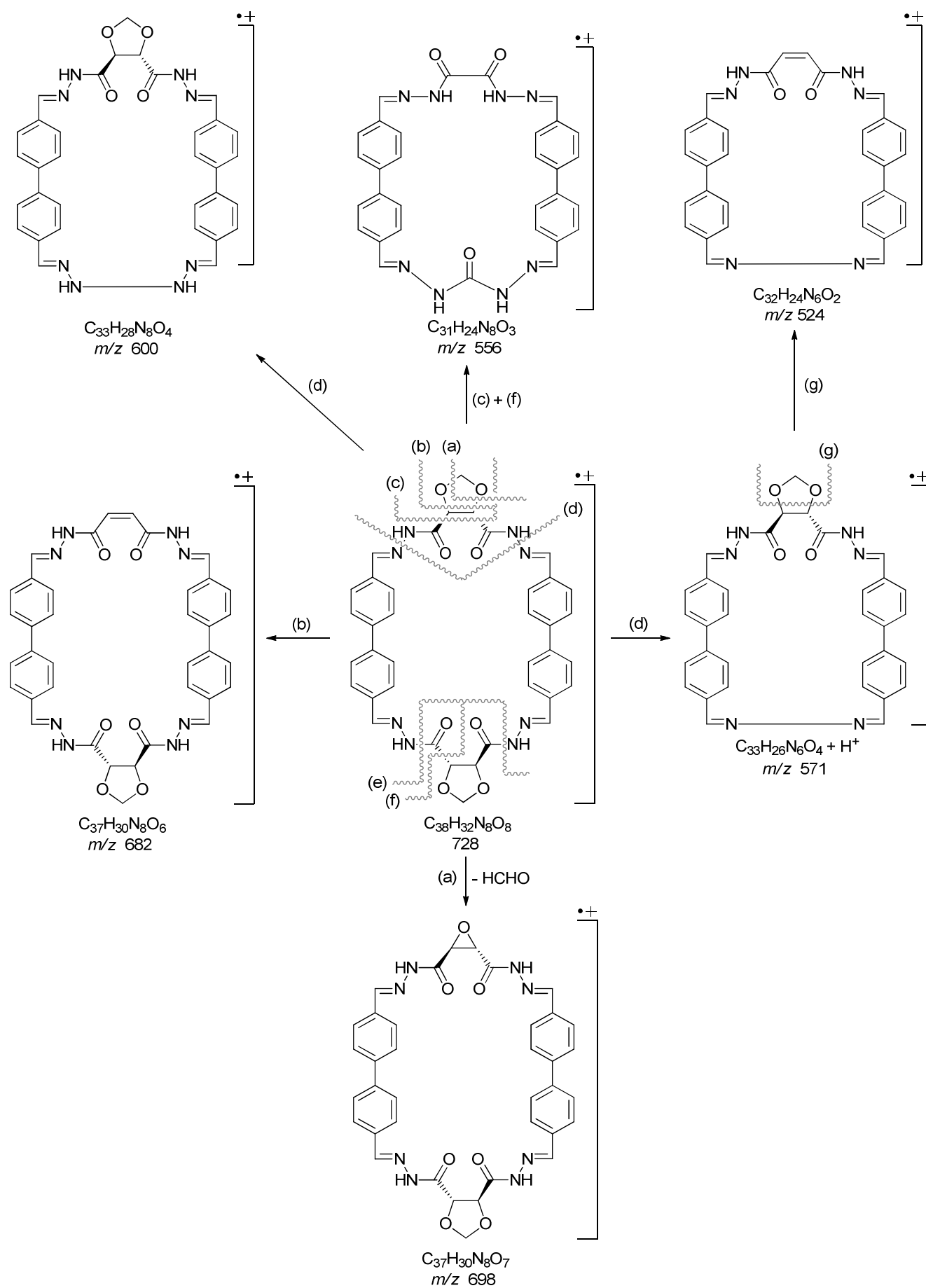


Figure 54. APCI-MS² spectrum for macrocycle (**12**) from DMSO (negative mode).



Scheme 11. Proposed fragmentation mechanism for macrocycle (**12**), positive mode.

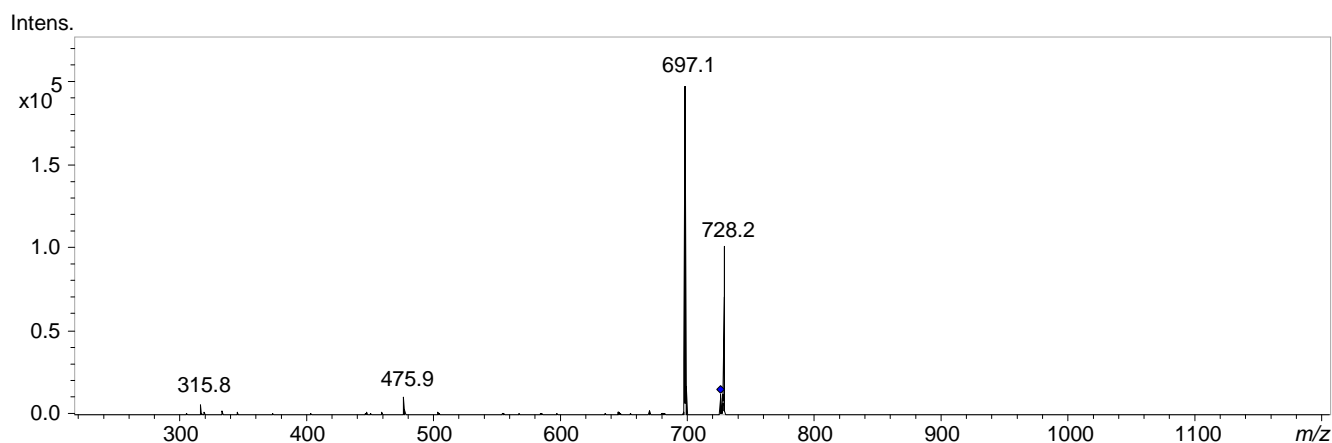
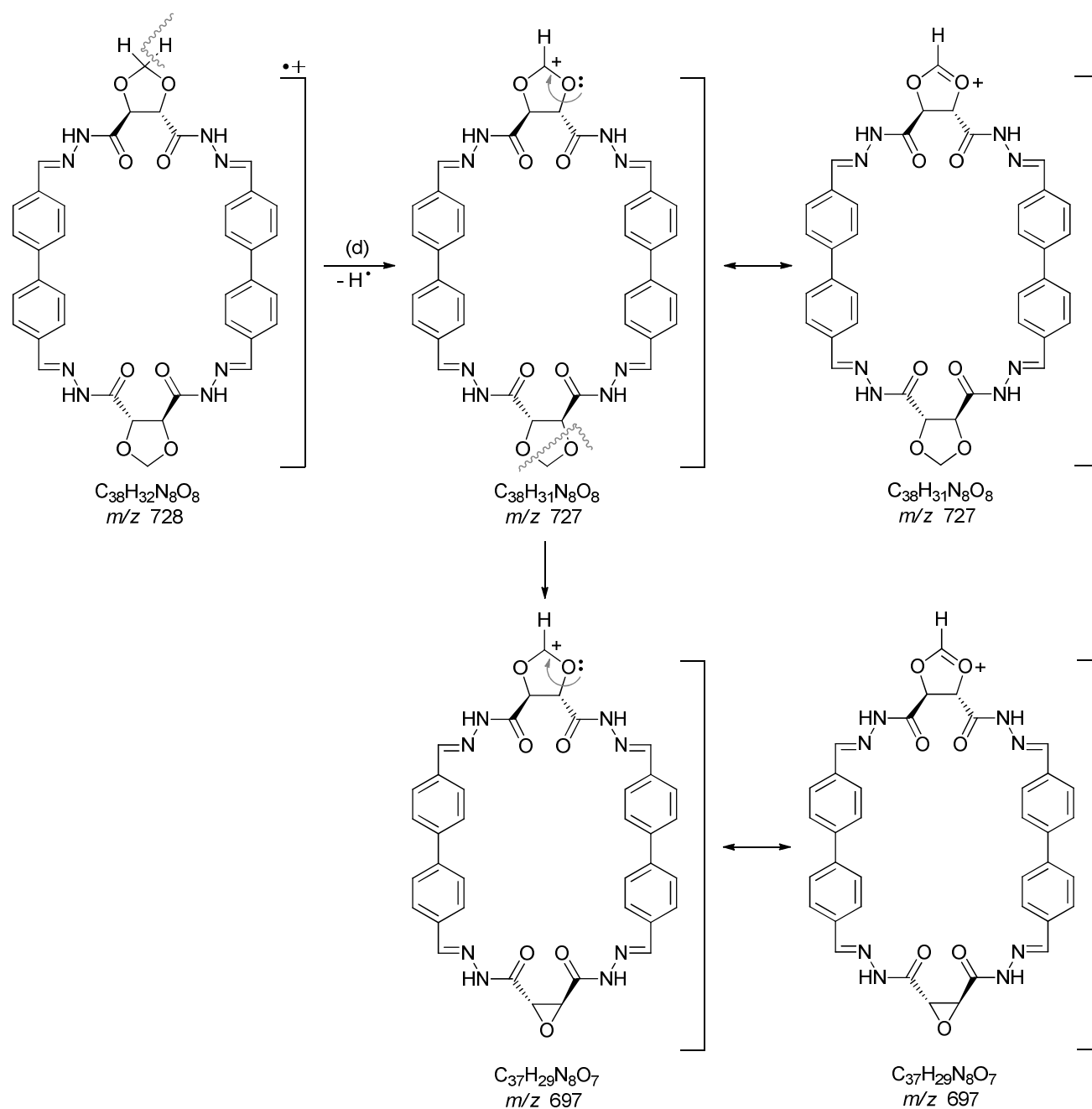


Figure 55. Tandem APCI-MS² spectrum for macrocycle (**12**) from DMSO (negative mode).



Scheme 12. Proposed fragmentation mechanism for macrocycle (**12**), negative mode.

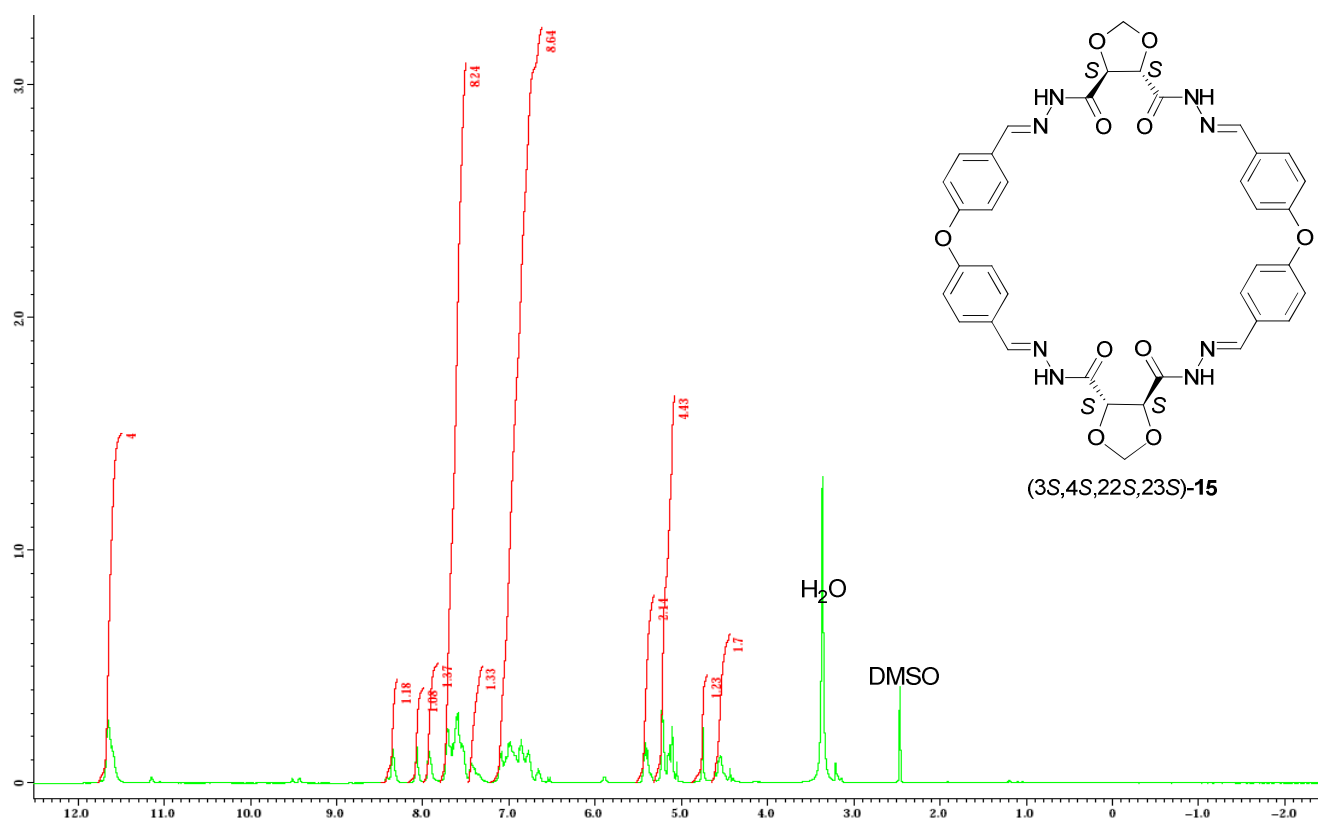


Figure 56. ^1H -NMR spectrum for macrocycle (**15**), DMSO- d_6 , 400 MHz.

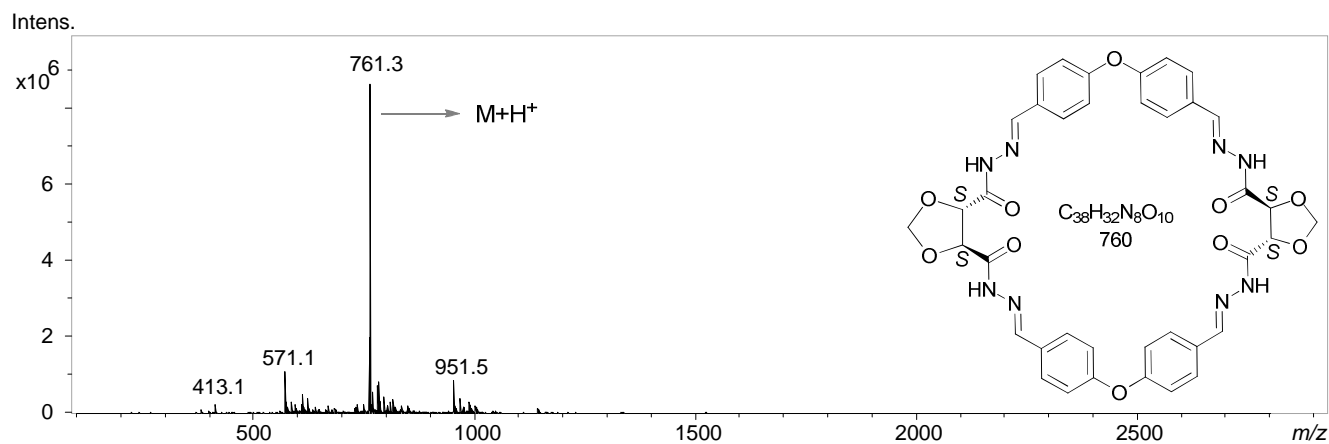


Figure 57. ESI-MS spectrum for macrocycle (**15**) from DMF and ACN (positive mode).

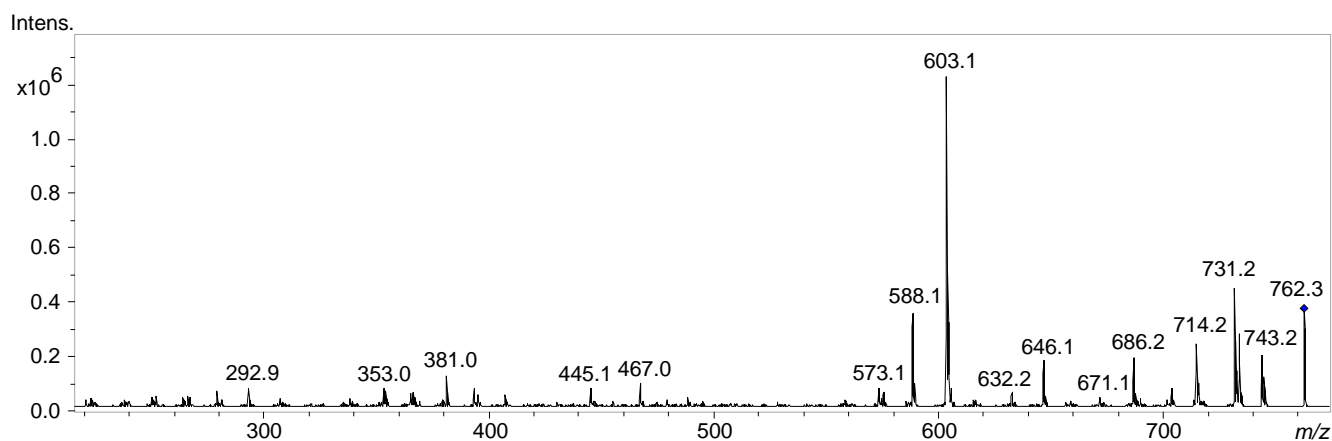
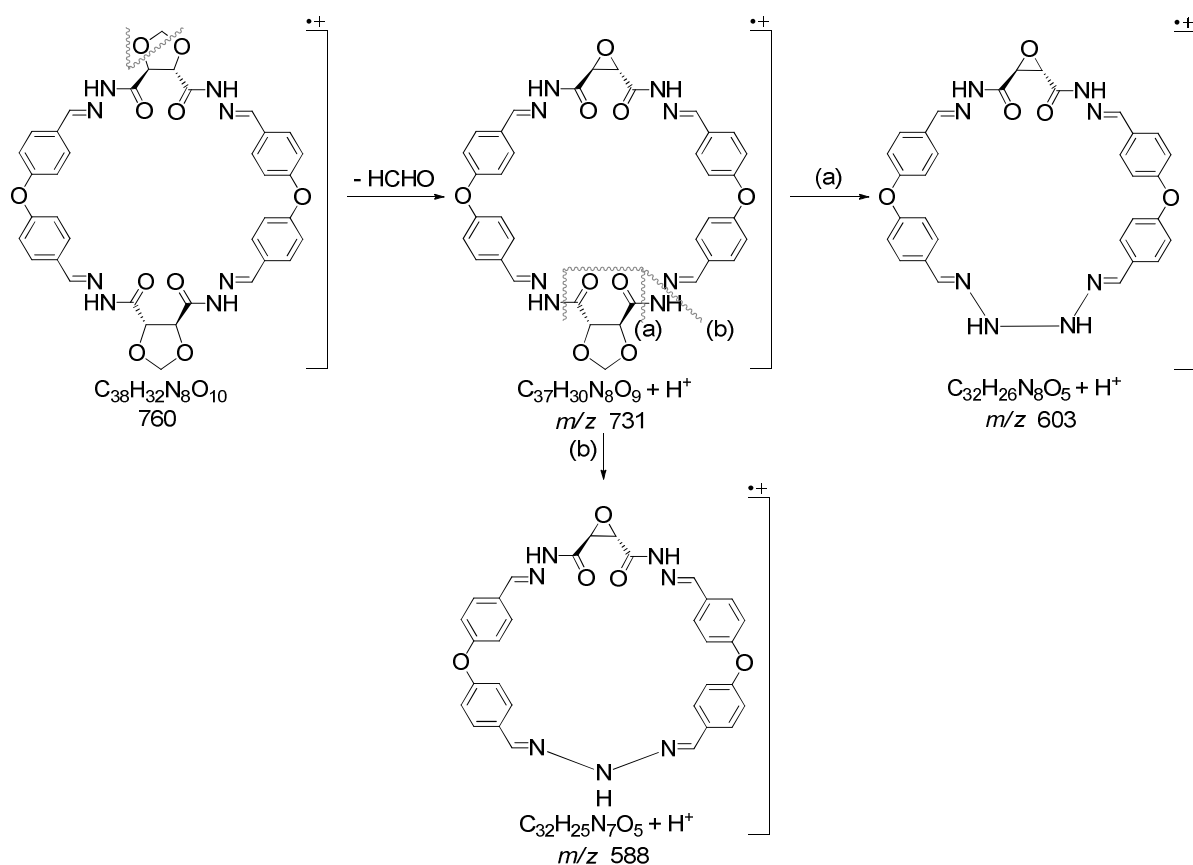


Figure 58. Tandem ESI- MS^2 spectrum for macrocycle (**15**) from DMF and ACN (positive mode).



Scheme 13. Proposed fragmentation mechanism for macrocycle (**15**), positive mode.

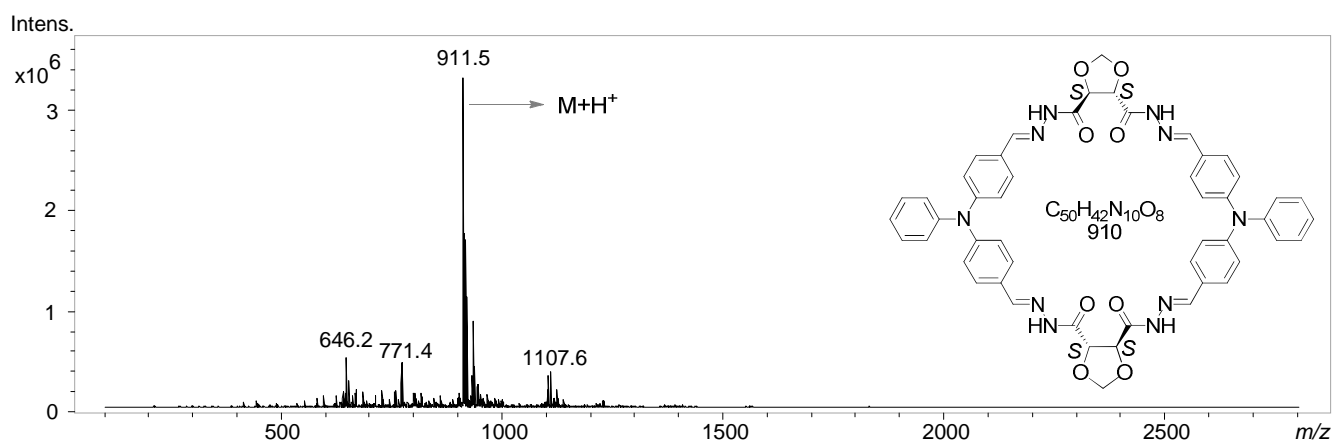


Figure 59. APCI-MS spectrum for macrocycle (**16**) from DMSO (positive mode).

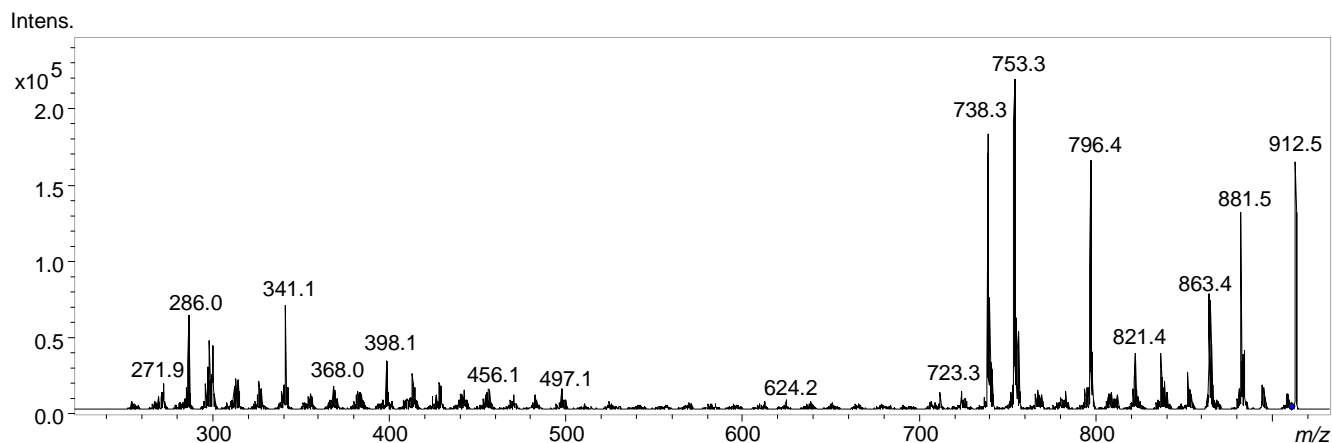
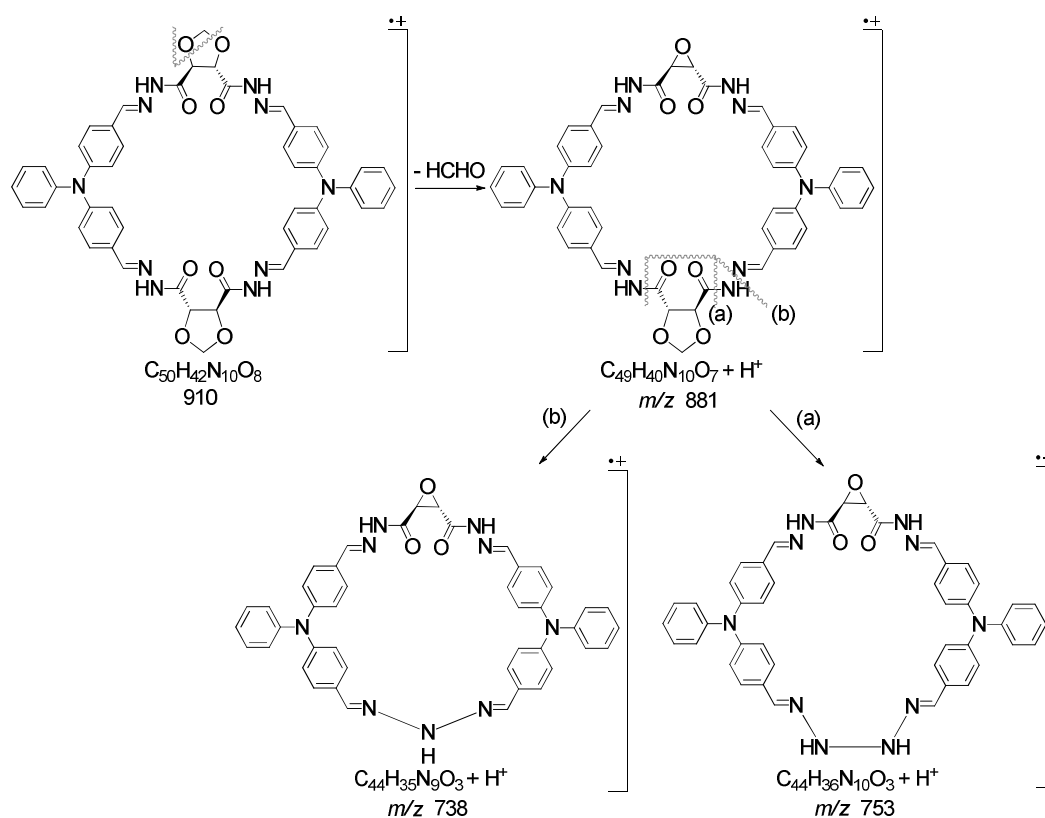


Figure 60. Tandem APCI-MS² spectrum for macrocycle (**16**) from DMSO (positive mode).



Scheme 14. Proposed fragmentation mechanism for macrocycle (16), positive mode.

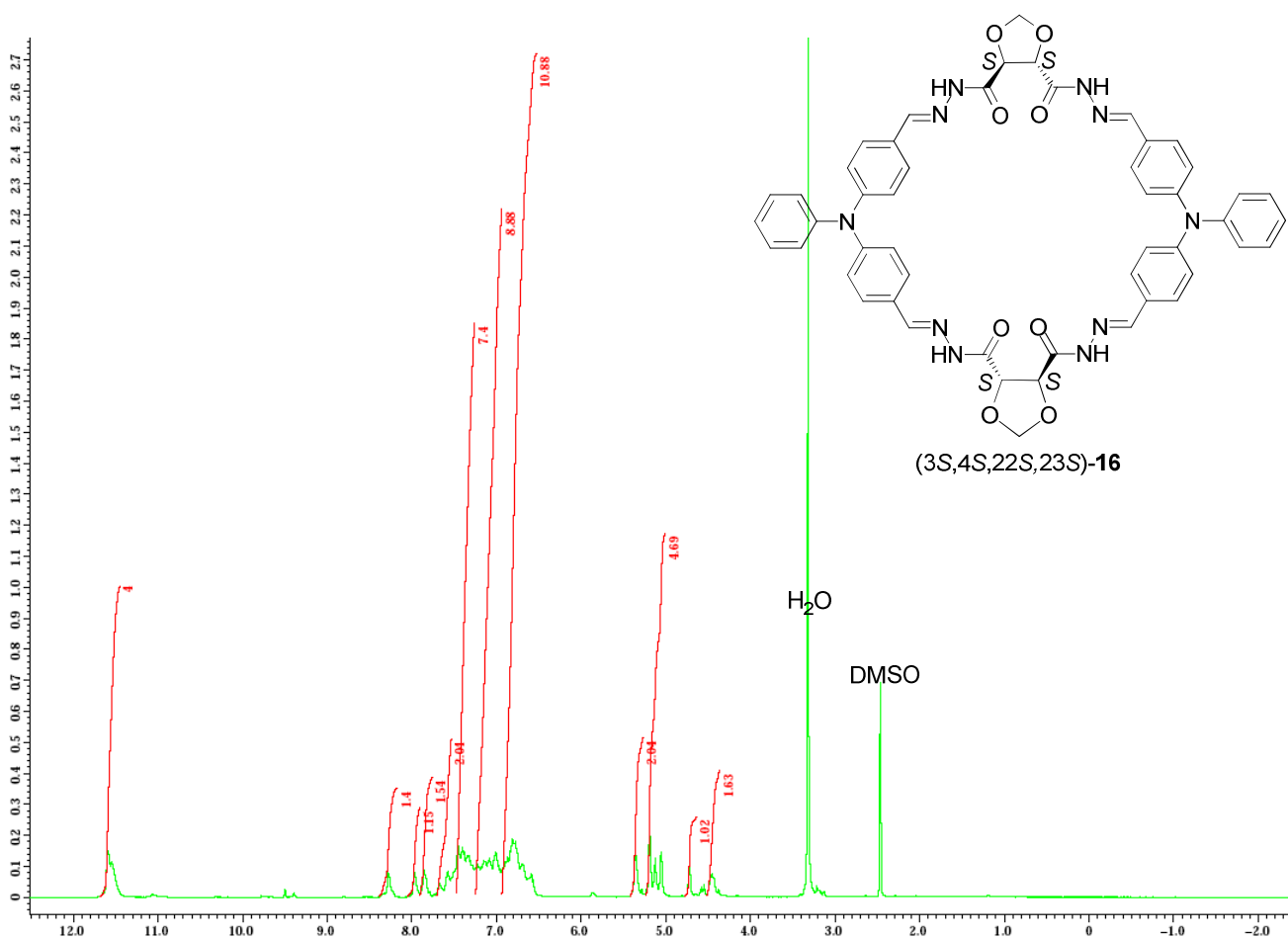


Figure 61. 1H -NMR spectrum for macrocycle (16), $DMSO-d_6$, 400 MHz.

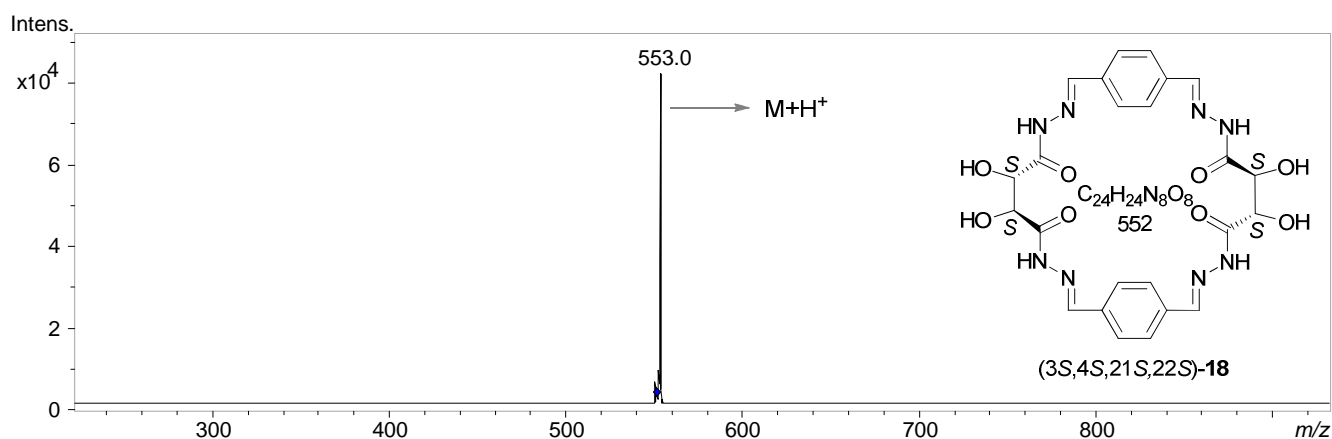


Figure 62. APCI-MS² spectrum for macrocycle (**18**) from DMSO (positive mode).

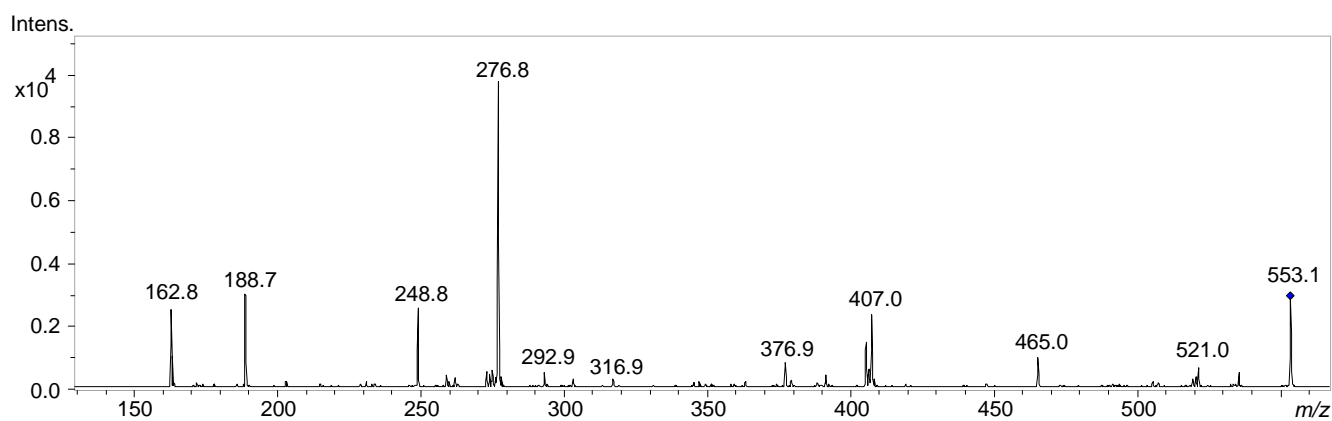
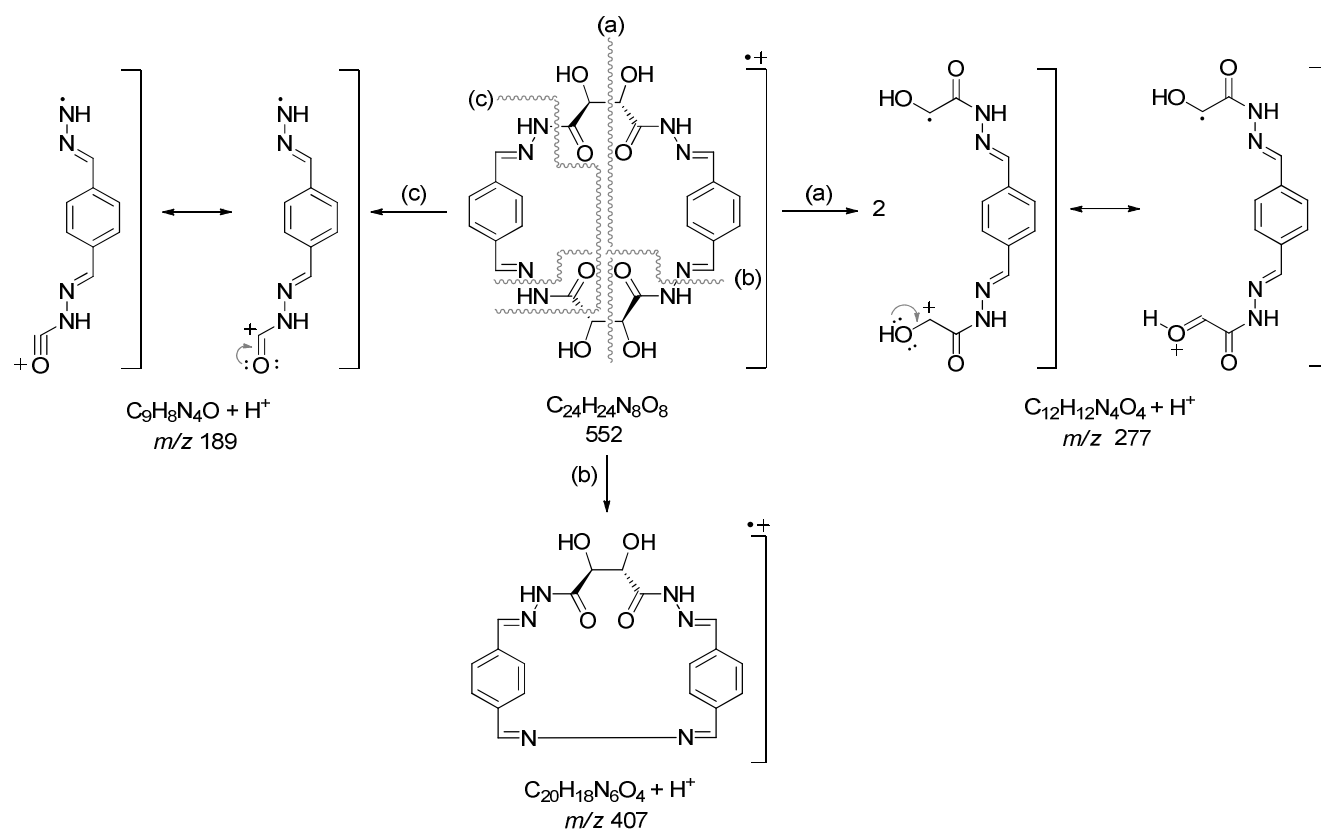


Figure 63. Tandem APCI-MS² spectrum for macrocycle (**18**) from DMSO (positive mode).



Scheme 15. Proposed fragmentation mechanism for macrocycle (**17**), positive mode.

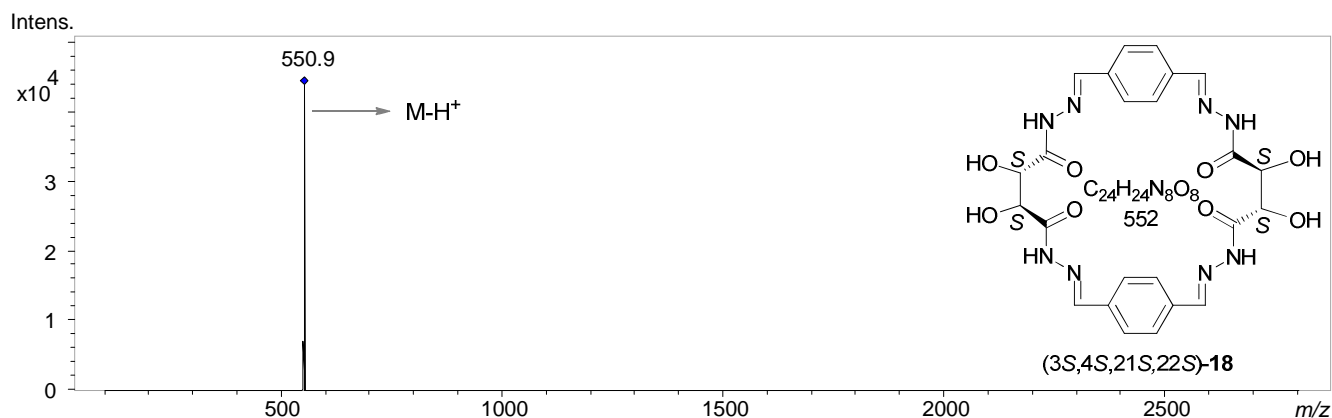


Figure 64. APCI-MS² spectrum for macrocycle (18) from DMSO (negative mode).

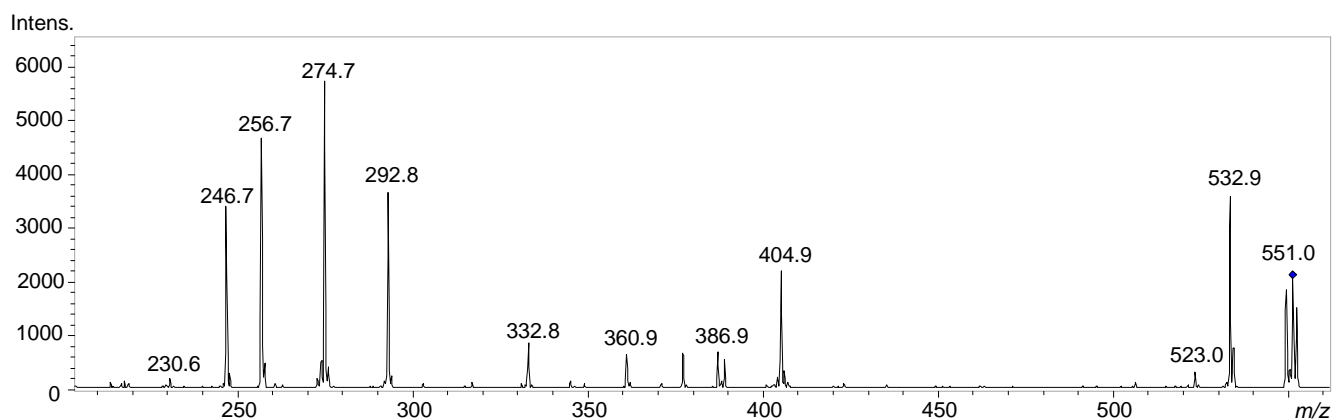
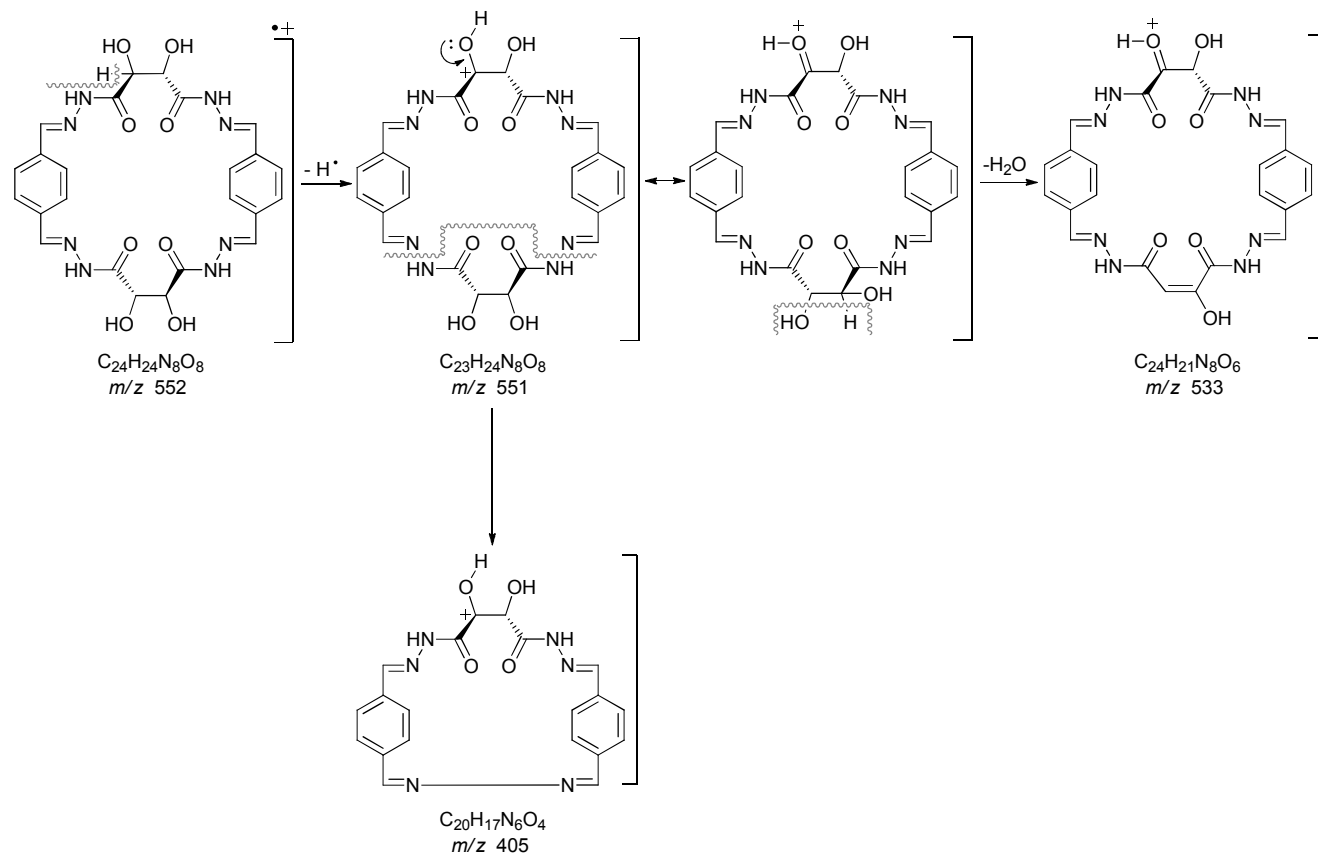


Figure 65. Tandem APCI-MS² spectrum for macrocycle (18) from DMSO (negative mode).



Scheme 16. Proposed fragmentation mechanism for macrocycle (18), negative mode.

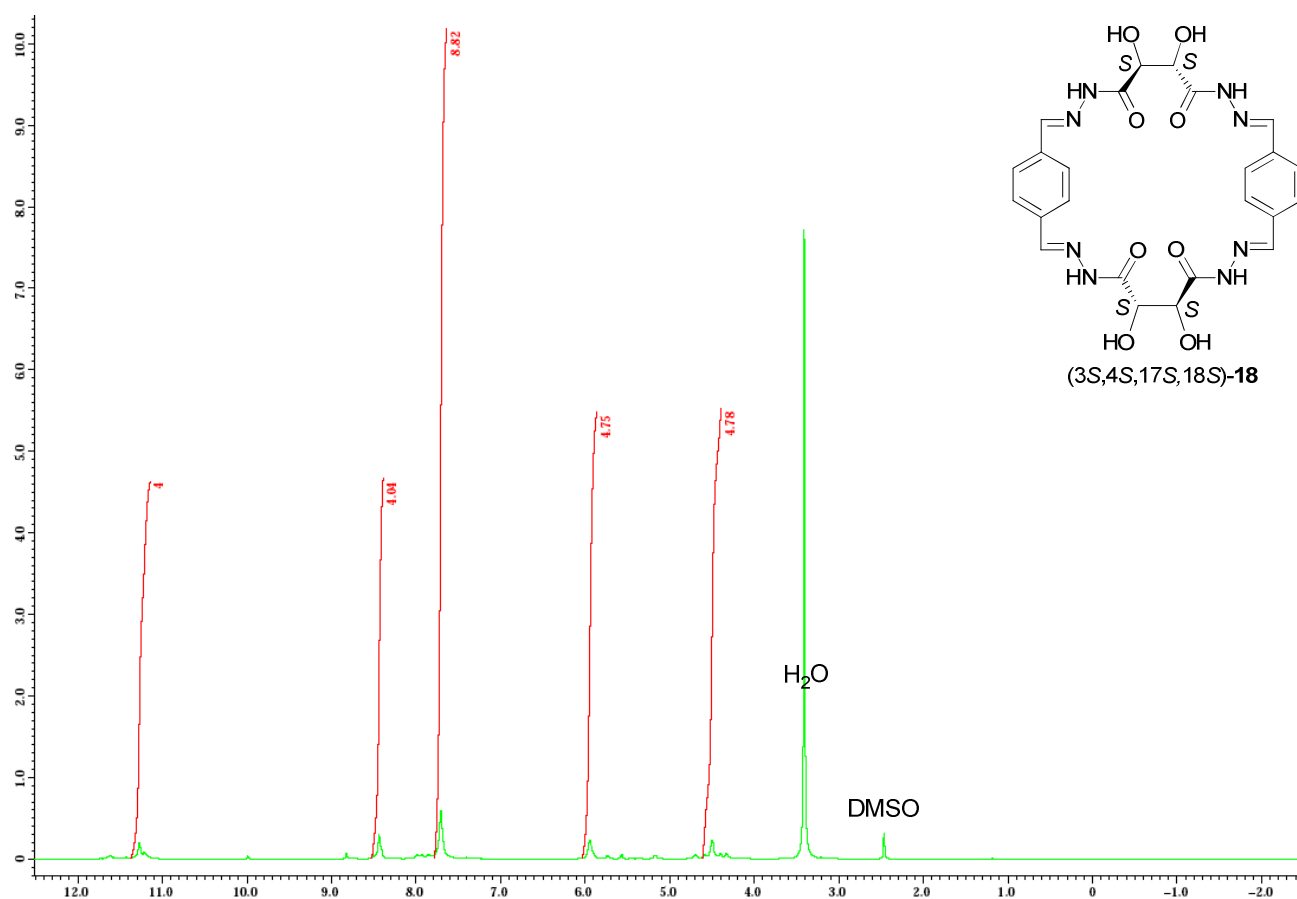


Figure 66. ^1H -NMR spectrum for macrocycle (18), DMSO- d_6 , 400 MHz.

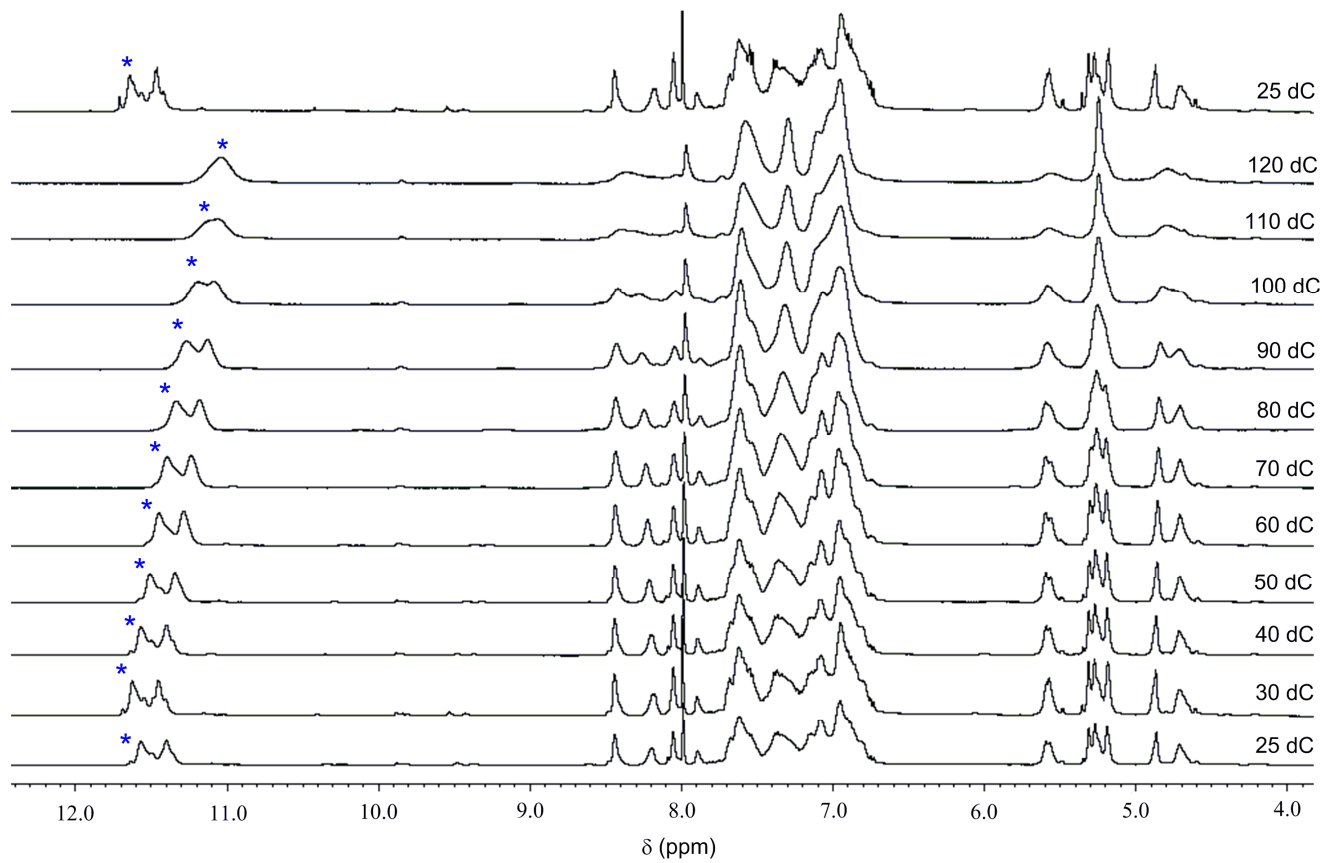


Figure 67. Stacked ^1H NMR spectra for macrocycle (14), 400 MHz, DMF- d_7 .

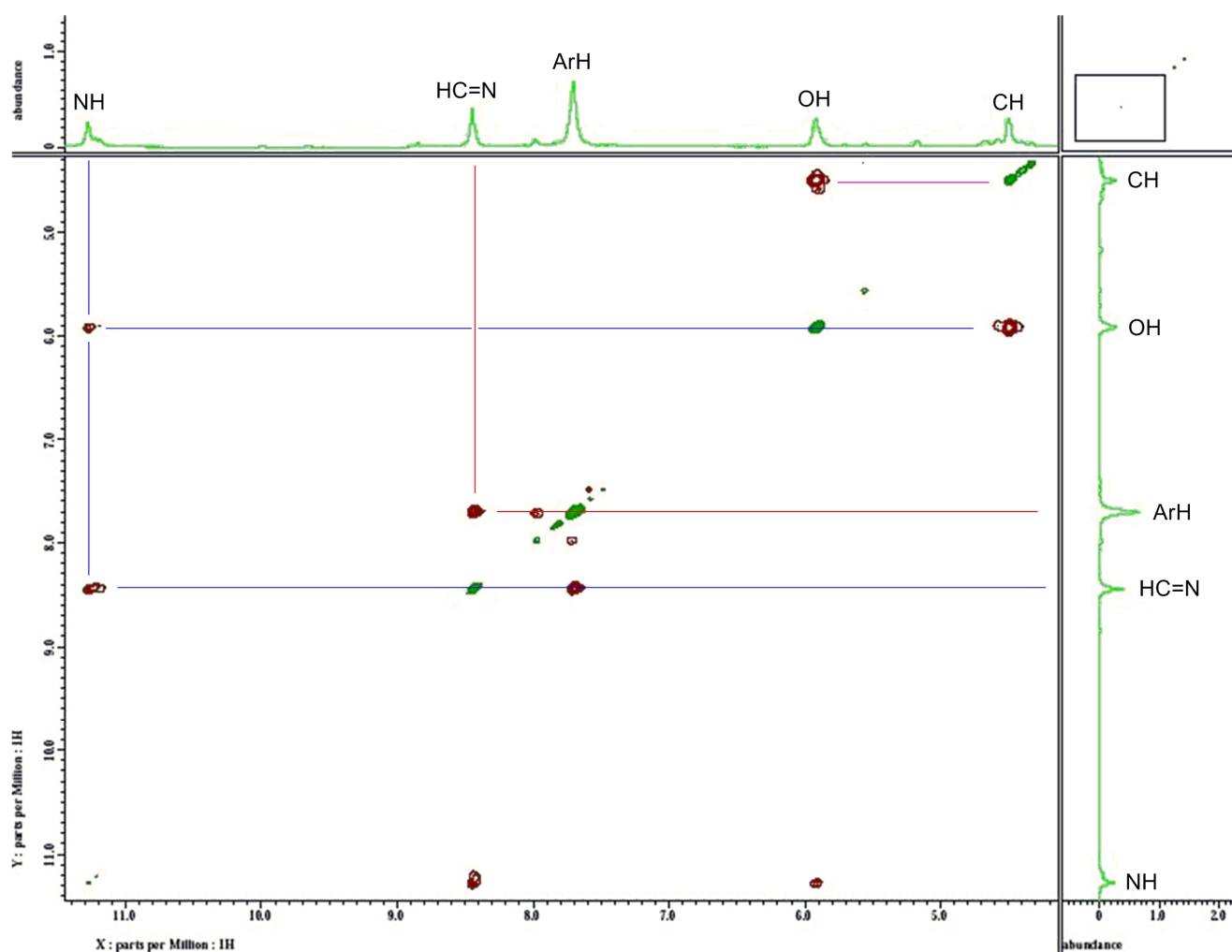


Figure 68. 2D-ROESY spectrum for macrocycle (**17**), 400 MHz, DMSO- d_6 .

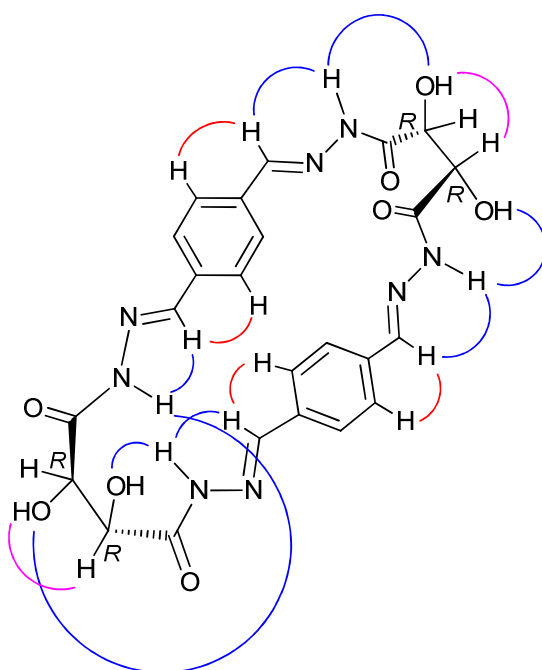


Figure 69. Through space interactions of different protons for macrocycle (**17**) as suggested by 2D-ROESY NMR spectrum.

Molecular modelling data for the computed structure (14a)

Geometry optimization, SemiEmpirical, PM3

Polak-Ribiere optimizer

Convergence limit = 0.0100000 Iteration limit = 50

Accelerate convergence = YES

Optimization algorithm = Polak-Ribiere

Criterion of RMS gradient = 0.0100 kcal/(Å mol) Maximum cycles = 3000

RHF Calculation:

Singlet state calculation

Number of electrons = 340

Number of Double Occupied Levels = 170

Charge on the System = 0

Total Orbitals = 314

ENERGIES AND GRADIENT

Total Energy = -242937.5595208 (kcal/mol)

Total Energy = -387.145596287 (a.u.)

Binding Energy = -12294.3055588 (kcal/mol)

Isolated Atomic Energy = -230643.2539620 (kcal/mol)

Electronic Energy = -2903965.4422912 (kcal/mol)

Core-Core Interaction = 2661027.8827704 (kcal/mol)

Heat of Formation = 44.9504412 (kcal/mol)

Gradient = 0.0079269 (kcal/mol/Å)

Molecular modelling data for the computed structure (14b)

Single Point, MolecularMechanics, AMBER

Total Energy = 119.979437 kcal/mol Gradient = 27.619543.

Bond = 50.4237 Angle = 16.5468 Dihedral = 61.4234 Vdw = 4.53074 Electrostatic = -12.9453.

Polak-Ribiere optimizer

Energy=37.585088 kcal/mol Gradient=0.009352 Converged=YES (864 cycles 1777 points).

Bond = 1.98755 Angle = 8.78296 Dihedral = 41.8076 Vdw = 4.14276 Electrostatic = -19.1358.

Supplementary Information:

Novel synthesis of enantiomerically pure dioxaspiro[4.5]decane tetra-carbohydrazide cyclophane macrocycles

Hany F. Nour, Agnieszka Golon, Adam Le-Gresley, and Nikolai Kuhnert*

****Corresponding Author:***

Prof. Dr. Nikolai Kuhnert, Fax: +49 421 200 3229; Tel: +49 421 200 3120; *E-mail:* n.kuhnert@jacobs-university.de, Jacobs University, Bremen, Germany.

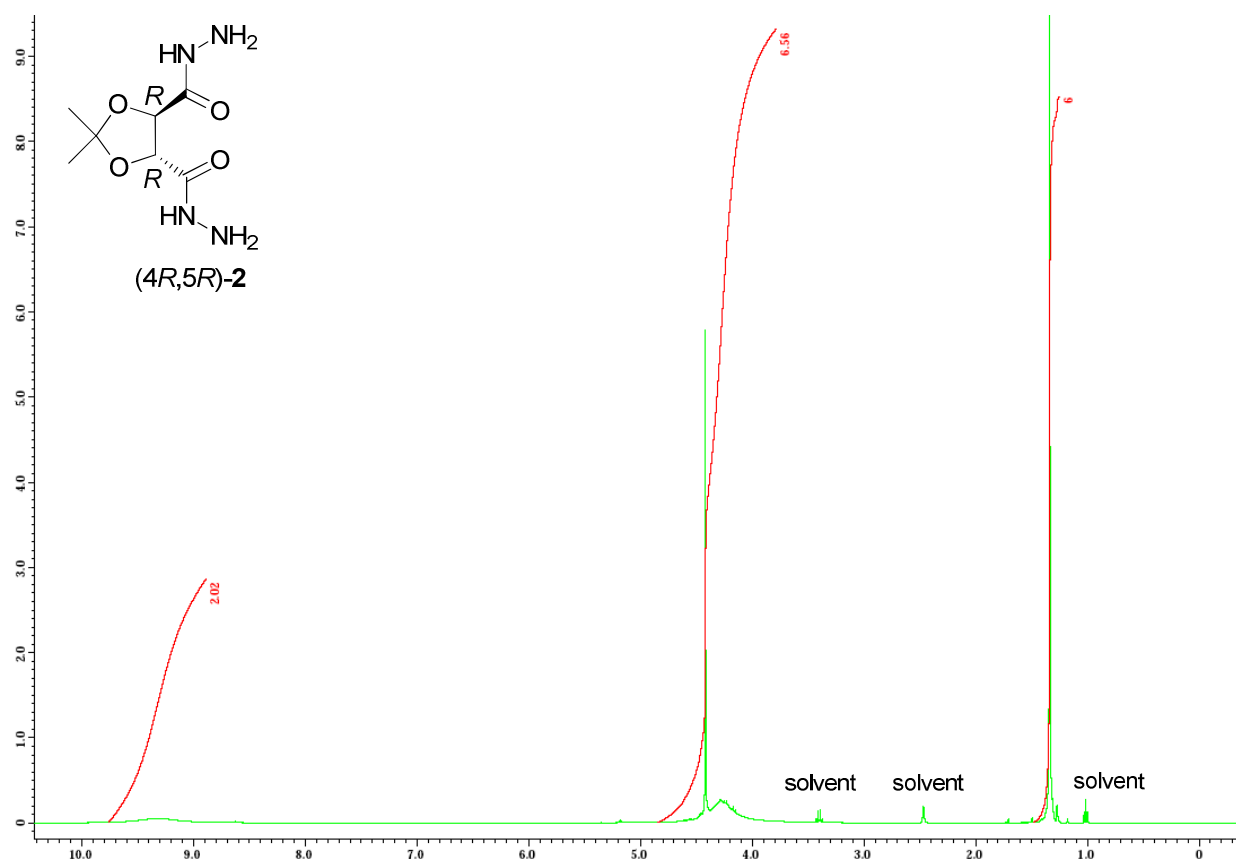


Figure 1. $^1\text{H-NMR}$ spectrum for dicarbohydrazide (**2**), DMSO- d_6 , 400 MHz.

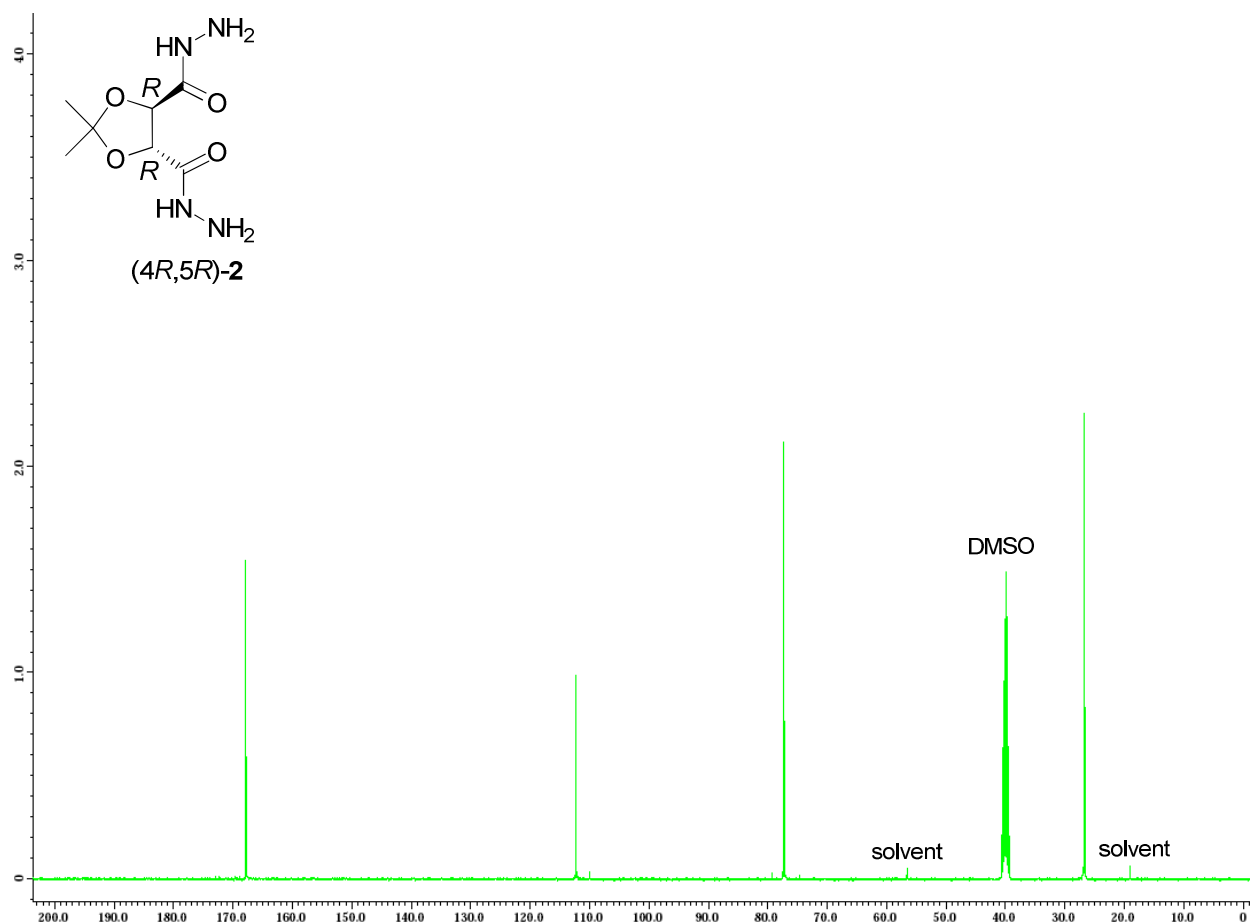


Figure 2. $^{13}\text{C-NMR}$ spectrum for dicarbohydrazide (**2**), DMSO- d_6 , 400 MHz.

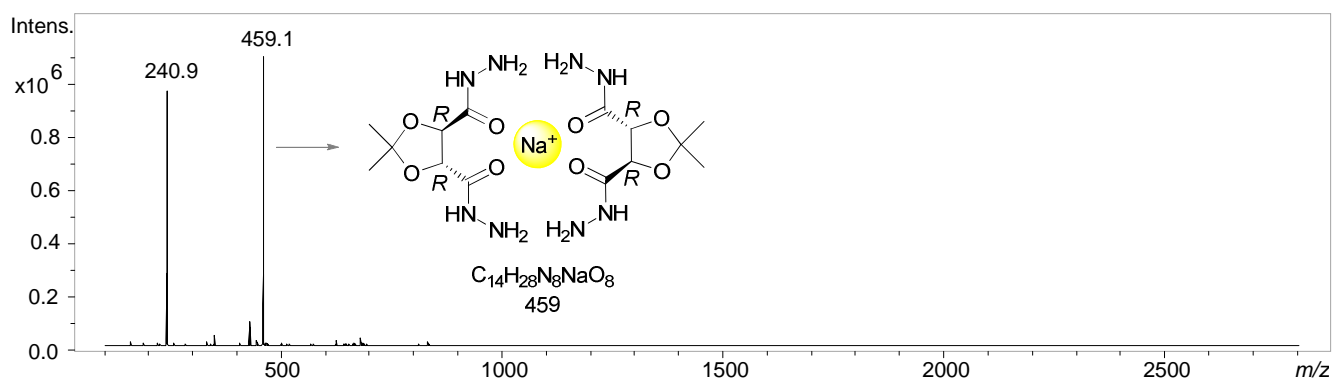


Figure 3. ESI-MS spectrum for dicarbohydrazide (2), from H₂O.

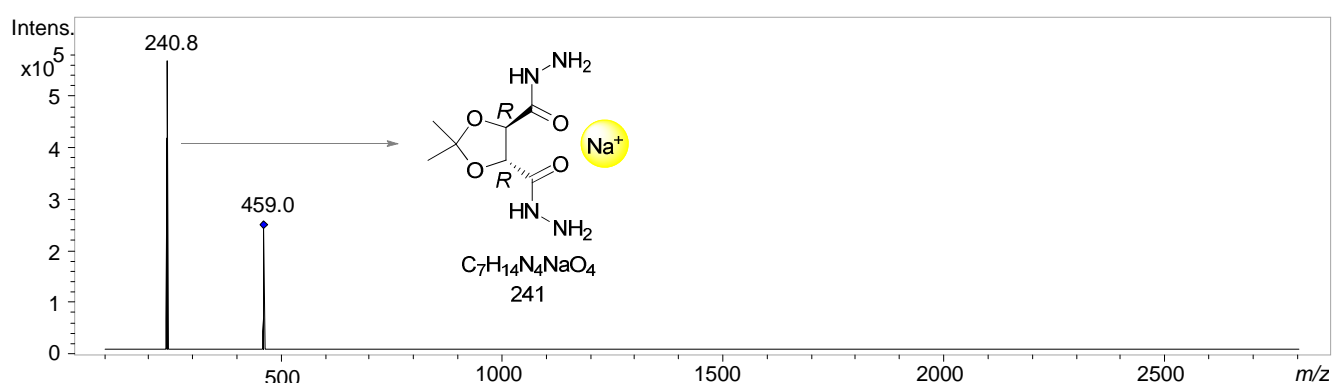


Figure 4. Tandem ESI-MS² spectrum for dicarbohydrazide (2), from H₂O.

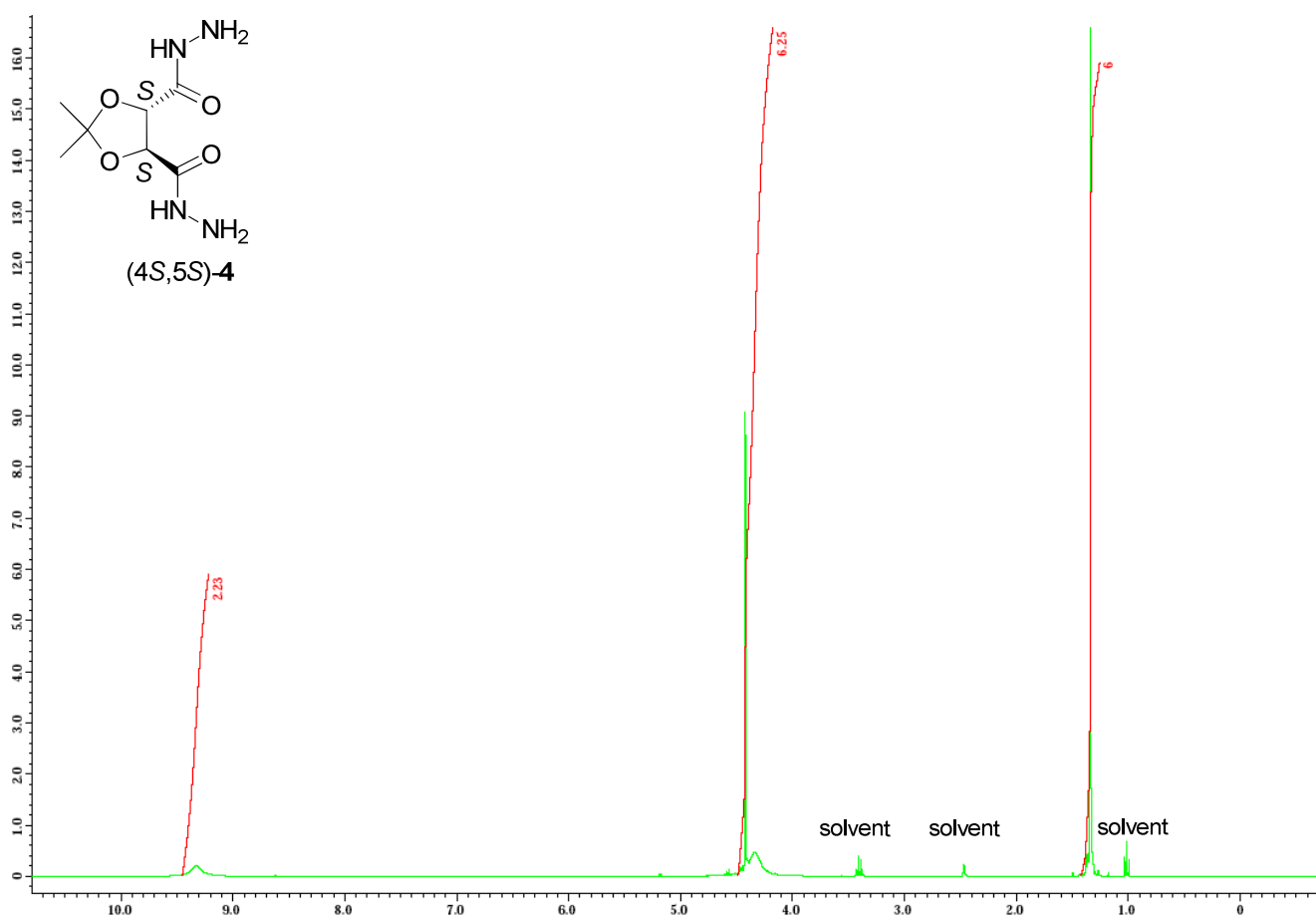


Figure 5. ¹H-NMR spectrum for dicarbohydrazide (4), DMSO-d₆, 400 MHz.

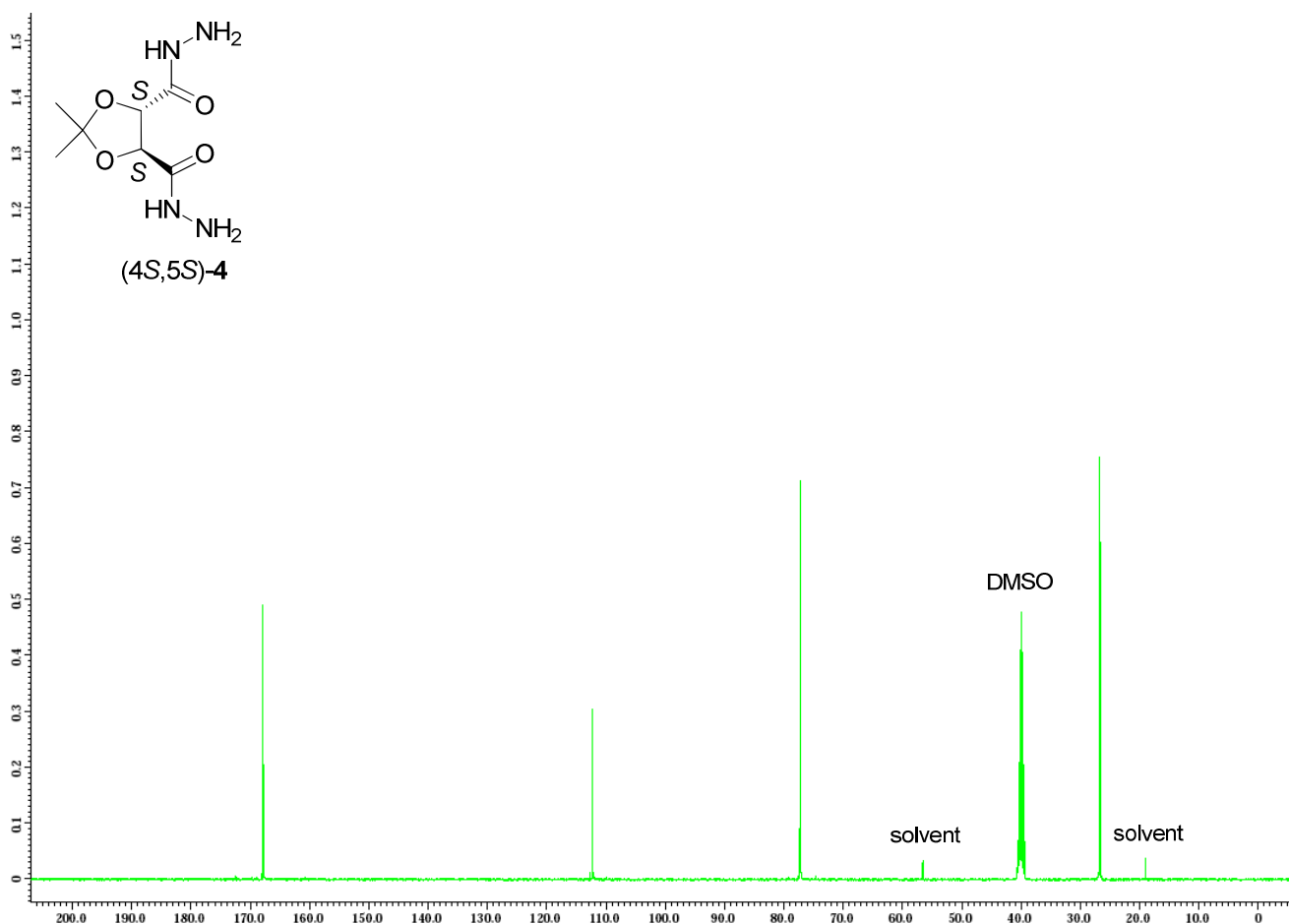


Figure 6. ^{13}C -NMR spectrum for dicarbohydrazide (**4**), DMSO- d_6 , 100 MHz.

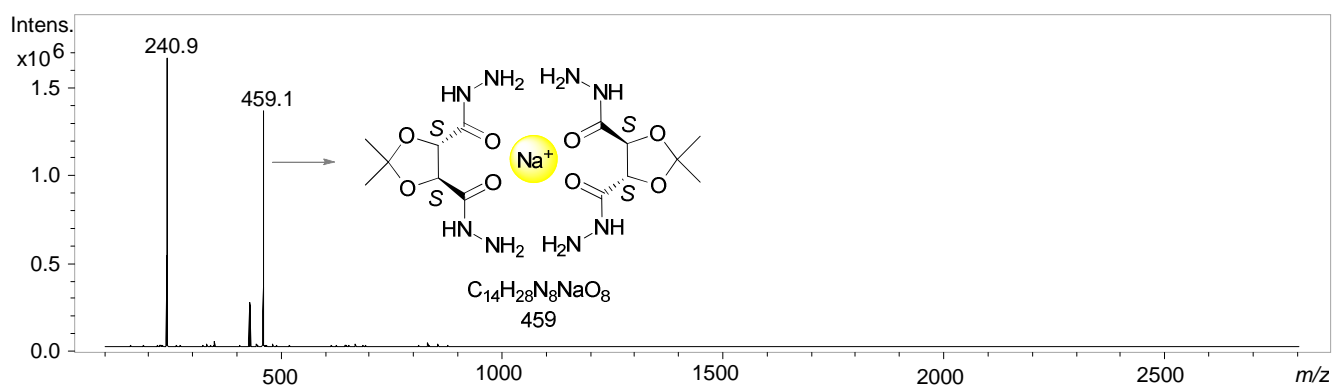


Figure 7. ESI-MS spectrum for dicarbohydrazide (**4**), from H_2O .

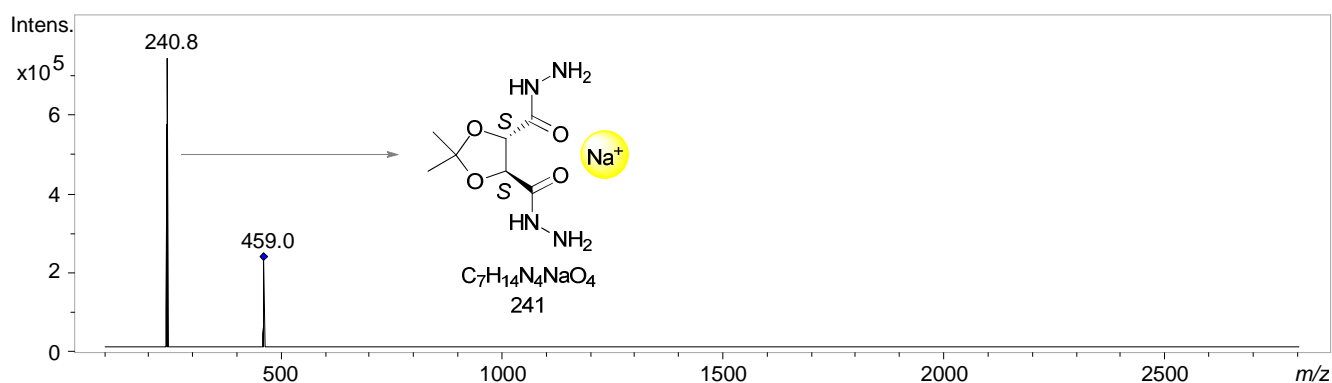


Figure 8. Tandem ESI- MS^2 spectrum for dicarbohydrazide (**4**), from H_2O .

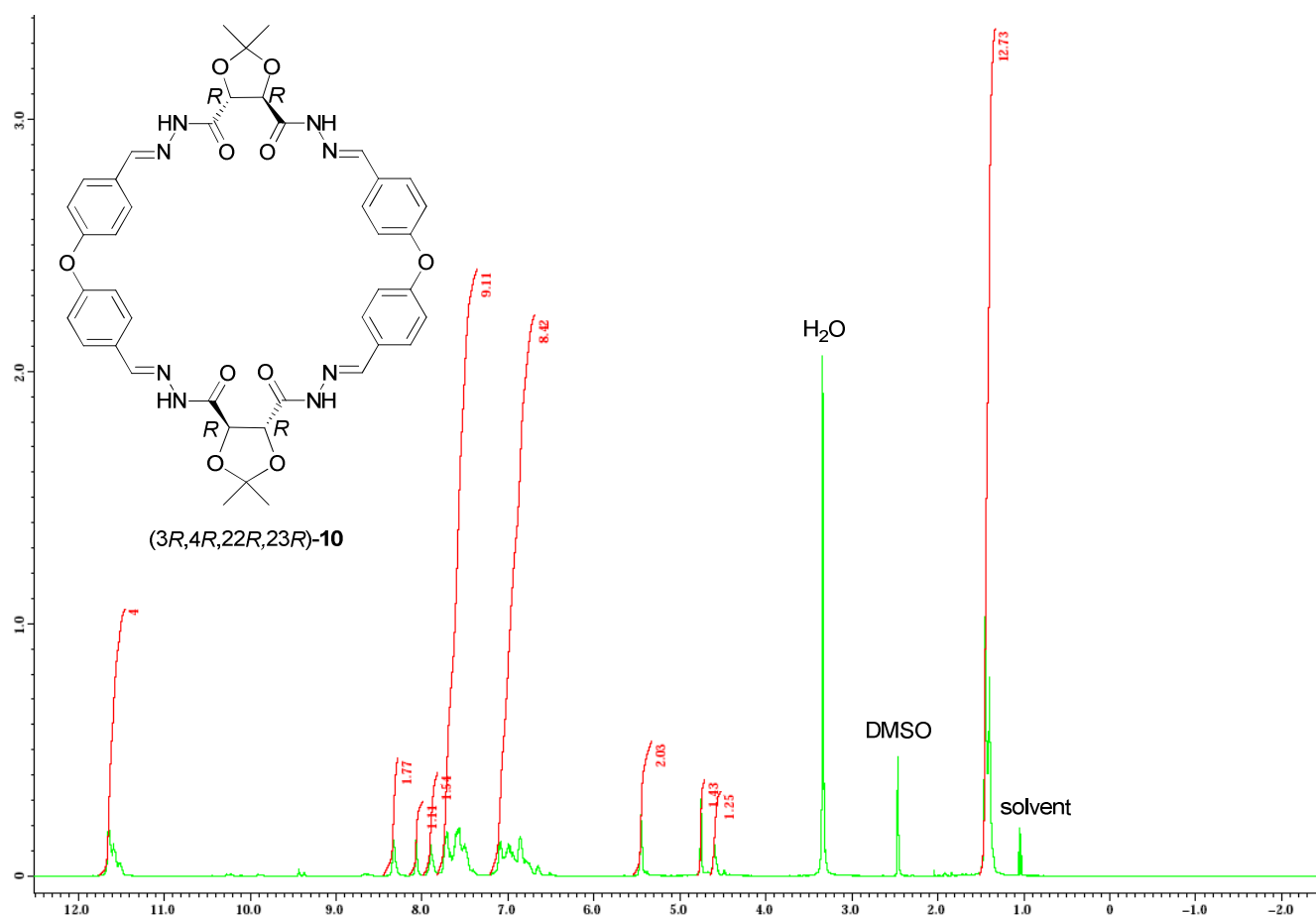


Figure 9. ^1H -NMR spectrum for macrocycle (**10**), DMSO- d_6 , 400 MHz.

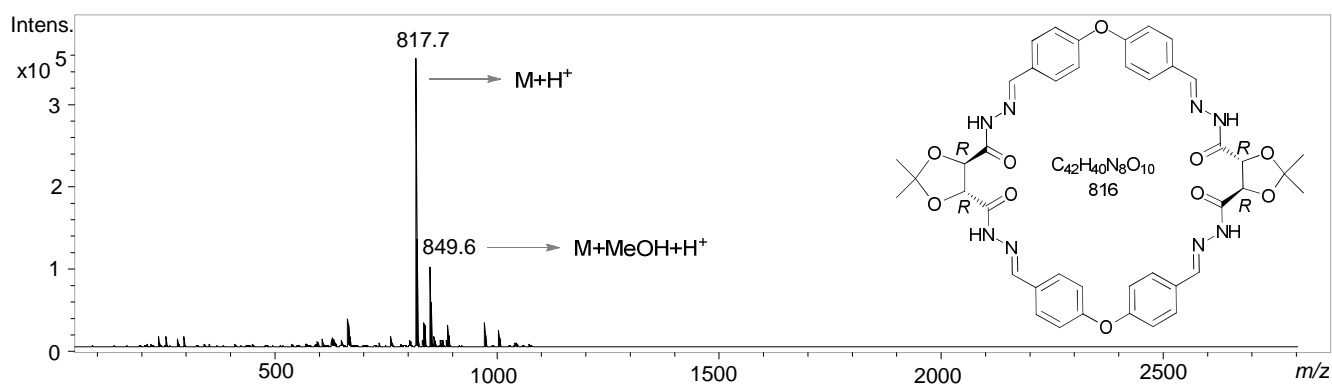


Figure 10. APCI-MS spectrum for macrocycle (**10**), from DMSO.

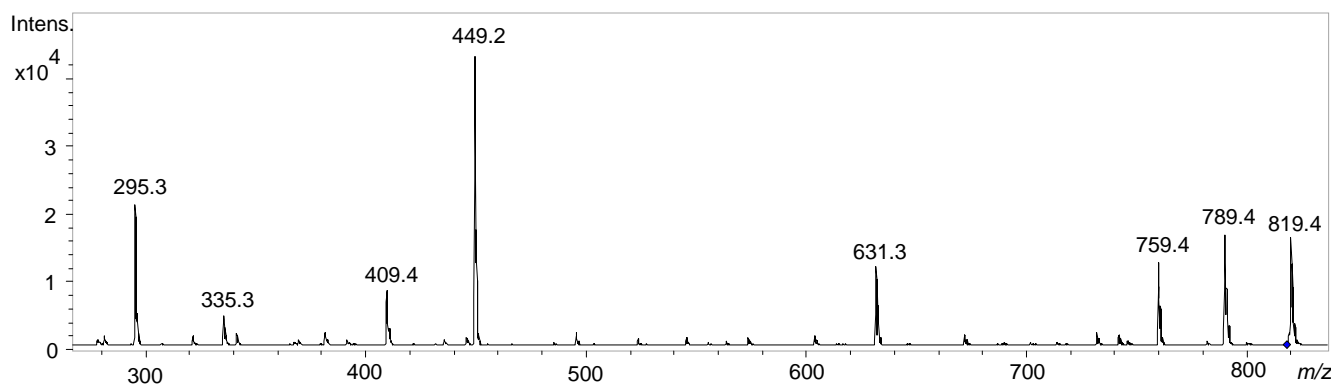


Figure 11. Tandem APCI-MS² spectrum for macrocycle (**10**), from DMSO.

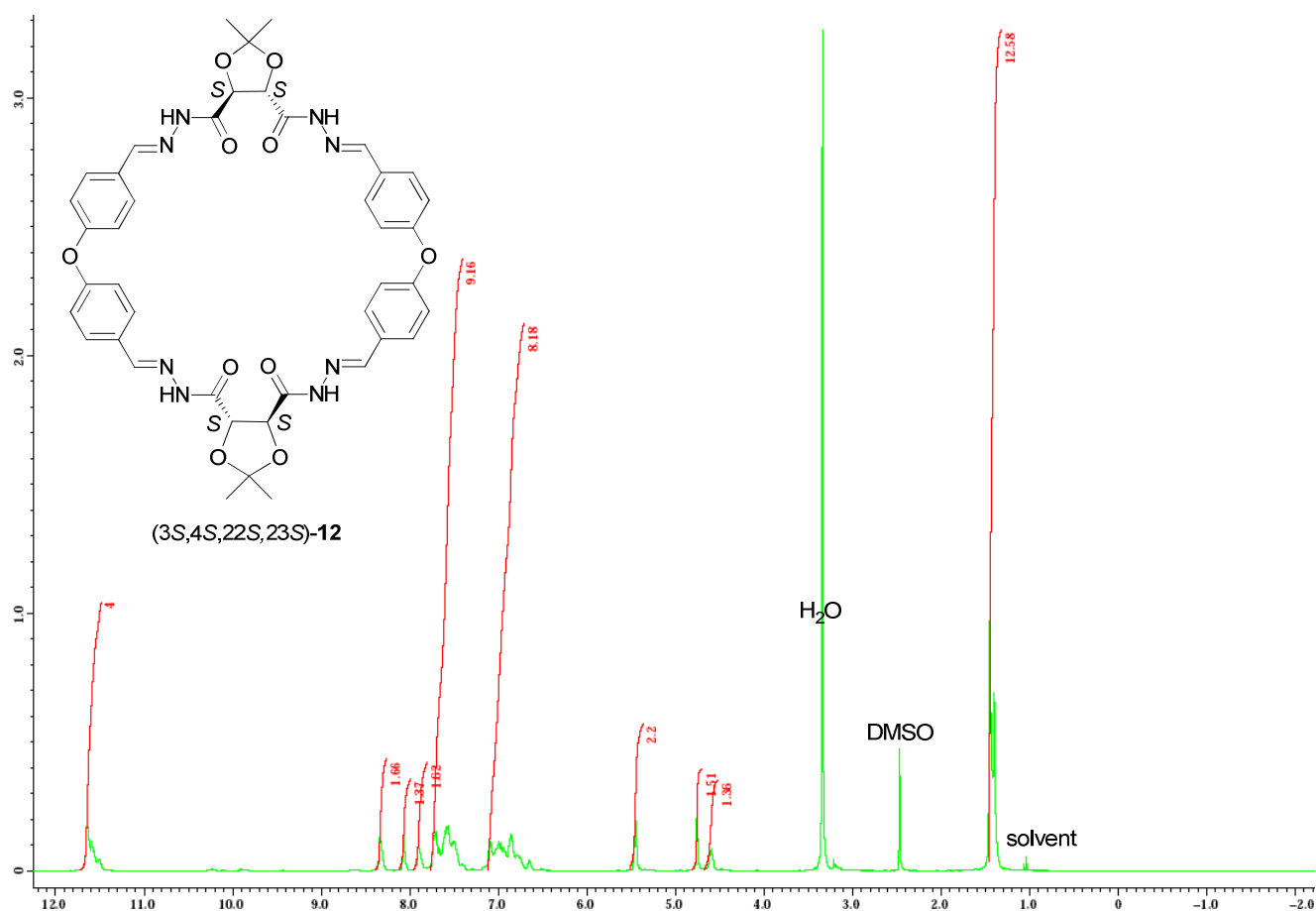


Figure 12. ¹H-NMR spectrum for macrocycle (12), DMSO-d₆, 400 MHz.

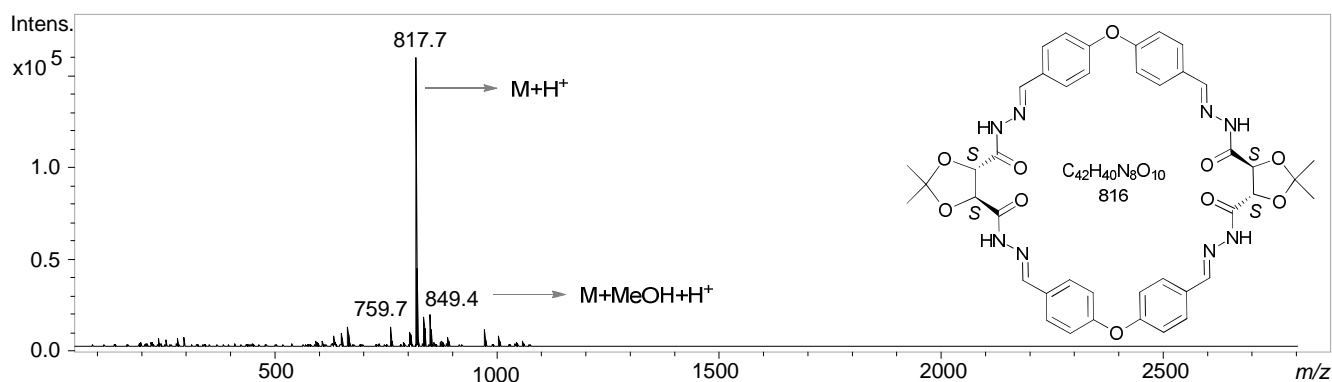


Figure 13. APCI-MS spectrum for macrocycle (12), from DMSO.

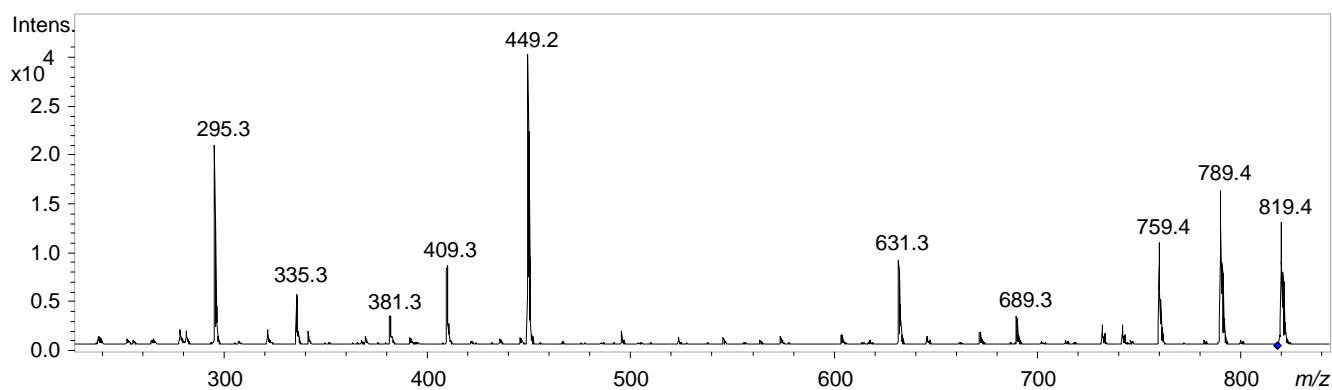


Figure 14. Tandem APCI-MS² spectrum for macrocycle (12), from DMSO.

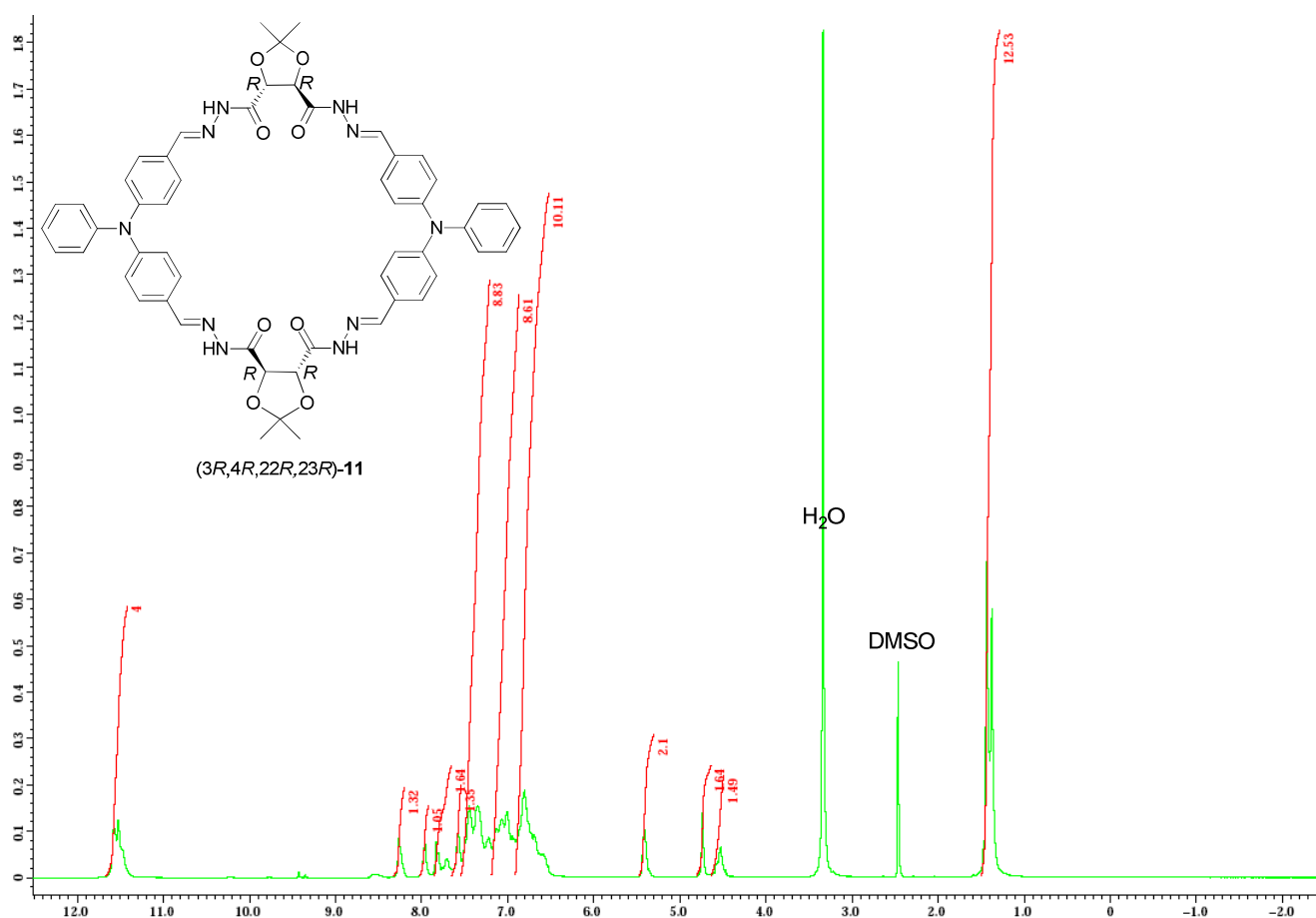


Figure 15. ¹H-NMR spectrum for macrocycle (**11**), DMSO-d₆, 400 MHz.

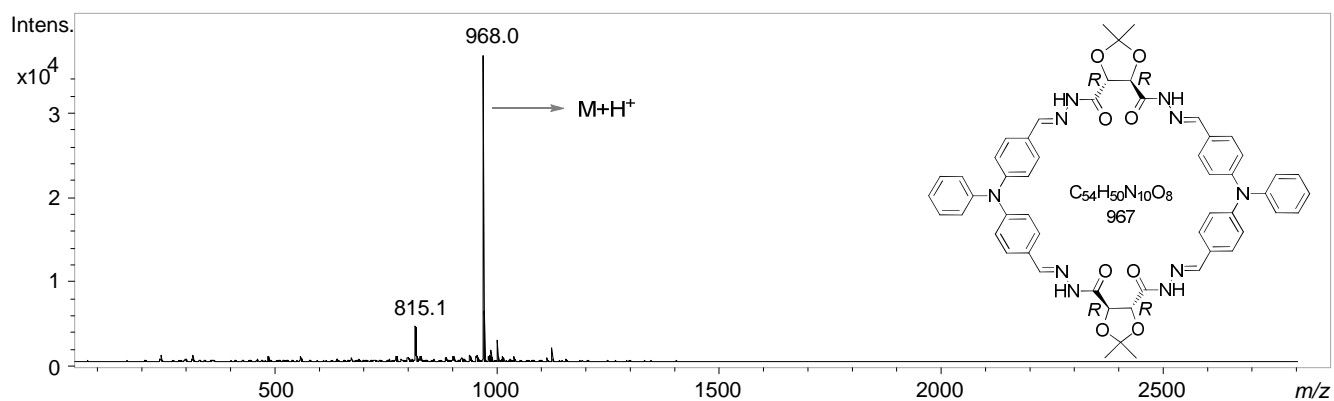


Figure 16. APCI-MS spectrum for macrocycle (**11**), from DMSO.

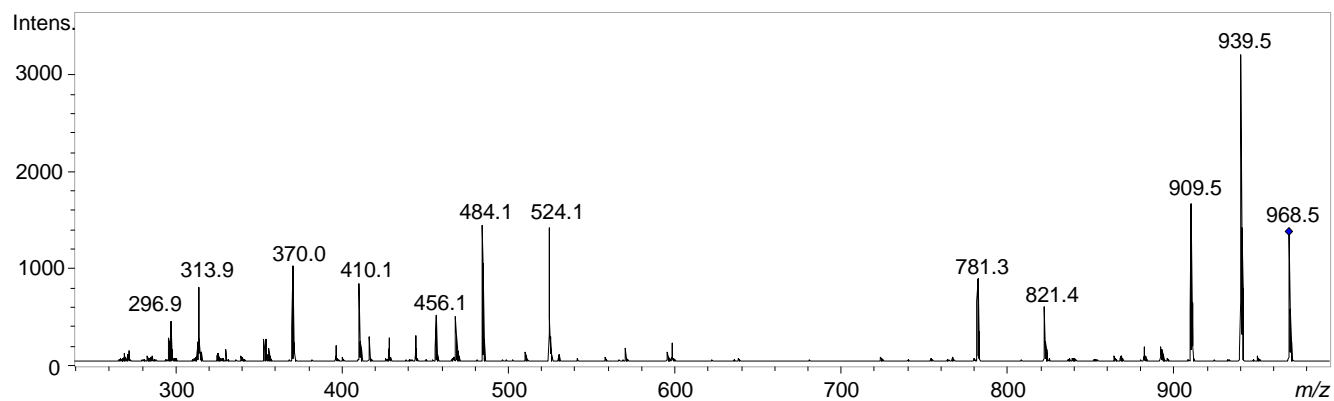
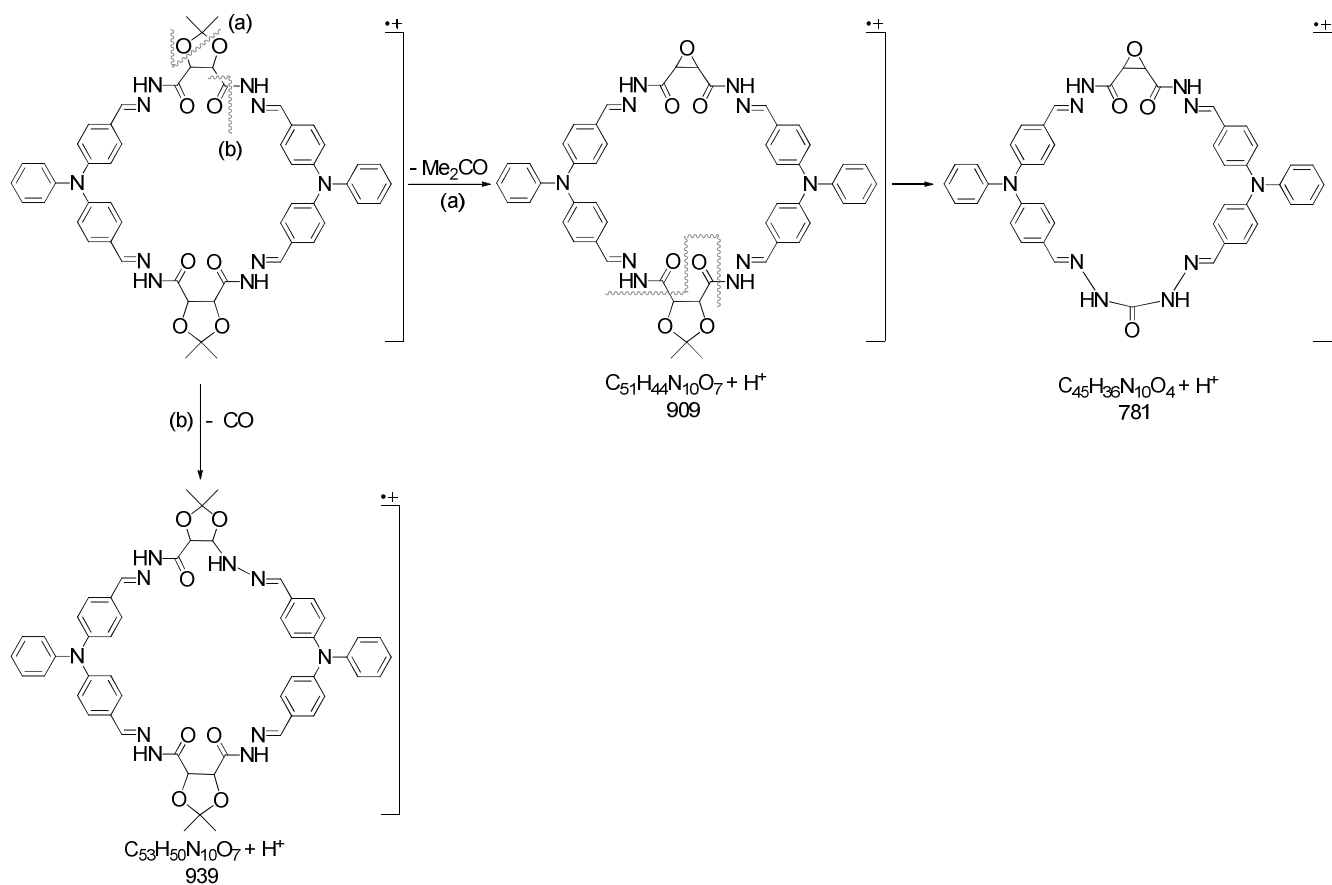


Figure 17. Tandem APCI-MS² spectrum for macrocycle (**11**), from DMSO.



Scheme 1. Suggested fragmentation mechanism for macrocycle (**11**).

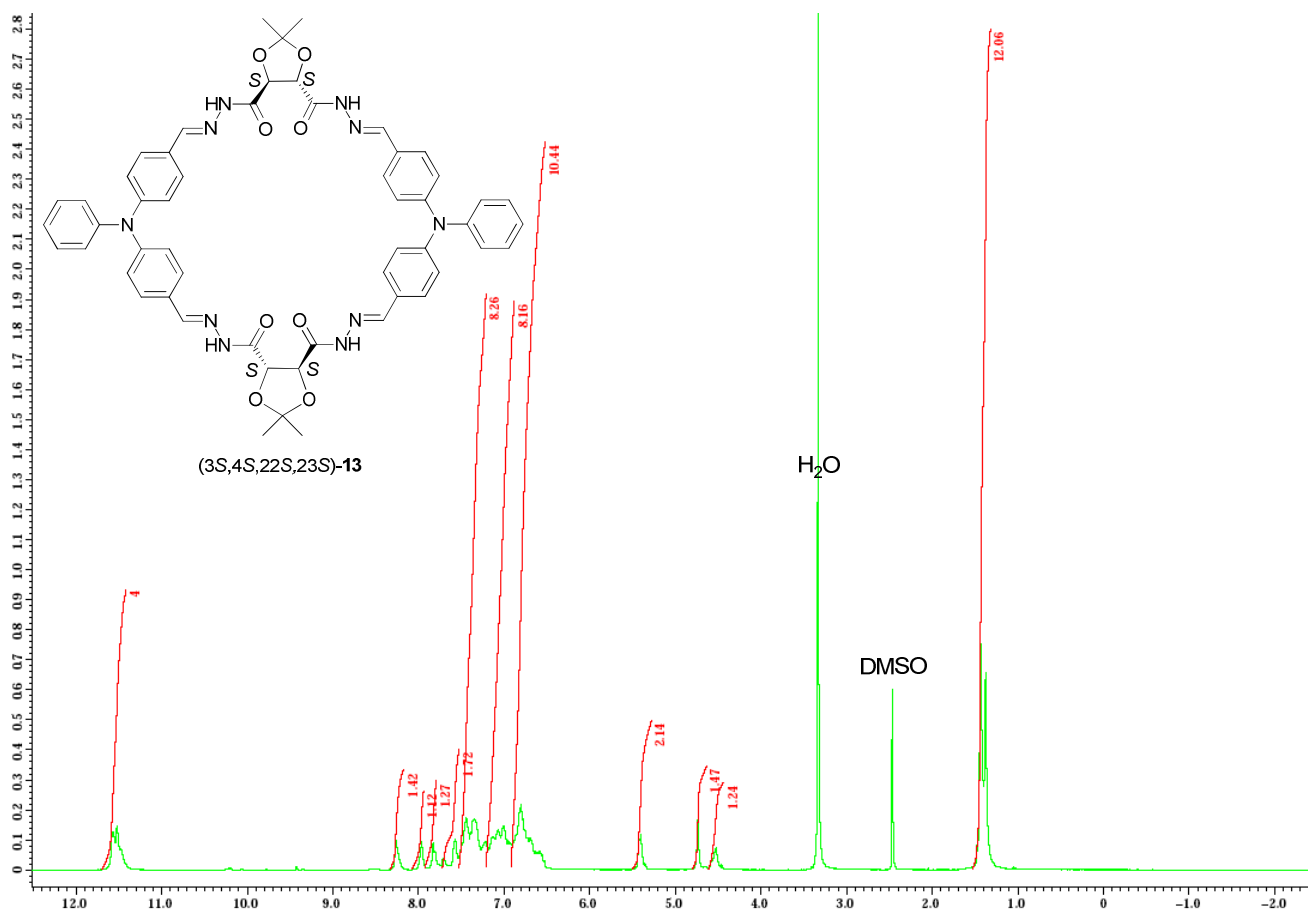


Figure 18. ¹H-NMR spectrum for macrocycle (**13**), DMSO-d₆, 400 MHz.

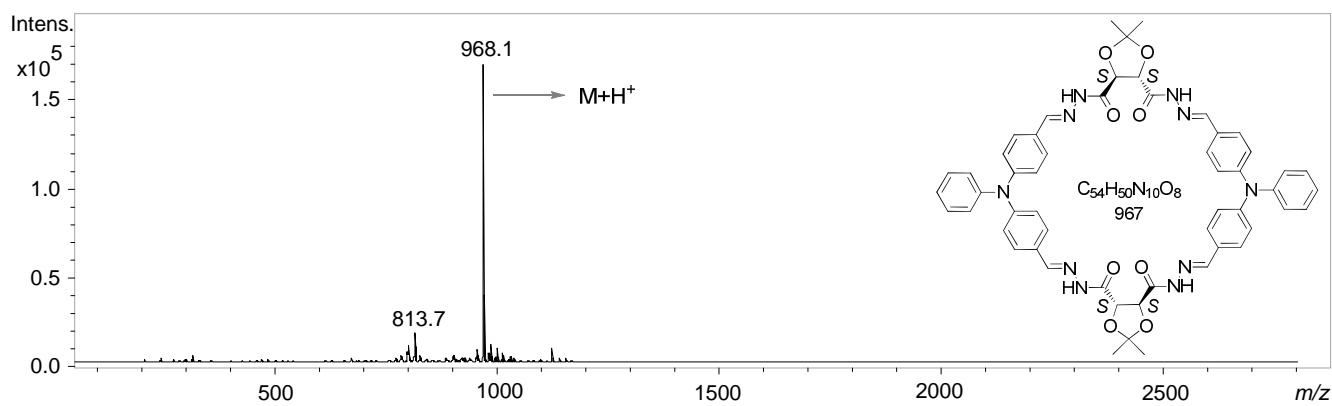


Figure 19. APCI-MS spectrum for macrocycle (13), from DMSO.

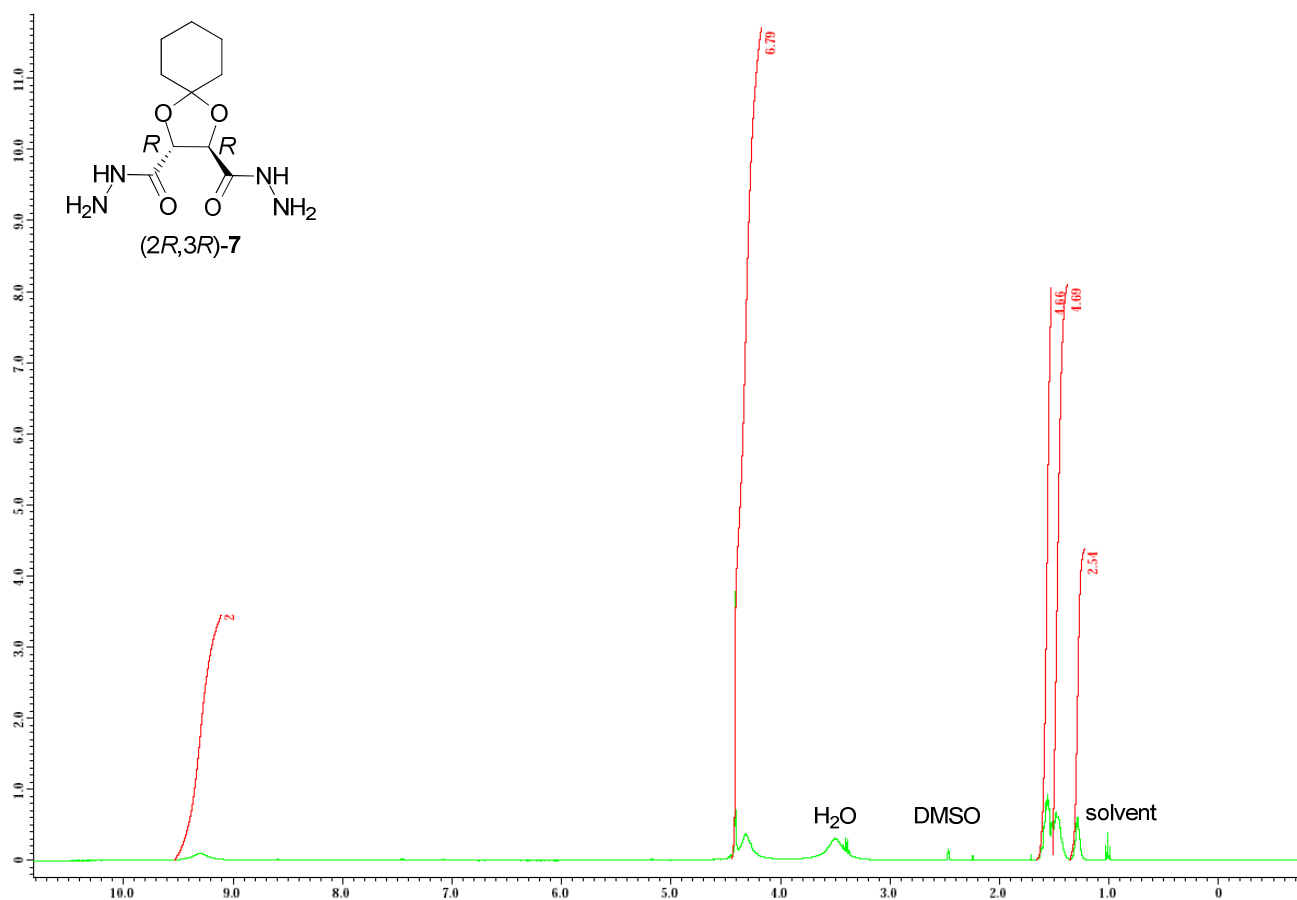


Figure 20. ¹H-NMR spectrum for dicarbohydrazide (7), DMSO-d₆, 400 MHz.

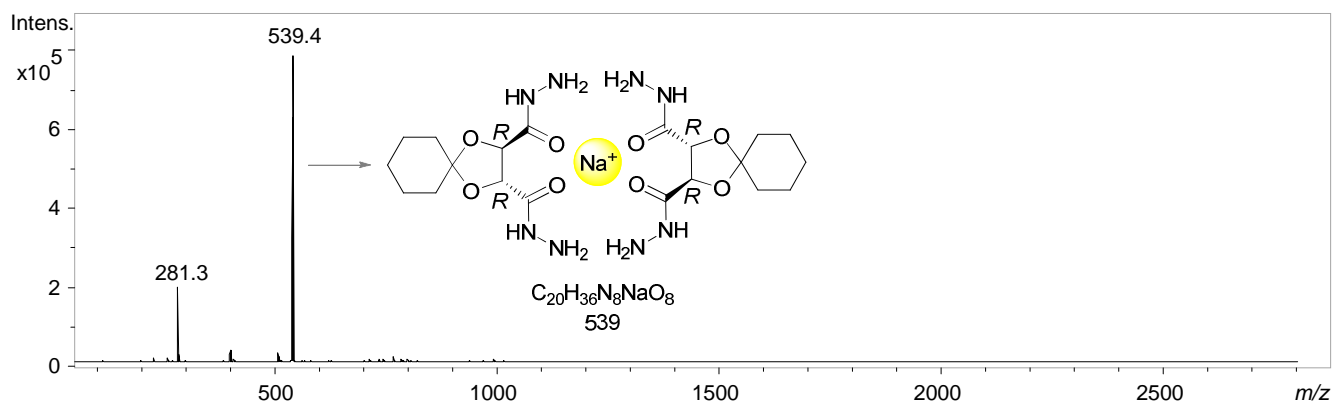


Figure 21. ESI-MS spectrum for dicarbohydrazide (7), from H₂O.

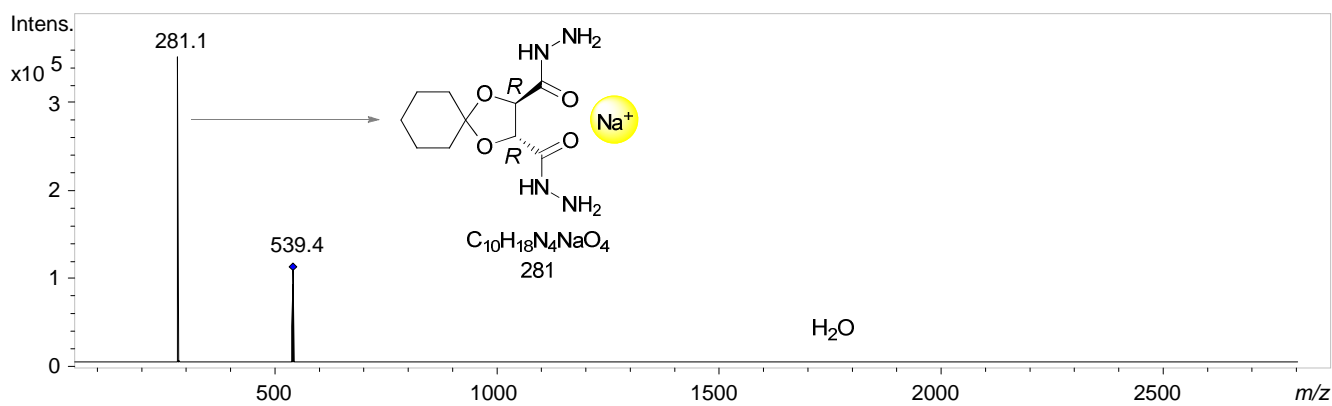


Figure 22. Tandem ESI-MS² spectrum for dicarbohydrazide (**7**), from H₂O.

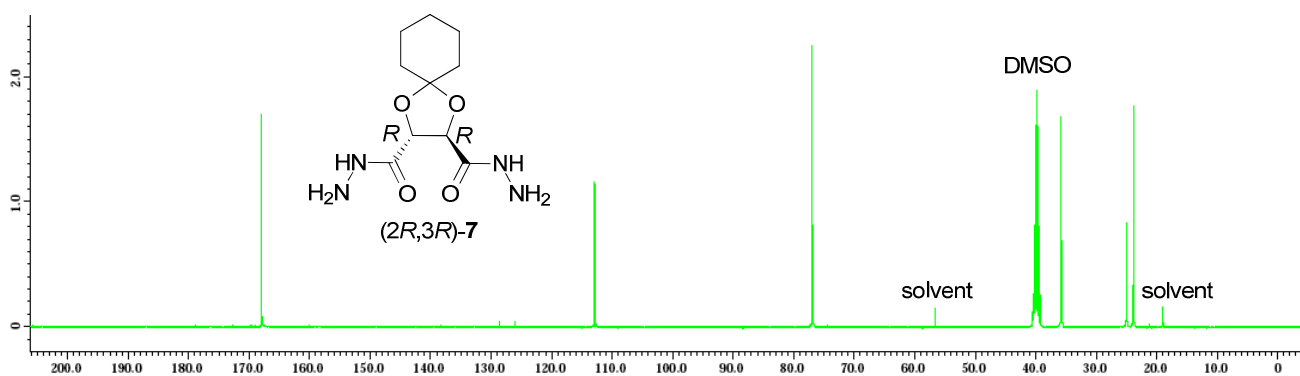


Figure 23. ¹³C-NMR spectrum for dicarbohydrazide (**7**), DMSO-d₆, 100 MHz.

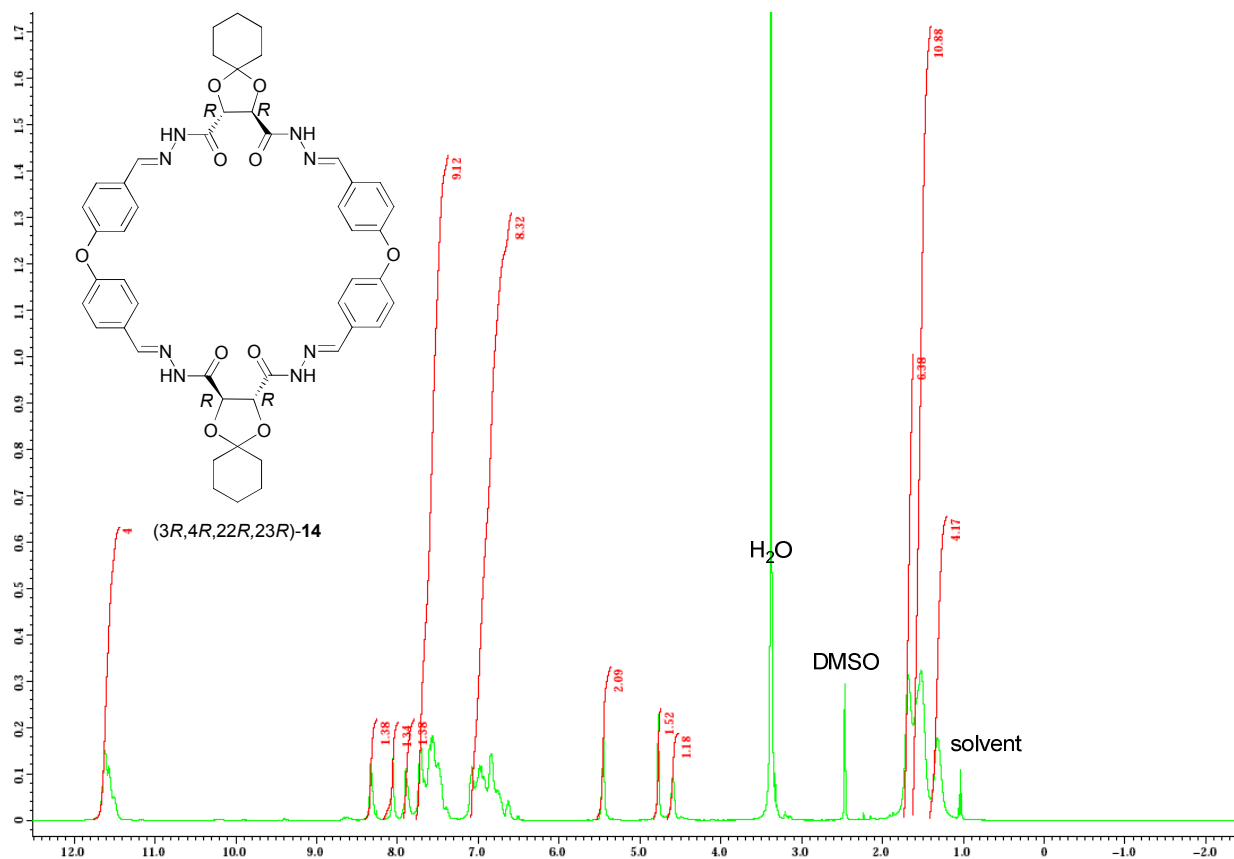


Figure 24. ¹H-NMR spectrum for macrocycle (**14**), DMSO-d₆, 400 MHz.

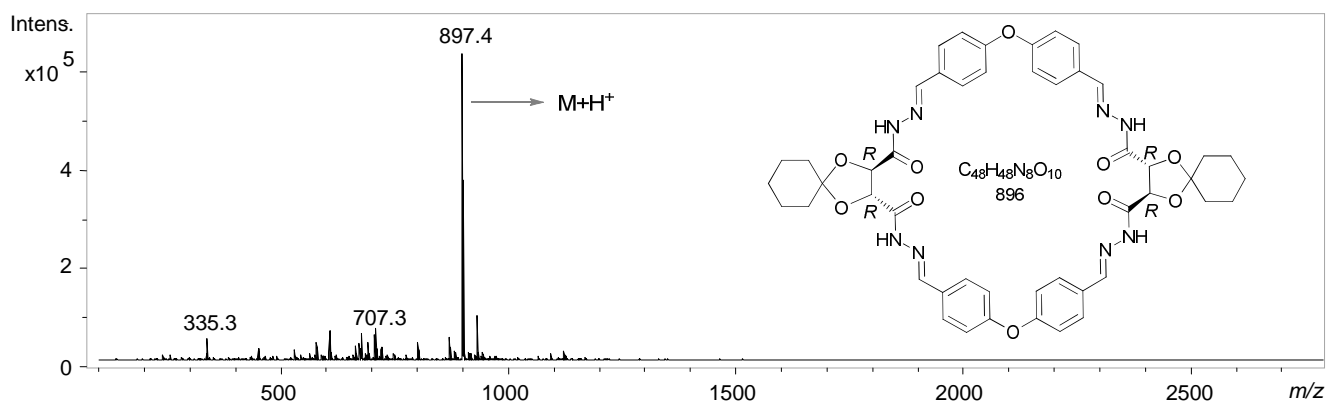


Figure 25. APCI-MS spectrum for macrocycle (**14**), from DMSO.

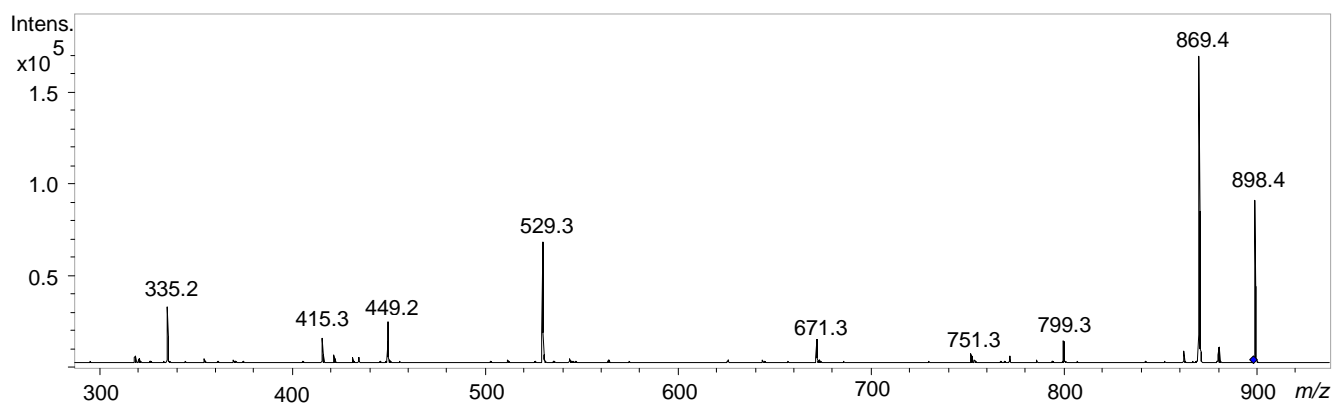


Figure 26. Tandem APCI-MS² spectrum for macrocycle (**14**), from DMSO.

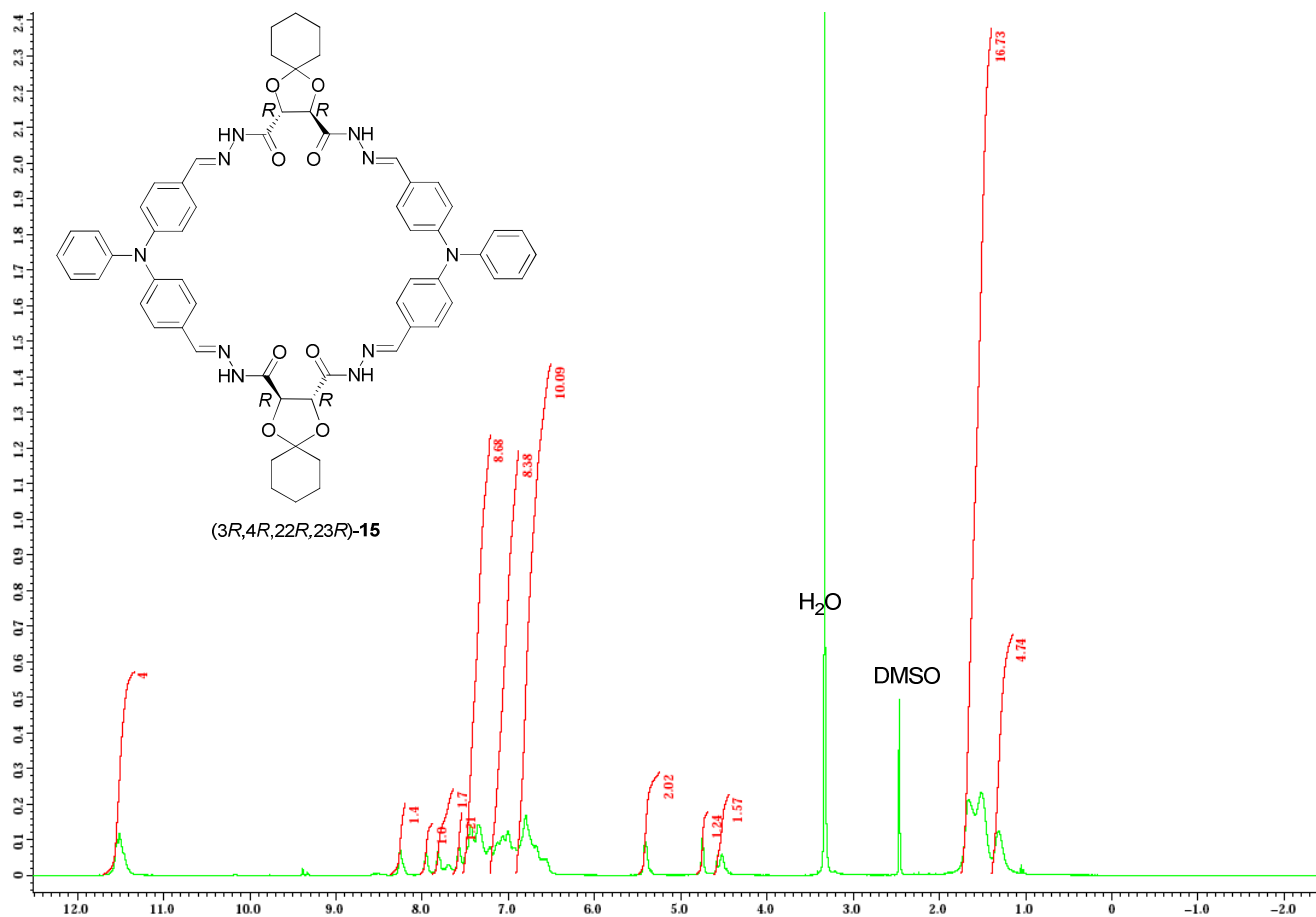


Figure 27. ^1H -NMR spectrum for macrocycle (**15**), DMSO- d_6 , 400 MHz.

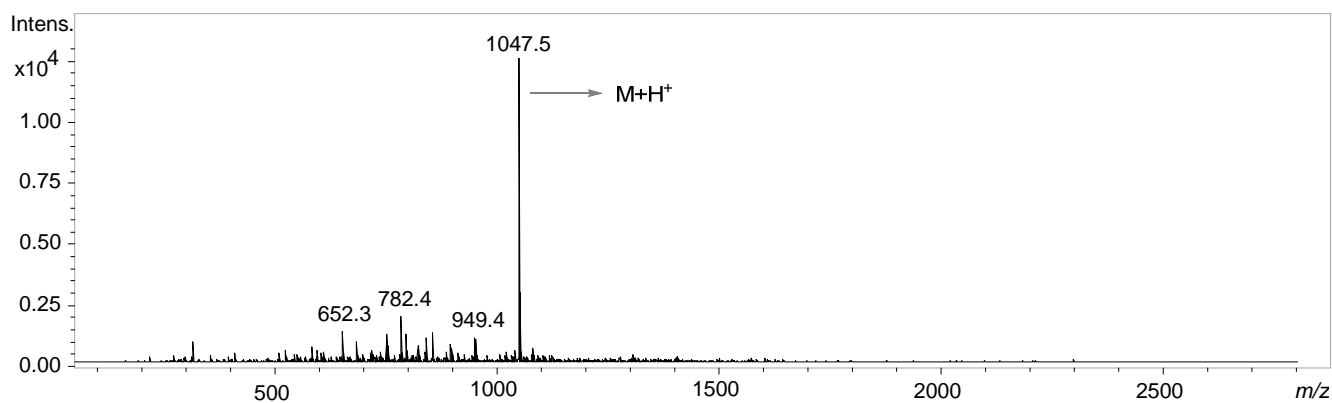
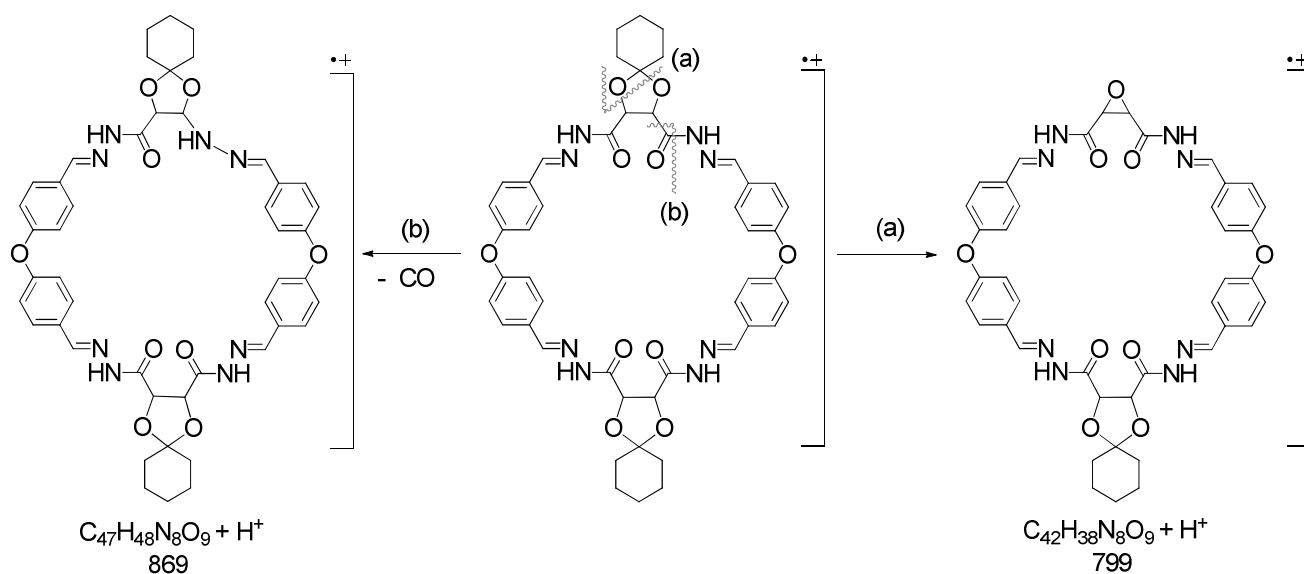


Figure 28. APCI-MS spectrum for macrocycle (15), from DMSO.



Scheme 2. Suggested fragmentation mechanism for macrocycle (15).

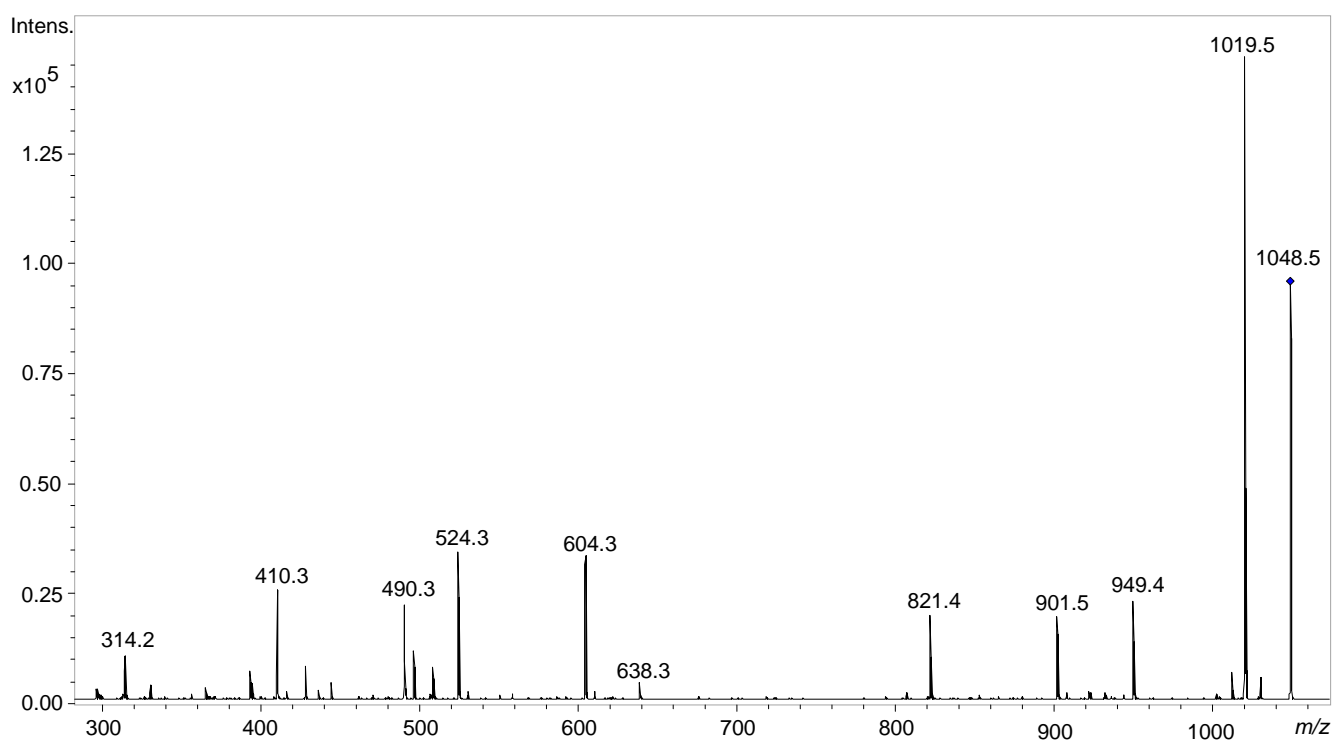
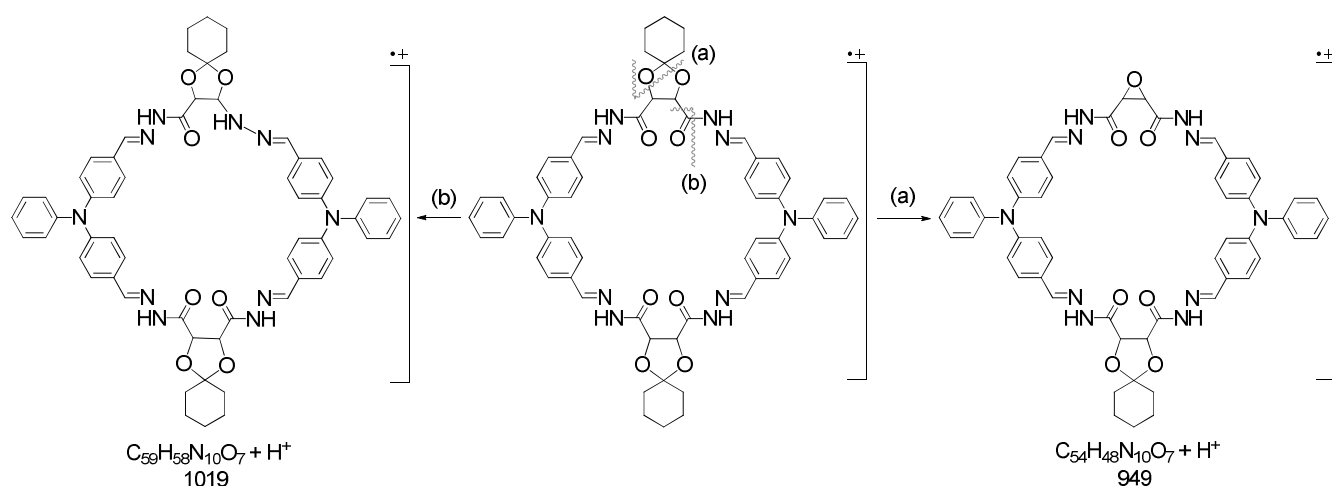


Figure 29. Tandem APCI-MS² spectrum for macrocycle (15), from DMSO.



Scheme 3. Suggested fragmentation mechanism for macrocycle (**15**).

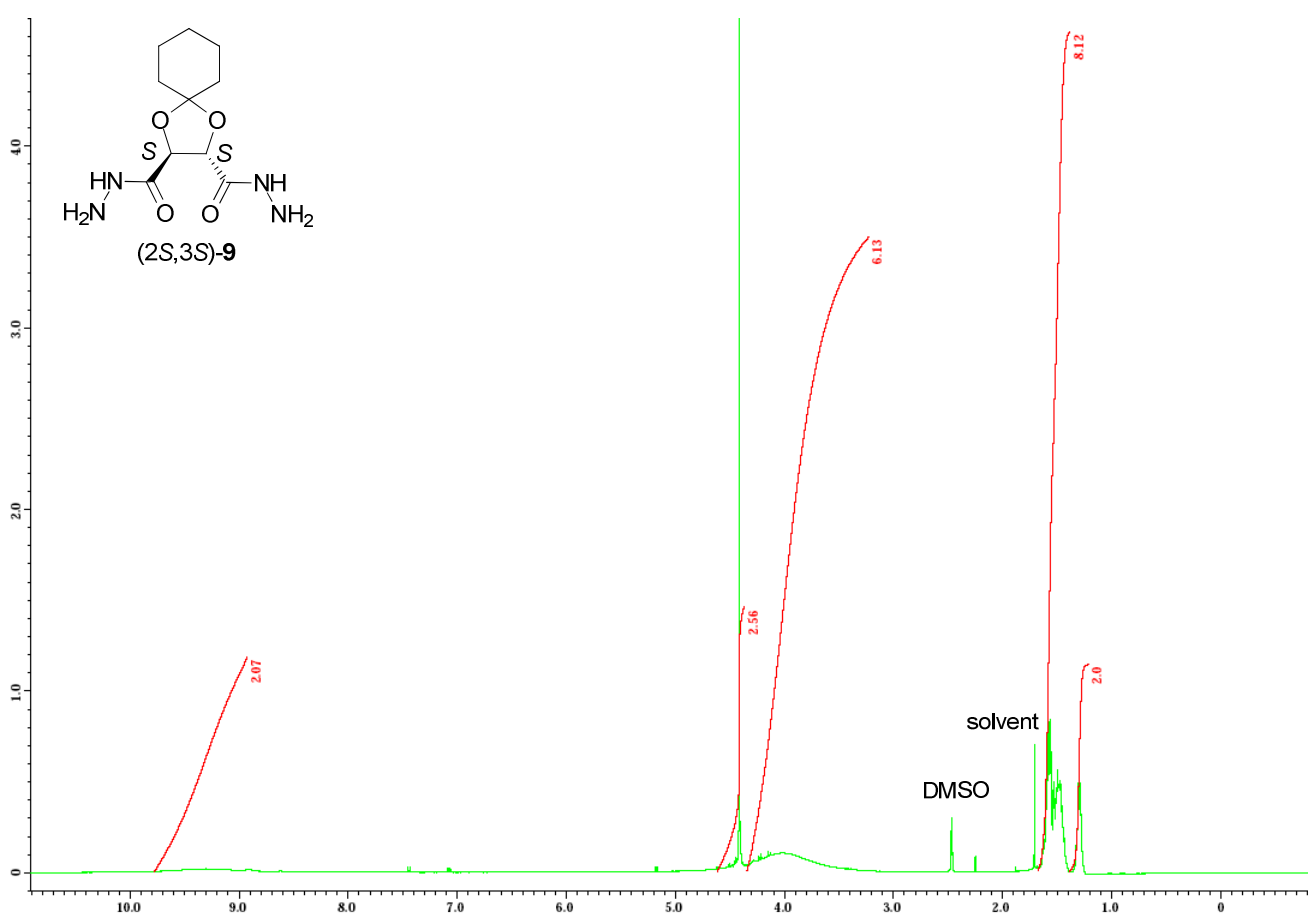


Figure 30. 1H -NMR spectrum for dicarbohydrazide (**9**), DMSO- d_6 , 400 MHz.

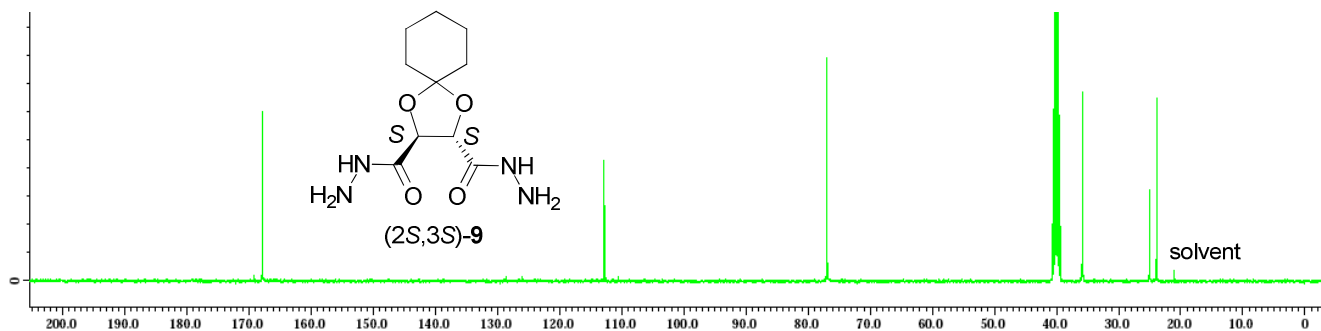


Figure 31. ^{13}C -NMR spectrum for dicarbohydrazide (**9**), DMSO- d_6 , 100 MHz.

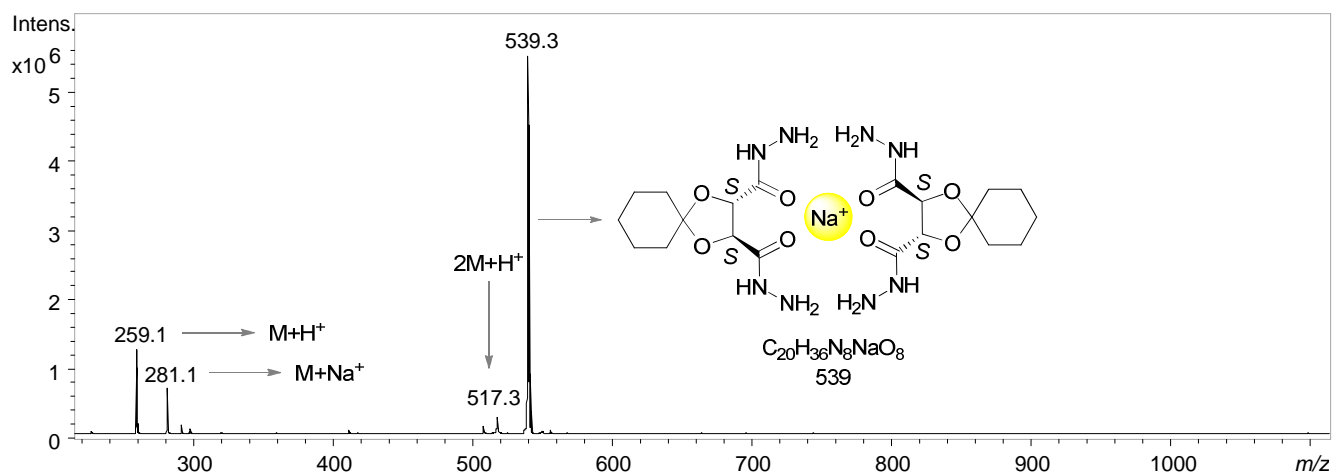


Figure 32. ESI-MS spectrum for dicarbohydrazide (**9**), from H₂O.

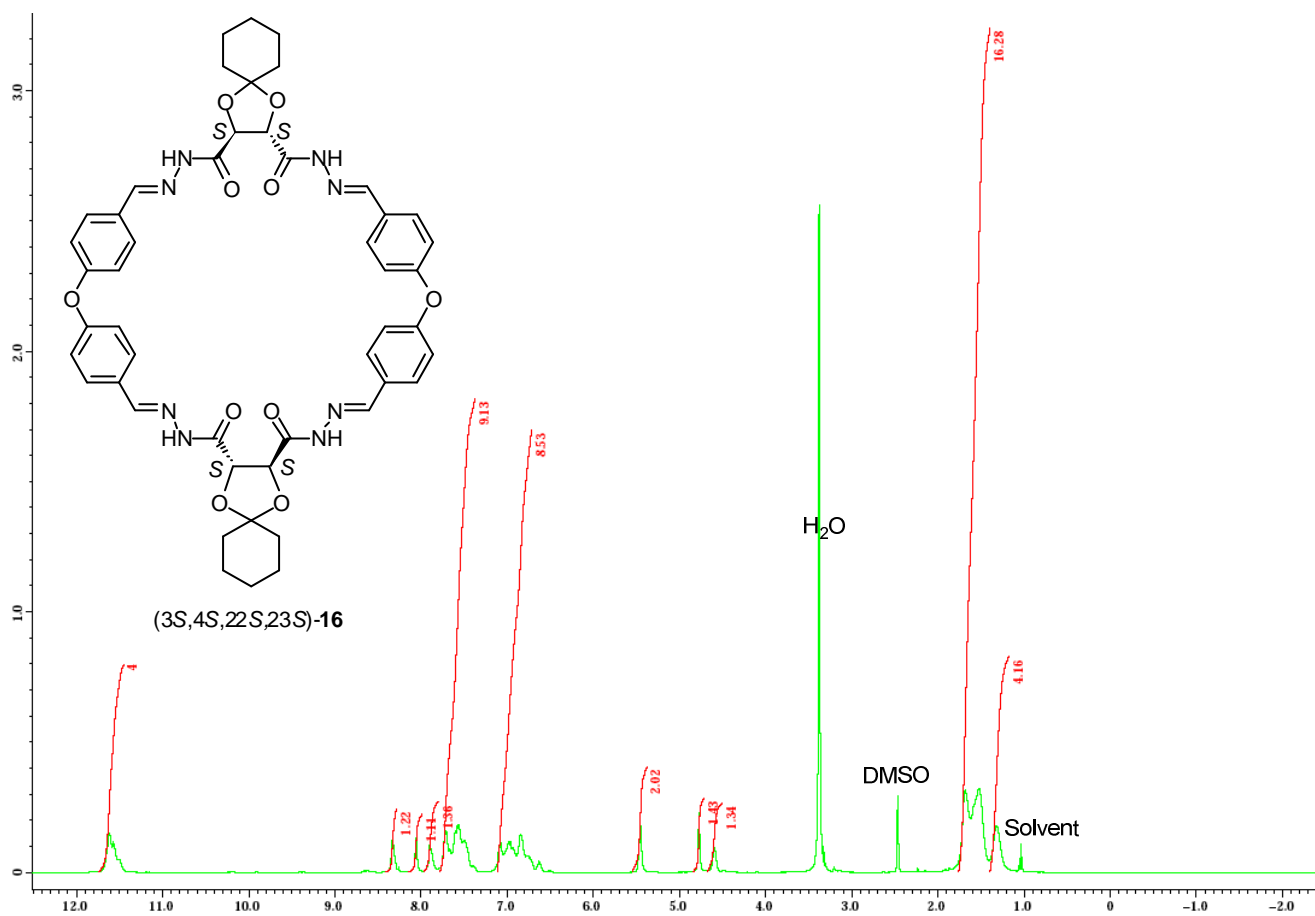


Figure 33. ¹H-NMR spectrum for macrocycle (**16**), DMSO-d₆, 400 MHz.

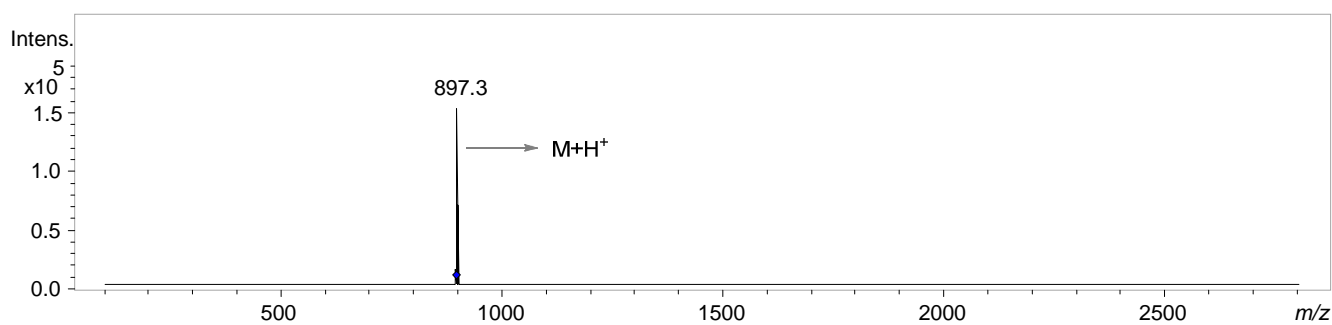


Figure 34. APCI-MS² spectrum for macrocycle (**16**), from DMSO.

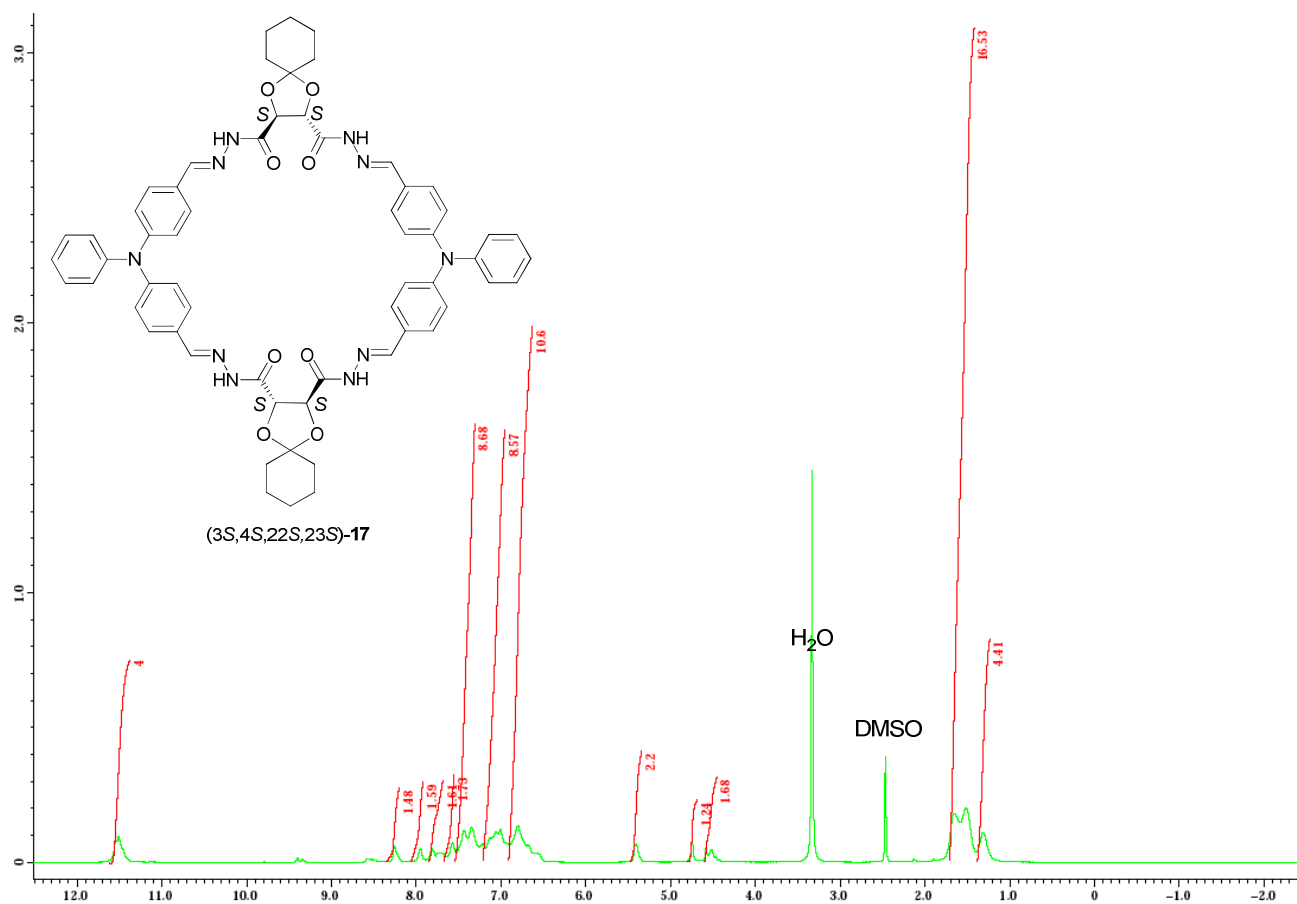


Figure 35. $^1\text{H-NMR}$ spectrum for macrocycle (17), DMSO- d_6 , 400 MHz.

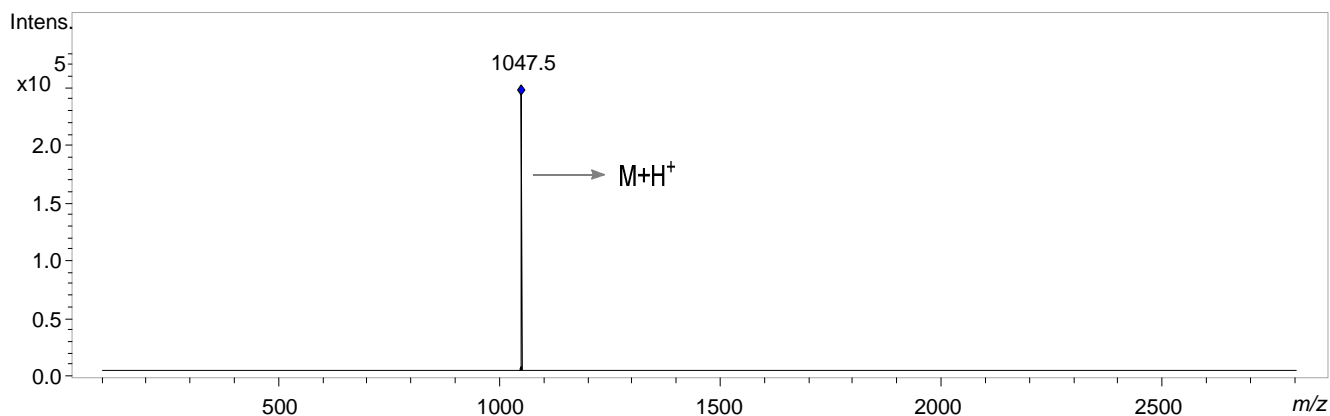


Figure 36. APCI- MS^2 spectrum for macrocycle (17), from DMSO.

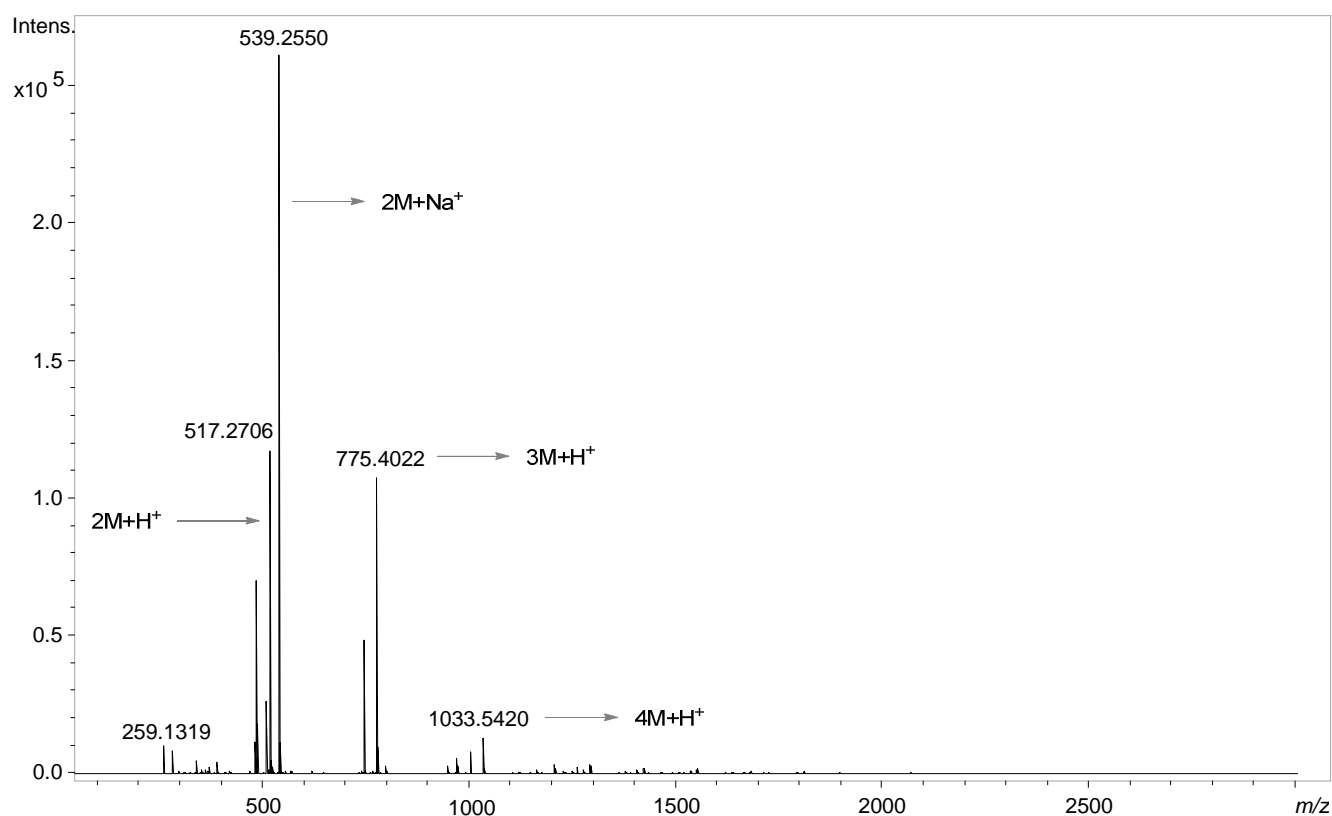


Figure 37. ESI-TOF MS spectrum for dicarbohydrazide (9) at high concentration in H₂O showing peaks corresponding to self-assembled dimeric, dimeric hosting a sodium ion, trimeric and tetrameric hydrogen bonded macrocycles.

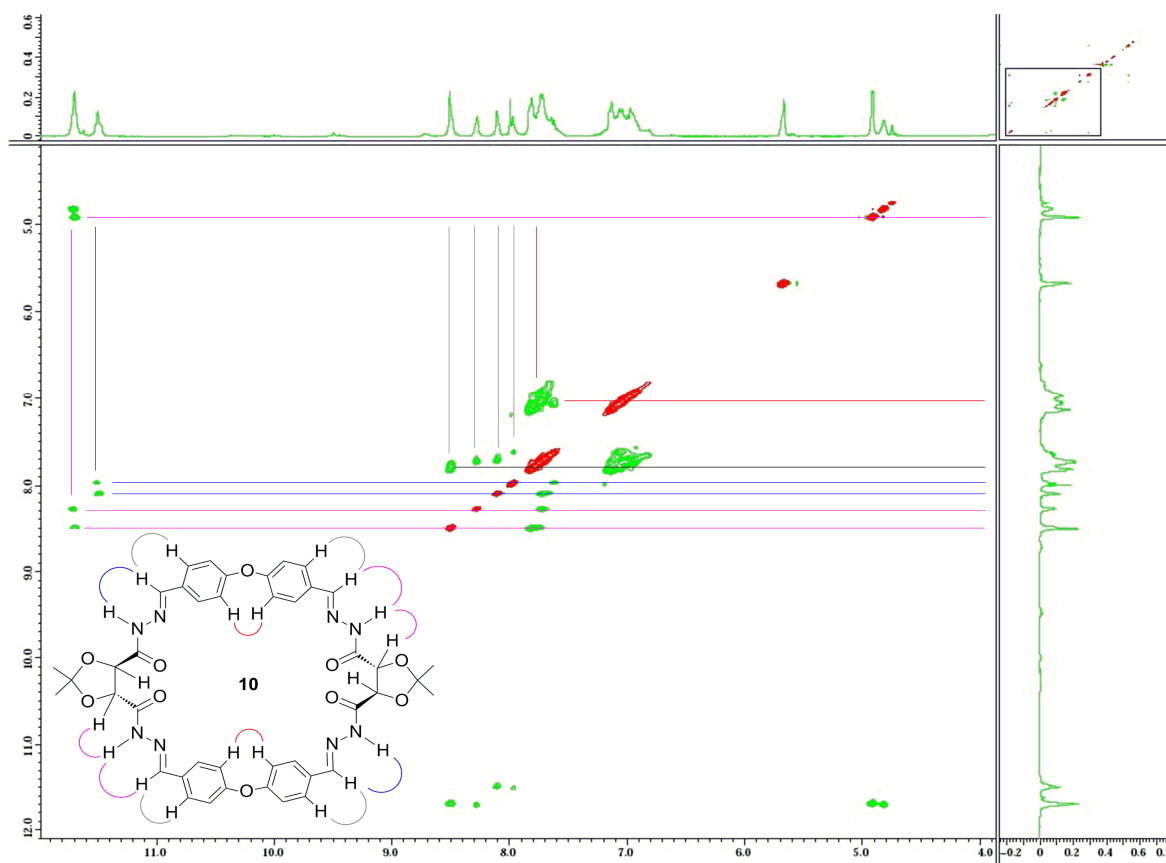


Figure 38. 2D-ROESY spectrum for macrocycle (10), DMF-d₇, 400 MHz.

Molecular modelling data for the computed structure (10a)

Geometry optimization, SemiEmpirical, PM3
Polak-Ribiere optimizer
Convergence limit = 0.0100000 Iteration limit = 50
Accelerate convergence = YES
Optimization algorithm = Polak-Ribiere
Criterion of RMS gradient = 0.0100 kcal/(Å mol) Maximum cycles = 1500
RHF Calculation:

Singlet state calculation
Number of electrons = 308
Number of Double Occupied Levels = 154
Charge on the System = 0
Total Orbitals = 280

ENERGIES AND GRADIENT

Total Energy = -226465.6896094 (kcal/mol)
Total Energy = -360.896003958 (a.u.)
Binding Energy = -10870.4299774 (kcal/mol)
Isolated Atomic Energy = -215595.2596320 (kcal/mol)
Electronic Energy = -2542033.7219103 (kcal/mol)
Core-Core Interaction = 2315568.0323009 (kcal/mol)
Heat of Formation = -109.3799774 (kcal/mol)
Gradient = 0.0074370 (kcal/mol/Å)

Molecular modelling data for the computed structure (10b)

Single Point, MolecularMechanics, AMBER.

Total Energy=113.852054 kcal/mol Gradient=28.306175.
Bond=42.8491 Angle=20.0809 Dihedral=48.1654 Vdw=-0.851527 Electrostatic=3.60814.

Polak-Ribiere optimizer

Energy=50.377868 kcal/mol Gradient=0.009025 Converged=YES (575 cycles 1229 points).
Bond=1.70422 Angle=11.4031 Dihedral=37.8273 Vdw=-2.26292 Electrostatic=1.70609.

Probing the dynamic reversibility and generation of dynamic combinatorial libraries in the presence of bacterial model oligopeptides as templating guests of tetra-carbohydrazide macrocycles using electrospray mass spectrometry

Hany F. Nour^{1,2}, Tuhidul Islam¹, Marcelo Fernández-Lahore¹ and Nikolai Kuhnert^{1*}

¹School of Engineering and Science, Centre for Nano and Functional Materials (NanoFun), Jacobs University, 28759 Bremen, Germany

²National Research Centre, Department of Photochemistry, El Behoose Street, P.O. Box 12622, Dokki, Cairo, Egypt

**Correspondence to:* N. Kuhnert, School of Engineering and Science, Jacobs University, P.O. Box 750 561, D-28725, Bremen, Germany, Fax: +49 421 200 3229, Tel: +49 421 200 3120. E-mail: n.kuhnert@jacobs-university.de

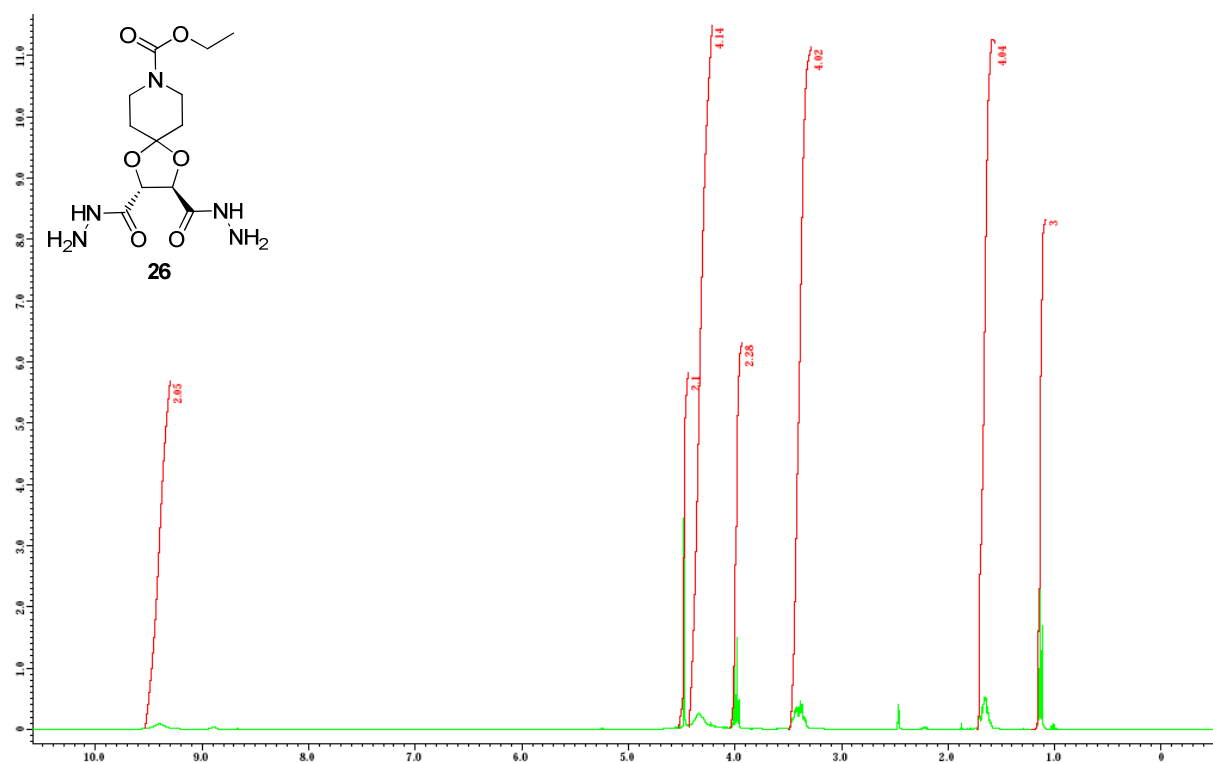


Figure 1. ^1H NMR spectrum for dicarbohydrazide **26** (400 MHz, DMSO-d_6).

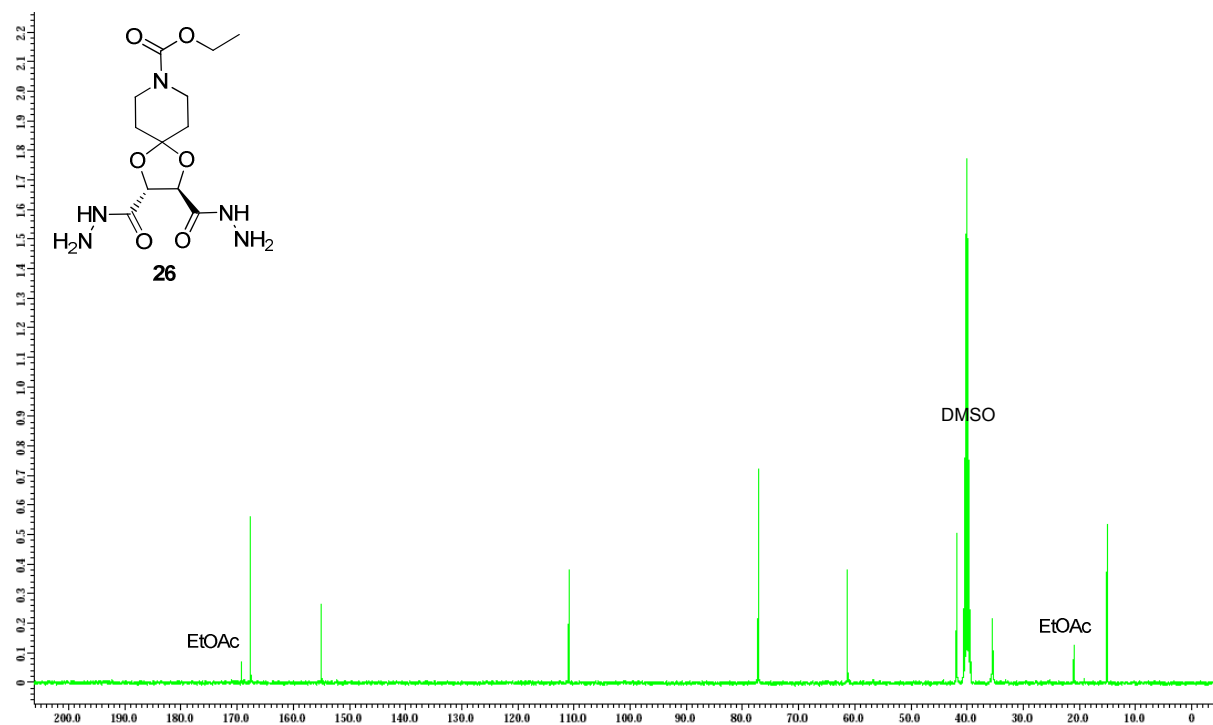
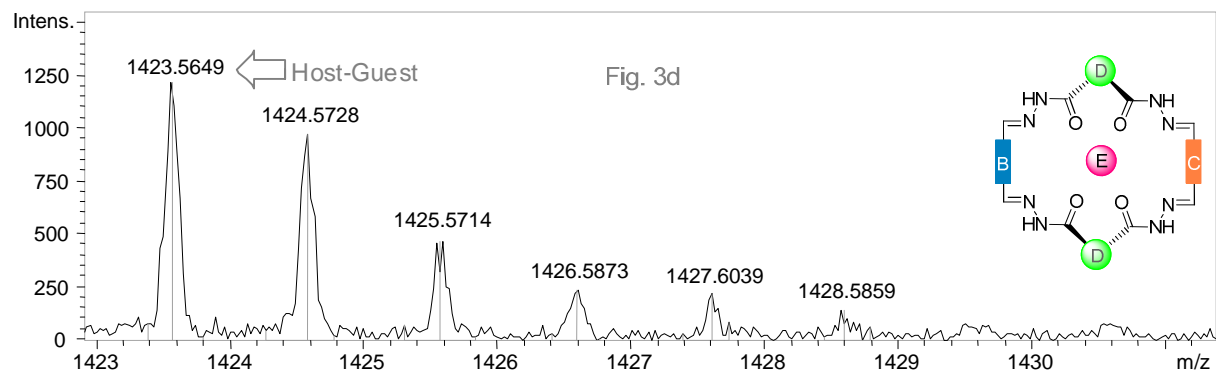
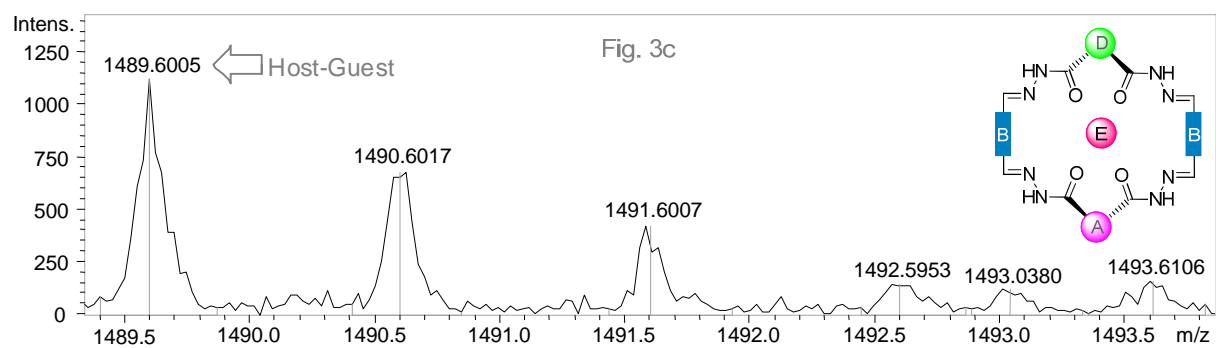
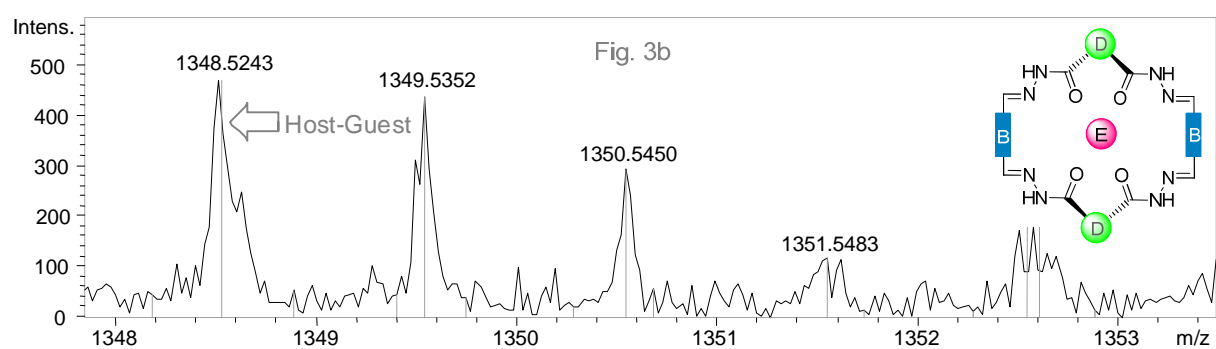
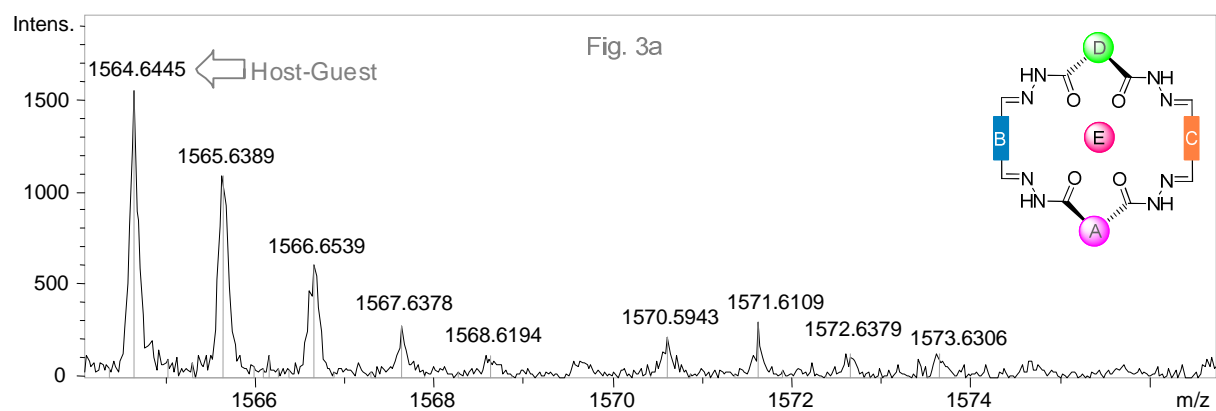
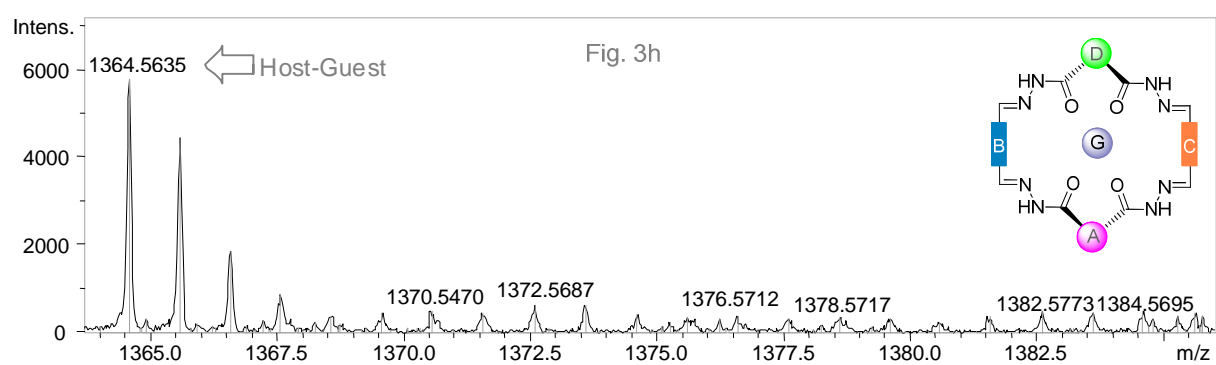
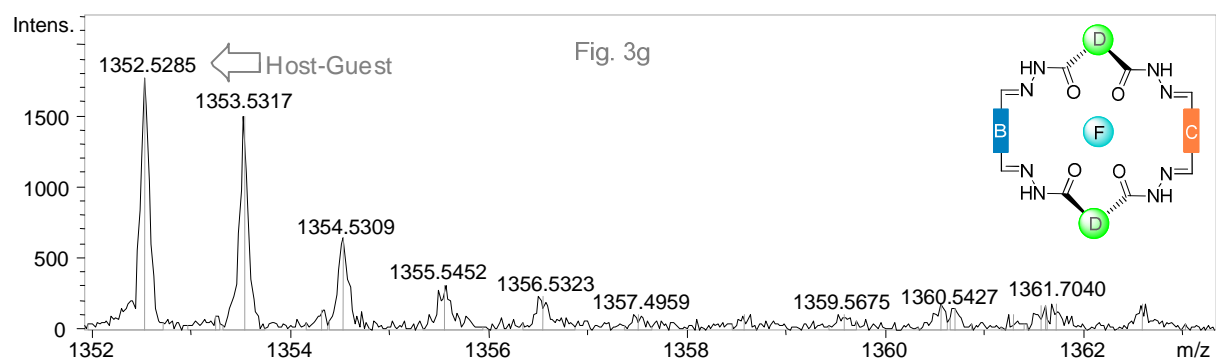
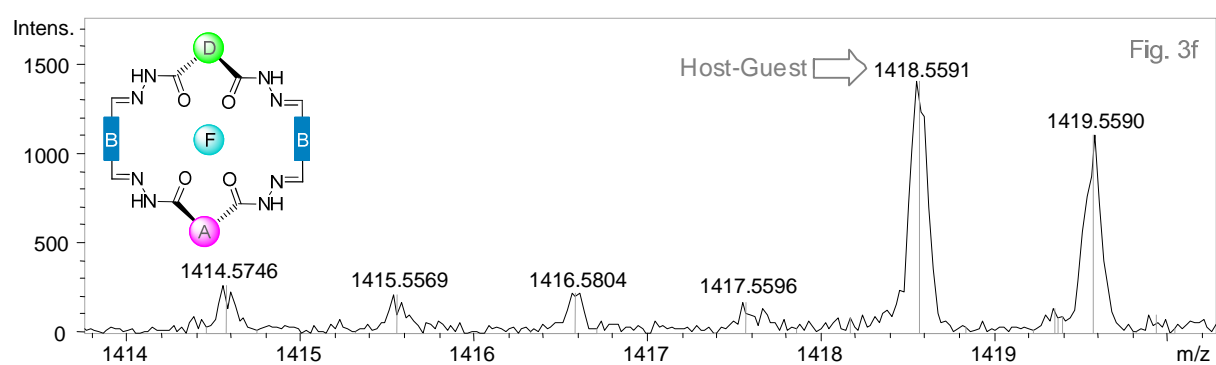
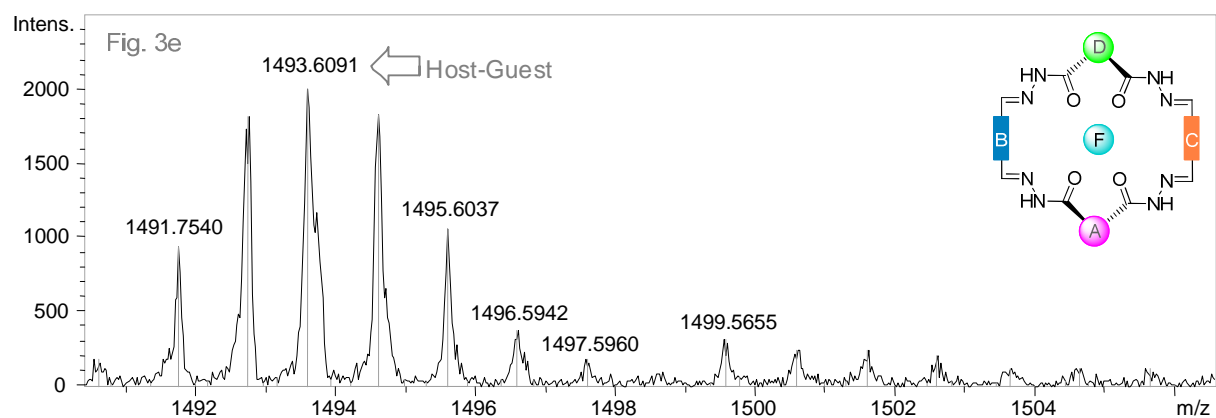
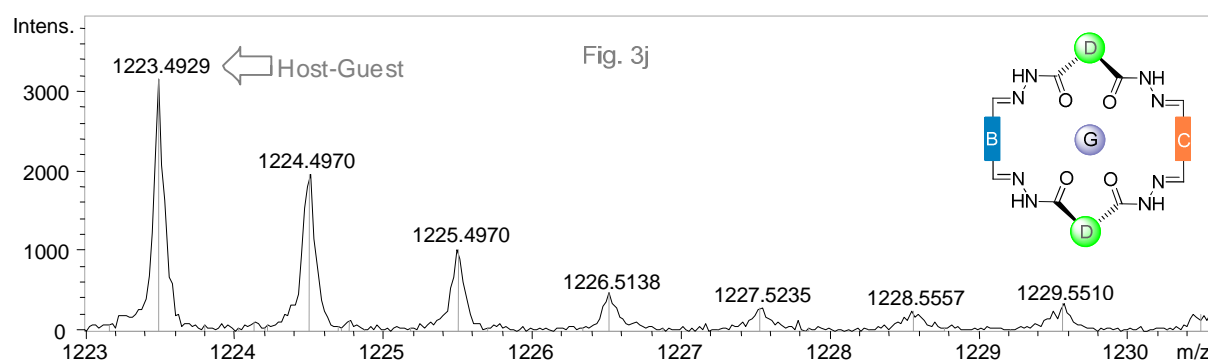
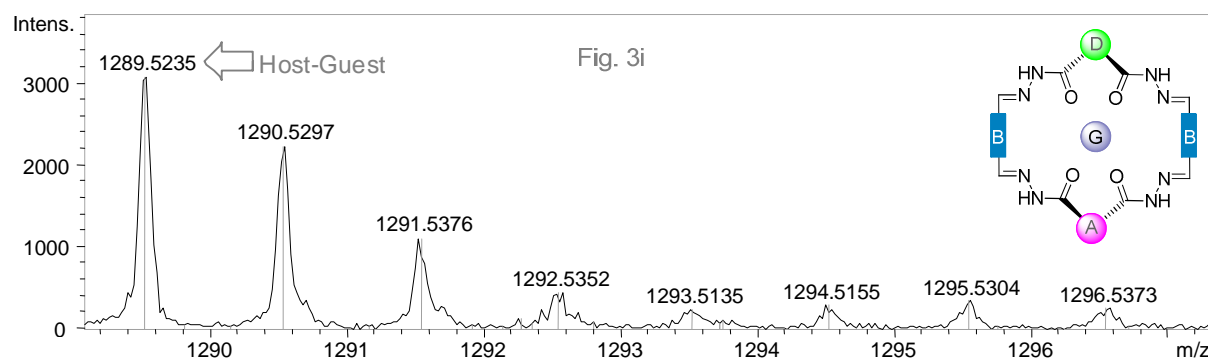


Figure 2. ^{13}C NMR spectrum for dicarbohydrazide **26** (100 MHz, DMSO-d_6).







Figures 3a-j. ESI-TOF mass spectra for host/guest complexes in the positive ion mode, products were detected as $[M+H]^+$ ions

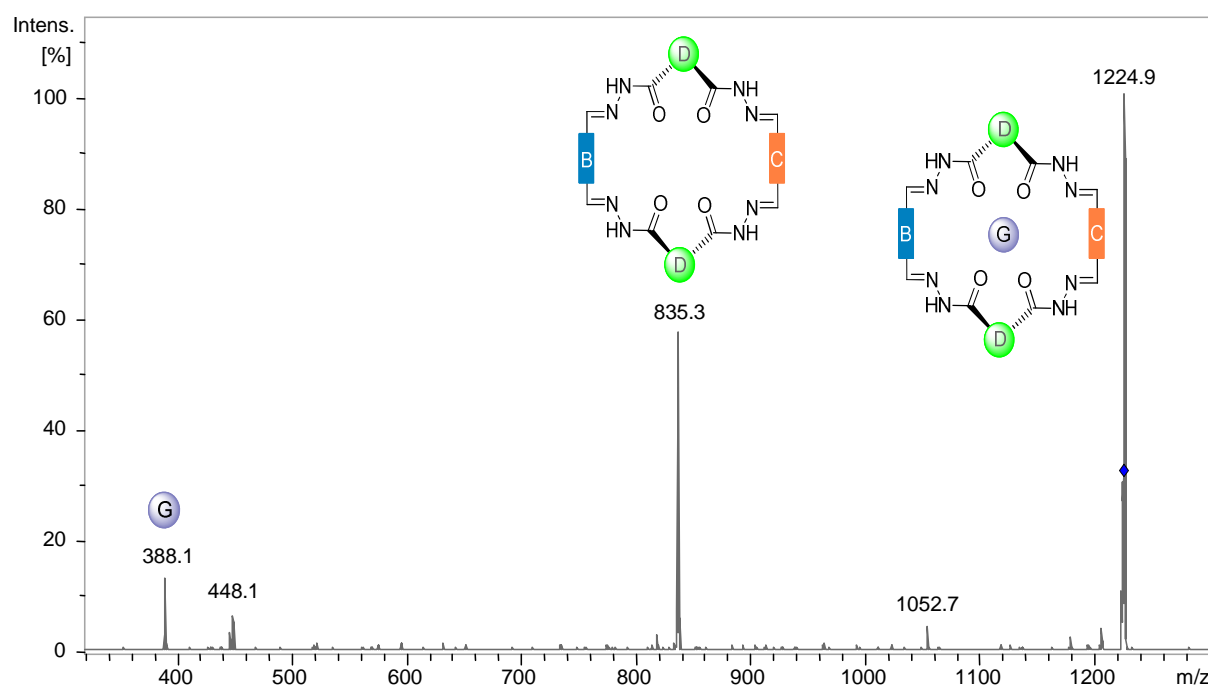


Figure 4. Tandem ESI-MS for host/guest complex **40** (m/z 1223.4929) in the positive ion mode.

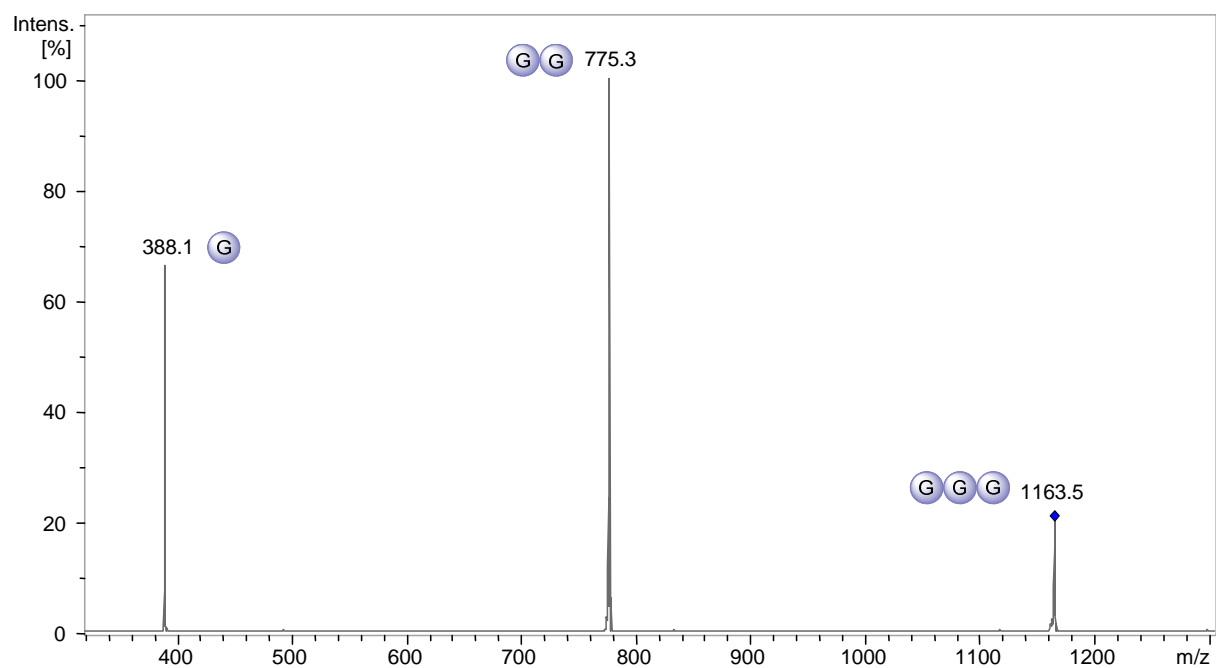


Figure 5. Tandem ESI-MS for self-assembled guest 43 (m/z 1162.6380) in the positive ion mode.

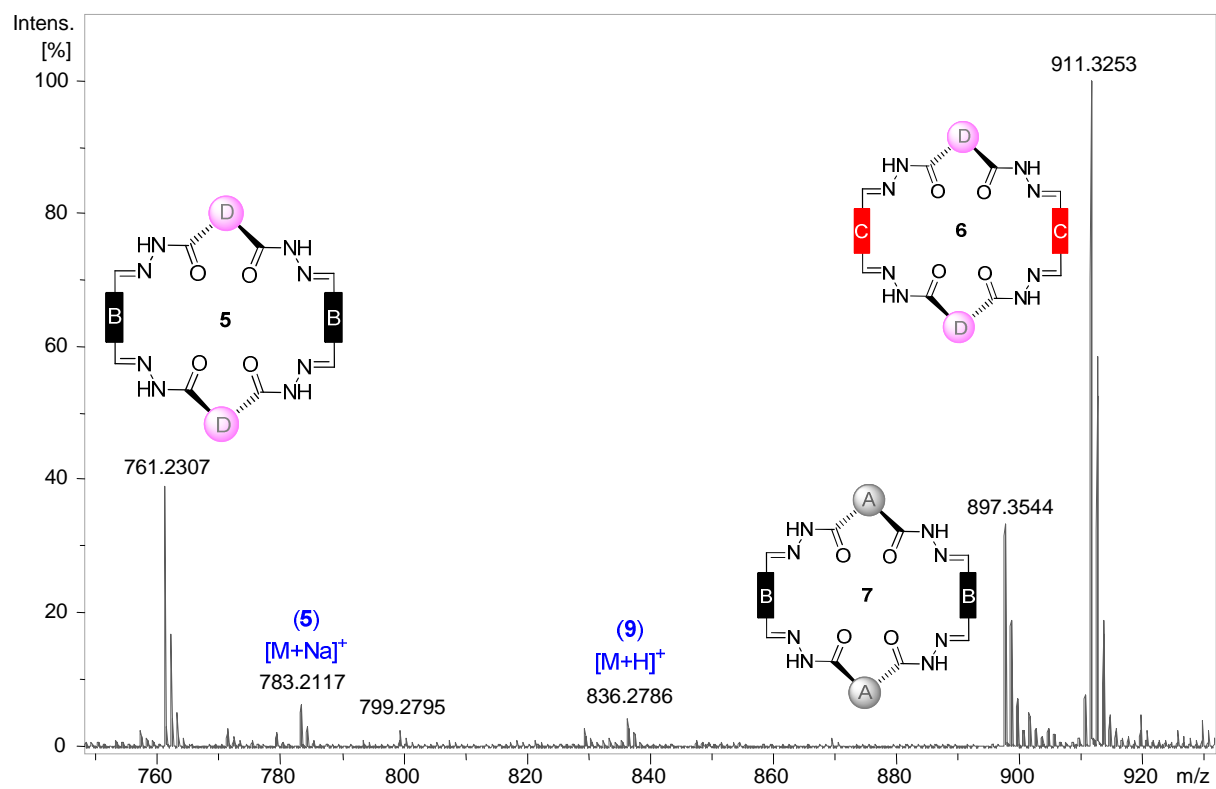


Figure 6. ESI-TOF mass spectrum for macrocycles **5-7**, spectrum recorded after 2 h in the positive ion mode, products were detected as $[M+H]^+$ ions.

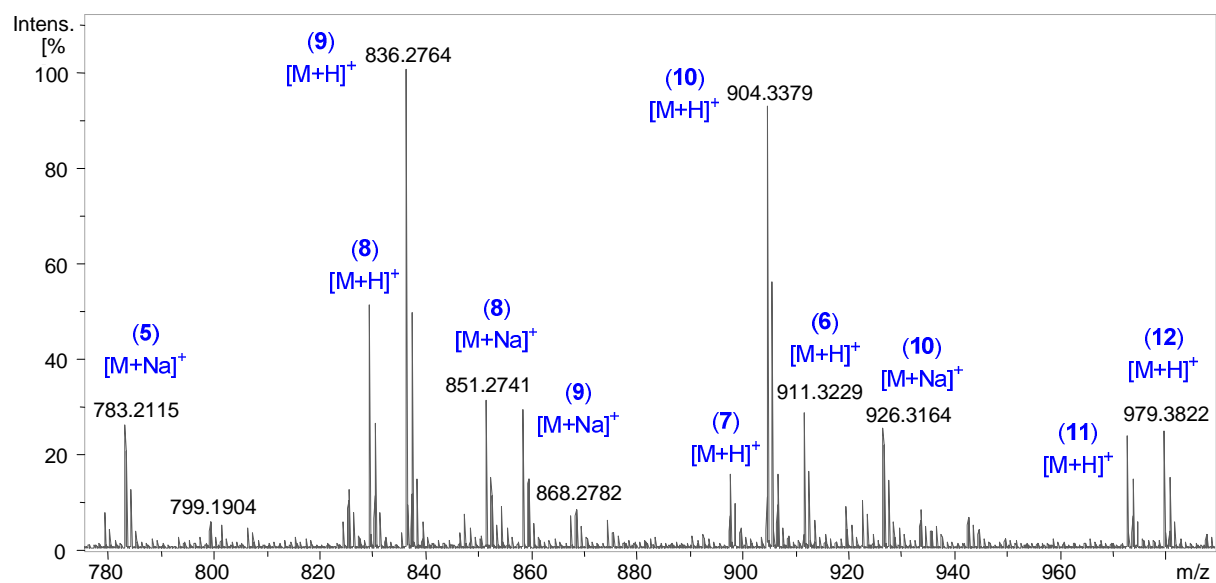
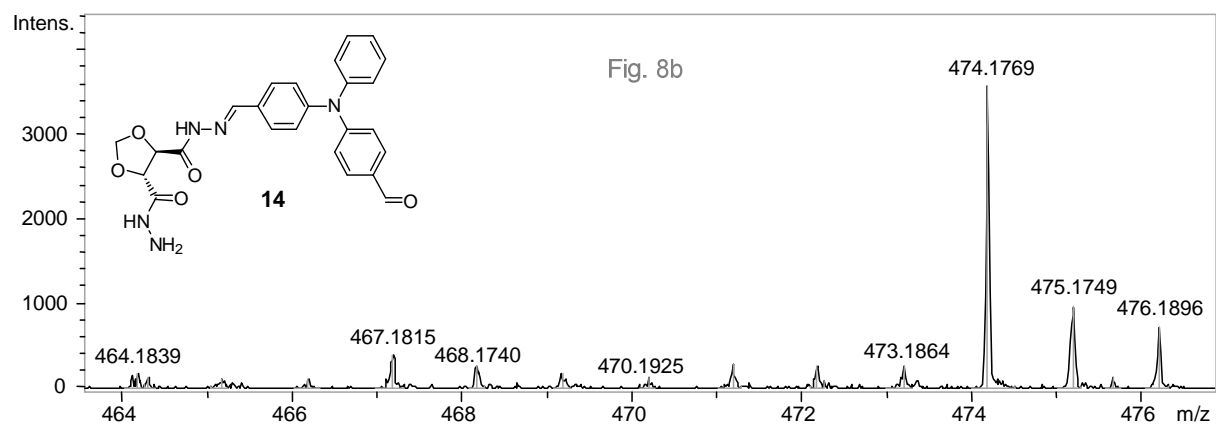
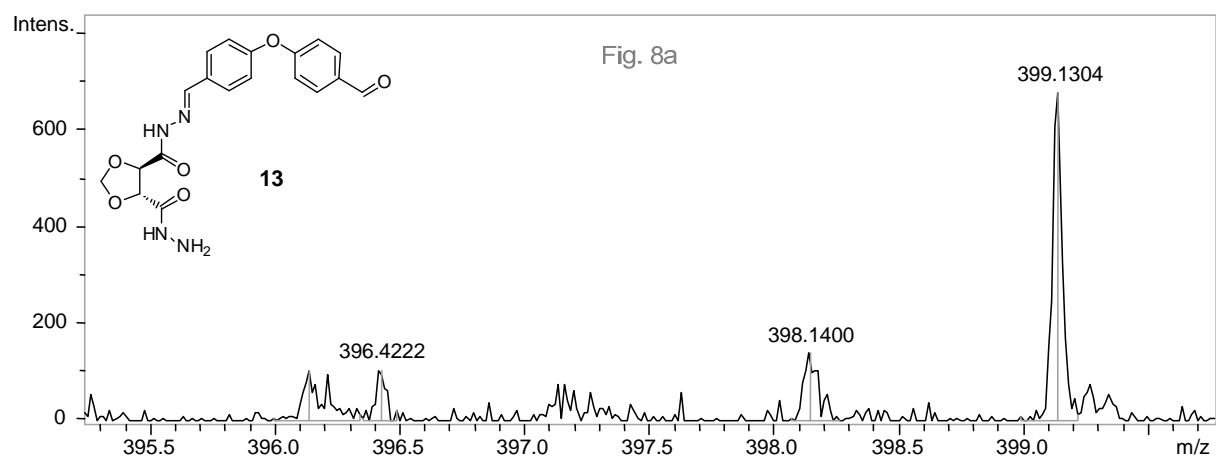
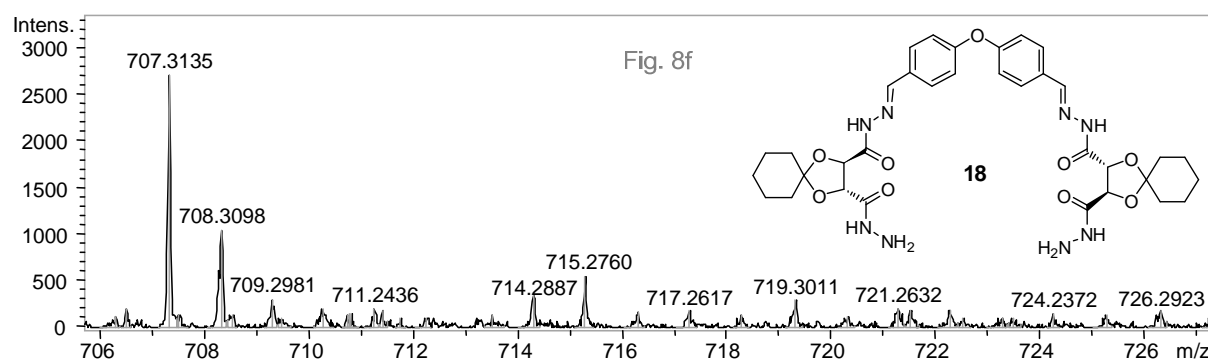
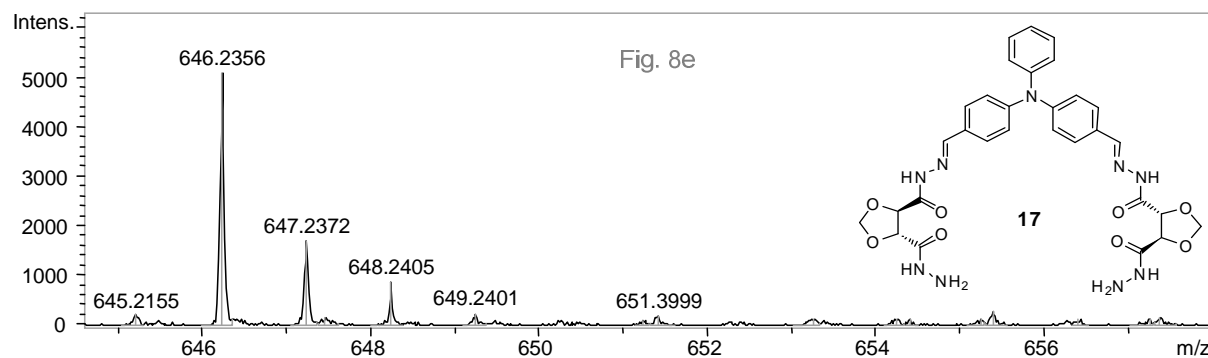
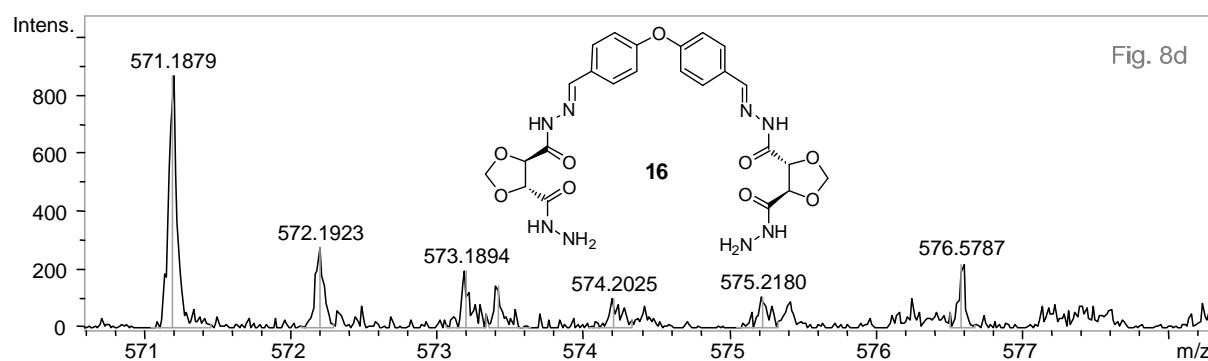
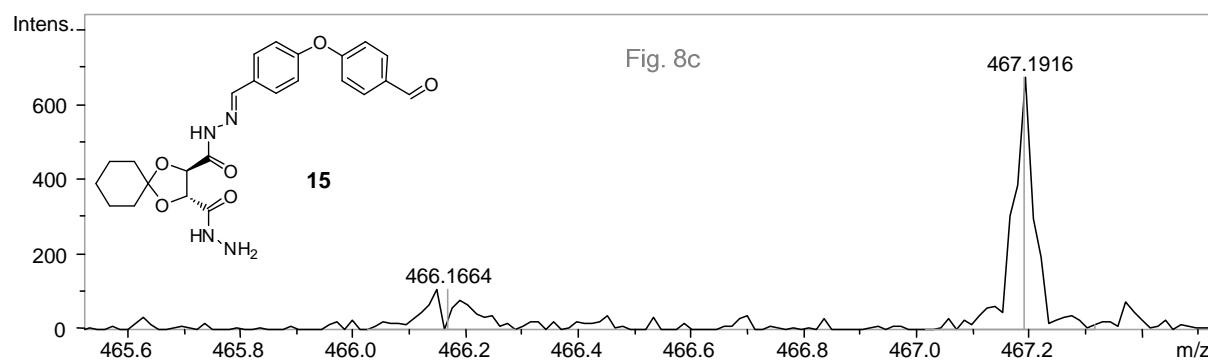
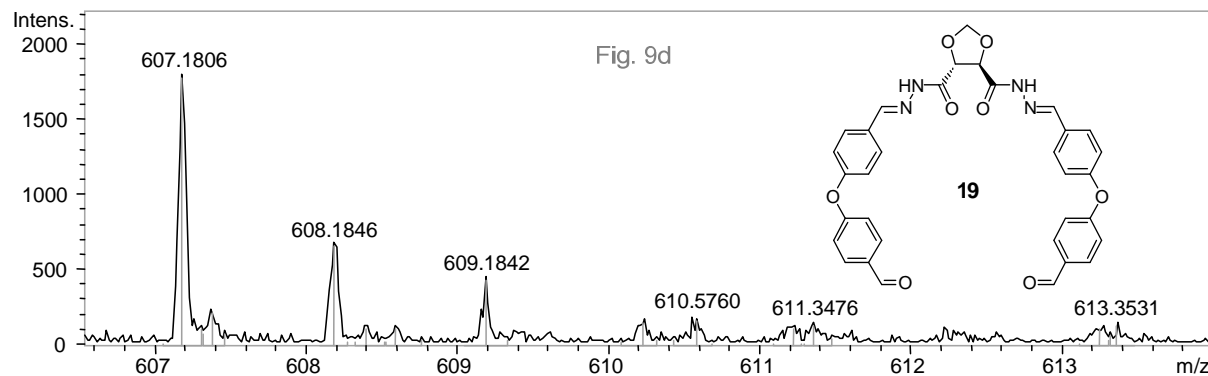
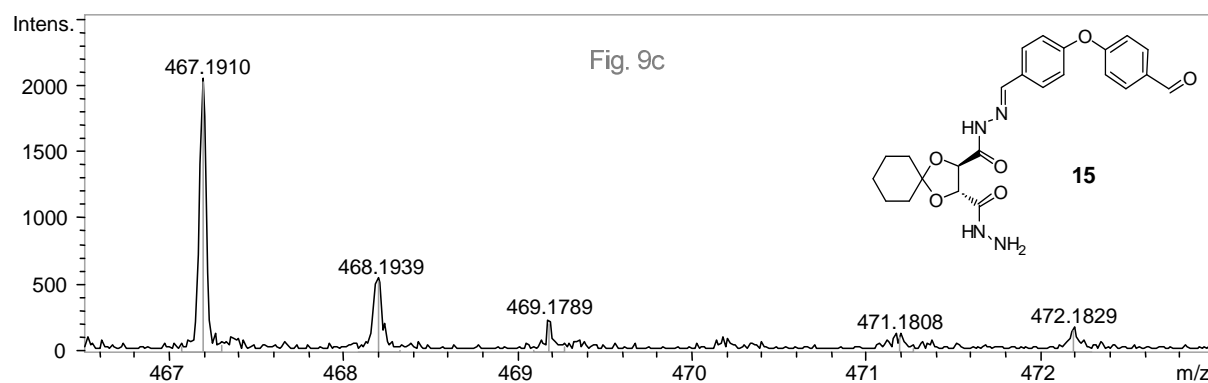
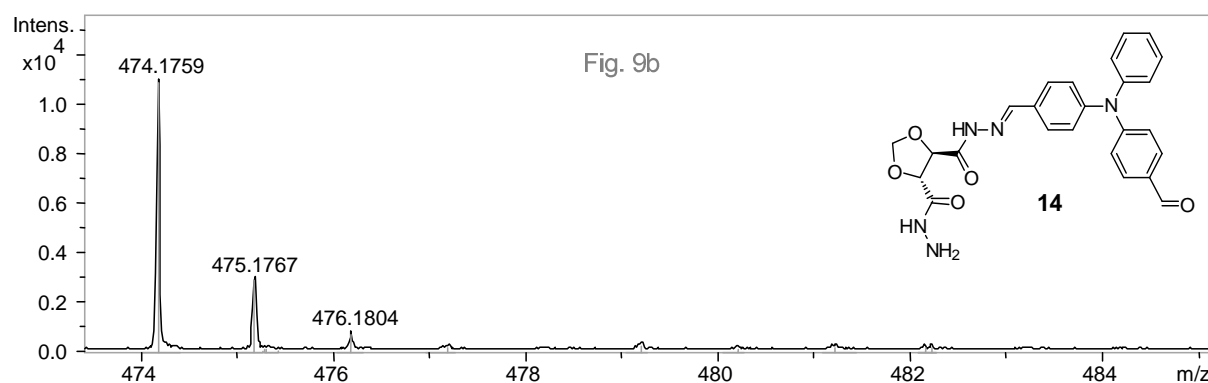
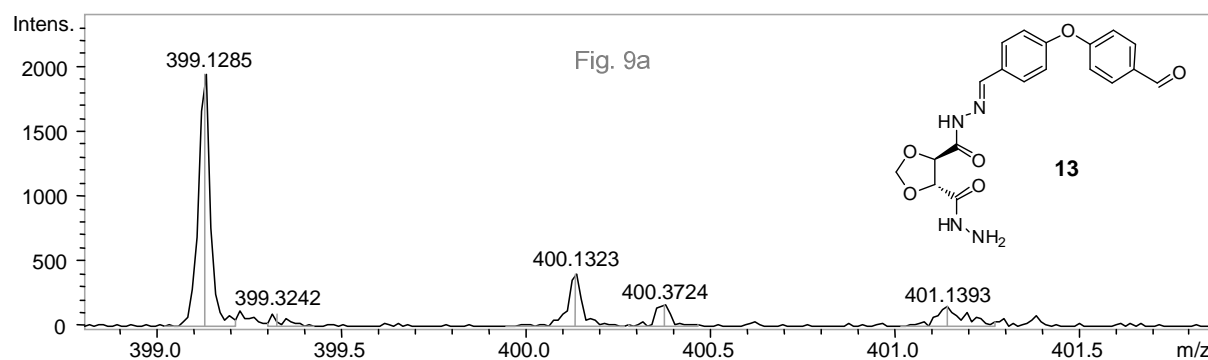


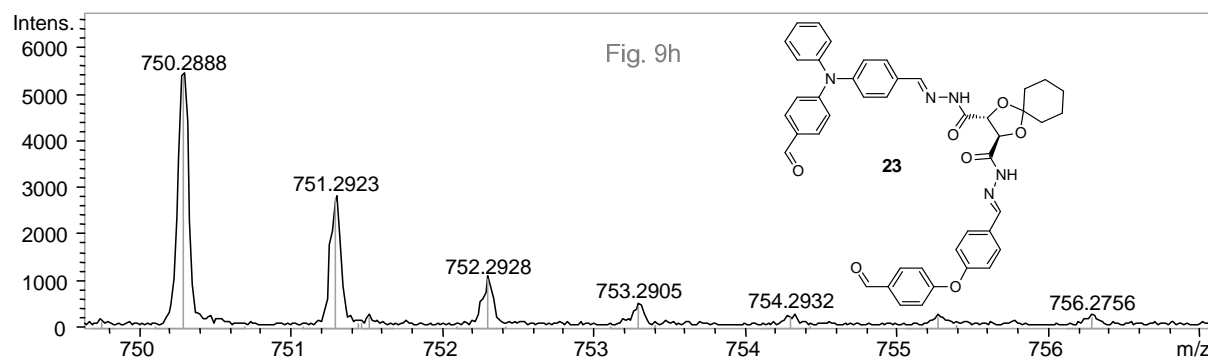
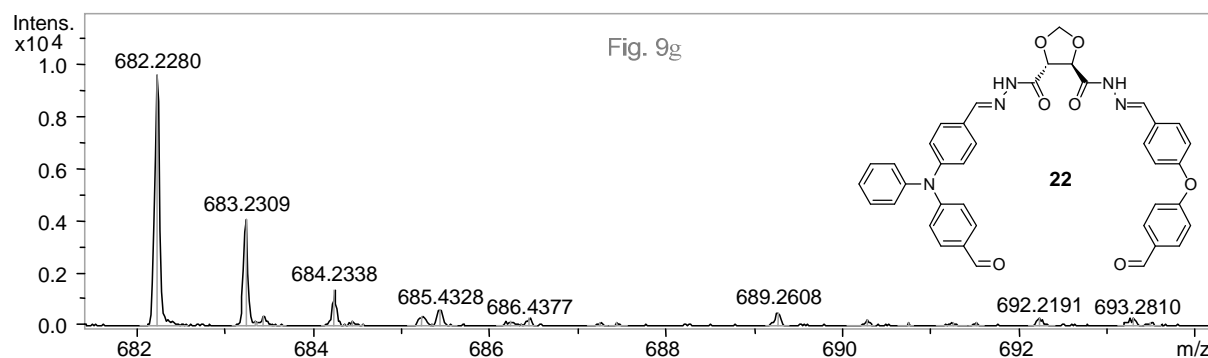
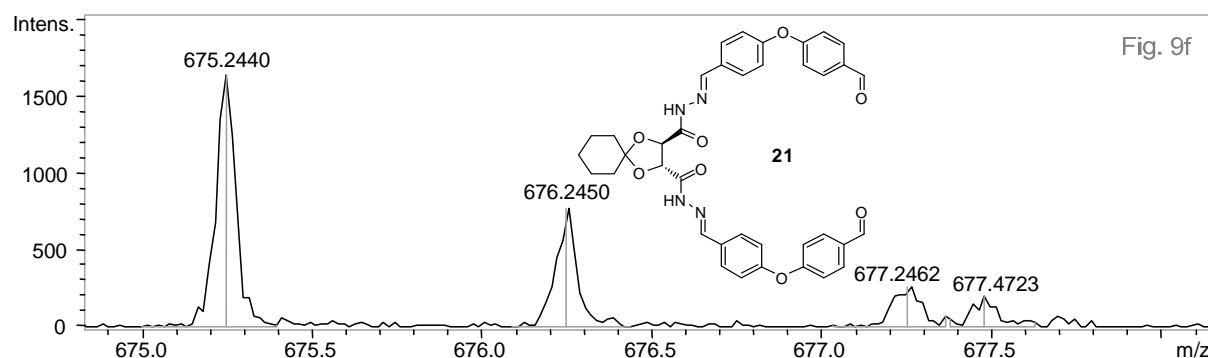
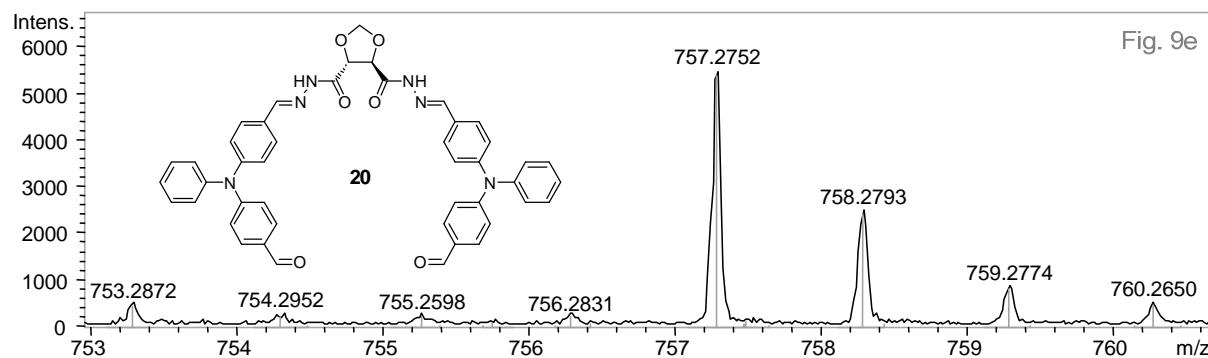
Figure 7. ESI-TOF mass spectrum for refluxing compounds **1-4**, spectrum recorded after 2 h in the positive ion mode, products were detected as $[M+H]^+$ and $[M+Na]^+$ ions.





Figures 8a-f. ESI-TOF mass spectra for intermediates **13-18** in the positive ion mode, products were detected as $[M+H]^+$ ions after 2 h of refluxing macrocycles **5-7**.





Figures 9a-h. ESI-TOF mass spectra for intermediates **13-15** and **19-23** in the positive ion mode, products were detected as $[M+H]^+$ ions after 2 h of refluxing compounds **1-4**.

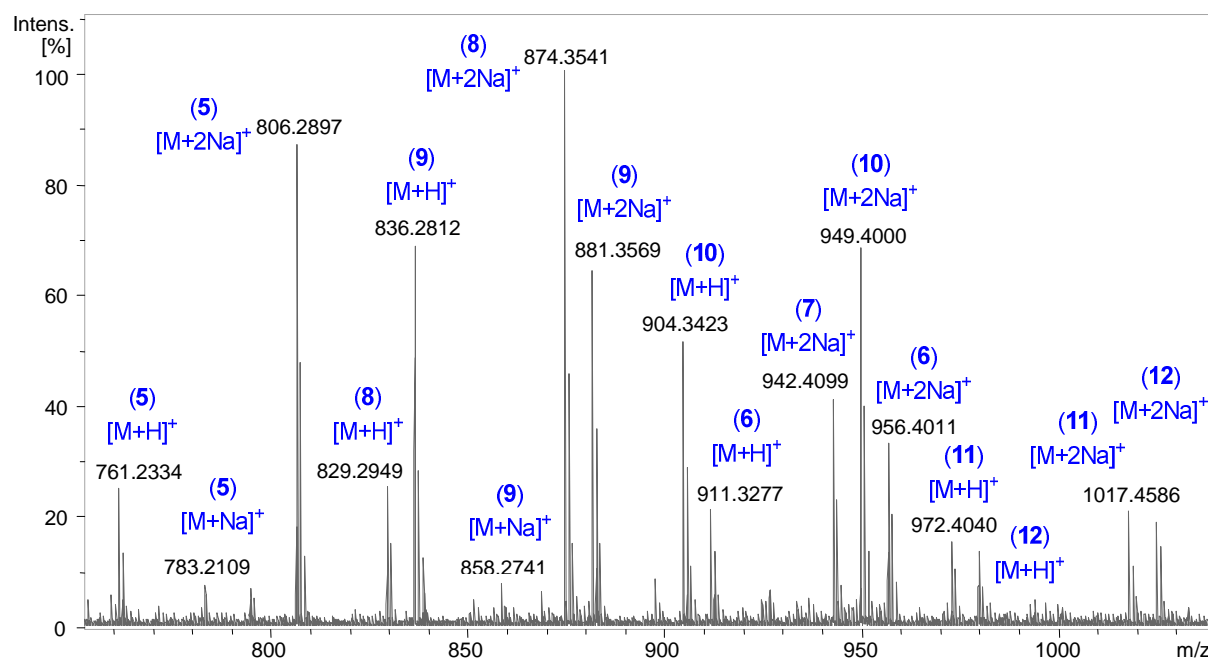


Figure 10. ESI-TOF mass spectrum at equilibration in the positive ion mode for the products of dynamic exchange reaction (Path (a), products were detected as $[M+H]^+$, $[M+Na]^+$ and $[M+2Na]^+$ ions).

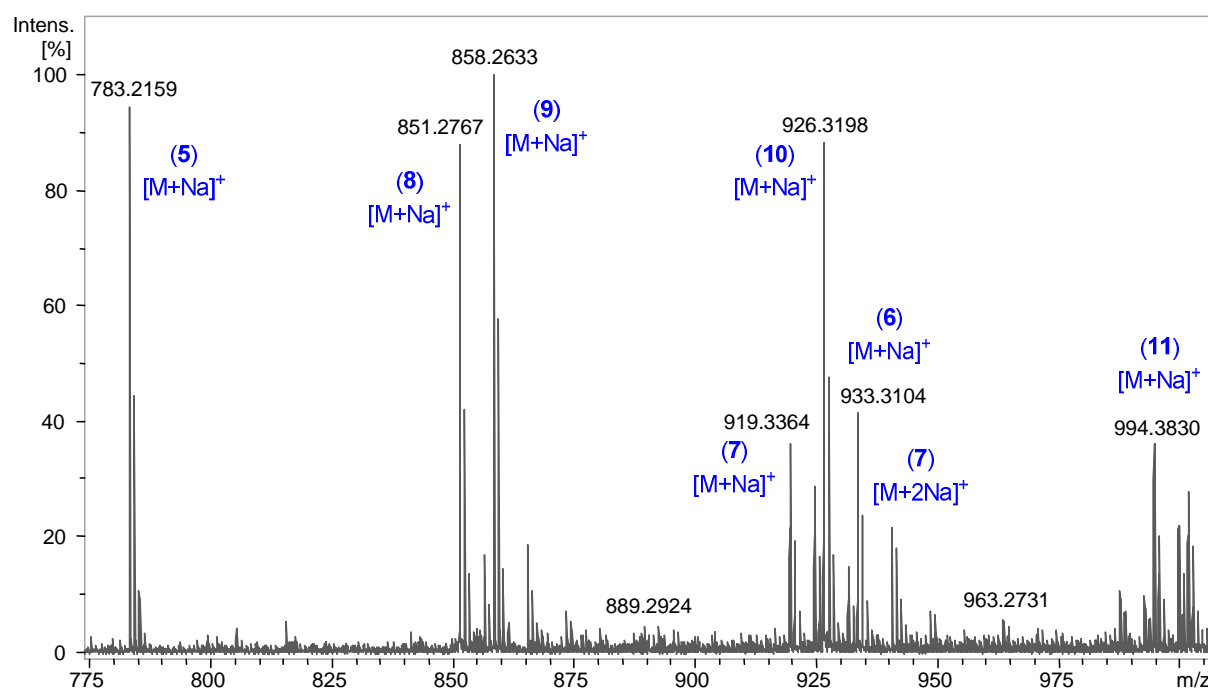


Figure 11. ESI-TOF mass spectrum at equilibration in the positive ion mode for the products of dynamic exchange reaction (Path (b), products were detected as $[M+Na]^+$ ions).

Table 1. High resolution ESI-TOF data for (a) refluxing macrocycles **5-7** (2 h, positive ion mode), (b) refluxing building block precursors **1-4** (2 h, positive ion mode).

Entry	Measured m/z		Molecular Formula	Theoretical m/z	Error [ppm]
5 ^{a,b}	761.2307 ^a	[M+H] ⁺	C ₃₈ H ₃₂ N ₈ O ₁₀	761.2314 ^a	0.9
	783.2115 ^b	[M+Na] ⁺	C ₃₈ H ₃₂ N ₈ O ₁₀	783.2134 ^b	2.3
6 ^{a,b}	911.3253 ^a	[M+H] ⁺	C ₅₀ H ₄₂ N ₁₀ O ₈	911.3260 ^a	0.7
	911.3229 ^b	[M+H] ⁺	C ₅₀ H ₄₂ N ₁₀ O ₈	911.3260 ^b	3.4
7 ^{a,b}	897.3544 ^a	[M+H] ⁺	C ₄₈ H ₄₈ N ₈ O ₁₀	897.3566 ^a	2.4
	919.3350 ^b	[M+Na] ⁺	C ₄₈ H ₄₈ N ₈ O ₁₀	919.3386 ^b	3.9
8 ^{a,b}	—	—	C ₄₃ H ₄₀ N ₈ O ₁₀	—	—
	851.2741 ^b	[M+Na] ⁺	C ₄₃ H ₄₀ N ₈ O ₁₀	851.2760 ^b	2.2
9 ^{a,b}	836.2786 ^a	[M+H] ⁺	C ₄₄ H ₃₇ N ₉ O ₉	836.2787 ^a	0.1
	836.2764 ^b	[M+H] ⁺	C ₄₄ H ₃₇ N ₉ O ₉	836.2787 ^b	2.7
10 ^{a,b}	—	—	C ₄₉ H ₄₅ N ₉ O ₉	—	—
	904.3379 ^b	[M+H] ⁺	C ₄₉ H ₄₅ N ₉ O ₉	904.3413 ^b	3.8
11 ^{a,b}	—	—	C ₅₄ H ₅₃ N ₉ O ₉	—	—
	972.3990 ^b	[M+H] ⁺	C ₅₄ H ₅₃ N ₉ O ₉	972.4039 ^b	5.0
12 ^{a,b}	—	—	C ₅₅ H ₅₀ N ₁₀ O ₈	—	—
	979.3822 ^b	[M+H] ⁺	C ₅₅ H ₅₀ N ₁₀ O ₈	979.3886 ^b	6.5

Supporting Information

Synthesis and ESI-MS Complexation Studies of Novel Chiral Tetra-(hydrazine-carboxamide) cyclophane Macrocycles

Hany F. Nour,^[a,b] Agnieszka Golon,^[a] Tuhidul Islam,^[a] Marcelo Fernández-Lahore,^[a] and Nikolai Kuhnert^{*[a]}

**Correspondence to:* N. Kuhnert, email: n.kuhnert@jacobs-university.de

[a] School of Engineering and Science, Centre for Nano and Functional Materials (NanoFun), Jacobs University, 28759 Bremen, Germany.

[a] National Research Centre, Department of Photochemistry, El Behoose Street, P.O. Box 12622, Dokki, Egypt.

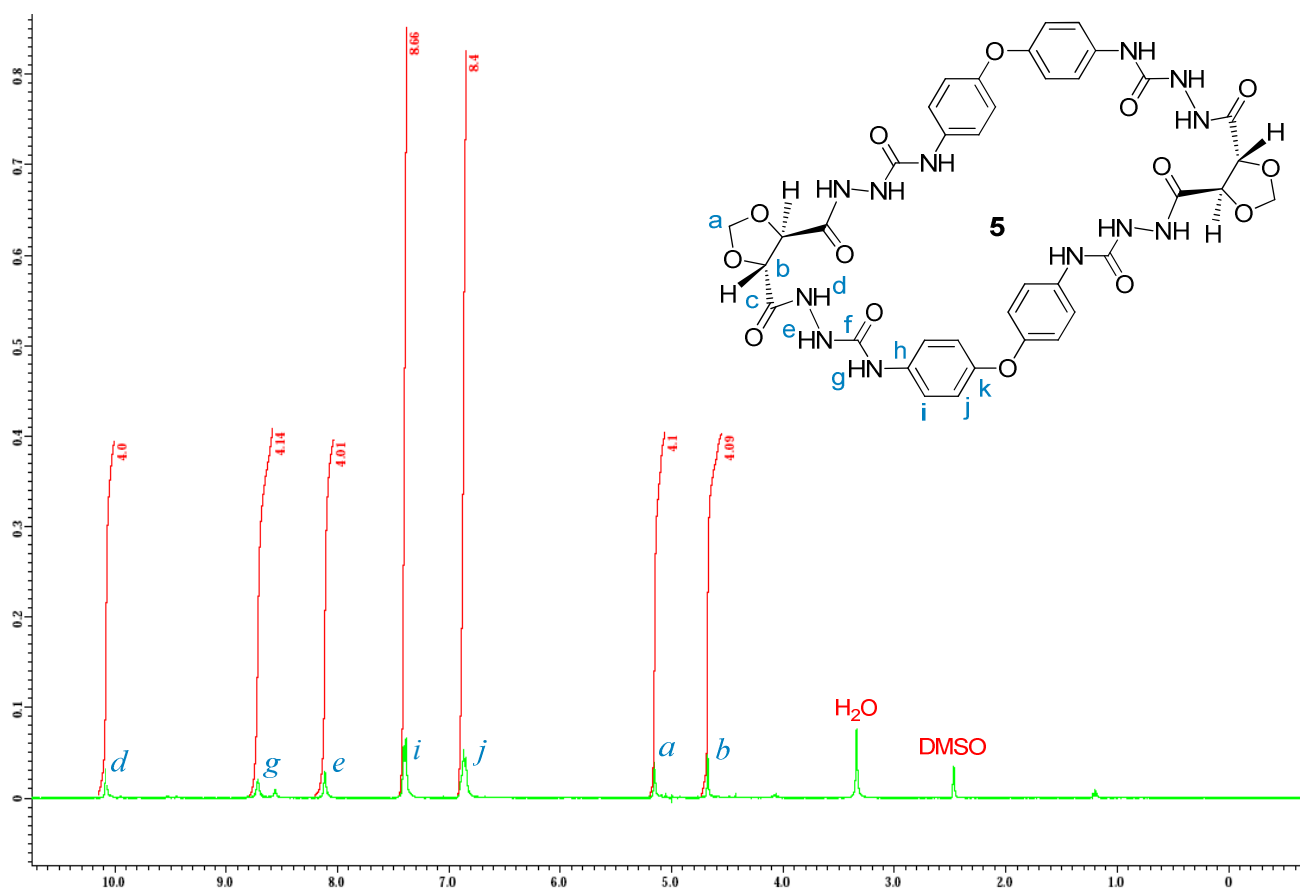


Figure 1. ^1H NMR spectrum for macrocycle **5** (DMSO- d_6 , 400 MHz).

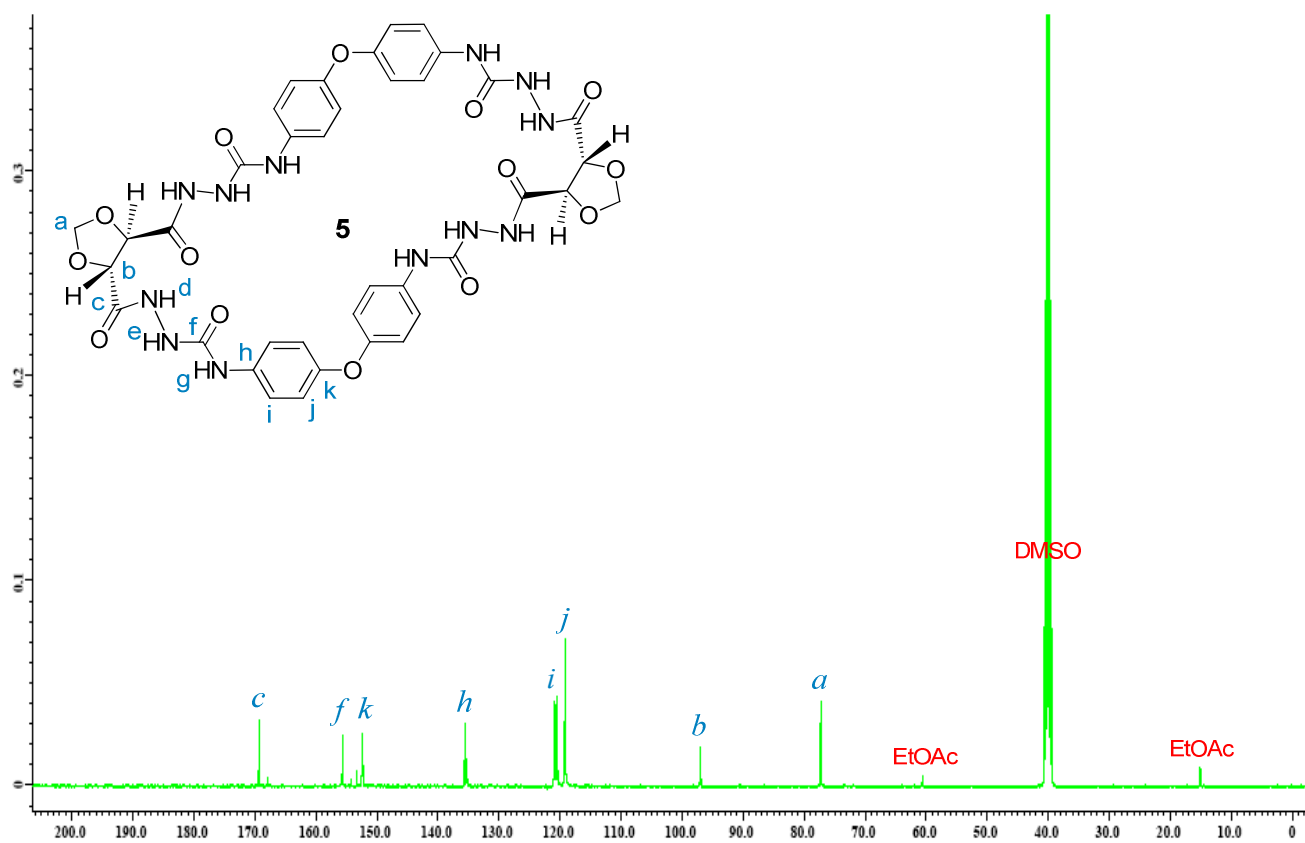


Figure 2. ^{13}C NMR spectrum for macrocycle **5** (DMSO- d_6 , 100 MHz).

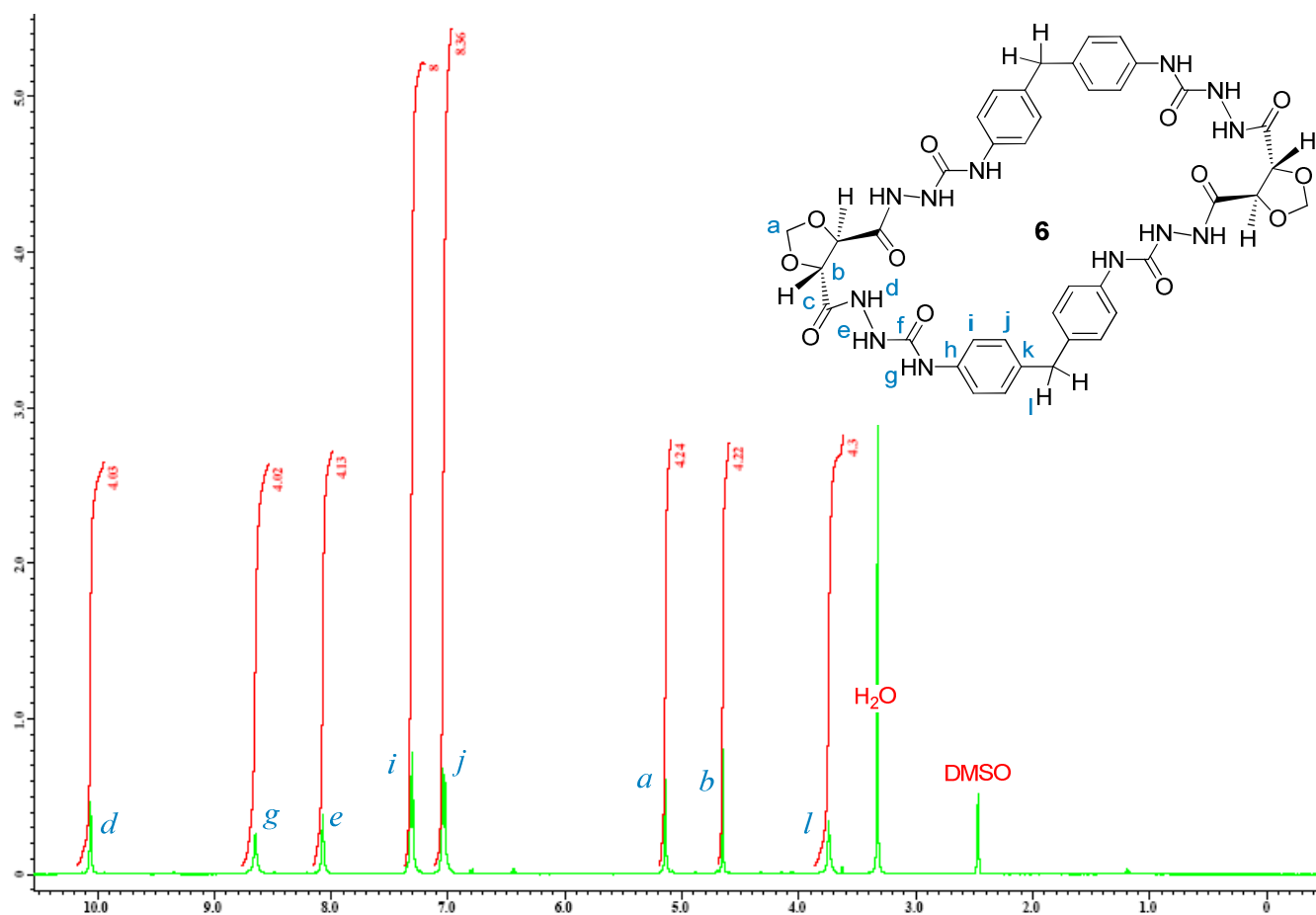


Figure 3. ^1H NMR spectrum for macrocycle **6** (DMSO-d_6 , 400 MHz).

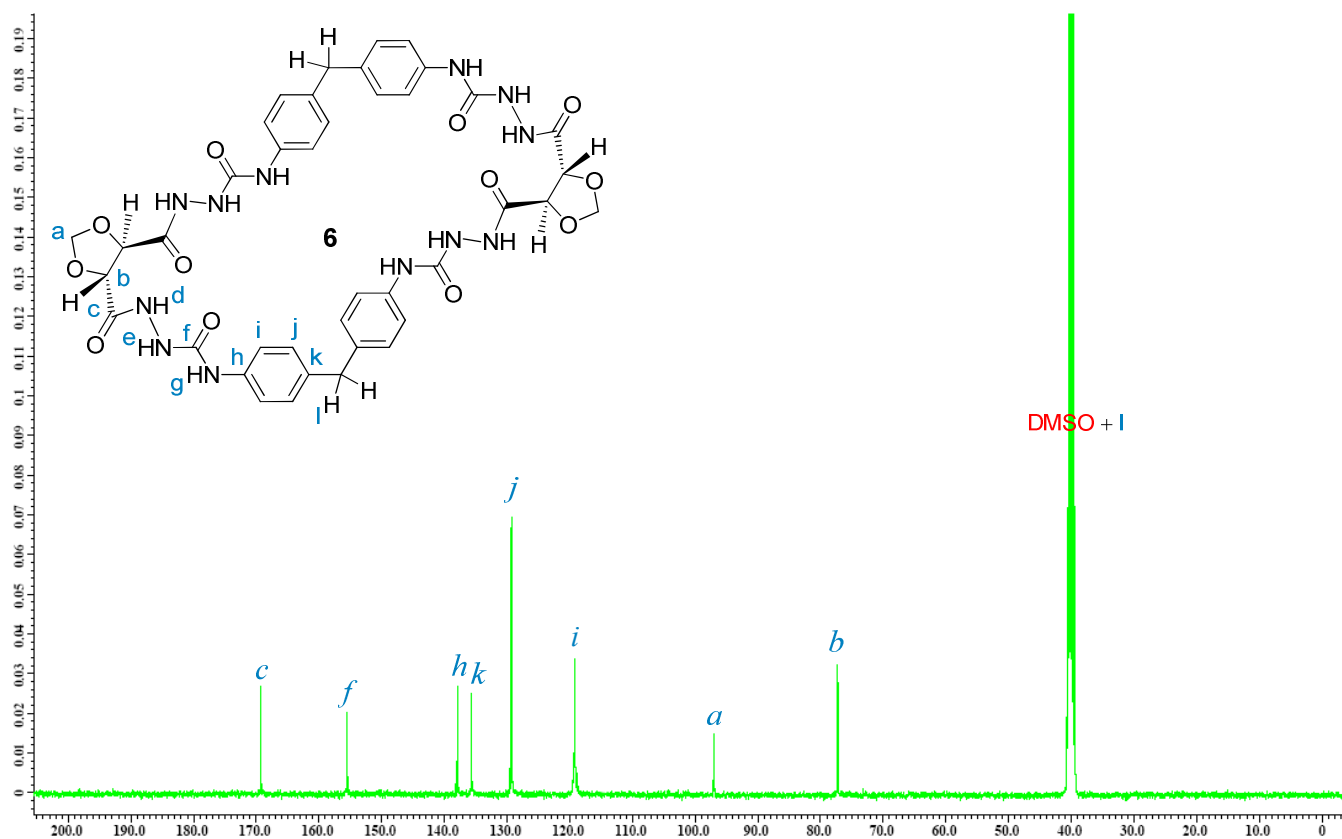


Figure 4. ^{13}C NMR spectrum for macrocycle **6** (DMSO-d_6 , 100 MHz).

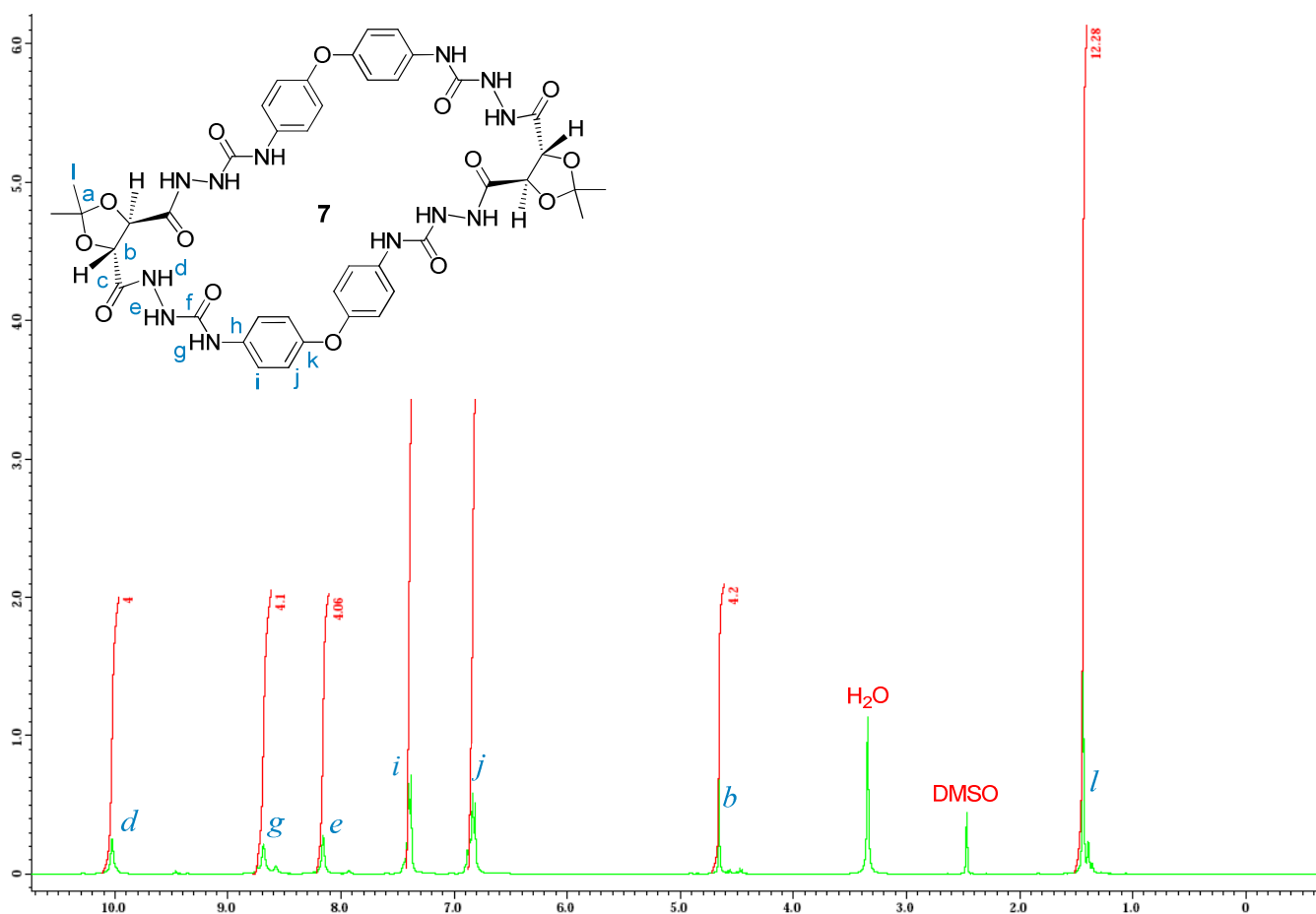


Figure 5. ^1H NMR spectrum for macrocycle **7** (DMSO-d_6 , 400 MHz).

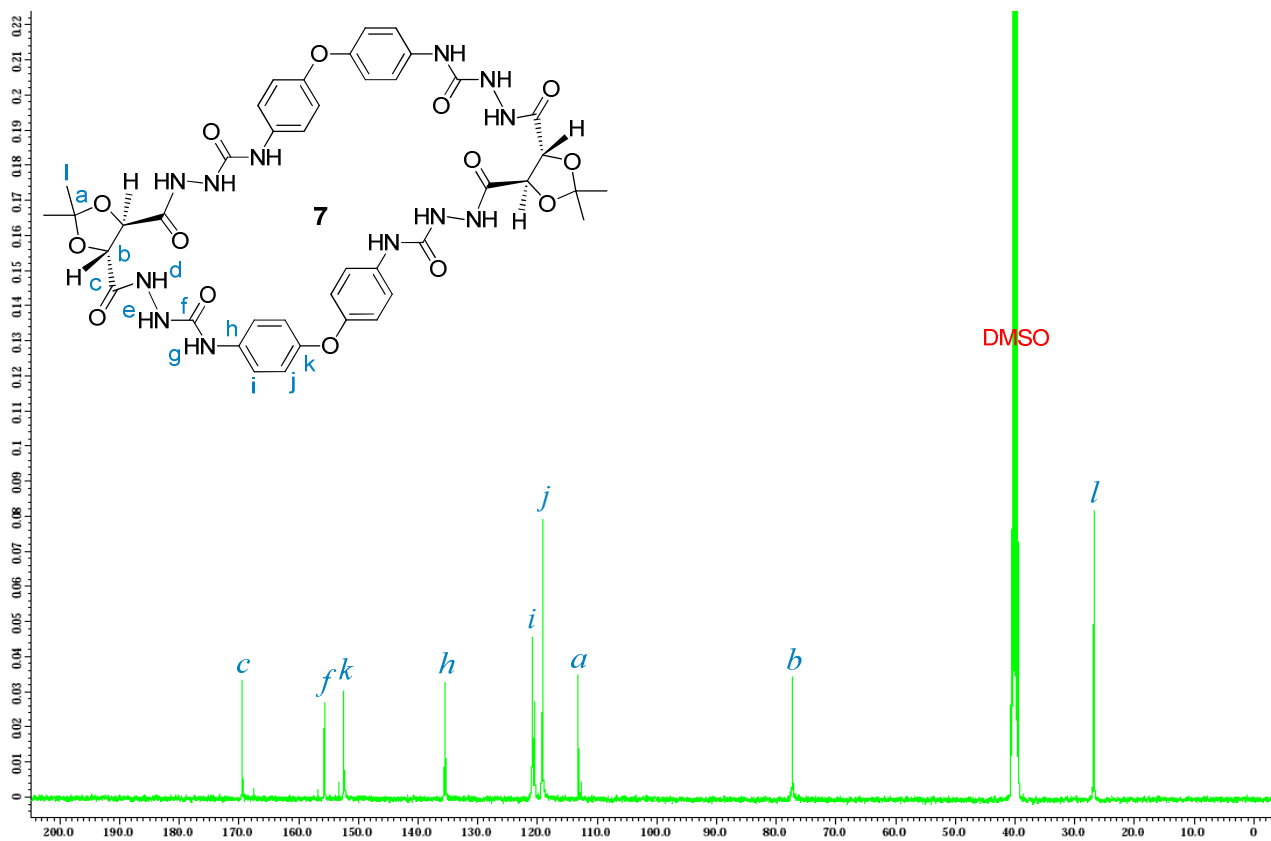


Figure 6. ^{13}C NMR spectrum for macrocycle **7** (DMSO-d_6 , 100 MHz).

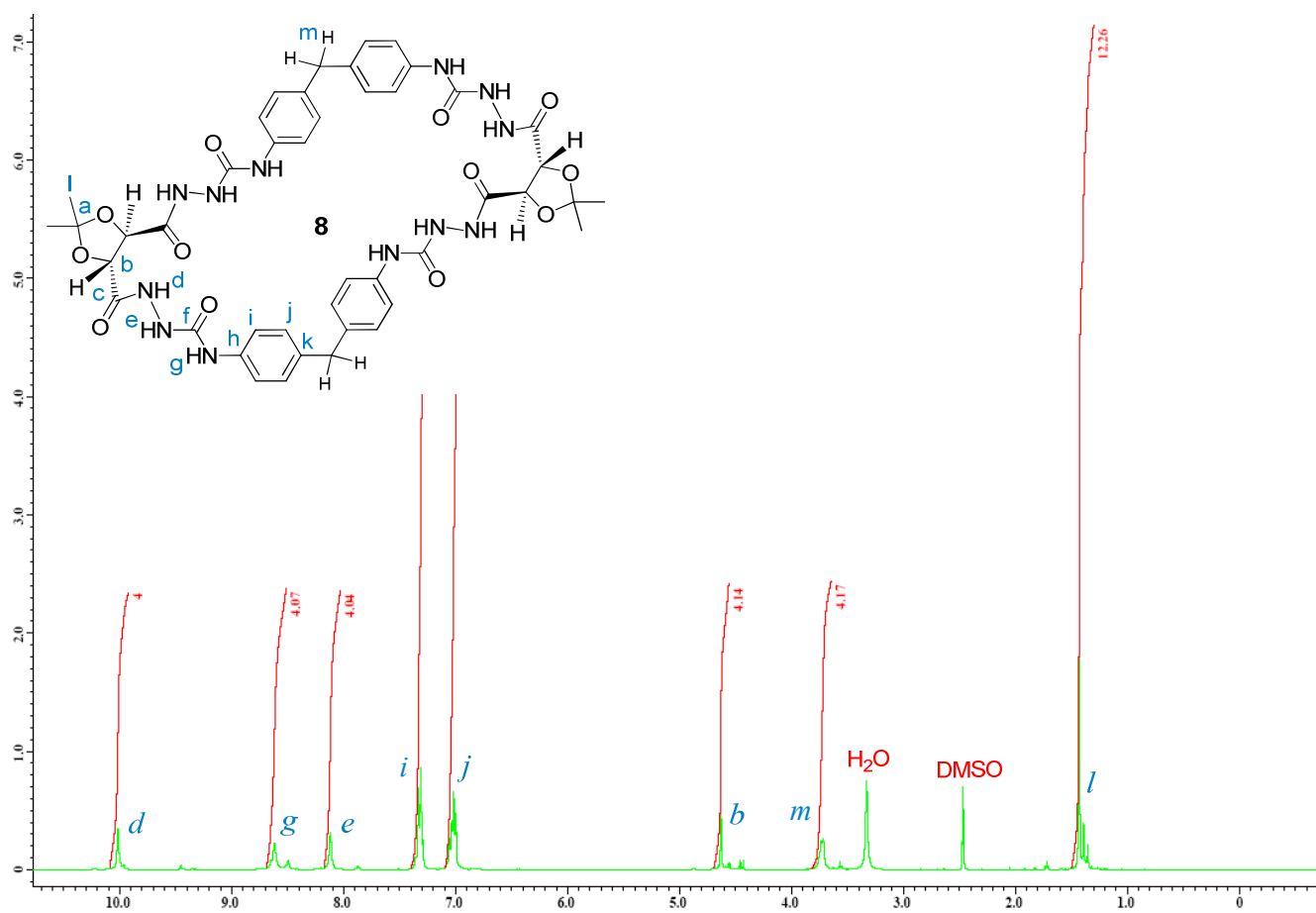


Figure 7. ^1H NMR spectrum for macrocycle **8** (DMSO- d_6 , 400 MHz).

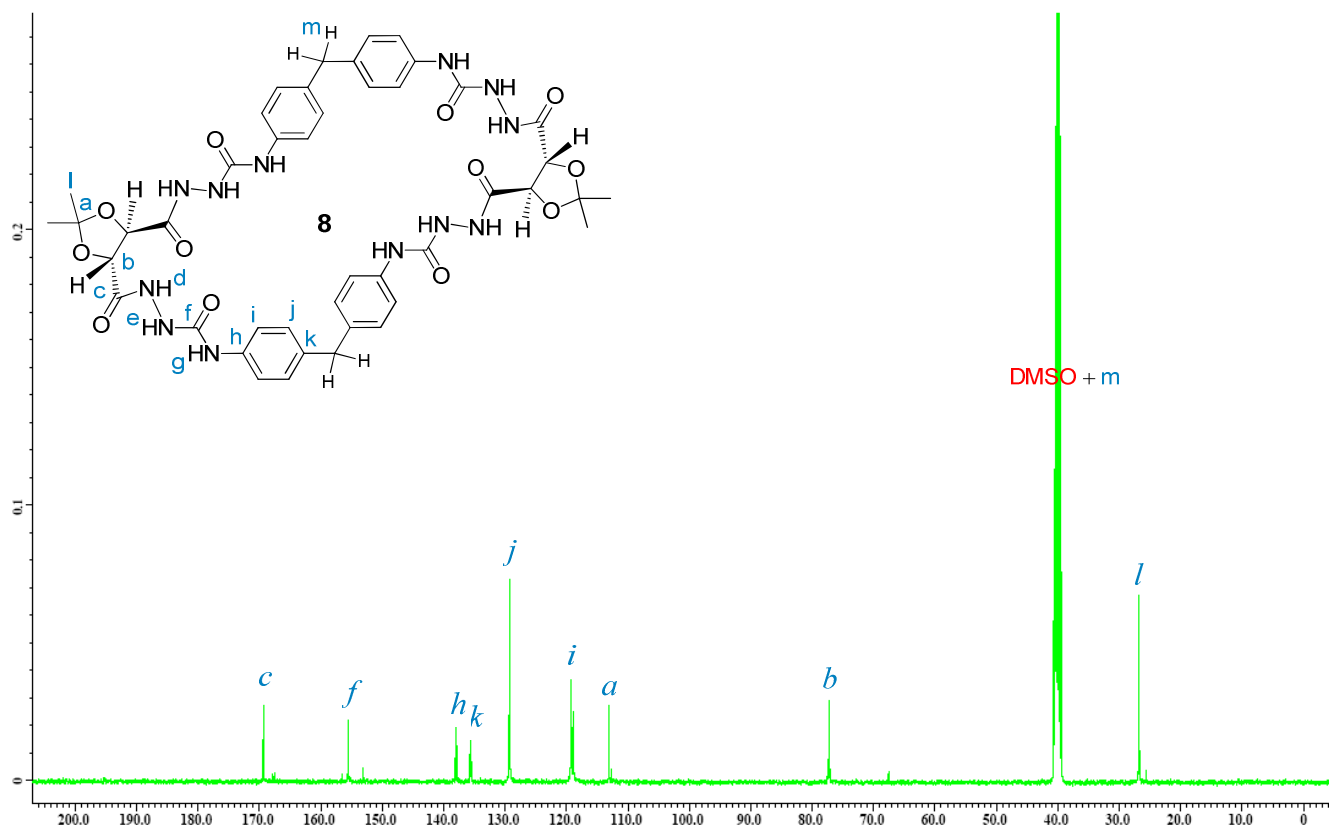


Figure 8. ^{13}C NMR spectrum for macrocycle **8** (DMSO- d_6 , 100 MHz).

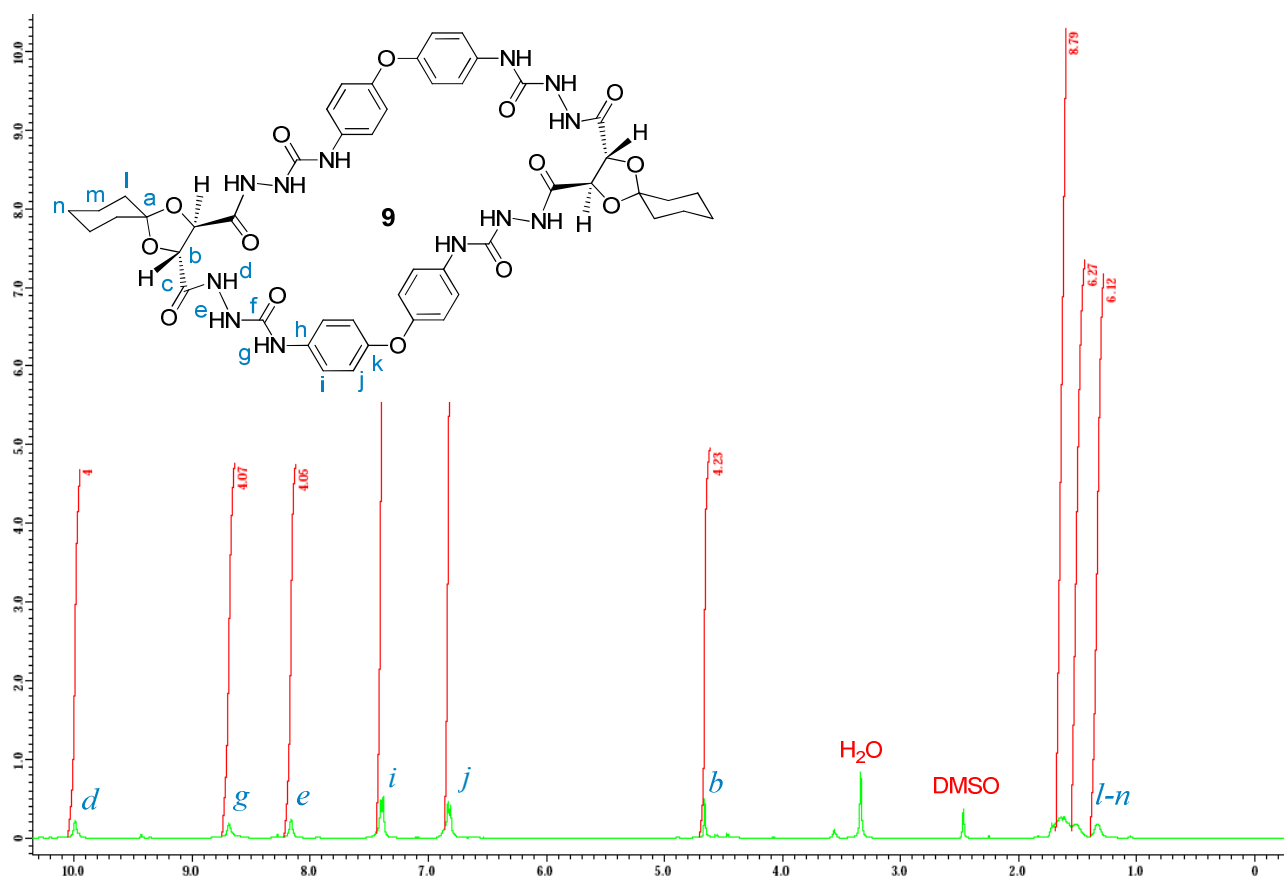


Figure 9. ^1H NMR spectrum for macrocycle **9** (DMSO-d_6 , 400 MHz).

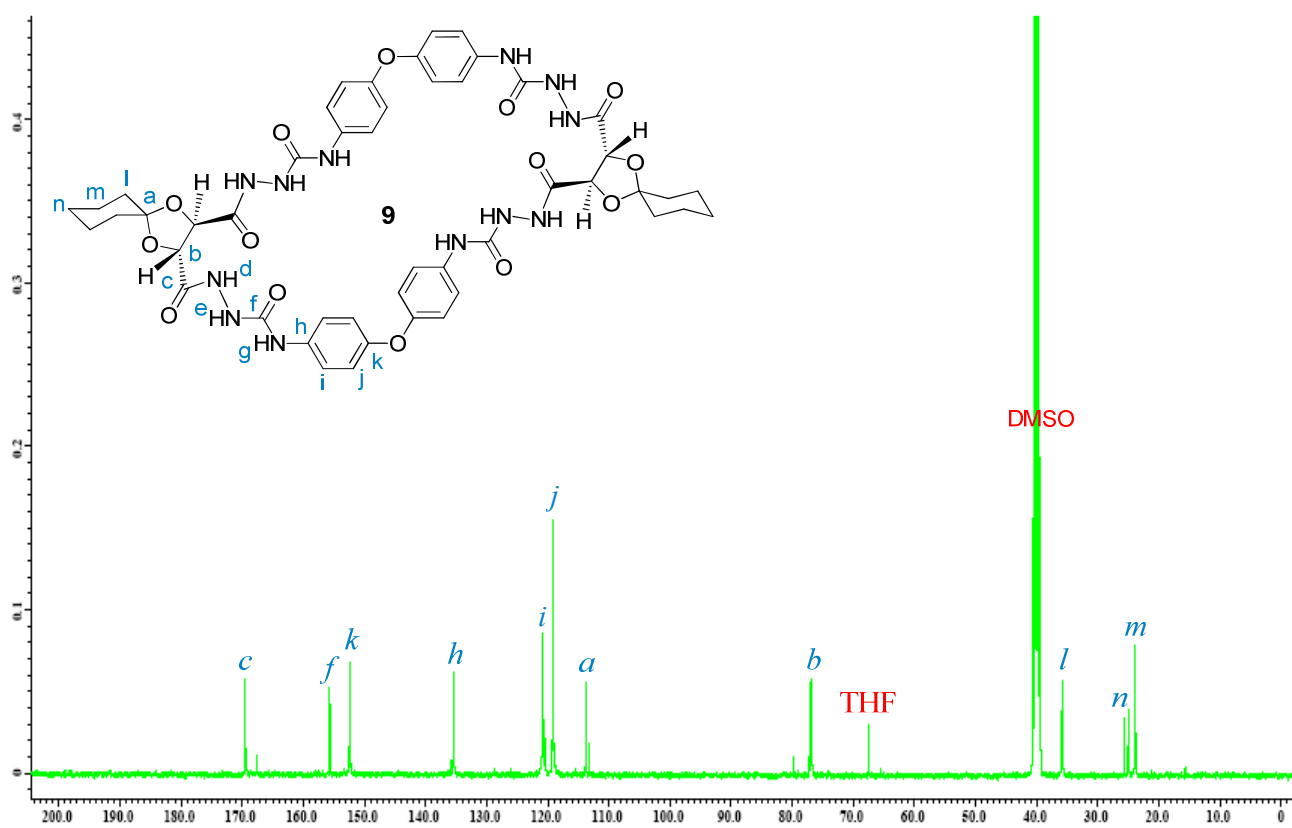


Figure 10. ^{13}C NMR spectrum for macrocycle **9** (DMSO-d_6 , 100 MHz).

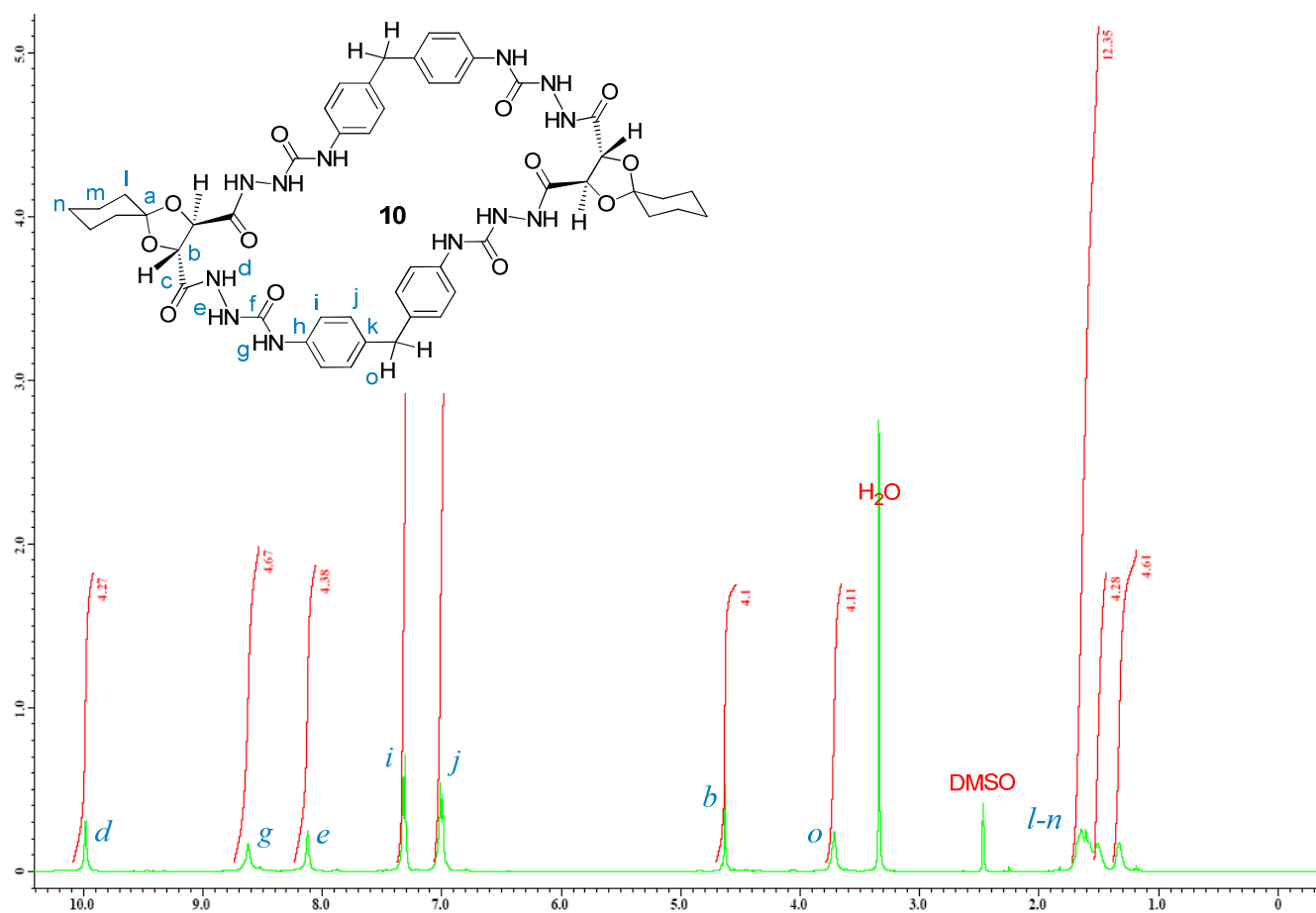


Figure 11. ¹H NMR spectrum for macrocycle **10** (DMSO-d₆, 400 MHz).

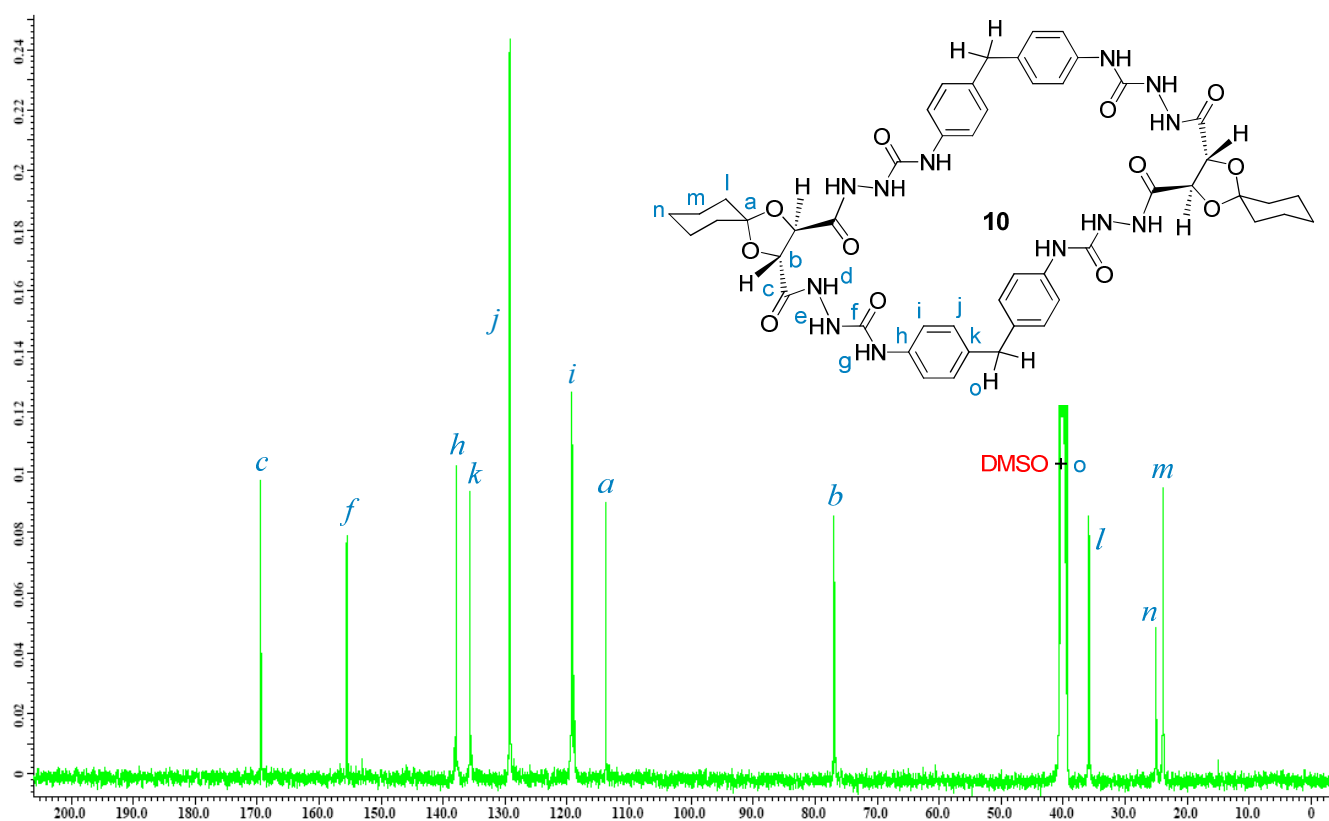


Figure 12. ¹³C NMR spectrum for macrocycle **10** (DMSO-d₆, 100 MHz).

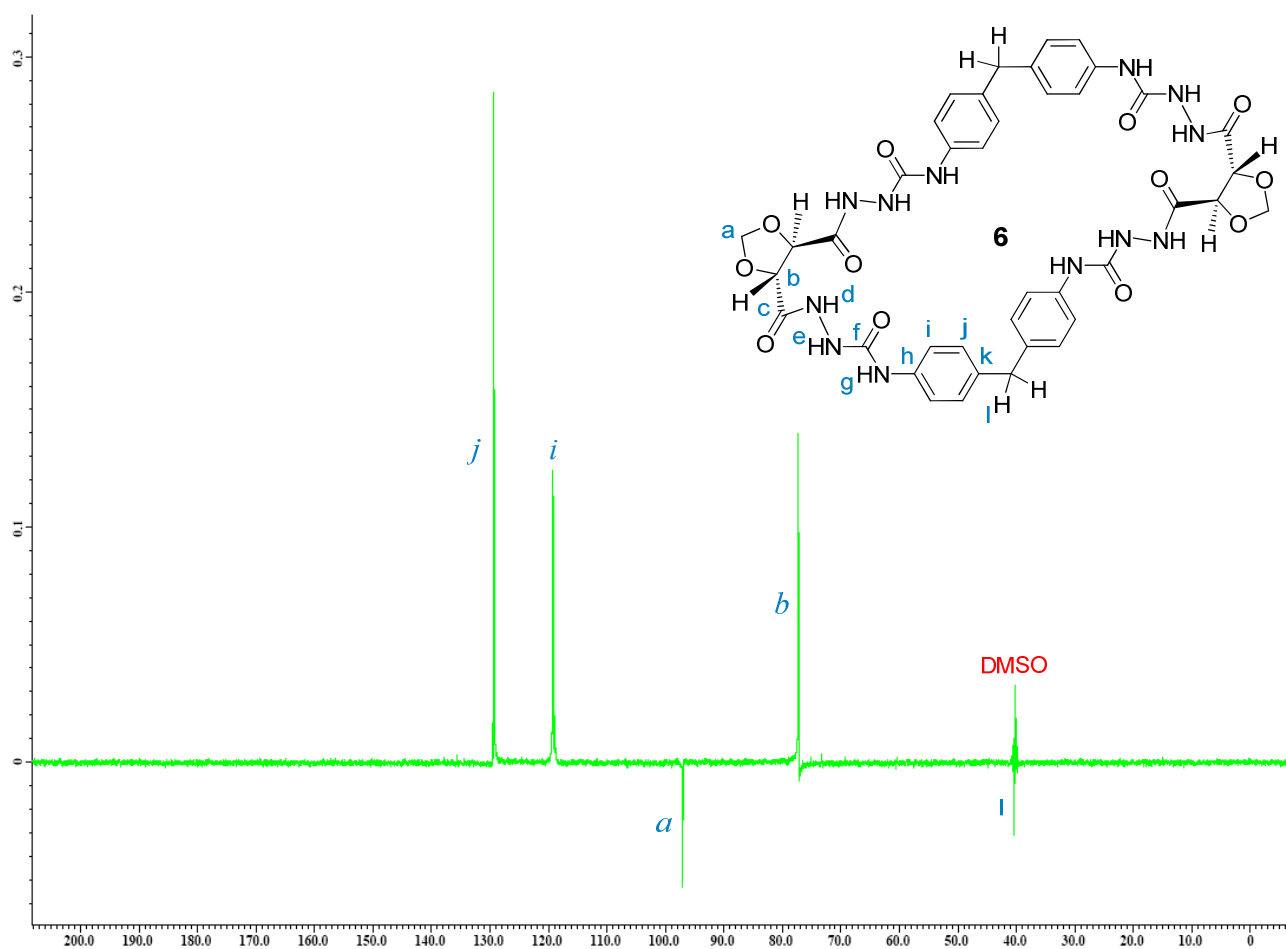


Figure 13. DEPT-135 spectrum for macrocycle **6** showing the CH₂ signal (DMSO-d₆, 100 MHz).

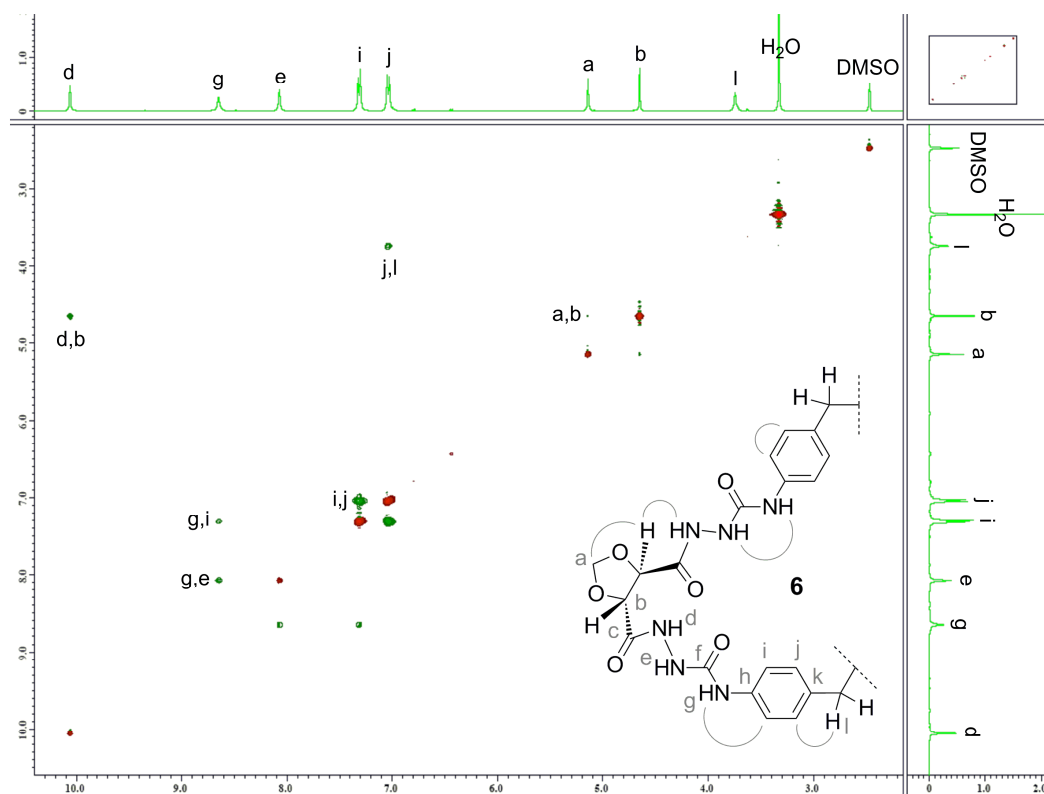


Figure 14. 2D ROESY spectrum for macrocycle **6**, DMSO-d₆.

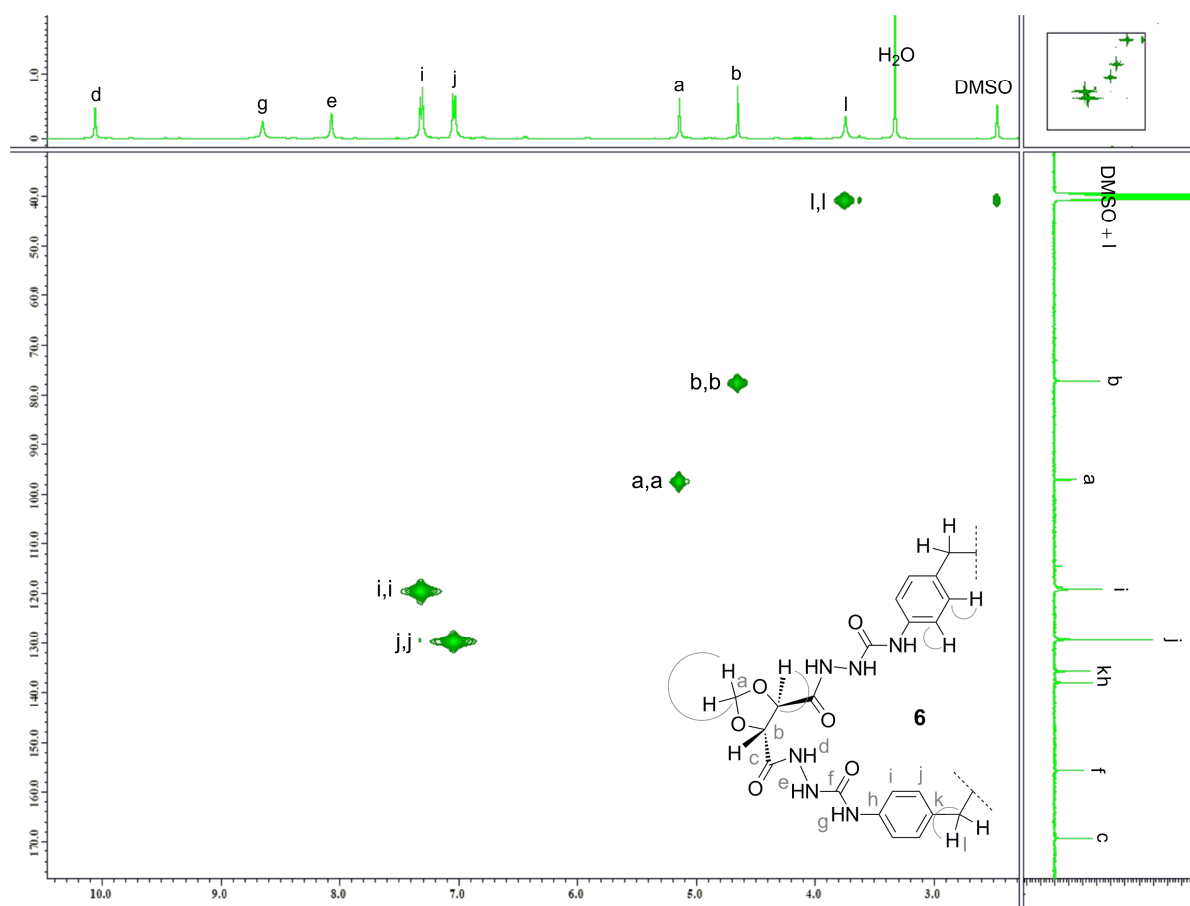


Figure 15. 2D HMQC spectrum for macrocycle **6**, DMSO- d_6 .

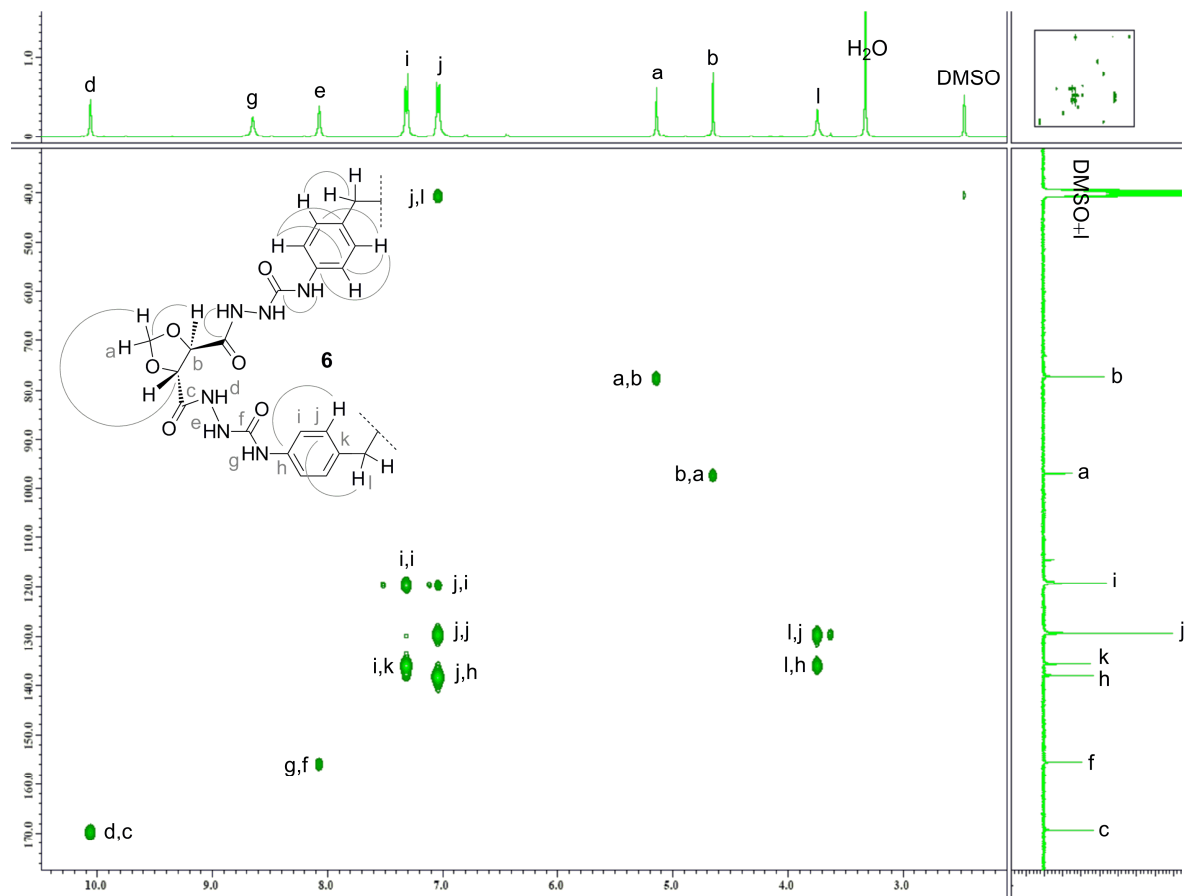


Figure 16. 2D HMBC spectrum for macrocycle **6**, DMSO- d_6 .

Scheme 1. General mechanism of fragmentation for the novel macrocycles 5-10

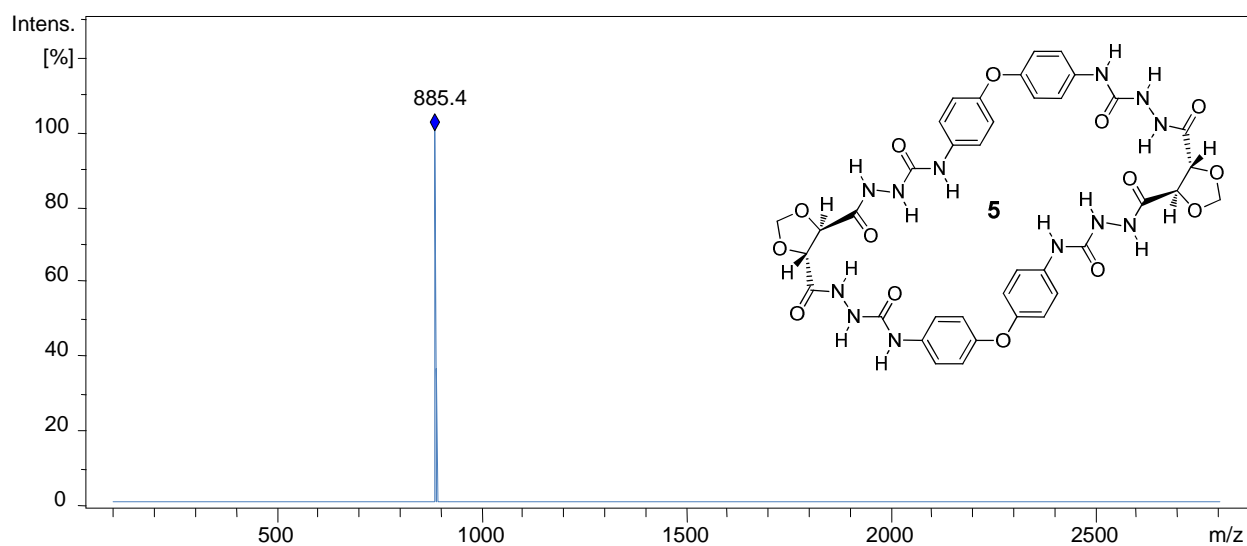
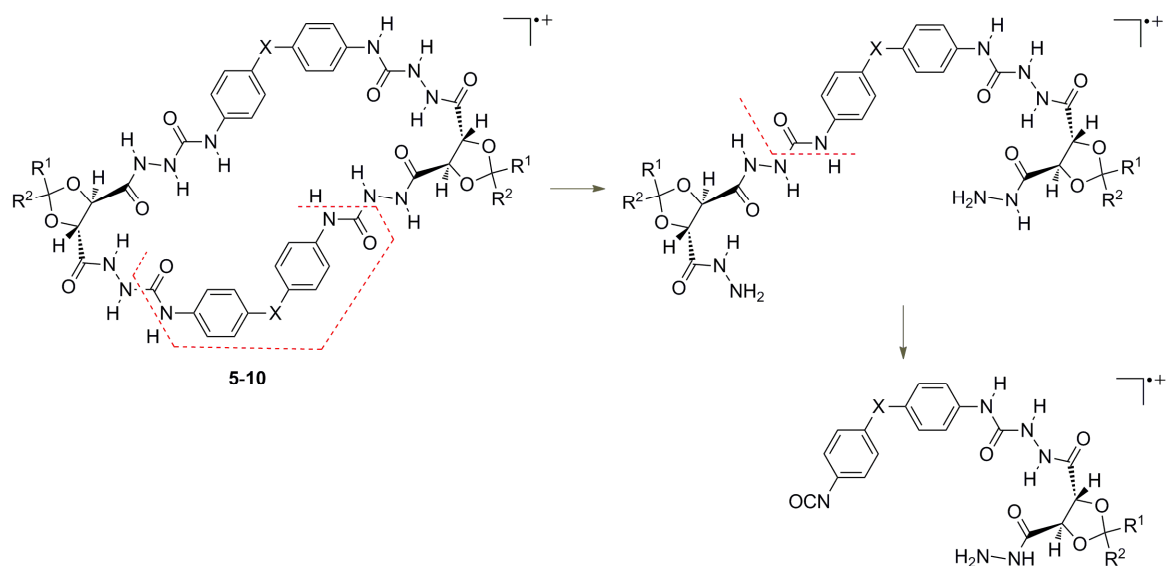


Figure 17. ESI-MS² for macrocycle **5** in the positive ion mode.

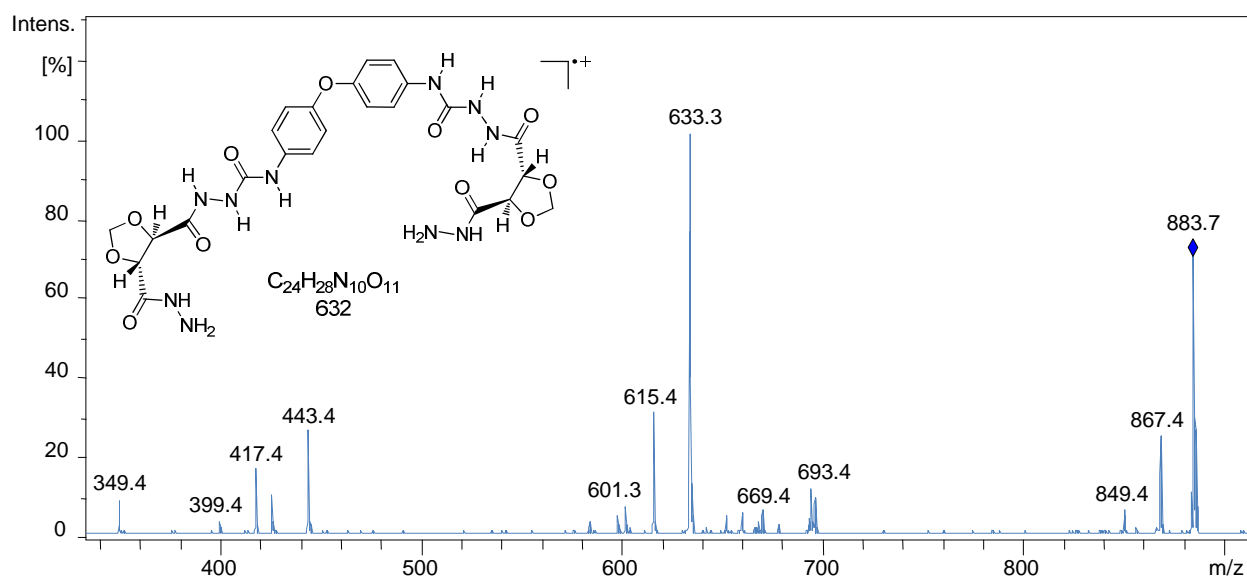


Figure 18. Tandem ESI-MS for macrocycle **5** in the positive ion mode.

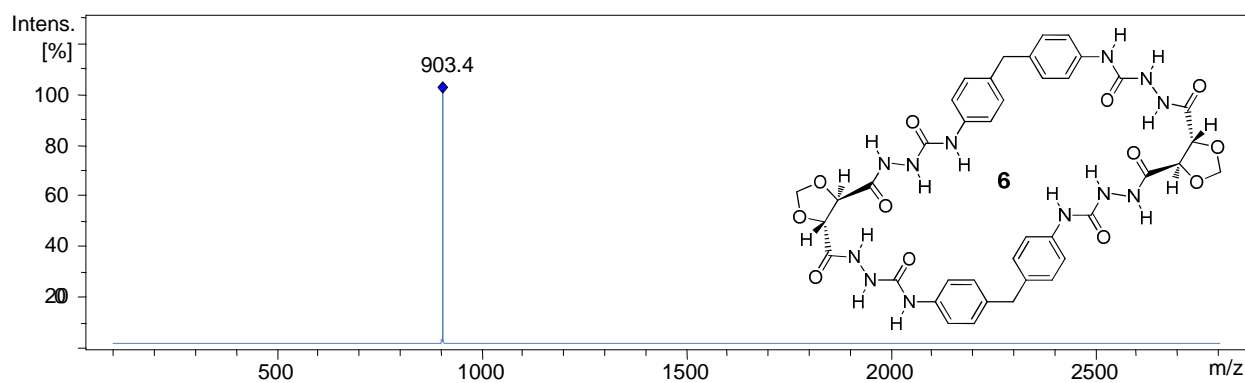


Figure 19. ESI-MS² for macrocycle **6** in the positive ion mode.

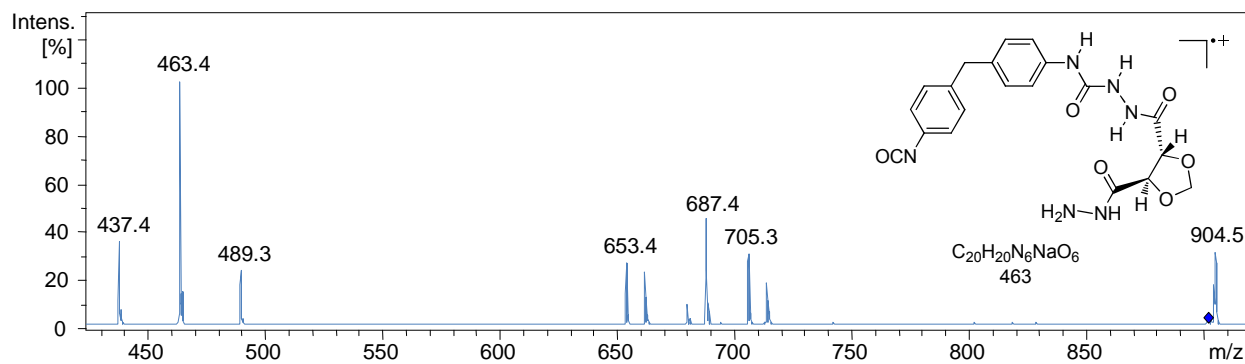


Figure 20. Tandem ESI-MS for macrocycle **6** in the positive ion mode.

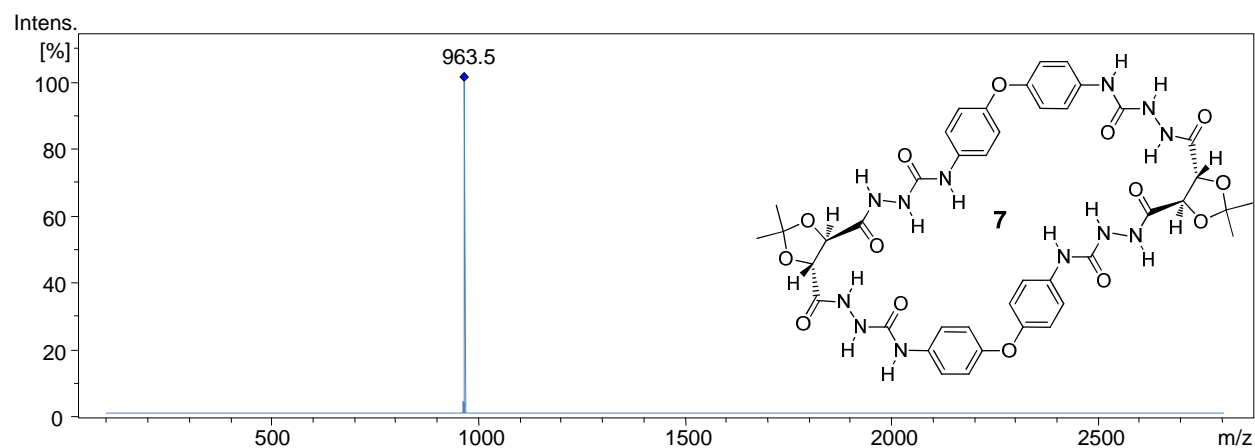


Figure 21. ESI-MS² for macrocycle **7** in the positive ion mode.

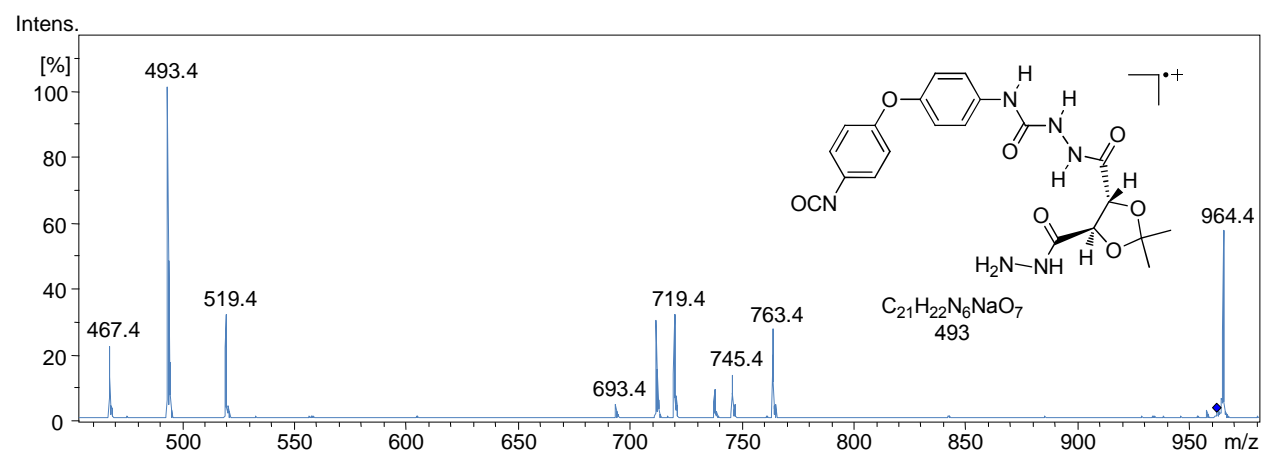


Figure 22. Tandem ESI-MS for macrocycle **7** in the positive ion mode.

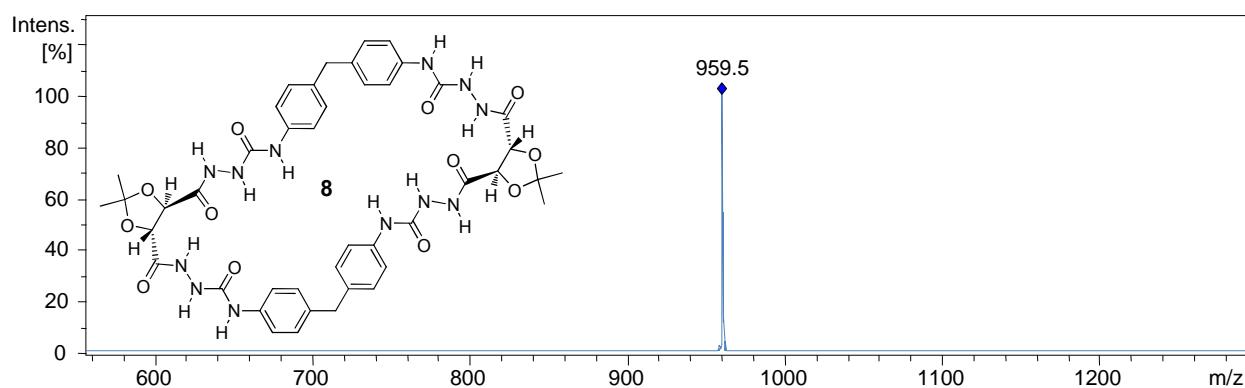


Figure 23. ESI-MS² for macrocycle **8** in the positive ion mode.

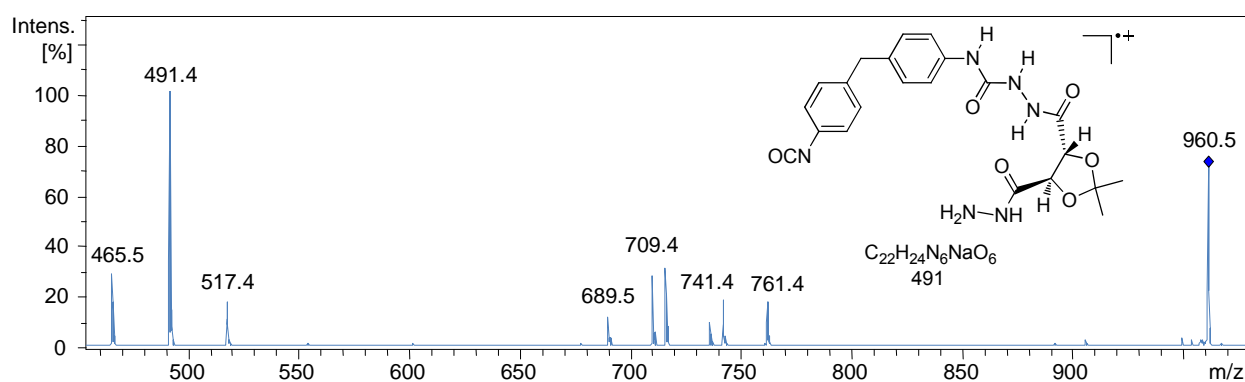


Figure 24. Tandem ESI-MS for macrocycle **8** in the positive ion mode.

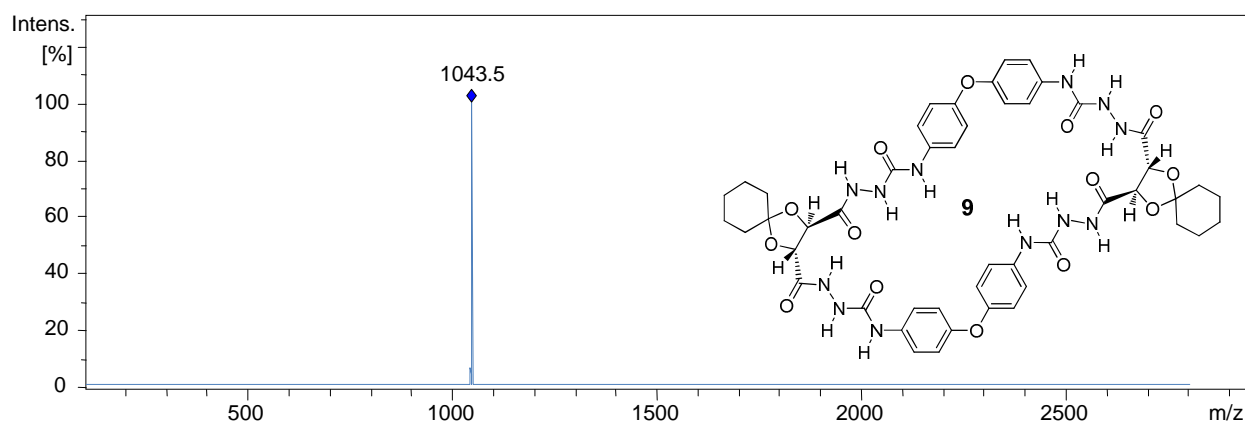


Figure 25. ESI-MS² for macrocycle **9** in the positive ion mode.

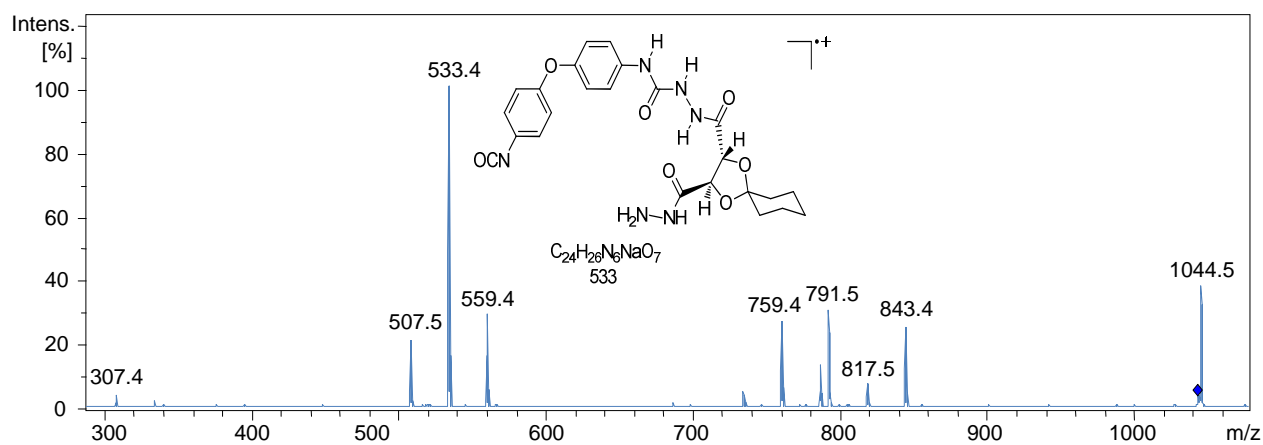


Figure 26. Tandem ESI-MS for macrocycle **9** in the positive ion mode.

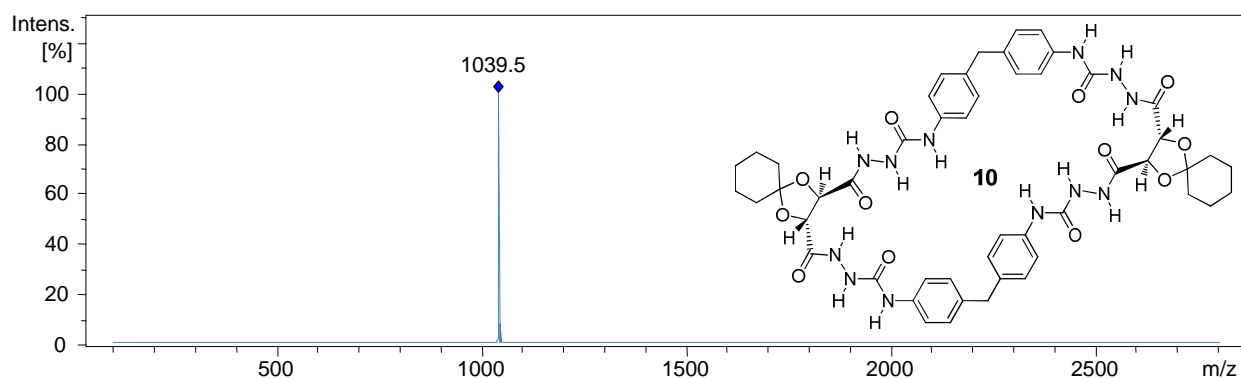


Figure 27. ESI-MS² for macrocycle **10** in the positive ion mode.

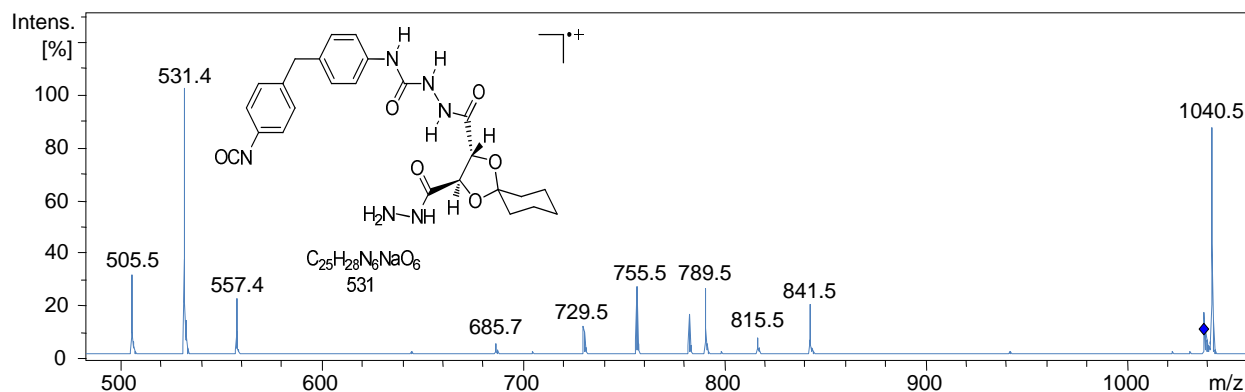


Figure 28. Tandem ESI-MS for macrocycle **10** in the positive ion mode.

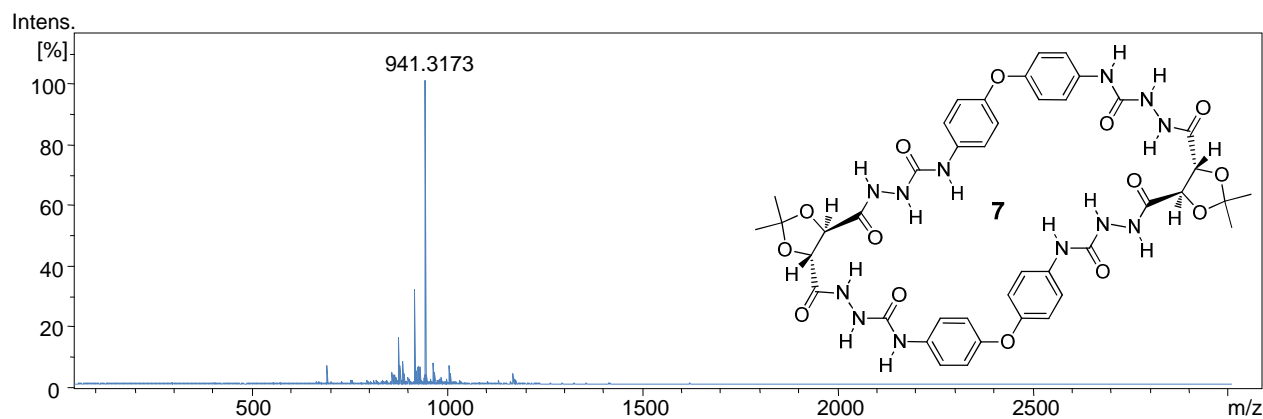


Figure 29. ESI-TOF/MS for free host **7** in the positive ion mode.

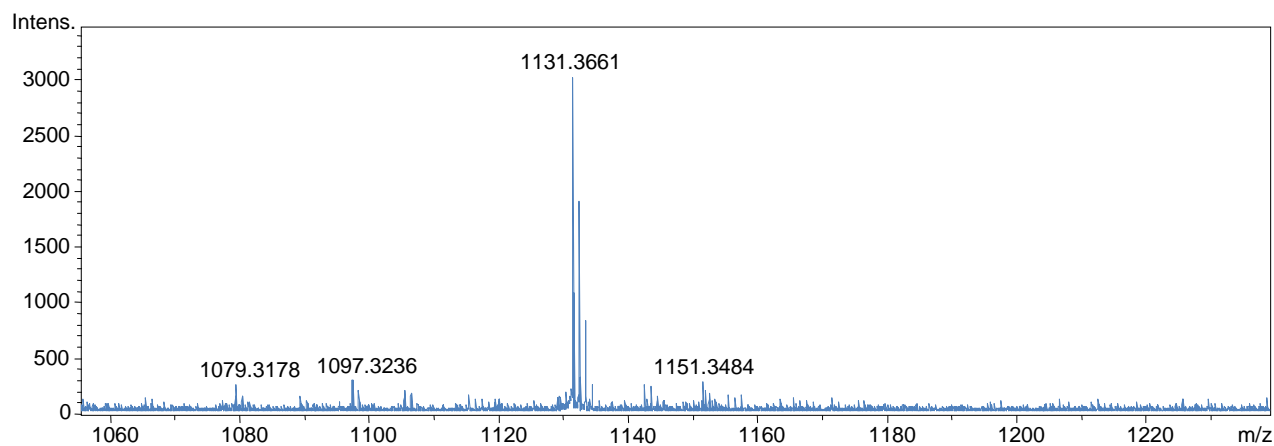


Figure 30. ESI-TOF/MS for host/guest complex **7/11** in the negative ion mode.

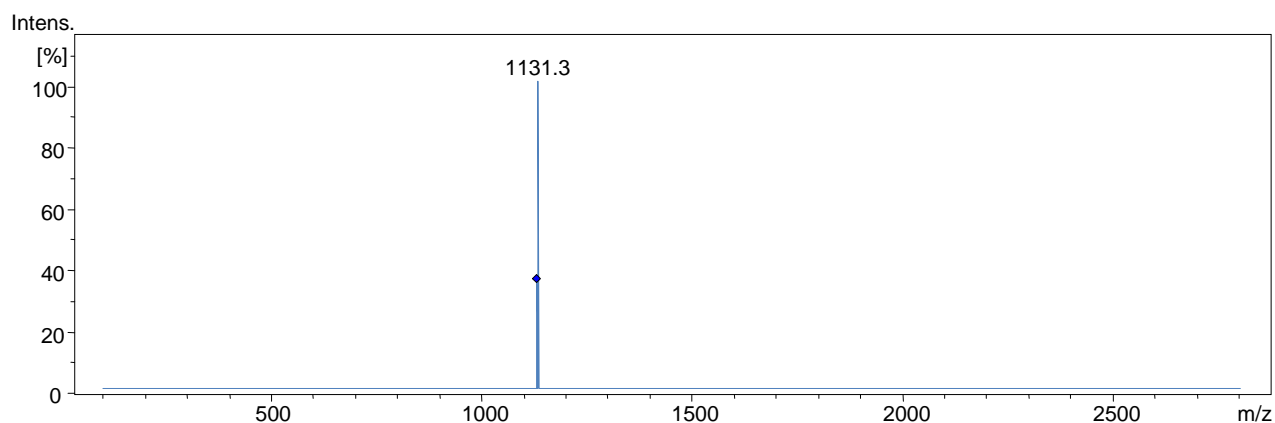


Figure 31. ESI-MS² for host/guest complex **7/11** in the negative ion mode.

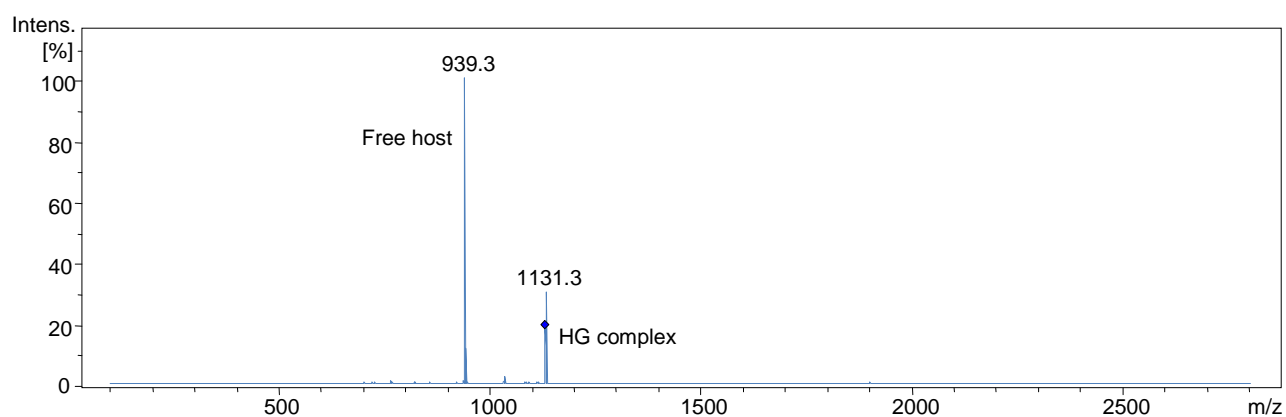


Figure 32. Tandem ESI-MS for host/guest complex **7/11** in the negative ion mode.

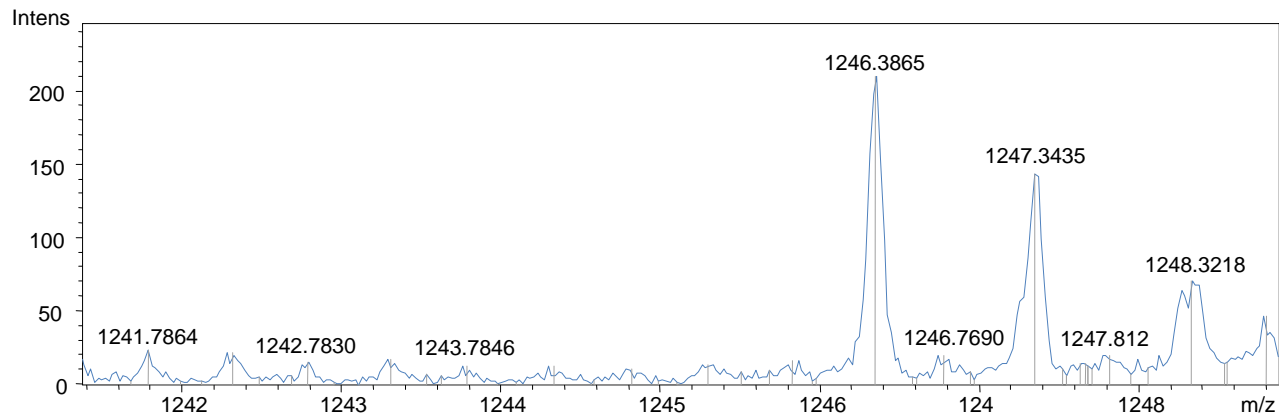


Figure 33. ESI-TOF/MS for host/guest complex **7/12** in the negative ion mode.

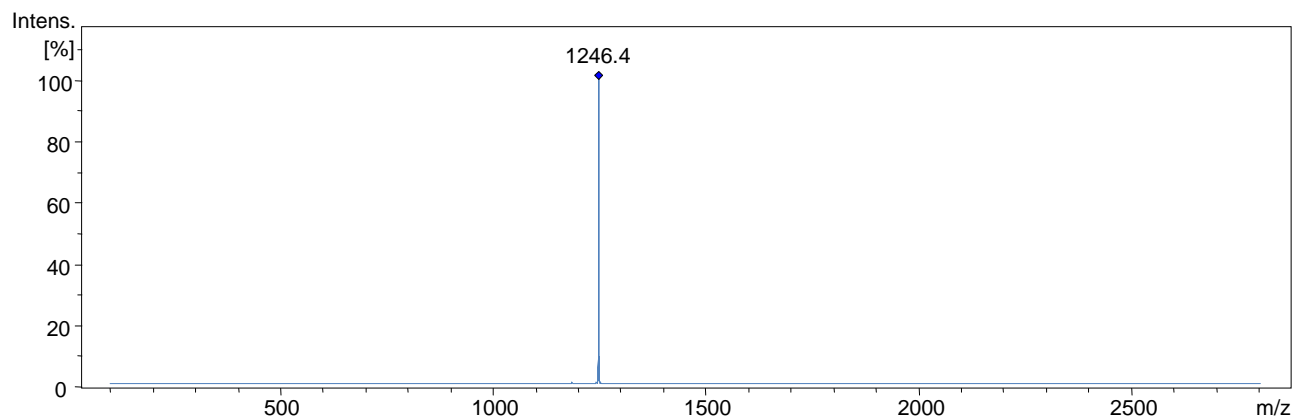


Figure 34. ESI-MS² for host/guest complex **7/12** in the negative ion mode.

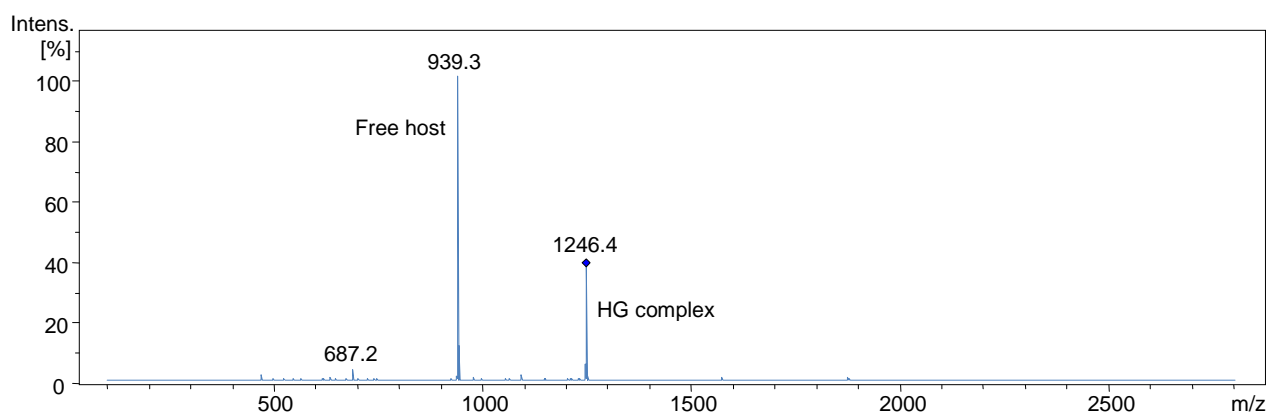


Figure 35. Tandem ESI-MS for host/guest complex **7/12** in the negative ion mode.

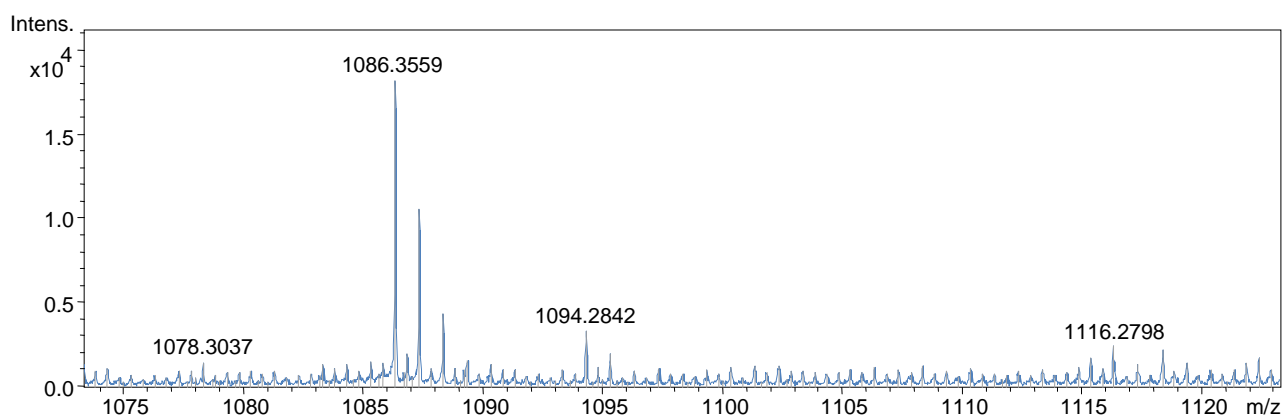


Figure 36. ESI-TOF/MS for host/guest complex **7/14** in the negative ion mode.

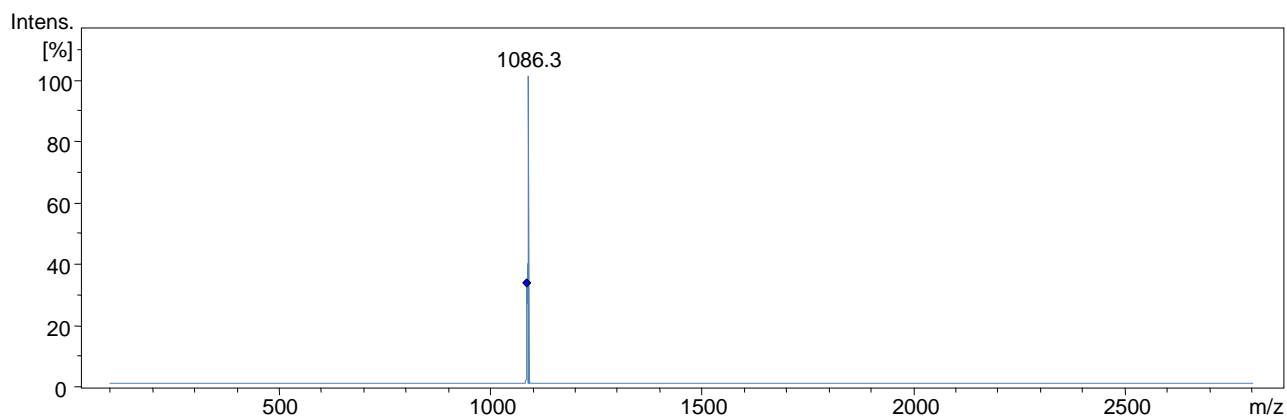


Figure 37. ESI-MS² for host/guest complex **7/14** in the negative ion mode.

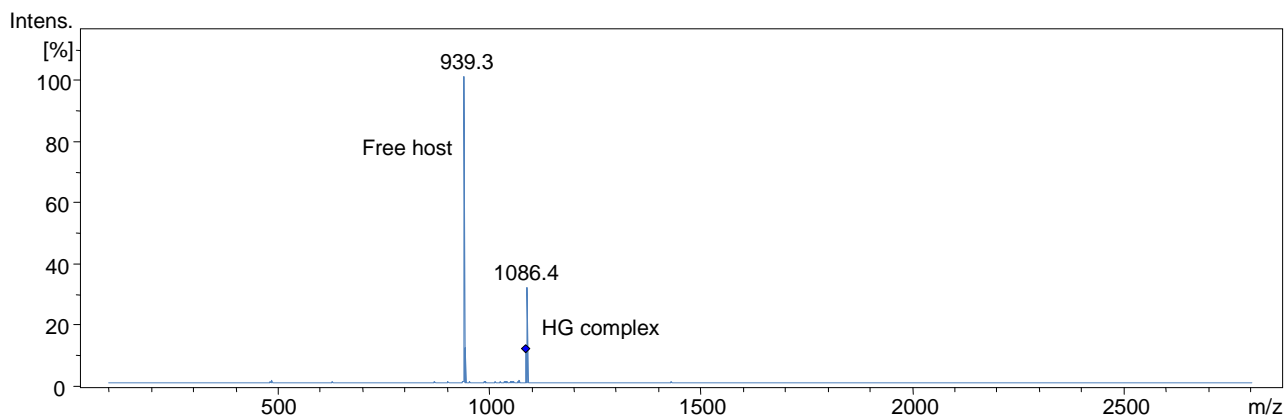


Figure 38. Tandem ESI-MS for host/guest complex **7/14** in the negative ion mode.

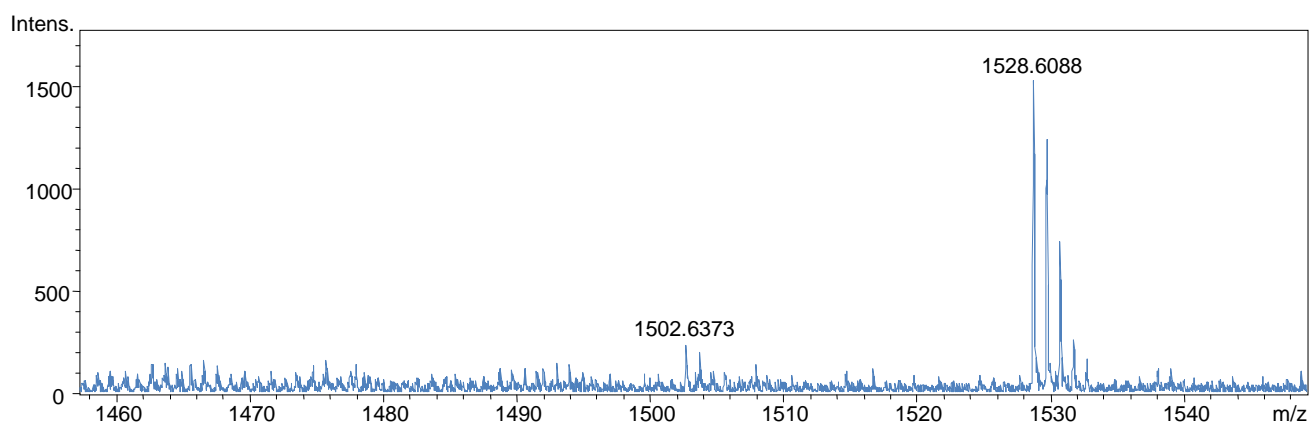


Figure 39. ESI-TOF/MS for host/guest complex **7/15** in the positive ion mode.

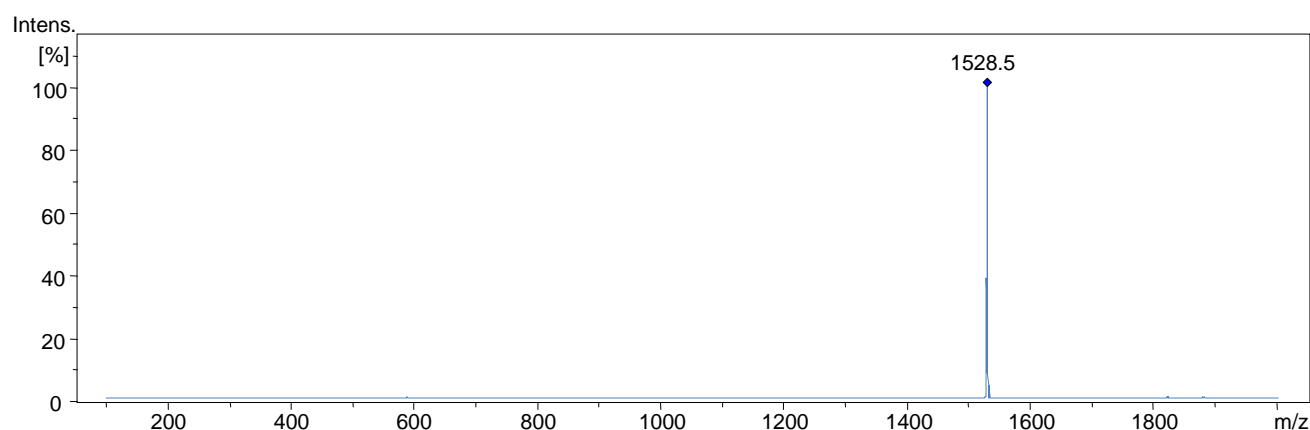


Figure 40. ESI- MS^2 for host/guest complex **7/15** in the positive ion mode.

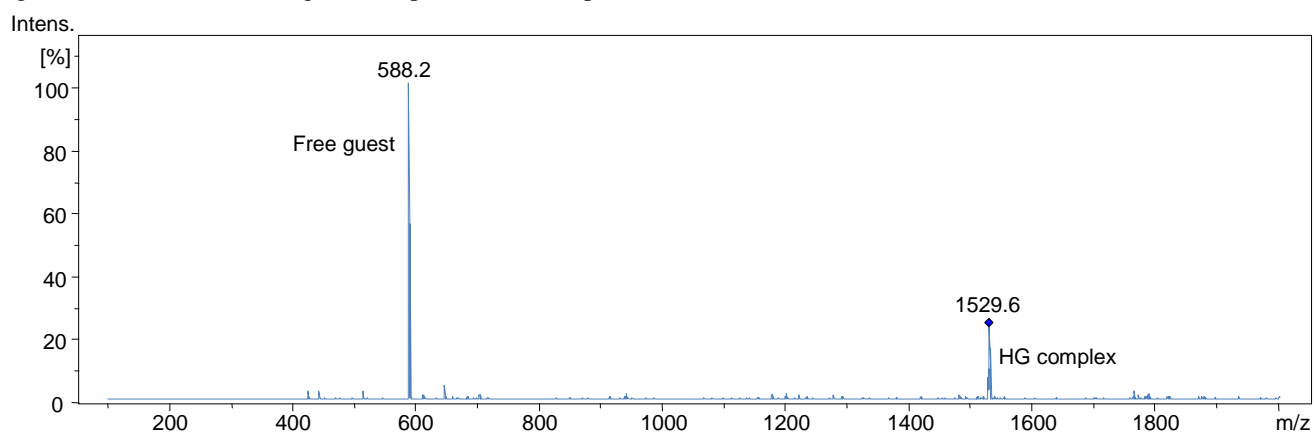


Figure 41. Tandem ESI-MS for host/guest complex **7/15** in the positive ion mode.

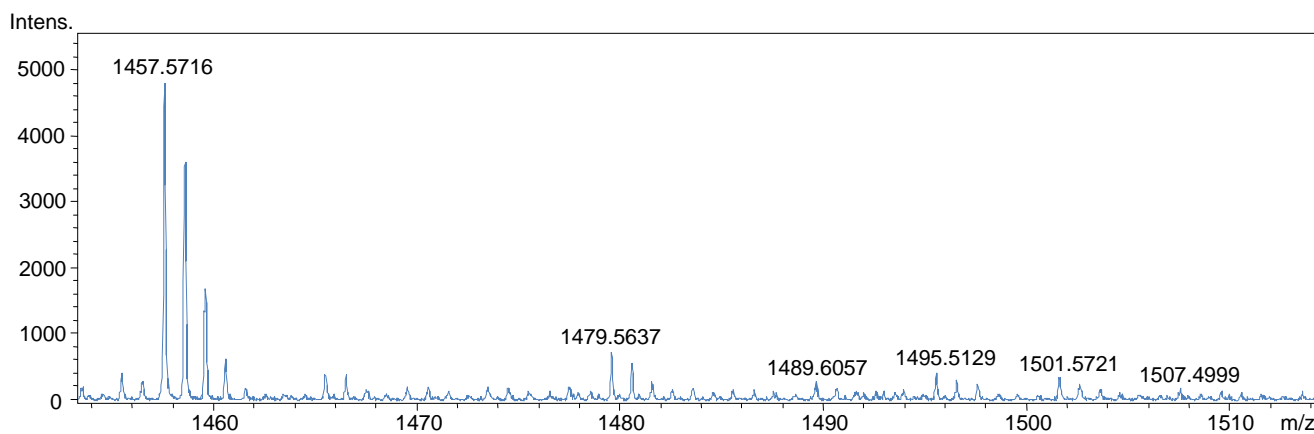


Figure 42. ESI-TOF/MS for host/guest complex **7/16** in the positive ion mode.

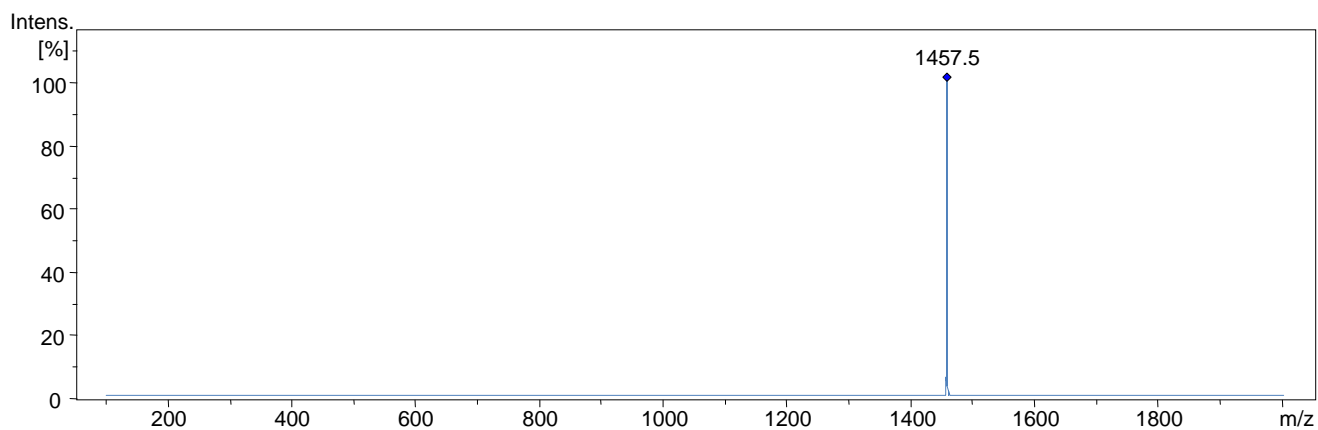


Figure 43. ESI-MS² for host/guest complex **7/16** in the positive ion mode.

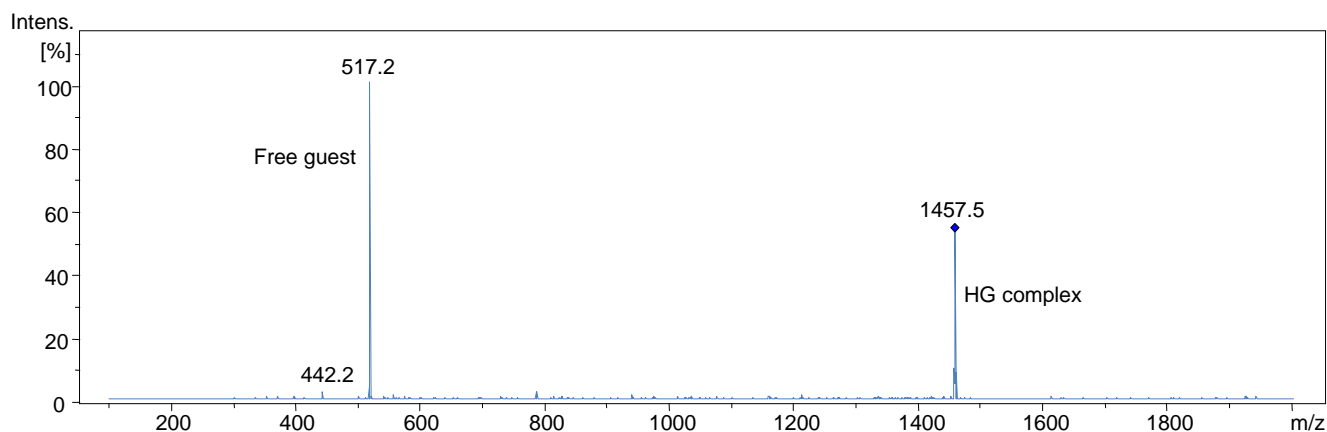


Figure 44. Tandem ESI-MS for host/guest complex **7/16** in the positive ion mode.

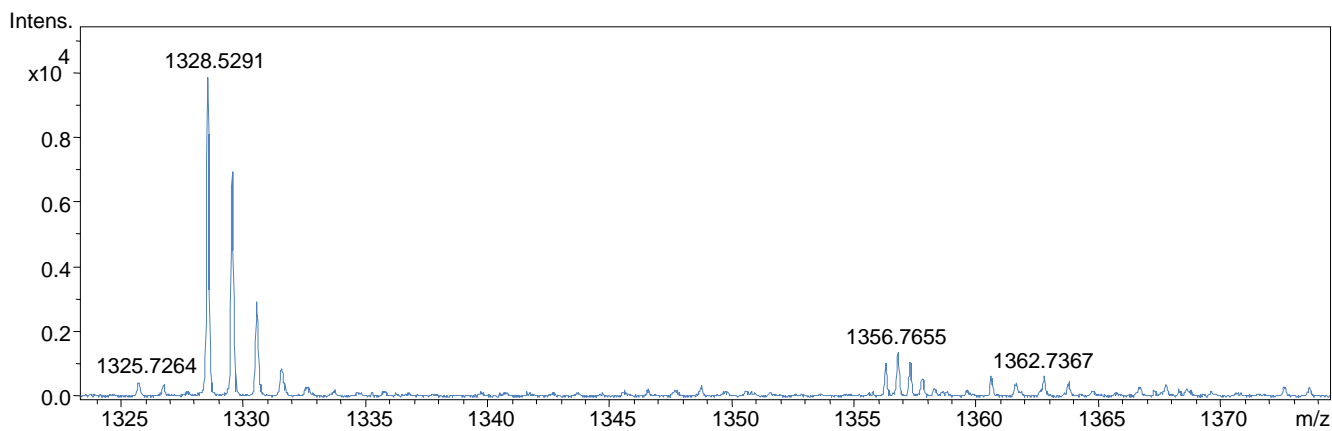


Figure 45. ESI-TOF/MS for host/guest complex **7/17** in the positive ion mode.

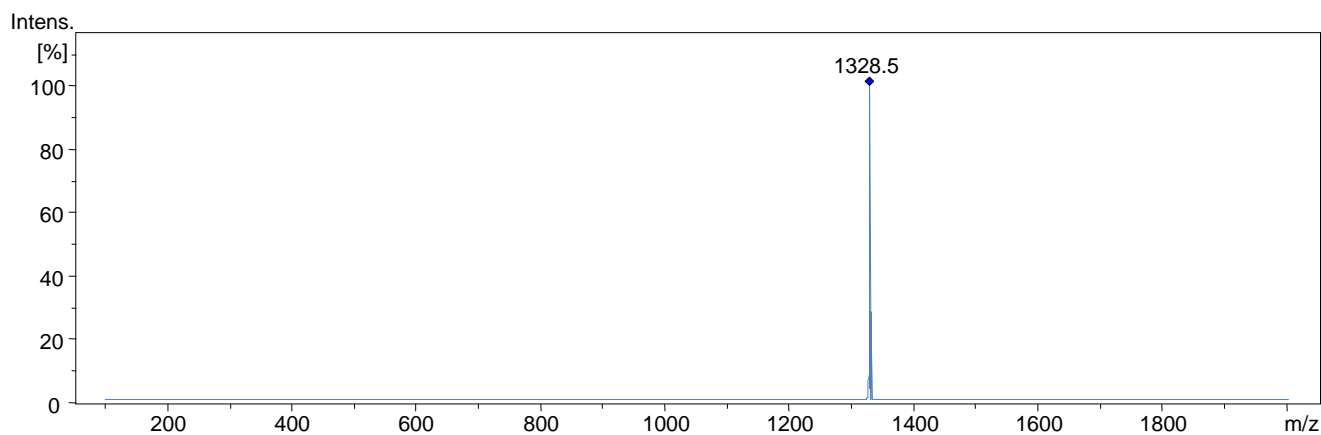


Figure 46. ESI-MS² for host/guest complex **7/17** in the positive ion mode.

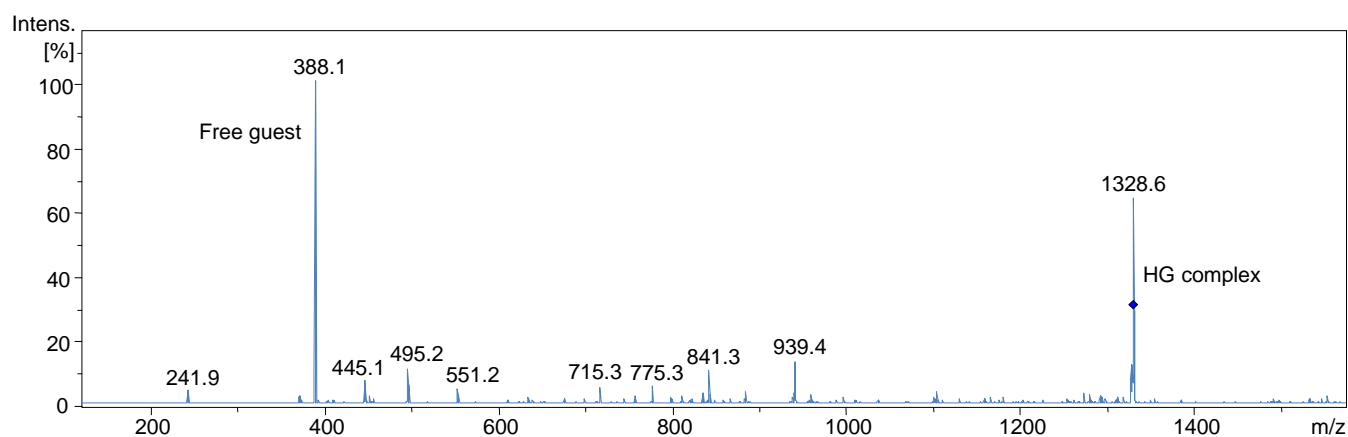


Figure 47. Tandem ESI-MS for host/guest complex **7/17** in the positive ion mode.

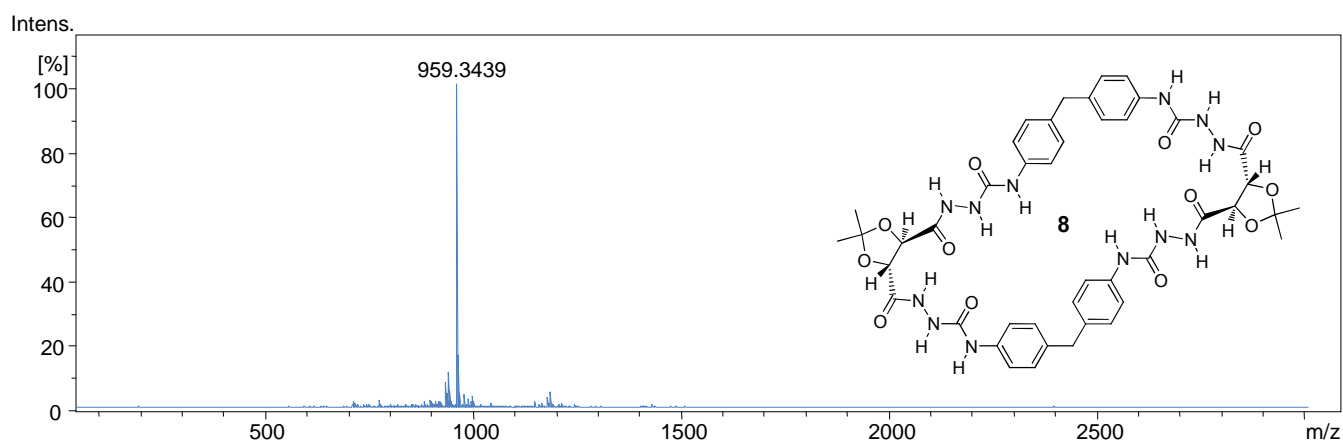


Figure 48. ESI-TOF/MS for free host **8** in the positive ion mode.

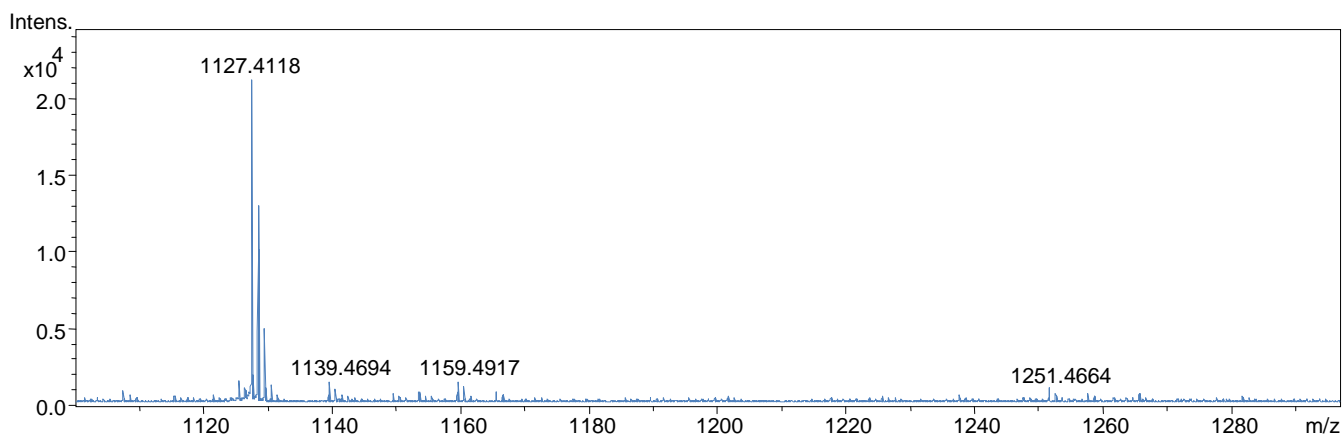


Figure 49. ESI-TOF/MS for host/guest complex **8/11** in the negative ion mode.

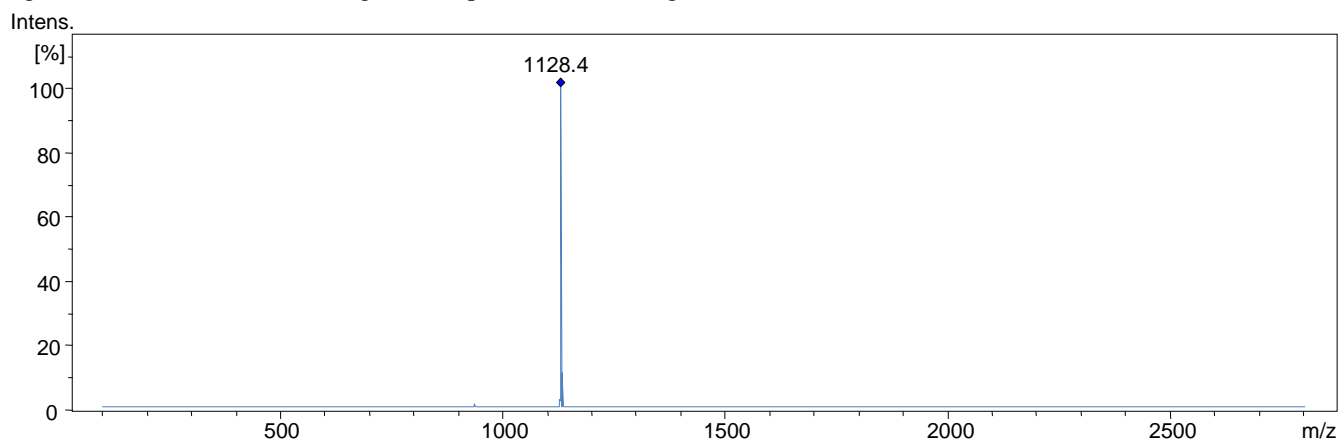


Figure 50. ESI-MS² for host/guest complex **8/11** in the negative ion mode.

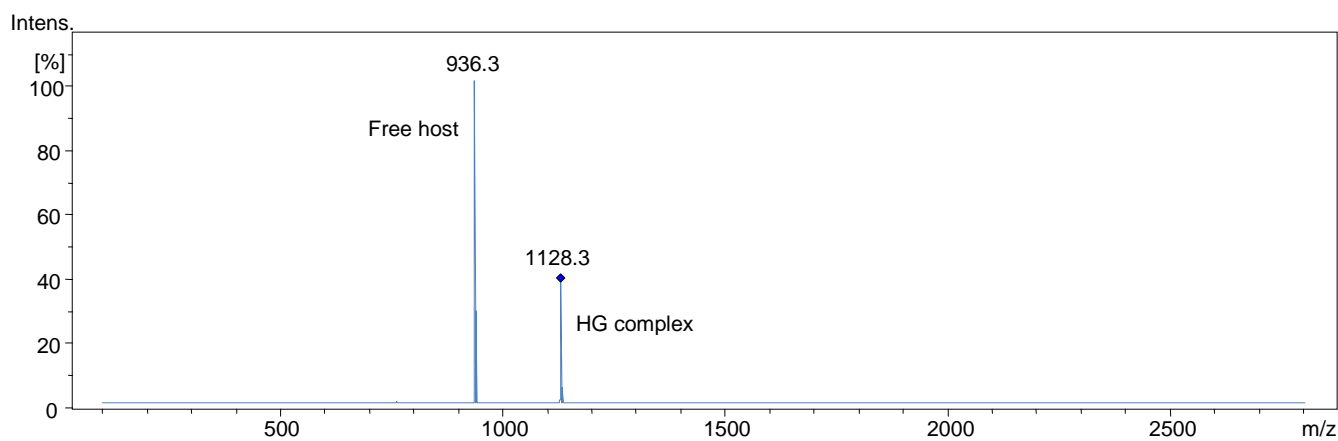


Figure 51. Tandem ESI-MS for host/guest complex **8/11** in the negative ion mode.

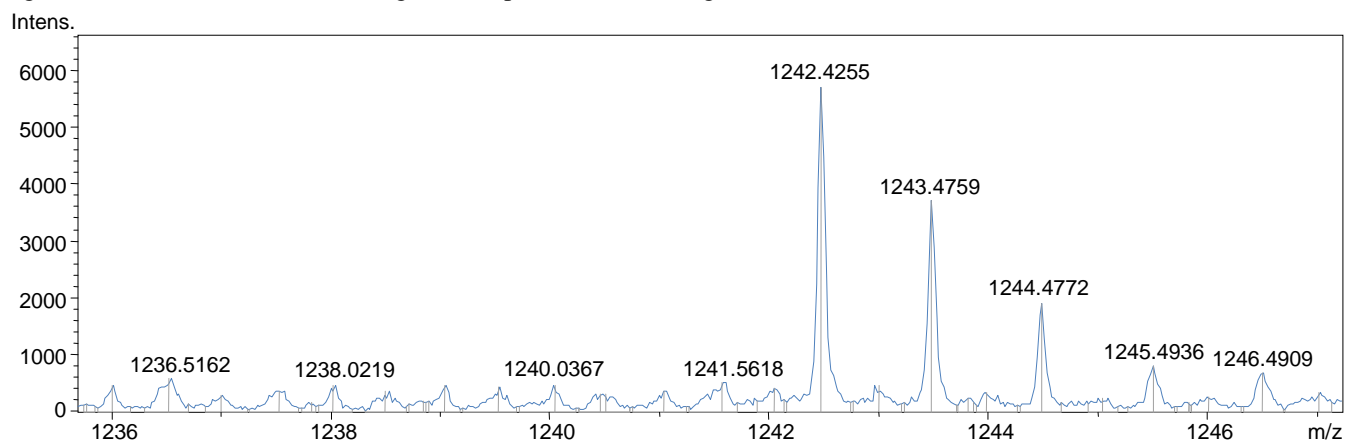


Figure 52. ESI-TOF/MS for host/guest complex **8/12** in the negative ion mode.

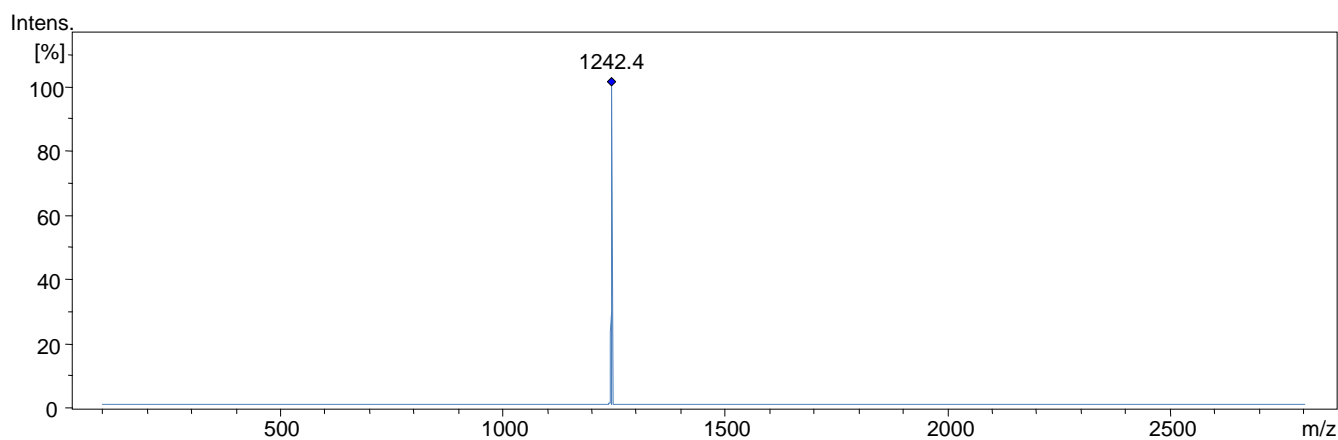


Figure 53. ESI-MS² for host/guest complex **8/12** in the negative ion mode.

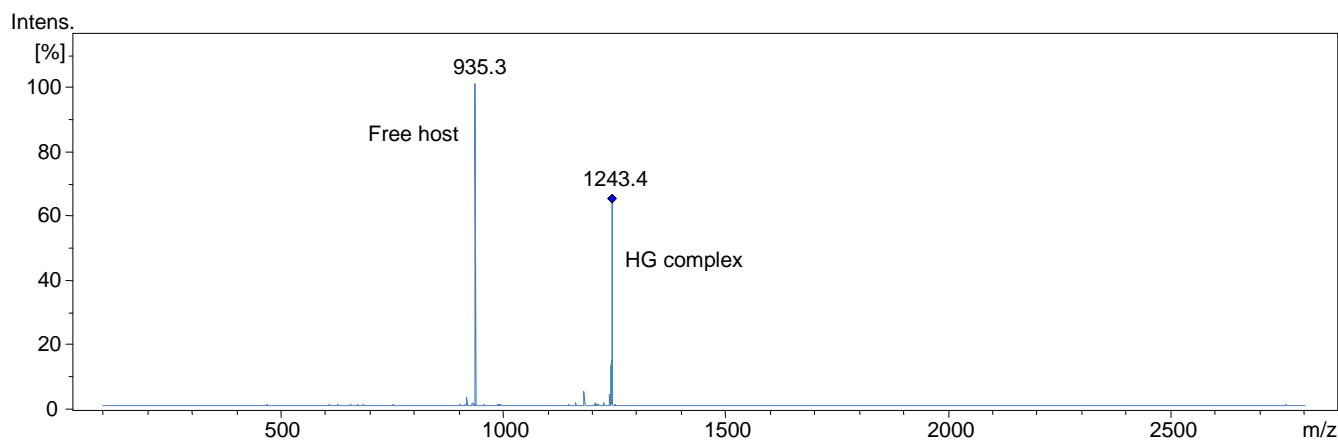


Figure 54. Tandem ESI-MS for host/guest complex **8/12** in the negative ion mode.

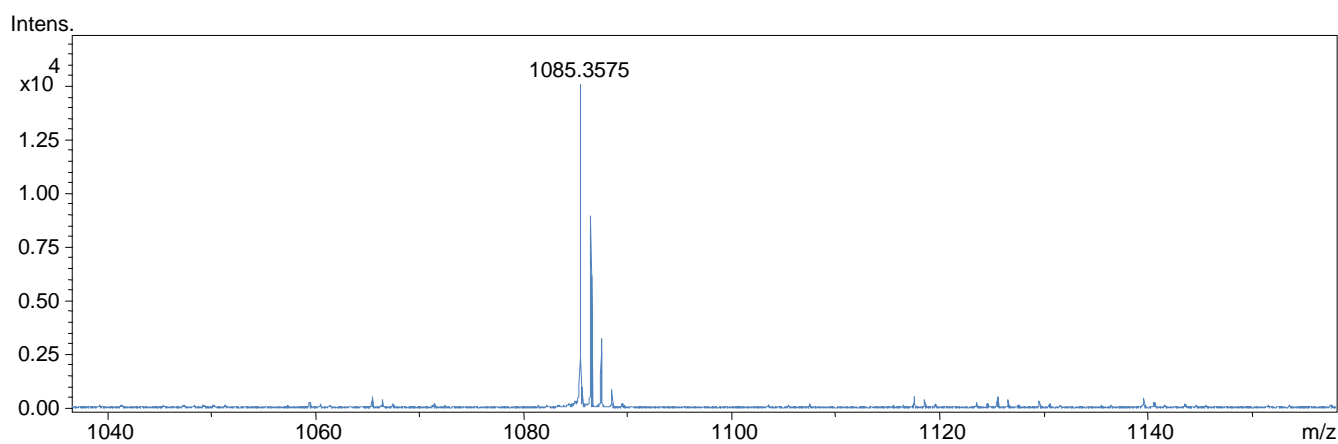


Figure 55. ESI-TOF/MS for host/guest complex **8/13** in the negative ion mode.

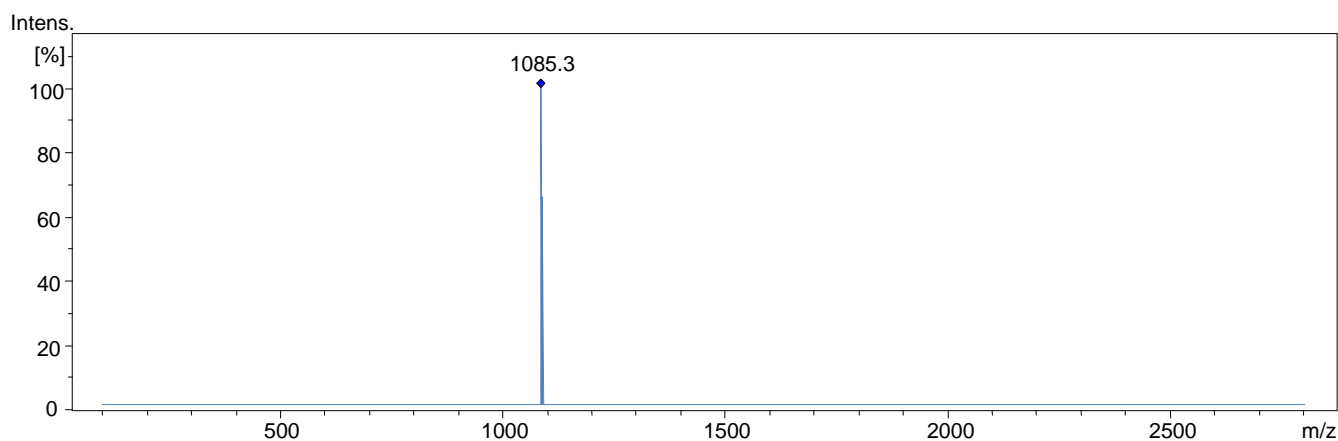


Figure 56. ESI- MS^2 for host/guest complex **8/13** in the negative ion mode.

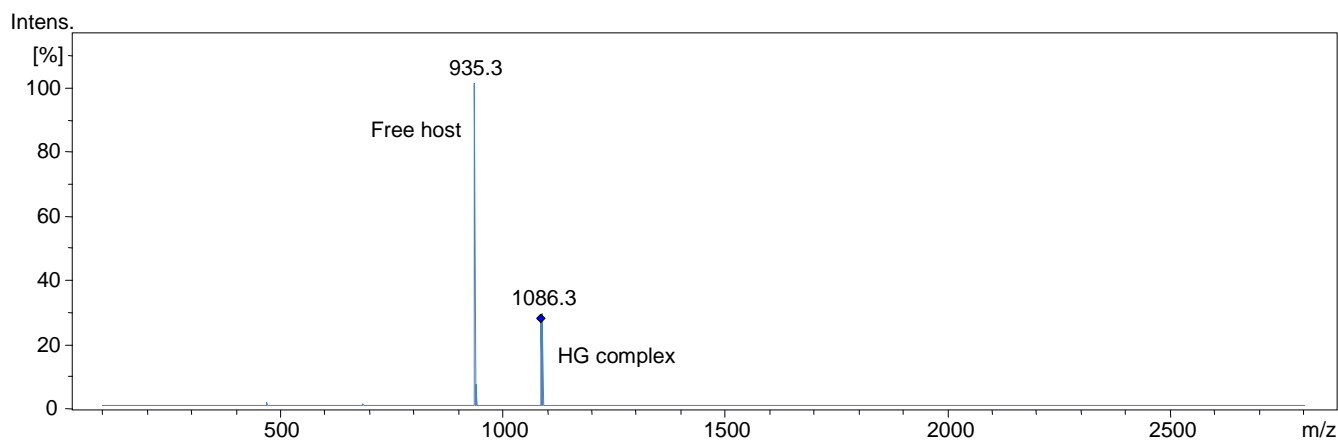


Figure 57. Tandem ESI-MS for host/guest complex **8/13** in the negative ion mode.

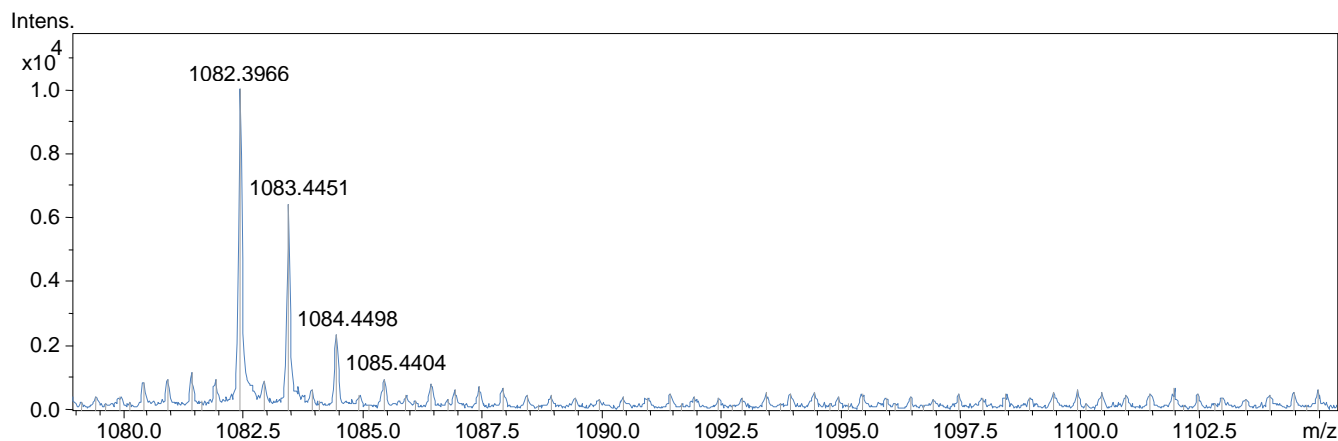


Figure 58. ESI-TOF/MS for host/guest complex **8/14** in the negative ion mode.

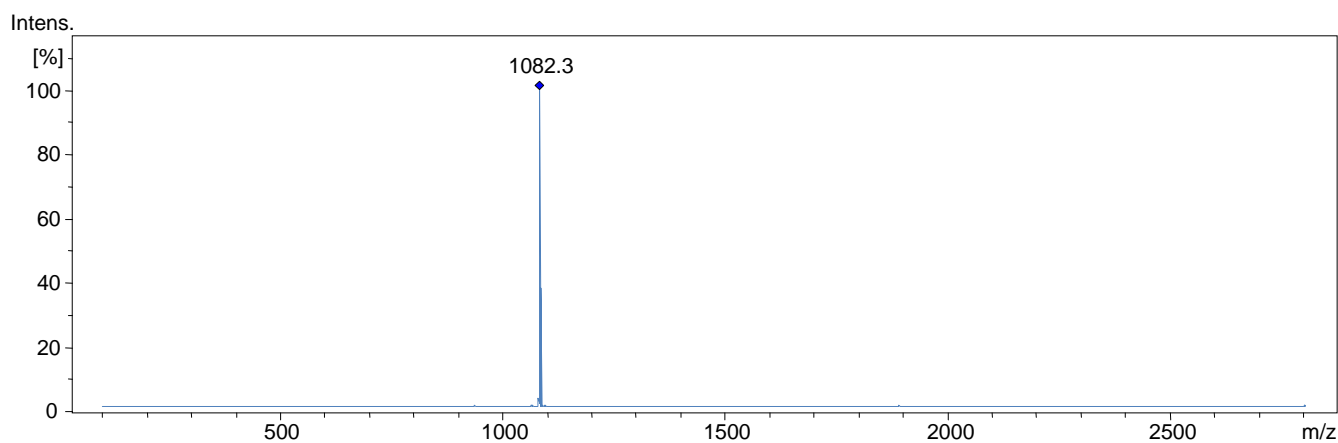


Figure 59. ESI-MS² for host/guest complex **8/14** in the negative ion mode.

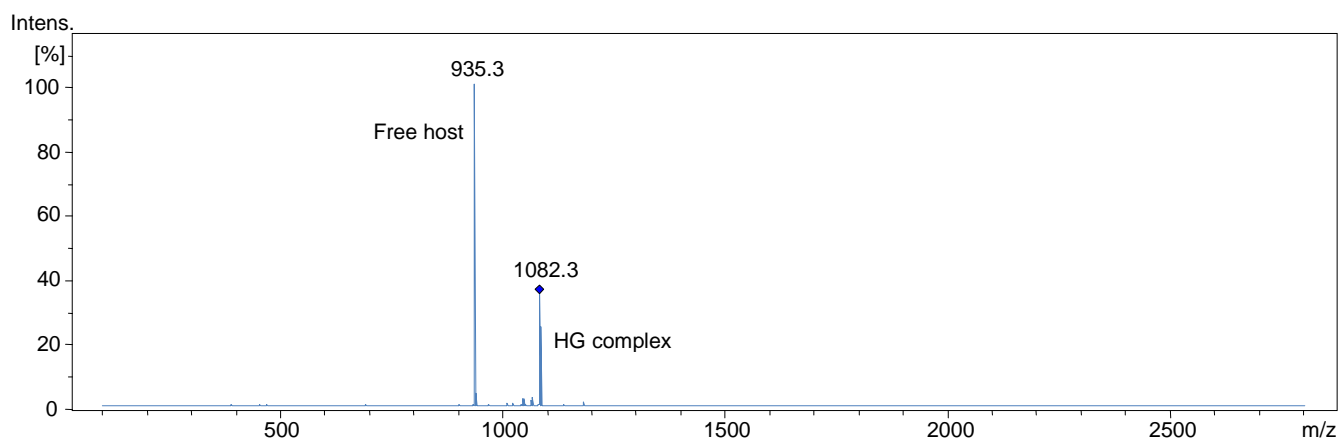


Figure 60. Tandem ESI-MS for host/guest complex **8/14** in the negative ion mode.

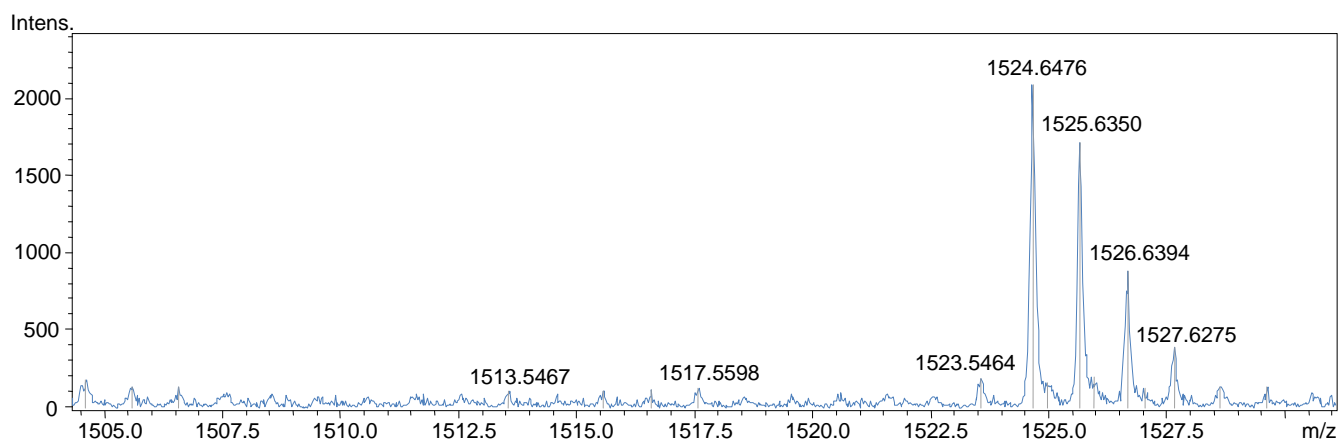


Figure 61. ESI-TOF/MS for host/guest complex **8/15** in the positive ion mode.

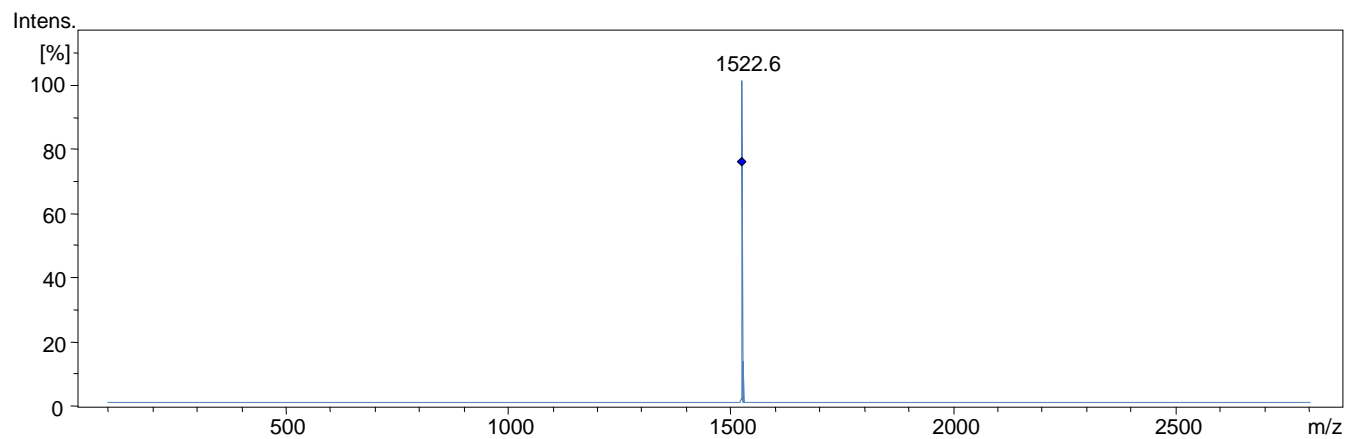


Figure 62. ESI-MS² for host/guest complex **8/15** in the negative ion mode.

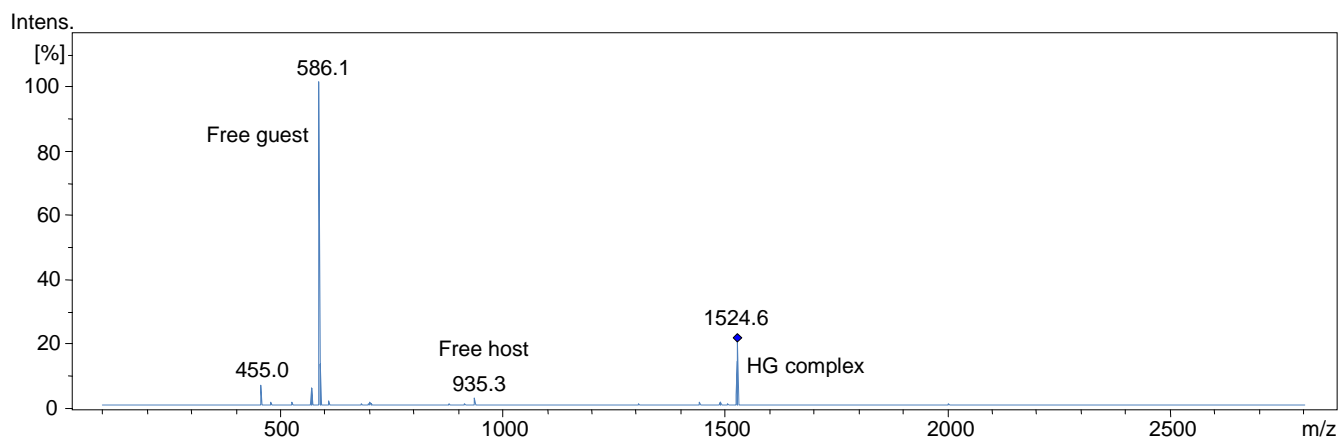


Figure 63. Tandem ESI-MS for host/guest complex **8/15** in the negative ion mode.

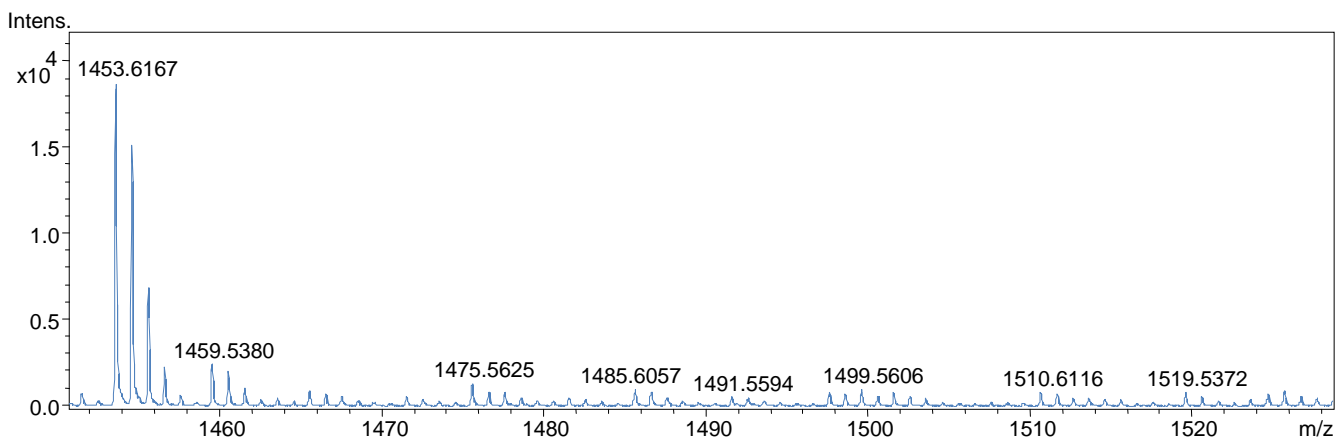


Figure 64. ESI-TOF/MS for host/guest complex **8/16** in the positive ion mode.

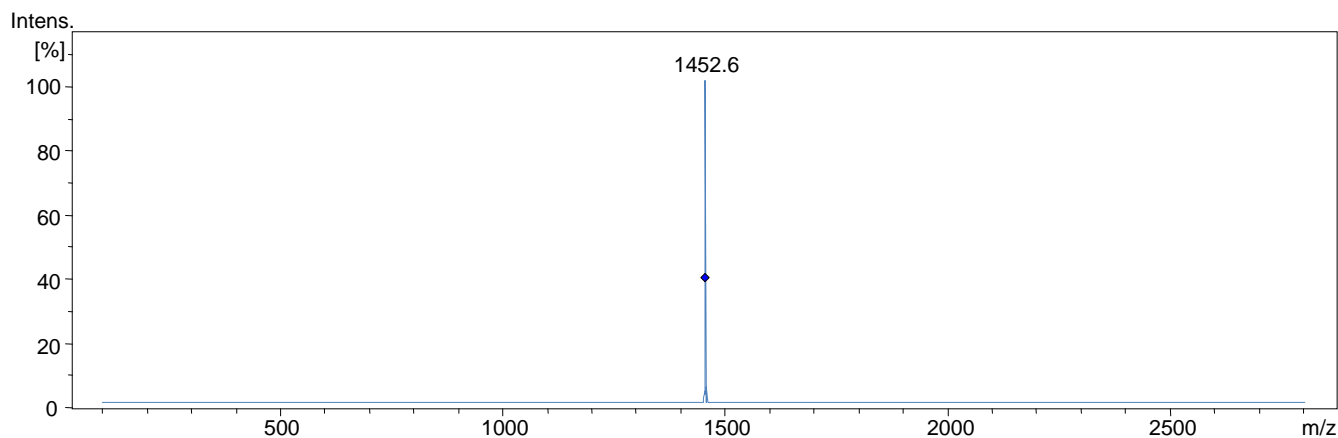


Figure 65. ESI-MS² for host/guest complex **8/16** in the negative ion mode.

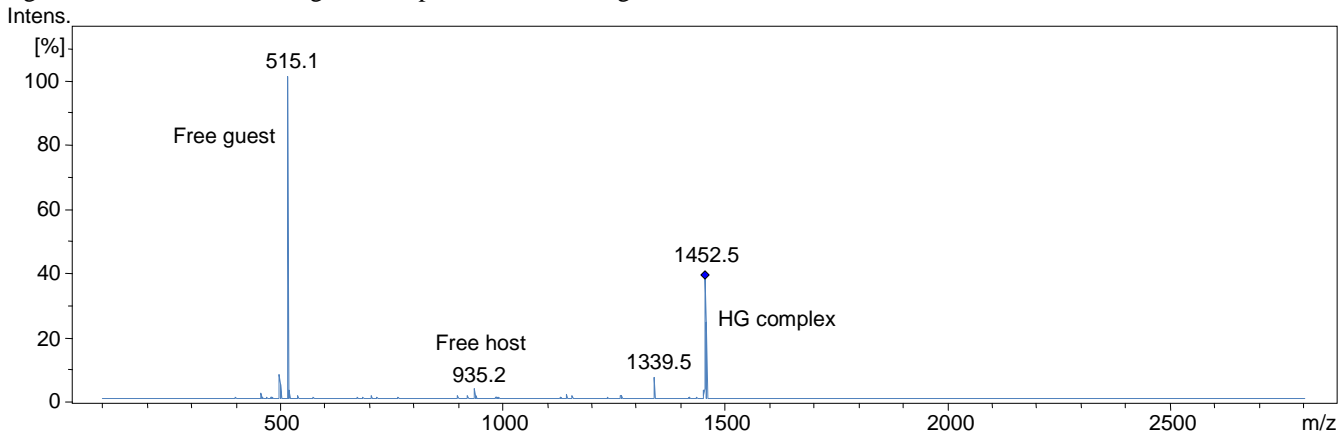


Figure 66. Tandem ESI-MS for host/guest complex **8/15** in the negative ion mode.

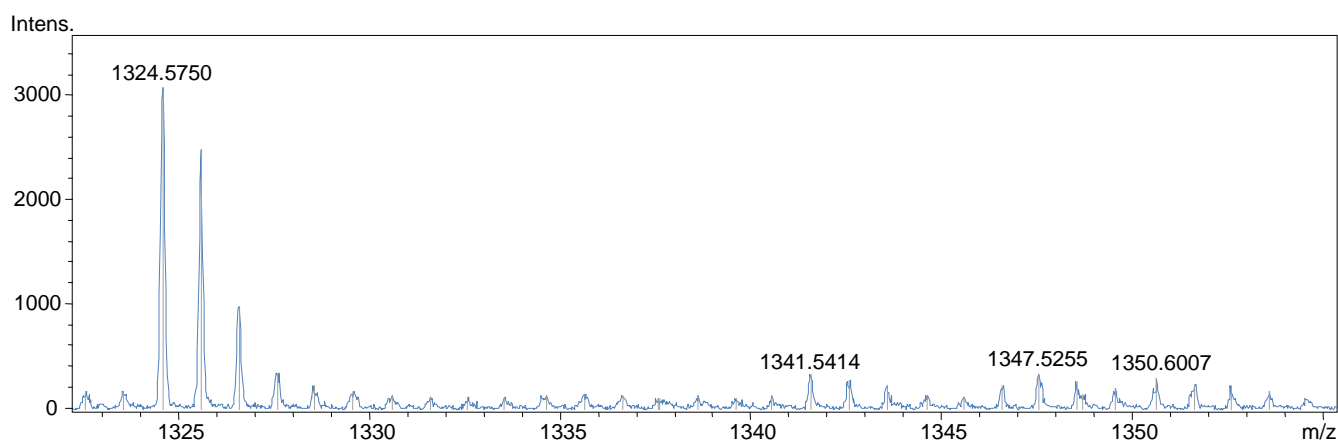


Figure 67. ESI-TOF/MS for host/guest complex **8/17** in the positive ion mode.

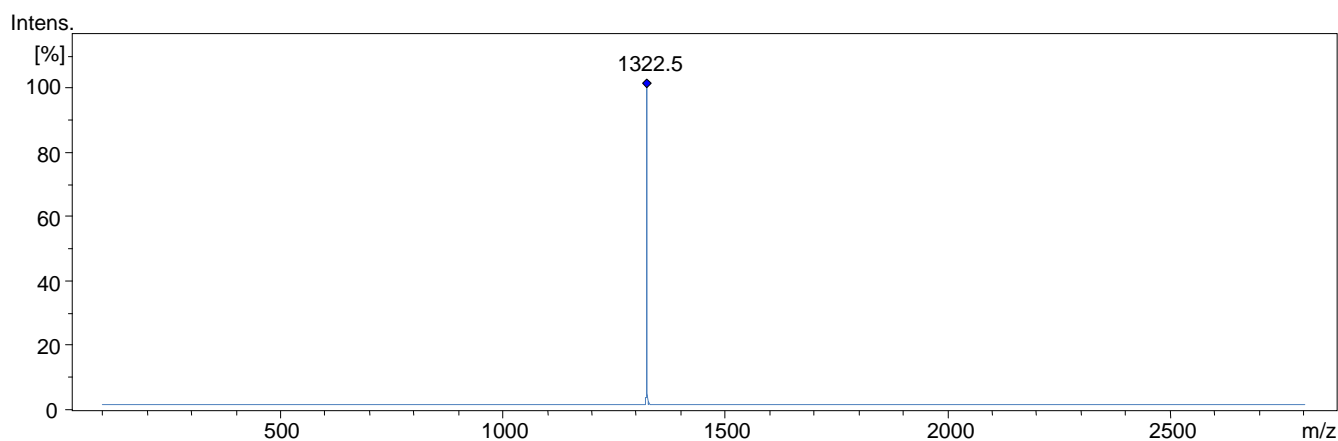


Figure 68. ESI-MS² for host/guest complex **8/17** in the negative ion mode.

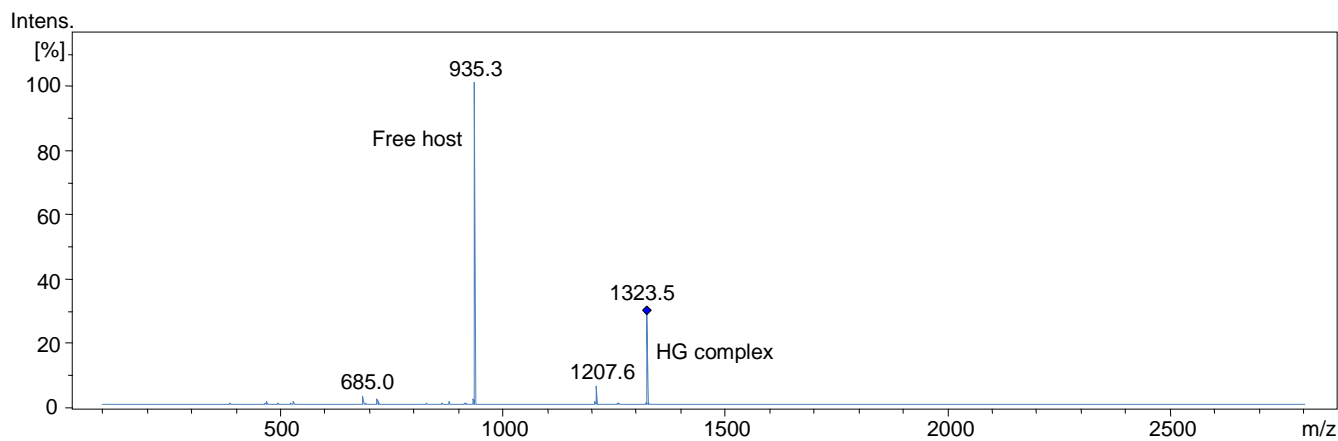


Figure 69. Tandem ESI-MS for host/guest complex **8/17** in the negative ion mode.

Conformer	E (Kcal.mol ⁻¹)	Gradient	Computational method
5a	5.38	0.009	MM+
5b	51.73	0.008	MM+
5c	46.56	0.009	MM+
B	1.17	0.009	MM+

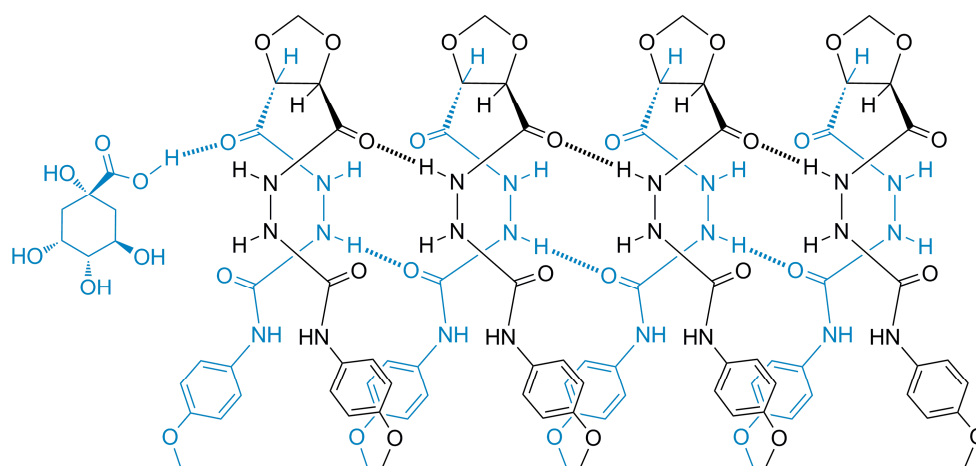
Table 1. Total energies for conformers **5a-c** and intermediate **B**.

Synthesis, self-assembly and ESI-MS complexation studies of novel chiral bis-*N*-substituted-hydrazinecarboxamide receptors

Hany F. Nour^{a,b}, Agnieszka Golon^a, Tuhidul Islam^a, Marcelo Fernández-Lahore^a and Nikolai Kuhnert^{a,*}

^a*School of Engineering and Science, Centre for Nano and Functional Materials (NanoFun), Jacobs University, 28759 Bremen, Germany*

^b*National Research Centre, Department of Photochemistry, El Behoose Street, P.O. Box 12622, Dokki, Egypt*



* Corresponding author: Tel.: +49-421-200-3120; Fax: +49-421-200-3229; e-mail: n.kuhnert@jacobs-university.de

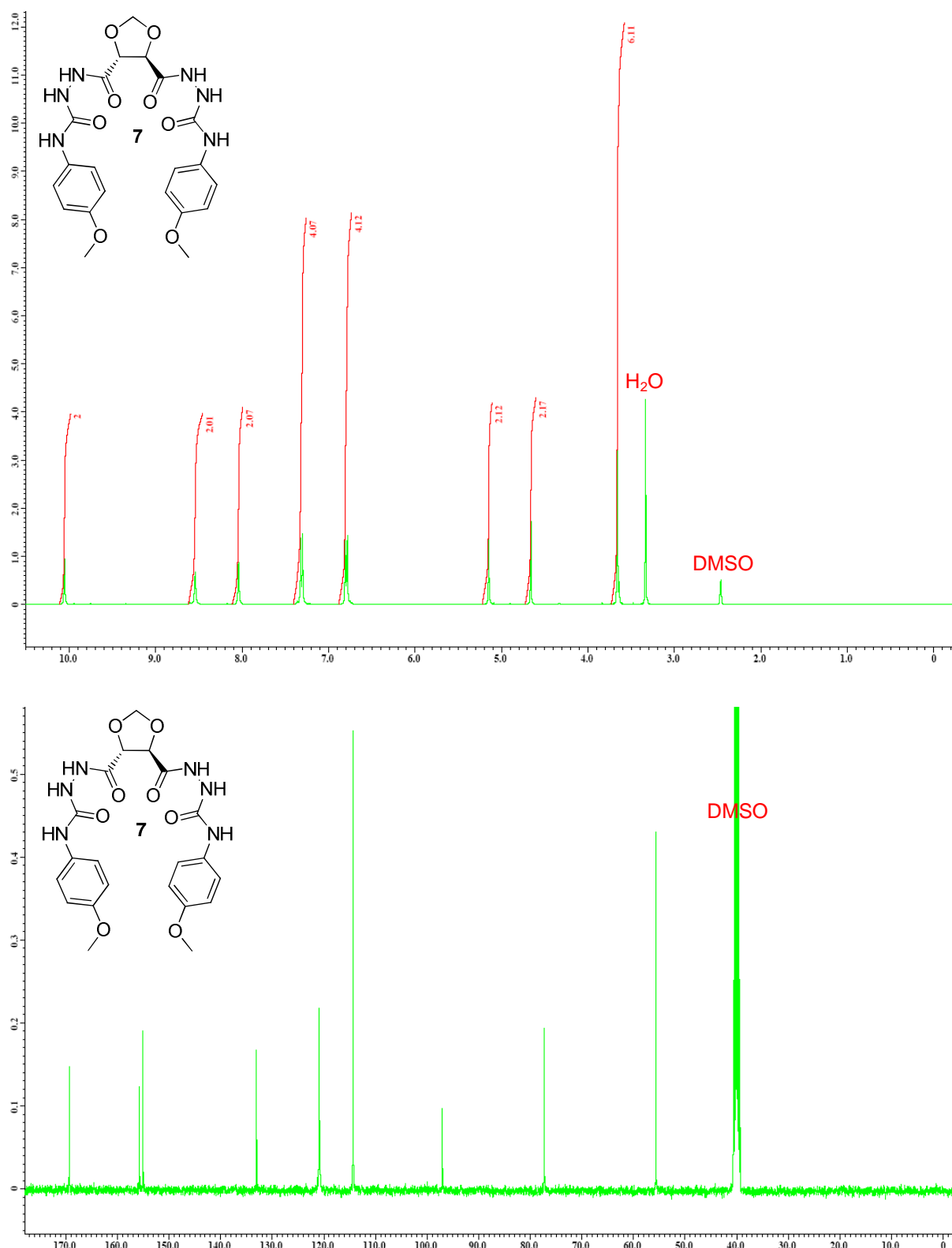


Figure 1. ¹H-NMR and ¹³C-NMR spectra for receptor 7 (DMSO-d₆, 400 MHz for ¹H-NMR and 100 MHz for ¹³C-NMR).

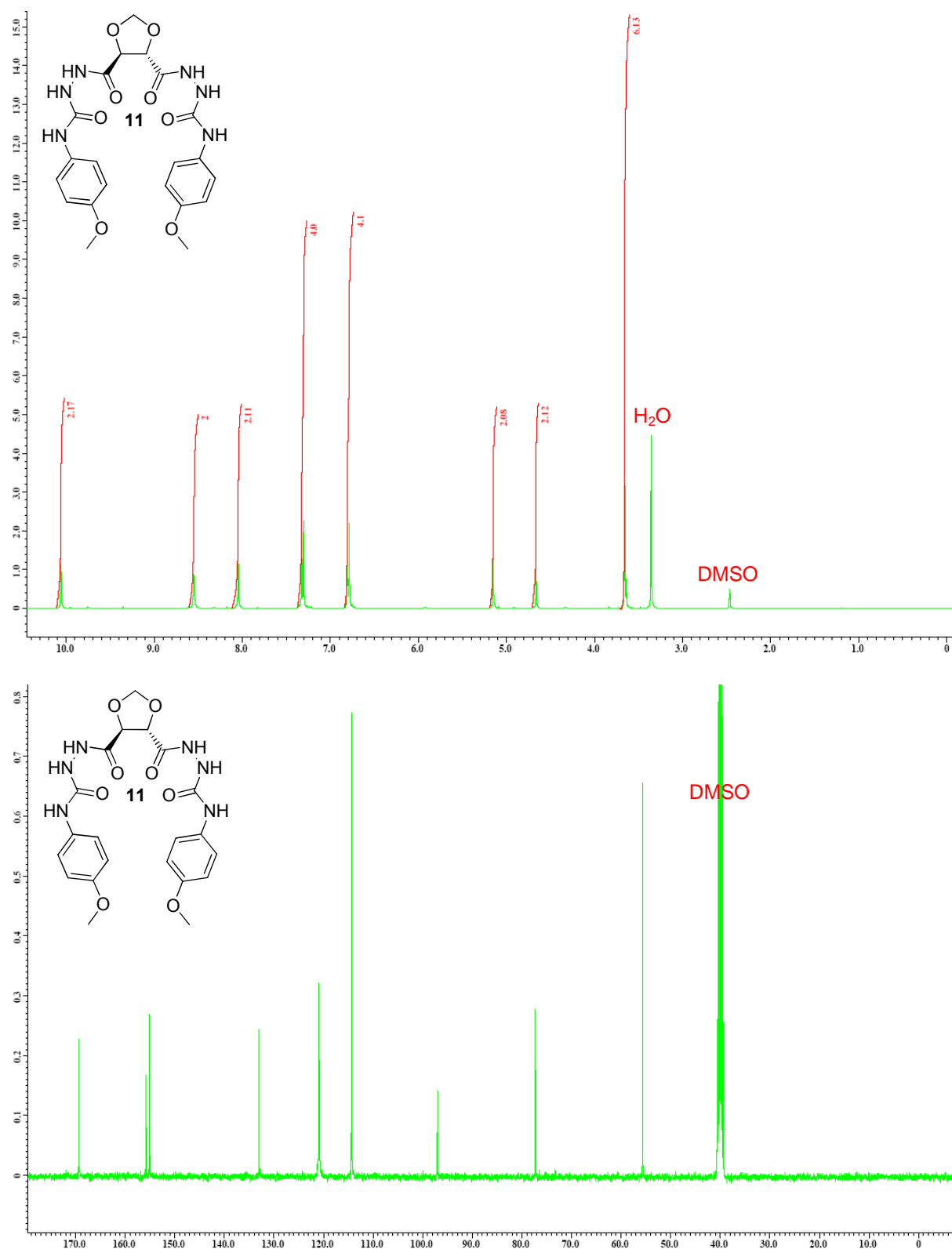


Figure 2. ¹H-NMR and ¹³C-NMR spectra for receptor **11** (DMSO-d₆, 400 MHz for ¹H-NMR and 100 MHz for ¹³C-NMR).

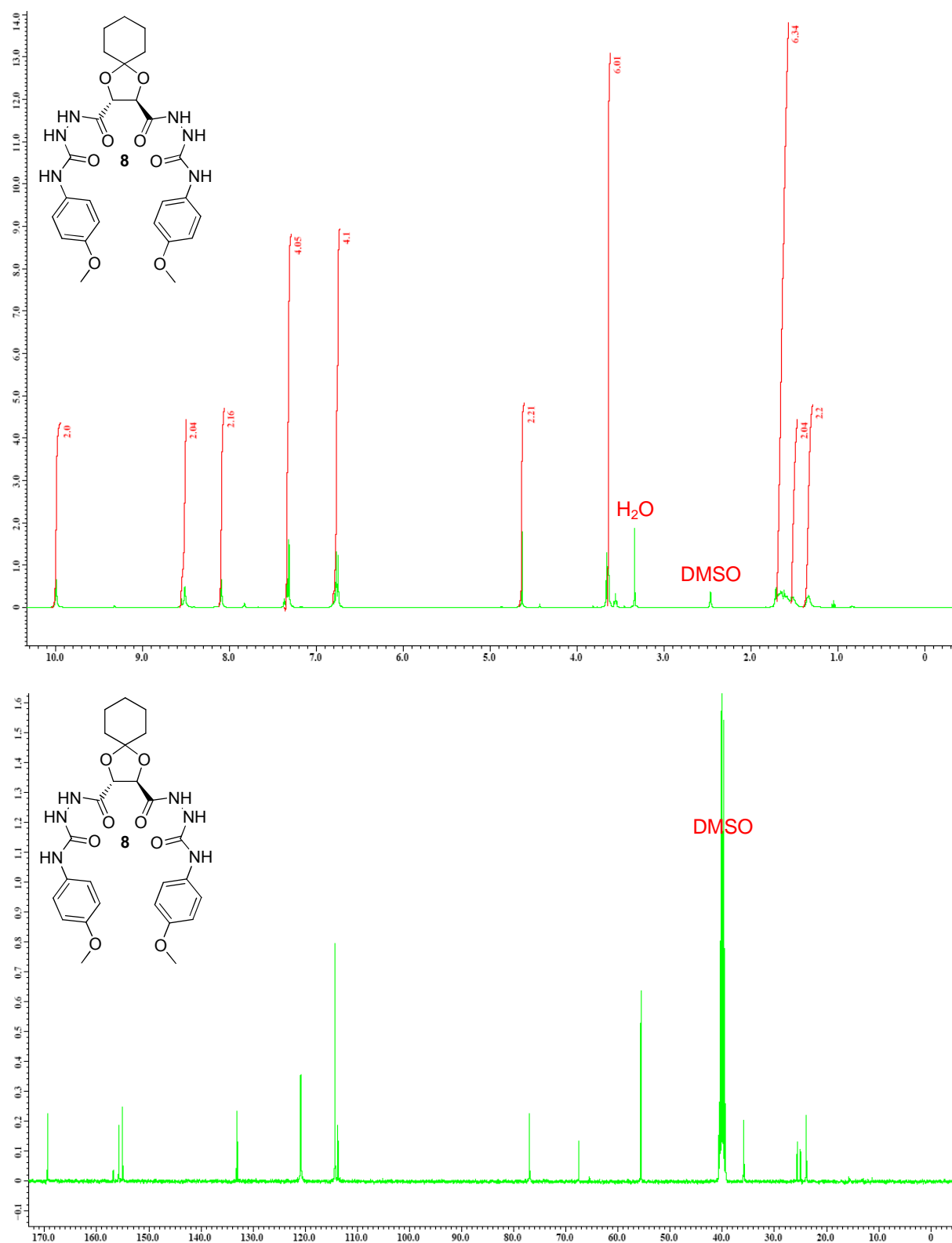


Figure 3. ¹H-NMR and ¹³C-NMR spectra for receptor **8** (DMSO-d₆, 400 MHz for ¹H-NMR and 100 MHz for ¹³C-NMR).

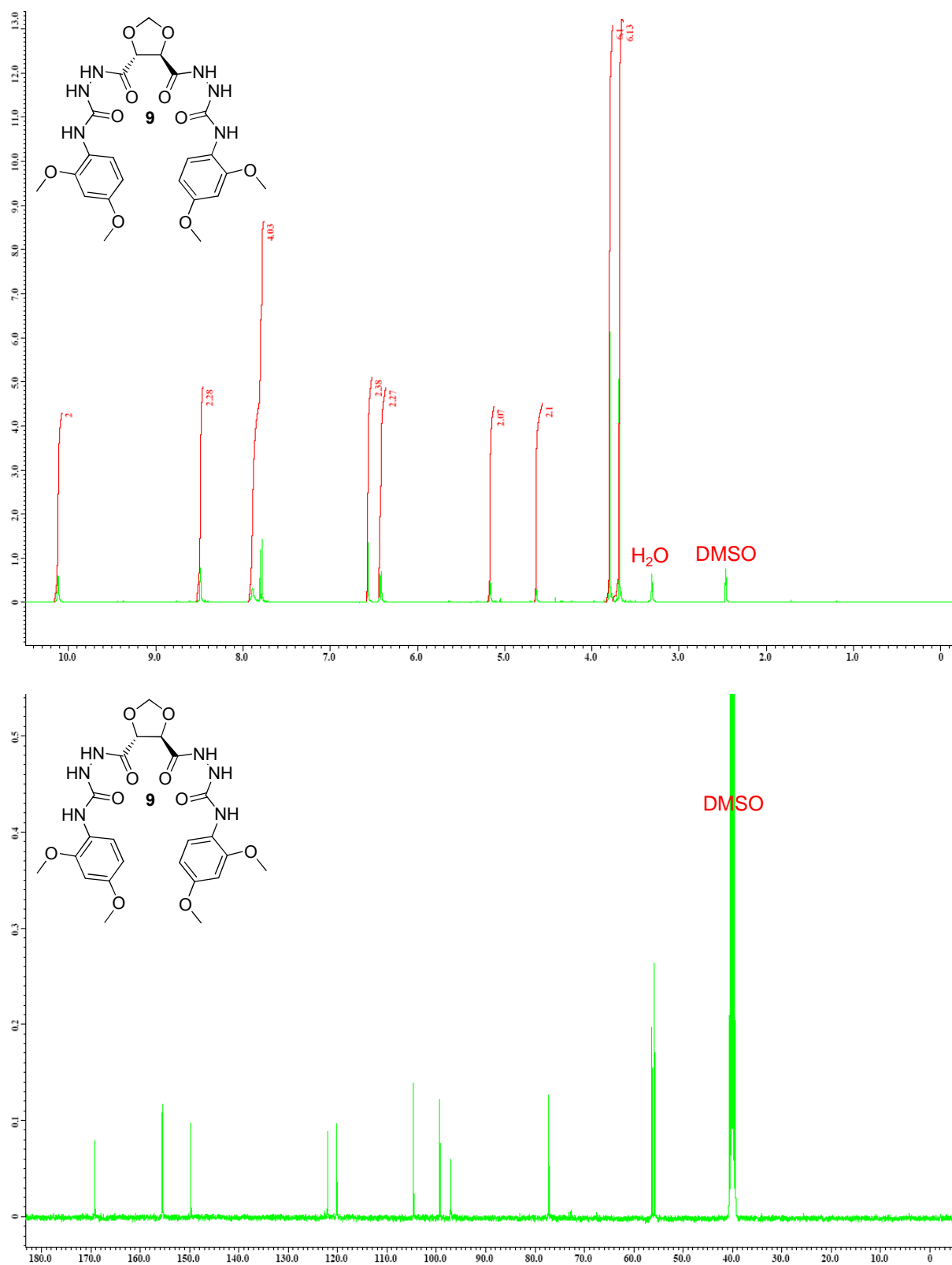


Figure 4. ^1H -NMR and ^{13}C -NMR spectra for receptor **9** (DMSO- d_6 , 400 MHz for ^1H -NMR and 100 MHz for ^{13}C -NMR).

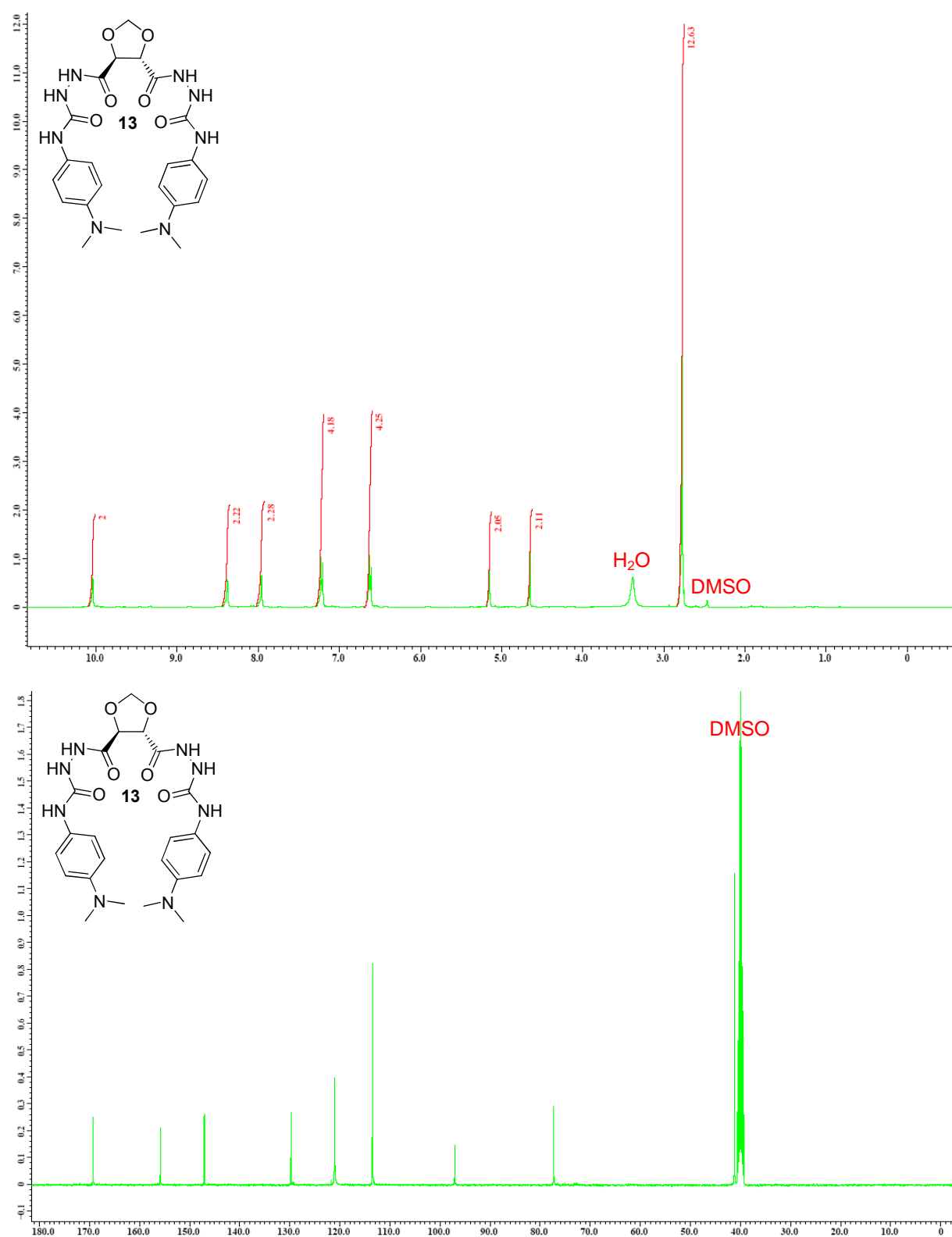


Figure 7. ¹H-NMR and ¹³C-NMR spectra for receptor **13** (DMSO-d₆, 400 MHz for ¹H-NMR and 100 MHz for ¹³C-NMR).

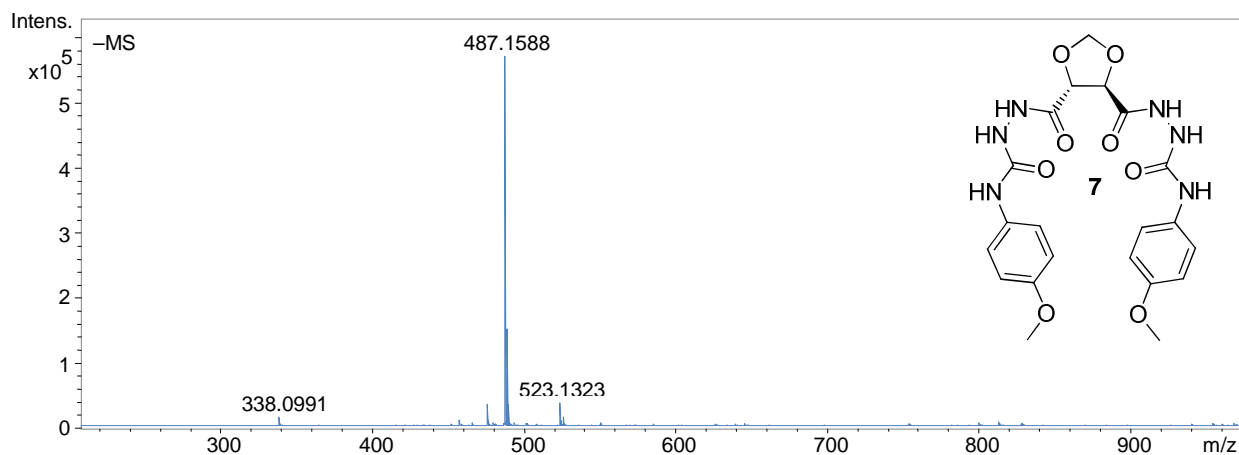


Figure 8. ESI-TOF/MS for receptor **7**.

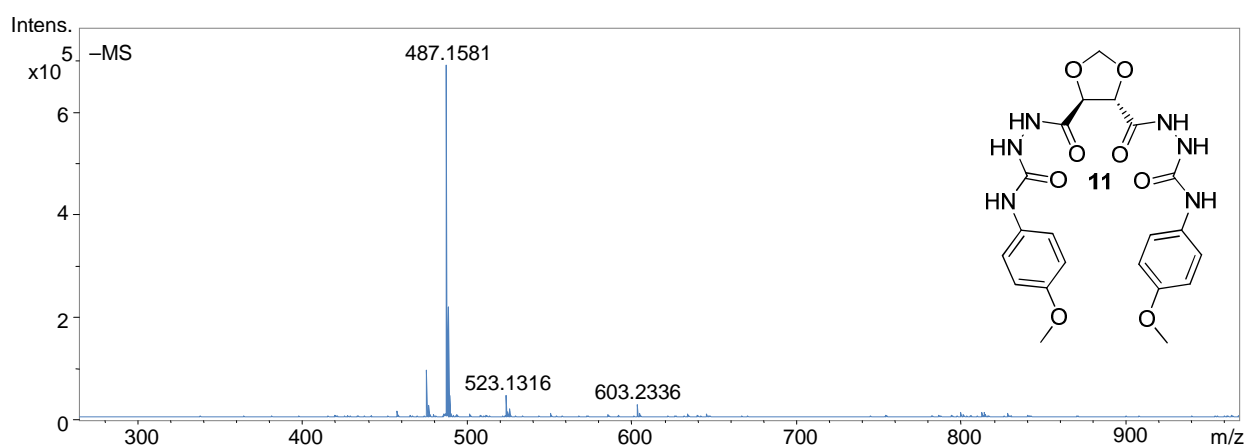


Figure 9. ESI-TOF/MS for receptor **11**.

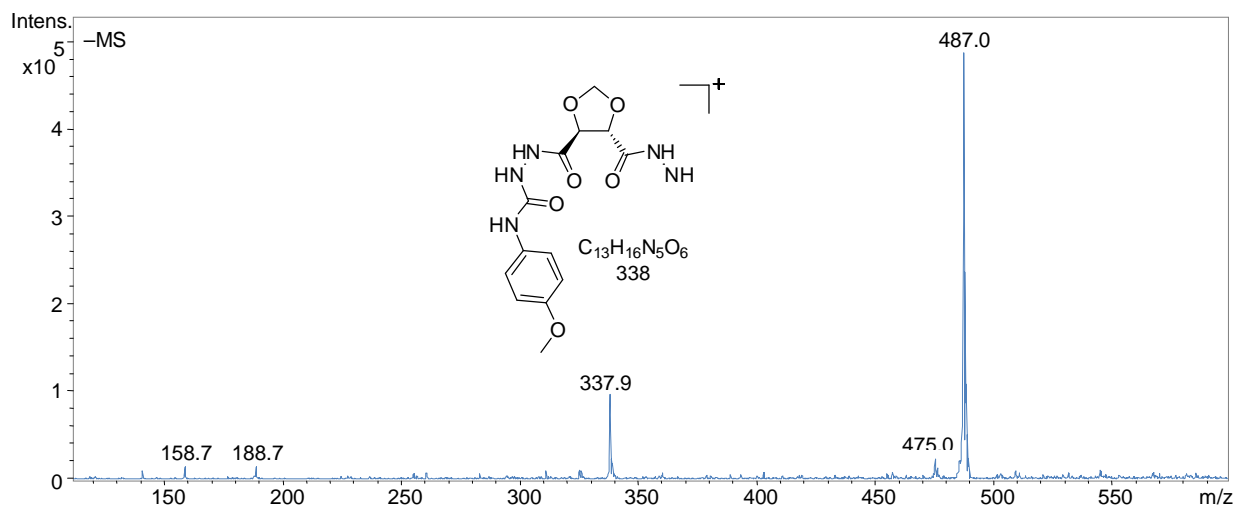


Figure 10. Tandem ESI-MS for receptor **11**.

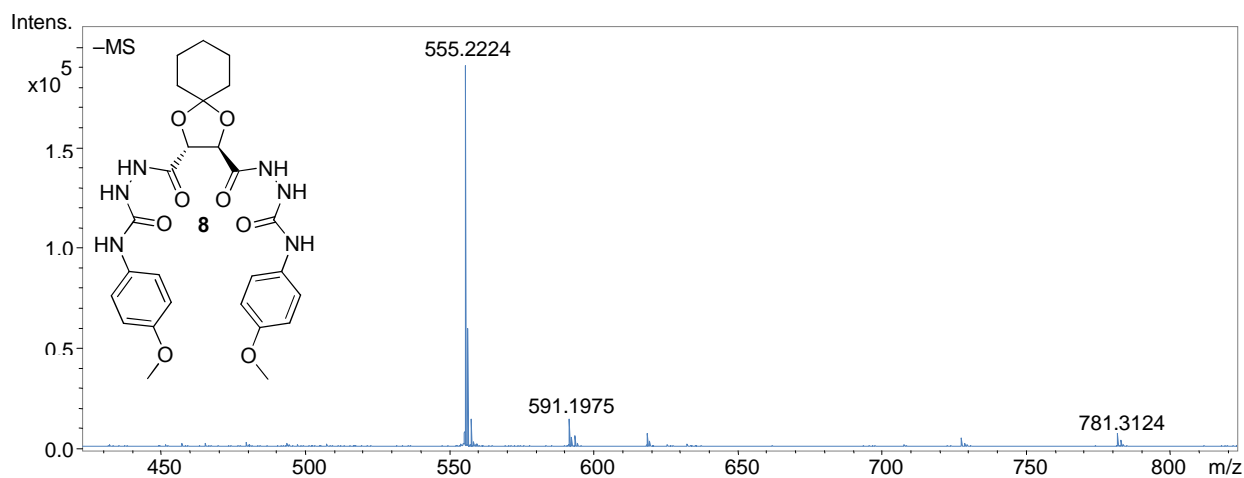


Figure 11. ESI-TOF/MS for receptor **8**.

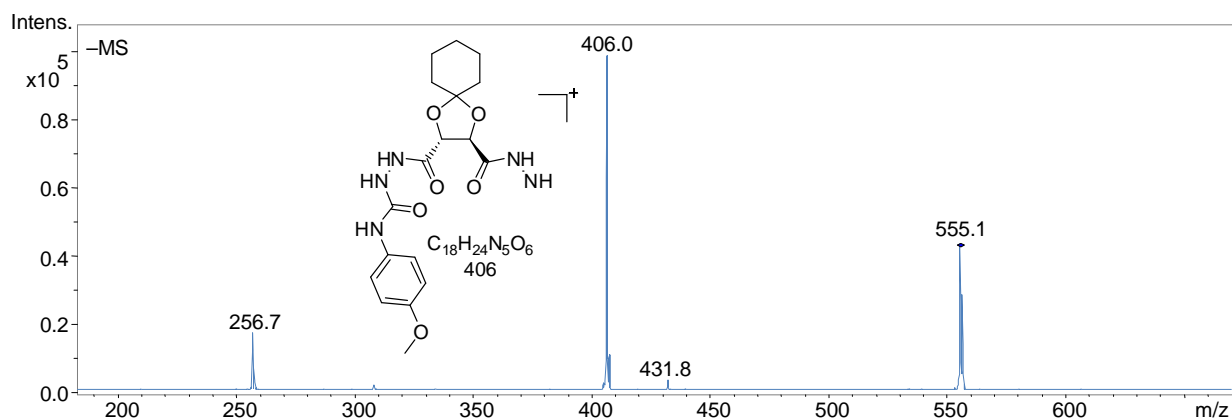


Figure 12. Tandem ESI-MS for receptor **8**.

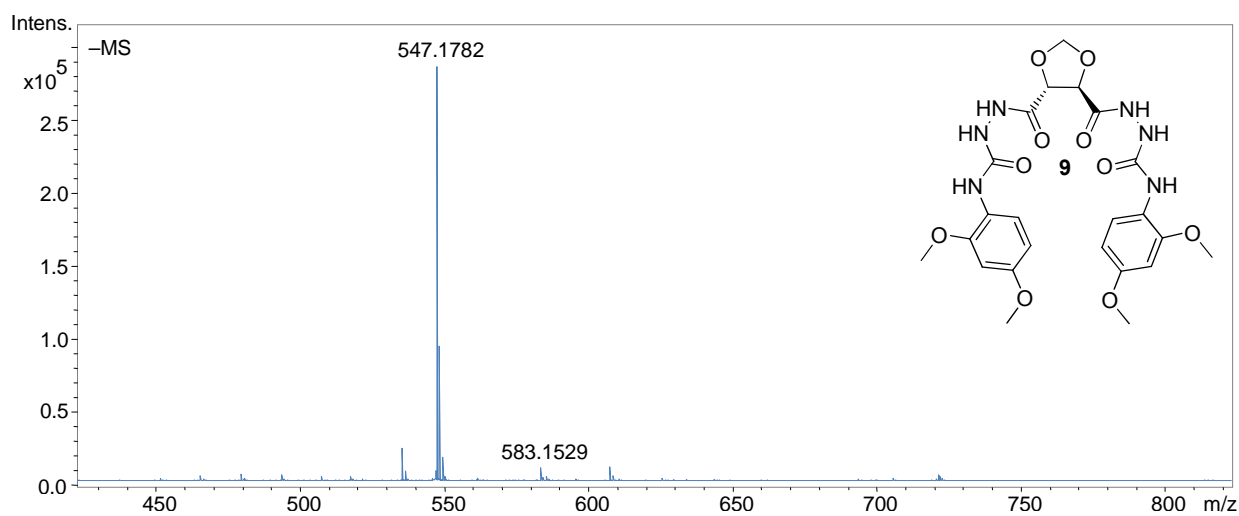


Figure 13. ESI-TOF/MS for receptor **9**.

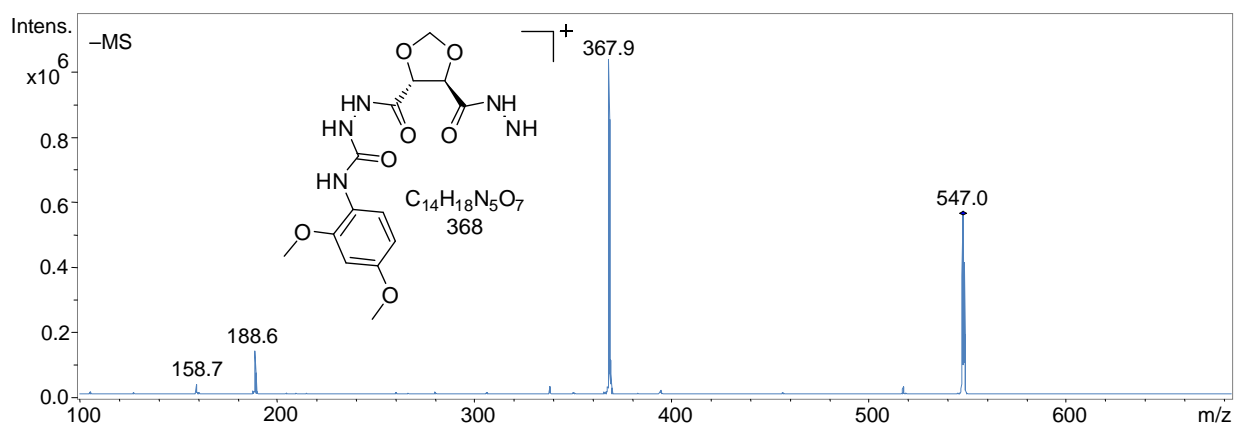


Figure 14. Tandem ESI-MS for receptor **9**.

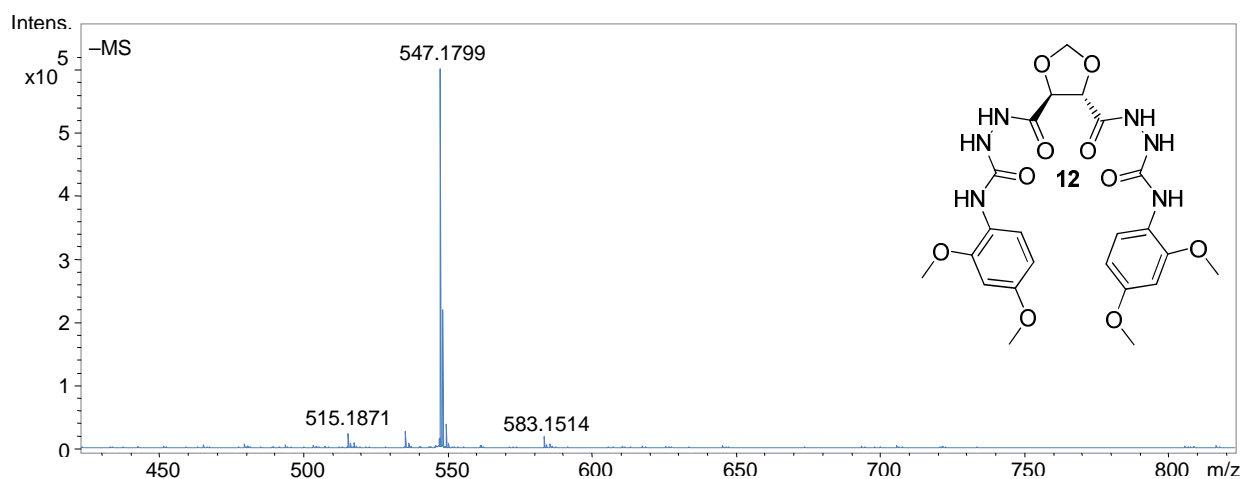


Figure 15. ESI-TOF/MS for receptor **12**.

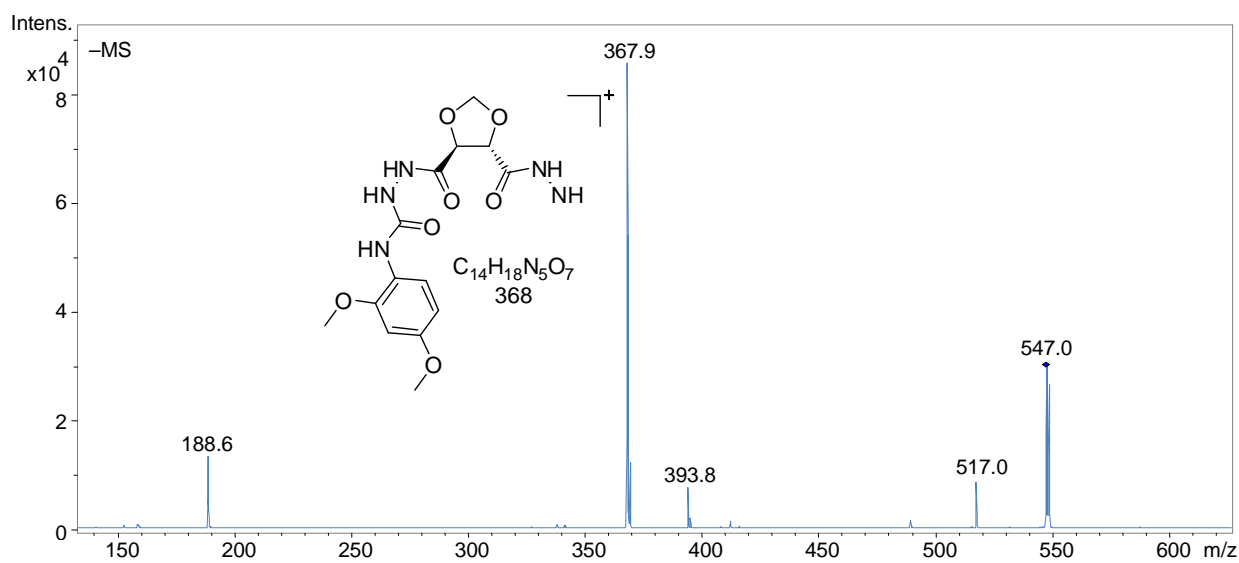


Figure 16. Tandem ESI-MS for receptor **12**.

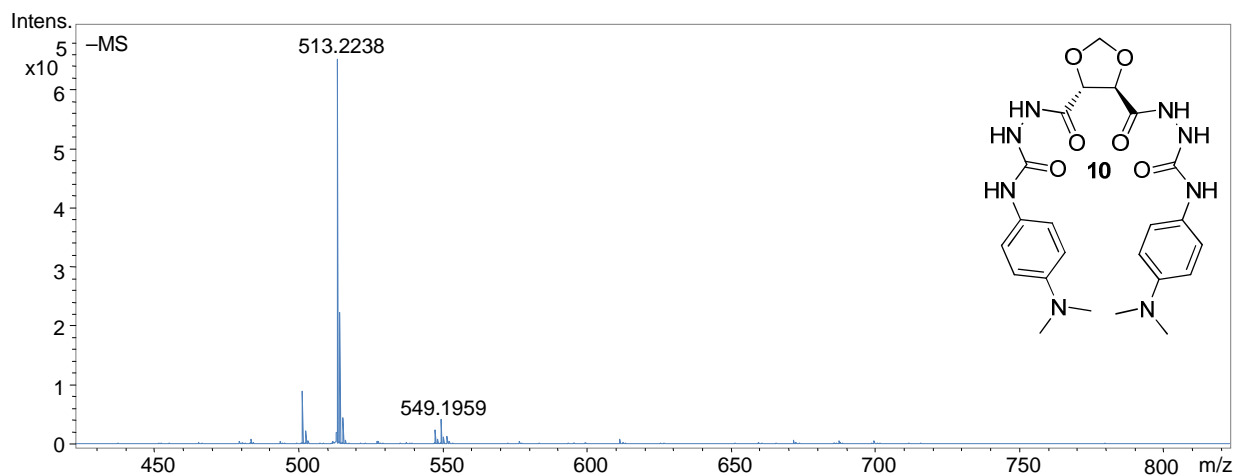


Figure 17. ESI-TOF/MS for receptor **10**.

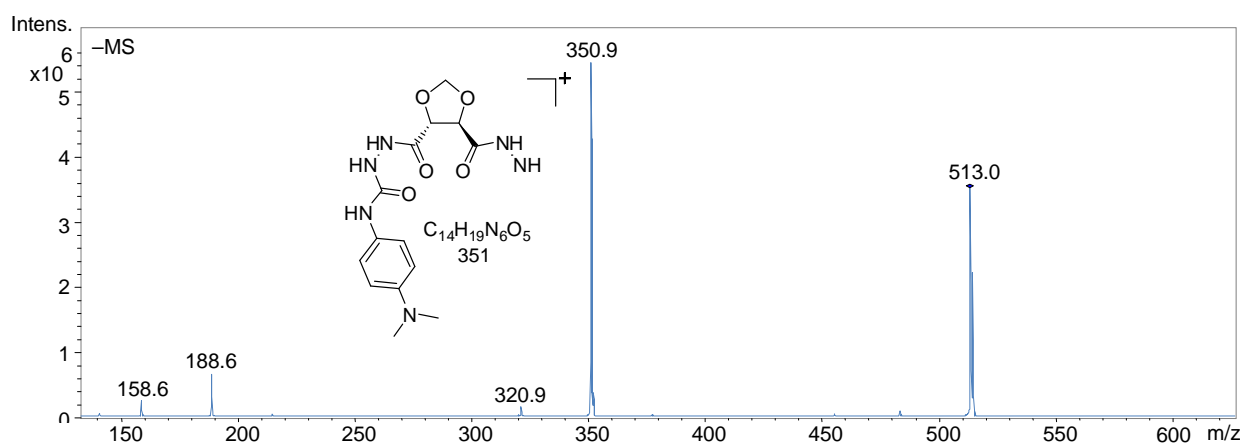


Figure 18. Tandem ESI-MS for receptor **10**.

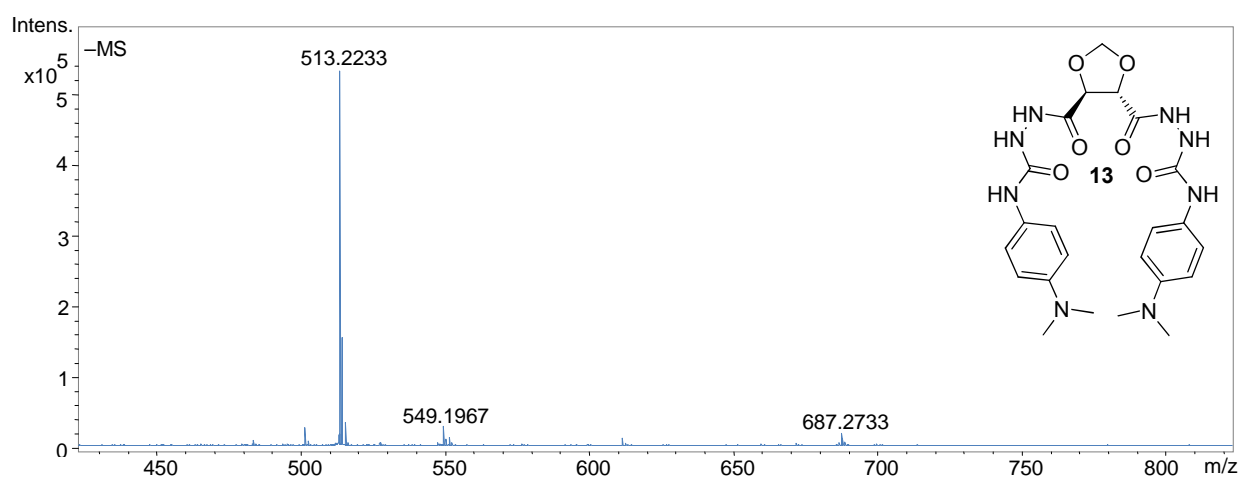


Figure 19. ESI-TOF/MS for receptor **13**.

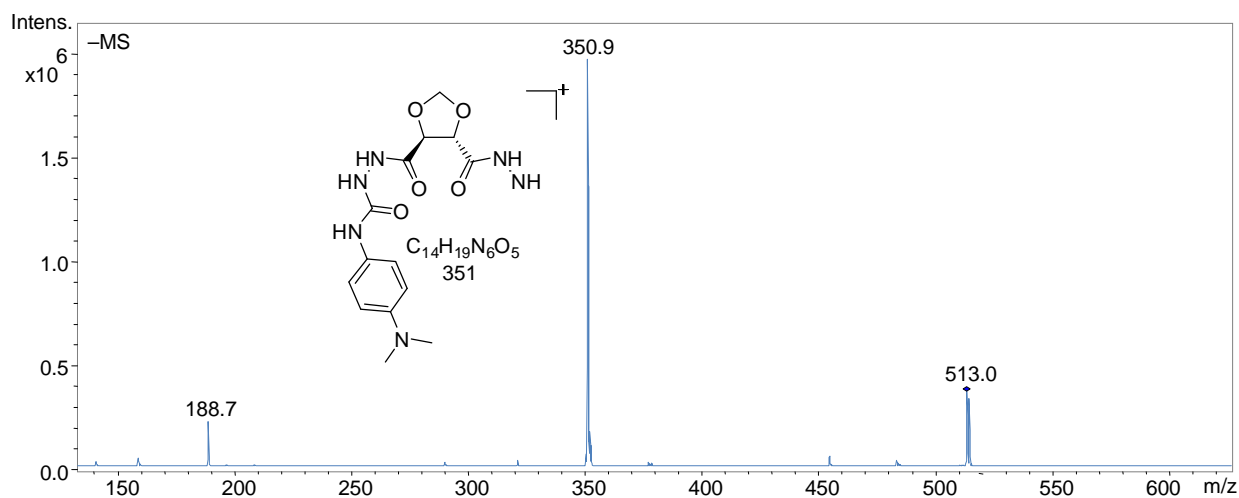


Figure 20. Tandem ESI-MS for receptor **13**.

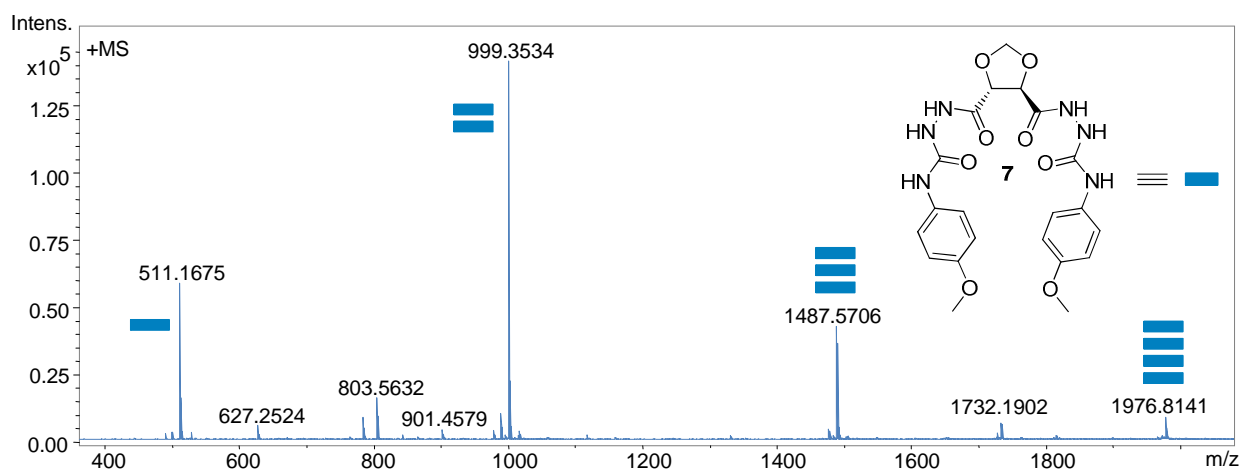


Figure 21. ESI-TOF/MS for receptor self-assembled receptor **7**.

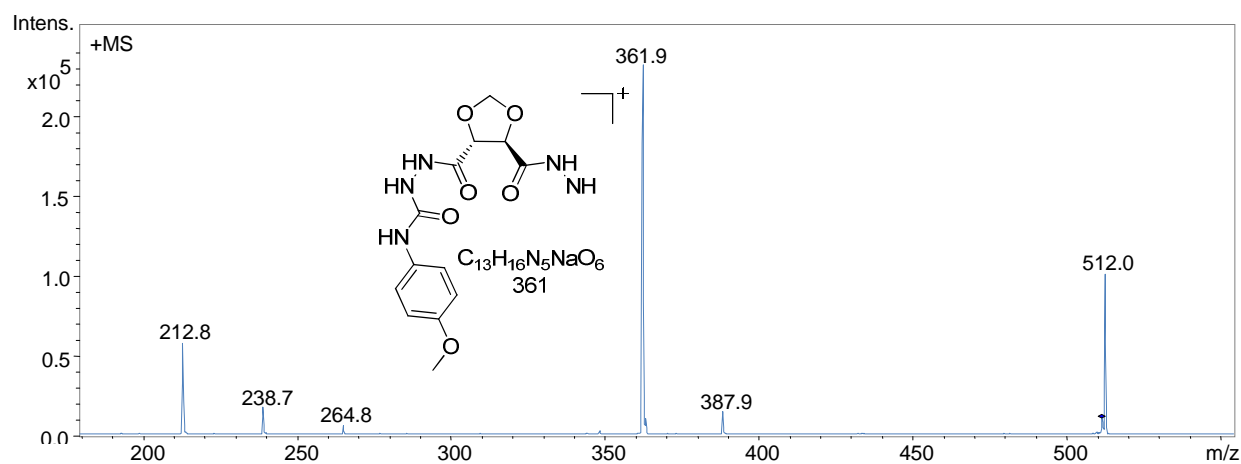


Figure 22. Tandem ESI-MS for receptor **7** (MS^2 for m/z 511).

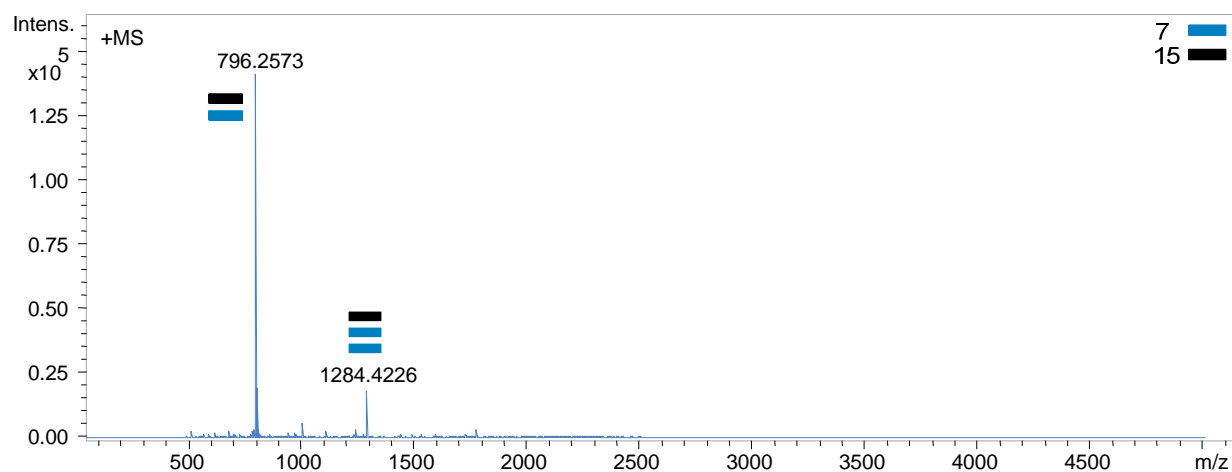


Figure 23. ESI-TOF/MS for host-guest complex 7/15.

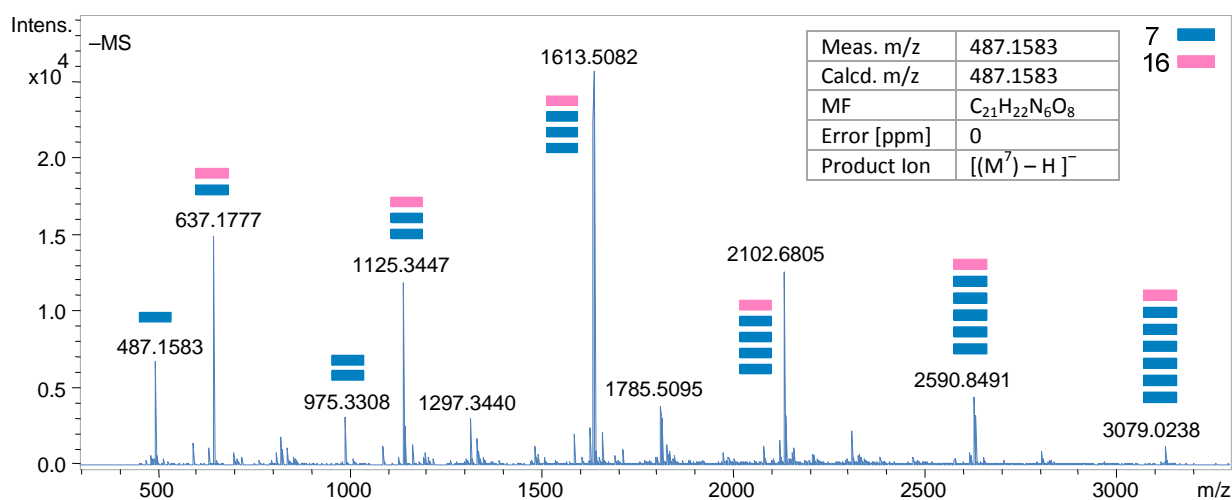


Figure 24. ESI-TOF/MS for host-guest complex 7/16.

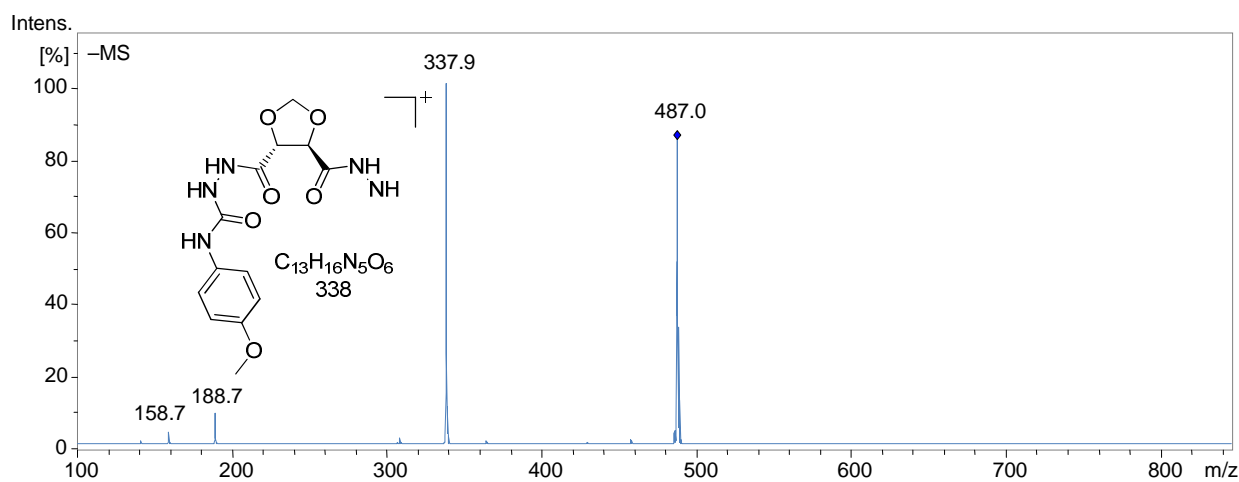


Figure 25. Tandem ESI-MS for host-guest complex 7/16 (MS^2 for m/z 487).

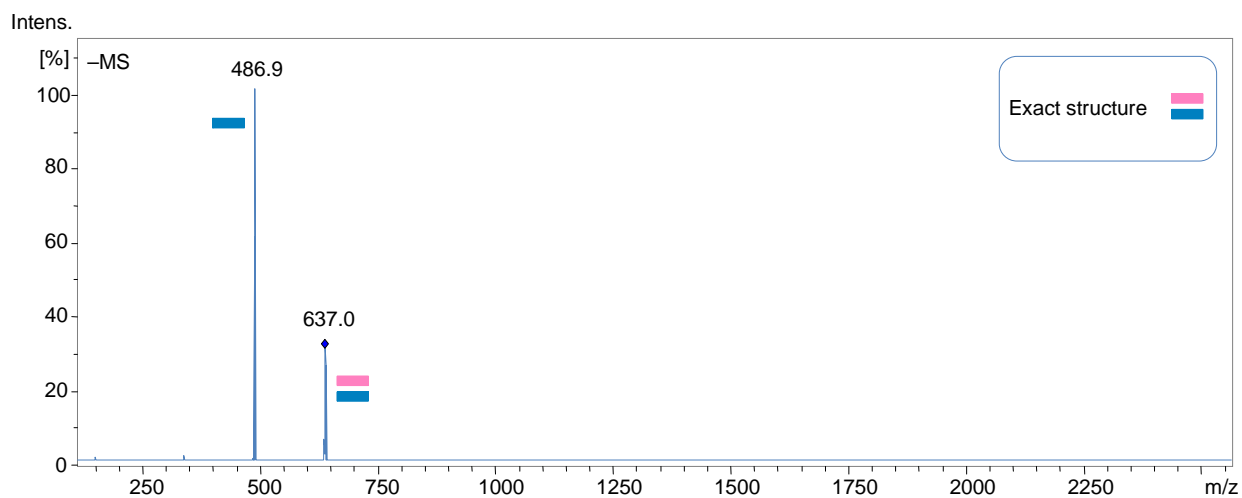


Figure 26. Tandem ESI-MS for host-guest complex **7/16** (MS² for m/z 637).

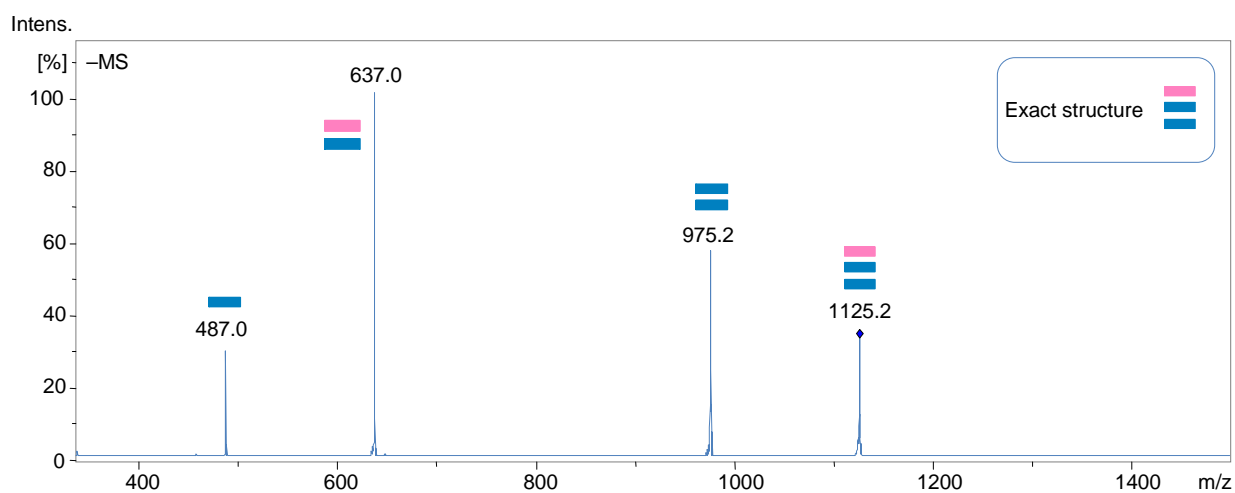


Figure 27. Tandem ESI-MS for host-guest complex **7/16** (MS² for m/z 1125).

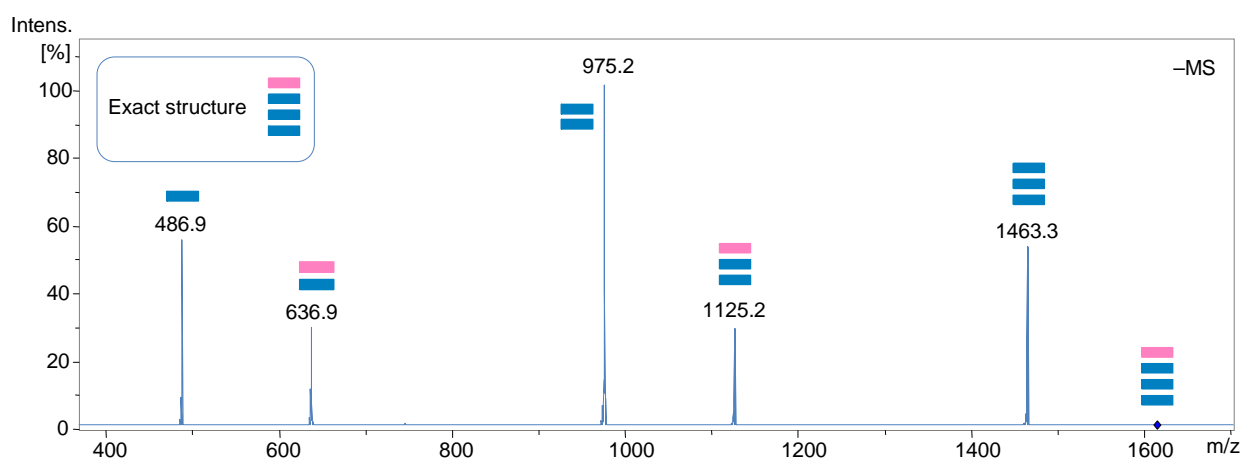


Figure 28. Tandem ESI-MS for host-guest complex **7/16** (MS² for m/z 1613).

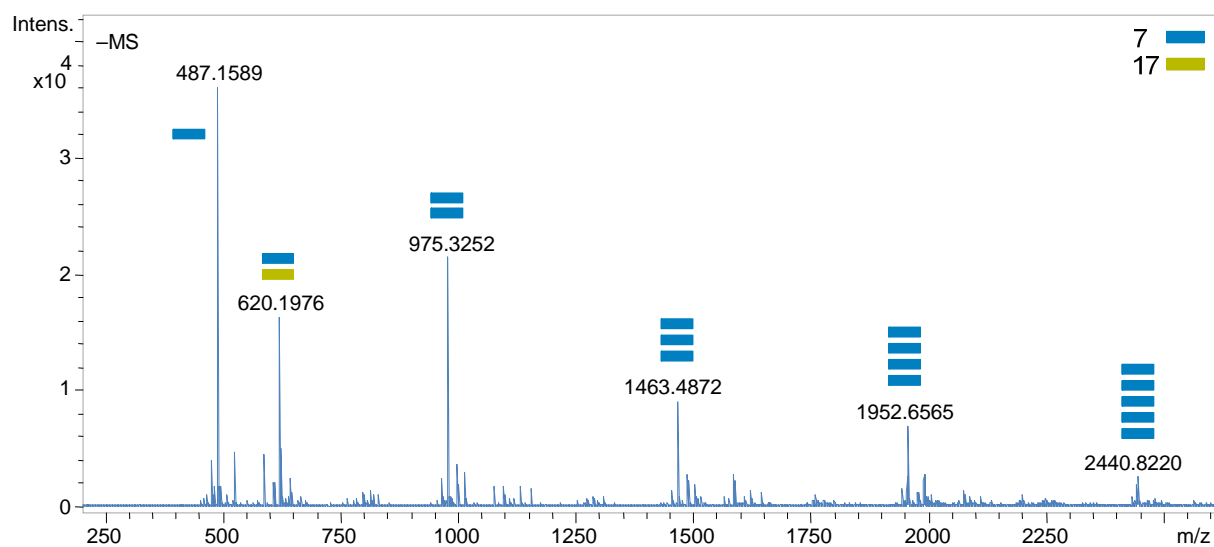


Figure 29. ESI-TOF/MS for host-guest complex 7/17.

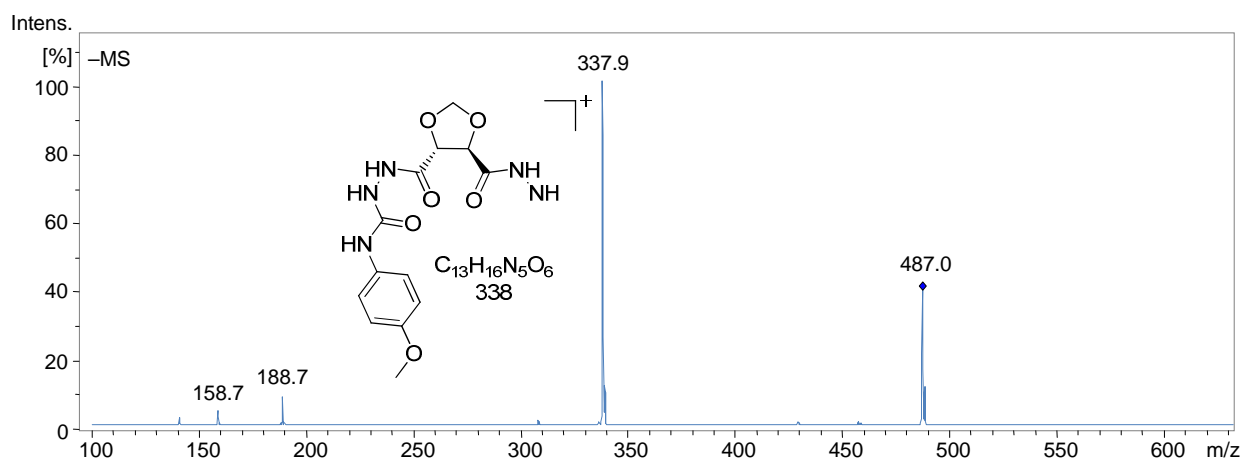


Figure 30. Tandem ESI-MS for host-guest complex 7/17 (MS^2 for m/z 487).

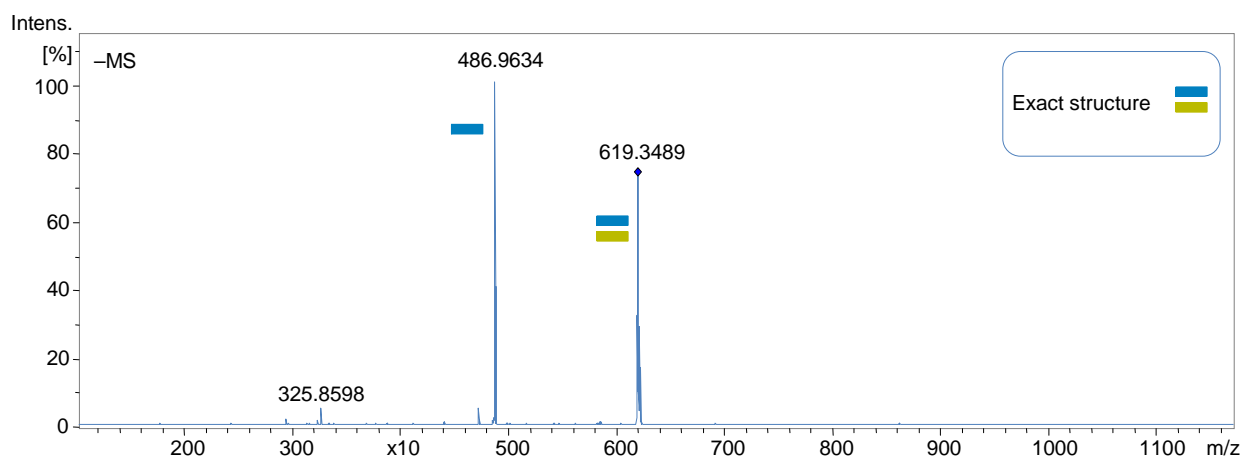


Figure 31. Tandem ESI-MS for host-guest complex 7/17 (MS^2 for m/z 620).

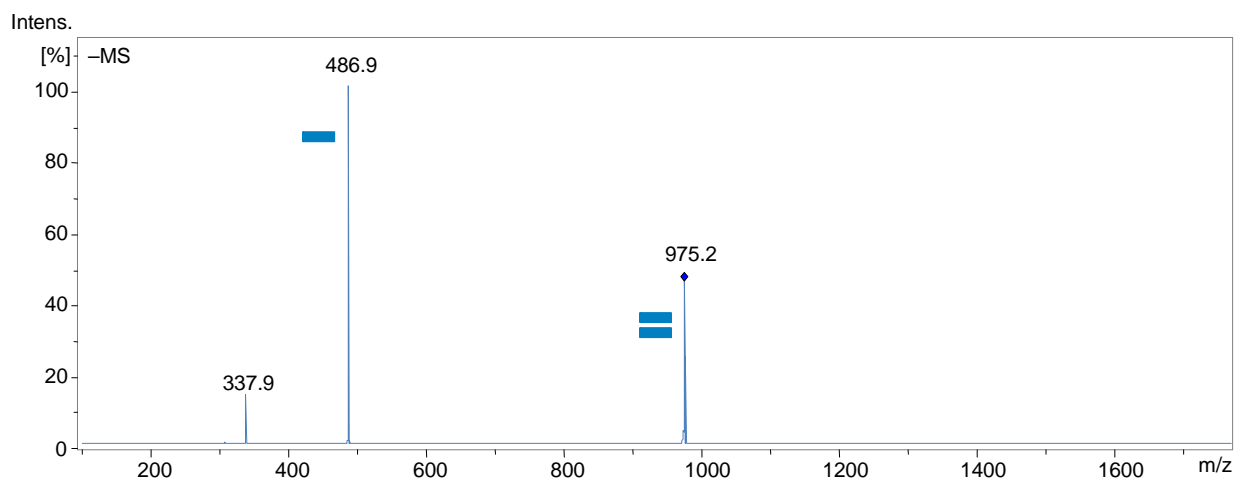


Figure 32. Tandem ESI-MS for host-guest complex **7/17** (MS² for m/z 975).

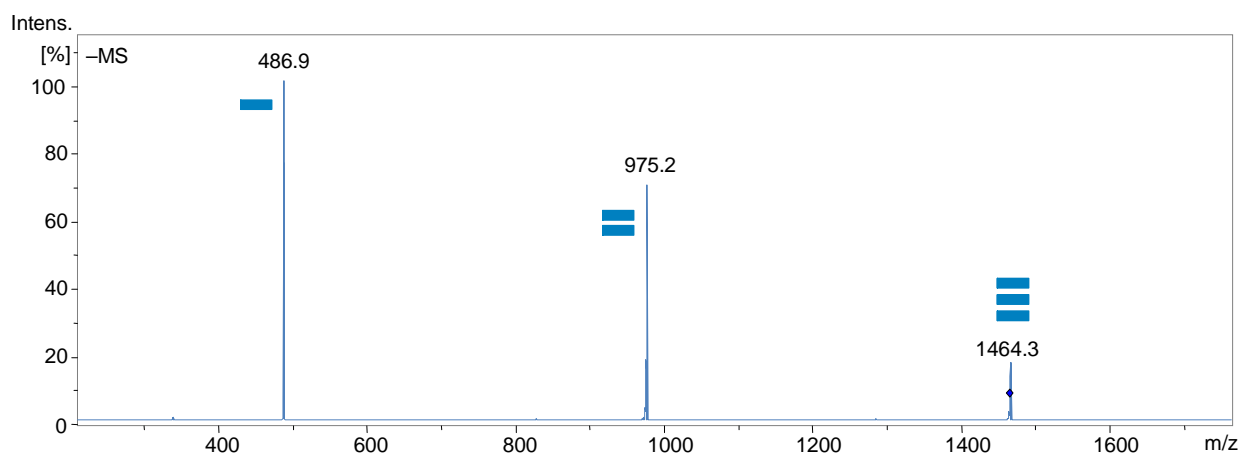


Figure 33. Tandem ESI-MS for host-guest complex **7/17** (MS² for m/z 1463).

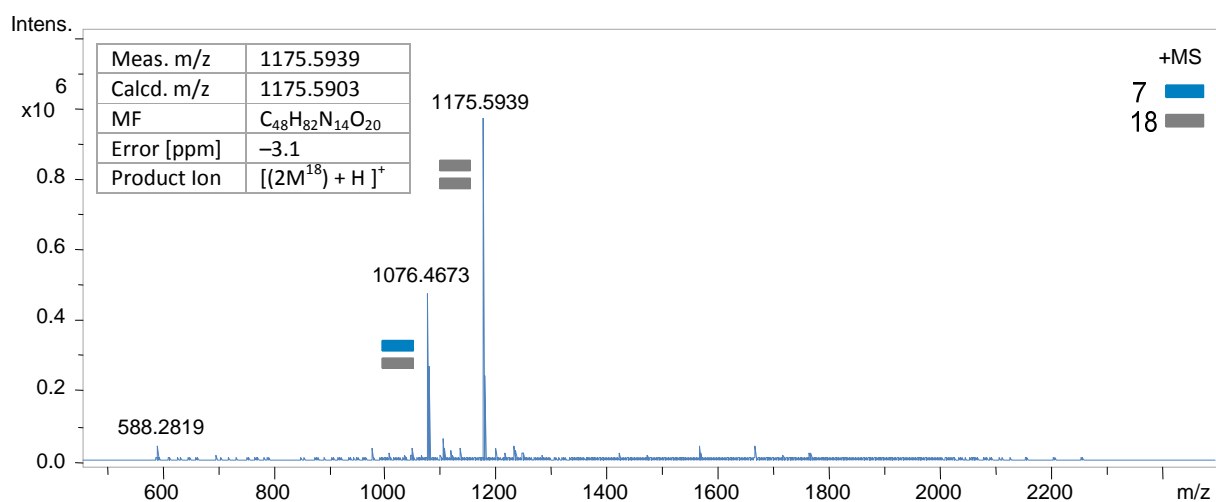


Figure 34. ESI-TOF/MS for host-guest complex **7/18**.

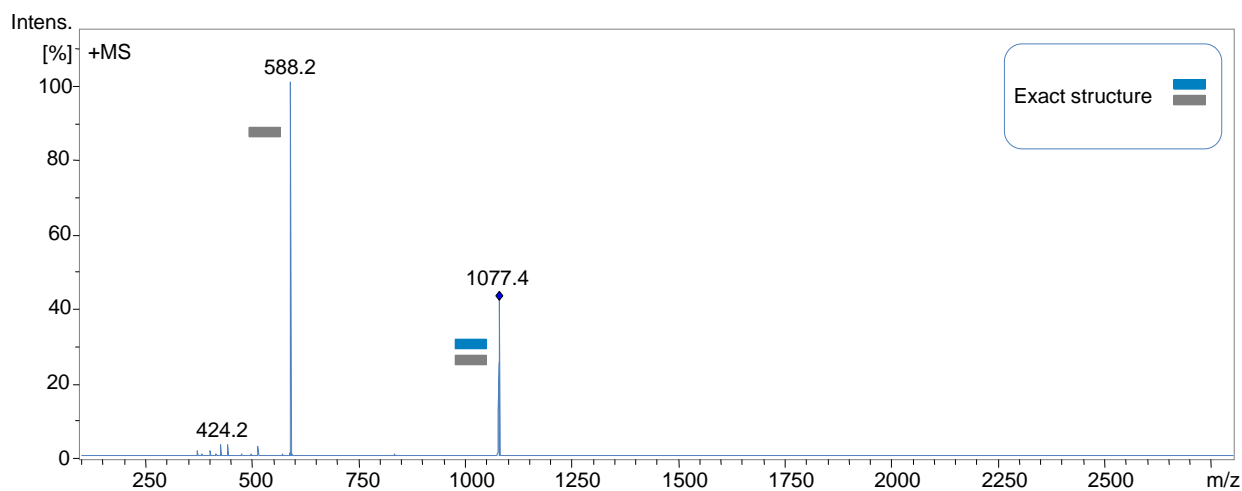


Figure 35. Tandem ESI-MS for host-guest complex **7/18** (MS² for m/z 1076).

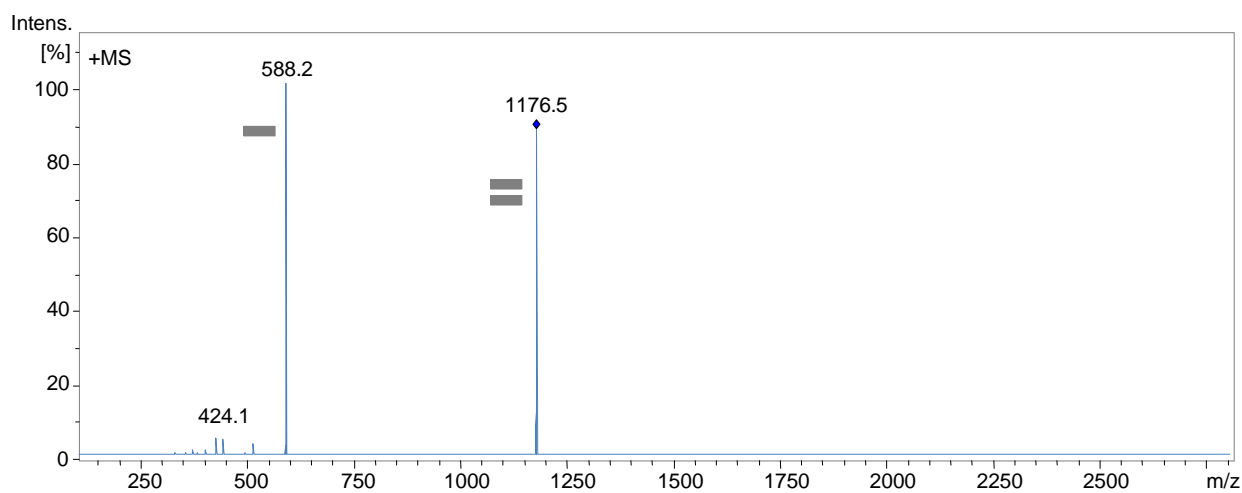


Figure 36. Tandem ESI-MS for host-guest complex **7/18** (MS² for m/z 1176).

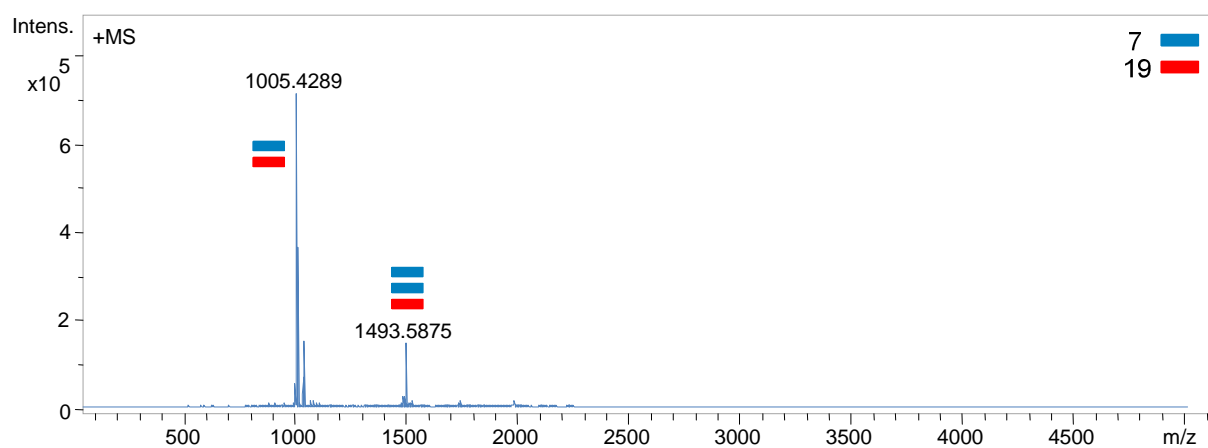


Figure 37. ESI-TOF/MS for host-guest complex **7/19**.

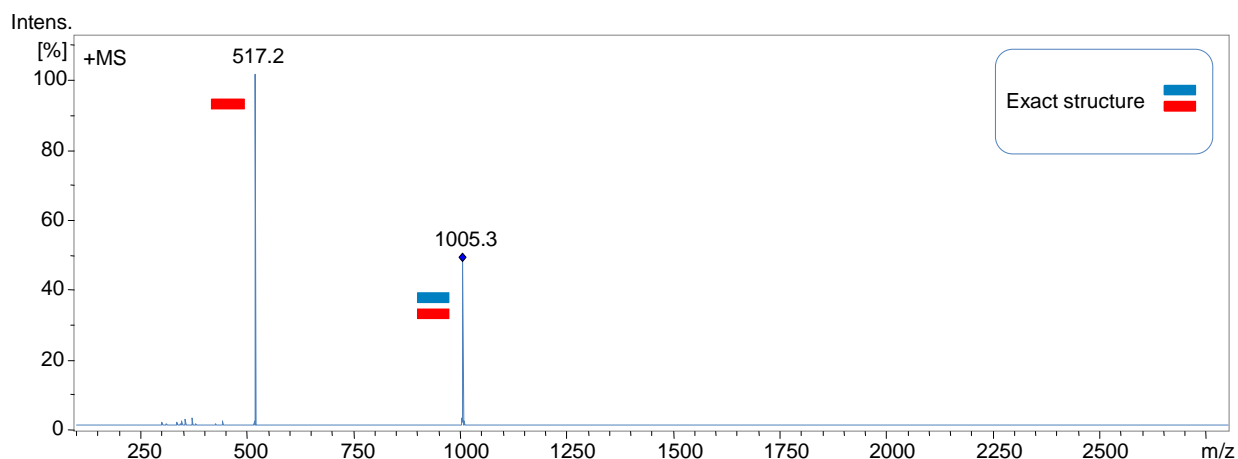


Figure 38. Tandem ESI-MS for host-guest complex **7/19** (MS^2 for m/z 1005).

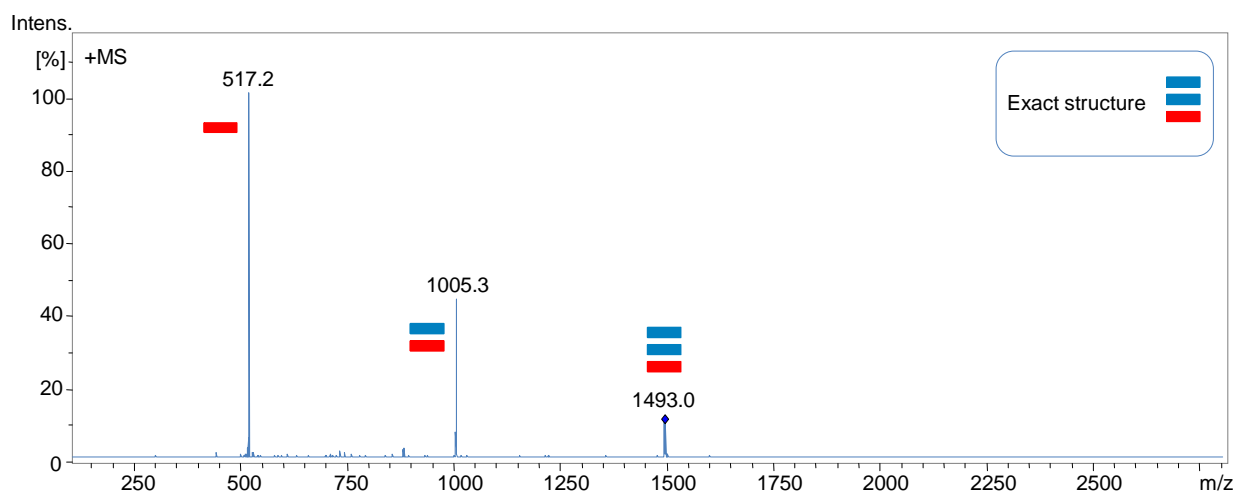


Figure 39. Tandem ESI-MS for host-guest complex **7/19** (MS^2 for m/z 1493).

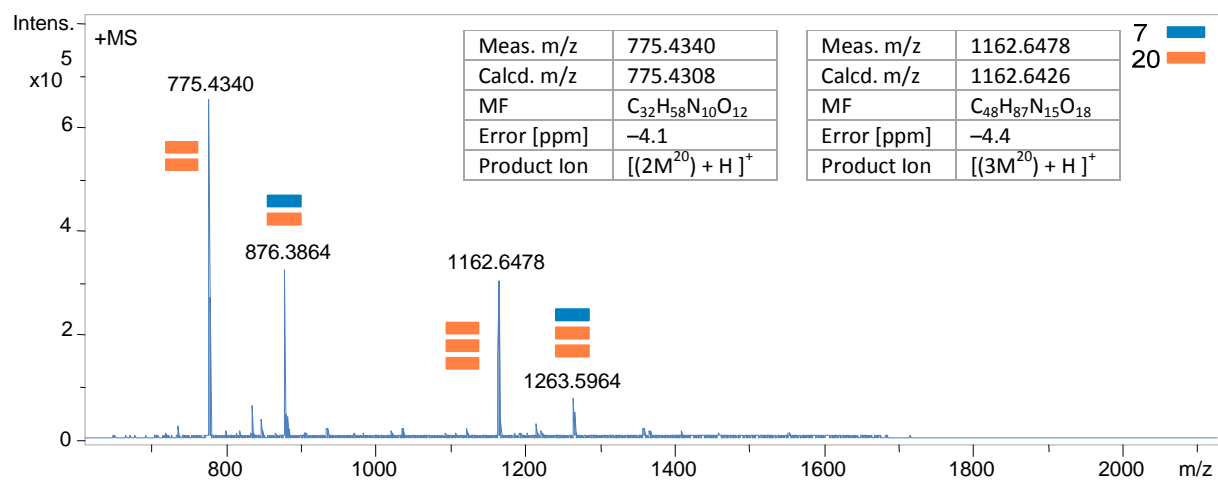


Figure 40. ESI-TOF/MS for host-guest complex **7/20**.

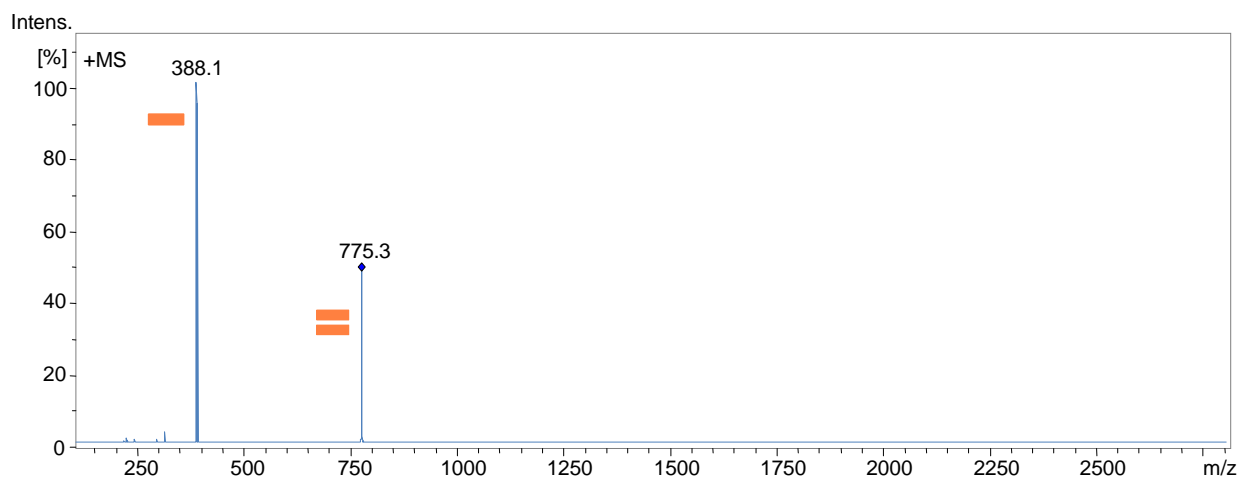


Figure 41. Tandem ESI-MS for host-guest complex **7/20** (MS^2 for m/z 775).

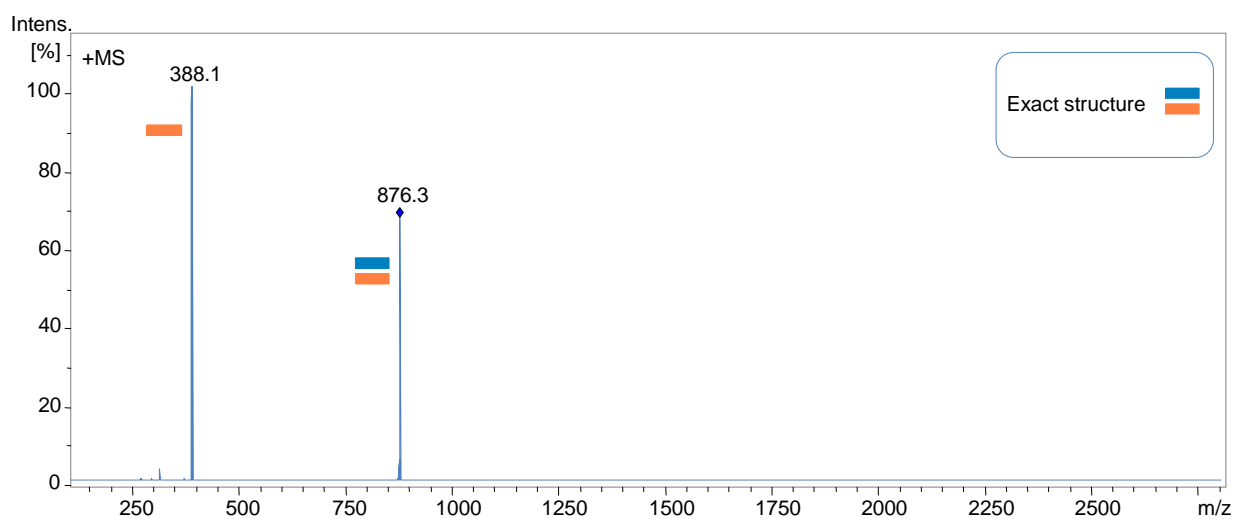


Figure 42. Tandem ESI-MS for host-guest complex **7/20** (MS^2 for m/z 876).

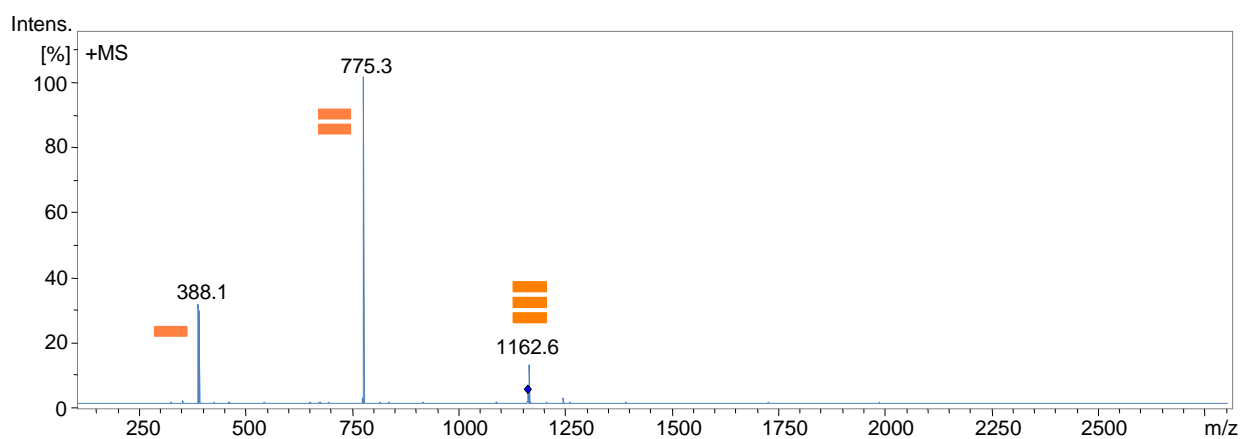


Figure 43. Tandem ESI-MS for host-guest complex **7/20** (MS^2 for m/z 1162).

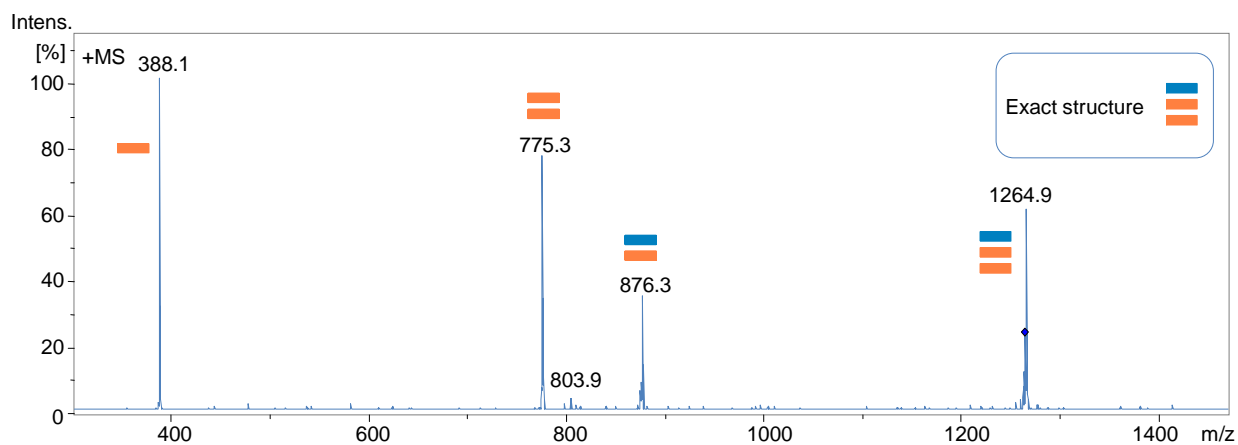


Figure 44. Tandem ESI-MS for host-guest complex **7/20** (MS^2 for m/z 1263).

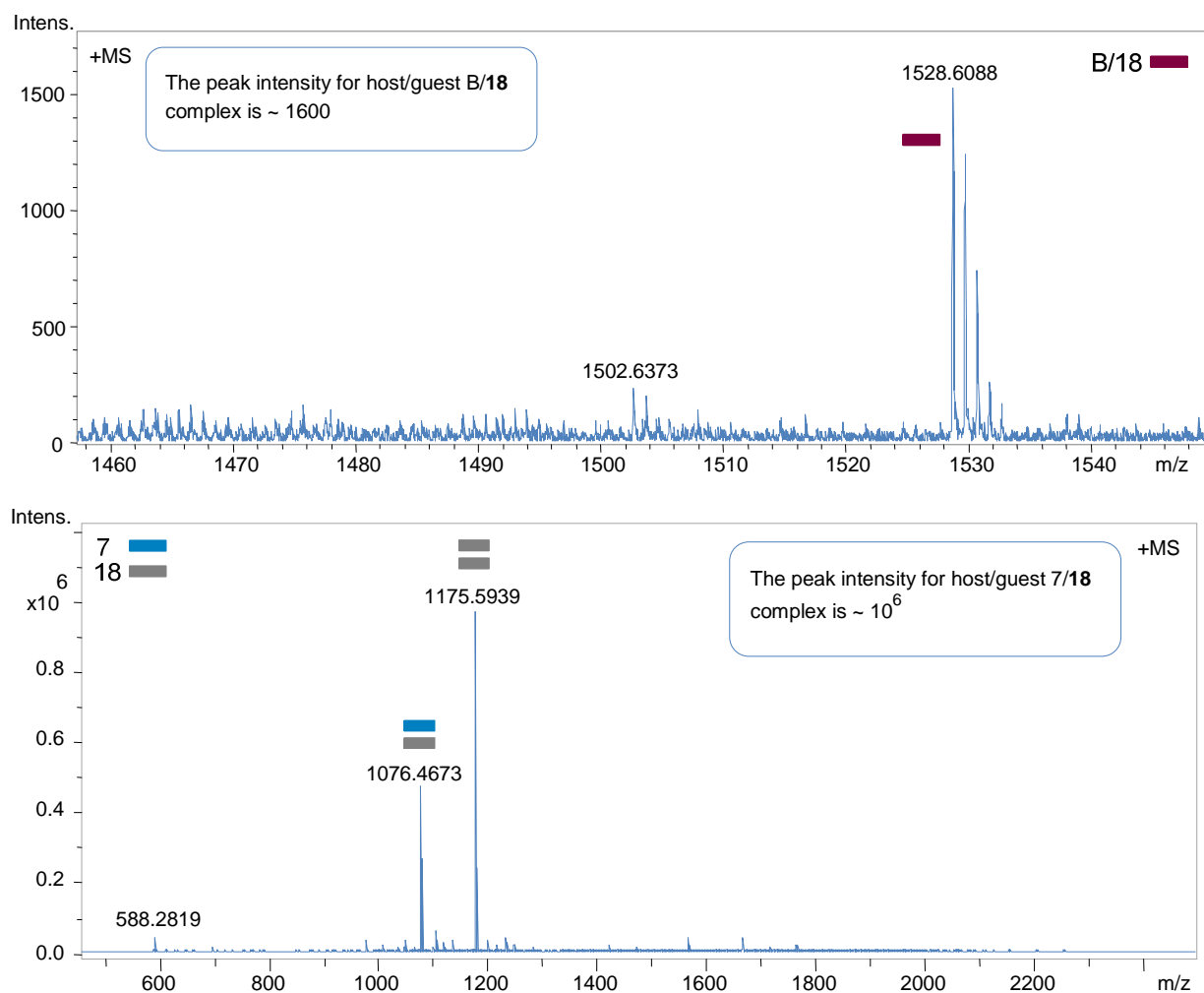


Figure 45. Comparison between ESI-TOF/MS for (receptor/guest, **7/18**) and (macrocycle/guest, **B/18**).

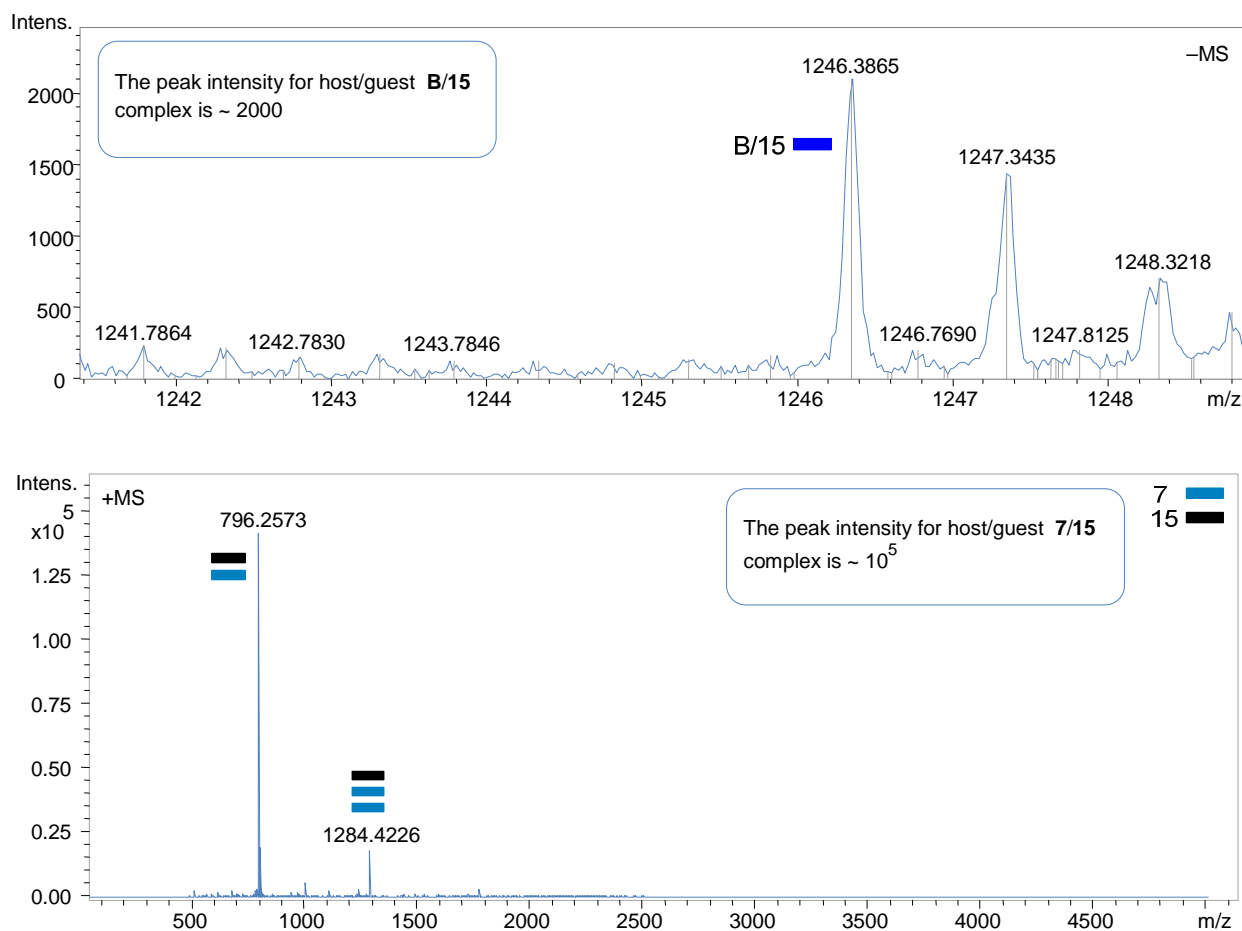


Figure 46. Comparison between ESI-TOF/MS for (receptor/guest, **7/15**) and (macrocycle/guest, **B/15**).

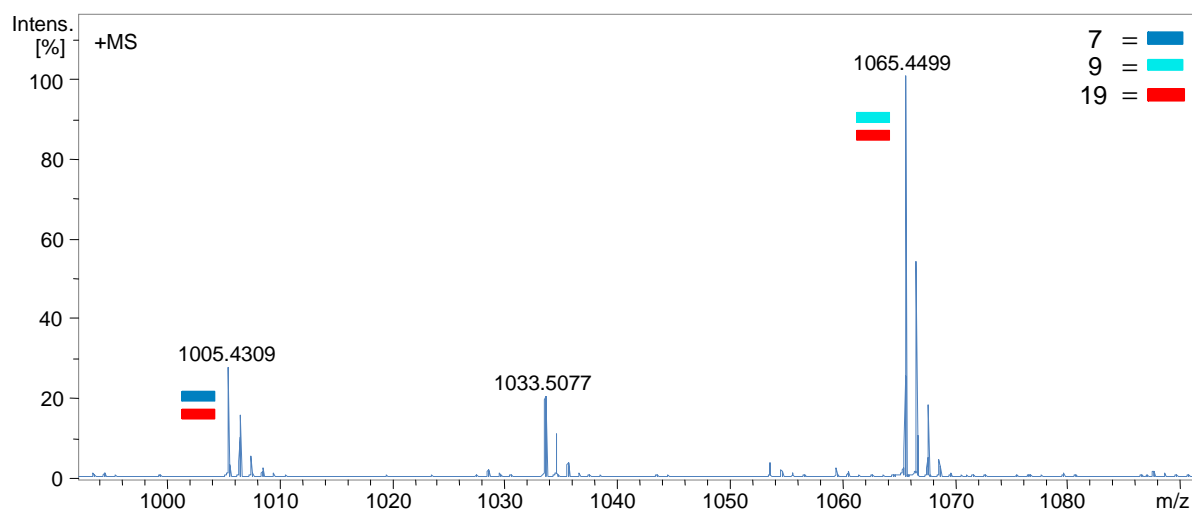


Figure 47. ESI-TOF/MS showing selective recognition of oligopeptide **19** by receptor **9**.

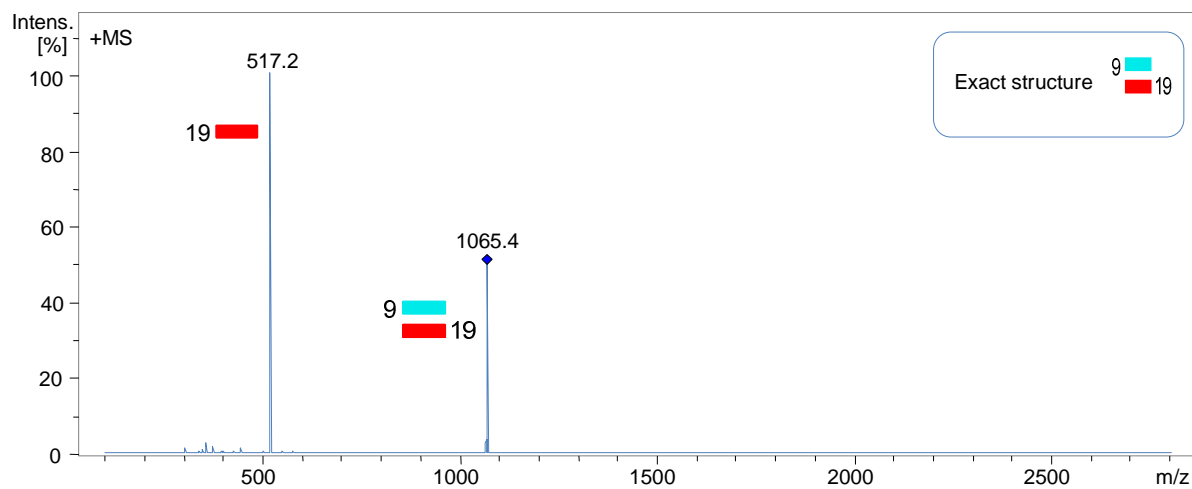


Figure 48. Tandem ESI-MS for host-guest complex (7 and 9)/19 (MS^2 for m/z 1065).

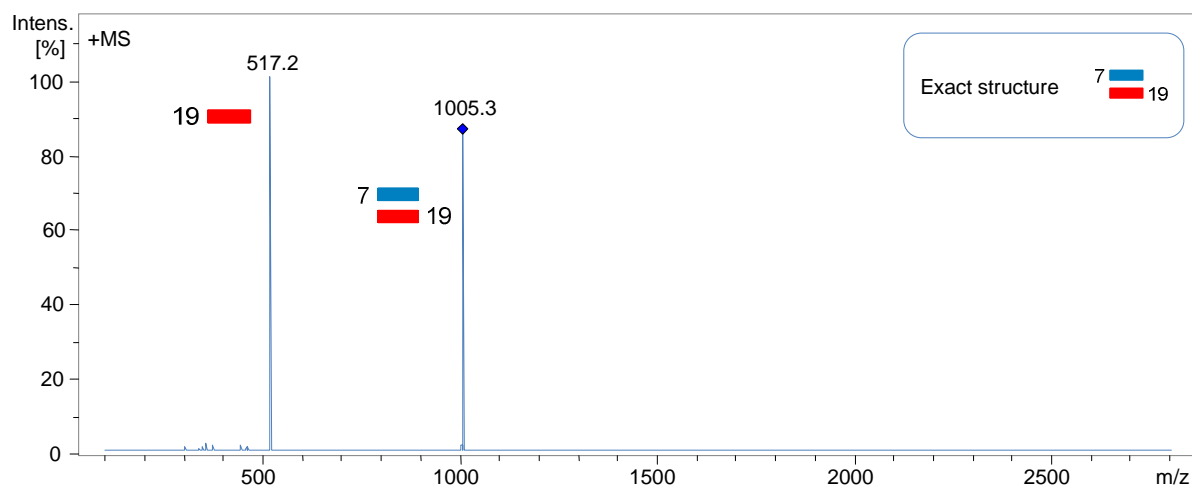


Figure 49. Tandem ESI-MS for host-guest complex (7 and 9)/19 (MS^2 for m/z 1005).

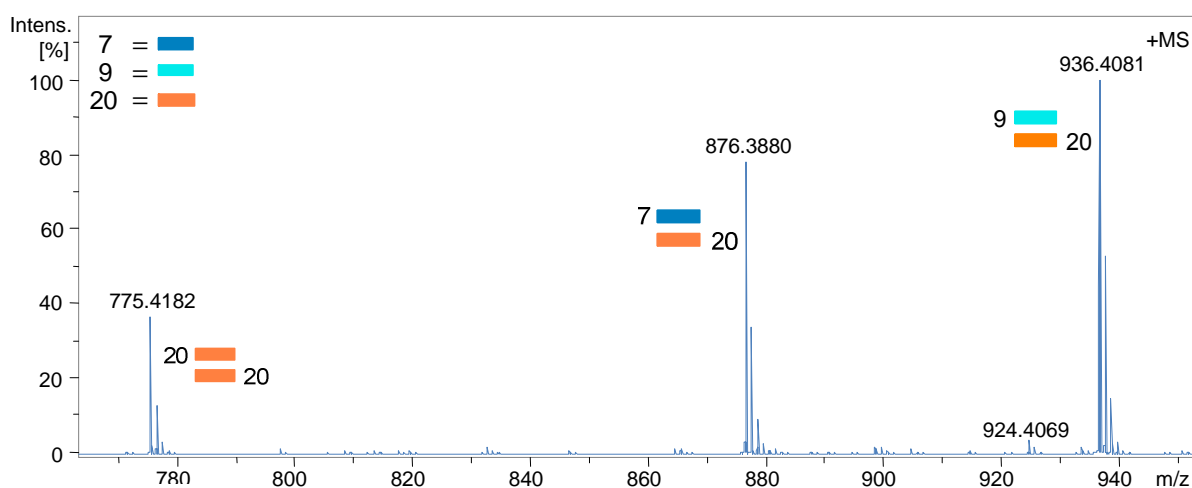


Figure 50. ESI-TOF/MS showing recognition of oligopeptide 20 by receptors 7 and 9.

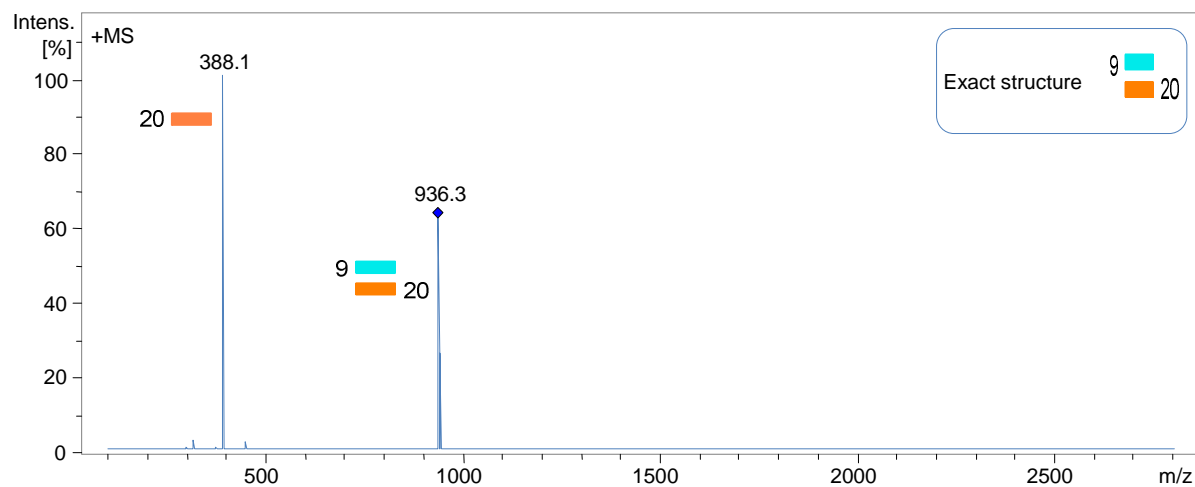


Figure 51. Tandem ESI-MS for host-guest complex (7 and 9)/20 (MS^2 for m/z 936).

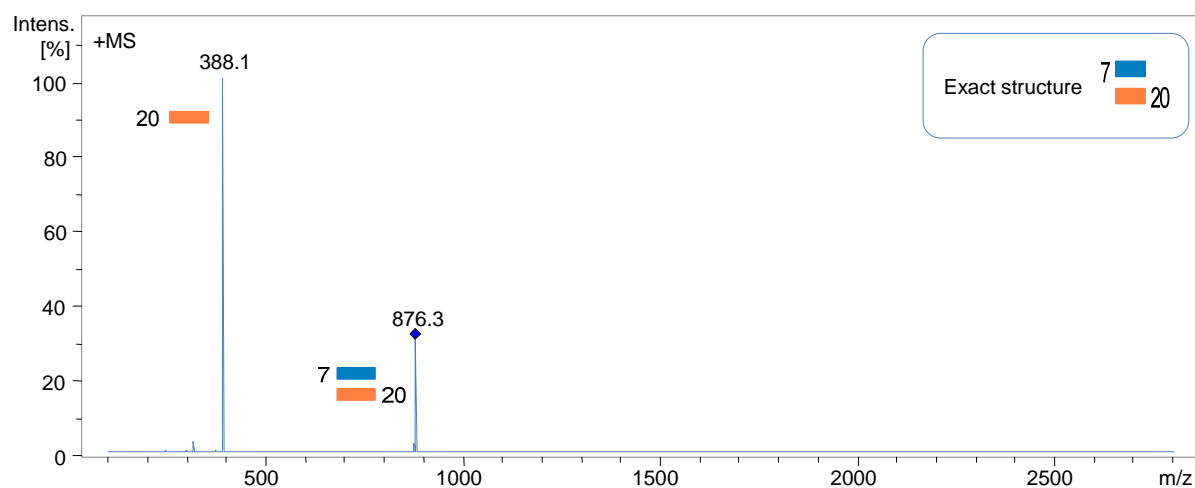


Figure 52. Tandem ESI-MS for host-guest complex (7 and 9)/20 (MS^2 for m/z 876).

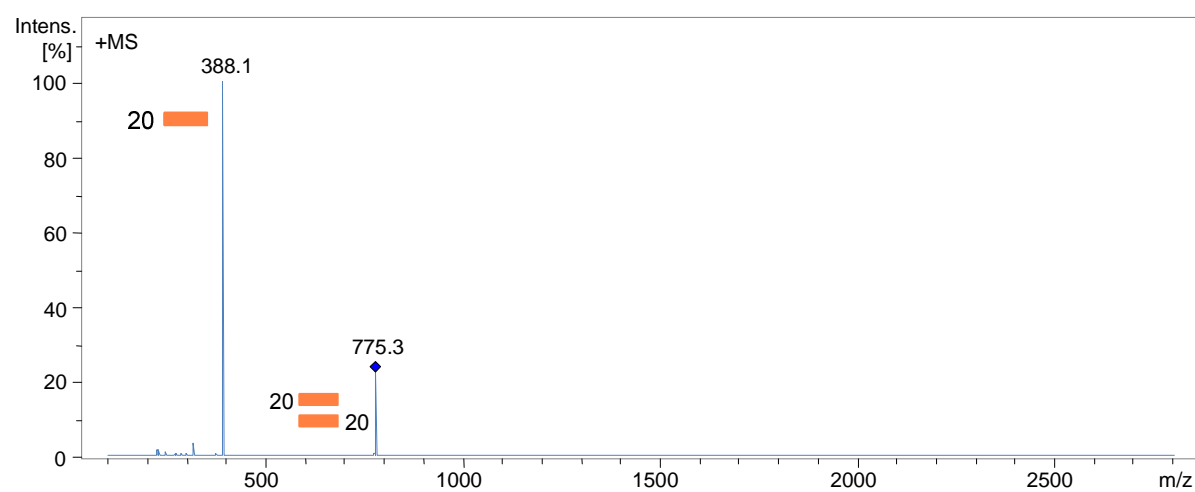


Figure 53. Tandem ESI-MS for host-guest complex (7 and 9)/20 (MS^2 for m/z 775).

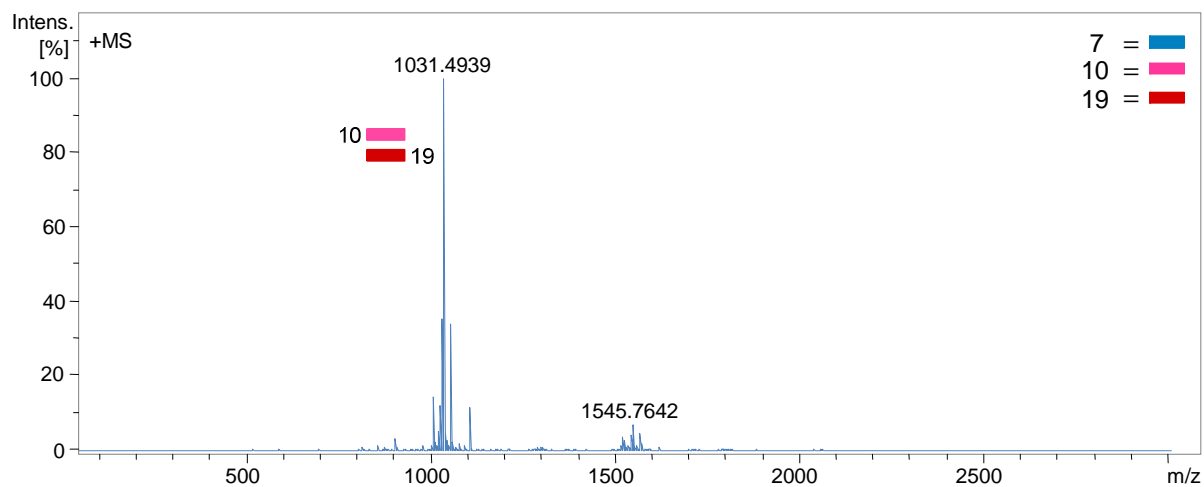


Figure 54. ESI-TOF/MS showing selective recognition of oligopeptide **19** by receptor **10**.

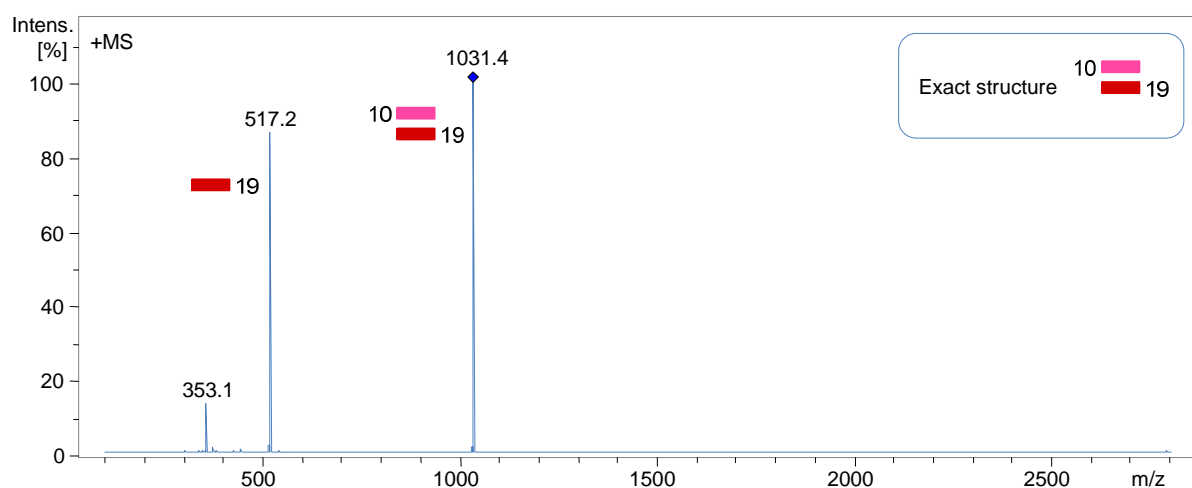


Figure 55. Tandem ESI-MS for host-guest complex (**7** and **10**)/**19** (MS^2 for m/z 1031).

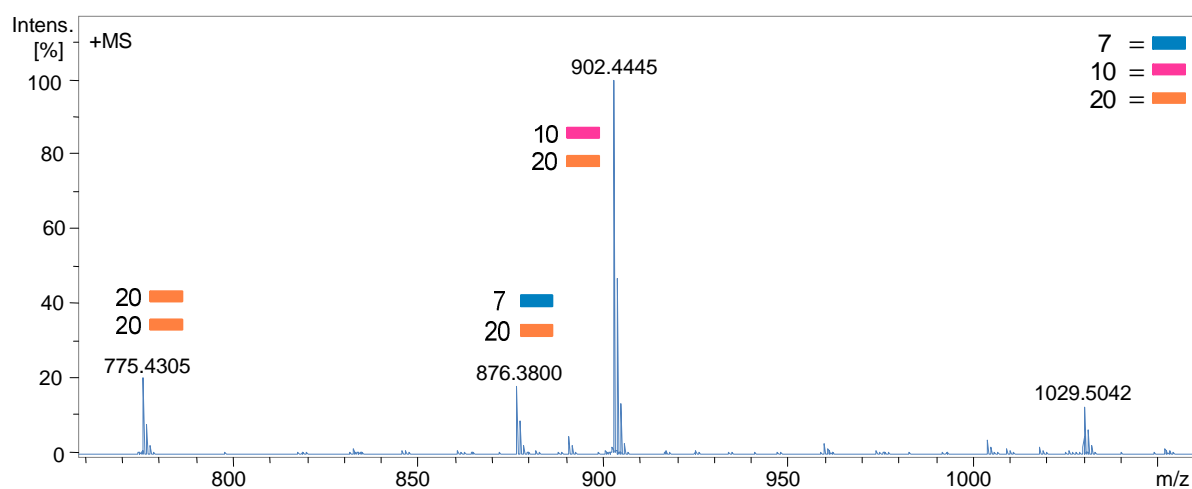


Figure 56. ESI-TOF/MS showing selective recognition of oligopeptide **20** by receptor **10**.

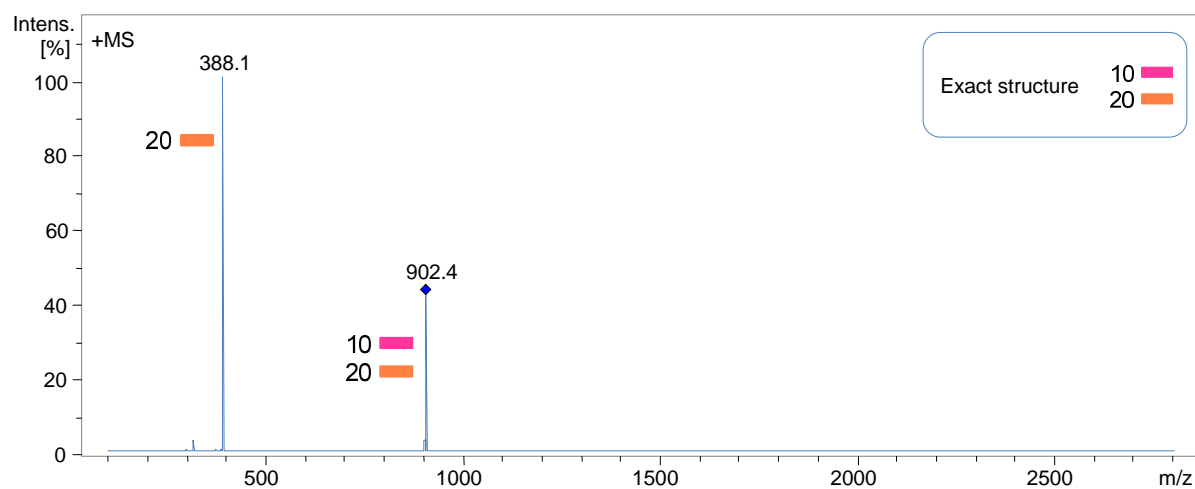


Figure 57. Tandem ESI-MS for host-guest complex (**7** and **10**)/**20** (MS^2 for m/z 902).

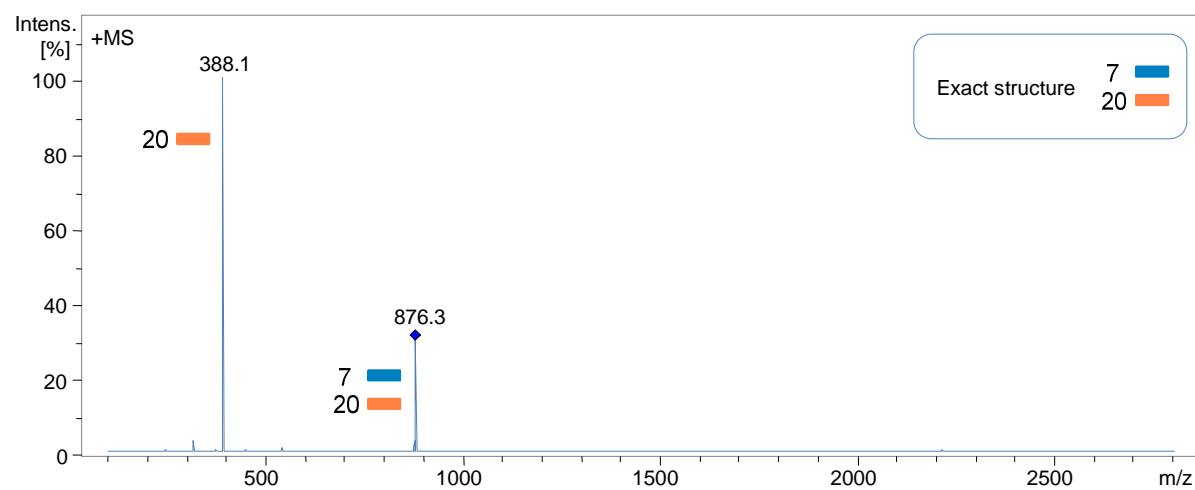


Figure 58. Tandem ESI-MS for host-guest complex (**7** and **10**)/**20** (MS^2 for m/z 876).

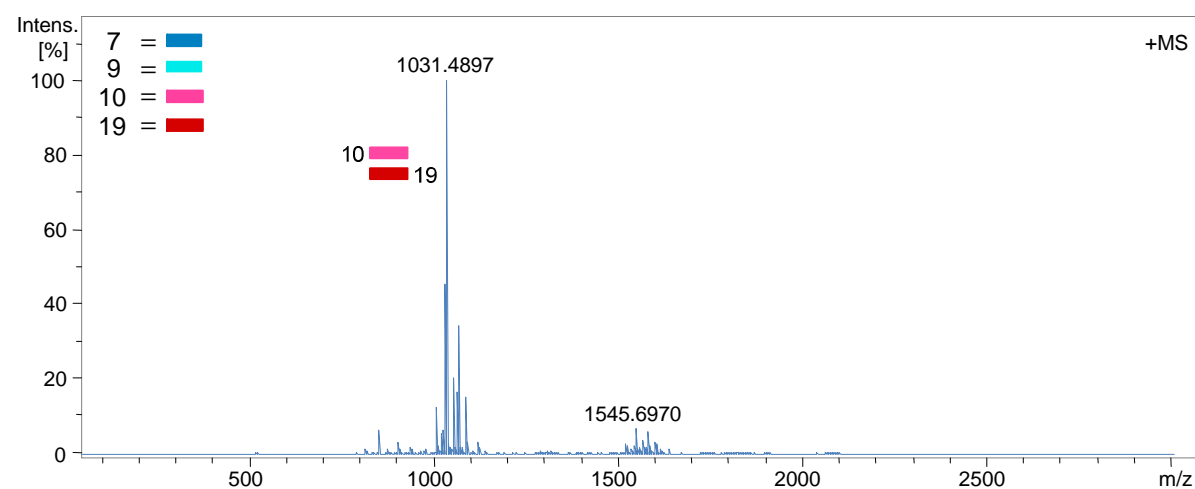


Figure 59. ESI-TOF/MS showing selective recognition of oligopeptide **19** by receptor **10**.

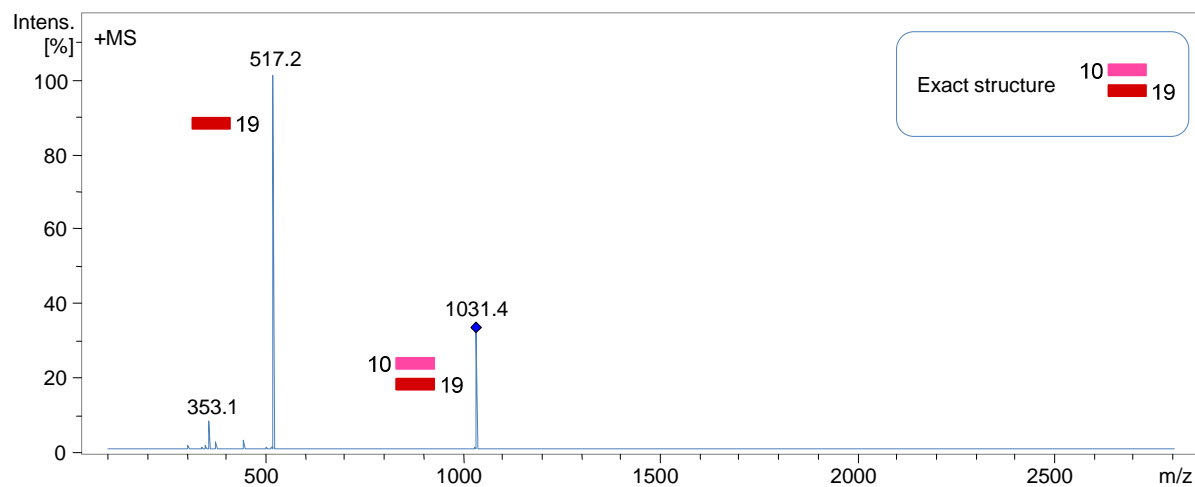


Figure 60. Tandem ESI-MS for host-guest complex (7, 9 and 10)/19 (MS^2 for m/z 1031).

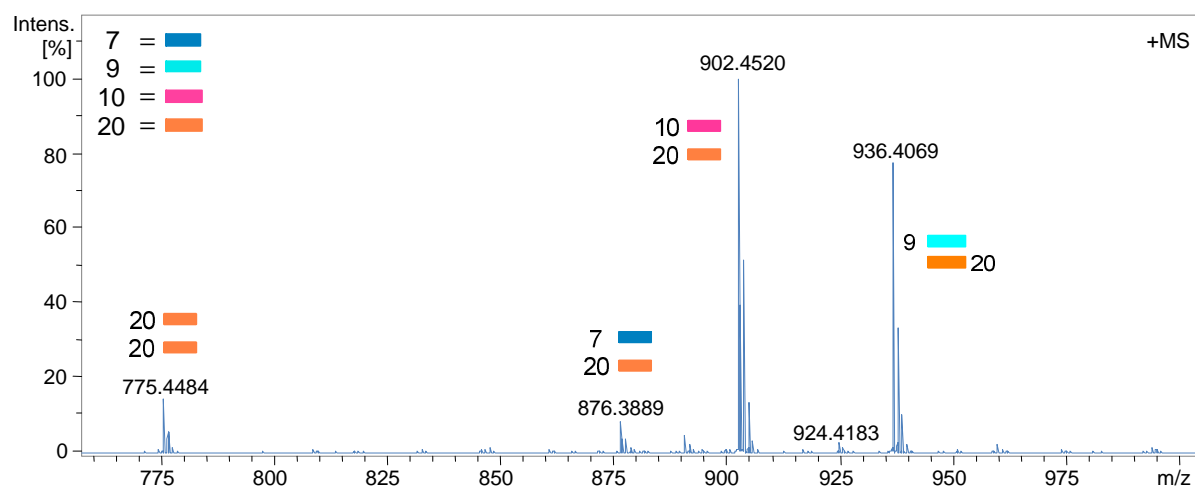


Figure 61. ESI-TOF/MS showing selective recognition of oligopeptide 19 by receptors 9 and 10.

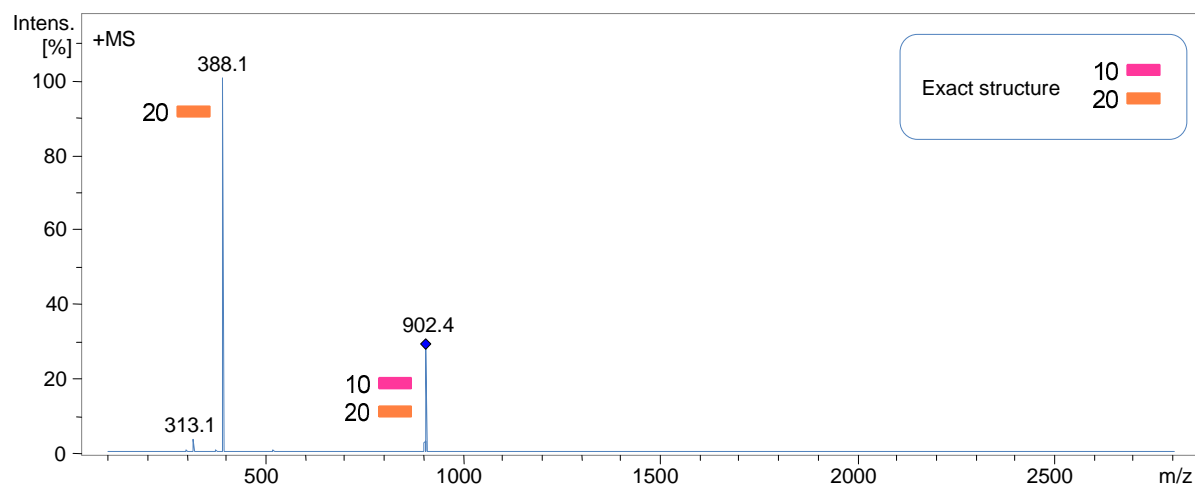


Figure 62. Tandem ESI-MS for host-guest complex (7, 9 and 10)/20 (MS^2 for m/z 902).

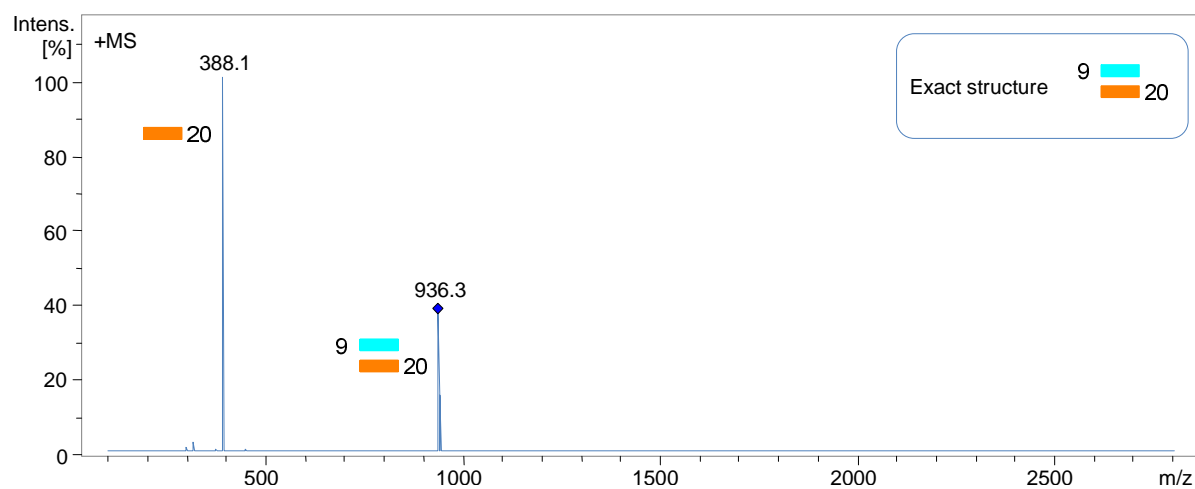


Figure 63. Tandem ESI-MS for host-guest complex (7, 9 and 10)/20 (MS^2 for m/z 936).

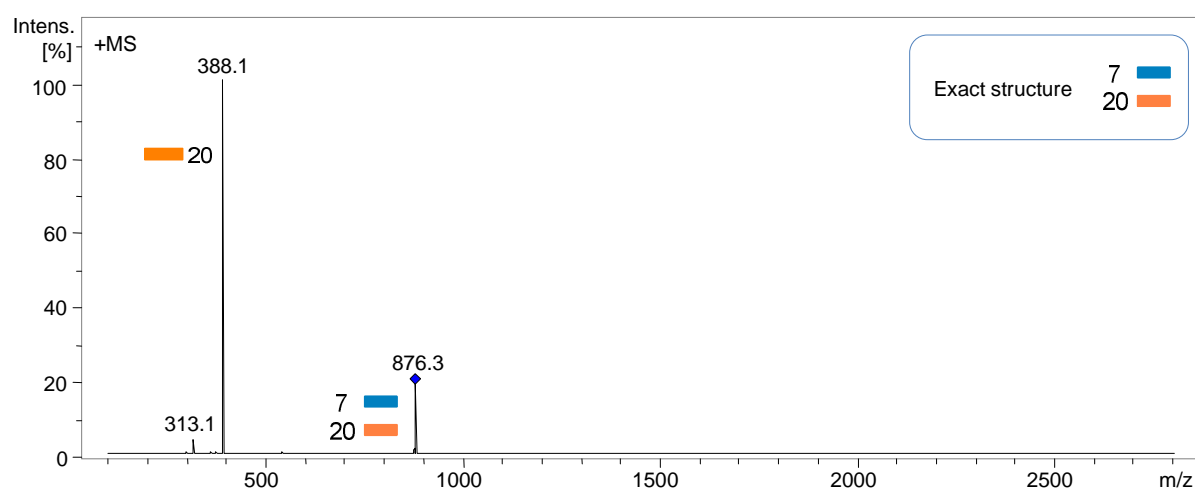


Figure 64. Tandem ESI-MS for host-guest complex (7, 9 and 10)/20 (MS^2 for m/z 876).

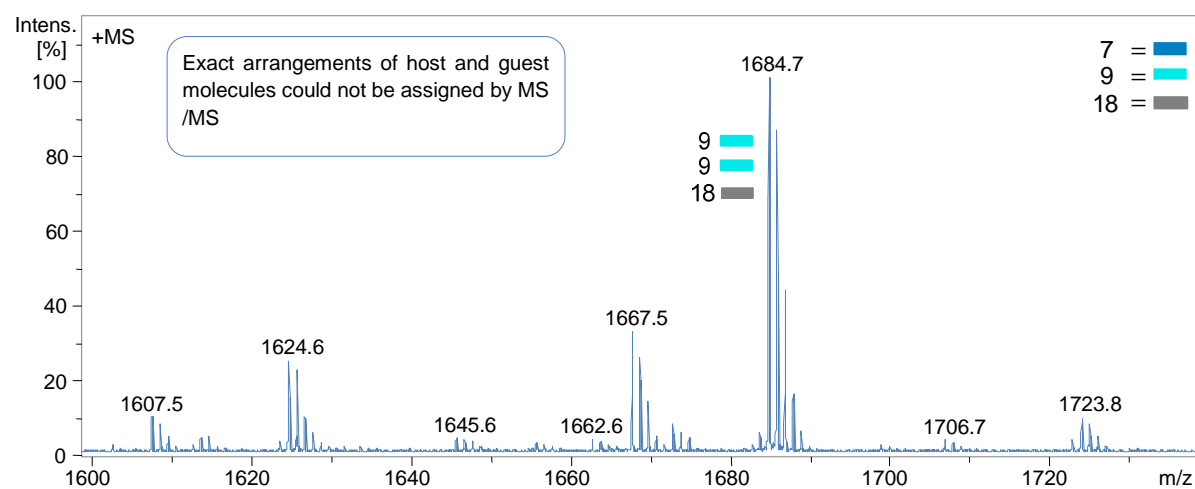


Figure 65. ESI-TOF/MS for higher Mwt complexes of receptor (7 and 10) with oligopeptide 18.

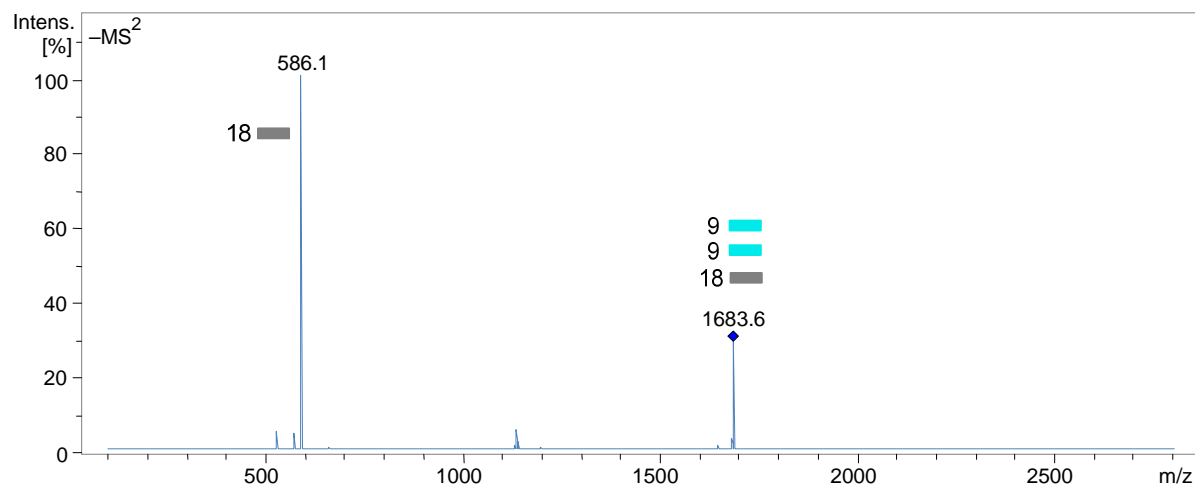


Figure 66. Tandem ESI-MS for higher Mwt complexes (7 and 10)/20 (MS^2 for m/z 1683).

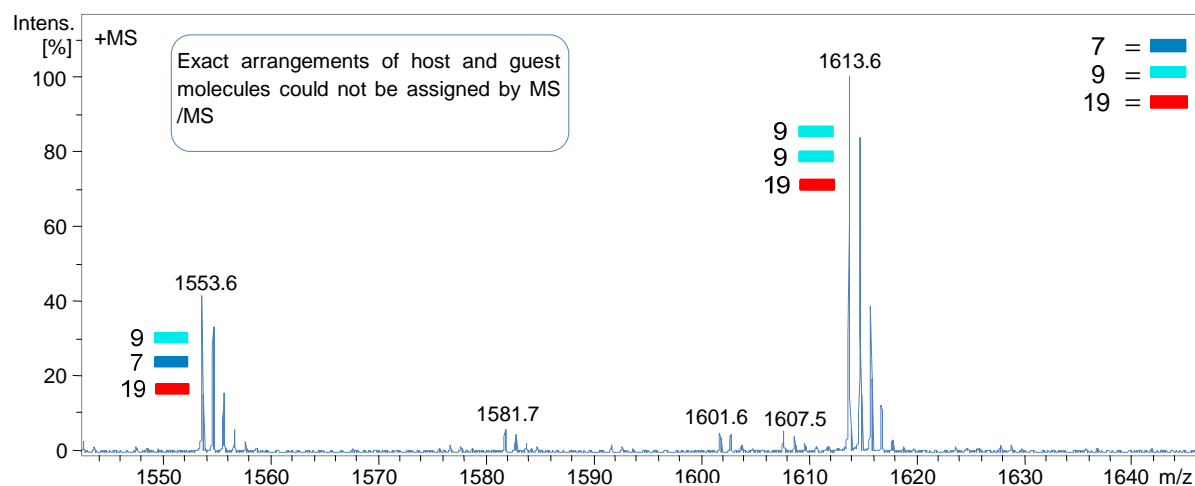


Figure 67. ESI-TOF/MS for higher Mwt complexes of receptor (7 and 9) with oligopeptide 19.

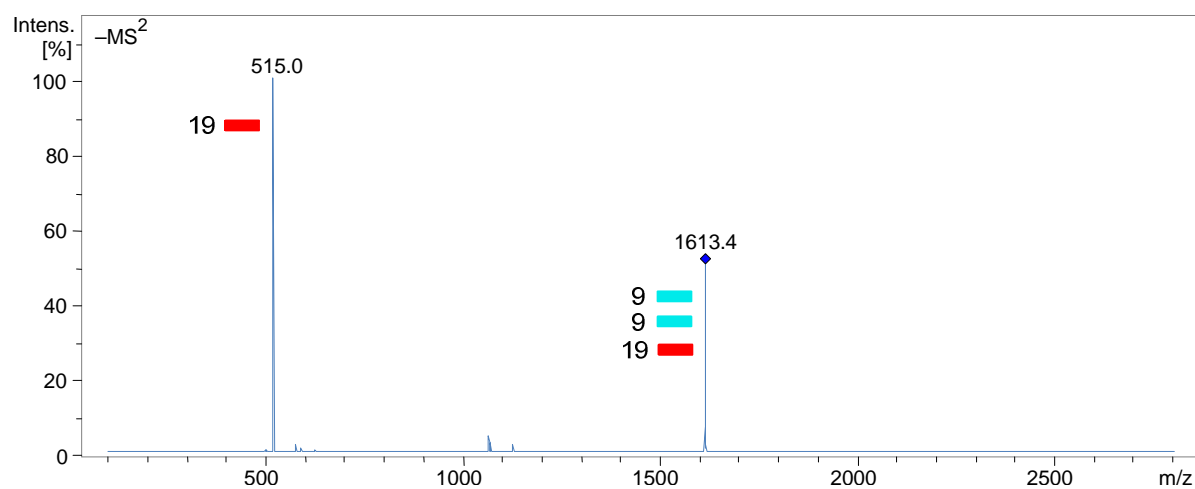


Figure 68. Tandem ESI-MS for higher Mwt complexes (7 and 9)/19 (MS^2 for m/z 1613).

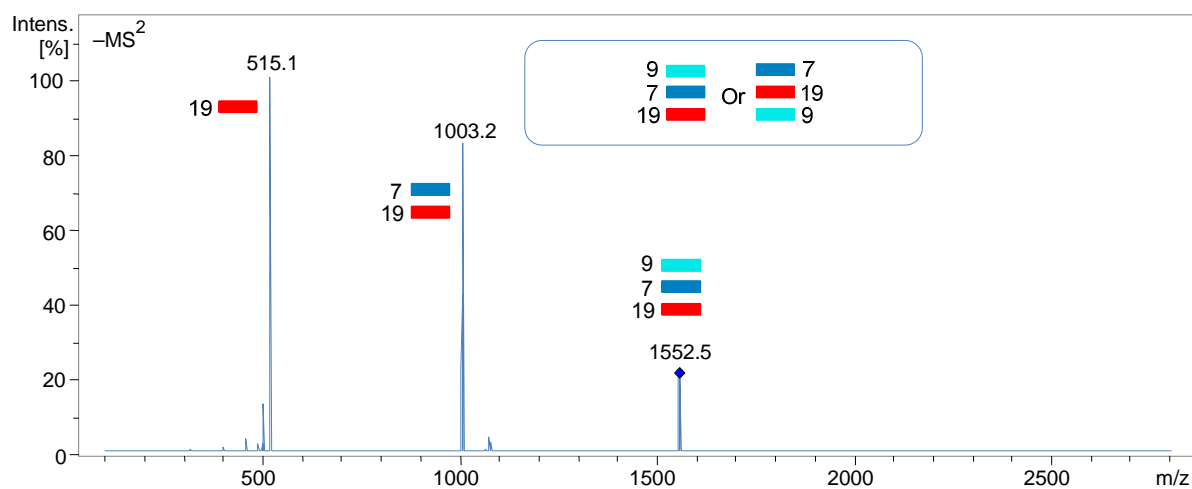


Figure 69. Tandem ESI-MS for higher Mwt complexes (7 and 9)/19 (MS^2 for m/z 1552).

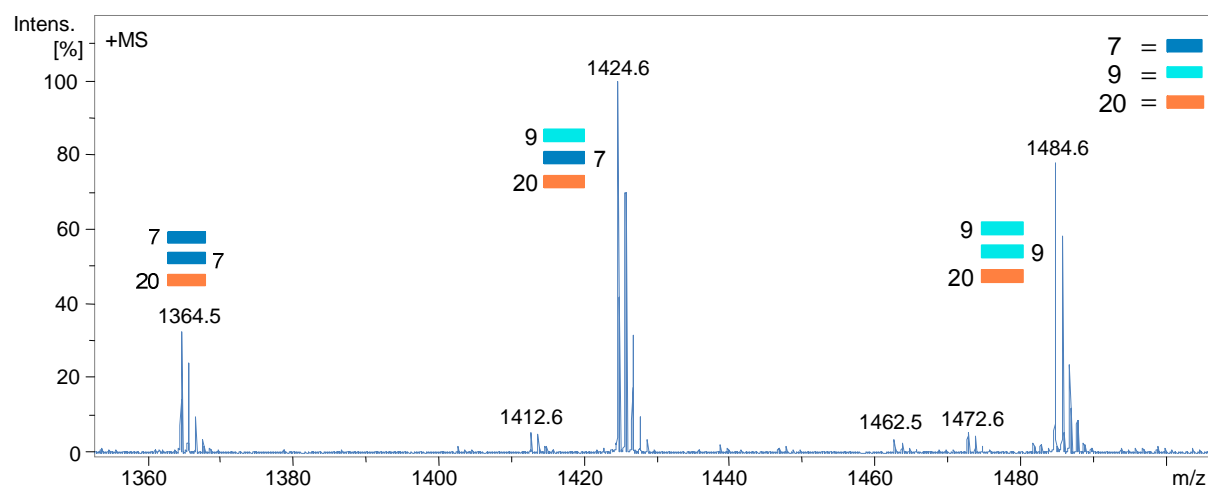


Figure 70. ESI-TOF/MS for higher Mwt complexes of receptor (7 and 9) with oligopeptide 20.

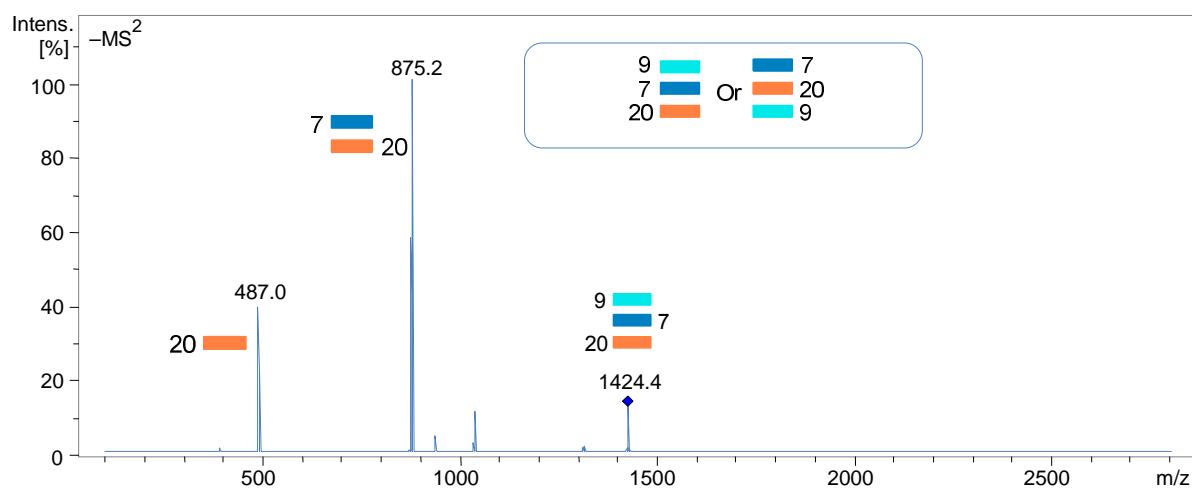


Figure 71. Tandem ESI-MS for higher Mwt complexes (7 and 9)/20 (MS^2 for m/z 1424).

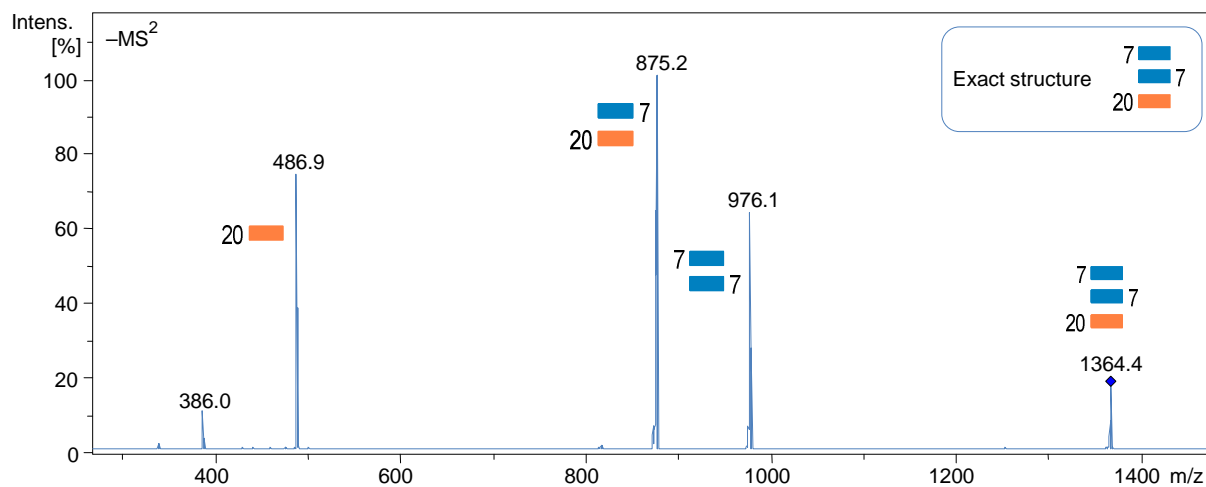


Figure 72. Tandem ESI-MS for higher Mwt complexes (**7** and **9**)/**20** (MS² for m/z 1364).

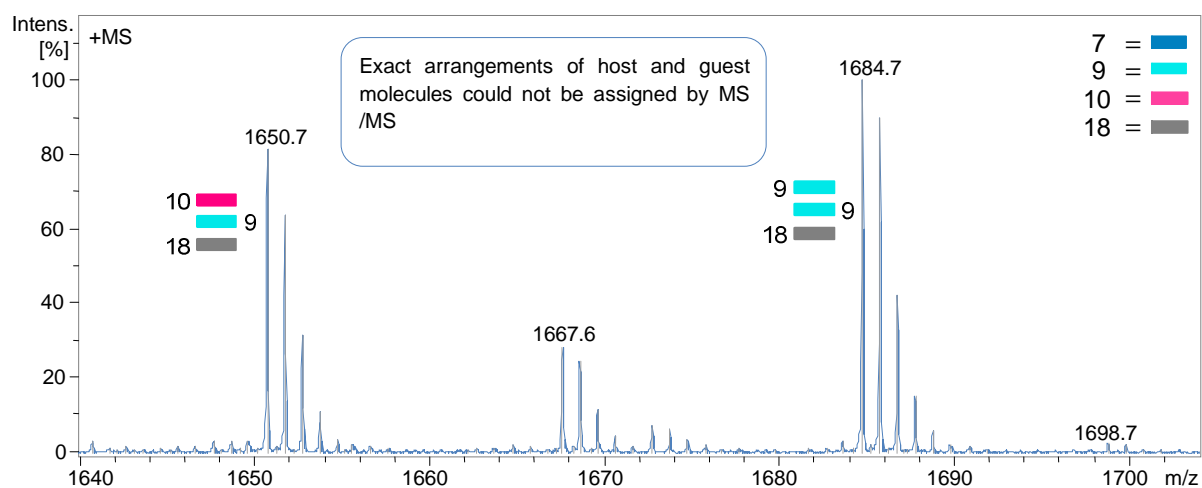


Figure 73. ESI-TOF/MS for higher Mwt complexes of receptor (**7**, **9** and **10**) with **18**.

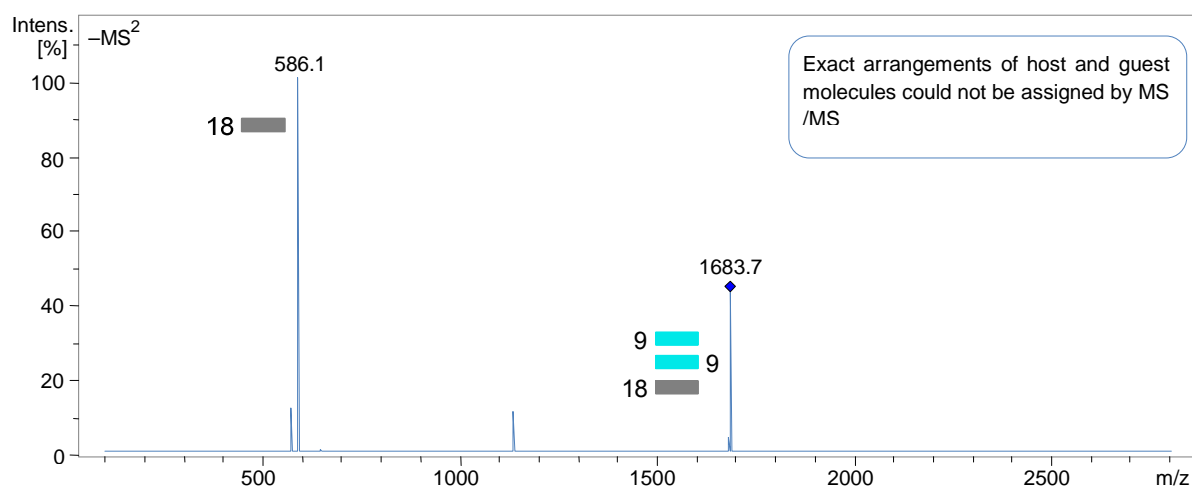


Figure 74. Tandem ESI-MS for higher Mwt complexes (**7**, **9** and **10**)/**18** (MS² for m/z 1683).

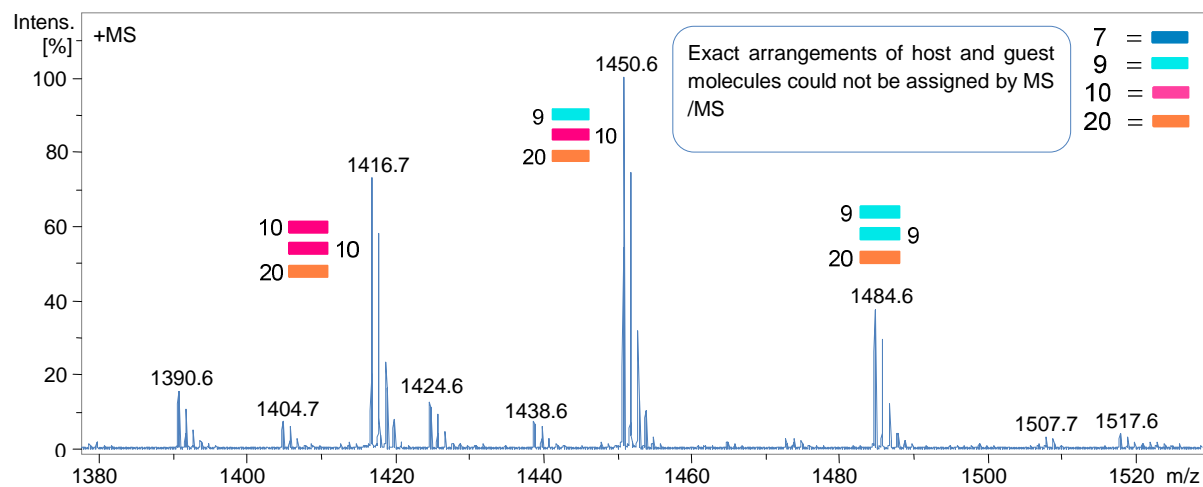


Figure 75. ESI-TOF/MS for higher Mwt complexes of receptor (**7**, **9** and **10**) with **20**.

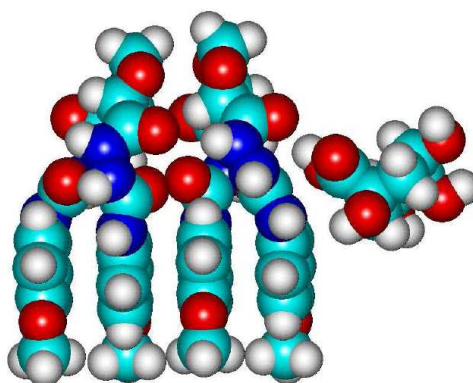


Figure 76. Proposed energy-minimized structure for two self-assembled molecules of receptor **7** recognizing D-(-)-quinic acid **14**. Structure was optimized at the MM+ level using HyperChem software (Release 8.0). Both hydrogen bonding and π - π stacking interactions participate in stabilizing the host-guest complexes.

Table 1. High resolution ESI-TOF/MS data for selective recognition of receptors **7**, **9** and **10** to oligo-peptide guests **19** and **20**

Host/Guest	Molecular Formula	^a Product Ions	Calcd. m/z	Meas. m/z	Error [ppm]
(7 and 9)/19	C ₄₄ H ₆₄ N ₁₂ O ₁₉	[(M ⁹ + M ¹⁹) + H] ⁺	1065.4483	1065.4499	−1.5
	C ₄₂ H ₆₀ N ₁₂ O ₁₇	[(M ⁷ + M ¹⁹) + H] ⁺	1005.4272	1005.4309	−3.7
	C ₆₅ H ₈₈ N ₁₈ O ₂₇	[(M ⁷ + M ⁹ + M ¹⁹) + H] ⁺	1553.6139	1553.6148	−0.6
	C ₆₇ H ₉₂ N ₁₈ O ₂₉	[(2M ⁹ + M ¹⁹) + H] ⁺	1613.6350	1613.6363	−0.8
(7 and 9)/20	C ₂₈ H ₅₈ N ₁₀ O ₁₅	[(2M ²⁰) + H] ⁺	775.4156	775.4182	−3.3
	C ₃₉ H ₅₇ N ₁₁ O ₁₆	[(M ⁹ + M ²⁰) + H] ⁺	936.4058	936.4081	−2.5
	C ₃₇ H ₅₃ N ₁₁ O ₁₄	[(M ⁷ + M ²⁰) + H] ⁺	876.3846	876.3880	−3.9
	C ₅₈ H ₇₇ N ₁₇ O ₂₂	[(2M ⁷ + M ²⁰) + H] ⁺	1364.5502	1364.5466	2.6
	C ₆₂ H ₈₅ N ₁₇ O ₂₆	[(2M ⁹ + M ²⁰) + H] ⁺	1484.5924	1484.5889	2.4
	C ₆₀ H ₈₁ N ₁₇ O ₂₄	[(M ⁷ + M ⁹ + M ²⁰) + H] ⁺	1424.5682	1424.5713	2.2
(7 and 10)/19	C ₄₄ H ₆₆ N ₁₄ O ₁₅	[(M ¹⁰ + M ¹⁹) + H] ⁺	1031.4905	1031.4939	−3.3
(7 and 10)/20	C ₃₉ H ₅₉ N ₁₃ O ₁₂	[(M ¹⁰ + M ²⁰) + H] ⁺	902.4479	902.4445	3.8
	C ₃₇ H ₅₃ N ₁₁ O ₁₄	[(M ⁷ + M ²⁰) + H] ⁺	876.3846	876.3800	5.3
	C ₃₂ H ₅₈ N ₁₀ O ₁₂	[(2M ²⁰) + H] ⁺	775.4308	775.4305	0.5
(7, 9 and 10)/19	C ₄₄ H ₆₆ N ₁₄ O ₁₅	[(M ¹⁰ + M ¹⁹) + H] ⁺	1031.4905	1031.4897	0.8
	C ₄₄ H ₆₄ N ₁₂ O ₁₉	[(M ⁹ + M ¹⁹) + H] ⁺	1065.4483	1065.4462	2.0
	C ₄₆ H ₆₀ N ₁₆ O ₁₂	[(2M ¹⁰) + H] ⁺	1029.4649	1029.4696	−4.5
	C ₄₆ H ₅₈ N ₁₄ O ₁₆	[(M ⁹ + M ¹⁰) + H] ⁺	1063.4228	1063.4250	−2.1
(7, 9 and 10)/20	C ₃₉ H ₅₇ N ₁₁ O ₁₆	[(M ⁹ + M ²⁰) + H] ⁺	936.4058	936.4069	−1.2
	C ₃₉ H ₅₉ N ₁₃ O ₁₂	[(M ¹⁰ + M ²⁰) + H] ⁺	902.4479	902.4520	−4.5
	C ₃₇ H ₅₃ N ₁₁ O ₁₄	[(M ⁷ + M ²⁰) + H] ⁺	876.3846	876.3889	−4.9
	C ₆₂ H ₈₈ N ₁₉ O ₂₂	[(M ⁹ + M ¹⁰ + M ²⁰) + H] ⁺	1450.6346	1450.6369	−1.6
	C ₆₂ H ₈₉ N ₂₁ O ₁₈	[(2M ¹⁰ + M ²⁰) + H] ⁺	1416.6767	1416.6775	−0.6
	C ₆₂ H ₈₅ N ₁₇ O ₂₆	[(2M ⁹ + M ²⁰) + H] ⁺	1484.5924	1484.5928	−0.2

^aESI-TOF/MS recorded in the positive ion mode.

Copyright permission for papers 1 and 3

Reproduced by permission of The Royal Society of Chemistry

- Paper 1 | H. Nour, M. Matei, B. Bassil, U. Kortz, N. Kuhnert, *Org. Biomol. Chem.*, **2011**, 9, 3258.
- Paper 3 | Hany F. Nour, Nadim Hourani and Nikolai Kuhnert, *Org. Biomol. Chem.*, **2012**, 10, 4381.

Dear Sir/Madam

I am writing to obtain permission for the use of my contribution to two articles published in "Org. Biomol. Chem.". I am a graduate student in the Department of Organic Chemistry at Jacobs University Bremen, Germany. I am a first author on the articles and I would like to include my contributions to the articles in my doctoral dissertation. The articles are:

1. Synthesis of tri-substituted biaryl based trianglimines: formation of C3-symmetrical and non-symmetrical regioisomers, *Org. Biomol. Chem.*, 2011,9, 3258-3271, DOI: 10.1039/C0OB00944J.
2. Synthesis of novel enantiomerically pure tetra-carbohydrazide cyclophane macrocycles, *Org. Biomol. Chem.*, 2012,10, 4381-4389, DOI: 10.1039/C2OB25171J.

Thank you for your consideration of this request.

Sincerely,

Hany Nour
Sager Strasse, 29B
28757, Bremen, Germany
Email: h.nour@jacobs-university.de

RE: Website Email: Copyright permission

CONTRACTS-COPYRIGHT (shared) [Contracts-Copyright@rsc.org]

Sent: Thursday, July 12, 2012 8:53 AM**To:** Nour, Hany Fathy

Dear Hany

The Royal Society of Chemistry (RSC) hereby grants permission for the use of your paper(s) specified below in the printed and microfilm version of your thesis. You may also make available the PDF version of your paper(s) that the RSC sent to the corresponding author(s) of your paper(s) upon publication of the paper(s) in the following ways: in your thesis via any website that your university may have for the deposition of theses, via your university's Intranet or via your own personal website. We are however unable to grant you permission to include the PDF version of the paper(s) on its own in your institutional repository. The Royal Society of Chemistry is a signatory to the STM Guidelines on Permissions (available on request).

Please note that if the material specified below or any part of it appears with credit or acknowledgement to a third party then you must also secure permission from that third party before reproducing that material.

Please ensure that the thesis states the following:

Reproduced by permission of The Royal Society of Chemistry

and include a link to the paper on the Royal Society of Chemistry's website.

Please ensure that your co-authors are aware that you are including the paper in your thesis.

Regards

Gill Cockhead
Publishing Contracts & Copyright Executive

Gill Cockhead (Mrs), Publishing Contracts & Copyright Executive
Royal Society of Chemistry, Thomas Graham House
Science Park, Milton Road, Cambridge CB4 0WF, UK
Tel +44 (0) 1223 432134, Fax +44 (0) 1223 423623
<http://www.rsc.org>

Copyright permission for paper 2

Reproduced by permission of John Wiley and Sons

- Paper 2 | H. Nour, A. López-Periago, N. Kuhnert, *Rapid Commun. Mass Spectrom.*, **2012**, 26, 1070.

JOHN WILEY AND SONS LICENSE TERMS AND CONDITIONS

Jul 17, 2012

This is a License Agreement between Hany Nour ("You") and John Wiley and Sons ("John Wiley and Sons") provided by Copyright Clearance Center ("CCC"). The license consists of your order details, the terms and conditions provided by John Wiley and Sons, and the payment terms and conditions.

All payments must be made in full to CCC. For payment instructions, please see information listed at the bottom of this form.

License Number	2951290933234
License date	Jul 17, 2012
Licensed content publisher	John Wiley and Sons
Licensed content publication	Rapid Communications in Mass Spectrometry
Licensed content title	Probing the mechanism and dynamic reversibility of trianglimine formation using real-time electrospray ionization time-of-flight mass spectrometry
Licensed content author	Hany F. Nour, Ana M. Lopez-Periago, Nikolai Kuhnert
Licensed content date	Mar 19, 2012
Start page	1070
End page	1080
Type of use	I don't see my intended use
Special requirements	Dear Sir, I am a graduate student in the Department of Organic Chemistry at Jacobs University Bremen, Germany. I am the first author on the article and I would like to ask for a permission for an additional electronic publication of the paper as part of my doctoral dissertation. Sincerely, Hany Nour
Order reference number	None

Permissions Request Requires Your Acceptance

Dear Mr. Hany Nour,

Thank you for your recent permission request, which was reviewed and approved by John Wiley and Sons. Prior to reusing this content, you must accept the license fee and terms.

To accept or decline this order, please click the link below to open RightsLink.

<https://s100.copyright.com/CustomerAdmin/FC.jsp?mac=EYGSVgmpVd6XXiQVoMAy1Qzz&oNum=500685843&pName=wiley>

(If the link above is displaying on two lines, it may not open your browser window properly. Copy and paste the entire link into your browser address field and try again.)

Order Details

Licensee:	Hany Nour
Order Date:	Jul 16, 2012
Order Number:	500685843
Publication:	Rapid Communications in Mass Spectrometry Probing the mechanism and dynamic reversibility of trianglimine formation using real-time electrospray ionization time-of-flight mass spectrometry
Title:	
Type of Use:	I don't see my intended use

Note: Payee for this order is Copyright Clearance Center.

B.3:v5.5

+1-877-622-5543 / Tel: +1-978-646-2777
customercare@copyright.com
<http://www.copyright.com>



This email was sent to: h.nour@jacobs-university.de

Please visit [Copyright Clearance Center](http://www.copyright.com) for more information.

This email was sent by Copyright Clearance Center
222 Rosewood Drive Danvers, MA 01923 USA

Curriculum Vitae

Hany Nour

Department of Photochemistry, National Research Centre,
El-Behoose street, Dokki, Cairo, Egypt, P.O. Box 12622.

Home Phone: +20483675330
Cell Phone: +201061402545

EMPLOYMENT HISTORY

- Jun 2007 - Present **Assistant Researcher**, National Research Centre, Department of Photochemistry, Egypt.
- May 2003 - Jun 2007 **Researcher Assistant**, National Research Centre, Department of Photochemistry, Egypt.

EDUCATION

- Sep 2012 **PhD** work at Jacobs University Bremen, Germany, Organic and Analytical Chemistry Laboratory.
“*The Development of Novel Antibiotics Using Chemical Evolution*”
Supervisor: Prof. Dr. Nikolai Kuhnert.
- Jun 2007 **Master of Science (MSc)** in Chemistry, Cairo University, Chemistry Department, Egypt.
“*Synthesis and Reactions of Some Heterocyclic Compounds Containing Nitrogen with Expected Antimicrobial Activity*”
Supervisors: Prof. Dr. Nabil Yousef and Prof. Dr. Mohamed Hegab.
- May 2002 **Bachelor**, El-Menoufia University, Chemistry Department, Egypt.
“*Very Good (83.03), third rank in class and Faculty*”

PUBLICATIONS

1. M. Hegab, A.-S. Abdel-fattah, N. Yousef, H. Nour, A. Mostafa, M. Ellithey, Synthesis, X-ray structure, and pharmacological activity of some 6,6-disubstituted chromeno[4,3-b]- and chromeno[3,4-c]-quinolines, *Arch. Pharm. Chem. Life Sci.*, **2007**, 340, 396.
2. M. Hegab, N. Yousef, H. Nour, M. Ellithey, Synthesis and pharmacological activities of some condensed 4-chloro-2,2-dialkyl chromen-3-carboxaldehyde derivatives, *Acta. Pharm.*, **2008**, 58, 15.
3. H. Nour, M. Matei, B. Bassil, U. Kortz, N. Kuhnert, Synthesis of tri-substituted biaryl based trianglimines: formation of C_3 -symmetrical and non-symmetrical regioisomers, *Org. Biomol. Chem.*, **2011**, 9, 3258.

4. H. Nour, A. López-Periago, N. Kuhnert, Probing the mechanism and dynamic reversibility of trianglimine formation using real-time electrospray ionization time-of-flight mass spectrometry, *Rapid Commun. Mass Spectrom.*, **2012**, 26, 1070.
5. H. Nour, N. Hourani, N. Kuhnert, Synthesis of novel enantiomerically pure tetra-carbohydrazide cyclophane macrocycles, *Org. Biomol. Chem.*, **2012**, 10, 4381.
6. H. Nour, A. Golon, A. Le Gresley, N. Kuhnert, Novel synthesis of enantiomerically pure dioxaspiro[4.5]decane tetra-carbohydrazide cyclophane macrocycles, *Chem. Eur. J.*, **2012**, *submitted manuscript*.
7. H. Nour, T. Islam, M. Fernández-Lahore, N. Kuhnert, Probing the dynamic reversibility and generation of dynamic combinatorial libraries in the presence of bacterial model oligopeptides as templating guests of tetra-carbohydrazide macrocycles using electrospray mass spectrometry, *Rapid Commun. Mass Spectrom.*, **2012**, *accepted manuscript*.
8. H. Nour, A. Golon, T. Islam, M. Fernández-Lahore, N. Kuhnert, Synthesis and ESI-MS complexation studies of novel chiral tetra-(hydrazinecarboxamide) cyclophane macrocycles, *manuscript*.
9. H. Nour, A. Golon, T. Islam, M. Fernández-Lahore, N. Kuhnert, Synthesis, self-assembly and ESI-MS complexation studies of novel chiral bis-*N*-substituted-hydrazinecarboxamide receptors, *manuscript*.
10. N. Kuhnert, F. Dairpoosh, R. Jaiswal, M. Matei, S. Deshpande, A. Golon, H. Nour, H. Karaköse, N. Hourani, Hill coefficients of dietary polyphenolic enzyme inhibitors: can beneficial health effects of dietary polyphenols be explained by allosteric enzyme denaturing?, *J. Chem. Biol.*, **2011**, 4, 109.

AWARDS

Apr 2008 - Sep 2012

DAAD scholarship